

**SAFETY ANALYSIS REPORT**  
on  
**THE HI-STAR 100 CASK SYSTEM**  
(Holtec International Storage, Transport, And Repository Cask System)

by

**Holtec International**

Holtec Center  
555 Lincoln Drive West  
Marlton, NJ 08053, USA  
([www.holtecinternational.com](http://www.holtecinternational.com))

USNRC Docket No. : 71-9261  
Holtec Report No. : HI-951251  
Quality Designation : Safety Significant \*

**Copyright Notice and Notice of Proprietary Information**

This document is a copyrighted intellectual property of Holtec International. All rights reserved. Excepting any part of this document, except for public domain citations included herein, by any person or entity except for the USNRC, a Holtec User Group (HUG) member company, or a foreign regulatory authority with jurisdiction over a HUG member's nuclear facility without written consent of Holtec International is unlawful.

---

\* The safety designation is pursuant to Holtec International's Quality Assurance Program.

**HOLTEC INTERNATIONAL**

DOCUMENT NUMBER: HI-951251

PROJECT NUMBER: 5014

DOCUMENT ISSUANCE AND REVISION STATUS										
DOCUMENT NAME: SAR on the HI-STAR 100 Cask System					DOCUMENT CATEGORY: <input checked="" type="checkbox"/> GENERIC <input type="checkbox"/> PROJECT SPECIFIC					
No.	Document Portion††	REVISION No. 15						REVISION No.		
		Author's Initials	Date Approved	VIR #	Author's Initials	Date Approved	VIR #	Author's Initials	Date Approved	VIR #
1.	1	TSM	10/11/10	361294						
2.	2	CWB	10/11/10	260690						
3.	3	IR	10/11/10	33301						
4.	4	TSM	10/11/10	649599						
5.	5	TSM	10/11/10	781083						
6.	6	SPA	10/11/10	306068						
7.	7	TSM	10/11/10	420365						
8.	8	TSM	10/11/10	582183						

**HOLTEC INTERNATIONAL**

DOCUMENT NUMBER: HI-951251

PROJECT NUMBER: 5014

DOCUMENT ISSUANCE AND REVISION STATUS										
DOCUMENT NAME: SAR on the HI-STAR 100 Cask System						DOCUMENT CATEGORY: <input checked="" type="checkbox"/> GENERIC <input type="checkbox"/> PROJECT SPECIFIC				
No.	Document Portion††	REVISION No. 12			REVISION No. 13			REVISION No. 14		
		Author's Initials	Date Approved	VIR #	Author's Initials	Date Approved	VIR #	Author's Initials	Date Approved	VIR #
1.	1	SPA	10/6/06	144688	TSM	12/10/09	262162	LEH	02/05/10	803463
2.	2	N/A	N/A	N/A	CWB	12/9/09	749163	JZ	02/05/10	892723
3.	3	ER	10/6/06	550348	IR	12/9/09	716045	IR	02/04/10	270643
4.	4	KC	10/6/06	240808	SPA	12/10/09	985580	SPA	02/04/10	880286
5.	5	SPA	10/6/06	967395	JGW	12/10/09	118204	JGW	02/04/10	826589
6.	6	SPA	10/6/06	351272	SPA	12/10/09	494396	SPA	02/04/10	130566
7.	7	N/A	N/A	N/A	TSM	12/10/09	542495	LEH	02/04/10	899988
8.	8	SPA	10/6/06	217910	TSM	12/10/09	782662	LEH	02/05/10	210451

†† Chapter or section number.

**DOCUMENT CATEGORIZATION**

In accordance with the Holtec Quality Assurance Manual and associated Holtec Quality Procedures (HQPs), this document is categorized as a:

- Calculation Package<sup>3</sup> (Per HQP 3.2)       Technical Report (Per HQP 3.2)(Such as a Licensing Report)
- Design Criterion Document (Per HQP 3.4)       Design Specification (Per HQP 3.4)
- Other (Specify):

**DOCUMENT FORMATTING**

The formatting of the contents of this document is in accordance with the instructions of HQP 3.2 or 3.4 except as noted below:

**DECLARATION OF PROPRIETARY STATUS**

- Nonproprietary       Holtec Proprietary (see note 4)       Privileged Intellectual Property (PIP)

Documents labeled Privileged Intellectual Property contain extremely valuable intellectual/commercial property of Holtec International. They cannot be released to external organizations or entities without explicit approval of a company corporate officer. The recipient of Holtec's proprietary or Top Secret document bears full and undivided responsibility to safeguard it against loss or duplication.

**Notes:**

1. This document has been subjected to review, verification and approval process set forth in the Holtec Quality Assurance Procedures Manual. Password controlled signatures of Holtec personnel who participated in the preparation, review, and QA validation of this document are saved in the N-drive of the company's network. The Validation Identifier Record (VIR) number is a random number that is generated by the computer after the specific revision of this document has undergone the required review and approval process, and the appropriate Holtec personnel have recorded their password-controlled electronic concurrence to the document.
2. A revision to this document will be ordered by the Project Manager and carried out if any of its contents is materially affected during evolution of this project. The determination as to the need for revision will be made by the Project Manager with input from others, as deemed necessary by him.
3. Revisions to this document may be made by adding supplements to the document and replacing the "Table of Contents", this page and the "Revision Log".
4. This document is Holtec Proprietary unless otherwise noted otherwise in Non-Proprietary versions.

## SAR SECTION REVISION STATUS, LIST OF AFFECTED SECTIONS AND REVISION SUMMARY

<b>SAR Report No.:</b> HI-951251	<b>SAR Revision Number:</b> 15	
<b>SAR Title:</b>	Safety Analysis Report on the HI-STAR 100 Cask System	
<p>This SAR is submitted to the USNRC in support of Holtec International's application to secure a CoC under 10CFR Part 71.</p> <p>SAR review and verification are controlled at the chapter level and changes are annotated at the section level.</p> <p>A section in a chapter is identified by two numerals separated by a decimal. Each section begins on a fresh page. Unless indicated as a "complete revision" in the summary description of change below, if any change in the content is made, then the change is indicated by a "bar" in the right page margin and the revision number (annotated in the footer) of the entire section (not including applicable figures) is changed. Figures are controlled individually at the latest SAR revision level for that particular figure. Sections and figures unchanged in the latest SAR revision indicate the revision level corresponding to the last changes made in the section/figure. Drawings are also controlled individually within the Holtec International drawing control system. The List of Effective Pages identifies and tracks the latest revision levels for all sections (including appendices and supplements) and figures.</p> <p>A summary description of change is provided below for each SAR chapter (by section as applicable). Minor editorial changes to this SAR are not described.</p>		
<b>Chapter 1</b>		
<b>Section No.</b>	<b>Current Revision No.</b>	<b>Summary Description of Change</b>
1.2	15	Table 1.2.3 Areal Density for Metamic neutron absorber updated to be consistent with Licensing Drawing for MPC-32.
1.4 and 1.1	15	Drawing revisions listed updated to reflect the latest licensing drawings included with the SAR.

<b>Chapter 2</b>		
<b>Section No.</b>	<b>Current Revision No.</b>	<b>Summary Description of Change</b>
2.3	15	Updated Table 2.3.7 to provide differentiation in crush strengths of AL-STAR impact limiter aluminum honeycomb materials for HI-STAR 100 and HI-STAR HB.
2.C	15	Figures added to provide overlay plots of the deceleration time histories predicted by LS-DYNA for all corresponding 9-meter drop orientations for the original impact limiter design and the new impact limiter design.
<b>Chapter 3</b>		
<b>Section No.</b>	<b>Current Revision No.</b>	<b>Summary Description of Change</b>
3.2	15	Table 3.2.1 revised to reflect the assumptions used for Aluminum thermal properties.
<b>Chapter 4</b>		
<b>Section No.</b>	<b>Current Revision No.</b>	<b>Summary Description of Change</b>
-	13	None
<b>Chapter 5</b>		
<b>Section No.</b>	<b>Current Revision No.</b>	<b>Summary Description of Change</b>
-	14	None
<b>Chapter 6</b>		
<b>Section No.</b>	<b>Current Revision No.</b>	<b>Summary Description of Change</b>
6.E	15	Editorial per ECO 5014-187.
<b>Chapter 7</b>		
<b>Section No.</b>	<b>Current Revision No.</b>	<b>Summary Description of Change</b>
-	14	None

<b>Chapter 8</b>		
<b>Section No.</b>	<b>Current Revision No.</b>	<b>Summary Description of Change</b>
8.1	15	Editorial updates to Metamic acceptance criteria.

**End of Change Descriptions**

**LIST OF EFFECTIVE PAGES FOR REVISION 15**

<u>Page(s)</u>	<u>Revision</u>
i through xiii	15
1.0-1 through 1.0-10	14
1.1-1	13
Fig. 1.1.1	7
Fig. 1.1.2	10
Fig. 1.1.3	10
Fig. 1.1.4	10
Fig. 1.1.5	10
1.2-1 through 1.2-79	15
Fig. 1.2.1	7
Fig. 1.2.2	7
Fig. 1.2.3	10
Fig. 1.2.4	10
Fig. 1.2.5	10
Fig. 1.2.6	7
Fig. 1.2.7	7
Fig. 1.2.8	10
Fig. 1.2.9	10
Fig. 1.2.10	13
Fig. 1.2.10A	10
Fig. 1.2.10B	10
Fig. 1.2.10C	10
Fig. 1.2.10D	10
Fig. 1.2.11	9
Fig. 1.2.11A	9
Fig. 1.2.12	Deleted
Fig. 1.2.13	4
Fig. 1.2.13A	10
Fig. 1.2.14	4
Fig. 1.2.15	10
Fig. 1.2.16	10
Fig. 1.2.17	10
Fig. 1.2.18	12
1.3-1 through 1.3-19	13
1.4-1 through 1.4-2	15
Drawings	See Section 1.4
1.5-1 through 1.5-2	13
1.6-1 through 1.6-3	13
1.A-1 through 1.A-7	10
Fig. 1.A.1 through Fig. 1.A.5	4
1.B-1 through 1.B-3	10
1.C-1 through 1.C-8	10
1.I-1 through 1.I-11	15
Fig. 1.I.1	13
Supplement 1.I Drawings	See Section 1.I.4
2.0-1 through 2.0-6	10
2.1-1 through 2.1-43	13
Fig. 2.1.1	7

## LIST OF EFFECTIVE PAGES FOR REVISION 15

<u>Page(s)</u>	<u>Revision</u>
Fig. 2.1.2	6
Fig. 2.1.3	10
Fig. 2.1.4	10
Fig. 2.1.5	4
Fig. 2.1.6	4
Fig. 2.1.7	4
Fig. 2.1.8	4
Fig. 2.1.9	4
Fig. 2.1.10	6
Fig. 2.1.11	4
Fig. 2.1.12	4
Fig. 2.1.13	4
Fig. 2.1.14	6
2.2-1 through 2.2-5	10
Fig. 2.2.1	4
2.3-1 through 2.3-12	15
Fig. 2.3.1	4
Fig. 2.3.2	7
2.4-1 through 2.4-7	14
2.5-1 through 2.5-18	14
Fig. 2.5.1	10
Fig. 2.5.2	10
Fig. 2.5.3 through 2.5.11	Deleted
Fig. 2.5.12	10
Fig. 2.5.13	10
2.6-1 through 2.6-68	14
Fig. 2.6.1	4
Fig. 2.6.2	4
Fig. 2.6.3	10
Fig. 2.6.4	10
Fig. 2.6.5	6
Fig. 2.6.6	10
Fig. 2.6.7	10
Fig. 2.6.8	6
Fig. 2.6.9	10
Fig. 2.6.10	10
Fig. 2.6.11	6
Fig. 2.6.12	7
Fig. 2.6.13	7
Fig. 2.6.14	7
Fig. 2.6.15	4
Fig. 2.6.16	8
Fig. 2.6.17	8
Fig. 2.6.18	8
Fig. 2.6.19	8
Fig. 2.6.19A	8
Fig. 2.6.19B	8
Fig. 2.6.19C	8
Fig. 2.6.20	10
Fig. 2.6.21	7

## LIST OF EFFECTIVE PAGES FOR REVISION 15

<u>Page(s)</u>	<u>Revision</u>
Fig. 2.6.22	6
Fig. 2.6.23	8
Fig. 2.6.24	10
Fig. 2.6.25	10
2.7-1 through 2.7-48	14
Fig. 2.7.1	10
Fig. 2.7.2	10
Fig. 2.7.3	10
Fig. 2.7.4	10
Fig. 2.7.5	6
Fig. 2.7.6	6
Fig. 2.7.7	8
Fig. 2.7.8	8
Fig. 2.7.9	8
Fig. 2.7.10	8
Fig. 2.7.11	8
Fig. 2.7.12	8
Fig. 2.7.13	8
Fig. 2.7.14	8
Fig. 2.7.15	8
Fig. 2.7.16	8
Fig. 2.7.17	8
Fig. 2.7.18	8
2.8-1	7
2.9-1 through 2.9-19	10
Fig. 2.9.1 through Fig. 2.9.9	8
2.10-1 through 2.10-2	14
2.11-1 through 2.11-3	14
2.A-1 through 2.A-28	15
Fig. 2.A.1.1	10
Fig. 2.A.1.2	10
Fig. 2.A.1.3	10
Fig. 2.A.2.1	10
Fig. 2.A.3.1	10
Fig. 2.A.4.1	10
Fig. 2.A.4.2	10
Fig. 2.A.4.3	10
Fig. 2.A.4.4	10
Fig. 2.A.5.1	10
Fig. 2.A.5.2	10
Fig. 2.A.5.3	10
Fig. 2.A.5.4	10
Fig. 2.A.5.5	10
Fig. 2.A.5.6	10
Fig. 2.A.5.7	10
Fig. 2.A.5.8	10
Fig. 2.A.5.9	10
Fig. 2.A.5.10	10
Fig. 2.A.5.11	10
Fig. 2.A.5.12	10

**LIST OF EFFECTIVE PAGES FOR REVISION 15**

<u>Page(s)</u>	<u>Revision</u>
Fig. 2.A.5.13	10
Fig. 2.A.5.14	10
Fig. 2.A.5.15	10
Fig. 2.A.5.15A	10
Fig. 2.A.5.15B	10
Fig. 2.A.5.15C	10
Fig. 2.A.5.16	10
Fig. 2.A.5.17	10
Fig. 2.A.5.17A	10
Fig. 2.A.5.18	10
Fig. 2.A.5.19	10
Fig. 2.a.5.19A	10
Fig. 2.A.5.20	10
Fig. 2.A.5.21	10
Fig. 2.A.5.21A	10
Fig. 2.A.6.1	10
Fig. 2.A.6.2	10
Fig. 2.A.6.3	10
Fig. 2.A.6.4	10
Fig. 2.A.6.5	10
Fig. 2.A.6.6	10
Fig. 2.A.7.1	10
Fig. 2.A.7.2	10
Fig. 2.A.7.3	10
Fig. 2.A.10.1	10
Fig. 2.A.10.2	10
Fig. 2.A.10.3	10
2.B-1	14
2.B-2	14
2.B-3	14
2.C-1 through 2.C-11	15
2.I-1 through 2.I-18	14
-----	
3.0-1 through 3.0-2	12
3.1-1 through 3.1-3	13
3.2-1 through 3.2-12	15
3.3-1 through 3.3-4	13
3.4-1 through 3.4-71	13
Fig. 3.4.1	6
Fig. 3.4.2	7
Fig. 3.4.3	7
Fig. 3.4.4	4
Fig. 3.4.5	7
Fig. 3.4.6	10
Fig. 3.4.7	6
Fig. 3.4.8	6
Fig. 3.4.9	Deleted
Fig. 3.4.10	10
Fig. 3.4.11	6
Fig. 3.4.12	7

**LIST OF EFFECTIVE PAGES FOR REVISION 15**

<u>Page(s)</u>	<u>Revision</u>
Fig. 3.4.13	7
Fig. 3.4.14	6
Fig. 3.4.15	Deleted
Fig. 3.4.16	6
Fig. 3.4.17	6
Fig. 3.4.18	Deleted
Fig. 3.4.19	7
Fig. 3.4.20	7
Fig. 3.4.21	Deleted
Fig. 3.4.22	7
Fig. 3.4.23	7
Fig. 3.4.24	8
Fig. 3.4.25	8
Fig. 3.4.26	8
Fig. 3.4.27	8
Fig. 3.4.28	8
3.5-1 through 3.5-10	10
Fig. 3.5.1	7
Fig. 3.5.2	6
Fig. 3.5.3	6
Fig. 3.5.4	6
Fig. 3.5.5	6
Fig. 3.5.6	7
Fig. 3.5.7	7
Fig. 3.5.8	7
Fig. 3.5.9	7
3.6-1 through 3.6-4	13
3.7-1 through 3.7-4	14
3.A-1 through 3.A-6	10
3.B-1 through 3.B-4	10
Fig 3.B-1	10
3.I-1 through 3.I-7	13
-----	
4.0-1	13
4.1-1 through 4.1-5	13
Fig. 4.1.1	8
Fig. 4.1.2	8
Fig. 4.1.3	8
Fig. 4.1.4	Deleted-13
4.2-1 through 4.2-30	13
4.3-1 through 4.3-2	13
4.4-1	13
4.A-1 through 4.A-3	8
4.B-1 through 4.B-5	10
4.I-1 through 4.I-16	13
-----	
5.0-1 through 5.0-2	10
5.1-1 through 5.1-21	13
Fig. 5.1.1	10
Fig. 5.1.2	6

## LIST OF EFFECTIVE PAGES FOR REVISION 15

<u>Page(s)</u>	<u>Revision</u>
5.2-1 through 5.2-59	13
5.3-1 through 5.3-11	14
Fig. 5.3.1	10
Fig. 5.3.2	10
Fig. 5.3.3	4
Fig. 5.3.4	10
Fig. 5.3.5	10
Fig. 5.3.6	7
Fig. 5.3.7	6
Fig. 5.3.8	6
Fig. 5.3.9	12
Fig. 5.3.10	10
Fig. 5.3.11	8
Fig. 5.3.12	8
5.4-1 through 5.4-45	13
Fig. 5.4.1	8
Fig. 5.4.2	10
5.5-1 through 5.5-4	13
5.6-1 through 5.6-3	10
5.A-1 through 5.A-3	7
5.B-1 through 5.B-6	7
5.C-1 through 5.C-33	10
5.I-1 through 5.I-6	14
-----	
6.1-1 through 6.1-17	14
6.2-1 through 6.2-58	14
6.3-1 through 6.3-18	14
Fig. 6.3.1	10
Fig. 6.3.1A	10
Fig. 6.3.2	10
Fig. 6.3.3	10
Fig. 6.3.4	10
Fig. 6.3.5	10
Fig. 6.3.6	4
Fig. 6.3.7	10
6.4-1 through 6.4-38	14
Fig. 6.4.1	9
Fig. 6.4.2	9
Fig. 6.4.3	9
Fig. 6.4.4	9
Fig. 6.4.5	9
Fig. 6.4.6	9
Fig. 6.4.7	9
Fig. 6.4.8	9
Fig. 6.4.9	10
Fig. 6.4.10	9
Fig. 6.4.11	10
Fig. 6.4.12	10
6.5-1	10
6.6-1	10

## LIST OF EFFECTIVE PAGES FOR REVISION 15

Page(s)	Revision
6.7-1 through 6.7-2	10
6.A-1 through 6.A-22	12
Fig. 6.A.1	7
Fig. 6.A.2	7
Fig. 6.A.3	7
Fig. 6.A.4	7
Fig. 6.A.5	7
Fig. 6.A.6	14
Fig. 6.A.7	10
6.B-1 through 6.B-2	7
Appendix 6.C	Deleted
6.D-1 through 6.D-46	10
6.E-1 through 6.E-125	15
Fig. 6.E.1	12
Fig. 6.E.2	12
Fig. 6.E.2a	12
Fig. 6.E.3	12
Fig. 6.E.4	12
Fig. 6.E.5	12
Fig. 6.E.6	12
Fig. 6.E.7	12
Fig. 6.E.8	12
Fig. 6.E.9	12
Fig. 6.E.10	12
Fig. 6.E.10a	12
Fig. 6.E.11	12
Fig. 6.E.12	12
Fig. 6.E.13	12
Fig. 6.E.14	12
Fig. 6.E.15	12
Fig. 6.E.16	12
Fig. 6.E.17	12
Fig. 6.E.18	not used
Fig. 6.E.19	not used
Fig. 6.E.20	not used
Fig. 6.E.21	12
Fig. 6.E.22	12
Fig. 6.E.23	12
Fig. 6.E.24	12
Fig. 6.E.25	12
Fig. 6.E.26	12
Fig. 6.E.27	12
Fig. 6.E.28	12
Fig. 6.E.29	12
Fig. 6.E.30	12
Fig. 6.E.31	12
Fig. 6.E.32	12
Fig. 6.E.33	12
Fig. 6.E.34	12
Fig. 6.E.35	12

**LIST OF EFFECTIVE PAGES FOR REVISION 15**

<u>Page(s)</u>	<u>Revision</u>
Fig. 6.E.36	12
Fig. 6.E.36a	12
Fig. 6.E.36b	12
Fig. 6.E.37	12
Fig. 6.E.38	12
Fig. 6.E.38a	12
Fig. 6.E.38b	12
Fig. 6.E.39	12
Fig. 6.E.40	12
Fig. 6.E.41	12
Fig. 6.E.42	12
Fig. 6.E.42a	12
Fig. 6.E.42b	12
Fig. 6.E.43	12
Fig. 6.E.44	12
Fig. 6.E.44a	12
Fig. 6.E.44b	12
Fig. 6.E.45	12
Fig. 6.E.46	12
Fig. 6.E.46a	12
Fig. 6.E.46b	12
Fig. 6.E.47	12
Fig. 6.E.48	12
Fig. 6.E.48a	12
Fig. 6.E.48b	12
Fig. 6.E.49	12
Fig. 6.E.50	12
Fig. 6.E.50a	12
Fig. 6.E.51	12
Fig. 6.E.51a	12
Fig. 6.E.52	12
Fig. 6.E.52a	12
Fig. 6.E.53	12
Fig. 6.E.53a	12
Fig. 6.E.54	12
Fig. 6.E.55	12
Fig. 6.E.55a	12
Fig. 6.E.55b	12
Fig. 6.E.56	12
Fig. 6.E.57	12
Fig. 6.E.58	12
Fig. 6.E.59	12
Fig. 6.E.60	12
Fig. 6.E.61	12
Fig. 6.E.62	12
Fig. 6.E.63	12
Fig. 6.E.64	12
Fig. 6.E.65	12
6.I-1 through 6.I-14	13
Fig.6.I.1 through Fig. 6.I.4	13

**LIST OF EFFECTIVE PAGES FOR REVISION 15**

<u>Page(s)</u>	<u>Revision</u>
7.0-1 through 7.0-2	13
7.1-1 through 7.1-8	14
Fig. 7.1.1	14
7.2-1 through 7.2-3	14
7.3-1 through 7.3-2	13
7.4-1	13
7.5-1	13
7.I-1	13
8.1-1 through 8.1-11	15
8.2-1 through 8.2-3	13
8.3-1	13
8.I-1	13

## TABLE OF CONTENTS

---

### CHAPTER 1: GENERAL INFORMATION

1.0	GENERAL INFORMATION.....	1.0-1
	1.0.1 Engineering Change Orders.....	1.0-3
1.1	INTRODUCTION .....	1.1-1
1.2	PACKAGE DESCRIPTION .....	1.2-1
	1.2.1 Packaging.....	1.2-1
	1.2.1.1 Gross Weight .....	1.2-2
	1.2.1.2 Materials of Construction, Dimensions, and Fabrication .....	1.2-2
	1.2.1.3 Impact Limiters.....	1.2-9
	1.2.1.4 Shielding .....	1.2-9
	1.2.1.5 Lifting and Tie-Down Devices .....	1.2-17
	1.2.1.6 Heat Dissipation.....	1.2-17
	1.2.1.7 Coolants .....	1.2-18
	1.2.1.8 Pressure Relief Systems.....	1.2-18
	1.2.1.9 Security Seal .....	1.2-19
	1.2.1.10 Design Life.....	1.2-19
	1.2.2 Operational Features .....	1.2-19
	1.2.2.1 Applicability of Operating Procedures for the Dual-Purpose HI-STAR 100 System .....	1.2-20
	1.2.3 Contents of Package.....	1.2-22
	1.2.3.1 Determination of Design Basis Fuel .....	1.2-23
	1.2.3.2 Design Payload for Intact Fuel .....	1.2-24
	1.2.3.3 Design Payload for Damaged Fuel and Fuel Debris.....	1.2-25
	1.2.3.4 Structural Payload Parameters .....	1.2-27
	1.2.3.5 Thermal Payload Parameters .....	1.2-27
	1.2.3.6 Radiological Payload Parameters .....	1.2-28
	1.2.3.7 Criticality Payload Parameters.....	1.2-29
	1.2.3.8 Non-Fuel Hardware and Neutron Sources.....	1.2-31
	1.2.3.9 Summary of Authorized Contents .....	1.2-32
1.3	DESIGN CODE APPLICABILITY .....	1.3-1

**TABLE OF CONTENTS (continued)**

---

1.4 DRAWINGS ..... 1.4-1

1.5 COMPLIANCE WITH 10CFR71 ..... 1.5-1

1.6 REFERENCES ..... 1.6-1

Appendix 1.A: Alloy X Description

Appendix 1.B: Holtite™ Material Data

Appendix 1.C: Miscellaneous Material Data

Supplement 1.I: General Description of the HI-STAR 100 System for Humboldt Bay

**CHAPTER 2: STRUCTURAL EVALUATION**

2.0 STRUCTURAL EVALUATION ..... 2.0-1

2.1 STRUCTURAL DESIGN ..... 2.1-1

    2.1.1 Discussion ..... 2.1-1

    2.1.2 Design Criteria ..... 2.1-5

        2.1.2.1 Loading and Load Combinations ..... 2.1-6

        2.1.2.2 Allowables ..... 2.1-11

        2.1.2.3 Brittle Fracture Failure ..... 2.1-14

        2.1.2.4 Impact Limiter ..... 2.1-16

        2.1.2.5 Buckling ..... 2.1-16

2.2 WEIGHTS AND CENTERS OF GRAVITY ..... 2.2-1

2.3 MECHANICAL PROPERTIES OF MATERIALS ..... 2.3-1

    2.3.1 Structural Materials ..... 2.3-1

        2.3.1.1 Alloy X ..... 2.3-1

        2.3.1.2 Carbon Steel, Low-Alloy, and Nickel Alloy Steel ..... 2.3-2

        2.3.1.3 Bolting Materials ..... 2.3-2

        2.3.1.4 Weld Material ..... 2.3-2

        2.3.1.5 Impact Limiter ..... 2.3-2

---

**TABLE OF CONTENTS (continued)**


---

2.3.2	Nonstructural Materials .....	2.3-5
2.3.2.1	Neutron Shield .....	2.3-5
2.3.2.2	Solid Neutron Absorber .....	2.3-5
2.3.2.3	Aluminum Heat Conduction Elements .....	2.3-5
2.4	GENERAL STANDARDS FOR ALL PACKAGES .....	2.4-1
2.4.1	Minimum Package Size .....	2.4-1
2.4.2	Tamperproof Feature .....	2.4-1
2.4.3	Positive Closure .....	2.4-1
2.4.4	Chemical and Galvanic Reactions .....	2.4-1
2.5	LIFTING AND TIE-DOWN STANDARDS .....	2.5-1
2.5.1	Lifting Devices .....	2.5-1
2.5.1.1	Overpack Trunnion Analysis .....	2.5-3
2.5.1.2	Stresses in the Overpack Closure Plate, Main Flange, and Baseplate During Lifting .....	2.5-4
2.5.1.3	MPC Lifting Analyses .....	2.5-6
2.5.2	Tie-Down Devices .....	2.5-7
2.5.2.1	Discussion .....	2.5-7
2.5.2.2	Equilibrium Equations to Determine the Tie-Down Forces .....	2.5-10
2.5.2.3	Longitudinal Loading .....	2.5-11
2.5.2.4	Vertical Load .....	2.5-11
2.5.2.5	Lateral Load .....	2.5-12
2.5.2.6	Numerical Results for Tie-Down Reactions .....	2.5-12
2.5.2.7	Structural Integrity of Pocket Trunnions on Applicable HI-STAR 100 Systems .....	2.5-14
2.5.3	Failure of Lifting and Tie-Down Devices .....	2.5-15
2.5.4	Conclusion .....	2.5-16
2.6	NORMAL CONDITIONS OF TRANSPORT .....	2.6-1
2.6.1	Heat .....	2.6-1
2.6.1.1	Summary of Pressures and Temperatures .....	2.6-1

---

**TABLE OF CONTENTS (continued)**


---

2.6.1.2	Differential Thermal Expansion .....	2.6-1
2.6.1.3	Stress Calculations .....	2.6-3
2.6.1.4	Comparison with Allowable Stresses .....	2.6-32
2.6.2	Cold.....	2.6-39
2.6.2.1	Differential Thermal Expansion .....	2.6-40
2.6.2.2	MPC Stress Analysis .....	2.6-41
2.6.2.3	Overpack Stress Analysis .....	2.6-41
2.6.3	Reduced External Pressure .....	2.6-46
2.6.4	Increased External Pressure .....	2.6-47
2.6.5	Vibration .....	2.6-47
2.6.6	Water Spray .....	2.6-47
2.6.7	Free Drop .....	2.6-48
2.6.8	Corner Drop .....	2.6-48
2.6.9	Compression .....	2.6-48
2.6.10	Penetration .....	2.6-48
2.7	HYPOTHETICAL ACCIDENT CONDITIONS.....	2.7-1
2.7.1	Free Drop .....	2.7-1
2.7.1.1	End Drop.....	2.7-8
2.7.1.2	Side Drop (Load Cases F3 (Table 2.1.6), E3 (Table 2.1.7), and 3 and 11 (Table 2.1.9) .....	2.7-14
2.7.1.3	Corner Drop .....	2.7-16
2.7.1.4	Oblique Drops.....	2.7-21
2.7.1.5	Comparison with Allowable Stresses .....	2.7-24
2.7.2	Puncture .....	2.7-25
2.7.3	Thermal.....	2.7-27
2.7.3.1	Summary of Pressures and Temperatures.....	2.7-27
2.7.3.2	Differential Thermal Expansion .....	2.7-29
2.7.3.3	Stress Calculations.....	2.7-30
2.7.3.4	Comparison of Fire Accident Results with Allowable Stresses ...	2.7-35
2.7.4	Immersion - Fissile Material.....	2.7-36

**TABLE OF CONTENTS (continued)**

2.7.5	Immersion - All Packages.....	2.7-36
2.7.6	Summary of Damage .....	2.7-37
2.8	SPECIAL FORM.....	2.8-1
2.9	FUEL RODS.....	2.9-1
2.10	MISCELLANEOUS ITEMS .....	2.10-1
2.10.1	Appendices.....	2.10-1
2.10.2	Summary of NUREG-1617/10CFR71 Compliance.....	2.10-1
2.11	REFERENCES .....	2.11-1

Appendix 2.A: Design, Testing, and Computer Simulation of the AL-STAR™ Impact Limiter  
 Appendix 2.B: Summary of Results for Structural Integrity of Damaged Fuel Canisters  
 Appendix 2.C: Evaluation of an Improved HI-STAR 100 Impact Limiter Design Based on LS-DYNA Drop Simulations  
 Supplement 2.I: HI-STAR HB Structural Evaluation

**CHAPTER 3: THERMAL EVALUATION**

3.0	INTRODUCTION .....	3.0-1
3.1	DISCUSSION .....	3.1-1
3.2	SUMMARY OF THERMAL PROPERTIES OF MATERIALS.....	3.2-1
3.3	TECHNICAL SPECIFICATIONS FOR COMPONENTS .....	3.3-1
3.3.1	Evaluation of Moderate Burnup Fuel .....	3.3-1

---

**TABLE OF CONTENTS (continued)**


---

3.4	THERMAL EVALUATION FOR NORMAL CONDITIONS OF TRANSPORT .....	3.4-1
3.4.1	Thermal Model.....	3.4-1
3.4.1.1	Analytical Model - General Remarks .....	3.4-1
3.4.1.2	Test Model .....	3.4-30
3.4.2	Maximum Temperatures Under Normal Transport Conditions.....	3.4-31
3.4.2.1	Maximum Accessible Surface Temperatures .....	3.4-33
3.4.3	Minimum Temperatures.....	3.4-33
3.4.3.1	Post Rapid Ambient Temperature Drop Overpack Cooldown Event.....	3.4-34
3.4.4	Maximum Internal Pressures .....	3.4-35
3.4.5	Maximum Thermal Stresses .....	3.4-35
3.4.6	Evaluation of System Performance for Normal Conditions of Transport .....	3.4-36
3.5	HYPOTHETICAL ACCIDENT THERMAL EVALUATION.....	3.5-1
3.5.1	Thermal Model.....	3.5-2
3.5.1.1	Analytical Model .....	3.5-2
3.5.1.2	Test Model .....	3.5-4
3.5.2	System Conditions and Environment.....	3.5-4
3.5.3	System Temperatures.....	3.5-4
3.5.4	Maximum Internal Pressure .....	3.5-6
3.5.5	Maximum Thermal Stresses .....	3.5-6
3.5.6	Evaluation of System Performance for the Hypothetical Accident Thermal Conditions .....	3.5-6
3.6	REGULATORY COMPLIANCE.....	3.6-1
3.7	REFERENCES .....	3.7-1

Appendix 3.A: Conservatism in the Thermal Analysis of the HI-STAR System

---

**TABLE OF CONTENTS (continued)**


---

Appendix 3.B: The Forced Helium Dehydration (FHD) System  
 Supplement 3.I: Thermal Evaluation of HI-STAR HB

**CHAPTER 4: CONTAINMENT**

4.0	INTRODUCTION .....	4.0-1
4.1	CONTAINMENT BOUNDARIES.....	4.1-1
4.1.1	Containment Vessel .....	4.1-1
4.1.2	Containment Penetrations .....	4.1-1
4.1.3	Seals and Welds .....	4.1-1
4.1.3.1	Containment Seals .....	4.1-2
4.1.3.2	Containment Welds.....	4.1-2
4.1.4	Closure .....	4.1-2
4.1.5	Damaged Fuel Container .....	4.1-3
4.2	REQUIREMENTS FOR NORMAL AND HYPOTHETICAL ACCIDENT CONDITIONS OF TRANSPORT.....	4.2-1
4.2.1	Containment Criteria.....	4.2-1
4.2.2	Containment of Radioactive Material.....	4.2-1
4.2.3	Pressurization of Containment Vessel .....	4.2-1
4.2.4	Assumptions.....	4.2-2
4.2.5	Analysis and Results .....	4.2-3
4.2.5.1	Volume in the Containment Vessel .....	4.2-4
4.2.5.2	Source Terms for Spent Nuclear Fuel Assemblies .....	4.2-4
4.2.5.3	Effective $A_2$ of Individual Contributors (Crud, Fines, Gases, and Volatiles).....	4.2-9
4.2.5.4	Releasable Activity .....	4.2-9
4.2.5.5	Effective $A_2$ for the Total Source Term.....	4.2-9
4.2.5.6	Allowable Radionuclide Release Rates .....	4.2-10
4.2.5.7	Allowable Leakage Rates at Operating Conditions.....	4.2-10

**TABLE OF CONTENTS (continued)**

4.2.5.8	Leakage Rate Acceptance Criteria for Test Conditions.....	4.2-11
4.2.5.9	Leak Test Sensitivity .....	4.2-12
4.3	REGULATORY COMPLIANCE.....	4.3-1
4.4	REFERENCES .....	4.4-1
Appendix 4.A: Bolt and Plug Torques		
Appendix 4.B: Manufacturer Seal Information		
Supplement 4.I: Containment Evaluation of Humboldt Bay Fuel in the HI-STAR HB		
<b>CHAPTER 5: SHIELDING EVALUATION</b>		
5.0	INTRODUCTION .....	5.0-1
5.1	DISCUSSION AND RESULTS .....	5.1-1
5.1.1	Normal Operations.....	5.1-2
5.1.2	Hypothetical Accident Conditions.....	5.1-5
5.2	SOURCE SPECIFICATION .....	5.2-1
5.2.1	Gamma Source.....	5.2-2
5.2.2	Neutron Source .....	5.2-4
5.2.3	Stainless Steel Clad Fuel Source .....	5.2-4
5.2.4	Non-fuel Hardware .....	5.2-5
5.2.4.1	BPRAs and TPDs.....	5.2-5
5.2.4.2	RCCAs.....	5.2-6
5.2.5	Choice of Design Basis Assembly .....	5.2-7
5.2.5.1	PWR Design Basis Assembly.....	5.2-8
5.2.5.2	BWR Design Basis Assembly .....	5.2-8
5.2.5.3	Decay Heat Loads.....	5.2-10
5.2.6	Thoria Rod Canister.....	5.2-10

---

**TABLE OF CONTENTS (continued)**


---

5.2.7	Fuel Assembly Neutron Sources.....	5.2-11
5.2.7.1	Dresden Unit 1 Neutron Source Assemblies .....	5.2-11
5.2.7.2	Trojan Nuclear Plant Neutron Source Assemblies .....	5.2-11
5.2.8	Trojan Non-Fuel Bearing Components, Damaged Fuel and Fuel Debris.....	5.2-12
5.3	MODEL SPECIFICATIONS.....	5.3-1
5.3.1	Description of the Radial and Axial Shielding Configuration.....	5.3-1
5.3.1.1	Fuel Configuration.....	5.3-3
5.3.1.2	Streaming Considerations .....	5.3-4
5.3.2	Regional Densities .....	5.3-5
5.4	SHIELDING EVALUATION .....	5.4-1
5.4.1	Streaming Through Radial Steel Fins and Pocket Trunnions.....	5.4-2
5.4.2	Damaged Fuel Post-Accident Shielding Evaluation.....	5.4-4
5.4.3	Mixed Oxide Fuel Evaluation.....	5.4-5
5.4.4	Stainless Steel Clad Fuel Evaluation .....	5.4-5
5.4.5	Dresden Unit 1 Antimony-Beryllium Neutron Sources .....	5.4-6
5.4.6	Thoria Rod Canister.....	5.4-7
5.4.7	Trojan Fuel Contents .....	5.4-8
5.4.8	Trojan Antimony-Beryllium Neutron Sources .....	5.4-8
5.5	REGULATORY COMPLIANCE.....	5.5-1
5.6	REFERENCES .....	5.6-1
Appendix 5.A:	Sample Input File for SAS2H	
Appendix 5.B:	Sample Input File for ORIGEN-S	
Appendix 5.C:	Sample Input File for MCNP	
Supplement 5.I:	Shielding Evaluation of the MPC-HB	

---

**TABLE OF CONTENTS (continued)**


---

**CHAPTER 6: CRITICALITY EVALUATION**

6.1	DISCUSSION AND RESULTS .....	6.1-2
6.2	SPENT FUEL LOADING .....	6.2-1
6.2.1	Definition of Assembly Classes.....	6.2-1
6.2.2	PWR Fuel Assemblies in the MPC-24.....	6.2-2
6.2.3	BWR Fuel Assemblies in the MPC-68 .....	6.2-3
6.2.4	Damaged BWR Fuel Assemblies and BWR Fuel Debris .....	6.2-5
6.2.5	Thoria Rod Canister.....	6.2-6
6.2.6	PWR Assemblies in the MPC-24E and MPC-24EF .....	6.2-6
6.2.7	PWR Intact Fuel, Damaged Fuel And Fuel Debris in the Trojan MPC-24E/EF .....	6.2-6
6.2.8	PWR Assemblies in the MPC-32.....	6.2-6
6.3	MODEL SPECIFICATION.....	6.3-1
6.3.1	Description of Calculational Model.....	6.3-1
6.3.2	Cask Regional Densities .....	6.3-3
6.3.3	Eccentric Positioning of Assemblies in Fuel Storage Cells.....	6.3-4
6.4	CRITICALITY CALCULATIONS.....	6.4-1
6.4.1	Calculational or Experimental Method.....	6.4-1
6.4.2	Fuel Loading or Other Contents Loading Optimization .....	6.4-2
6.4.2.1	Internal and External Moderation .....	6.4-2
6.4.2.2	Partial Flooding.....	6.4-5
6.4.2.3	Clad Gap Flooding.....	6.4-5
6.4.2.4	Preferential Flooding .....	6.4-6
6.4.2.5	Hypothetical Accident Conditions of Transport.....	6.4-7

**TABLE OF CONTENTS (continued)**

6.4.3	Criticality Results .....	6.4-7
6.4.4	Damaged Fuel Container for BWR Fuel .....	6.4-9
6.4.5	Fuel Assemblies with Missing Rods.....	6.4-11
6.4.6	Thoria Rod Canister.....	6.4-11
6.4.7	Sealed Rods Replacing BWR Water Rods .....	6.4-11
6.4.8	Neutron Sources in Fuel Assemblies .....	6.4-11
6.4.9	PWR Damaged Fuel and Fuel Debris.....	6.4-12
6.4.9.1	Bounding Intact Assemblies .....	6.4-13
6.4.9.2	Bare Fuel Rod Arrays .....	6.4-13
6.4.9.3	Results for MPC-24E and MPC-24EF.....	6.4-15
6.4.9.4	Results for Trojan MPC-24E and MPC-24EF .....	6.4-15
6.4.10	Non-fuel Hardware in PWR Fuel Assemblies.....	6.4-15
6.4.11	Reactivity Effect of Potential Fixed Neutron Absorber Damage .....	6.4-16
6.4.12	Fixed Neutron Absorber Material.....	6.4-16
6.4.13	Reactivity Effect of Manufacturing Variations .....	6.4-17
6.5	CRITICALITY BENCHMARK EXPERIMENTS .....	6.5-1
6.6	REGULATORY COMPLIANCE.....	6.6-1
6.7	REFERENCES .....	6.7-1
	Appendix 6.A: Benchmark Calculations	
	Appendix 6.B: Distributed Enrichments in BWR Fuel	
	Appendix 6.C: Deleted	
	Appendix 6.D: Sample Input Files	
	Appendix 6.E: Burnup Credit in the MPC-32	
	Supplement 6.I: Criticality Evaluation of Humboldt Bay Fuel in the MPC-HB	
	<b>CHAPTER 7: OPERATING PROCEDURES</b>	
7.0	INTRODUCTION .....	7.0-1

**TABLE OF CONTENTS (continued)**

7.1	PROCEDURE FOR LOADING AND PREPARATION FOR TRANSPORT OF THE HI-STAR 100 SYSTEM .....	7.1-1
7.1.1	Overview of HI-STAR Loading Operations.....	7.1-1
7.1.2	Preparation of HI-STAR for Loading.....	7.1-1
7.1.3	Loading of Contents into HI-STAR.....	7.1-1
7.1.4	Closure of HI-STAR.....	7.1-5
7.1.5	Preparation of HI-STAR for Transport.....	7.1-6
7.2	PROCEDURE FOR UNLOADING THE HI-STAR 100 SYSTEM.....	7.2-1
7.2.1	Receipt of Package from Carrier.....	7.2-1
7.2.2	Removal of Contents.....	7.2-2
7.3	PREPARATION OF AN EMPTY PACKAGE FOR TRANSPORT.....	7.3-1
7.4	PROCEDURE FOR PREPARING THE HI-STAR 100 OVERPACK FOR TRANSPORT FOLLOWING A PERIOD OF STORAGE.....	7.4-1
7.5	REFERENCES .....	7.5-1

Supplement 7.I: Operating Procedures of the HI-STAR HB System

**CHAPTER 8: ACCEPTANCE TESTS AND MAINTENANCE PROGRAM**

8.0	INTRODUCTION .....	8.1-1
8.1	ACCEPTANCE TESTS.....	8.1-1
8.1.1	Visual Inspections and Measurements.....	8.1-1
8.1.2	Weld Examinations.....	8.1-2

---

**TABLE OF CONTENTS (continued)**


---

8.1.3	Structural and Pressure Tests .....	8.1-2
8.1.3.1	Lifting Trunnions .....	8.1-2
8.1.3.2	Pressure Testing .....	8.1-3
8.1.3.3	Pneumatic Testing of the Neutron Shield Enclosure Vessel .....	8.1-4
8.1.4	Leakage Tests .....	8.1-4
8.1.5	Component and Material Tests .....	8.1-5
8.1.5.1	Valves, Relief Devices, and Fluid Transport Devices .....	8.1-5
8.1.5.2	Seals and Gaskets .....	8.1-5
8.1.5.3	Transport Impact Limiter .....	8.1-6
8.1.5.4	Neutron Shielding Material .....	8.1-6
8.1.5.5	Neutron Absorber Material .....	8.1-7
8.1.5.6	Gamma Shielding .....	8.1-11
8.1.6	Thermal Tests .....	8.1-11
8.2	MAINTENANCE PROGRAM .....	8.2-1
8.2.1	Structural and Pressure Tests .....	8.2-1
8.2.2	Leakage Tests .....	8.2-1
8.2.3	Component and Material Tests .....	8.2-2
8.2.4	Shielding .....	8.2-2
8.2.5	Thermal Tests .....	8.2-2
8.2.6	Miscellaneous Tests .....	8.2-2
8.3	REFERENCES .....	8.3-1

Supplement 8.I: Acceptance Tests and Maintenance Program

## CHAPTER 1: GENERAL INFORMATION

### 1.0 GENERAL INFORMATION

This Safety Analysis Report (SAR) for Holtec International's HI-STAR 100 packaging is a compilation of information and analyses to support a United States Nuclear Regulatory Commission (NRC) licensing review as a spent nuclear fuel transportation package (Docket No. 71-9261) under requirements specified in 10CFR71 [1.0.1] and 49CFR173 [1.0.2]. This SAR supports NRC approval and issuance of Certificate of Compliance No. 9261, issued under the provisions and definitions in 10CFR71, Subpart D, for the design Model: HI-STAR 100 as an acceptable Type B(U)F-96 packaging for transport by exclusive use shipment (10CFR71.47).

The HI-STAR 100 packaging complies with the requirements of 10CFR71 for a Type B(U)F-96 package. The HI-STAR 100 packaging does not have a maximum normal operating pressure (MNOP) greater than 700 kPa (100 lb/in<sup>2</sup>). The HI-STAR 100 internal design pressure is specified in Table 2.1.1 as 100 psig to calculate bounding stress values. Section 3.4 calculates the MNOP (reported in Table 3.4.15) and demonstrates that the value remains below the design value specified in Table 2.1.1. No pressure relief device is provided on the HI-STAR 100 containment boundary, as discussed in Subsection 1.2.1.8. Therefore, there is no pressure relief device that would allow the release of radioactive material under the tests specified in 10CFR71.73. Analyses that demonstrate that the HI-STAR 100 packaging complies with the requirements of Subparts E and F of 10CFR71 are provided in this SAR. Specific reference to each section of the SAR that is used to specifically address compliance to 10CFR71 is provided in Table 1.0.2. Therefore, the HI-STAR 100 packaging to transport spent nuclear fuel should be designated B(U)F-96.

The HI-STAR 100 Criticality Safety Index (CSI) is zero, as an unlimited number of packages is subcritical under the procedures specified in 10CFR71.59(a). Section 6.1 provides the determination of the CSI. The Transport Index (TI) based on radiation is in excess of 10 for the HI-STAR 100 Packaging with design basis fuel contents. Therefore, the HI-STAR 100 Packaging must be transported by exclusive use shipment (10CFR71.47).

The HI-STAR 100 packaging design, fabrication, assembly, and testing shall be performed in accordance with Holtec International's quality assurance program. Holtec International's quality assurance program was originally developed to meet NRC requirements delineated in 10CFR50, Appendix B, and was expanded to include provisions of 10CFR71, Subpart H, and 10CFR72, Subpart G, for structures, systems, and components designated as important to safety. NRC approval of Holtec International's quality assurance program is documented by the Quality Assurance Program Approval for Radioactive material Packages (NRC Form 311), Approval Number 0784, Docket No. 71-0784.

This SAR has been prepared in the format and content suggested in NRC Regulatory Guide 7.9 [1.0.3]. The purpose of this chapter is to provide a general description of the design features and transport capabilities of the HI-STAR 100 packaging including its intended use. This chapter provides a summary description of the packaging, operational features, and contents, and provides reasonable assurance that the package will meet the regulations and operating objectives. Table 1.0.1 contains a listing of the terminology and notation used in preparing this SAR.

This SAR was initially prepared prior to the issuance of the draft version of NUREG-1617 [1.0.5]. To aid NRC review, additional tables and references have been added to facilitate the location of information needed to demonstrate compliance with 10CFR71 as outlined by NUREG-1617. Table 1.0.2 provides a matrix of the 10CFR71 requirements as outlined in NUREG-1617, the format requirements of Regulatory Guide 7.9, and reference to the applicable SAR section(s) that address(es) each topic.

The HI-STAR 100 System is a dual purpose system, certified under 10 CFR 71 and 10 CFR 72. The HI-STAR 100 Final Safety Analysis Report (FSAR) [1.0.6] supports Certificate of Compliance No. 1008 for HI-STAR 100 to store spent nuclear fuel at an Independent Spent Fuel Storage Installation (ISFSI) facility under requirements of 10CFR72, Subpart L [1.0.4] (Docket Number 72-1008).

Within this report, all figures, tables and references cited are identified by the double decimal system m.n.i, where m is the chapter number, n is the section number, and i is the sequential number. Thus, for example, Figure 1.1.1 is the first figure in Section 1.1 of Chapter 1 (which is the next section in this chapter).

Revision of this document was made on a section level. Therefore, if any change occurs on a page, the entire section was updated to the current revision. The locations of specific text changes are indicated by revision bars in the margin of the page. Figures are controlled individually at the latest SAR revision level for that particular figure. Sections and figures unchanged in the latest SAR revision indicate the revision level corresponding to the last changes made in the section/figure. Drawings are also controlled individually within the Holtec International drawing control system.

The HI-STAR 100 Version HB (also called HI-STAR HB) is a shorter variation of the HI-STAR 100 specifically designed for Humboldt Bay fuel [1.0.8]. Information pertaining to the HI-STAR HB System is generally contained in supplements to each chapter identified by a Roman numeral "I" (i.e., Chapter 1 and Supplement 1.I). Certain sections of the main SAR are also affected and are appropriately modified for continuity with the "I" supplements. Unless superseded or specifically modified by information in the "I" supplements, the information in the main SAR chapters is applicable to the HI-STAR HB System.

Through revision 11 of this SAR, discussions were presented that described MPC designs called the MPC-24EF, and MPC-68F. These designs contain features required to classify them as secondary containments, which was necessary for transportation of fuel debris under an earlier version of 10 CFR 71, and were the only MPC designs allowed to be loaded with fuel debris. Recent changes to 10 CFR 71 have eliminated the need for secondary containment of fuel debris. The F-canister designs have been retained in this SAR; however, any requirements regarding the secondary containment function of these canisters have been removed.

1.0.1 Engineering Change Orders

The changes authorized by Holtec Engineering Change Orders (ECOs) for the following licensed components are reflected in this revision of this SAR (see Supplement(s) to this chapter for listing of additional ECOs for respective applicable licensed components).

MPC-68/68F Basket: 1021-62, 63, 64, 78, 80, 89, 97, 102 and 103.

MPC-24 Basket: 1022-58, 59, 67, 68, 76 and 81.

MPC-24E/24EF Basket: 1022-67, 68, 76 and 81.

MPC-32 Basket: 1023-31, 32, 33, 43, 45, 46, 50, 54, 55 and 60.

HI-STAR 100 overpack: None.

MPC Enclosure Vessel: 1021-94, 96, 99 and 102; 1022-73, 75, 78 and 80; 1023-51, 54, 57 and 59; 5014-164 (MPC-Fuel Spacers: 1021-95, 100, 101 and 104; 1022-74, 79 and 82; and 1023-52, 58 and 62).

HI-STAR 100 Assembly for Transport: None.

Ancillary Equipment: AL-STAR Impact Limiters - 5014-176.

Trojan Equipment: None.

Table 1.0.1

## TERMINOLOGY AND NOTATION

**ALARA** is an acronym for As Low As Reasonably Achievable.

**AL-STAR™** is the trademark name of the HI-STAR 100 impact limiter.

**Boral** is a generic term to denote an aluminum-boron carbide cermet manufactured in accordance with U.S. Patent No. 4027377. The individual material supplier may use another trade name to refer to the same product.

**Boral™** means Boral manufactured by AAR Advanced Structures.

**BWR** is an acronym for boiling water reactor.

**C.G.** is an acronym for center of gravity.

**Commercial Spent Fuel or CSF** refers to nuclear fuel used to produce energy in a commercial nuclear power plant.

**Containment System Boundary** means the enclosure formed by the overpack inner shell welded to a bottom plate and top flange plus the bolted closure plate with dual seals and the vent and drain port plugs with seals.

**Containment System** means the HI-STAR 100 overpack that forms the containment boundary of the packaging intended to contain the radioactive material during transport.

**Cooling Time (or post-irradiation cooling time)** for a spent fuel assembly is the time between reactor shutdown and the time the spent fuel assembly is loaded into the MPC.

**Critical Characteristic** means a feature of a component or assembly that is necessary for the proper safety function of the component or assembly. Critical characteristics of a material are those attributes that have been identified, in the associated material specification, as necessary to render the material's intended function.

**Criticality Safety Index (CSI)** is the dimensionless number (rounded up to the next tenth) assigned to and placed on the label of a fissile material package, to designate the degree of control of accumulation of packages containing fissile material during transportation.

**Damaged Fuel Assembly** is a fuel assembly with known or suspected cladding defects, as determined by a review of records, greater than pinhole leaks or hairline cracks, empty fuel rod locations that are not filled with dummy fuel rods, missing structural components such as grid spacers, whose structural integrity has been impaired such that geometric rearrangement of fuel or gross failure of the cladding is expected based on engineering evaluations, or that cannot be handled

by normal means. Fuel assemblies that cannot be handled by normal means due to fuel cladding damage are considered FUEL DEBRIS.

**Damaged Fuel Container (or Canister)** means a specially designed enclosure for damaged fuel assemblies or fuel debris which permits gaseous and liquid media to escape while minimizing dispersal of gross solid particulates.

**Enclosure Vessel (or MPC Enclosure Vessel)** means the pressure vessel defined by the cylindrical shell, baseplate, port cover plates, lid, closure ring, and associated welds that provides confinement for the helium gas contained within the MPC. The Enclosure Vessel (EV) and the fuel basket together constitute the multi-purpose canister.

**Exclusive use** means the sole use by a single consignor of a conveyance for which all initial, intermediate, and final loading and unloading are carried out in accordance with the direction of the consignor or consignee. The consignor and the carrier must ensure that loading or unloading is performed by personnel having radiological training and resources appropriate for safe handling of the consignment. The consignor must issue specific instructions, in writing, for maintenance of exclusive use shipment controls, and include them with the shipping paper information provided to the carrier by the consignor.

**FSAR** is an acronym for Final Safety Analysis Report (10CFR72).

**Fuel Basket** means a honeycomb structural weldment with square openings which can accept a fuel assembly of the type for which it is designed.

**Fuel Debris** is ruptured fuel rods, severed fuel rods, loose fuel pellets, or fuel assemblies with known or suspected defects which cannot be handled by normal means due to fuel cladding damage, including containers and structures supporting these parts. Fuel debris also includes certain Trojan plant-specific fuel material contained in Trojan Failed Fuel Cans.

**HI-STAR 100 overpack or overpack** means the cask that receives and contains the sealed multi-purpose canisters containing spent nuclear fuel. It provides the containment boundary for radioactive materials, gamma and neutron shielding, and a set of lifting trunnions for handling. Certain overpack models also include optional pocket trunnions for upending and downending.

**HI-STAR 100 System or HI-STAR 100 Packaging** consists of the MPC sealed within the HI-STAR 100 overpack with impact limiters installed.

**Holtite™** is the trade name for all present and future neutron shielding materials formulated under Holtec International's R&D program dedicated to developing shielding materials for application in dry storage and transport systems. The Holtite development program is an ongoing experimentation effort to identify neutron shielding materials with enhanced shielding and temperature tolerance characteristics. Holtite-A™ is the first and only shielding material qualified under the Holtite R&D program. As such, the terms Holtite and Holtite-A may be used interchangeably throughout this SAR.

**Holtite™-A** is a trademarked Holtec International neutron shield material.

**Humboldt Bay Damaged Fuel Container (or Canister)** is a Holtec damaged fuel container custom-designed for Humboldt Bay plant damaged fuel and fuel debris.

**Impact Limiter** means a set of fully-enclosed energy absorbers that are attached to the top and bottom of the overpack during transport. The impact limiters are used to absorb kinetic energy resulting from normal and hypothetical accident drop conditions. The HI-STAR impact limiters are called AL-STAR.

**Important to Safety (ITS)** means a function or condition required to transport spent nuclear fuel safely; to prevent damage to spent nuclear fuel, and to provide reasonable assurance that spent nuclear fuel can be received, handled, packaged, transported, and retrieved without undue risk to the health and safety of the public.

**Intact Fuel Assembly** is defined as a fuel assembly without known or suspected cladding defects greater than pinhole leaks and hairline cracks, and which can be handled by normal means. Fuel assemblies without fuel rods in fuel rod locations shall not be classified as Intact Fuel Assemblies unless dummy fuel rods are used to displace an amount of water greater than or equal to that displaced by the original fuel rod(s).

**Load-and-Go** is a term used in this SAR that means the practice of loading spent fuel into the HI-STAR 100 System packaging and placing the packaging into transportation service under 10 CFR 71, without first deploying the system at an Independent Spent Fuel Storage Installation (ISFSI) under 10 CFR 72.

**Maximum Normal Operating Pressure (MNOP)** means the maximum gauge pressure that would develop in the containment system in a period of 1 year under the heat condition specified in 10CFR71.71(c)(1), in the absence of venting, external cooling by an ancillary system, or operational controls during transport.

**Maximum Reactivity** means the highest possible k-effective including bias, uncertainties, and calculational statistics evaluated for the worst-case combination of fuel basket manufacturing tolerances.

**MGDS** is an acronym for Mined Geological Depository System.

**MPC Fuel Basket** means the honeycombed composite cell structure utilized to maintain subcriticality of the spent nuclear fuel. The number and size of the storage cells depends on the type of spent nuclear fuel to be transported. Each MPC fuel basket has sheathing welded to the storage cell walls for retaining the neutron absorber. The neutron absorber is a commercially-available thermal neutron poison material composed of boron carbide and aluminum.

**Multi-Purpose Canister (MPC)** means the sealed canister consisting of a honeycombed fuel basket for spent nuclear fuel storage, contained in a cylindrical canister shell (the MPC Enclosure Vessel). There are different MPCs with different fuel basket geometries for storing PWR or BWR fuel. All MPCs except the Trojan and Humboldt Bay plant MPCs have identical exterior dimensions. The Trojan plant MPCs have the same outside diameter, but are approximately nine inches shorter than the generic MPC design. The Humboldt Bay plant MPCs have the same outside diameter, but are approximately 6.3 feet shorter. MPC is an acronym for multi-purpose canister. Many of the MPCs used as part of the HI-STAR 100 Packaging are identical to the MPCs authorized for use in the HI-STAR 100 Storage (Docket No. 72-1008) and HI-STORM 100 Storage (72-1014) [1.0.7] CoCs to the extent that many of the particular MPC models are authorized for use under both CoCs.

**Neutron Absorber Material** is a generic term used in this SAR to indicate any neutron absorber material qualified for use in the HI-STAR 100 System MPCs.

**Neutron Shielding** means Holtite, a material used in the overpack to thermalize and capture neutrons emanating from the radioactive spent nuclear fuel.

**Neutron Sources** means specially designed inserts for fuel assemblies that produce neutrons for startup of the reactor. The specific types of neutron sources authorized for transportation in the HI-STAR 100 System are discussed in Section 1.2.3.

**Non-fuel Hardware, or NFH**, means Burnable Poison Rod Assemblies (BPRAs), Thimble Plug Devices (TPDs), Control Rod Assemblies (CRAs), Axial Power Shaping Rods (APSRs), Wet Annular Burnable Absorbers (WABAs), Rod Cluster Control Assemblies (RCCAs), Control Element Assemblies (CEAs), water displacement guide tube plugs, orifice rod assemblies, and vibration suppressor inserts. The specific types of NFH authorized for transportation in the HI-STAR 100 System are discussed in Section 1.2 of this SAR.

**Packaging** means the HI-STAR 100 System consisting of a single HI-STAR 100 overpack, a set of impact limiters, and a multi-purpose canister (MPC). It excludes all lifting devices, rigging, transporters, saddle blocks, welding machines, and auxiliary equipment (such as the drying and helium backfill system) used during fuel loading operations and preparation for off-site transportation.

**Package** means the HI-STAR 100 System plus the licensed radioactive contents loaded for transport.

**Planar-Average Initial Enrichment** is the average of the distributed fuel rod initial enrichments within a given axial plane of the assembly lattice.

**PWR** is an acronym for pressurized water reactor.

**Reactivity** is used synonymously with effective multiplication factor or k-effective.

**SAR** is an acronym for Safety Analysis Report (10CFR71).

**Single Failure Proof** means that the handling system is designed so that a single failure will not result in the loss of the capability of the system to safely retain the load.

**SNF** is an acronym for spent nuclear fuel.

**STP** is Standard Temperature (298°K) and Pressure (1 atm) conditions.

**Transport Index (TI)** means the dimensionless number (rounded up to the next tenth) placed on the label of a package, to designate the degree of control to be exercised by the carrier during transportation. The transport index is the number determined by multiplying the maximum radiation level in mSv/hr at one meter (3.3 ft) from the external surface of the package by 100 (equivalent to the maximum radiation level in mrem/hr at one meter (3.3 ft)).

**Trojan Damaged Fuel Container (or Canister)** is a Holtec damaged fuel container custom-designed for Trojan plant damaged fuel and fuel debris. Trojan plant damaged fuel and fuel debris not loaded into a Trojan Failed Fuel Can must be loaded into a Trojan Damaged Fuel Container.

**Trojan Failed Fuel Can (FFC)** is a non-Holtec designed Trojan plant-specific damaged fuel container that may be loaded with Trojan plant damaged fuel assemblies, Trojan fuel assembly metal fragments (e.g., portions of fuel rods, grid assemblies, bottom nozzles, etc.), a Trojan fuel rod storage container, a Trojan Fuel Debris Process Can Capsule, or a Trojan Fuel Debris Process Can.

**Trojan Failed Fuel Can Spacer** is a square, structural steel tube with a baseplate designed to be placed inside one Trojan Failed Fuel Can to occupy any space between the top of the contents and the top of the FFC in order to minimize movement of the FFC contents during transportation.

**Trojan Fuel Debris Process Can** is a Trojan plant-specific canister containing fuel debris (metal fragments) and was used to process organic media removed from the Trojan plant spent fuel pool during cleanup operations in preparation for spent fuel pool decommissioning. Trojan Fuel Debris Process Cans are loaded into Trojan Fuel Debris Process Can Capsules or directly into Trojan Failed Fuel Cans.

**Trojan Fuel Debris Process Can Capsule** is a Trojan plant-specific canister that contains up to five Trojan Fuel Debris Process Cans and is vacuumed, purged, backfilled with helium, and then seal-welded closed.

**Undamaged fuel assemblies** are fuel assemblies where all the exterior rods in the assembly are visually inspected and shown to be intact. The interior rods of the assembly are in place; however the cladding of these rods is of unknown condition. This definition only applies to Humboldt Bay fuel assembly array/class 6x6D and 7x7C.

**ZR** means any zirconium-based fuel cladding material authorized for use in a commercial nuclear power plant reactor. Any reference to Zircaloy fuel cladding in this SAR applies to any zirconium-based fuel cladding material.

Table 1.0.2

## HI-STAR 100 SAR CORRELATION WITH 10CFR71 AND REGULATORY GUIDE 7.9

<b>RG 7.9 Section</b>	<b>10CFR Part 71 Section</b>	<b>HI-STAR SAR Section</b>
1.1	71.31(a)(1), 71.31(a)(2), 71.31(a)(3), 71.31(c), 71.33(a)(1), 71.33(a)(3), 71.35(b), 71.37, 71.59	1.0, 1.1, 1.2, 1.5
1.2	71.31(a)(1), 71.33(a)(2), 71.33(a)(4), 71.33(a)(5), 71.33(a)(6), 71.33(b), 71.43(b)	1.2, 1.3, 1.4
None	71.31(a)(2), 71.35(a), 71.41(a)	1.5
1.3	None	Appendices 1.A, 1.B, and 1.C
2.1, 2.2	71.31(a)(1), 71.31(c), 71.33	2.1, 2.2
2.3, 2.4	71.43(d)	2.3, 2.4
2.5	71.45	2.5
2.6, 2.7	71.31(a)(2), 71.35(a), 71.41(a), 71.61, 71.71, 71.73	2.6, 2.7
2.6	71.35(a), 71.41(a), 71.43(f), 71.51(a)(1), 71.55(d)(4), 71.71	2.6
2.7	71.35(a), 71.41(a), 71.73	2.7
None	71.61	2.7
None	71.85(b)	8.1.3
2.10	None	2.10
3.1	71.31(a)(1), 71.31(c), 71.33(a)(5), 71.33(a)(6), 71.33(b)(1), 71.33(b)(3), 71.33(b)(5), 71.33(b)(7), 71.33(b)(8), 71.51(c)	Chapters 1 & 2, Sections 3.0, 3.1, 3.4, 3.6
3.2, 3.3	71.31(a)(1), 71.33(a)(5)	Chapters 1 & 2, Sections 3.0, 3.1, 3.4, 3.6
None	71.31(a)(2), 71.35(a), 71.41(a)	3.0, 3.1, 3.4, 3.5, 3.6
None	71.43(g)	3.0, 3.4, 3.6
3.4	71.43(f), 71.51(a)(1), 71.71	3.0, 3.4, 3.6
3.5	71.73	3.0, 3.5, 3.6
3.6	None	N/A
4.1	71.31(a)(1), 71.31(c), 71.33(a)(4), 71.33(a)(5), 71.33(b)(1), 71.33(b)(3), 71.33(b)(5), 71.33(b)(7), 71.43(c), 71.43(d), 71.43(e)	4.0, 4.1, 4.2, 4.3
4.2	71.31(a)(2), 71.35(a), 71.41(a), 71.43(f), 71.43(h), 71.51(a)(1), 71.51(c)	4.2, 4.3
4.3	71.31(a)(2), 71.35(a),	4.2, 4.3

Table 1.0.2 (continued)

## HI-STAR 100 SAR CORRELATION WITH 10CFR71 AND REGULATORY GUIDE 7.9

RG 7.9 Section	10CFR Part 71 Section	HI-STAR SAR Section
	71.41(a), 71.51(a)(2), 71.51(c)	
4.4	71.63	4.2, 4.3
4.5	None	-
5.1	71.31(a)(1), 71.31(c), 71.33(a)(5)	5.1
5.2	71.31(a)(1), 71.33(b)(1), 71.33(b)(2), 71.33(b)(3)	5.2
5.3	71.31(a), 71.31(b)	5.3
5.4	71.31(a)(2), 71.35(a), 71.41(a), 71.43(f), 71.47(b), 71.51(a)(1), 71.51(a)(2)	5.1, 5.4, 5.5
5.5	None	Appendices 5.A, 5.B, 5.C
6.1	71.31(a)(1), 71.31(c), 71.33(a)(5), 71.35(b), 71.59(b)	6.1
6.2	71.31(a)(1), 71.33(b)(1), 71.33(b)(2), 71.33(b)(3), 71.83	6.2
6.3	71.31(a)(2), 71.35(a), 71.41(a)	6.3
6.4	71.35, 71.43(f), 71.51(a)(1), 71.55(b), 71.55(d), 71.55(e), 71.59	6.4, Appendix 6.E
6.5	71.31(a)(2), 71.35	6.5, Appendix 6.A, Appendix 6.E
6.6	None	6.2, 6.4, Appendices 6.B, 6.C, 6.D
7.1	71.31(c), 71.35(c), 71.43(g), 71.47(b), 71.47(c), 71.47(d), 71.87, 71.89	7.1
7.2	71.35(c)	7.2
7.3	71.87(i)	7.3
None	71.35(c)	7.0
7.4	None	-
8.1	71.31(c), 71.37(b), 71.85(a), 71.85(b), 71.85(c), 71.87(g), 71.93(b)	8.1
8.2	71.31(c), 71.37(b), 71.87(b), 71.87(g), 71.93(b)	8.2

Notes:

“-“ There is no HI-STAR SAR section that addresses this.

## 1.1 INTRODUCTION

HI-STAR 100 (acronym for Holtec International Storage, Transport and Repository) is a spent nuclear fuel (SNF) packaging designed to be in general compliance with the U.S. Department of Energy's (DOE) original design procurement specifications for multi-purpose canisters and large transportation casks [1.1.1], [1.1.2].

The HI-STAR 100 System consists of a sealed, metal multi-purpose canister, herein abbreviated as the "MPC", contained within an overpack with impact limiters. Figure 1.1.1 provides a pictorial view of the HI-STAR 100 System. The HI-STAR 100 System is designed to accommodate a wide variety of spent fuel assemblies in a single overpack design by utilizing different MPC basket designs. The exterior dimensions of all MPCs (except the custom-designed Trojan and Humboldt Bay MPCs) are identical to allow the use of a single overpack design. The Trojan plant MPCs are approximately nine inches shorter than the generic Holtec MPC design and have the same outer diameter. The Humboldt Bay MPCs are approximately 6.3 feet shorter than the generic Holtec MPC design and have the same outer diameter. Each of the MPCs has different design features (e.g., fuel baskets) to accommodate distinct fuel characteristics. Each MPC is identified by the maximum quantity of fuel assemblies it is capable of receiving. The MPC-24, -24E, and -24EF each can contain a maximum of 24 PWR assemblies; the MPC-32 can contain up to 32 PWR assemblies; the MPC-68 and -68F each can contain a maximum of 68 BWR fuel assemblies; and the MPC-HB for Humboldt Bay can contain up to 80 fuel assemblies. Figure 1.1.2 depicts the HI-STAR 100 with two of its major constituents, the MPC and the overpack, in a cutaway view. This view does not include depiction of the spacer required for the Trojan version of the MPC-24E/EF design, which is shorter than the Holtec generic design. The spacer is required for the shorter MPC to ensure the design characteristics of the HI-STAR 100 System (e.g., center-of-gravity, MPC lid-to-overpack closure plate gap, etc.) remain bounded by the supporting analyses. See Figure 1.1.5 for a depiction of the Trojan MPC spacer. A drawing of the Trojan MPC spacer is also included in Section 1.4. A summary of the qualification of the spacer for performing its design function is provided in Section 2.7.1.1.

Figure 1.1.2 also indicates that the overpack pocket trunnions are optional appurtenances. Overpack serial numbers 1020-001 through 1020-007 include the pocket trunnions, while later serial number overpacks do not. The impact of this design change on vehicle tie down methods and qualification analyses are discussed in Section 2.5 of this SAR. The pocket trunnions are not part of the qualified vehicle tie-down system for the package. Figure 1.1.3 provides an elevation cross sectional view of an MPC, and Figure 1.1.4 contains an elevation cross sectional view of the HI-STAR 100 overpack.

The HI-STAR 100 System is designed for both storage and transport. The HI-STAR 100 System's multi-purpose design reduces SNF handling operations and thereby enhances radiological protection. Once SNF is loaded and the MPC and overpack are sealed, the HI-STAR 100 System can be positioned on site for temporary or long-term storage or transported directly off-site. The HI-STAR 100 System's ability to both store and transport SNF eliminates repackaging.

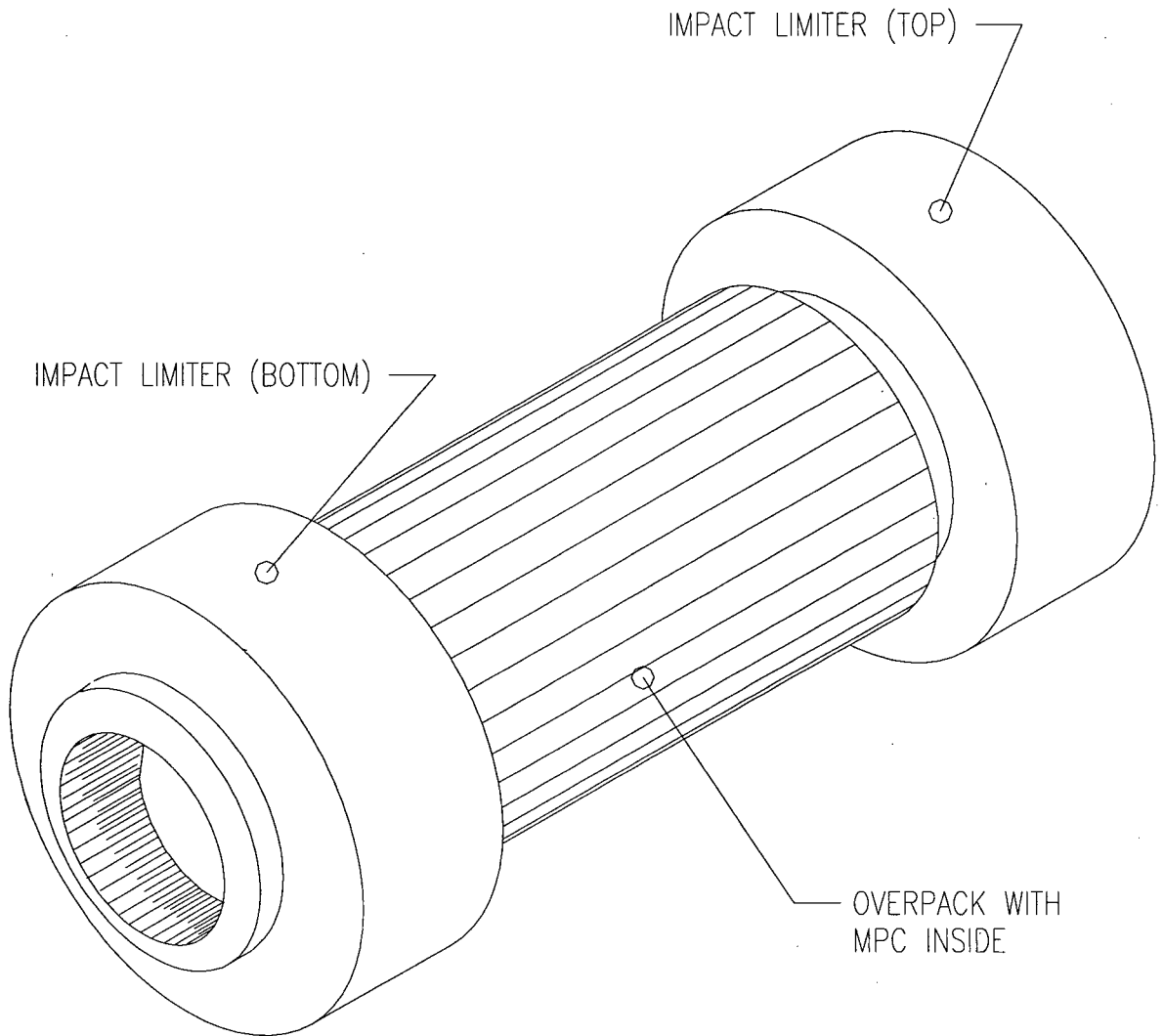


FIGURE 1.1.1; PICTORIAL VIEW OF  
HI-STAR 100 PACKAGE

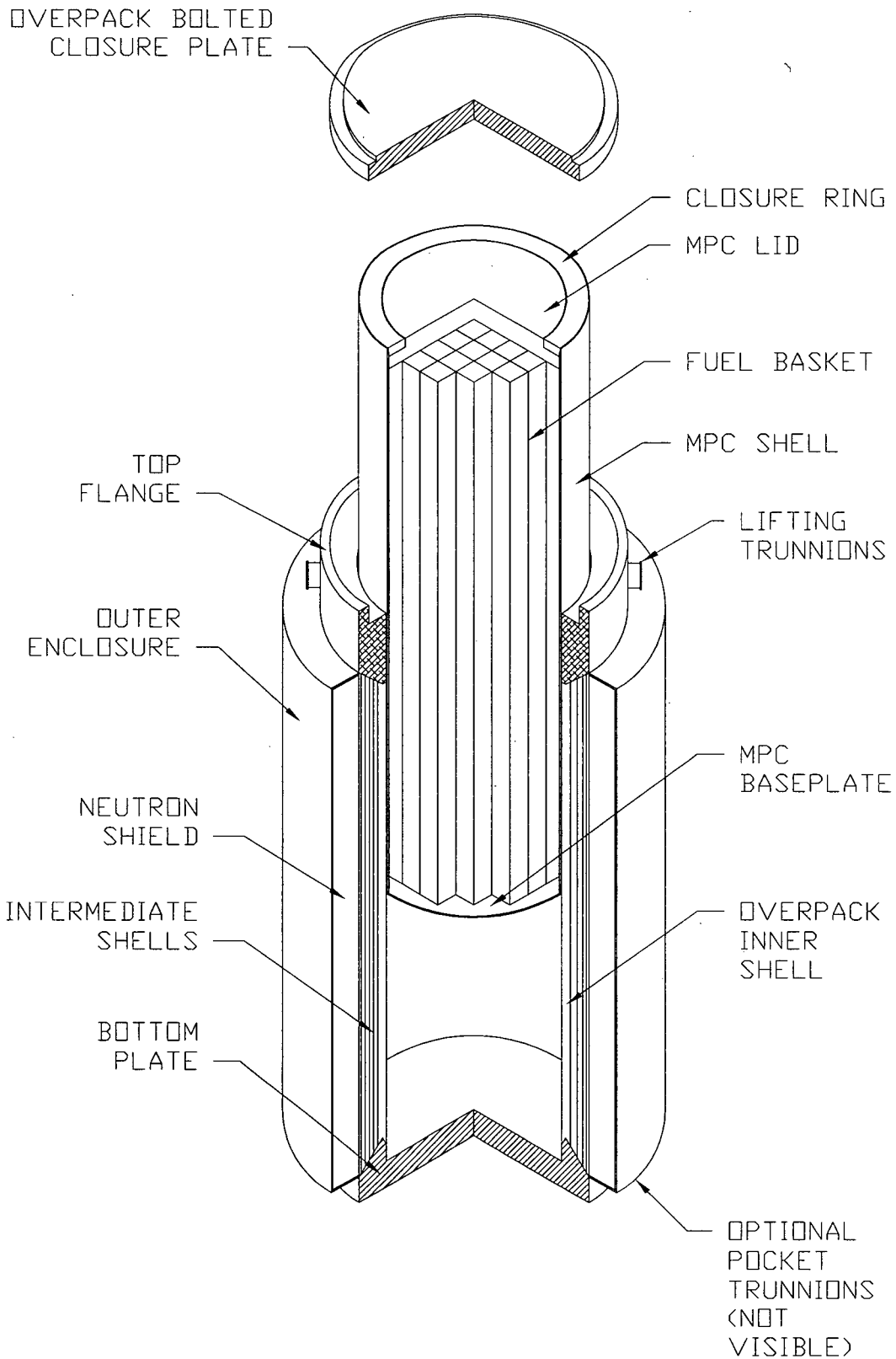


FIGURE 1.1.2; HI-STAR 100 OVERPACK WITH MPC PARTIALLY INSERTED

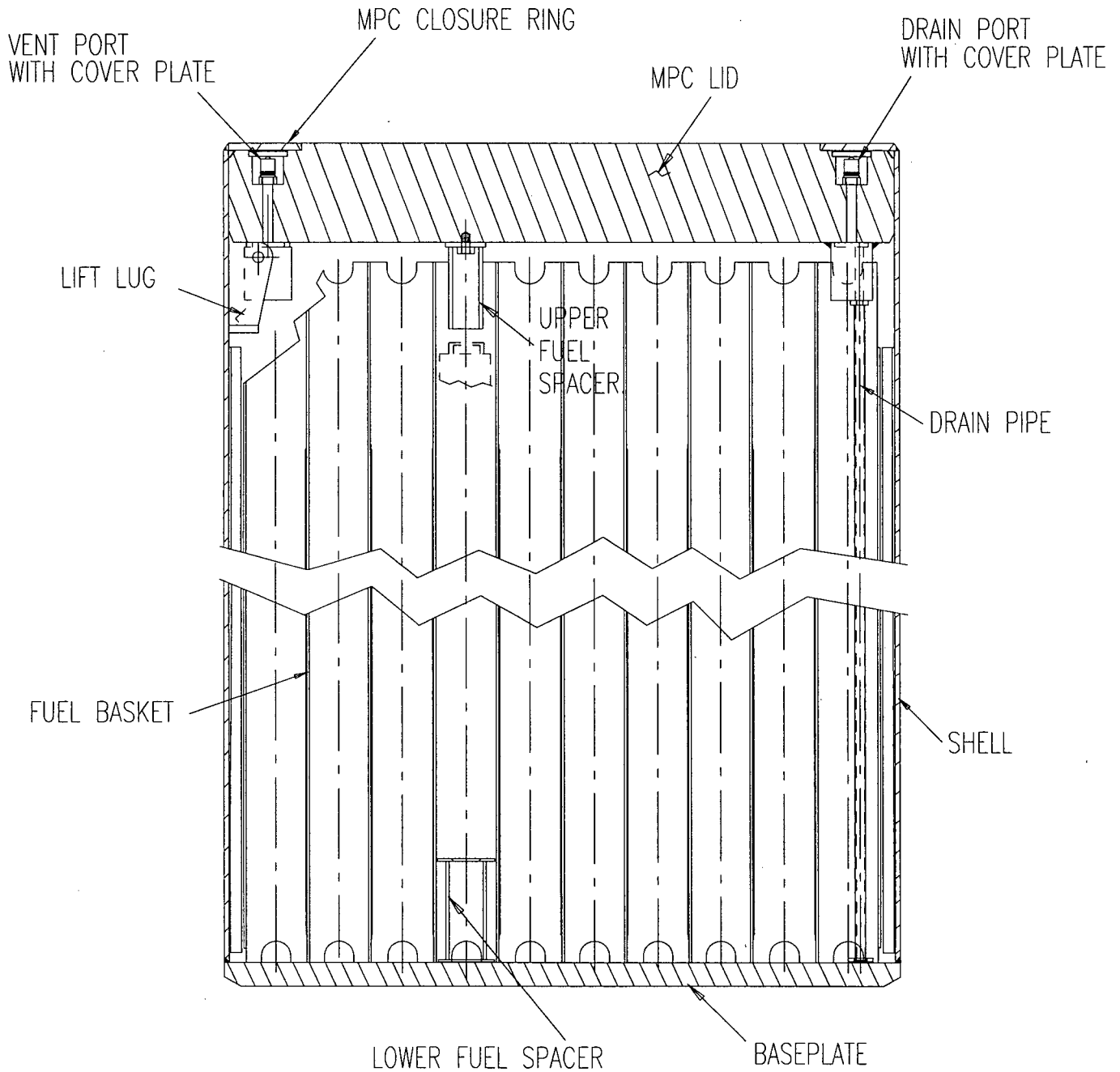


FIGURE 1.1.3; CROSS SECTION ELEVATION VIEW OF MPC

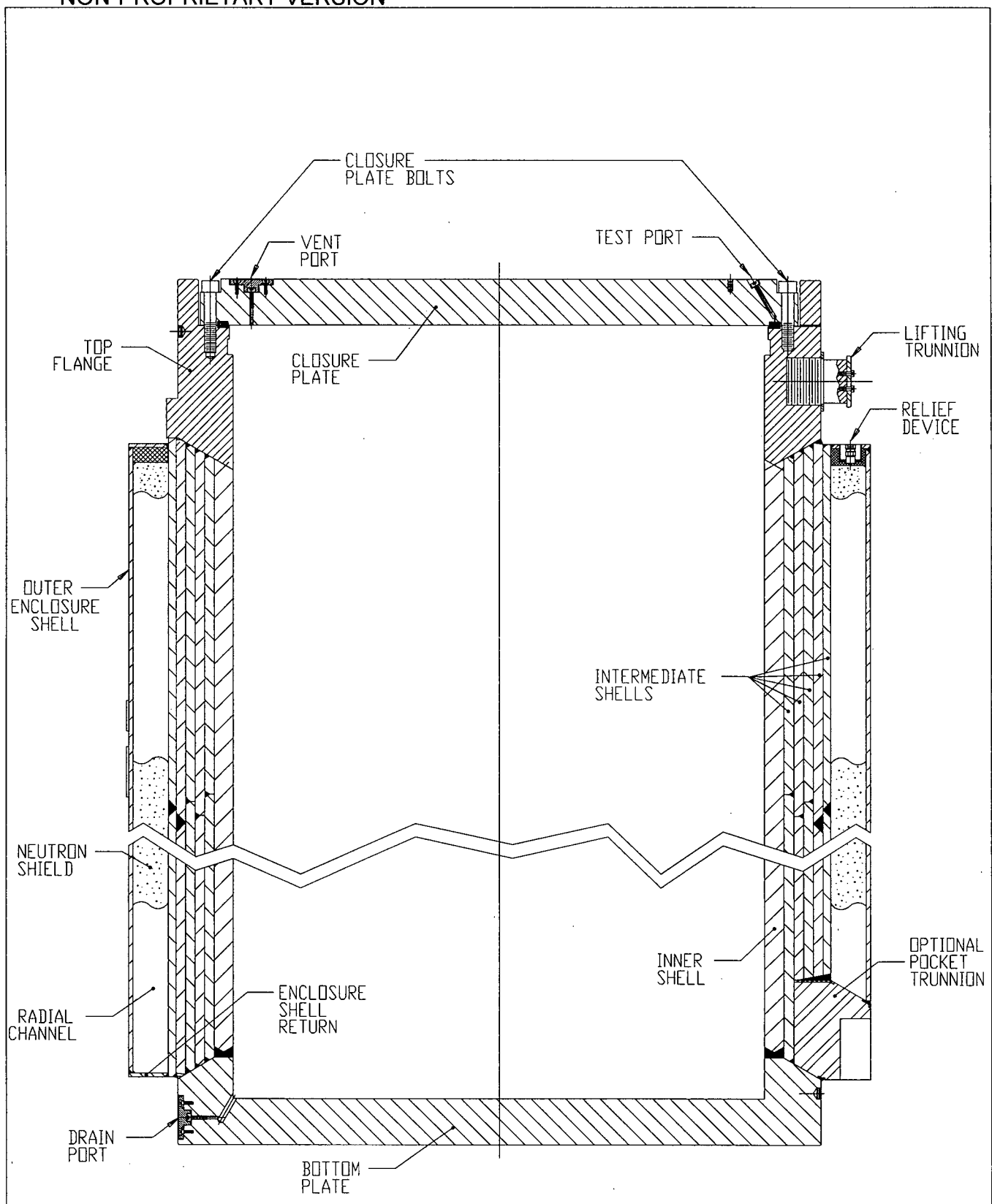


FIGURE 1.1.4; CROSS SECTION ELEVATION VIEW OF OVERPACK

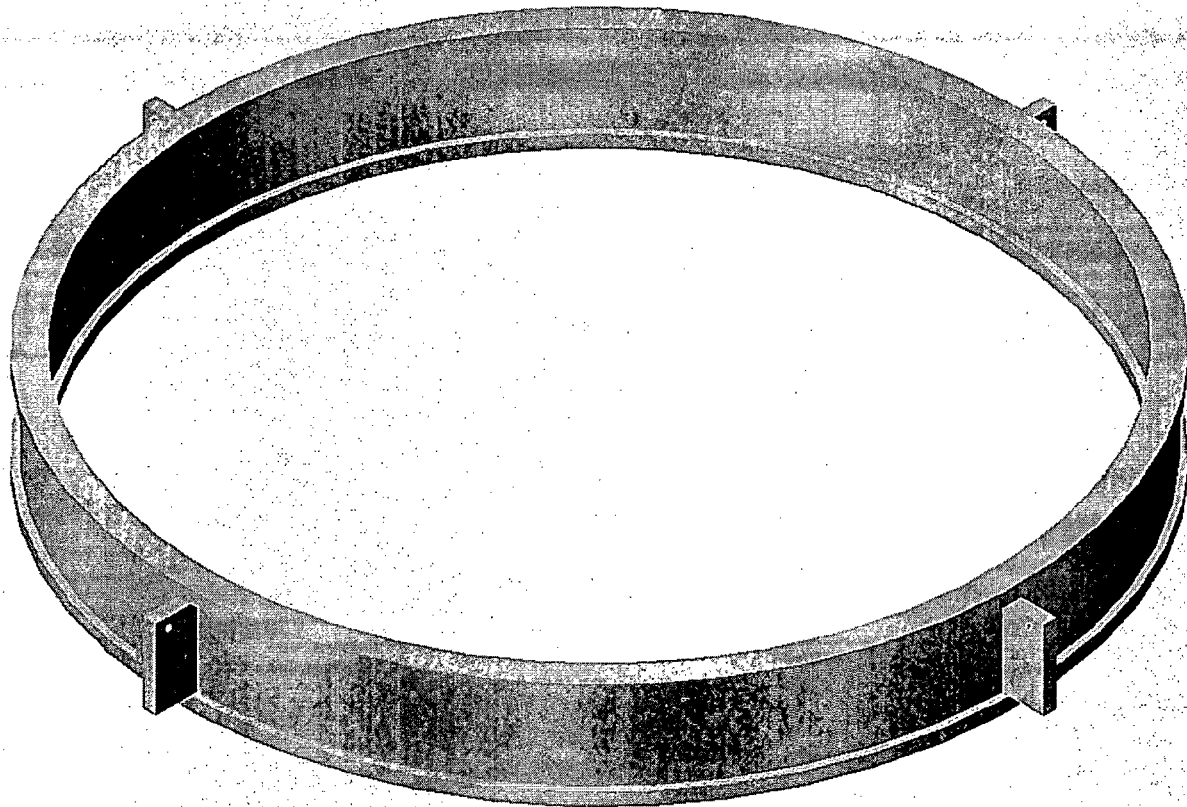


FIGURE 1.1.5; TROJAN MPC SPACER

## 1.2 PACKAGE DESCRIPTION

### 1.2.1 Packaging

The HI-STAR 100 System consists of an MPC designed for BWR or PWR spent nuclear fuel, an overpack that provides the containment boundary and a set of impact limiters that provide energy absorption capability for the normal and hypothetical accident conditions of transport. Each of these components is described below, including information with respect to component fabrication techniques and designed safety features. This discussion is supplemented by a set of drawings in Section 1.4. Section 1.3 provides the HI-STAR 100 design code applicability and details any alternatives to the ASME Code.

Before proceeding to present detailed physical data on HI-STAR 100, it is contextual to summarize the design attributes that set it apart from the prior generation of spent fuel transportation packages.

There are several features in the HI-STAR 100 System design that increase its effectiveness with respect to the safe transport of spent nuclear fuel (SNF). Some of the principal features of the HI-STAR 100 System that enhance its effectiveness are:

- the honeycomb design of the MPC fuel basket
- the effective distribution of neutron and gamma shielding materials within the system
- the high heat rejection capability
- the structural robustness of the multi-shell overpack construction

The honeycomb design of the MPC fuel baskets renders the basket into a multi-flanged plate weldment where all structural elements (box walls) are arrayed in two orthogonal sets of plates. Consequently, the walls of the cells are either completely coplanar (no offset) or orthogonal with each other. There is complete edge-to-edge continuity between contiguous cells.

Among the many benefits of the honeycomb construction is the uniform distribution of the metal mass over the body of the basket (in contrast to the “box and spacer disk” construction where the support plates are localized mass points). Physical reasoning suggests that a uniformly distributed mass provides a more effective shielding barrier than can be obtained from a non-uniform (box and spacer disk) basket. In other words, the honeycomb basket is a more effective radiation attenuation device.

The complete cell-to-cell connectivity inherent in the honeycomb basket structure provides an uninterrupted heat transmission path, making the HI-STAR 100 MPC an effective heat rejection device.

The multi-layer shell construction in the overpack provides a natural barrier against crack propagation in the radial direction across the overpack structure. If, during a hypothetical

accident (impact) event, a crack was initiated in one layer, the crack could not propagate to the adjacent layer. Additionally, it is highly unlikely that a crack would initiate as the thinner layers are more ductile than a thicker plate.

In this Safety Analysis Report the HI-STAR 100 System design is demonstrated to have predicted responses to accident conditions that are clearly acceptable with respect to certification requirements for post-accident containment system integrity, maintenance of subcriticality margin, dose rates, and adequate heat rejection capability. Table 1.2.18 presents a summary of the HI-STAR 100 System performance against these aspects of post-accident performance at two levels. At the first level, the integrity of the MPC boundary prevents release of radioactive material or helium from the MPC, and ingress of moderator. The integrity of the MPC is demonstrated by the analysis of the response of this high quality, ASME Code, Section III, Subsection NB-designed, pressure vessel to the accident loads while in the overpack. With this demonstration of MPC integrity, the excellent performance results listed in the second column of Table 1.2.18 constitute an acceptable basis for certification of the HI-STAR 100 System for the safe transport of spent nuclear fuel. However, no credit is taken for MPC integrity for certification of the HI-STAR 100 System for the transport of intact or damaged fuel assemblies.

The HI-STAR 100 System provides a large margin of safety. The third column in Table 1.2.18 summarizes the performance if the MPC is postulated to suffer gross failure in the post-accident analysis. Even with this postulated failure, the performance of the HI-STAR 100 System is acceptable for the transport of intact and damaged fuel assemblies, showing the defense-in-depth methodology incorporated into the HI-STAR 100 System.

The containment boundary of the HI-STAR 100 System is shown to satisfy the special requirements of 10CFR71.61 for irradiated nuclear fuel shipments.

#### 1.2.1.1 Gross Weight

The gross weight of the HI-STAR 100 System depends on which of the MPCs is loaded into the HI-STAR 100 overpack for shipment. Table 2.2.1 summarizes the maximum calculated component weights for the HI-STAR 100 overpack, impact limiters, and each MPC loaded to maximum capacity with design basis SNF. The maximum gross transport weight of the HI-STAR 100 System is to be marked on the packaging nameplate.

#### 1.2.1.2 Materials of Construction, Dimensions, and Fabrication

All materials used to construct the HI-STAR 100 System are ASME Code materials, except the neutron shield, neutron poison, optional aluminum heat conduction elements, thermal expansion foam, seals, pressure relief devices, aluminum honeycomb, pipe couplings, and other material classified as Not Important to Safety. The specified materials of construction along with outline dimensions for important-to-safety items are provided in the drawings in Section 1.4.

The materials of construction and method of fabrication are further detailed in the subsections that follow. Section 1.3 provides the codes applicable to the HI-STAR 100 packaging for

materials, design, fabrication, and inspection, including NRC-approved alternatives to the ASME Code.

#### 1.2.1.2.1 HI-STAR 100 Overpack

The HI-STAR 100 overpack is a heavy-walled steel cylindrical vessel. The inner diameter of the overpack is approximately 68-3/4 inches and the height of the internal cavity is usually 191-1/8 inches, however, shorter overpacks are available to meet site-specific requirements. Refer to Supplement 1.I for details of the Humboldt Bay HI-STAR HB. The overpack inner cavity is sized to accommodate the MPCs. The outer diameter of the overpack is approximately 96 inches and the height is approximately 203-1/4 inches, however, shorter overpacks are available to meet site-specific requirements. Refer to Supplement 1.I for details of the Humboldt Bay HI-STAR HB.

Figure 1.2.1 provides a cross sectional elevation view of the overpack containment boundary. The overpack containment boundary is formed by a steel inner shell welded at the bottom to a bottom plate and, at the top, to a heavy top flange with a bolted closure plate. Two concentric grooves are machined into the closure plate for the seals. The closure plate is recessed into the top flange and the bolted joint is configured to protect the closure bolts and seals in the event of a drop accident. The closure plate has test and vent ports that are closed by a threaded port plug with a seal. The bottom plate has a drain port that is also closed by a threaded port plug with a seal. The containment boundary forms an internal cylindrical cavity for housing the MPC.

The outer surface of the overpack inner shell is buttressed with intermediate shells of gamma shielding that are installed in a manner to ensure a permanent state of contact between adjacent layers. Besides serving as an effective gamma shield, these layers provide additional strength to the overpack to resist puncture or penetration. Except in the HI-STAR HB (refer to Supplement 1.I), radial channels are vertically welded to the outside surface of the outermost intermediate shell at equal intervals around the circumference. These radial channels act as fins for improved heat conduction to the overpack outer enclosure shell surface and as cavities for retaining and protecting the neutron shielding. The enclosure shell is formed by welding enclosure shell panels between each of the channels to form additional cavities. Neutron shielding material is placed into each of the radial cavity segments formed by the radial channels, the outermost intermediate shell, and the enclosure shell panels. The exterior flats of the radial channels and enclosure shell panels form the overpack outer enclosure shell (Figure 1.2.2). Atop the outer enclosure shell, pressure relief devices (e.g., rupture disks) are positioned in a recessed area. The relief devices relieve internal pressure that may develop as a result of the fire accident and subsequent off-gassing of the neutron shield material. Within each radial channel, a layer of silicone sponge is positioned to act as a thermal expansion foam to compress as the neutron shield expands in the axial direction. Appendix 1.C provides material information on the thermal expansion foam. Figure 1.2.2 provides a mid-plane cross section view of the overpack, depicting the inner shell, intermediate shells, radial channels, outer enclosure shell, and neutron shield. Refer to drawings in Supplement 1.I for HI-STAR HB.

The exposed steel surfaces (except seal seating surfaces) of the overpack and the intermediate shell layers are coated to prevent corrosion. Coating materials are chosen based on the expected

service conditions, considering the dual purpose certification status of the HI-STAR 100 System under 10 CFR 72 for spent fuel storage as well as transportation. The coatings applied to the overpack exposed exterior and interior surfaces are specified on the drawings in Section 1.4. The material data on the coatings is provided in Appendix 1.C. The inner cavity of the overpack is coated with a material appropriate to its high temperatures and the exterior of the overpack is coated with a material appropriate for fuel pool operations and environmental exposure. The coating applied to the intermediate shells acts as a surface preservative and is not exposed to the fuel pool or ambient environment.

Lifting trunnions are attached to the overpack top flange for lifting and rotating the cask body between vertical and horizontal positions. The lifting trunnions are located 180° apart in the sides of the top flange. On overpack serial numbers 1020-001 through 1020-007, pocket trunnions are welded to the lower side of the overpack 180° apart to provide a pivoting axis for rotation. The pocket trunnions are slightly off-center to ensure proper rotation direction of the overpack. As shown in Figure 1.1.4, the trunnions do not protrude beyond the cylindrical envelope of the overpack outer enclosure shell. This feature reduces the potential for direct impact on a trunnion in the event of an overpack side impact. After fabrication of HI-STAR overpack serial number 1020-007, the pocket trunnions were deleted from the overpack design.

#### 1.2.1.2.2 Multi-Purpose Canisters

##### 1.2.1.2.2.1 General Description

In this subsection, discussion of those attributes applicable to all of the MPC models is provided. Differences among the models are discussed in subsequent subsections. Specifications for the authorized contents of each MPC model, including non-fuel hardware and neutron sources are provided in Section 1.2.3.

The HI-STAR 100 MPCs are welded cylindrical structures with flat ends. Each MPC is an assembly consisting of a honeycombed fuel basket, a baseplate, a canister shell, a lid with vent and drain ports and cover plates, and a closure ring. The outer diameter of all MPCs and cylindrical height of each generic design MPC is fixed (see discussion in Subsection 1.2.1.2.2.3 regarding Trojan plant-specific MPCs and Supplement 1.I for Humboldt Bay plant-specific MPCs). The number of spent nuclear fuel storage locations in each of the MPCs depends on the fuel assembly characteristics. As the generic MPCs are interchangeable, they correspondingly have identical exterior dimensions. The outer dimension of the MPC is nominally 68-3/8 inches and the length is nominally 190-1/4 inches. Figures 1.2.3-1.2.5 depict the cross sectional views of the different MPCs. Drawings of the MPCs are provided in Section 1.4. Key system data for the HI-STAR 100 System are outlined in Tables 1.2.2 and 1.2.3.

The generic MPC-24/24E/24EF and Trojan plant MPC-24E/EF differ in construction from the MPC-32 and MPC-68/68F in one important aspect: the fuel cells are physically separated from one another by a flux trap between each cell for criticality control (Figures 1.2.3 and 1.2.4). All MPC baskets are formed from an array of plates welded to each other, such that a honeycomb structure is created that resembles a multi-flanged, closed-section beam in its structural characteristics.

The MPC fuel basket is positioned and supported within the MPC shell by a series of basket supports welded to the inside of the MPC shell. In the peripheral area created by the basket, the MPC shell, and the basket supports, optional aluminum heat conduction elements are installed in some early production MPC-68 and MPC-68F models (see Figure 1.2.3). These heat conduction elements are fabricated from thin aluminum alloy 1100 in shapes and a design that allows a snug fit in the confined spaces and ease of installation. The heat conduction elements are along the full length of the MPC basket, except at the drain pipe location, to create a nonstructural thermal connection that facilitates heat transfer from the basket to the shell. In their operating condition, the heat conduction elements conform to, and contact the MPC shell and basket walls. In SAR Revision 10, a refined thermal analysis, described in Chapter 3, has allowed the elimination of these heat conduction elements from the MPC design, thus giving this design feature “optional” status.

Lifting lugs attached to the inside surface of the MPC canister shell serve to permit placement of the empty MPC into the overpack, and are considered non-structural, non-pressure retaining attachments to the MPC pressure boundary. The lifting lugs also serve to axially locate the MPC lid prior to welding. These internal lifting lugs are not used to handle a loaded MPC, since the MPC lid blocks access to the lifting lugs.

The top of the HI-STAR 100 MPC incorporates a redundant closure system. Figure 1.2.6 provides a sketch of the MPC closure details. The MPC lid is a circular plate (fabricated from one piece, or two pieces - split top and bottom) that is edge-welded to the MPC shell. If the two-piece lid design is employed, only the top piece is analyzed as part of the enclosure vessel pressure boundary. The bottom piece acts primarily as a radiation shield and is attached to the top piece with a non-structural, non-pressure retaining weld, as depicted on the MPC enclosure vessel drawing in Section 1.4. The MPC lid is equipped with vent and drain ports that are used to remove moisture and gas from the MPC and backfill the MPC with a specified pressure of inert gas (helium). The vent and drain ports are sealed closed by cover plates welded to the MPC lid before the closure ring is installed. The closure ring is a circular ring edge-welded to the MPC shell and MPC lid. The MPC lid provides sufficient rigidity to allow the entire MPC loaded with SNF to be lifted by the threaded holes in the MPC lid during transfer from the storage-only HI-STORM 100 System to the HI-STAR 100 overpack for transportation. Threaded insert plugs are installed to provide shielding when the threaded holes are not in use.

All MPCs are designed to handle intact fuel assemblies, damaged fuel assemblies, and fuel classified as fuel debris. Damaged fuel and fuel debris must be transported in damaged fuel containers or other approved damaged/failed fuel canister. At this time, BWR damaged fuel and fuel debris from Dresden Unit 1 is certified for transportation in the MPC-68 and the MPC-68F. Humboldt Bay damaged fuel and fuel debris will be transported in the MPC-HB (refer to Supplement 1.1). Similarly, only PWR damaged fuel and fuel debris from the Trojan plant is certified for transportation in the Trojan plant-specific MPC-24E and the MPC-24EF. The definitions, and applicable specifications for all authorized contents, including the requirements for canning certain fuel, are provided in Subsection 1.2.3.

Intact SNF can be placed directly into the MPC. Damaged SNF and fuel debris must be placed into a Holtec damaged fuel container or other authorized canister for transportation inside the MPC and the HI-STAR 100 overpack. Figures 1.2.10 through 1.2.11 provide sketches of the containers authorized for transportation of damaged fuel and fuel debris in the HI-STAR 100 System. One Dresden Unit 1 Thoria rod canister, shown in Figure 1.2.11A, is also authorized for transportation in HI-STAR 100.

The MPC-68 and MPC-24E enclosure vessels have been slightly modified to further strengthen the lid-to-shell joint area. These MPCs are given the “F” suffix (hence, MPC-68F and MPC-24EF)<sup>†</sup>. The differences between the standard and “F-model” MPC lid-to-shell joints are shown on Figure 1.2.17, and include a thickened upper shell, a larger lid-to-shell weld size, and a correspondingly smaller lid diameter. The design of the rest of the enclosure vessel is identical between the standard MPC and the “F-model” MPC.

#### 1.2.1.2.2.2 MPC-24/24E/24EF

The MPC-24 is designed to transport up to 24 PWR intact fuel assemblies meeting the limits specified in Subsection 1.2.3. The MPC 24E is designed to transport up to 24 PWR intact and up to four PWR damaged fuel assemblies in damaged fuel containers. The MPC-24EF is designed to transport up to 24 PWR intact fuel assemblies and up to four PWR damaged fuel assemblies or fuel assemblies classified as fuel debris. At this time, however, generic PWR damaged fuel and fuel debris are not authorized for transportation in the MPC-24E/EF.

All MPC-24-series fuel baskets employ the flux trap design for criticality control, as shown in the drawings in Section 1.4. The fuel basket design for the MPC-24E is an enhanced MPC-24 basket layout designed to improve the fuel storage geometry for criticality control. The fuel basket design of the MPC-24EF is identical to the MPC-24E. The MPC-24E/EF basket designs also employ a higher <sup>10</sup>B loading than the MPC-24, as shown in Table 1.2.3. The differences between the MPC-24EF enclosure vessel design and the MPC-24/24E enclosure vessel are discussed in Subsection 1.2.1.2.2.1.

#### 1.2.1.2.2.3 Trojan Plant MPC-24E/EF

The Trojan plant MPC-24E and -24EF models are designs that have been customized for that plant’s fuel and the concrete storage cask being used at the Trojan plant Independent Spent Fuel Storage Installation (ISFSI) (Docket 72-0017). The design features that are unique to the Trojan plant MPCs are specifically noted on the MPC enclosure vessel and MPC-24E/EF fuel basket drawings in Section 1.4. These differences include:

- a shorter MPC fuel basket and cavity length to match the shorter Trojan fuel assembly length
- shorter corner fuel storage cell lengths to accommodate the Trojan Failed Fuel Cans

<sup>†</sup> The drawing in Section 1.4 also denotes an MPC-68FF canister design. However, the MPC-68FF is not authorized for use in transportation under the HI-STAR 100 10 CFR 71 CoC.

- a different fuel storage cell and flux trap dimension in the corner cells to accommodate the Trojan Failed Fuel Cans
- a different configuration of the flow holes at the bottom of the fuel basket (rectangular vs. semi-circular)

All other design features in the Trojan MPCs are identical to the generic MPC-24E/EF design. The HI-STAR 100 overpack design has not been modified for the Trojan MPC design.

The technical analyses described in this SAR were verified in most cases to bound the Trojan-specific design features. Where necessary, Trojan plant-specific evaluations were performed and are summarized in the appropriate SAR section. To accommodate the shorter Trojan plant MPC length in a standard-length HI-STAR 100 overpack, a spacer was designed for installation into the overpack above the Trojan MPC (see Figure 1.1.5 and the drawing in Section 1.4) for transportation in the standard-length HI-STAR 100 overpack. This spacer prevents the MPC from moving more than the MPC was analyzed to move in the axial direction and serves to transfer the axial loads from the MPC lid to the overpack top closure plate within the limits of the supporting analyses. See Section 2.7.1.1 for additional discussion of the spacer used with the Trojan MPC design. Hereafter in this SAR, the Trojan plant-specific MPC design is only distinguished from the generic MPC-24E/EF design when necessary to describe unique evaluations performed for those MPCs.

#### 1.2.1.2.2.4 MPC-32

The MPC-32 is designed to transport up to 32 PWR intact fuel assemblies meeting the specifications in Subsection 1.2.3. Damaged fuel and fuel debris are not permitted to be transported in the MPC-32. The MPC-32 enclosure vessel design is identical to the MPC-24/24E enclosure vessel design as shown on the drawings in Section 1.4. The MPC-32 fuel basket does not employ flux traps for criticality control. Credit for burnup of the fuel is taken in the criticality analyses for accident conditions and to meet the requirements of 10 CFR 71.55(b). Because the MPC is designed to preclude the intrusion of moderator under all normal and credible accident conditions of transport, the moderator intrusion condition analyzed as required by 10 CFR 71.55(b) is a non-mechanistic event for the HI-STAR 100 System.

#### 1.2.1.2.2.5 MPC-68/68F

The MPC-68 is designed to transport up to 68 BWR intact fuel assemblies and damaged fuel assemblies meeting the specifications in Subsection 1.2.3. Zircaloy channels are permitted. At this time, only damaged fuel from the Dresden Unit 1 plant is authorized for transportation in the MPC-68. The MPC-68F is designed to transport only fuel and other authorized material from the Dresden Unit 1 plant meeting the specifications in Subsection 1.2.3. The sole difference between the MPC-68 and MPC-68F fuel basket design is a reduction in the required  $^{10}\text{B}$  areal density in the neutron absorber. A reduction in the required  $^{10}\text{B}$  areal density of the neutron absorber is possible for the MPC-68F due to limited types of fuel and low enrichments permitted

to be transported in this MPC model. The differences between the MPC-68F enclosure vessel design and the MPC-68 enclosure vessel are discussed in Subsection 1.0.

#### 1.2.1.2.2.6 Alloy X

The HI-STAR MPC is constructed entirely from stainless steel alloy materials (except for the neutron absorber and aluminum vent and drain cap seal washers in all MPCs, and the aluminum heat conduction elements in the first several production units of MPC-68 and MPC-68F). No carbon steel parts are used in the design of the HI-STAR 100 MPC. Concerns regarding interaction of coated carbon steel materials and various MPC operating environments [1.2.1] are not applicable to the HI-STAR MPCs. All structural components in a HI-STAR MPC will be fabricated of Alloy X, a designation that warrants further explanation.

Alloy X is a fictitious material that should be acceptable as a Mined Geological Depository System (MGDS) waste package and that meets the thermophysical properties set forth in this document.

At this time, there is considerable uncertainty with respect to the material of construction for an MPC that would be acceptable as a waste package for the MGDS. Candidate materials being considered for acceptability by the DOE include:

- Type 316
- Type 316LN
- Type 304
- Type 304LN

The DOE material selection process is primarily driven by corrosion resistance in the potential environment of the MGDS. As the decision regarding a suitable material to meet disposal requirements is not imminent, this application requests approval for use of any one of the four Alloy X materials.

For the MPC design and analysis, Alloy X (as defined in this SAR) may be one of the following materials. Any steel part in an MPC may be fabricated from any of the acceptable Alloy X materials listed below, except that all steel pieces comprising the MPC shell (i.e., the 1/2" thick cylinder) must be fabricated from the same Alloy X stainless steel type:

- Type 316
- Type 316LN
- Type 304
- Type 304LN

The Alloy X approach is accomplished by qualifying the MPC for all mechanical, structural, neutronic, radiological, and thermal conditions using material thermophysical properties that are the least favorable for the entire group for the analysis in question. For example, when calculating the rate of heat rejection to the outside environment, the value of thermal conductivity used is the lowest for the candidate material group. Similarly, the stress analysis

calculations use the lowest value of the ASME Code allowable stress intensity for the entire group. Stated differently, we have defined a material, which is referred to as Alloy X, whose thermophysical properties, from the MPC design perspective, are the least favorable of the candidate materials group. The evaluation of the Alloy X constituents to determine the least favorable properties is provided in Appendix 1.A.

The Alloy X approach is conservative because no matter which material is ultimately utilized, the Alloy X approach guarantees that the performance of the MPC will exceed the analytical predictions contained in this document.

#### 1.2.1.3 Impact Limiters

The HI-STAR 100 overpack is fitted with aluminum honeycomb impact limiters, termed AL-STAR™, one at each end, once the overpack is positioned and secured in the transport frame. The impact limiters ensure the inertia loadings during the normal and hypothetical accident conditions of transport are maintained below design levels. The impact limiter design is discussed further in Chapter 2 and drawings are provided in Section 1.4.

#### 1.2.1.4 Shielding

The HI-STAR 100 System is provided with shielding to minimize personnel exposure. The HI-STAR 100 System will be transported by exclusive use shipment to ensure the external radiation requirements of 10CFR71.47 are met. During transport, a personnel barrier is installed to restrict access to the overpack to protect personnel from the HI-STAR 100 exterior surface temperature in accordance with 10CFR71.43(g). The personnel barrier provides a stand-off equal to the exterior radial dimension of the impact limiters. Figure 1.2.8 provides a sketch of the personnel barrier being installed.

The initial attenuation of gamma and neutron radiation emitted by the radioactive spent fuel is provided by the MPC fuel basket structure built from inter-welded plates and Boral neutron poison panels with sheathing attached to the fuel cell walls. The MPC canister shell, baseplate, and lid provide additional thicknesses of steel to further reduce gamma radiation and, to a smaller extent, neutron radiation at the outer MPC surfaces. No shielding credit is taken for the aluminum heat conduction elements installed in some of the early production MPC-68 and MPC-68F units.

The primary HI-STAR 100 shielding is located in the overpack and consists of neutron shielding and additional layers of steel for gamma shielding. Neutron shielding is provided around the outside circumferential surface of the overpack. Gamma shielding is provided by the overpack inner, intermediate and enclosure shells with additional axial shielding provided by the bottom plate and the top closure plate. During transport, the impact limiters will provide incremental gamma shielding and provide additional distance from the radiation source at the ends of the package. An additional circular segment of neutron shielding is contained within each impact limiter to provide neutron attenuation.

#### 1.2.1.4.1 Neutron Absorber Materials

Both Boral and Metamic are neutron absorber materials made of B<sub>4</sub>C and Aluminum. Boral is used in the MPC-24/24E/24EF, MPC-32, MPC-68/68F, and Trojan MPC-24E/24EF. Metamic is used in MPC-24/24E/24EF, MPC-68, and MPC-32 Models. Metamic is the only neutron absorber used in the MPC-HB (See drawing package in Supplement 1.I).

##### 1.2.1.4.1.1 Boral Neutron Absorber

Boral is a thermal neutron poison material composed of boron carbide and aluminum alloy 1100. Boron carbide is a compound having a high boron content in a physically stable and chemically inert form. The boron carbide contained in Boral is a fine granulated powder that conforms to ASTM C-750-80 nuclear grade Type III. The aluminum alloy 1100 is a lightweight metal with high tensile strength that is protected from corrosion by a highly resistant oxide film. The two materials, boron carbide and aluminum, are chemically compatible and ideally suited for long-term use in the radiation, thermal, and chemical environment of a nuclear reactor, spent fuel pool, or dry cask.

The documented historical applications of Boral, in environments comparable to those in spent fuel pools and fuel storage casks, dates to the early 1950s (the U.S. Atomic Energy Commission's AE-6 Water-Boiler Reactor [1.2.2]). Technical data on the material was first printed in 1949, when the report "Boral: A New Thermal Neutron Shield" was published [1.2.3]. In 1956, the first edition of the "Reactor Shielding Design Manual" [1.2.4], contains a section on Boral and its properties.

In the research and test reactors built during the 1950s and 1960s, Boral was frequently the material of choice for control blades, thermal-column shutters, and other items requiring very good thermal-neutron absorption properties. It is in these reactors that Boral has seen its longest service in environments comparable to today's applications.

Boral found other uses in the 1960s, one of which was a neutron poison material in baskets used in the shipment of irradiated, enriched fuel rods from Canada's Chalk River laboratories to Savannah River. Use of Boral in shipping containers continues, with Boral serving as the poison in many cask designs.

Boral has been licensed by the NRC for use in numerous BWR and PWR spent fuel storage racks and has been extensively used in international nuclear installations.

Boral has been exclusively used in fuel storage applications in recent years. Its use in spent fuel pools as the neutron absorbing material can be attributed to its proven performance and several unique characteristics, such as:

- The content and placement of boron carbide provides a very high removal cross section for thermal neutrons.

- Boron carbide, in the form of fine particles, is homogeneously dispersed throughout the central layer of the Boral panels.
- The boron carbide and aluminum materials in Boral do not degrade as a result of long-term exposure to radiation.
- The neutron absorbing central layer of Boral is clad with permanently bonded surfaces of aluminum.
- Boral is stable, strong, durable, and corrosion resistant.

Boral absorbs thermal neutrons without physical change or degradation of any sort from the anticipated exposure to gamma radiation and heat. The material does not suffer loss of neutron attenuation capability when exposed to high levels of radiation dose.

Holtec International's QA Program ensures that Boral is manufactured under the control and surveillance of a Quality Assurance/Quality Control Program that conforms to the requirements of 10CFR71, Subpart H and 10CFR72, Subpart G. Holtec International has procured over 200,000 panels of Boral from AAR Advanced Structures for over 20 projects. Boral has always been purchased with a minimum  $^{10}\text{B}$  loading requirement. Coupons extracted from production runs were tested using the "wet chemistry" procedure. The actual  $^{10}\text{B}$  loading, out of thousands of coupons tested, has never been found to fall below the design specification. The size of this coupon database is sufficient to provide confidence that all future procurements will continue to yield Boral with full compliance with the stipulated minimum loading. Furthermore, the surveillance, coupon testing, and material tracking processes that have so effectively controlled the quality of Boral are expected to continue to yield Boral of similar quality in the future. Nevertheless, to add another layer of insurance, only 75%  $^{10}\text{B}$  credit of the fixed neutron absorber is assumed in the criticality analysis.

Operating experience in nuclear plants with fuel loading of Boral equipped MPCs as well as laboratory test data indicate that the aluminum used in the manufacture of the Boral may react with water, resulting in the generation of hydrogen. The numerous variables (i.e., aluminum particle size, pool temperature, pool chemistry, etc.) that influence the extent of the hydrogen produced make it impossible to predict the amount of hydrogen that may be generated during MPC loading or unloading at a particular plant. Therefore, due to the variability in hydrogen generation from the Boral-water reaction, the operating procedures in Chapter 7 describe steps to monitor and mitigate combustible gas accumulation beneath the MPC lid during loading and unloading operations when an ignition event could occur (i.e., when the space beneath the MPC lid is open to the welding or cutting operation).

#### 1.2.1.4.1.2 METAMIC<sup>®</sup>

METAMIC<sup>®</sup> is a neutron absorber material developed by the Reynolds Aluminum Company in the mid-1990s for spent fuel reactivity control in dry and wet storage applications. Metallurgically, METAMIC<sup>®</sup> is a metal matrix composite (MMC) consisting of a matrix of 6061 aluminum alloy reinforced with Type 1 ASTM C-750 boron carbide. METAMIC<sup>®</sup> is

characterized by extremely fine aluminum (325 mesh or better) and boron carbide powder. Typically, the average B<sub>4</sub>C particle size is between 10 and 15 microns. As described in the U.S. patents held by Holtec International<sup>1,2</sup>, the high performance and reliability of METAMIC<sup>®</sup> derives from the particle size distribution of its constituents, rendered into a metal matrix composite by the powder metallurgy process. This yields excellent and uniform homogeneity.

The powders are carefully blended without binders or other additives that could potentially adversely influence performance. The maximum percentage of B<sub>4</sub>C that can be dispersed in the aluminum alloy 6061 matrix is approximately 40 wt.%, although extensive manufacturing and testing experience is limited to approximately 31 wt.%. The blend of powders is isostatically compacted into a green billet under high pressure and vacuum sintered to near theoretical density.

According to the manufacturer, billets of any size can be produced using this technology. The billet is subsequently extruded into one of a number of product forms, ranging from sheet and plate to angle, channel, round and square tube, and other profiles. For the METAMIC<sup>®</sup> sheets used in the MPCs, the extruded form is rolled down into the required thickness.

METAMIC<sup>®</sup> has been subjected to an extensive array of tests sponsored by the Electric Power Research Institute (EPRI) that evaluated the functional performance of the material at elevated temperatures (up to 900°F) and radiation levels (1E+11 rads gamma). The results of the tests documented in an EPRI report (Ref. [1.2.17]) indicate that METAMIC<sup>®</sup> maintains its physical and neutron absorption properties with little variation in its properties from the unirradiated state. The main conclusions provided in the above-referenced EPRI report are summarized below:

- The metal matrix configuration produced by the powder metallurgy process with a complete absence of open porosity in METAMIC<sup>®</sup> ensures that its density is essentially equal to the theoretical density.
- The physical and neutronic properties of METAMIC<sup>®</sup> are essentially unaltered under exposure to elevated temperatures (750° F - 900° F).
- No detectable change in the neutron attenuation characteristics under accelerated corrosion test conditions has been observed.

In addition, independent measurements of boron carbide particle distribution show extremely small particle-to-particle distance<sup>†</sup> and near-perfect homogeneity.

---

<sup>1</sup> U.S. Patent No. 5,965,829, "Radiation Absorbing Refractory Composition".

<sup>2</sup> U.S. Patent No. 6,042,779, "Extrusion Fabrication Process for Discontinuous Carbide Particulate Metal Matrix Composites and Super, Hypereutectic Al/Si."

<sup>†</sup> Medium measured neighbor-to-neighbor distance is 10.08 microns according to the article, "METAMIC Neutron Shielding", by K. Anderson, T. Haynes, and R. Kazmier, EPRI Boraflex Conference, November 19-20, 1998.

An evaluation of the manufacturing technology underlying METAMIC<sup>®</sup> as disclosed in the above-referenced patents and of the extensive third-party tests carried out under the auspices of EPRI makes METAMIC<sup>®</sup> an acceptable neutron absorber material for use in the MPCs. Holtec's technical position on METAMIC<sup>®</sup> is also supported by the evaluation carried out by other organizations.

Consistent with its role in reactivity control, all METAMIC<sup>®</sup> material procured for use in the Holtec MPCs will be qualified as important-to-safety (ITS) Category A item. ITS category A manufactured items, as required by Holtec's NRC-approved Quality Assurance program, must be produced to essentially preclude the potential of an error in the procurement of constituent materials and the manufacturing processes. Accordingly, material and manufacturing control processes must be established to eliminate the incidence of errors, and inspection steps must be implemented to serve as an independent set of barriers to ensure that all critical characteristics defined for the material by the cask designer are met in the manufactured product.

All manufacturing and in-process steps in the production of METAMIC<sup>®</sup> shall be carried out using written procedures. As required by the company's quality program, the material manufacturer's QA program and its implementation shall be subject to review and ongoing assessment, including audits and surveillances as set forth in the applicable Holtec QA procedures to ensure that all METAMIC<sup>®</sup> panels procured meet with the requirements appropriate for the quality genre of the MPCs. Additional details pertaining to the qualification and production tests for METAMIC<sup>®</sup> are summarized in Subsection 8.1.5.5.2.

Because of the absence of interconnected porosities, the time required to dehydrate a METAMIC<sup>®</sup>-equipped MPC is expected to be less compared to an MPC containing Boral.

NUREG/CR-5661 (Ref. [1.2.20]) recommends limiting poison material credit to 75% of the minimum <sup>10</sup>B loading because of concerns for potential "streaming" of neutrons, and allows for greater percentage credit in criticality analysis "if comprehensive acceptance tests, capable of verifying the presence and uniformity of the neutron absorber, are implemented". The value of 75% is characterized in NUREG/CR-5661 as a very conservative value, based on experiments with neutron poison containing relatively large B<sub>4</sub>C particles, such as BORAL with an average particle size in excess of 100 microns. METAMIC<sup>®</sup>, however, has a much smaller particle size of typically between 10 and 15 microns on average. Any streaming concerns would therefore be drastically reduced.

Analyses performed by Holtec International show that the streaming due to particle size is practically non-existent in METAMIC<sup>®</sup>. Further, EPRI's neutron attenuation measurements on 31 and 15 B<sub>4</sub>C weight percent METAMIC<sup>®</sup> showed that METAMIC<sup>®</sup> exhibits very uniform <sup>10</sup>B areal density. This makes it easy to reliably establish and verify the presence and microscopic and macroscopic uniformity of the <sup>10</sup>B in the material. Therefore, 90% credit can be applied to the minimum <sup>10</sup>B areal density in the criticality calculations, i.e. a 10% penalty can be applied. This 10% penalty is considered conservative since there are no significant remaining uncertainties in the <sup>10</sup>B areal density. In Chapter 8 the qualification and production tests for METAMIC<sup>®</sup> to support 90% <sup>10</sup>B credit are specified. With 90% credit, the target weight percent of boron carbide in METAMIC<sup>®</sup> is 31, consistent with the test coupons used in the EPRI

evaluations [1.2.17]. The maximum permitted value is 33.0 wt% to allow for necessary fabrication flexibility.

Because METAMIC<sup>®</sup> is a solid material, there is no capillary path through which spent fuel pool water can penetrate METAMIC<sup>®</sup> panels and chemically react with aluminum in the interior of the material to generate hydrogen. Any chemical reaction of the outer surfaces of the METAMIC<sup>®</sup> neutron absorber panels with water to produce hydrogen occurs rapidly and reduces to an insignificant amount in a short period of time. Nevertheless, operating procedures in Chapter 7 describe steps to monitor and mitigate combustible gas accumulation beneath the MPC lid during loading and unloading operations when an ignition event could occur (i.e., when the space beneath the MPC lid is open to the welding or cutting operation).

Mechanical properties of 31 wt.% METAMIC<sup>®</sup>, based on coupon tests of the material in the as-fabricated condition and after 48 hours of an elevated temperature state at 900°F, are summarized below from the EPRI report [1.2.17].

Mechanical Properties of 31wt.% B <sub>4</sub> C METAMIC		
Property	As-Fabricated	After 48 hours of 900°F Temperature Soak
Yield Strength (psi)	32937 ± 3132	28744 ± 3246
Ultimate Strength (psi)	40141 ± 1860	34608 ± 1513
Elongation (%)	1.8 ± 0.8	5.7 ± 3.1

The required flexural strain of the neutron absorber to ensure that it will not fracture when the supporting basket wall flexes, due to the worst case lateral inertial loading is 0.2%, which is the flexural strain of the Alloy X basket panel material. The 1% minimum elongation of 31wt.% B<sub>4</sub>C METAMIC<sup>®</sup> indicated by the above table means that a large margin of safety against cracking exists, so there is no need to perform testing of the METAMIC<sup>®</sup> for mechanical properties.

EPRI's extensive characterization effort [1.2.17], which was focused on 15 and 31 wt.% B<sub>4</sub>C METAMIC<sup>®</sup> served as the principal basis for a recent USNRC SER for 31wt.% B<sub>4</sub>C METAMIC for used in wet storage [1.2.18]. Additional studies on METAMIC<sup>®</sup> [1.2.19], EPRI's and others work provide the confidence that 31wt.% B<sub>4</sub>C METAMIC<sup>®</sup> will perform its intended function in the MPCs. Finally to further substantiate the performance of Metamic (with maximum B<sub>4</sub>C of up to 33%), Holtec has performed robust independent qualification testing as documented in Holtec Proprietary Report [1.2.21].

#### 1.2.1.4.2 Holtite-A<sup>™</sup> Neutron Shielding

The specification for the overpack and impact limiter neutron shield material is predicated on functional performance criteria. These criteria are:

- Attenuation of neutron radiation and associated neutron capture to appropriate levels;

- Durability of the shielding material under normal conditions, in terms of thermal, chemical, mechanical, and radiation environments;
- Stability of the homogeneous nature of the shielding material matrix;
- Stability of the shielding material in mechanical or thermal accident conditions to the desired performance levels; and
- Predictability of the manufacturing process under adequate procedural control to yield an in-place neutron shield of desired function and uniformity.

Other aspects of a shielding material, such as ease of handling and prior nuclear industry use, are also considered, within the limitations of the main criteria. Final specification of a shield material is a result of optimizing the material properties with respect to the main criteria, along with the design of the shield system, to achieve the desired shielding results.

Holtite-A is the only approved neutron shield material that fulfills the aforementioned criteria. Holtite-A is a poured-in-place solid borated synthetic neutron-absorbing polymer. Holtite-A is specified with a nominal B<sub>4</sub>C loading of 1 weight percent for the HI-STAR 100 System. Appendix 1.B provides the Holtite-A material properties germane to its function as a neutron shield. Holtec has performed confirmatory qualification tests on Holtite-A under the company's QA program.

In the following, a brief summary of the performance characteristics and properties of Holtite-A is provided.

#### Density

The nominal specific gravity of Holtite-A is 1.68 g/cm<sup>3</sup> as specified in Appendix 1.B. To conservatively bound any potential weight loss at the design temperature and any inability to reach the theoretical density, the density is reduced by 4% to 1.61 g/cm<sup>3</sup>. The density used for the shielding analysis is assumed to be 1.61 g/cm<sup>3</sup> to underestimate the shielding capabilities of the neutron shield.

#### Hydrogen

The nominal weight concentration of hydrogen is 6.0%. However, all shielding analyses conservatively assume 5.9% hydrogen by weight in the calculations.

#### Boron Carbide

Boron carbide dispersed within Holtite-A in finely dispersed powder form is present in 1% (nominal) weight concentration. Holtite-A may be specified with a B<sub>4</sub>C content of up to 6.5 weight percent. For the HI-STAR 100 System, Holtite-A is specified with a nominal B<sub>4</sub>C weight percent of 1%.

### Design Temperature

The design temperature of Holtite-A is set at 300°F. The maximum spatial temperature of Holtite-A under all normal operating conditions must be demonstrated to be below this design temperature.

### Thermal Conductivity

It is evident from Figure 1.2.2 that Holtite-A is directly in the path of heat transmission from the inside of the overpack to its outside surface. For conservatism, however, the design basis thermal conductivity of Holtite-A under heat rejection conditions is set equal to zero, except for HI-STAR HB. The reverse condition occurs under a postulated fire event when the thermal conductivity of Holtite-A aids in the influx of heat to the stored fuel in the fuel basket. The thermal conductivity of Holtite-A is conservatively set at 1 Btu/hr-ft-°F for all fire accident analyses.

The Holtite-A neutron shielding material is stable at normal design temperatures over the long term and provides excellent shielding properties for neutrons.

#### 1.2.1.4.3 Gamma Shielding Material

For gamma shielding, HI-STAR 100 utilizes carbon steel in plate stock form. Instead of utilizing a thick forging, the gamma shield design in the HI-STAR 100 overpack borrows from the concept of layered vessels from the field of ultra-high pressure vessel technology. The shielding is made from successive layers of plate stock. The fabrication of the shell begins by rolling the inner shell plate and making the longitudinal weld seam. Each layer of the intermediate shells is constructed from two halves. The two halves of the shell are precision sheared, beveled, and rolled to the required radii. The two halves of the second layer are wrapped around the first shell. Each shell half is positioned in its location and while applying pressure using a specially engineered fixture, the halves are tack welded. The beveled edges to be joined are positioned to make contact or have a slight gap. The second layer is made by joining the two halves using two longitudinal welds. Successive layers are assembled in a like manner. Thus, the welding of every successive shell provides a certain inter-layer contact (Figure 1.2.7).

A thick structural component radiation barrier is thus constructed with four key features, namely:

- The number of layers can be increased as necessary to realize the required design objectives.
- The layered construction is ideal to stop propagation of flaws.
- The thinner plate stock is much more ductile than heavy forgings used in other designs.
- Post-weld heat treatment is not required by the ASME Code, simplifying fabrication.

#### 1.2.1.5 Lifting and Tie-Down Devices

The HI-STAR 100 overpack is equipped with two lifting trunnions located in the top flange. The lifting trunnions are designed in accordance with 10CFR71.45, NUREG-0612 [1.2.11], and ANSI N14.6 [1.3.3], manufactured from a high strength alloy, and are installed in threaded openings. The lifting trunnions may be secured in position by optional locking pads, shaped to make conformal contact with the curved overpack. Once the locking pad is bolted in position, the inner diameter is sized to restrain the trunnion from backing out. The two off-center pockets located near the overpack bottom plate on overpack serial numbers 1020-001 through 1020-007 are pocket trunnions. The pocket trunnions were eliminated from the design after serial number 1020-007 was fabricated and are no longer considered qualified tie-down devices. However, the pocket trunnions on these overpacks may still be used for normal handling activities such as upending and downending.

The lifting, upending, and downending of the HI-STAR 100 System requires the use of external handling devices. A lifting yoke is utilized when the cask is to be lifted or set in a vertical orientation. For those overpacks that have been fabricated with the pocket trunnions, transport and rotation cradles may include rotation trunnions that interface with the pocket trunnions to provide a pivot axis. A lift yoke may be connected to the lifting trunnions and the crane hook used for upending or downending the HI-STAR 100 System by rotating on the pocket trunnions for these overpacks. For those overpacks fabricated without pocket trunnions, the overpack must be transferred into the transport saddle with appropriate lift rigging. If an overpack having pocket trunnions is secured to the transport vehicle without engaging the pocket trunnions, plugs are required to be installed in the pocket to provide radiation shielding (see the overpack drawing in Section 1.4).

For transportation, the HI-STAR 100 System is engineered to be mounted on a transport frame secured to the transporter bed. Figure 1.2.8 provides a sketch of the HI-STAR 100 System secured for transport and the drawing in Section 1.4 provides additional details. The transport frame has a lower saddle with attachment points for belly slings around the cask body designed to prevent excessive vertical or lateral movement of the cask during normal transportation. The impact limiters affixed to both ends of the cask are designed to transmit the design basis axial loads into the cradle structure. See Section 2.5 for discussion of the qualification of tie-down devices.

The top of the MPC lid is equipped with four threaded holes that allow lifting of the loaded MPC. These holes allow the loaded MPC to be raised and/or lowered from the HI-STAR overpack. For users of the HI-STORM 100 Dry Storage System, MPC handling operations are performed using a HI-TRAC transfer cask of the HI-STORM 100 System (Docket No. 72-1014). The HI-TRAC transfer cask allows the sealed MPC loaded with spent fuel to be transferred from the HI-STORM 100 overpack (storage-only) to the HI-STAR 100 overpack, or vice versa. The threaded holes in the MPC lid are designed in accordance with NUREG-0612 and ANSI N14.6 and are plugged during transportation to prevent radiation streaming.

#### 1.2.1.6 Heat Dissipation

The HI-STAR 100 System can safely transport SNF by maintaining the fuel cladding temperature below the limits specified in Table 1.2.3 for normal and accident conditions. These limits have been established consistent with the guidance in NRC Interim Staff Guidance (ISG) document No. 11, Revision 3 (Ref. [1.2.14]). The temperature of the fuel cladding is dependent on the decay heat and the heat dissipation capabilities of the cask. The total heat load per BWR and PWR MPC is identified in Table 1.2.3. The SNF decay heat is passively dissipated without any mechanical or forced cooling.

The HI-STAR 100 System must meet the requirements of 10 CFR 71.43(g) for the accessible surface temperature limit. To meet this requirement the HI-STAR 100 System is shipped as an exclusive use shipment and includes an engineered personnel barrier during transport.

The primary heat transfer mechanisms in the HI-STAR 100 System are conduction and surface radiation.

The free volume of the MPC and the annulus between the external surface of the MPC and the inside surface of the overpack containment boundary are filled with 99.995% pure helium gas during fuel loading operations. Table 1.2.3 specifies the acceptance criteria for helium fill pressure in the MPC internal cavity. Besides providing an inert dry atmosphere for the fuel cladding, the helium also provides conductive heat transfer across any gaps between the metal surfaces inside the MPC and in the annulus between the MPC and overpack containment boundary. Metal conduction transfers the heat throughout the MPC fuel basket, through the MPC aluminum heat conduction elements (if installed) and shell, through the overpack inner shell, intermediate shells, steel radial connectors and finally, to the outer neutron shield enclosure shell. The most adverse temperature profiles and thermal gradients for the HI-STAR 100 System with each of the MPCs are discussed in detail in Chapter 3. The thermal analysis in Chapter 3 no longer takes credit for the aluminum heat conduction elements and they have been designated as optional equipment.

#### 1.2.1.7 Coolants

There are no coolants utilized in the HI-STAR 100 System. As discussed in Subsection 1.2.1.6 above, helium is sealed within the MPC internal cavity. The annulus between the MPC outer surface and overpack containment boundary is also purged and filled with helium gas.

#### 1.2.1.8 Pressure Relief Systems

No pressure relief system is provided on the HI-STAR 100 packaging containment boundary.

The sole pressure relief devices are provided in the overpack outer enclosure (Figure 1.1.4). The overpack outer enclosure contains the neutron shield material. Normal loadings will not cause the rupture disks to open. The rupture disks are installed to relieve internal pressure in the neutron shield cavities caused by the fire accident. The overpack outer enclosure is not designed as a pressure vessel. Correspondingly, the rupture disks are designed to open at relatively low pressures as stated below.

Relief Device location	Set pressure, psig
Overpack outer enclosure	30, +/- 5

#### 1.2.1.9 Security Seal

The HI-STAR 100 packaging provides a security seal that while intact, provides evidence that the package has not been opened by unauthorized persons. When installed, the impact limiters cover all penetrations into the HI-STAR 100 packaging containment boundary. Therefore, the security seal is placed to ensure that the impact limiters are not removed which thereby ensures that the package has not been opened. As shown on the HI-STAR transport assembly drawing in Section 1.4, security seals are provided on one impact limiter attachment bolt on the top impact limiter and through two adjacent bolts on the bottom impact limiter. A hole is provided in the head of the bolt and the impact limiter. Lock wire shall be threaded through the hole and joined with a security seal.

#### 1.2.1.10 Design Life

The design life of the HI-STAR 100 System is 40 years. This is accomplished by using materials of construction with a long proven history in the nuclear industry and specifying materials known to withstand their operating environments with little to no degradation. A maintenance program, as specified in Chapter 8, is also implemented to ensure the HI-STAR 100 System will exceed its design life of 40 years. The design considerations that assure the HI-STAR 100 System performs as designed throughout the service life include the following:

#### HI-STAR Overpack

- Exposure to Environmental Effects
- Material Degradation
- Maintenance and Inspection Provisions

#### MPC

- Corrosion
- Structural Fatigue Effects
- Maintenance of Helium Atmosphere
- Allowable Fuel Cladding Temperatures
- Neutron Absorber Boron Depletion

#### 1.2.2 Operational Features

Table 1.2.7 provides the sequence of basic operations necessary to load fuel and prepare the HI-STAR 100 System for transport. More detailed guidance for transportation-related loading, unloading, and handling operations is provided in Chapter 7 and is supported by the drawings in

Section 1.4. A summary of the loading and unloading operations is provided below. Figures 1.2.9 and 1.2.16 provide a pictorial view of the loading and unloading operations, respectively.

#### 1.2.2.1 Applicability of Operating Procedures for the Dual-Purpose HI-STAR 100 System

The HI-STAR 100 System is a dual-purpose system certified for use as a dry storage cask under 10 CFR 72 and as a transportation package under 10 CFR 71. In addition, the MPC is certified for use under 10 CFR 72 in the storage-only HI-STORM 100 System (a ventilated concrete cask system). Therefore, it is possible that the HI-STAR 100 overpack and/or the MPC may be loaded, prepared, and sealed under the operating procedures for storage, delineated in the HI-STAR 100 storage FSAR (Docket 72-1008) or the HI-STORM 100 storage FSAR (Docket 72-1014) or under a site specific storage license. In those cases, the operating procedures governing MPC and overpack preparation for storage would apply. The MPC and HI-STAR 100 overpack, as applicable, must be confirmed to meet all requirements of the Part 71 Certificate of Compliance before being released for shipment.

For those instances where the MPC is being loaded and shipped off-site in a HI-STAR 100 overpack under 10 CFR 71 without first being deployed at an ISFSI (known as "load-and-go" operations), the operating procedures in Chapter 7 (and summarized below) apply for preparation of the MPC and HI-STAR overpack. For those cases where the MPC is transferred from storage in a HI-STORM overpack to a HI-STAR overpack for shipment, the operating procedures in Chapter 7 (and summarized below) govern the preparation activities for the HI-STAR overpack.

#### Loading Operations

At the start of loading operations; the overpack is configured with the closure plate removed. The lift yoke is used to position the overpack in the designated preparation area or setdown area for overpack inspection and MPC insertion. The annulus is filled with plant demineralized water and an annulus seal is installed. The seal prevents contact between spent fuel pool water and the MPC shell reducing the possibility of contaminating the outer surfaces of the MPC. The MPC is then filled with spent fuel pool water or plant demineralized water. The overpack and MPC are lowered into the spent fuel pool for fuel loading using the lift yoke. Pre-selected assemblies are loaded into the MPC and a visual verification of the assembly identification is performed.

While still underwater, a thick shielding lid (the MPC lid) is installed. The lift yoke is remotely engaged to the overpack lifting trunnions and is used to lift the overpack close to the spent fuel pool surface. The MPC lift bolts (securing the MPC lid to the lift yoke) are removed. As the overpack is removed from the spent fuel pool, the lift yoke and overpack are sprayed with demineralized water to help remove contamination.

The overpack is removed from the pool and placed in the designated preparation area. The top surfaces of the MPC lid and the top flange of the overpack are decontaminated. The annulus seal is removed, and an annulus shield is installed. The annulus shield provides additional personnel shielding at the top of the annulus and also prevents small items from being dropped into the annulus (foreign material exclusion). If used, the Automated Welding System (AWS) is installed. The MPC water level is lowered slightly (See Chapter 7 for steps describing

monitoring and mitigation of combustible gas accumulation). The MPC lid is seal-welded using the AWS. Liquid penetrant examinations are performed on the root and final passes and ultrasonic examination is also performed on the MPC lid-to-shell weld or, in place of the ultrasonic examination, the weld may be inspected by multiple-pass liquid penetrant examination at approximately every 3/8 inch of weld depth. At the appropriate time in the sequence of activities, based on the type of test performed (hydrostatic or pneumatic), a pressure test of the MPC enclosure vessel is performed.

The Forced Helium Dehydration (FHD) System is connected to the MPC and is used to remove residual water from the MPC and reduce the level of moisture in the MPC to acceptable levels. This is accomplished by recirculating dry, heated helium through the MPC cavity to absorb the moisture. When the helium exiting the MPC is determined to meet the required moisture limit, the MPC is considered sufficiently dried for transportation (see Section 3.4.1.1.16 for a description of the FHD System).

Following MPC drying operations, the MPC is backfilled with a predetermined amount of helium gas. The helium backfill ensures adequate heat transfer and provides an inert atmosphere for fuel cladding integrity.

The MPC closure ring is then placed on the MPC, aligned, tacked in place, and seal welded, providing redundant closure of the MPC enclosure vessel closure welds. Tack welds are visually examined, and the root and/or final welds (depending on the number of weld passes required) are inspected using the liquid penetrant examination technique to ensure weld integrity. The annulus shield is removed and the remaining water in the annulus is drained. The AWS is removed. The overpack closure plate is installed and the bolts are torqued. The overpack annulus is dried using the vacuum drying system (VDS).

The overpack annulus is backfilled with helium gas for heat transfer and seal testing. Concentric metallic seals in the overpack closure plate prevent the leakage of the helium gas from the annulus and provide the containment boundary to the release of radioactive materials. The seals on the overpack vent and drain port plugs are leak tested along with the overpack closure plate inner seal. Cover plates with metallic seals are installed over the overpack vent and drain ports to provide redundant closure of the overpack penetrations. A port plug with a metallic seal is installed in the overpack closure plate test port to provide fully redundant closure of all overpack penetrations.

The overpack is surveyed for removable contamination and secured on the transport vehicle with impact limiters installed, the security seals are attached, and the personnel barrier is installed. The HI-STAR 100 packaging is then ready for transport.

#### Unloading Operations

The HI-STAR 100 System unloading procedures describe the general actions necessary to prepare the MPC for unloading, cool the stored fuel assemblies in the MPC (if necessary), flood the MPC cavity, remove the lid welds, unload the spent fuel assemblies, and recover the overpack and empty MPC. Special precautions are outlined to ensure personnel safety during the

unloading operations, and to prevent the risk of MPC overpressurization and thermal shock to the stored spent fuel assemblies.

After removing the impact limiters, the overpack and MPC are positioned in the designated preparation area. At the site's discretion, a gas sample is drawn from the overpack annulus and analyzed. The gas sample provides an indication of MPC enclosure vessel performance. The annulus is depressurized, the overpack closure plate is removed, and the annulus is filled with plant demineralized water. The annulus shield is installed to protect the annulus from debris produced from the lid removal process. Similarly, overpack top surfaces are covered with a protective fire-retarding blanket.

The Weld Removal System (WRS) is positioned on the MPC lid. The MPC closure ring is core drilled over the locations of the vent and drain port cover plates. The MPC closure ring and vent and drain port cover plates are core drilled to the extent necessary to allow access by the Remote Valve Operating Assemblies (RVOAs). Local ventilation is established around the vent and drain ports. The RVOAs are connected to allow access to the MPC cavity for re-flooding operations.

The MPC cavity gas is verified to be below an appropriate temperature (approximately 200°F) to allow water flooding. Depending on the time since initial fuel loading and the age and burnup of the contained fuel, mechanical cooling of the MPC cavity gas may or may not be required to ensure the cavity gas temperature meets the acceptance criterion. A thermal evaluation should be performed to determine the MPC bulk cavity gas temperature at the time of unloading. Based on that thermal evaluation, if the MPC cavity gas temperature does not already meet the acceptance limit, any appropriate means to cool the cavity gas may be employed to reduce the gas temperature to the acceptance criterion. Typically, this may involve intrusive means, such as recirculation cooling of the MPC cavity helium, or non-intrusive means, such as cooling of the exterior surface of the MPC enclosure vessel with water or air. The thermal evaluation should include an evaluation of the cooling process, if required, to determine the appropriate criteria for the cooling process, such as fluid flow rate(s), fluid temperature(s), and the cooling duration required to meet the acceptance criterion. Following fuel cool-down (if required), the MPC is flooded with water. The WRS is positioned for MPC lid-to-shell weld removal. The WRS is then removed with the MPC lid left in place.

The annulus shield is removed and the annulus seal is installed and pressurized. The MPC lid is rigged to the lift yoke and the lift yoke is engaged to overpack lifting trunnions. The overpack is placed in the spent fuel pool and the MPC lid is removed. All fuel assemblies are returned to the spent fuel storage racks. The overpack and MPC are returned to the designated preparation area. The annulus water is drained and the MPC and overpack are dispositioned for re-use or waste.

### 1.2.3 Contents of Package

The HI-STAR 100 packaging is classified as a Type B package under 10CFR71. As the HI-STAR 100 System is designed to transport spent nuclear fuel, the maximum activity of the contents requires that the HI-STAR 100 packaging be classified as Category I in accordance with Regulatory Guide 7.11 [1.2.10]. This section delineates the authorized contents permitted for

shipment in the HI-STAR 100 System, including fuel assembly types; non-fuel hardware; neutron sources; physical parameter limits for fuel assemblies and sub-components; enrichment, burnup, cooling time, decay heat limits, and core operating parameters as applicable; location requirements; and requirements for canning the material. See Supplement I for the contents of the HI-STAR HB.

#### 1.2.3.1 Determination of Design Basis Fuel

The HI-STAR 100 package is designed to transport most types of fuel assemblies generated in the commercial U.S. nuclear industry. Boiling-water reactor (BWR) fuel assemblies have been supplied by General Electric (GE), Siemens (SPC), Exxon Nuclear, ANF, UNC, ABB Combustion Engineering, Allis-Chalmers (AC) and Gulf Atomic. Pressurized-water reactor (PWR) fuel assemblies are generally supplied by Westinghouse, Babcock & Wilcox, ANF, and ABB Combustion Engineering. ANF, Exxon, and Siemens are historically the same manufacturing company under different ownership. Within this report, SPC is used to designate fuel manufactured by ANF, Exxon, or Siemens. Publications such as Refs. [1.2.6], [1.2.7], and [1.2.15] provide a comprehensive description of fuel discharged from U.S. reactors. A central object in the design of the HI-STAR 100 System is to ensure that a majority of SNF discharged from the U.S. reactors can be transported in one of the MPCs.

The cell openings in the fuel basket have been sized to accommodate all BWR and PWR assemblies listed in Refs. [1.2.6], [1.2.7], and [1.2.15], except as noted below. Similarly, the cavity length of the MPC has been set at a dimension that permits transportation of most types of PWR fuel assemblies and BWR fuel assemblies with or without fuel channels. The one exception is as follows:

- The South Texas Units 1 & 2 SNF, and CE 16x16 System 80<sup>TM</sup> SNF are too long to be accommodated in the available MPC cavity length.

In addition to satisfying the cross sectional and length compatibility, the active fuel region of the SNF must be enveloped in the axial direction by the neutron absorber located in the MPC fuel basket. Alignment of the neutron absorber with the active fuel region is ensured by the use of upper and lower fuel spacers suitably designed to support the bottom and restrain the top of the fuel assembly. The spacers axially position the SNF assembly such that its active fuel region is properly aligned with the neutron absorber in the fuel basket. Figure 1.2.15 provides a pictorial representation of the fuel spacers positioning the fuel assembly active fuel region. Both the upper and lower fuel spacers are designed to perform their function under normal and hypothetical accident conditions of transport. Due to the shorter, custom MPC design for Trojan plant fuel, only lower fuel spacers are needed for certain fuel assemblies that do not contain integral control rod assemblies. This creates the potential for a slight misalignment between the active fuel region of a fuel assembly and the neutron absorber panels affixed to the cell walls of the Trojan MPCs. This condition is addressed in the criticality evaluations described in Chapter 6.

In summary, the geometric compatibility of the SNF with the MPC designs does not require the definition of a design basis fuel assembly. This, however, is not the case for structural, containment, shielding, thermal-hydraulic, and criticality criteria. In fact, the same fuel type in a

category (PWR or BWR) may not control the cask design in all of the above-mentioned criteria. To ensure that no SNF listed in Refs. [1.2.6], [1.2.7], and [1.2.15] that is geometrically admissible in the HI-STAR MPC is precluded from loading, it is necessary to determine the governing fuel specification for each analysis criteria. To make the necessary determinations, potential candidate fuel assemblies for each qualification criteria were considered. Table 1.2.8 lists the PWR fuel assemblies evaluated. These fuel assemblies were evaluated to define the governing design criteria for PWR fuel. The BWR fuel assembly designs evaluated are listed in Table 1.2.9. Tables 1.2.10 and 1.2.11 provide the fuel characteristics determined to be acceptable for transport in the HI-STAR 100 System. Each "array/class" listed in these tables represents a bounding set of parameters for one or more fuel assembly types. The array/classes are defined in SAR Section 6.2. Table 1.2.12 lists the BWR and PWR fuel assembly designs that are found to govern for the qualification criteria, namely reactivity, shielding, and thermal. Thermal is broken down into three criteria, namely: 1) fuel assembly effective planar conductivity, 2) fuel basket effective axial conductivity, and 3) MPC density and heat capacity. Substantiating results of analyses for the governing assembly types are presented in the respective chapters dealing with the specific qualification topic. Tables 1.2.10, 1.2.11, and 1.2.21 through 1.2.36 provide the specific limits for all material authorized to be transported in the HI-STAR 100 System. Additional information on the design basis fuel definition is presented in the following subsections.

#### 1.2.3.2 Design Payload for Intact Fuel

Intact fuel assemblies are defined as fuel assemblies without known or suspected cladding defects greater than pinhole leaks and hairline cracks, and which can be handled by normal means. The design payload for intact fuel to be transported in the HI-STAR 100 System is provided in Tables 1.2.10, 1.2.11, and 1.2.22 through 1.2.36. The placement of a single stainless steel clad fuel assembly in an MPC necessitates that all fuel assemblies (stainless steel clad or Zircaloy clad) stored in that MPC meet the maximum heat generation requirements for stainless steel clad fuel. Stainless steel clad fuel assemblies are not authorized for transportation in the MPC-68F or MPC-32.

Fuel assemblies without fuel rods in fuel rod locations cannot be classified as intact fuel unless dummy fuel rods, which occupy a volume equal to or greater than the original fuel rods, replace the missing rods prior to loading. Any intact fuel assembly that falls within the geometric, thermal, and nuclear limits established for the design basis intact fuel assembly can be safely transported in the HI-STAR 100 System.

Some Trojan fuel assemblies not loaded into DFCs or FFCs show conditions of minor impairments on some grid straps [1.2.16]. These conditions, as determined by visual inspection of the assemblies, consist of small portions of grid straps that are missing or bent. The worst condition is the exposure of a single fuel rod on the periphery of one grid strap. These conditions do not meet the definition of damaged fuel in the CoC, since the impairment is minor, no grid spacers are missing, and the overall structural integrity of the assembly is not affected. Such assemblies are therefore classified as intact assemblies.

The fuel characteristics specified in Tables 1.2.10, 1.2.11, and 1.2.21 have been evaluated in this SAR and are acceptable for transport in the HI-STAR 100 System.

#### 1.2.3.3 Design Payload for Damaged Fuel and Fuel Debris

Damaged fuel and fuel debris are defined in Table 1.0.1. The only PWR damaged fuel and fuel debris authorized for transportation in the HI-STAR 100 System is that from the Trojan plant. The only BWR damaged fuel and fuel debris authorized for transportation in the HI-STAR 100 System is that from the Dresden Unit 1 and Humboldt Bay plants.

Damaged fuel may only be transported in the MPC-24E, MPC-24EF, MPC-68, or MPC-68F as shown in Tables 1.2.23 through 1.2.26. Fuel debris may only be transported in the MPC-24EF and the MPC-68F as shown in Tables 1.2.24 and 1.2.26. Damaged fuel and fuel debris must be transported in stainless steel Holtec damaged fuel containers (DFCs) or other approved stainless steel damaged/failed fuel canister in the HI-STAR 100 System. The list of approved damaged/failed fuel canisters and associated SAR figures are provided below:

- Holtec-designed Dresden Unit 1 Damaged Fuel Container (Figure 1.2.10)
- Sierra Nuclear-designed Trojan Failed Fuel Can (Figure 1.2.10A) containing Trojan damaged fuel, fuel debris, or Trojan Fuel debris process cans; or containing Trojan Fuel Debris Process Can Capsules (Figure 1.2.10C), which themselves contain Trojan Fuel Debris Process Cans (Figure 1.2.10B).
- Holtec-designed Damaged Fuel Container for Trojan plant fuel (Figure 1.2.10D)
- Dresden Unit 1's TN Damaged Fuel Container (Figure 1.2.11)
- Dresden Unit 1's Thoria Rod Canister (Figure 1.2.11A)
- Holtec-designed Humboldt Bay Damaged Fuel Container (refer to Supplement 1.I)

##### 1.2.3.3.1 BWR Damaged Fuel and Fuel Debris

Dresden Unit 1 (UO<sub>2</sub> fuel rods and MOX fuel rods) fuel arrays (Assembly Classes 6x6A, 6x6B, 6x6C, 7x7A, and 8x8A) are authorized for transportation as damaged fuel in the MPC-68 and damaged fuel or fuel debris in the MPC-68F. No other BWR damaged fuel or fuel debris is authorized for transportation.

The limits for transporting Dresden Unit 1 damaged fuel and fuel debris are given in Table 1.2.23 and 1.2.24. The placement of a single damaged fuel assembly in an MPC-68 or MPC-68F, or a single fuel debris damaged fuel container in an MPC-68F necessitates that all fuel assemblies (intact, damaged, or debris) placed in that MPC meet the maximum heat generation requirements specified in Tables 1.2.23 and 1.2.24.

The fuel characteristics specified in Tables 1.2.11, 1.2.23 and 1.2.24 for Dresden Unit 1 fuel arrays have been evaluated in this SAR and are acceptable for transport as damaged fuel or fuel debris in the HI-STAR 100 System. Because of the long cooling time, small size, and low weight of spent fuel assemblies qualified as damaged fuel or fuel debris, the DFC and its contents are bounded by the structural, thermal, and shielding analyses performed for the intact BWR design basis fuel. Separate criticality analysis of the bounding fuel assembly for the damaged fuel and fuel debris has been performed in Chapter 6.

The fuel characteristics specified in Table 1.2.11 for the Dresden Unit 1 fuel arrays (Assembly Classes 6x6A, 6x6B, 6x6C, 7x7A, and 8x8A) have been evaluated in this SAR and are acceptable for transport as damaged fuel or fuel debris in the HI-STAR 100 System after being placed in a damaged fuel container.

Refer to Supplement 1.I for information regarding Humboldt Bay damaged fuel and fuel debris.

#### 1.2.3.3.2 PWR Damaged Fuel and Fuel Debris

The PWR damaged fuel and fuel debris authorized for transportation in the HI-STAR 100 System is limited to that from the Trojan plant. The limits for transporting Trojan plant damaged fuel and fuel debris in the Trojan MPC-24E/EF are given in Tables 1.2.10, 1.2.25 and 1.2.26. All Trojan plant damaged fuel, and fuel debris listed below is authorized for transportation in the HI-STAR 100 System [1.2.12]:

- Damaged fuel assemblies in Trojan failed fuel cans
- Damaged fuel assemblies in Holtec's Trojan plant PWR damaged fuel container
- Fuel assemblies classified as fuel debris in Trojan failed fuel cans
- Trojan fuel assemblies classified as fuel debris in Holtec's Trojan damaged fuel container
- Fuel debris consisting of loose fuel pellets, fuel pellet fragments, and fuel assembly metal fragments (portions of fuel rods, portions of grid assemblies, bottom nozzles, etc.) in Trojan failed fuel cans
- Trojan fuel debris process cans loaded into Trojan fuel debris process can capsules and then into Trojan failed fuel cans. The fuel debris process cans contain fuel debris (metal fragments) and were used to process organic media removed from the Trojan spent fuel pool during cleanup operations in preparation for decommissioning the pool. The fuel debris process cans have metallic filters in the can bottom and lid that allowed removal of water and organic media using high temperature steam, while retaining the solid

residue from the processed media and fuel debris inside the process can<sup>†</sup>. Up to five process cans can be loaded into a process can capsule, which is vacuumed, purged, backfilled with helium, and seal-welded closed to provide a sealed containment for the fuel debris.

One Trojan Failed Fuel Can is not completely filled with fuel debris. Therefore, a stainless steel failed fuel can spacer is installed in this FFC to minimize movement of the fuel debris during normal transportation and hypothetical accident conditions. The spacer is a long, square tube with a baseplate that rests atop the fuel debris inside the Trojan FFC. A drawing of the Trojan failed fuel can spacer is provided in Section 1.4. A summary of the structural analysis of the FFC spacer is provided in Section 2.6.1.3.1.3.

#### 1.2.3.4 Structural Payload Parameters

The main physical parameters of an SNF assembly applicable to the structural evaluation are the fuel assembly length, envelope (cross sectional dimensions), and weight. These parameters, which define the mechanical and structural design, are listed in Tables 1.2.22 through 1.2.27 for the various MPC models. The centers of gravity reported in Chapter 2 are based on the maximum fuel assembly weight. Upper and lower fuel spacers (as appropriate) maintain the axial position of the fuel assembly within the MPC basket and, therefore, the location of the center of gravity. The upper and lower spacers are designed to withstand normal and accident conditions of transport. An axial clearance of approximately 2 inches is provided to account for the irradiation and thermal growth of the fuel assemblies. The suggested upper and lower fuel spacer lengths are listed in Tables 1.2.16 and 1.2.17. Due to the custom design of the Trojan MPCs, only lower fuel spacers are required with Trojan plant fuel assemblies not containing non-fuel hardware or neutron sources. In order to qualify for transport in the HI-STAR 100 MPC, the SNF must satisfy the physical parameters listed in Tables 1.2.21 through 1.2.36, as applicable.

#### 1.2.3.5 Thermal Payload Parameters

The principal thermal design parameter for the fuel is the peak fuel cladding temperature, which is a function of the maximum heat generation rate per assembly and the decay heat removal capabilities of the HI-STAR 100 System. The maximum heat generation rate per assembly for the design basis fuel assembly is based on the fuel assembly type with the lowest thermal performance characteristics. The parameters that define this decay heat design basis fuel are listed in Table 1.2.12. The governing thermal parameters to ensure that the range of SNF discussed previously are bounded by the thermal analysis discussed in detail and specified in Chapter 3. By utilizing these bounding thermal parameters, the calculated peak fuel rod cladding temperatures are conservative for the actual spent fuel assemblies, which are apt to have a higher thermal conductivity.

The peak fuel cladding temperature limit for normal conditions of transport is 400°C (752°F), which is consistent with the guidance in ISG-11, Revision 3 [1.2.14]. Tables 1.2.21 through

<sup>†</sup> The Trojan Fuel Debris Process Cans were used in the spent fuel pool cleanup effort conducted as part of plant decommissioning. This project is complete and not associated with certification of Trojan fuel debris for transportation in the HI-STAR 100 System under 10 CFR 71.

1.2.27 provide the maximum heat generation for all fuel assemblies authorized for transportation in the HI-STAR 100 System. The basis for these limits is discussed in Chapter 3.

Finally, the axial variation in the heat emission rate in the design basis fuel is defined based on the axial burnup distribution. For this purpose, the data provided in Refs. [1.2.8], [1.2.9], and [1.2.12] are utilized and summarized in Table 1.2.15 and Figures 1.2.13, 1.2.13A, and 1.2.14, for reference. These distributions are representative of fuel assemblies with the design burnup levels considered. These distributions are used for analysis only, and do not provide a criteria for fuel assembly acceptability for transport in the HI-STAR 100 System.

#### 1.2.3.6 Radiological Payload Parameters

The principal radiological design criteria are the 10CFR71.47 and 10CFR71.51 radiation dose rate and release requirements for the HI-STAR 100 System. The radiation dose rate is directly affected by the gamma and neutron source terms of the SNF assembly.

The gamma and neutron sources are separate and are affected differently by enrichment, burnup, and cool time. It is recognized that, at a given burnup, the radiological source terms increase monotonically as the initial enrichment is reduced. The shielding design basis fuel assembly is, therefore, evaluated for different combinations of maximum burnup, minimum cooling time, and minimum enrichment. The shielding design basis intact fuel assembly thus bounds all other intact fuel assemblies.

The design basis dose rates can be met by a variety of burnup levels, cooling times, and minimum enrichments. Tables 1.2.21 through 1.2.36 include the burnup and cooling time values that meet the radiological dose rate requirements for all authorized contents to be transported in each MPC model. The allowable maximum burnup, minimum cooling time, and minimum enrichment limits were chosen strictly based on the dose rate requirements. All allowable burnup, cooling time, and minimum enrichment combinations result in calculated dose rates less than the regulatory dose rate limits.

Table 1.2.15 and Figures 1.2.13, 1.2.13A, and 1.2.14 provide the axial distribution for the radiological source term for PWR and BWR fuel assemblies, and for Trojan plant-specific fuel, based on the actual burnup distribution. The axial burnup distributions are representative of fuel assemblies with the design basis burnup levels considered. These distributions are used for analysis only, and do not provide criteria for fuel assembly acceptability for transport in the HI-STAR 100 System.

Thoria rods placed in Dresden Unit 1 Thoria Rod Canisters meeting the requirements of Table 1.2.21 and Dresden Unit 1 fuel assemblies with one Antimony-Beryllium neutron source have been qualified for transport. Up to one Dresden Unit 1 Thoria Rod Canister plus any combination of damaged fuel assemblies in damaged fuel containers and intact fuel, up to a total of 68 may be transported.

### 1.2.3.7 Criticality Payload Parameters

As discussed earlier, the MPC-68/68F and MPC-32 feature a basket without flux traps. In these fuel baskets, there is one panel of neutron absorber between adjacent fuel assemblies. The MPC-24/24E/24EF employs a construction wherein two neighboring fuel assemblies are separated by two panels of neutron absorber with a water gap between them (flux trap construction). The MPC-24 flux trap basket can accept a much higher enrichment fuel than a non-flux trap basket without taking credit for fuel assembly burnup in the criticality analysis. The maximum initial  $^{235}\text{U}$  enrichment for PWR and BWR fuel authorized for transport is specified by fuel array/class in Tables 1.2.10 and 1.2.11, respectively. Trojan plant fuel is limited to a lower maximum initial enrichment of 3.7 wt.%  $^{235}\text{U}$  compared to other fuel in its array/class, based on the specific analysis performed for the custom-designed Trojan MPCs containing only Trojan plant fuel.

The minimum  $^{10}\text{B}$  areal density in the neutron absorber panels for each MPC model is shown in Table 1.2.3. Values for MPC-HB are found in Supplement 1.I.

For all MPCs, the  $^{10}\text{B}$  loading areal density used for analysis is conservatively established below the minimum values shown in Table 1.2.3. For Boral, the value used in the analysis is 75% of the minimum  $^{10}\text{B}$  areal density, while for METAMIC, 90% of the minimum value can be used to demonstrate that the reactivity under the most adverse accumulation of tolerances and biases is less than 0.95. The reduction in  $^{10}\text{B}$  areal density credit meets NUREG-1617 [1.0.5], which requires up to a 25% reduction in  $^{10}\text{B}$  areal density credit. A large body of sampling data accumulated by Holtec from thousands of manufactured Boral panels indicates the average  $^{10}\text{B}$  areal densities to be approximately 15% greater than the specified minimum.

Credit for burnup of the fuel, in accordance with the intent of the guidance in Interim Staff Guidance Document 8 (ISG-8) [1.2.13], is taken in the criticality analysis to allow the transportation of certain PWR fuel assemblies in MPC-32. Burnup credit is a required input to qualify PWR fuel for transportation in the MPC-32, considering the inleakage of moderator (i.e., unborated water) under accident conditions. This hypothetical event is non-credible given the double barrier design engineered into the HI-STAR 100 System with the fully welded MPC enclosure vessel (designed for 60 g's) surrounded by the sealed overpack, which is designed for deep submersion under water (greater than 650 feet submersion) without breach. The details of the burnup credit analyses are provided in Chapter 6, including detailed discussion of how the recommendations of ISG-8 were implemented. Exceptions to some of the recommendations in ISG-8 were necessary (e.g., partial credit for fission products) in order to develop burnup versus enrichment curves that can be practically implemented at the plants. These exceptions are described in Chapter 6.

#### 1.2.3.7.1 Core Operating Parameters<sup>†</sup>

For burnup credit in the MPC-32, assemblies must meet certain operating limits during their in-core depletion. These limits are listed in Table 1.2.27. For each assembly, the parameters Soluble

<sup>†</sup> This subsection is included by reference into Appendix A of the CoC.

Boron Concentration (SBC), Specific Power (SP), and Moderator Temperature (MT) must be calculated using the following equations. In these equations, and the symbols used therein, the subscript  $i$  denotes the cycle. The summation ( $\sum$ ) in these equation is to be performed over all cycles  $i$  that the assembly was in the core.

Given

$B_i$  Assembly-average burnup for cycle  $i$   
 $BC_i$  Core-average burnup for cycle  $i$   
 $SB_i$  Average In-Core Soluble Boron Concentration for cycle  $i$   
 $T_i$  Length of Cycle  
 $CIT_i$  Core Inlet Temperature  
 $COT_i$  Core Outlet temperature

the values to compared to the limits in Table 1.2.27 are to be calculated as follows:

Soluble Boron:

$$SB = \sum (SB_i * B_i) / \sum B_i$$

Assembly Average Specific Power:

$$SP = \sum B_i / \sum T_i$$

Assembly Average Moderator Temperature:

$$CFC_i = B_i/BC_i \quad \text{Correction Factor; if } CFC_i < 1 \text{ then set } CFC_i = 1$$

$$MT = \sum (B_i * (CIT_i + CFC_i * (COT_i - CIT_i))) / \sum B_i$$

#### 1.2.3.7.2 Burnup Measurements<sup>††</sup>

For the MPC-32, the burnup value that is used to qualify the assembly by comparison with the limits listed in Table 1.2.34 shall be confirmed by burnup measurements using one of the following three approaches:

- Burnup measurements of every assembly to be loaded without correlation to reactor records on burnup. In this case, the measured burnup value is used for comparison with the limit, but shall be reduced by the uncertainty of the burnup measurement.
- Burnup measurements of every assembly based on correlation to reactor records on burnup. In this case, the reactor record burnup value is used for the comparison with the limit, but shall be reduced by the uncertainty of the reactor record burnup value compared to the measured burnup, combined with the uncertainty of the burnup measurement. The

<sup>††</sup> This subsection is included by reference into Appendix A of the CoC.

uncertainty of the reactor burnup value shall be determined at a 95 percent confidence level. Burnup measurements for another plant may be used if it is shown that they are applicable to the fuel to be qualified. This applicability review shall include a comparison of the fuel type, general core design and operation, and method for calculating burnup, and shall be supplemented by confirmatory burnup measurements.

- Burnup measurements of a sampling of the fuel assemblies. In this case a database of measured burnup, either based on correlation to reactor records on burnup or independent of reactor records must be provided to justify the adequacy of the sampling approach. The assigned burnup value shall be adjusted by the applicable method described above.

#### 1.2.3.7.3 Combined Burnup and Enrichment Curves

In addition to the minimum burnup requirements for the MPC-32 for burnup credit (Table 1.2.34), there are also maximum burnup limits based on the dose rate requirements (Tables 1.2.32 and 1.2.33). As a result, there is an acceptable burnup range for each enrichment. As an example, Figure 1.2.18 shows the lower burnup limits for B&W 15x15 assemblies (solid line), Configuration A, together with the upper burnup limits for assemblies with Zircaloy grid spacers (dashed lines). Acceptable assemblies must have a burnup between these two lines.

#### 1.2.3.8 Non-Fuel Hardware and Neutron Sources

BWR fuel is permitted to be stored with or without Zircaloy channels. Control blades and stainless steel channels are not authorized for transportation in the HI-STAR 100 System. Dresden Unit 1 (D-1) neutron sources are authorized for transportation as shown in Tables 1.2.23 and 1.2.24. The D-1 neutron sources are single, long rods containing Sb-Be source material that fits into a water rod location in a D-1 fuel assembly.

Except for Trojan plant fuel, no PWR non-fuel hardware or neutron sources are authorized for transportation in the HI-STAR 100 System. For Trojan plant fuel only, the following non-fuel hardware and neutron sources are permitted for transportation in specific quantities as shown in Tables 1.2.25 and 1.2.26:

- Rod Cluster Control Assemblies (RCCAs) with cladding made of Type 304 stainless steel and Ag-In-Cd neutron absorber material.
- Burnable Poison Rod Assemblies (BPRAs) with cladding made of Type 304 stainless steel and borosilicate glass tube neutron poison material.
- Thimble Plug Devices made of Type 304 stainless steel.
- Neutron source assemblies with cladding made of Type 304 stainless steel - two (2) californium primary source assemblies and four (4) antimony-beryllium secondary source assemblies.

These devices are designed with thin rods of varying length and materials as discussed above, that fit into the fuel assembly guide tubes within the fuel rod lattice. The upper fittings for each device can vary to accommodate the handling tool (grapple) design. During reactor operation, the positions of the RCCAs are controlled by the operator using the control rod drive system, while the BPRAs, TPDs, and neutron sources stay fully inserted.

A complete list of the authorized non-fuel hardware and neutron sources, including appropriate limits on the characteristics of this material, is provided in Tables 1.2.23 through 1.2.36, as applicable.

#### 1.2.3.9 Summary of Authorized Contents

The criticality safety index for the HI-STAR 100 Package is zero. A fuel assembly is acceptable for transport in a HI-STAR 100 System if it fulfills the following criteria.

- a. It satisfies the physical parameter characteristics listed in Tables 1.2.10 or 1.2.11, as applicable.
- b. It satisfies the cooling time, decay heat, burnup, enrichment, and other limits specified in Tables 1.2.21 through 1.2.36, as applicable.

A damaged fuel assembly shall be transported in a damaged fuel container or other authorized damaged/failed fuel canister, and shall meet the characteristics specified in Tables 1.2.23 through 1.2.26 for transport in the MPC-68, MPC-68F, MPC-24E, or MPC-24EF. Fuel classified as fuel debris shall be placed in a damaged fuel container or other authorized damaged/failed fuel canister and shall meet the characteristics specified in Tables 1.2.24 or 1.2.26 for transport in the MPC-68F or MPC-24EF.

Stainless steel clad fuel assemblies shall meet the characteristics specified in Tables 1.2.22 through 1.2.33 for transport in the MPC-24, MPC-24E, MPC-24EF, or MPC-68.

MOX BWR fuel assemblies shall meet the requirements of Tables 1.2.23 or 1.2.24 for intact and damaged fuel/fuel debris.

Thoria rods placed in Dresden Unit 1 Thoria Rod Canisters meeting the requirements of Table 1.2.21 and Dresden Unit 1 fuel assemblies with one Antimony-Beryllium neutron source have been qualified for transport. Up to one Dresden Unit 1 Thoria Rod Canister plus any combination of damaged fuel assemblies in damaged fuel containers and intact fuel, up to a total of 68 may be transported.

Dresden Unit 1 fuel assemblies with one Antimony-Beryllium neutron source are authorized for loading in the MPC-68 or MPC-68F.

Table 1.2.2 summarizes the key system data for the HI-STAR 100 System. Table 1.2.3 summarizes the key parameters and limits for the HI-STAR 100 MPCs. Tables 1.2.10, 1.2.11, and 1.2.21 through 1.2.36 and other tables referenced from these tables provide the limiting

conditions for all material to be transported in the HI-STAR 100 System. Refer to Supplement 1.I for HI-STAR HB.

Table 1.2.1

TABLE INTENTIONALLY DELETED

Table 1.2.2

## SUMMARY OF KEY SYSTEM DATA FOR HI-STAR 100

PARAMETER	VALUE (Nominal)	
Types of MPCs in this SAR	6†	4 for PWR 2 for BWR
MPC capacity	MPC-24	Up to 24 intact ZR or stainless steel clad PWR fuel assemblies
	MPC-24E	Up to 24 intact ZR or stainless steel clad PWR fuel assemblies. Up to four (4) Trojan plant fuel assemblies classified as damaged fuel, each in a Trojan Failed Fuel Can or a Holtec damaged fuel container, and the complement intact fuel assemblies.
	MPC-24EF	Up to 24 intact ZR or stainless steel clad PWR fuel assemblies. Up to four (4) Trojan plant fuel assemblies classified as damaged fuel or fuel debris, each in a Trojan Failed Fuel Can or a Holtec damaged fuel container; or other Trojan fuel debris stored in Trojan Process Cans either placed directly into a Trojan Failed Fuel Can or placed inside Trojan Process Can Capsules and then in Trojan Failed Fuel Cans; and the complement intact fuel assemblies.
	MPC-32	Up to 32 intact ZR clad PWR fuel assemblies.
	MPC-68	Up to 68 intact ZR or stainless steel clad BWR fuel assemblies or damaged ZR clad fuel assemblies* in damaged fuel containers within an MPC-68
	MPC-68F	Up to 4 damaged fuel containers with ZR clad BWR fuel debris* and the complement intact or damaged* ZR clad BWR fuel assemblies within an MPC-68F.  *Only damaged fuel and fuel debris from Dresden Unit 1 is authorized for transportation in the MPC-68 and MPC-68F.

† - excluding MPC-HB. See Supplement I.

Table 1.2.3  
KEY PARAMETERS FOR HI-STAR 100 MULTI-PURPOSE CANISTERS

PARAMETER	PWR	BWR
Unloaded MPC weight (lb)	See Table 2.2.1	See Table 2.2.1
Minimum Boral neutron absorber <sup>10</sup> B loading (g/cm <sup>2</sup> )	0.0267 (MPC-24) 0.0372 (MPC-24E/EF) 0.0372 (MPC-32)	0.0372 (MPC-68) 0.01 (MPC-68F)
Minimum Metamic neutron absorber <sup>10</sup> B loading (g/cm <sup>2</sup> )	0.0267 (MPC-24) 0.0372 (MPC-24E/EF) 0.0310 (MPC-32)	0.0310 (MPC-68)
Pre-disposal service life (years)	40	40
Design temperature, max./min. (°F)	725 <sup>†</sup> /-40 <sup>††</sup>	725 <sup>†</sup> /-40 <sup>††</sup>
Design Internal pressure (psig)		
Normal Conditions	100	100
Off-normal Conditions	100	100
Accident Conditions	200	200
Total heat load, max. (kW)	20.0	18.5
Maximum permissible peak fuel cladding temperature (°F)	752° (normal conditions) 1058° (accident conditions)	752° (normal conditions) 1058° (accident conditions)
MPC internal environment Helium filled (psig)	≥ 0 and ≤ 44.8 psig <sup>†††</sup> at a reference temperature of 70°F	≥ 0 and ≤ 44.8 psig <sup>†††</sup> at a reference temperature of 70°F
MPC external environment/overpack internal environment Helium filled initial pressure (psig, at STP)	≥ 10 and ≤ 14	≥ 10 and ≤ 14
Maximum permissible reactivity including all uncertainty and biases	<0.95	<0.95
End closure(s)	Welded	Welded
Fuel handling	Opening compatible with standard grapples	Opening compatible with standard grapples
Heat dissipation	Passive	Passive

† Maximum normal condition design temperature for the MPC fuel basket. A complete listing of design temperatures for all components is provided in Table 2.1.2

†† Temperature based on minimum ambient temperature (10CFR71.71(c)(2)) and no fuel decay heat load.

††† This value represents the nominal backfill value used in the thermal analysis, plus 2 psig operating tolerance. Based on the MPC pressure results in Table 3.4.15 and the pressure limits specified in Table 2.1.1, there is sufficient analysis margin to accommodate this operating tolerance.

Tables 1.2.4 through 1.2.6  
INTENTIONALLY DELETED

Table 1.2.7

## HI-STAR 100 LOADING OPERATIONS DESCRIPTION

Site-specific handling and operating procedures will be prepared, reviewed, and approved by each owner/user.	
1	Overpack and MPC lowered into the fuel pool without closure plate and MPC lid
2	Fuel assemblies transferred to the MPC fuel basket
3	MPC lid lowered onto the MPC
4	Overpack/MPC assembly moved to the decon pit and MPC lid welded in place, examined, and pressure tested
5	MPC dewatered, dried, backfilled with helium, and the vent/drain port cover plates and closure ring welded
6	Overpack drained and external surfaces decontaminated
7	Overpack seals and closure plate installed and bolts pre-tensioned
8	Overpack cavity dried, backfilled with helium, and helium leak tested
9	HI-STAR 100 System transferred to transport bay
10	HI-STAR 100 placed onto transport saddles, tied down, impact limiters and personnel barrier installed, and package surveyed for release for transport.

Table 1.2.8

## PWR FUEL ASSEMBLIES EVALUATED TO DETERMINE DESIGN BASIS SNF

Assembly Class	Array Type
B&W 15x15	All
B&W 17x17	All
CE 14x14	All
CE 16x16	All except System 80™
WE 14x14	All
WE 15x15	All
WE 17x17	All
St. Lucie	All
Ft. Calhoun	All
Haddam Neck (Stainless Steel Clad)	All
San Onofre 1 (Stainless Steel Clad, except MOX)	All
Indian Point 1	All

Table 1.2.9

## BWR FUEL ASSEMBLIES EVALUATED TO DETERMINE DESIGN BASIS SNF

Assembly Class	Array Type			
GE BWR/2-3	All 7x7	All 8x8	All 9x9	All 10x10
GE BWR/4-6	All 7x7	All 8x8	All 9x9	All 10x10
Humboldt Bay	All 6x6	All 7x7 (Zircaloy Clad)		
Dresden-1	All 6x6	All 8x8		
LaCrosse (Stainless Steel Clad)	All			

Table 1.2.10  
PWR FUEL ASSEMBLY CHARACTERISTICS (Note 1)

Fuel Assembly Array/Class	14x14A	14x14B	14x14C	14x14D	14x14E
Clad Material (Note 2)	ZR	ZR	ZR	SS	ZR
Design Initial U (kg/assy.) (Note 3)	≤ 407	≤ 407	≤ 425	≤ 400	≤ 206
Initial Enrichment (MPC-24, 24E, and 24EF) (wt % <sup>235</sup> U)	≤ 4.6 (24) ≤ 5.0 (24E/24EF)	≤ 4.6 (24) ≤ 5.0 (24E/24EF)	≤ 4.6 (24) ≤ 5.0 (24E/24EF)	≤ 4.0 (24) ≤ 5.0 (24E/24EF)	≤ 5.0
Initial Enrichment (MPC-32) (wt % <sup>235</sup> U) (Note 5)	N/A	N/A	N/A	N/A	N/A
No. of Fuel Rod Locations	179	179	176	180	173
Fuel Clad O.D. (in.)	≥ 0.400	≥ 0.417	≥ 0.440	≥ 0.422	≥ 0.3415
Fuel Clad I.D. (in.)	≤ 0.3514	≤ 0.3734	≤ 0.3880	≤ 0.3890	≤ 0.3175
Fuel Pellet Dia. (in.)	≤ 0.3444	≤ 0.3659	≤ 0.3805	≤ 0.3835	≤ 0.3130
Fuel Rod Pitch (in.)	≤ 0.556	≤ 0.556	≤ 0.580	≤ 0.556	Note 6
Active Fuel Length (in.)	≤ 150	≤ 150	≤ 150	≤ 144	≤ 102
No. of Guide and/or Instrument Tubes	17	17	5 (Note 4)	16	0
Guide/Instrument Tube Thickness (in.)	≥ 0.017	≥ 0.017	≥ 0.038	≥ 0.0145	N/A

Table 1.2.10 (continued)  
PWR FUEL ASSEMBLY CHARACTERISTICS (Note 1)

Fuel Assembly Array/Class	15x15A	15x15B	15x15C	15x15D	15x15E	15x15F
Clad Material (Note 2)	ZR	ZR	ZR	ZR	ZR	ZR
Design Initial U (kg/assy.) (Note 3)	≤ 464	≤ 464	≤ 464	≤ 475	≤ 475	≤ 475
Initial Enrichment (MPC-24, 24E, and 24EF (wt % <sup>235</sup> U))	≤ 4.1 (24) ≤ 4.5 (24E/24EF)					
Initial Enrichment (MPC-32) (wt % <sup>235</sup> U) (Note 5)	N/A	(Note5)	N/A	(Note5)	(Note5)	(Note5)
No. of Fuel Rod Locations	204	204	204	208	208	208
Fuel Clad O.D. (in.)	≥ 0.418	≥ 0.420	≥ 0.417	≥ 0.430	≥ 0.428	≥ 0.428
Fuel Clad I.D. (in.)	≤ 0.3660	≤ 0.3736	≤ 0.3640	≤ 0.3800	≤ 0.3790	≤ 0.3820
Fuel Pellet Dia. (in.)	≤ 0.3580	≤ 0.3671	≤ 0.3570	≤ 0.3735	≤ 0.3707	≤ 0.3742
Fuel Rod Pitch (in.)	≤ 0.550	≤ 0.563	≤ 0.563	≤ 0.568	≤ 0.568	≤ 0.568
Active Fuel Length (in.)	≤ 150	≤ 150	≤ 150	≤ 150	≤ 150	≤ 150
No. of Guide and/or Instrument Tubes	21	21	21	17	17	17
Guide/Instrument Tube Thickness (in.)	≥ 0.0165	≥ 0.015	≥ 0.0165	≥ 0.0150	≥ 0.0140	≥ 0.0140

Table 1.2.10 (continued)  
PWR FUEL ASSEMBLY CHARACTERISTICS (Note 1)

Fuel Assembly Array/Class	15x15G	15x15H	16x16A	17x17A	17x17B	17x17C
Clad Material (Note 2)	SS	ZR	ZR	ZR	ZR	ZR
Design Initial U (kg/assy.) (Note 3)	≤ 420	≤ 475	≤ 443	≤ 467	≤ 467	≤ 474
Initial Enrichment (MPC-24, 24E, and 24EF) (wt % <sup>235</sup> U)	≤ 4.0 (24) ≤ 4.5 (24E/24EF)	≤ 3.8 (24) ≤ 4.2 (24E/24EF)	≤ 4.6 (24) ≤ 5.0 (24E/24EF)	≤ 4.0 (24) ≤ 4.4 (24E/24EF)	≤ 4.0 (24) ≤ 4.4 (24E/24EF) (Note 7)	≤ 4.0 (24) ≤ 4.4 (24E/24EF)
Initial Enrichment (MPC-32) (wt % <sup>235</sup> U) (Note 5)	N/A	(Note5)	N/A	(Note5)	(Note5)	(Note5)
No. of Fuel Rod Locations	204	208	236	264	264	264
Fuel Clad O.D. (in.)	≥ 0.422	≥ 0.414	≥ 0.382	≥ 0.360	≥ 0.372	≥ 0.377
Fuel Clad I.D. (in.)	≤ 0.3890	≤ 0.3700	≤ 0.3320	≤ 0.3150	≤ 0.3310	≤ 0.3330
Fuel Pellet Dia. (in.)	≤ 0.3825	≤ 0.3622	≤ 0.3255	≤ 0.3088	≤ 0.3232	≤ 0.3252
Fuel Rod Pitch (in.)	≥ 0.563	≥ 0.568	≥ 0.506	≥ 0.496	≥ 0.496	≥ 0.502
Active Fuel Length (in.)	≤ 144	≤ 150	≤ 150	≤ 150	≤ 150	≤ 150
No. of Guide and/or Instrument Tubes	21	17	5 (Note 4)	25	25	25
Guide/Instrument Tube Thickness (in.)	≥ 0.0145	≥ 0.0140	≥ 0.0400	≥ 0.016	≥ 0.014	≥ 0.020

Table 1.2.10 (continued)  
PWR FUEL ASSEMBLY CHARACTERISTICS

## Notes:

1. All dimensions are design nominal values. Maximum and minimum dimensions are specified to bound variations in design nominal values among fuel assemblies within a given array/class.
2. ZR designates any zirconium-based fuel cladding material authorized for use in a commercial power reactor.
3. Design initial uranium weight is the nominal uranium weight specified for each assembly by the fuel manufacturer or reactor user. For each PWR fuel assembly, the total uranium weight limit specified in this table may be increased up to 2.0 percent for comparison with users' fuel records to account for manufacturer's tolerances.
4. Each guide tube replaces four fuel rods.
5. "NA" means that this array/class is not authorized for transportation in the MPC-32. For authorized array/classes, minimum assembly average burnup and maximum enrichment is specified in Table 1.2.34.
6. This fuel assembly array/class includes only the Indian Point Unit 1 fuel assembly. This fuel assembly has two pitches in different sectors of the assembly. These pitches are 0.441 inches and 0.453 inches.
7. Trojan plant-specific fuel is governed by the limits specified for array/class 17x17B and will be transported in the custom-designed Trojan MPC-24E/EF canisters. The Trojan MPC-24E/EF design is authorized to transport only Trojan plant fuel with a maximum initial enrichment of 3.7 wt.% <sup>235</sup>U.

Table 1.2.11  
BWR FUEL ASSEMBLY CHARACTERISTICS (Note 1)

Fuel Assembly Array/Class	6x6A	6x6B	6x6C	7x7A	7x7B	8x8A
Clad Material (Note 2)	ZR	ZR	ZR	ZR	ZR	ZR
Design Initial U (kg/assy.) (Note 3)	≤ 110	≤ 110	≤ 110	≤ 100	≤ 195	≤ 120
Maximum Planar-Average Initial Enrichment (wt % <sup>235</sup> U)	≤ 2.7	≤ 2.7 for the UO <sub>2</sub> rods. See Note 4 for MOX rods.	≤ 2.7	≤ 2.7	≤ 4.2	≤ 2.7
Initial Maximum Rod Enrichment (wt % <sup>235</sup> U)	≤ 4.0	≤ 4.0	≤ 4.0	≤ 5.5	≤ 5.0	≤ 4.0
No. of Fuel Rod Locations	35 or 36	35 or 36 (up to 9 MOX rods)	36	49	49	63 or 64
Fuel Clad O.D. (in.)	≥ 0.5550	≥ 0.5625	≥ 0.5630	≥ 0.4860	≥ 0.5630	≥ 0.4120
Fuel Clad I.D. (in.)	≤ 0.5105	≤ 0.4945	≤ 0.4990	≤ 0.4204	≤ 0.4990	≤ 0.3620
Fuel Pellet Dia. (in.)	≤ 0.4980	≤ 0.4820	≤ 0.4880	≤ 0.4110	≤ 0.4910	≤ 0.3580
Fuel Rod Pitch (in.)	≤ 0.710	≤ 0.710	≤ 0.740	≤ 0.631	≤ 0.738	≤ 0.523
Active Fuel Length (in.)	≤ 120	≤ 120	≤ 77.5	≤ 80	≤ 150	≤ 120
No. of Water Rods (Note 11)	1 or 0	1 or 0	0	0	0	1 or 0
Water Rod Thickness (in.)	> 0	> 0	N/A	N/A	N/A	≥ 0
Channel Thickness (in.)	≤ 0.060	≤ 0.060	≤ 0.060	≤ 0.060	≤ 0.120	≤ 0.100

Table 1.2.11 (continued)  
BWR FUEL ASSEMBLY CHARACTERISTICS (Note 1)

Fuel Assembly Array/Class	8x8B	8x8C	8x8D	8x8E	8x8F	9x9A
Clad Material (Note 2)	ZR	ZR	ZR	ZR	ZR	ZR
Design Initial U (kg/assy) (Note 3)	≤ 185	≤ 185	≤ 185	≤ 185	≤ 185	≤ 177
Maximum Planar-Average Initial Enrichment (wt % <sup>235</sup> U)	≤ 4.2	≤ 4.2	≤ 4.2	≤ 4.2	≤ 4.0	≤ 4.2
Initial Maximum Rod Enrichment (wt % <sup>235</sup> U)	≤ 5.0	≤ 5.0	≤ 5.0	≤ 5.0	≤ 5.0	≤ 5.0
No. of Fuel Rod Locations	63 or 64	62	60 or 61	59	64	74/66 (Note 5)
Fuel Clad O.D. (in.)	≥ 0.4840	≥ 0.4830	≥ 0.4830	≥ 0.4930	≥ 0.4576	≥ 0.4400
Fuel Clad I.D. (in.)	≤ 0.4295	≤ 0.4250	≤ 0.4230	≤ 0.4250	≤ 0.3996	≤ 0.3840
Fuel Pellet Dia. (in.)	≤ 0.4195	≤ 0.4160	≤ 0.4140	≤ 0.4160	≤ 0.3913	≤ 0.3760
Fuel Rod Pitch (in.)	≤ 0.642	≤ 0.641	≤ 0.640	≤ 0.640	≤ 0.609	≤ 0.566
Design Active Fuel Length (in.)	≤ 150	≤ 150	≤ 150	≤ 150	≤ 150	≤ 150
No. of Water Rods (Note 11)	1 or 0	2	1 - 4 (Note 7)	5	N/A (Note 12)	2
Water Rod Thickness (in.)	≥ 0.034	> 0.00	> 0.00	≥ 0.034	≥ 0.0315	> 0.00
Channel Thickness (in.)	≤ 0.120	≤ 0.120	≤ 0.120	≤ 0.100	≤ 0.055	≤ 0.120

Table 1.2.11 (continued)  
BWR FUEL ASSEMBLY CHARACTERISTICS (Note 1)

Fuel Assembly Array/Class	9x9 B	9x9 C	9x9 D	9x9 E (Note 13)	9x9 F (Note 13)	9x9 G
Clad Material (Note 2)	ZR	ZR	ZR	ZR	ZR	ZR
Design Initial U (kg/assy.) (Note 3)	≤ 177	≤ 177	≤ 177	≤ 177	≤ 177	≤ 177
Maximum Planar-Average Initial Enrichment (wt % <sup>235</sup> U)	≤ 4.2	≤ 4.2	≤ 4.2	≤ 4.0	≤ 4.0	≤ 4.2
Initial Maximum Rod Enrichment (wt % <sup>235</sup> U)	≤ 5.0	≤ 5.0	≤ 5.0	≤ 5.0	≤ 5.0	≤ 5.0
No. of Fuel Rod Locations	72	80	79	76	76	72
Fuel Clad O.D. (in.)	≥ 0.4330	≥ 0.4230	≥ 0.4240	≥ 0.4170	≥ 0.4430	≥ 0.4240
Fuel Clad I.D. (in.)	≤ 0.3810	≤ 0.3640	≤ 0.3640	≤ 0.3640	≤ 0.3860	≤ 0.3640
Fuel Pellet Dia. (in.)	≤ 0.3740	≤ 0.3565	≤ 0.3565	≤ 0.3530	≤ 0.3745	≤ 0.3565
Fuel Rod Pitch (in.)	≤ 0.572	≤ 0.572	≤ 0.572	≤ 0.572	≤ 0.572	≤ 0.572
Design Active Fuel Length (in.)	≤ 150	≤ 150	≤ 150	≤ 150	≤ 150	≤ 150
No. of Water Rods (Note 11)	1 (Note 6)	1	2	5	5	1 (Note 6)
Water Rod Thickness (in.)	> 0.00	≥ 0.020	≥ 0.0300	≥ 0.0120	≥ 0.0120	≥ 0.0320
Channel Thickness (in.)	≤ 0.120	≤ 0.100	≤ 0.100	≤ 0.120	≤ 0.120	≤ 0.120

Table 1.2.11 (continued)  
BWR FUEL ASSEMBLY CHARACTERISTICS (Note 1)

Fuel Assembly Array/Class	10x10 A	10x10 B	10x10 C	10x10 D	10x10 E
Clad Material (Note 2)	ZR	ZR	ZR	SS	SS
Design Initial U (kg/assy.) (Note 3)	≤ 186	≤ 186	≤ 186	≤ 125	≤ 125
Maximum Planar-Average Initial Enrichment (wt % <sup>235</sup> U)	≤ 4.2	≤ 4.2	≤ 4.2	≤ 4.0	≤ 4.0
Initial Maximum Rod Enrichment (wt % <sup>235</sup> U)	≤ 5.0	≤ 5.0	≤ 5.0	≤ 5.0	≤ 5.0
No. of Fuel Rod Locations	92/78 (Note 8)	91/83 (Note 9)	96	100	96
Fuel Clad O.D. (in.)	≥ 0.4040	≥ 0.3957	≥ 0.3780	≥ 0.3960	≥ 0.3940
Fuel Clad I.D. (in.)	≤ 0.3520	≤ 0.3480	≤ 0.3294	≤ 0.3560	≤ 0.3500
Fuel Pellet Dia. (in.)	≤ 0.3455	≤ 0.3420	≤ 0.3224	≤ 0.3500	≤ 0.3430
Fuel Rod Pitch (in.)	≤ 0.510	≤ 0.510	≤ 0.488	≤ 0.565	≤ 0.557
Design Active Fuel Length (in.)	≤ 150	≤ 150	≤ 150	≤ 83	≤ 83
No. of Water Rods (Note 11)	2	1 (Note 6)	5 (Note 10)	0	4
Water Rod Thickness (in.)	≥ 0.030	> 0.00	≥ 0.031	N/A	≥ 0.022
Channel Thickness (in.)	≤ 0.120	≤ 0.120	≤ 0.055	≤ 0.080	≤ 0.080

Table 1.2.11 (continued)  
BWR FUEL ASSEMBLY CHARACTERISTICS

## NOTES:

1. All dimensions are design nominal values. Maximum and minimum dimensions are specified to bound variations in design nominal values among fuel assemblies within a given array/class.
2. ZR designates any zirconium-based fuel cladding material authorized for use in a commercial power reactor.
3. Design initial uranium weight is the nominal uranium weight specified for each assembly by the fuel manufacturer or reactor user. For each BWR fuel assembly, the total uranium weight limit specified in this table may be increased up to 1.5 percent for comparison with users' fuel records to account for manufacturer tolerances.
4.  $\leq 0.635$  wt. %  $^{235}\text{U}$  and  $\leq 1.578$  wt. % total fissile plutonium ( $^{239}\text{Pu}$  and  $^{241}\text{Pu}$ ), (wt. % of total fuel weight, i.e.,  $\text{UO}_2$  plus  $\text{PuO}_2$ ).
5. This assembly class contains 74 total rods; 66 full length rods and 8 partial length rods.
6. Square, replacing nine fuel rods.
7. Variable.
8. This assembly contains 92 total fuel rods; 78 full length rods and 14 partial length rods.
9. This assembly class contains 91 total fuel rods; 83 full length rods and 8 partial length rods.
10. One diamond-shaped water rod replacing the four center fuel rods and four rectangular water rods dividing the assembly into four quadrants.
11. These rods may also be sealed at both ends and contain ZR material in lieu of water.
12. This assembly is known as "QUAD+." It has four rectangular water cross segments dividing the assembly into four quadrants.
13. For the SPC 9x9-5 fuel assembly, each fuel rod must meet either the 9x9E or the 9x9F set of limits or clad O.D., clad I.D., and pellet diameter.

Table 1.2.12

## DESIGN BASIS FUEL ASSEMBLY FOR EACH DESIGN CRITERION

<b>Criterion</b>	<b>MPC-68/68F</b>	<b>MPC-24/24E/24EF/32</b>
Reactivity	SPC 9x9-5 (Array/Class 9x9E/F)	B&W 15x15 (Array/Class 15x15F)
Shielding (Source Term)	GE 7x7	B&W 15x15
Fuel Assembly Effective Planar Thermal Conductivity	GE 11 9x9	<u>W</u> 17x17 OFA
Fuel Basket Effective Axial Thermal Conductivity	GE 7x7	<u>W</u> 14x14 OFA
MPC Density and heat Capacity	Dresden 6x6	<u>W</u> 14x14 OFA

Tables 1.2.13 and 1.2.14

INTENTIONALLY DELETED

Table 1.2.15

## NORMALIZED DISTRIBUTION BASED ON BURNUP PROFILE

<b>GENERIC FUEL DISTRIBUTION<sup>†</sup></b>			
<b>Interval</b>	<b>Axial Distance From Bottom of Active Fuel (% of Active Fuel Length)</b>	<b>PWR Fuel Normalized Distribution</b>	<b>BWR Fuel Normalized Distribution</b>
1	0% to 4-1/6%	0.5485	0.2200
2	4-1/6% to 8-1/3%	0.8477	0.7600
3	8-1/3% to 16-2/3%	1.0770	1.0350
4	16-2/3% to 33-1/3%	1.1050	1.1675
5	33-1/3% to 50%	1.0980	1.1950
6	50% to 66-2/3%	1.0790	1.1625
7	66-2/3% to 83-1/3%	1.0501	1.0725
8	83-1/3% to 91-2/3%	0.9604	0.8650
9	91-2/3% to 95-5/6%	0.7338	0.6200
10	95-5/6% to 100%	0.4670	0.2200
<b>TROJAN PLANT FUEL DISTRIBUTION<sup>††</sup></b>			
<b>Interval</b>	<b>Axial Distance From Bottom of Active Fuel (% of Active Fuel Length)</b>	<b>Normalized Distribution</b>	
1	0% to 5%	0.59	
2	5% to 10%	0.89	
3	10% to 15%	1.03	
4	15% to 20%	1.07	
5	20% to 25%	1.09	
6	25% to 45%	1.10	
7	45% to 70%	1.09	
8	70% to 75%	1.07	
9	75% to 80%	1.05	
10	80% to 85%	1.02	
11	85% to 90%	0.96	
12	90% to 95 %	0.82	
13	95% to 100%	0.56	

<sup>†</sup> References [1.2.8] and [1.2.9]

<sup>††</sup> Reference [1.2.12]

Table 1.2.16

## SUGGESTED PWR UPPER AND LOWER FUEL SPACER LENGTHS (Note 1)

Fuel Assembly Type	Assembly Length w/o NFH <sup>†</sup> (in.)	Location of Active Fuel from Bottom (in.)	Max. Active Fuel Length (in.)	Upper Fuel Spacer Length (in.)	Lower Fuel Spacer Length (in.)
CE 14x14	157	4.1	137	9.5	10
CE 16x16	176.8	4.7	150	0	0
BW 15x15	165.7	8.4	141.8	6.7	4.1
W 17x17 OFA	159.8	3.7	144	8.2	8.5
W 17x17S	159.8	3.7	144	8.2	8.5
W 17x17V5H	160.1	3.7	144	7.9	8.5
W 15x15	159.8	3.7	144	8.2	8.5
W 14x14S	159.8	3.7	145.2	9.2	7.5
W 14x14 OFA	159.8	3.7	144	8.2	8.5
Ft. Calhoun	146	6.6	128	10.25	20.25
St. Lucie 2	158.2	5.2	136.7	10.25	8.05
B&W 15x15 SS	137.1	3.873	120.5	19.25	19.25
W 15x15 SS	137.1	3.7	122	19.25	19.25
W 14x14 SS	137.1	3.7	120	19.25	19.25
Indian Point 1	137.2	17.705	101.5	18.75	20.0

Notes: 1. These fuel spacer lengths are not applicable to Trojan plant fuel. Trojan plant fuel spacer lengths are determined uniquely for the custom-designed Trojan MPC-24E/EF, as necessary, based on the presence of non-fuel hardware. They are sized to maintain the active fuel within the envelope of the neutron absorber affixed to the cell walls and allow for an approximate 2-inch gap between the fuel and the MPC lid. See Chapter 6 for discussion of potential misalignments between the active fuel and the neutron absorber.

<sup>†</sup> NFH is an abbreviation for non-fuel hardware, including control components. Fuel assemblies with control components may require shorter fuel spacers.

Table 1.2.17

## SUGGESTED BWR UPPER AND LOWER FUEL SPACER LENGTHS (Note 1)

Fuel Assembly Type	Assembly Length (in.)	Location of Active Fuel from Bottom (in.)	Max. Active Fuel Length (in.)	Upper Fuel Spacer Length (in.)	Lower Fuel Spacer Length (in.)
GE/2-3	171.2	7.3	150	4.8	0
GE/4-6	176.2	7.3	150	0	0
Dresden 1	134.4	11.2	110	18	28.0
Dresden 1 Damaged Fuel or Fuel Debris	142.1 <sup>†</sup>	11.2	110	17	16.9
LaCrosse	102.5	10.5	83	37	37.5

Notes: 1. Each user shall specify the fuel spacer lengths based on their fuel length and allowing an approximate 2-inch gap between the fuel and the MPC lid. See Chapter 6 for discussion of potential misalignments between the active fuel and the neutron absorber.

<sup>†</sup> Fuel length includes the damaged fuel container.

Table 1.2.18

SUMMARY OF HI-STAR 100 SYSTEM POST-ACCIDENT PERFORMANCE

Aspect of Post-Accident Performance	Results with Demonstrated Integrity of MPC Enclosure Vessel	Results with Postulated Gross Failure of MPC Enclosure Vessel
Containment Boundary Integrity	The overpack containment boundary is standard air leak tested to $4.3 \times 10^{-6}$ atm cm <sup>3</sup> /s (helium). Boundary is shown to withstand all hypothetical accident conditions. Therefore, there will be no detectable release of radioactive materials.	The overpack containment boundary is leak tested to $4.3 \times 10^{-6}$ atm cm <sup>3</sup> /s (helium). The overpack containment boundary is shown to withstand all hypothetical accident conditions. Therefore, the overpack containment boundary meets the accident condition leakage rates.
Maintenance of Subcritical Margins (Maximum $k_{eff}$ )	The MPC enclosure vessel is seal welded and there is no breach of the MPC. The bolted closure overpack containment boundary has been shown to prevent water immersion. Therefore, the maximum reactivity of the fuel in a dry MPC is less than 0.5.	The bolted closure overpack containment boundary has been shown to prevent water immersion. Therefore, the maximum reactivity of the fuel in a dry MPC is less than 0.5. Assuming the MPC is fully flooded with water, the reactivity is shown to be below the regulatory requirement of 0.95 including uncertainties and bias.
Adequate Shielding	The MPC enclosure vessel boundary has no effect on the dose rates of the HI-STAR 100 System.	Failure of the MPC enclosure vessel to maintain a release boundary has no effect on the dose rates of the HI-STAR 100 System.
Adequate Heat Rejection (Peak Fuel Cladding Temperature)	The MPC enclosure vessel maintains the helium and the peak fuel cladding temperature is demonstrated to remain below 800°F in the post-fire hypothetical accident condition.	<p>Assuming the MPC internal helium fill pressure is released into the overpack containment, the pressure within the small annulus would rise to equalize with the MPC internal pressure. There would be a corresponding slight pressure decrease in the MPC enclosure vessel. The comparatively small volume of the annulus and pressure differential results in the slight pressure change. This will have a negligibly small effect on the peak fuel cladding temperature.</p> <p>The overpack containment boundary is demonstrated to withstand all hypothetical accident conditions. Therefore, there is no credible mechanism for the release of the helium.</p>

Tables 1.2.19 and 1.2.20  
INTENTIONALLY DELETED

Table 1.2.21

## DESIGN CHARACTERISTICS FOR THORIA RODS IN D-1 THORIA ROD CANISTERS

PARAMETER	MPC-68 or MPC-68F
Cladding Type	ZR
Composition	98.2 wt.% ThO <sub>2</sub> , 1.8 wt.% UO <sub>2</sub> with an enrichment of 93.5 wt. % <sup>235</sup> U
Number of Rods Per Thoria Canister	≤ 18
Decay Heat Per Thoria Canister	≤ 115 watts
Post-Irradiation Fuel Cooling Time and Average Burnup Per Thoria Canister	Cooling time ≥ 18 years and average burnup ≤ 16,000 MWD/MTIHM
Initial Heavy Metal Weight	≤ 27 kg/canister
Fuel Cladding O.D.	≥ 0.412 inches
Fuel Cladding I.D.	≤ 0.362 inches
Fuel Pellet O.D.	≤ 0.358 inches
Active Fuel Length	≤ 111 inches
Canister Weight	≤ 550 lbs., including Thoria Rods
Canister Material	Type 304 SS

Table 1.2.22

## LIMITS FOR MATERIAL TO BE TRANSPORTED IN MPC-24

PARAMETER	VALUE
Fuel Type	Uranium oxide, PWR intact fuel assemblies meeting the limits in Table 1.2.10 for the applicable array/class
Cladding Type	ZR or Stainless Steel (SS) as specified in Table 1.2.10 for the applicable array/class
Maximum Initial Enrichment	As specified in Table 1.2.10 for the applicable array/class
Post-irradiation Cooling Time, Average Burnup, and Minimum Initial Enrichment per Assembly	ZR clad: As specified in Table 1.2.28 or Table 1.2.29, as applicable SS clad: As specified in Table 1.2.30
Decay Heat Per Assembly	ZR clad: $\leq 833$ Watts SS clad: $\leq 488$ Watts
Fuel Assembly Length	$\leq 176.8$ in. (nominal design)
Fuel Assembly Width	$\leq 8.54$ in. (nominal design)
Fuel Assembly Weight	$\leq 1,680$ lbs
Other Limitations	<ul style="list-style-type: none"> <li>▪ Quantity is limited to up to 24 PWR intact fuel assemblies.</li> <li>▪ Non-fuel hardware and neutron sources not permitted.</li> <li>▪ Damaged fuel assemblies and fuel debris not permitted.</li> <li>▪ Trojan plant fuel not permitted.</li> </ul>

Table 1.2.23

LIMITS FOR MATERIAL TO BE TRANSPORTED IN MPC-68

PARAMETER	VALUE (Note 1)			
Fuel Type(s)	Uranium oxide, BWR intact fuel assemblies meeting the limits in Table 1.2.11 for the applicable array/class, with or without Zircaloy channels	Uranium oxide, BWR damaged fuel assemblies meeting the limits in Table 1.2.11 for array/class 6x6A, 6x6C, 7x7A, or 8x8A, with or without Zircaloy channels, placed in Damaged Fuel Containers (DFCs)	Mixed Oxide (MOX) BWR intact fuel assemblies meeting the limits in Table 1.2.11 for array/class 6x6B, with or without Zircaloy channels	Mixed Oxide (MOX) BWR damaged fuel assemblies meeting the limits in Table 1.2.11 for array/class 6x6B, with or without Zircaloy channels, placed in Damaged Fuel Containers (DFCs)
Cladding Type	ZR or Stainless Steel (SS) as specified in Table 1.2.11 for the applicable array/class	ZR	ZR	ZR
Maximum Initial Planar-Average and Rod Enrichment	As specified in Table 1.2.11 for the applicable array/class	As specified in Table 1.2.11 for the applicable array/class	As specified in Table 1.2.11 for array/class 6x6B	As specified in Table 1.2.11 for array/class 6x6B
Post-irradiation Cooling Time, Average Burnup, and Minimum Initial Enrichment per Assembly	ZR clad: As specified in Table 1.2.31 except as provided in Notes 2 and 3 SS clad: Note 4	Cooling time $\geq 18$ years, average burnup $\leq 30,000$ MWD/MTU, and minimum initial enrichment $\geq 1.45$ wt. % $^{235}\text{U}$ .	Cooling time $\geq 18$ years, average burnup $\leq 30,000$ MWD/MTIHM, and minimum initial enrichment $\geq 1.8$ wt. % $^{235}\text{U}$ .	Cooling time $\geq 18$ years, average burnup $\leq 30,000$ MWD/MTIHM, and minimum initial enrichment $\geq 1.8$ wt. % $^{235}\text{U}$ .
Decay Heat Per Assembly	ZR clad: $\leq 272$ Watts (Note 5)  SS clad: $\leq 83$ Watts	$\leq 115$ Watts	$\leq 115$ Watts	$\leq 115$ Watts

Table 1.2.23 (cont'd)

## LIMITS FOR MATERIAL TO BE TRANSPORTED IN MPC-68

PARAMETER	VALUE (Note 1)			
Fuel Assembly Length	≤ 176.2 in. (nominal design)	≤ 135.0 in. (nominal design)	≤ 135.0 in. (nominal design)	≤ 135.0 in. (nominal design)
Fuel Assembly Width	≤ 5.85 in. (nominal design)	≤ 4.70 in. (nominal design)	≤ 4.70 in. (nominal design)	≤ 4.70 in. (nominal design)
Fuel Assembly Weight	≤ 700 lbs (including channels)	≤ 550 lbs, (including channels and DFC)	≤ 400 lbs, (including channels)	≤ 550 lbs, (including channels and DFC)
Quantity per MPC	Up to 68 BWR intact fuel assemblies	Up to 68 BWR damaged and/or intact fuel assemblies	Up to 68 BWR intact fuel assemblies	Up to 68 BWR damaged and/or intact fuel assemblies
Other Limitations	<ul style="list-style-type: none"> <li>▪ Quantity is limited to up to one (1) Dresden Unit 1 thoria rod canister meeting the specifications listed in Table 1.2.21 plus any combination of Dresden Unit 1 damaged fuel assemblies in DFCs and intact fuel assemblies up to a total of 68.</li> <li>▪ Stainless steel channels are not permitted.</li> <li>▪ Fuel debris is not permitted.</li> <li>▪ Dresden Unit 1 fuel assemblies with one antimony-beryllium neutron source are permitted. The antimony-beryllium neutron source material shall be in a water rod location.</li> </ul>			

## Notes:

1. A fuel assembly must meet the requirements of any one column and the other limitations to be authorized for transportation.
2. Array/class 6x6A, 6x6C, 7x7A, and 8x8A fuel assemblies shall have a cooling time  $\geq 18$  years, an average burnup  $\leq 30,000$  MWD/MTU, and a minimum initial enrichment  $\geq 1.45$  wt. %  $^{235}\text{U}$ .
3. Array/class 8x8F fuel assemblies shall have a cooling time  $\geq 10$  years, an average burnup  $\leq 27,500$  MWD/MTU, and a minimum initial enrichment  $\geq 2.4$  wt. %  $^{235}\text{U}$ .
4. SS-clad fuel assemblies shall have a cooling time  $\geq 16$  years, an average burnup  $\leq 22,500$  MWD/MTU, and a minimum initial enrichment  $\geq 3.5$  wt. %  $^{235}\text{U}$ .
5. Array/class 8x8F fuel assemblies shall have a decay heat  $\leq 183.5$  Watts.

Table 1.2.24

## LIMITS FOR MATERIAL TO BE TRANSPORTED IN MPC-68F

PARAMETER	VALUE (Notes 1 and 2)			
Fuel Type(s)	Uranium oxide, BWR intact fuel assemblies meeting the limits in Table 1.2.11 for array/class 6x6A, 6x6C, 7x7A, or 8x8A, with or without Zircaloy channels	Uranium oxide, BWR damaged fuel assemblies or fuel debris meeting the limits in Table 1.2.11 for array/class 6x6A, 6x6C, 7x7A, or 8x8A, with or without Zircaloy channels, placed in Damaged Fuel Containers(DFCs)	Mixed Oxide (MOX) BWR intact fuel assemblies meeting the limits in Table 1.2.11 for array/class 6x6B, with or without Zircaloy channels	Mixed Oxide (MOX) BWR damaged fuel assemblies or fuel debris meeting the limits in Table 1.2.11 for array/class 6x6B, with or without Zircaloy channels, placed in Damaged Fuel Containers (DFCs))
Cladding Type	ZR	ZR	ZR	ZR
Maximum Initial Planar-Average and Rod Enrichment	As specified in Table 1.2.11 for the applicable array/class	As specified in Table 1.2.11 for the applicable array/class	As specified in Table 1.2.11 for array/class 6x6B	As specified in Table 1.2.11 for array/class 6x6B
Post-irradiation Cooling Time, Average Burnup, and Minimum Initial Enrichment per Assembly	Cooling time $\geq 18$ years, average burnup $\leq 30,000$ MWD/MTU, and minimum initial enrichment $\geq 1.45$ wt. % $^{235}\text{U}$ .	Cooling time $\geq 18$ years, average burnup $\leq 30,000$ MWD/MTU, and minimum initial enrichment $\geq 1.45$ wt. % $^{235}\text{U}$ .	Cooling time $\geq 18$ years, average burnup $\leq 30,000$ MWD/MTIHM, and minimum initial enrichment $\geq 1.8$ wt. % $^{235}\text{U}$ .	Cooling time $\geq 18$ years, average burnup $\leq 30,000$ MWD/MTIHM, and minimum initial enrichment $\geq 1.8$ wt. % $^{235}\text{U}$ .
Decay Heat Per Assembly	$\leq 115$ Watts	$\leq 115$ Watts	$\leq 115$ Watts	$\leq 115$ Watts

Table 1.2.24 (cont'd)

LIMITS FOR MATERIAL TO BE TRANSPORTED IN MPC-68F

PARAMETER	VALUE (Note 1)			
Fuel Assembly Length	≤ 135.0 in. (nominal design)	≤ 135.0 in. (nominal design)	≤ 135.0 in. (nominal design)	≤ 135.0 in. (nominal design)
Fuel Assembly Width	≤ 4.70 in. (nominal design)	≤ 4.70 in. (nominal design)	≤ 4.70 in. (nominal design)	≤ 4.70 in. (nominal design)
Fuel Assembly Weight	≤ 400 lbs (including channels)	≤ 550 lbs (including channels and DFC)	≤ 400 lbs (including channels)	≤ 550 lbs (including channels and DFC)
Other Limitations	<ul style="list-style-type: none"> <li>▪ Quantity is limited to up to four (4) DFCs containing Dresden Unit 1 uranium oxide or MOX fuel debris. The remaining fuel storage locations may be filled with array/class 6x6A, 6x6B, 6x6C, 7x7A, and 8x8A fuel assemblies of the following type, as applicable:                             <ul style="list-style-type: none"> <li>- uranium oxide BWR intact fuel assemblies</li> <li>- MOX BWR intact fuel assemblies</li> <li>- uranium oxide BWR damaged fuel assemblies in DFCs</li> <li>- MOX BWR damaged fuel assemblies in DFCs</li> <li>- up to one (1) Dresden Unit 1 thoria rod canister meeting the specifications listed in Table 1.2.21</li> </ul> </li> <li>▪ Stainless steel channels are not permitted.</li> <li>▪ Dresden Unit 1 fuel assemblies with one antimony-beryllium neutron source are permitted. The antimony-beryllium neutron source material shall be in a water rod location.</li> </ul>			

Notes:

1. A fuel assembly must meet the requirements of any one column and the other limitations to be authorized for transportation.
2. Only fuel from Dresden Unit 1 is permitted for transportation in the MPC-68F.

Table 1.2.25

## LIMITS FOR MATERIAL TO BE TRANSPORTED IN MPC-24E

PARAMETER	VALUE (Note 1)	
Fuel Type	Uranium oxide PWR intact fuel assemblies meeting the limits in Table 1.2.10 for the applicable array/class	Trojan plant damaged fuel meeting the limits in Table 1.2.10 for array/class 17x17B, placed in a Holtec Damaged Fuel Container (DFC) designed for Trojan plant fuel or a Trojan Failed Fuel Can (FFC)
Cladding Type	ZR or Stainless Steel (SS) assemblies as specified in Table 1.2.10 for the applicable array/class	ZR
Maximum Initial Enrichment	As specified in Table 1.2.10 for the applicable array/class	3.7 wt. % <sup>235</sup> U
Post-irradiation Cooling Time, Average Burnup, and Minimum Initial Enrichment per Assembly (except Trojan plant fuel and non-fuel hardware)	ZR clad: As specified in Table 1.2.28 or 1.2.29, as applicable SS clad: As specified in Table 1.2.30	Not applicable
Post-irradiation Cooling Time, Average Burnup, and Minimum Initial Enrichment per Assembly for Trojan plant fuel	As specified in Table 1.2.35	As specified in Table 1.2.35
Post-irradiation Cooling Time and Burnup for Trojan plant Non-fuel Hardware and Neutron Sources	As specified in Table 1.2.36	Not applicable
Decay Heat Per Assembly (except for Trojan plant fuel)	ZR clad: ≤ 833 Watts SS clad: ≤ 488 Watts	Not applicable
Decay heat per Assembly for Trojan plant fuel	≤ 725 Watts	≤ 725 Watts

Table 1.2.25 (cont'd)

LIMITS FOR MATERIAL TO BE TRANSPORTED IN MPC-24E

PARAMETER	VALUE (Note 1)	
Fuel Assembly Length	≤ 176.8 in. (nominal design)	≤ 169.3 in. (nominal design)
Fuel Assembly Width	≤ 8.54 in. (nominal design)	≤ 8.43 in. (nominal design)
Fuel Assembly Weight	≤ 1680 lbs (including non-fuel hardware)	≤ 1680 lbs (including DFC or Failed Fuel Can)
Other Limitations	<ul style="list-style-type: none"> <li>▪ Quantity per MPC: up to 24 PWR intact fuel assemblies. For Trojan plant fuel only, up to four (4) damaged fuel assemblies may be stored in fuel storage locations 3, 6, 19, and/or 22. The remaining fuel storage locations may be filled with Trojan plant intact fuel assemblies.</li> <li>▪ Trojan plant fuel must be transported in the custom-designed Trojan MPCs with the MPC spacer installed (see Figure 1.1.5). Fuel from other plants is not permitted to be transported in the Trojan MPCs.</li> <li>▪ Except for Trojan plant fuel, the fuel assemblies shall not contain non-fuel hardware. Trojan intact fuel assemblies containing non-fuel hardware may be transported in any fuel storage location.</li> <li>▪ Trojan plant damaged fuel assemblies must be transported in a Holtec DFC for Trojan plant fuel or a Trojan plant FFC.</li> <li>▪ One (1) Trojan plant Sb-Be and/or two (2) Cf neutron sources, each in a Trojan plant intact fuel assembly may be transported in any one MPC. Each neutron source may be transported in any fuel storage location.</li> <li>▪ Fuel debris is not authorized for transportation in the MPC-24E.</li> <li>▪ Trojan plant non-fuel hardware and neutron sources may not be transported in the same fuel storage location with damaged fuel assemblies.</li> </ul>	

Notes:

1. A fuel assembly must meet the requirements of any one column and the other limitations to be authorized for transportation.

Table 1.2.26

LIMITS FOR MATERIAL TO BE TRANSPORTED IN MPC-24EF

PARAMETER	VALUE (Note 1)		
Fuel Type	Uranium oxide PWR intact fuel assemblies meeting the limits in Table 1.2.10 for the applicable array/class	Trojan plant damaged fuel meeting the limits in Table 1.2.10 for array/class 17x17B, placed in a Holtec Damaged Fuel Container (DFC) designed for Trojan plant fuel or a Trojan Failed Fuel Can (FFC)	Trojan plant Fuel Debris Process Can Capsules and/or Trojan plant fuel assemblies classified as fuel debris, for which the original fuel assemblies meet the applicable criteria in Table 1.2.10 for array/class 17x17B, placed in a Holtec Damaged Fuel Container (DFC) designed for Trojan plant fuel or a Trojan Failed Fuel Can (FFC)
Cladding Type	ZR or Stainless Steel (SS) assemblies as specified in Table 1.2.10 for the applicable array/class	ZR	ZR
Maximum Initial Enrichment	As specified in Table 1.2.10 for the applicable array/class	$\leq 3.7$ wt. % <sup>235</sup> U	$\leq 3.7$ wt. % <sup>235</sup> U
Post-irradiation Cooling Time, Average Burnup, and Minimum Initial Enrichment per Assembly (except Trojan plant fuel and non-fuel hardware)	ZR clad: As specified in Table 1.2.28 or 1.2.29, as applicable SS clad: As specified in Table 1.2.30	Not applicable	Not applicable
Post-irradiation Cooling Time, Average Burnup, and Minimum Initial Enrichment per Assembly for Trojan plant fuel	As specified in Table 1.2.35	As specified in Table 1.2.35	As specified in Table 1.2.35

Table 1.2.26 (cont'd)

## LIMITS FOR MATERIAL TO BE TRANSPORTED IN MPC-24EF

PARAMETER	VALUE (Note 1)		
Post-irradiation Cooling Time and Burnup for Trojan plant Non-fuel Hardware and Neutron Sources	As specified in Table 1.2.36	As specified in Table 1.2.36	As specified in Table 1.2.36
Decay Heat Per Assembly (except for Trojan plant fuel)	ZR clad: $\leq 833$ Watts SS clad: $\leq 488$ Watts	Not applicable	Not applicable
Decay heat per Assembly for Trojan plant fuel	$\leq 725$ Watts	$\leq 725$ Watts	$\leq 725$ Watts
Fuel Assembly Length	$\leq 176.8$ in. (nominal design)	$\leq 169.3$ in. (nominal design)	$\leq 169.3$ in. (nominal design)
Fuel Assembly Width	$\leq 8.54$ in. (nominal design)	$\leq 8.43$ in. (nominal design)	$\leq 8.43$ in. (nominal design)
Fuel Assembly Weight	$\leq 1680$ lbs (including non-fuel hardware)	$\leq 1680$ lbs (including DFC or Failed Fuel Can)	$\leq 1680$ lbs (including DFC or Failed Fuel Can)

Table 1.2.26 (cont'd)

LIMITS FOR MATERIAL TO BE TRANSPORTED IN MPC-24EF

<p>Other Limitations</p>	<ul style="list-style-type: none"> <li>▪ Quantity per MPC: Up to 24 PWR intact fuel assemblies. For Trojan plant fuel only, up to four (4) damaged fuel assemblies, fuel assemblies classified as fuel debris, and/or Trojan Fuel Debris Process Can Capsules may be stored in fuel storage locations 3, 6, 19, and/or 22. The remaining fuel storage locations may be filled with Trojan plant intact fuel assemblies.</li> <li>▪ Trojan plant fuel must be transported in the custom-designed Trojan MPCs with the MPC spacer installed (see Figure 1.1.5). Fuel from other plants is not permitted to be transported in the Trojan MPCs.</li> <li>▪ Except for Trojan plant fuel, the fuel assemblies shall not contain non-fuel hardware or neutron sources. Trojan intact fuel assemblies containing non-fuel hardware may be transported in any fuel storage location.</li> <li>▪ Trojan plant damaged fuel assemblies, fuel assemblies classified as fuel debris, and Fuel Debris Process Can Capsules must be transported in a Trojan Failed Fuel Can or a Holtec DFC for Trojan plant fuel.</li> <li>▪ One (1) Trojan plant Sb-Be and/or two (2) Cf neutron sources, each in a Trojan plant intact fuel assembly may be transported in any one MPC. Each neutron source may be transported in any fuel storage location.</li> </ul>
--------------------------	--

Notes:

1. A fuel assembly must meet the requirements of any one column and the other limitations to be authorized for transportation.

Table 1.2.27

## LIMITS FOR MATERIAL TO BE TRANSPORTED IN MPC-32

PARAMETER	VALUE
Fuel Type	Uranium oxide, PWR intact fuel assemblies meeting the limits in Table 1.2.10 for array/classes 15x15D, E, F, and H and 17x17A, B, and C
Cladding Type	ZR
Maximum Initial Enrichment	As specified in Table 1.2.34 for the applicable array/class
Post-irradiation Cooling Time, Average Burnup, and Minimum Initial Enrichment per Assembly	As specified in Table 1.2.32 or Table 1.2.33, as applicable
Decay Heat Per Assembly	$\leq 625$ Watts
Minimum Cooling time	5 years
Minimum Burnup per Assembly	As specified in Table 1.2.34 for the applicable array/class
Fuel Assembly Length	$\leq 176.8$ in. (nominal design)
Fuel Assembly Width	$\leq 8.54$ in. (nominal design)
Fuel Assembly Weight	$\leq 1,680$ lbs
Operating Parameters During Irradiation of the Assembly (See Subsection 1.2.3.7.1)	
Average in-core soluble boron concentration	$\leq 1000$ ppmb
Average Moderator Temperature	$\leq 601$ K for array/classes 15x15D, E, F and H $\leq 610$ K for array/classes 17x17A, B and C
Average Specific Power	$\leq 47.36$ kW/kg-U for array/classes 15x15D, E, F and H $\leq 61.61$ kW/kg-U for array/classes 17x17A, B and C

Other Limitations	<ul style="list-style-type: none"><li>▪ Quantity is limited to up to 32 PWR intact fuel assemblies in the above-specified array/classes only.</li><li>▪ Non-fuel hardware and neutron sources not permitted.</li><li>▪ Damaged fuel assemblies and fuel debris not permitted.</li><li>▪ Trojan plant fuel not permitted.</li></ul>
-------------------	--

Table 1.2.28

FUEL ASSEMBLY COOLING, AVERAGE BURNUP, AND MINIMUM ENRICHMENT  
LIMITS FOR TRANSPORTATION IN MPC-24/24E/24EF; PWR FUEL WITH ZR  
CLADDING AND WITH NON-ZIRCALOY IN-CORE GRID SPACERS

ASSEMBLY POST-IRRADIATION COOLING TIME (years)	ASSEMBLY BURNUP (MWD/MTU)	ASSEMBLY ENRICHMENT (wt. % <sup>235</sup> U)
≥ 9	≤ 24,500	≥ 2.3
≥ 11	≤ 29,500	≥ 2.6
≥ 13	≤ 34,500	≥ 2.9
≥ 15	≤ 39,500	≥ 3.2
≥ 18	≤ 44,500	≥ 3.4

Table 1.2.29

FUEL ASSEMBLY COOLING, AVERAGE BURNUP, AND MINIMUM ENRICHMENT  
LIMITS FOR TRANSPORTATION IN MPC-24/24E/24EF; PWR FUEL WITH ZR  
CLADDING AND WITH ZIRCALOY IN-CORE GRID SPACERS

ASSEMBLY POST-IRRADIATION COOLING TIME (years)	ASSEMBLY BURNUP (MWD/MTU)	ASSEMBLY ENRICHMENT (wt. % <sup>235</sup> U)
≥ 6	≤ 24,500	≥ 2.3
≥ 7	≤ 29,500	≥ 2.6
≥ 9	≤ 34,500	≥ 2.9
≥ 11	≤ 39,500	≥ 3.2
≥ 14	≤ 44,500	≥ 3.4

Table 1.2.30

FUEL ASSEMBLY COOLING, AVERAGE BURNUP, AND MINIMUM ENRICHMENT  
LIMITS FOR TRANSPORTATION IN MPC-24/24E/24EF; PWR FUEL WITH  
STAINLESS STEEL CLADDING

<b>ASSEMBLY POST-IRRADIATION COOLING TIME (years)</b>	<b>ASSEMBLY BURNUP (MWD/MTU)</b>	<b>ASSEMBLY ENRICHMENT (wt. % <sup>235</sup>U)</b>
$\geq 19$	$\leq 30,000$	$\geq 3.1$
$\geq 24$	$\leq 40,000$	$\geq 3.1$

Table 1.2.31

FUEL ASSEMBLY COOLING, AVERAGE BURNUP, AND MINIMUM ENRICHMENT  
LIMITS FOR TRANSPORTATION IN MPC-68

ASSEMBLY POST-IRRADIATION COOLING TIME (years)	ASSEMBLY BURNUP (MWD/MTU)	ASSEMBLY ENRICHMENT (wt. % <sup>235</sup> U)
≥ 5	≤ 10,000	≥ 0.7
≥ 7	≤ 20,000	≥ 1.35
≥ 8	≤ 24,500	≥ 2.1
≥ 9	≤ 29,500	≥ 2.4
≥ 11	≤ 34,500	≥ 2.6
≥ 14	≤ 39,500	≥ 2.9
≥ 19	≤ 44,500	≥ 3.0

Table 1.2.32

FUEL ASSEMBLY COOLING, AVERAGE BURNUP, AND MINIMUM ENRICHMENT LIMITS FOR TRANSPORTATION IN MPC-32; PWR FUEL WITH ZR CLADDING AND WITH NON-ZIRCALOY IN-CORE GRID SPACERS

<b>ASSEMBLY POST-IRRADIATION COOLING TIME (years)</b>	<b>ASSEMBLY BURNUP (MWD/MTU)</b>	<b>ASSEMBLY ENRICHMENT (wt. % <sup>235</sup>U)</b>
≥ 12	≤ 24,500	≥ 2.3
≥ 14	≤ 29,500	≥ 2.6
≥ 16	≤ 34,500	≥ 2.9
≥ 19	≤ 39,500	≥ 3.2
≥ 20	≤ 42,500	≥ 3.4

Table 1.2.33

FUEL ASSEMBLY COOLING, AVERAGE BURNUP, AND MINIMUM ENRICHMENT  
LIMITS FOR TRANSPORTATION IN MPC-32; PWR FUEL WITH ZR CLADDING  
AND WITH ZIRCALOY IN-CORE GRID SPACERS

ASSEMBLY POST-IRRADIATION COOLING TIME (years)	ASSEMBLY BURNUP (MWD/MTU)	ASSEMBLY ENRICHMENT (wt. % <sup>235</sup> U)
≥ 8	≤ 24,500	≥ 2.3
≥ 9	≤ 29,500	≥ 2.6
≥ 12	≤ 34,500	≥ 2.9
≥ 14	≤ 39,500	≥ 3.2
≥ 19	≤ 44,500	≥ 3.4

Table 1.2.34

FUEL ASSEMBLY MAXIMUM ENRICHMENT AND MINIMUM BURNUP  
REQUIREMENTS FOR TRANSPORTATION IN MPC-32

FUEL ASSEMBLY ARRAY/CLASS	Configuration (Note 2)	Maximum Enrichment (wt% <sup>235</sup> U)	MINIMUM BURNUP (B) AS A FUNCTION OF INITIAL ENRICHMENT (E) (Note 1)  (GWD/MTU)
15x15D, E, F, H	A	4.65	$B = +(1.6733) * E^3 - (18.72) * E^2$ $+ (80.5967) * E - 88.3$
	B	4.38	$B = +(2.175) * E^3 - (23.355) * E^2$ $+ (94.77) * E - 99.95$
	C	4.48	$B = +(1.9517) * E^3 - (21.45) * E^2$ $+ (89.1783) * E - 94.6$
	D	4.45	$B = +(1.93) * E^3 - (21.095) * E^2$ $+ (87.785) * E - 93.06$
17x17A, B, C	A	4.49	$B = +(1.08) * E^3 - (12.25) * E^2$ $+ (60.13) * E - 70.86$
	B	4.04	$B = +(1.1) * E^3 - (11.56) * E^2$ $+ (56.6) * E - 62.59$
	C	4.28	$B = +(1.36) * E^3 - (14.83) * E^2$ $+ (67.27) * E - 72.93$
	D	4.16	$B = +(1.4917) * E^3 - (16.26) * E^2$ $+ (72.9883) * E - 79.7$

## Notes:

1. E = Initial enrichment, i.e., for 4.05wt. %, E = 4.05.
2. See Table 1.2.37

Table 1.2.35

TROJAN PLANT FUEL ASSEMBLY COOLING, AVERAGE BURNUP, AND MINIMUM  
ENRICHMENT LIMITS (Note 1)

Post-irradiation Cooling Time (years)	Assembly Burnup (MWD/MTU)	Assembly Minimum Enrichment (wt. % <sup>235</sup> U)
≥ 16	≤ 42,000	≥ 3.09
≥ 16	≤ 37,500	≥ 2.6
≥ 16	≤ 30,000	≥ 2.1

## Notes:

1. Each fuel assembly must only meet one set of limits (i.e., one row).

Table 1.2.36

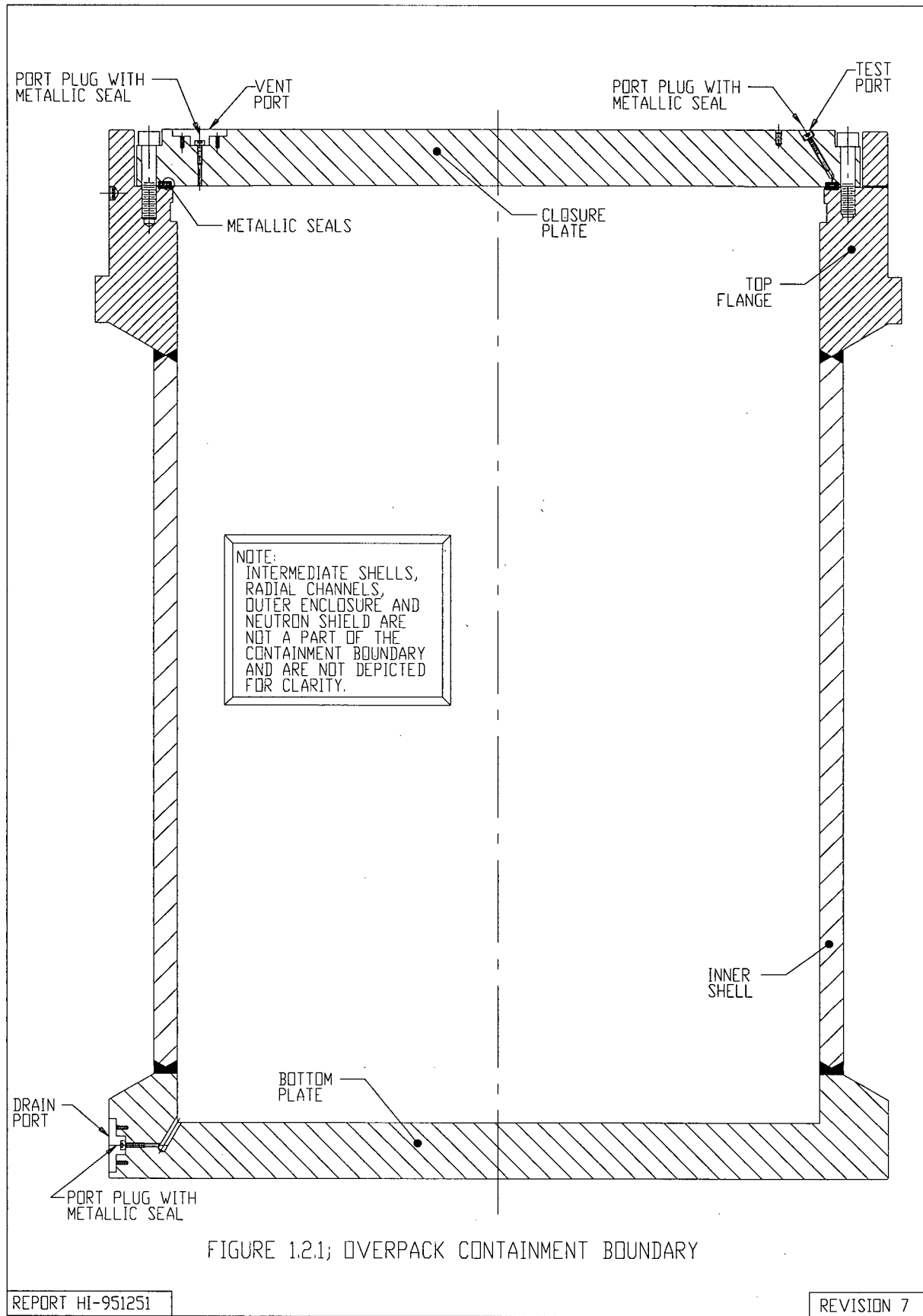
TROJAN PLANT NON-FUEL HARDWARE AND NEUTRON SOURCE COOLING AND  
BURNUP LIMITS

Type Of Hardware or Neutron Source	Burnup (MWD/MTU)	Post-irradiation Cooling Time (years)
BPRAs	$\leq 15,998$	$\geq 24$
TPDs	$\leq 118,674$	$\geq 11$
RCCAs	$\leq 125,515$	$\geq 9$
Cf neutron source	$\leq 15,998$	$\geq 24$
Sb-Be neutron source with 4 source rods, 16 burnable poison rods, and 4 thimble plug rods	$\leq 45,361$	$\geq 19$
Sb-Be neutron source with 4 source rods and 20 thimble plug rods	$\leq 88,547$	$\geq 9$

Table 1.2.37

## LOADING CONFIGURATIONS FOR THE MPC-32

Configuration	Assembly Specifications
A	<ul style="list-style-type: none"> <li>○ Assemblies that have not been located in any cycle under a control rod bank that was permitted to be inserted during full power operation (per plant operating procedures); or</li> <li>○ Assemblies that have been located under a control rod bank that was permitted to be inserted during full power operation (per plant operating procedures), but where it can be demonstrated, based on operating records, that the insertion never exceeded 8 inches from the top of the active length during full power operation.</li> </ul>
B	<ul style="list-style-type: none"> <li>○ Of the 32 assemblies in a basket, up to 8 assemblies can be from core locations where they were located under a control rod bank, that was permitted to be inserted more than 8 inches during full power operation. There is no limit on the duration (in terms of burnup) under this bank.</li> <li>○ The remaining assemblies in the basket must satisfy the same conditions as specified for configuration A.</li> </ul>
C	<ul style="list-style-type: none"> <li>○ Of the 32 assemblies in a basket, up to 8 assemblies can be from core locations where they were located under a control rod bank, that was permitted to be inserted more than 8 inches during full power operation. Location under such a control rod bank is limited to 20 GWd/mtU of the assembly.</li> <li>○ The remaining assemblies in the basket must satisfy the same conditions as specified for configuration A.</li> </ul>
D	<ul style="list-style-type: none"> <li>○ Of the 32 assemblies in a basket, up to 8 assemblies can be from core locations where they were located under a control rod bank, that was permitted to be inserted more than 8 inches during full power operation. Location under such a control rod bank is limited to 30 GWd/mtU of the assembly.</li> <li>○ The remaining assemblies in the basket must satisfy the same conditions as specified for configuration A.</li> </ul>



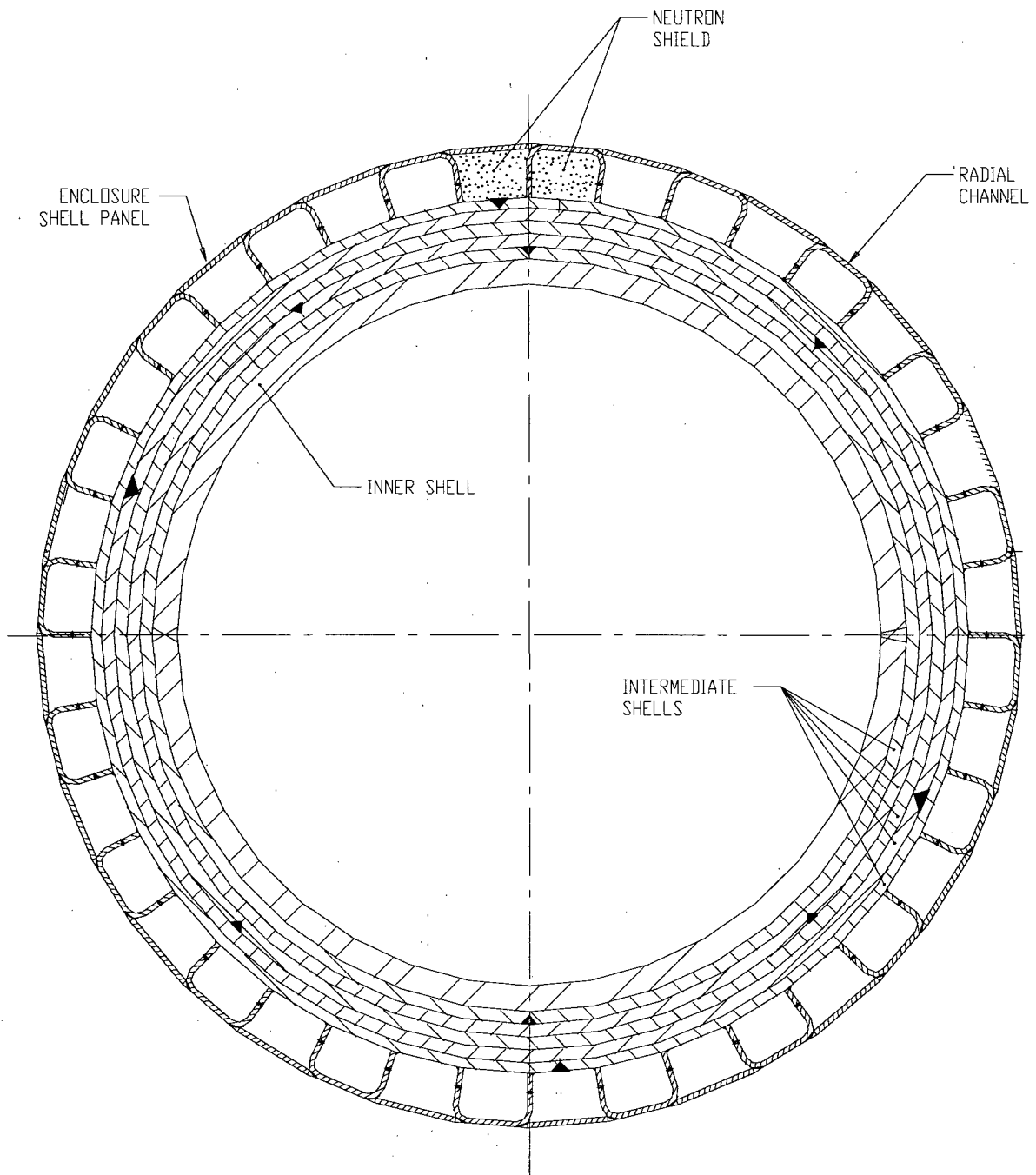


FIGURE 1.2.2; OVERPACK MID-PLANE CROSS SECTION

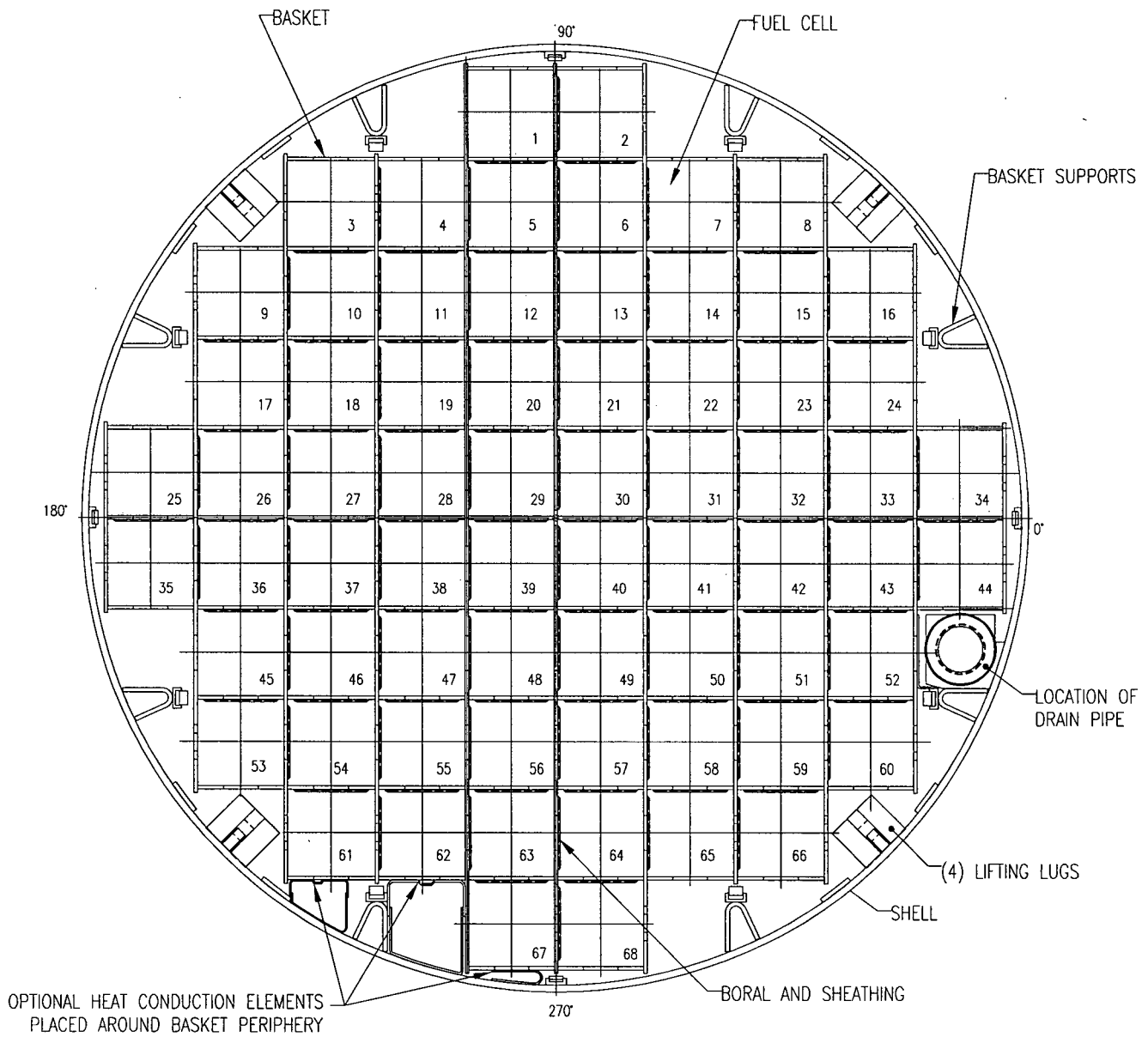


FIGURE 1.2.3; MPC-68/68F CROSS SECTION VIEW

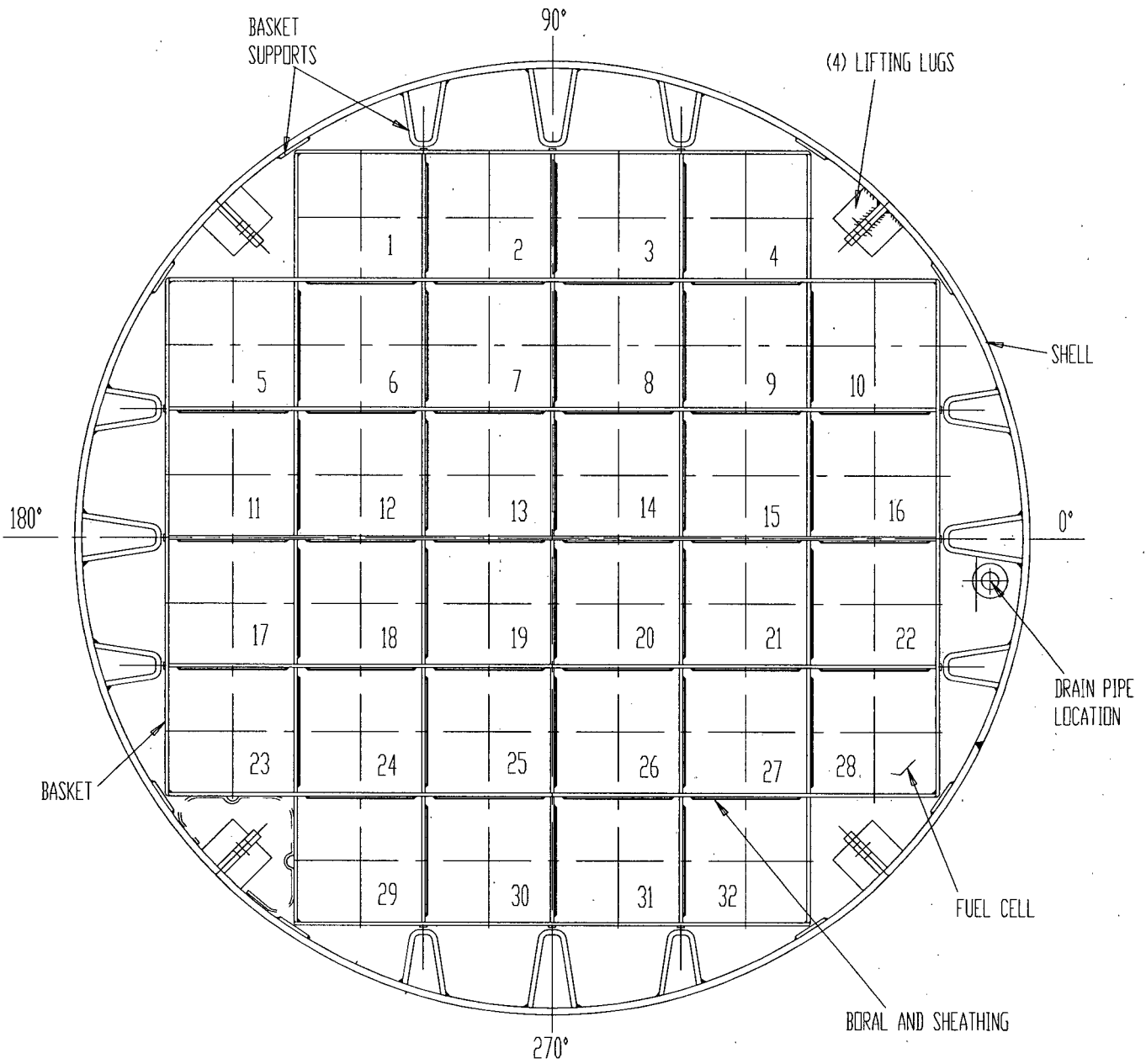


FIGURE 1.2.4; MPC-32 CROSS SECTION VIEW

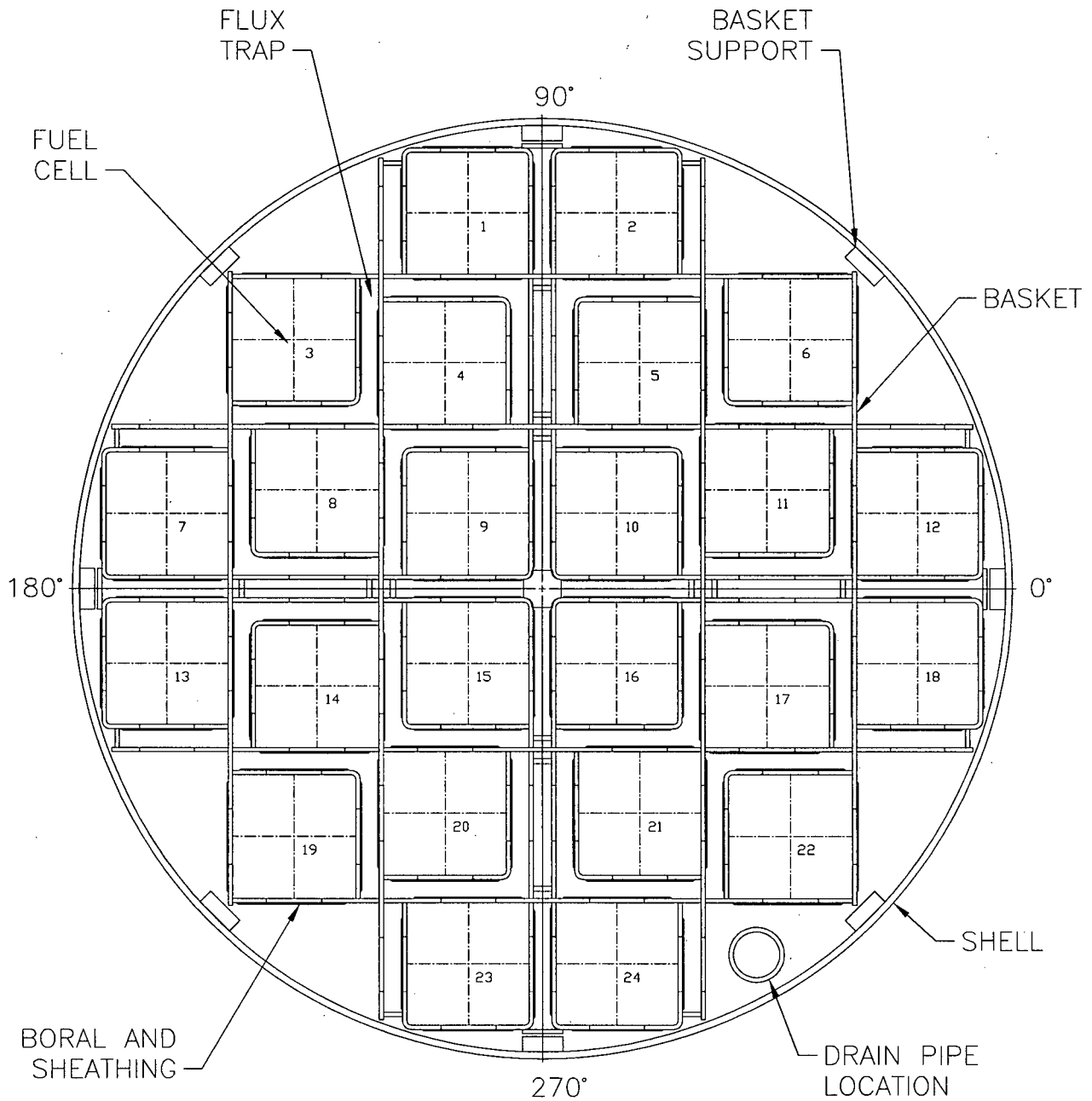


FIGURE 1.2.5; MPC-24/E/EF CROSS SECTION VIEW

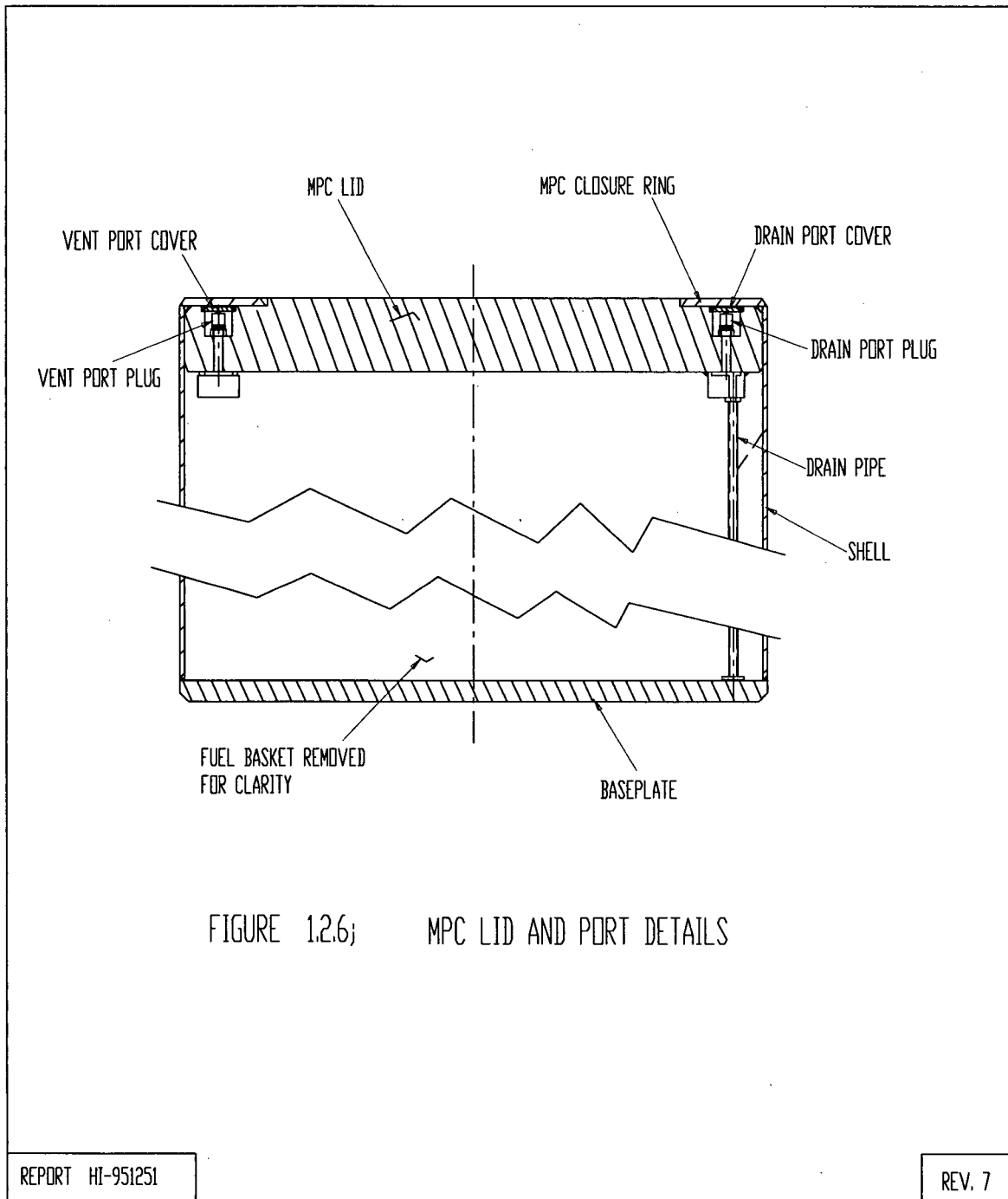
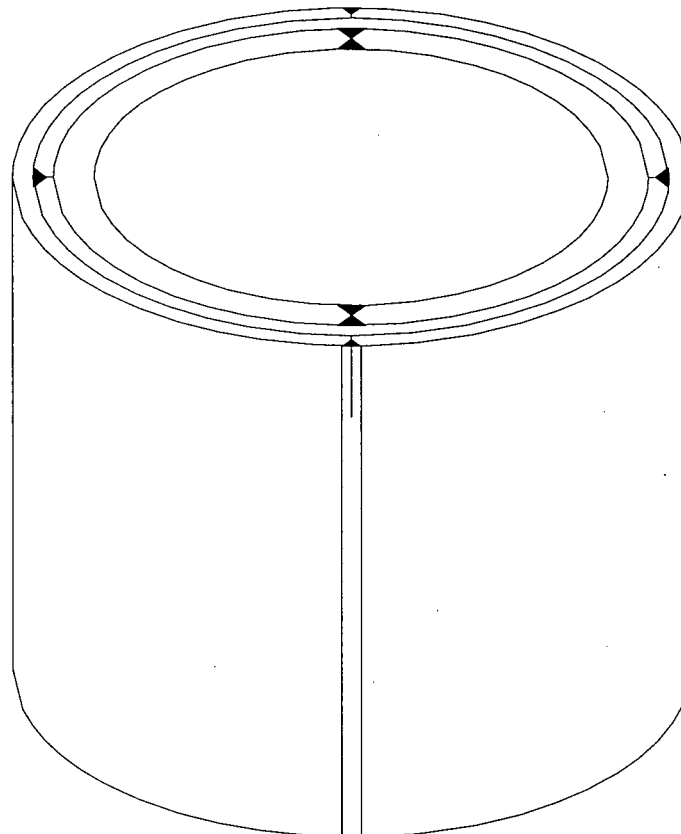


FIGURE 1.2.6; MPC LID AND PORT DETAILS

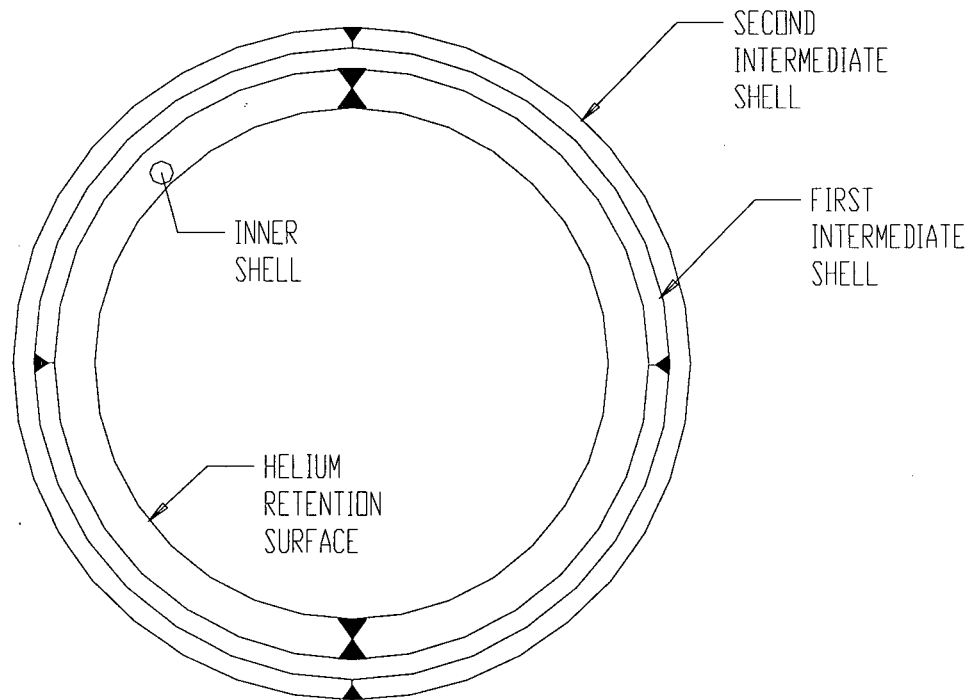
REPORT HI-951251

REV. 7

G:\SAR DOCUMENTS\HI-STAR SAR\FIGURES\REVISION 7\CHAPTER 1\FIG1\_2\_6



ISOMETRIC VIEW OF CENTRAL REGION OF THE OVERPACK



CROSS SECTION AT MID-HEIGHT  
FIGURE 1.2.7; HI-STAR 100 OVERPACK SHELL LAYERING

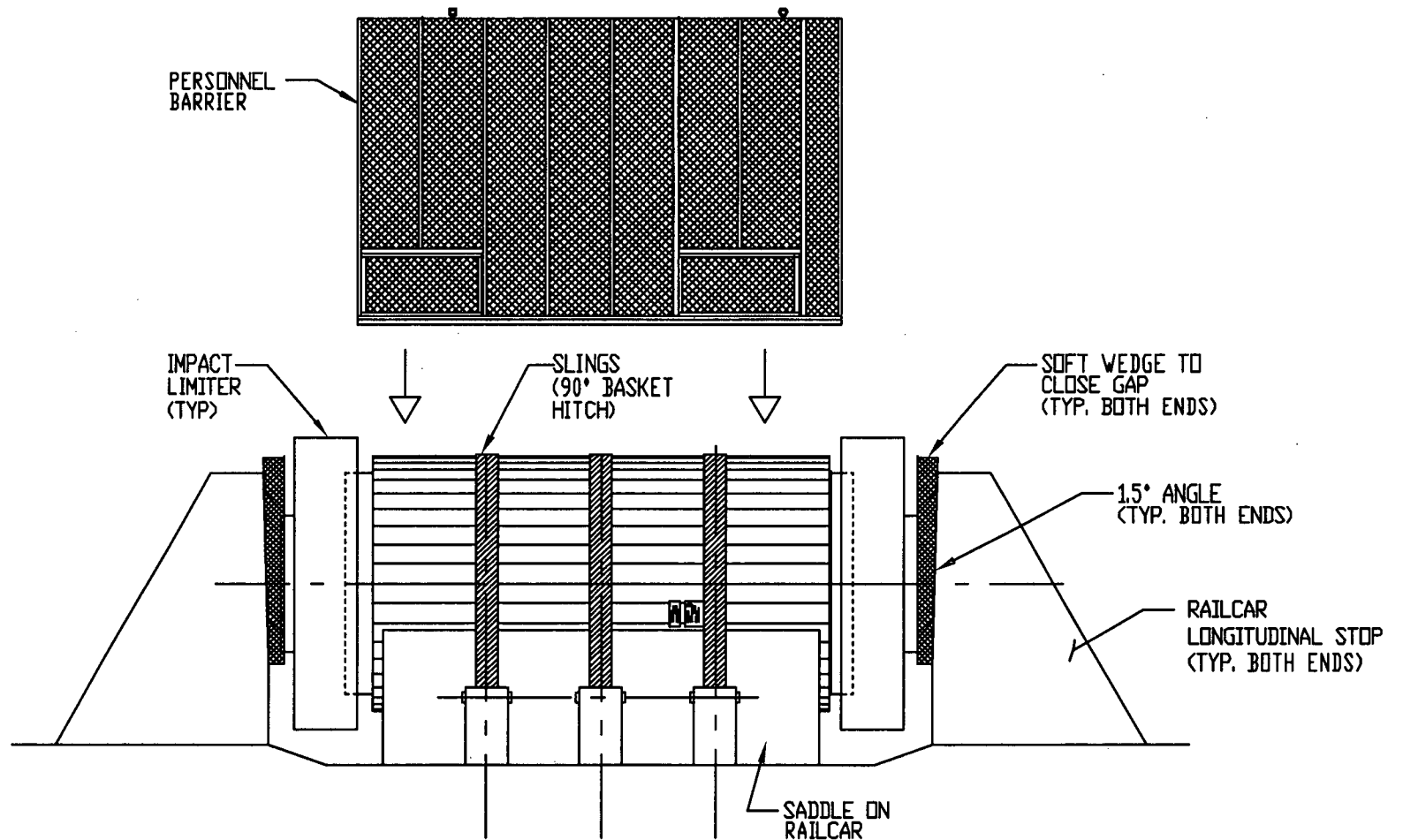
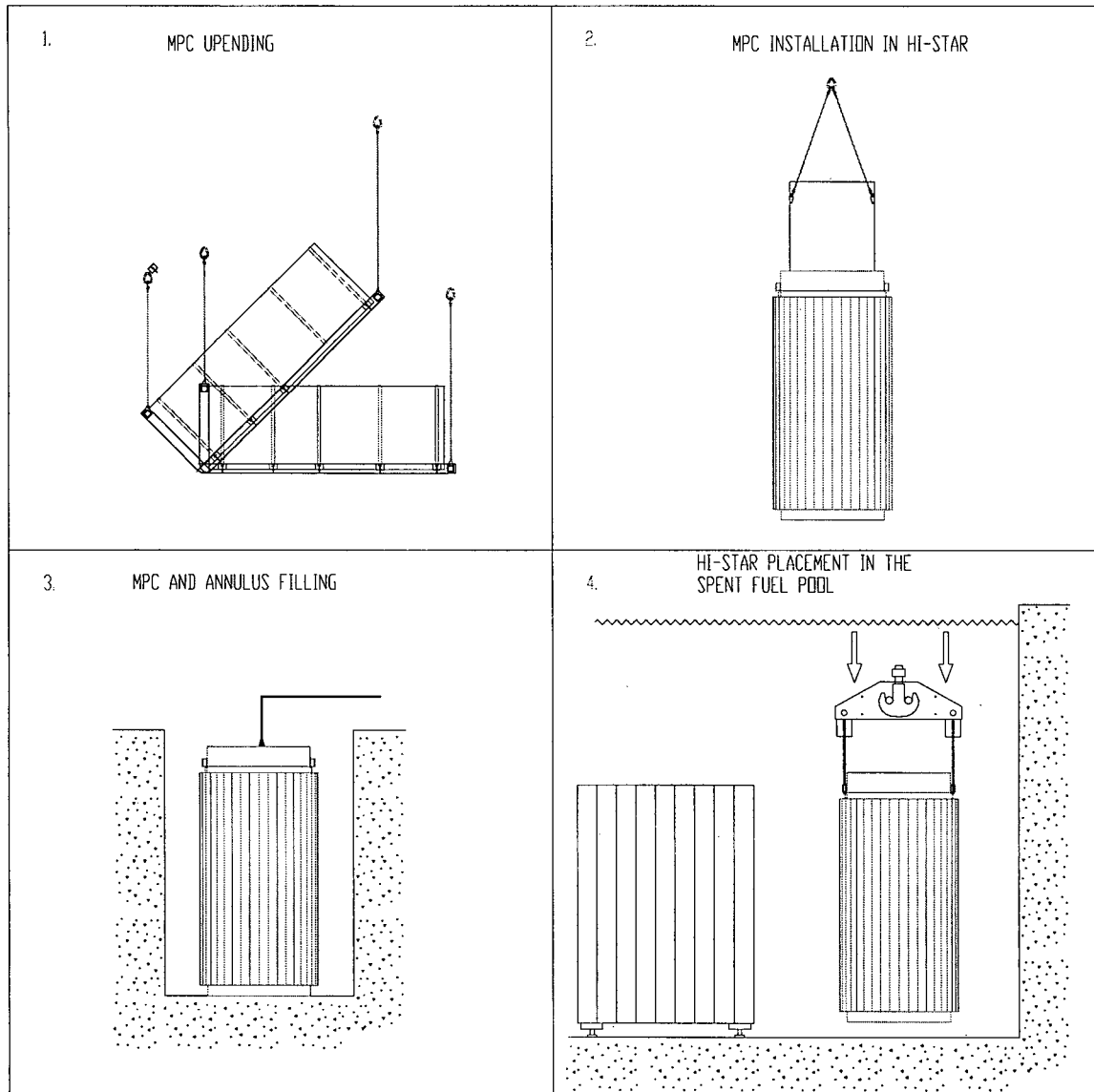
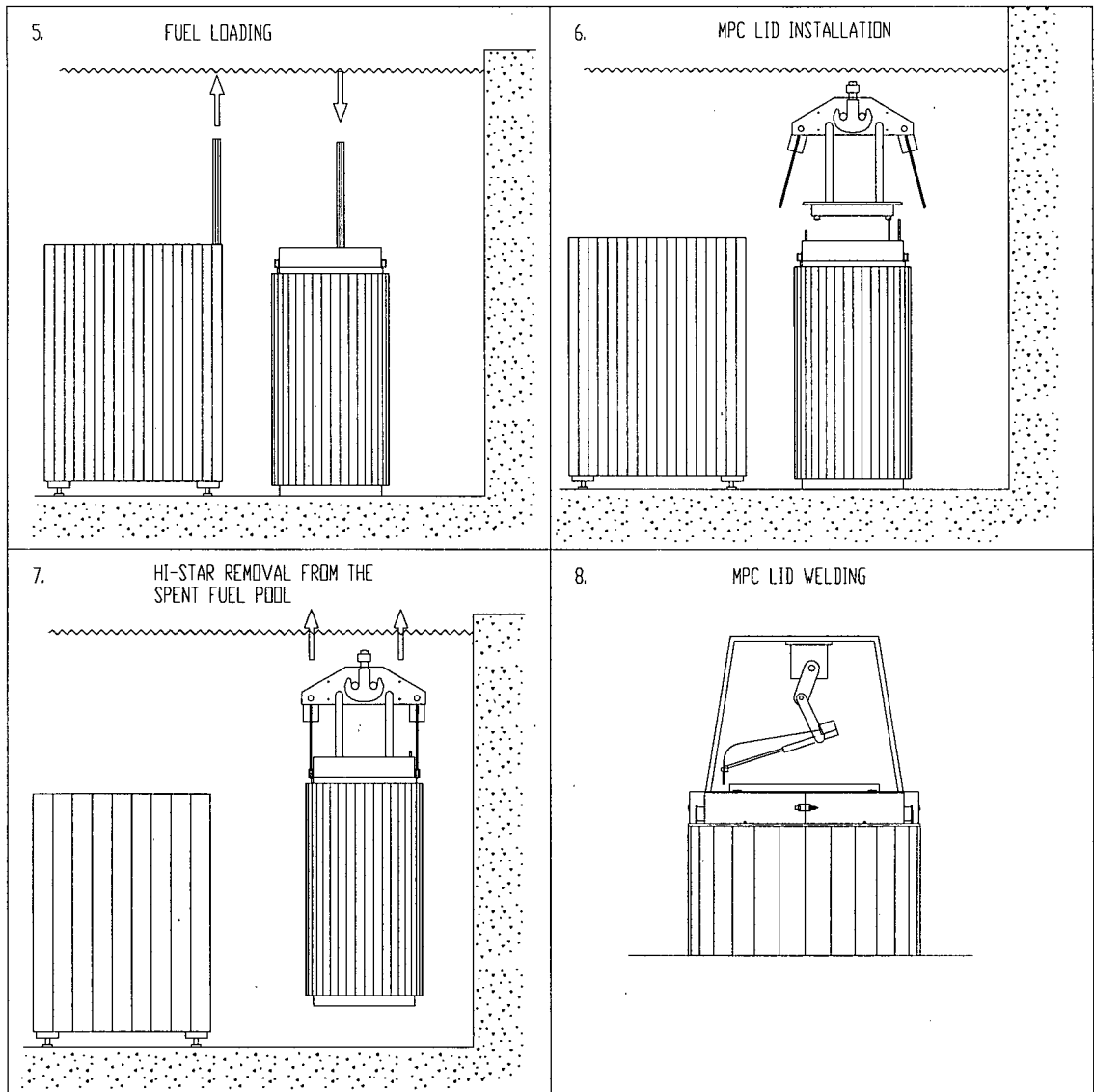


FIGURE 1.2.8; HI-STAR 100 TRANSPORT CONFIGURATION



**Figure 1.2.9; Major HI-STAR 100 Loading Operations (Sheet 1 of 3)**



**Figure 1.2.9; Major HI-STAR 100 Loading Operations (Sheet 2 of 3)**

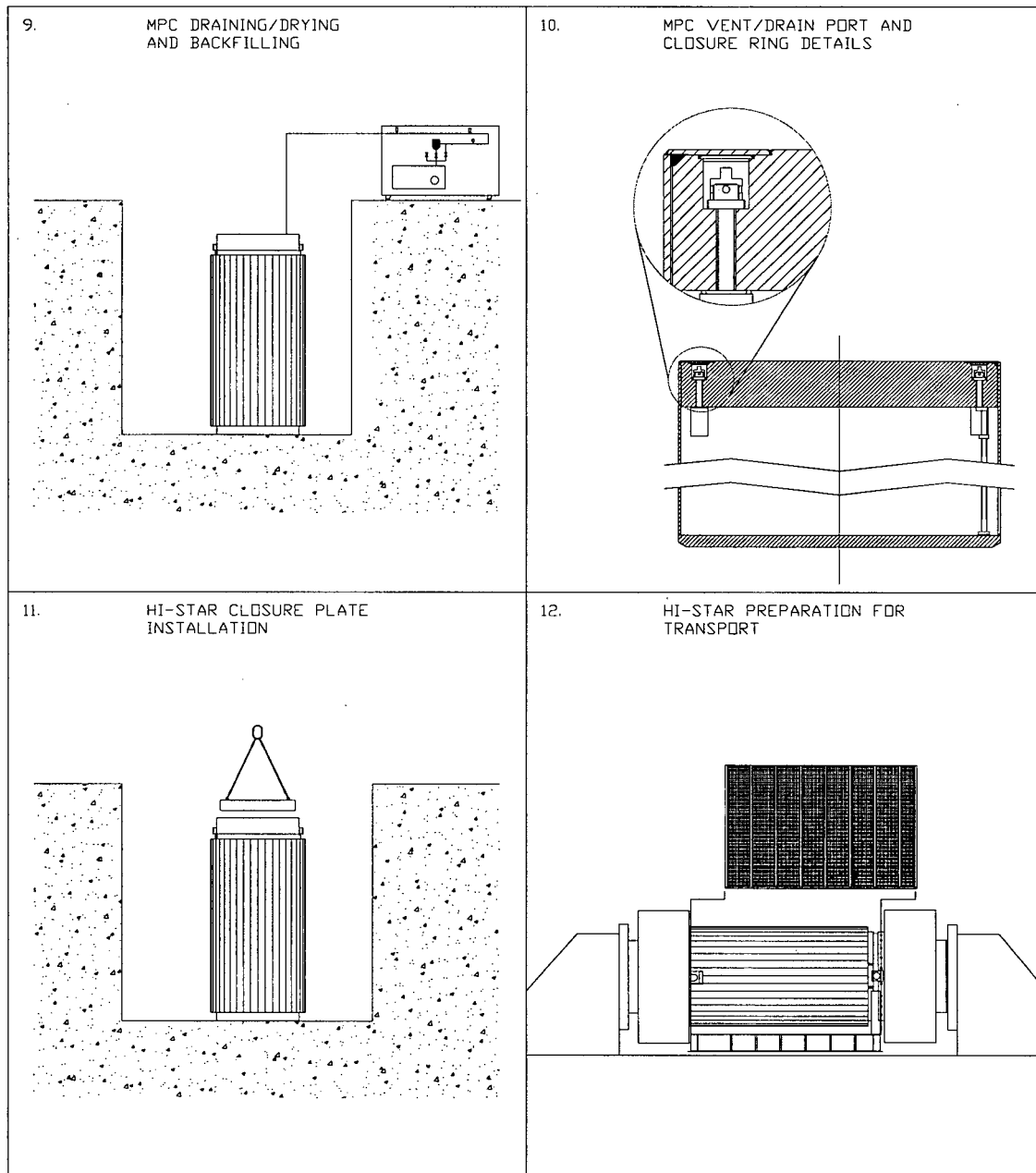
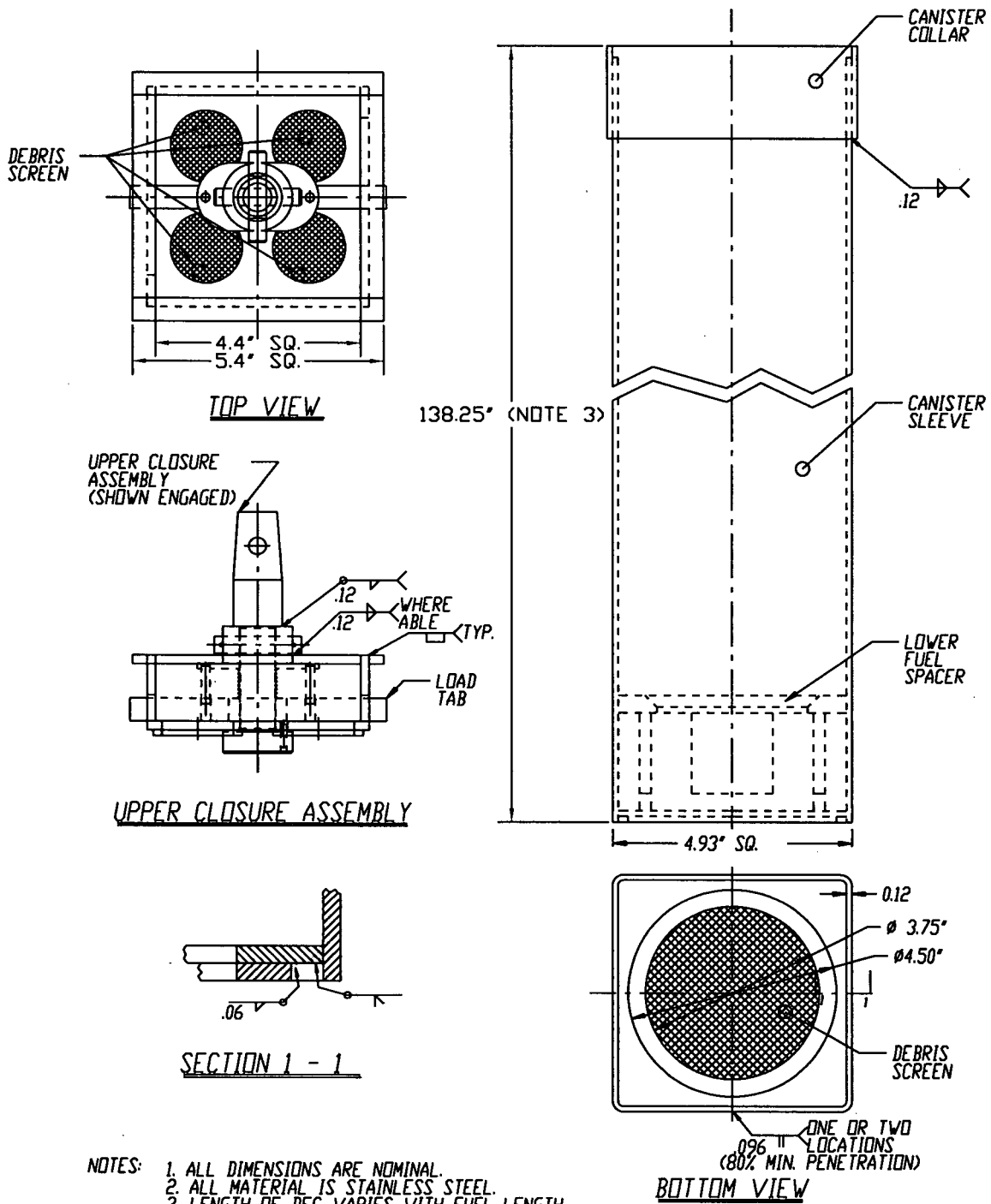


**Figure 1.2.9; Major HI-STAR 100 Loading Operations (Sheet 3 of 3)**



- NOTES:
1. ALL DIMENSIONS ARE NOMINAL.
  2. ALL MATERIAL IS STAINLESS STEEL.
  3. LENGTH OF DFC VARIES WITH FUEL LENGTH.

FIGURE 1.2.10; HOLTEC DAMAGED FUEL CONTAINER FOR DRESDEN UNIT-1 SNF

REPORT HI-951251

G:\SAR DOCUMENTS\HI-STAR SAR\FIGURES\REVISION 10\CHAPTER1\FIG1\_2\_10R10 REV. 13

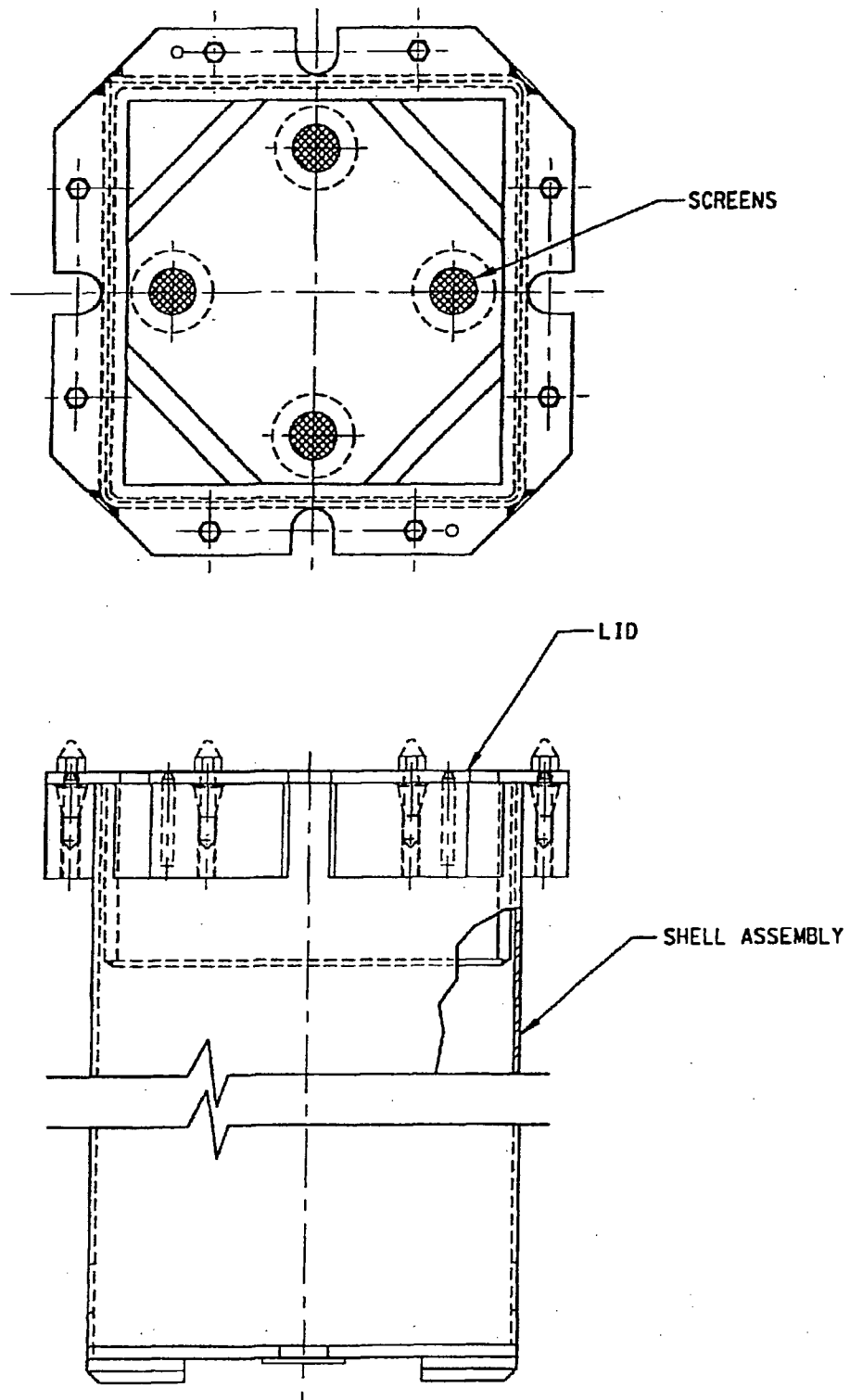


FIGURE 1.2.10A; TROJAN FAILED FUEL CAN

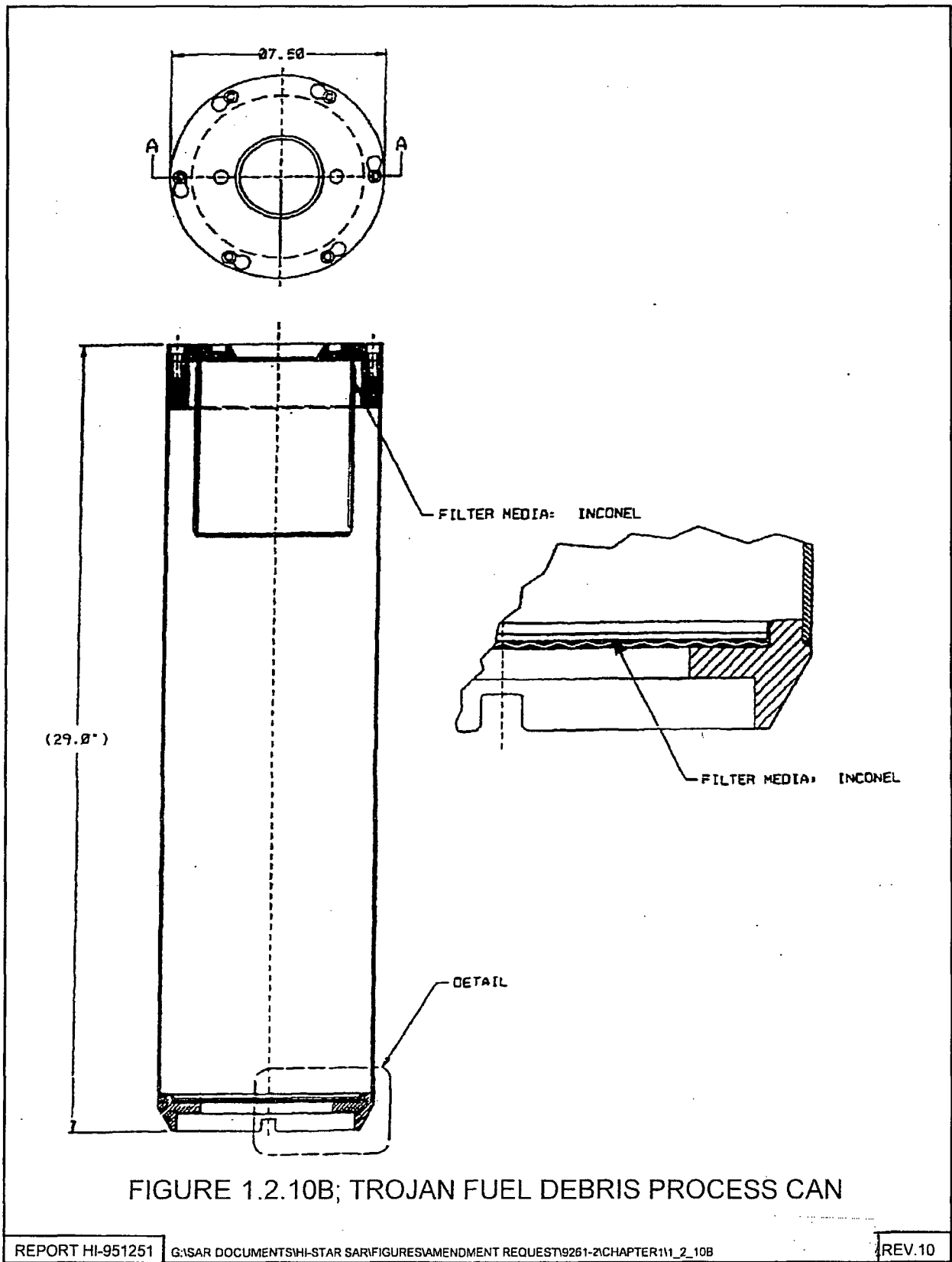


FIGURE 1.2.10B; TROJAN FUEL DEBRIS PROCESS CAN

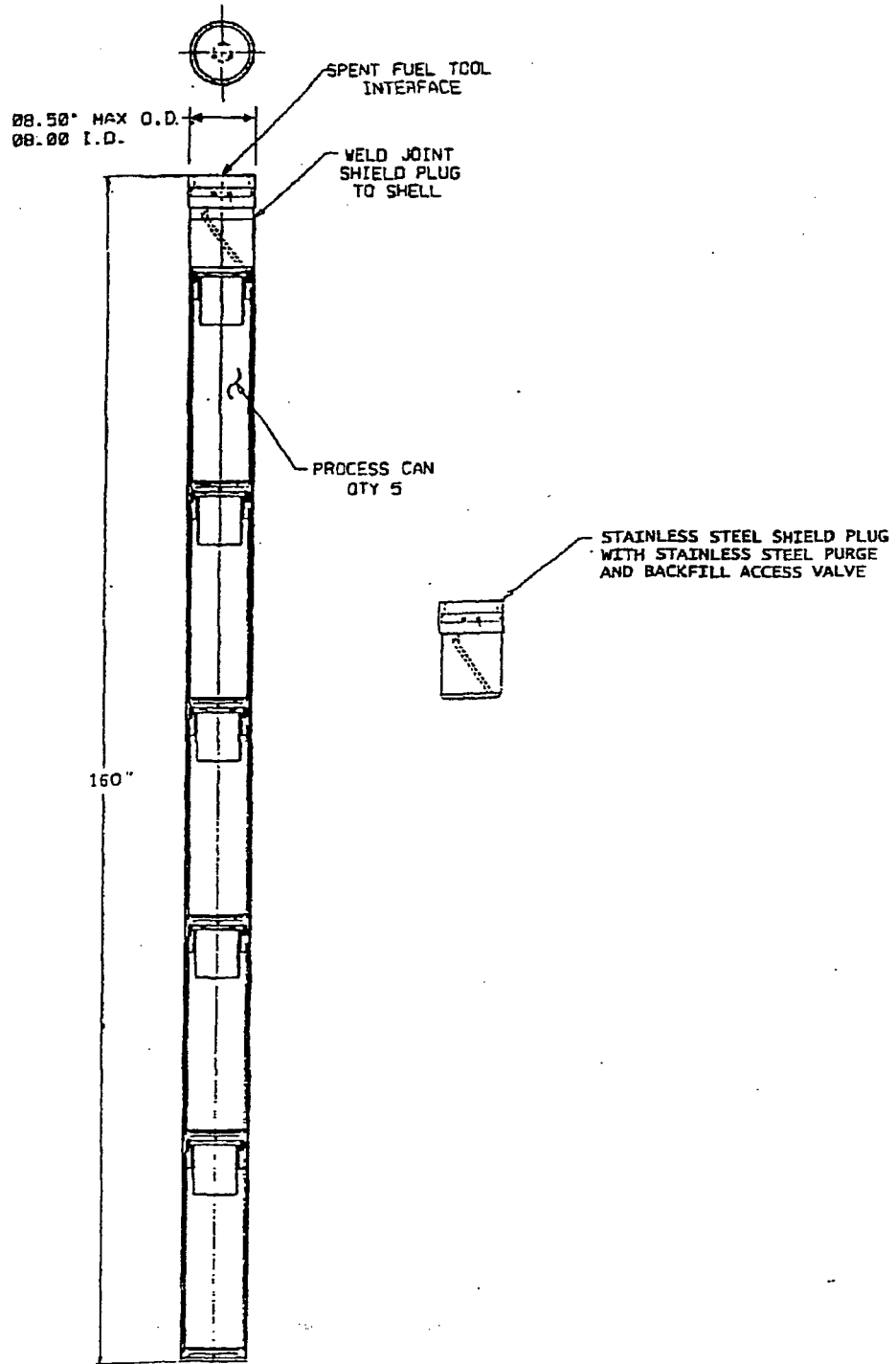


FIGURE 1.2.10C; TROJAN FUEL DEBRIS PROCESS CAN CAPSULE

NON-PROPRIETARY VERSION

NOTES:

1. ALL DIMENSIONS ARE APPROXIMATE.
2. ALL MATERIAL IS STAINLESS STEEL.

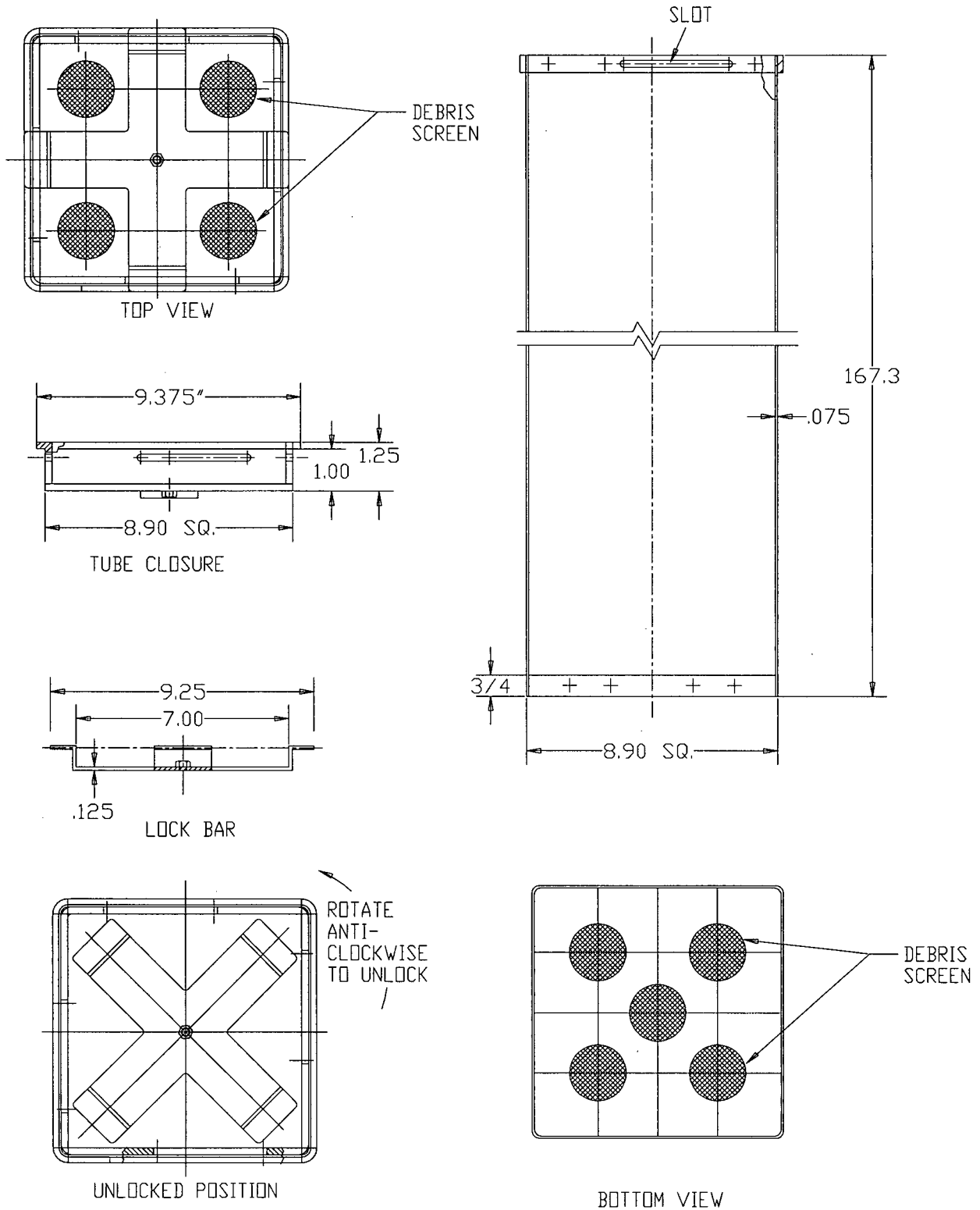


FIGURE 1.2.10D; HOLTEC DAMAGED FUEL CONTAINER FOR TROJAN PLANT SNF IN MPC-24E/24EF

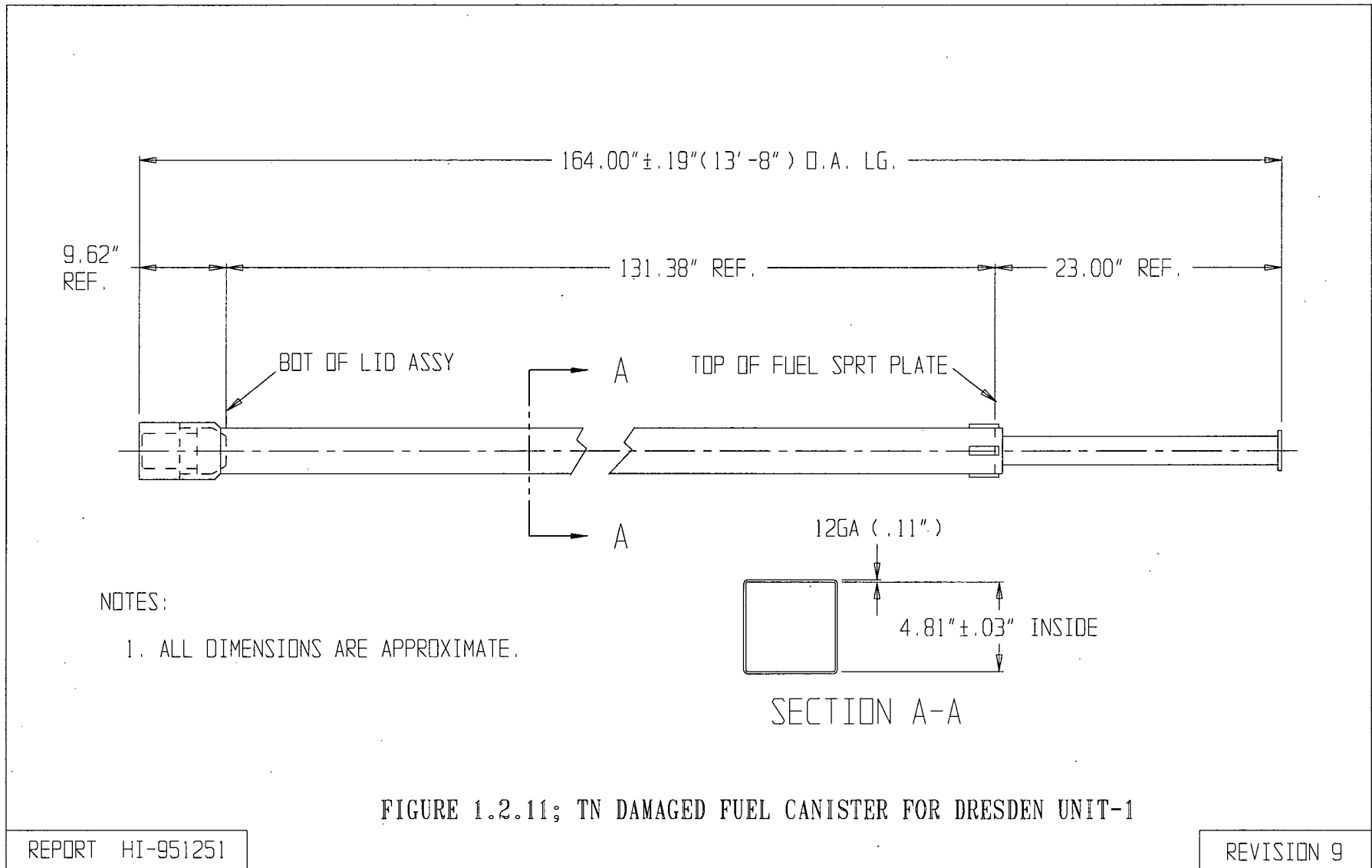


FIGURE 1.2.11; TN DAMAGED FUEL CANISTER FOR DRESDEN UNIT-1

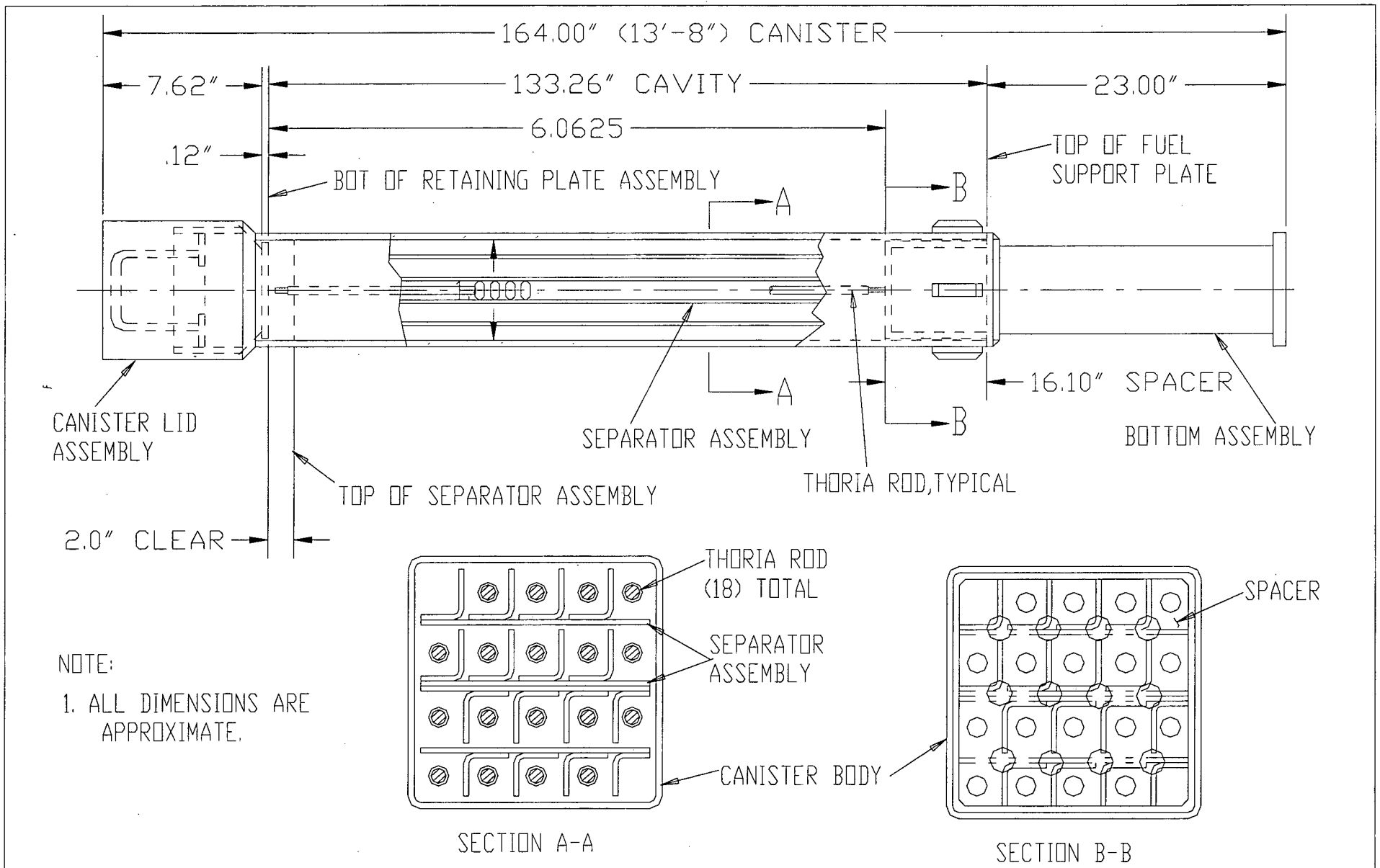


FIGURE 12.11A; TN THORIA ROD CANISTER FOR DRESDEN UNIT-1

FIGURE 1.2.12

INTENTIONALLY DELETED

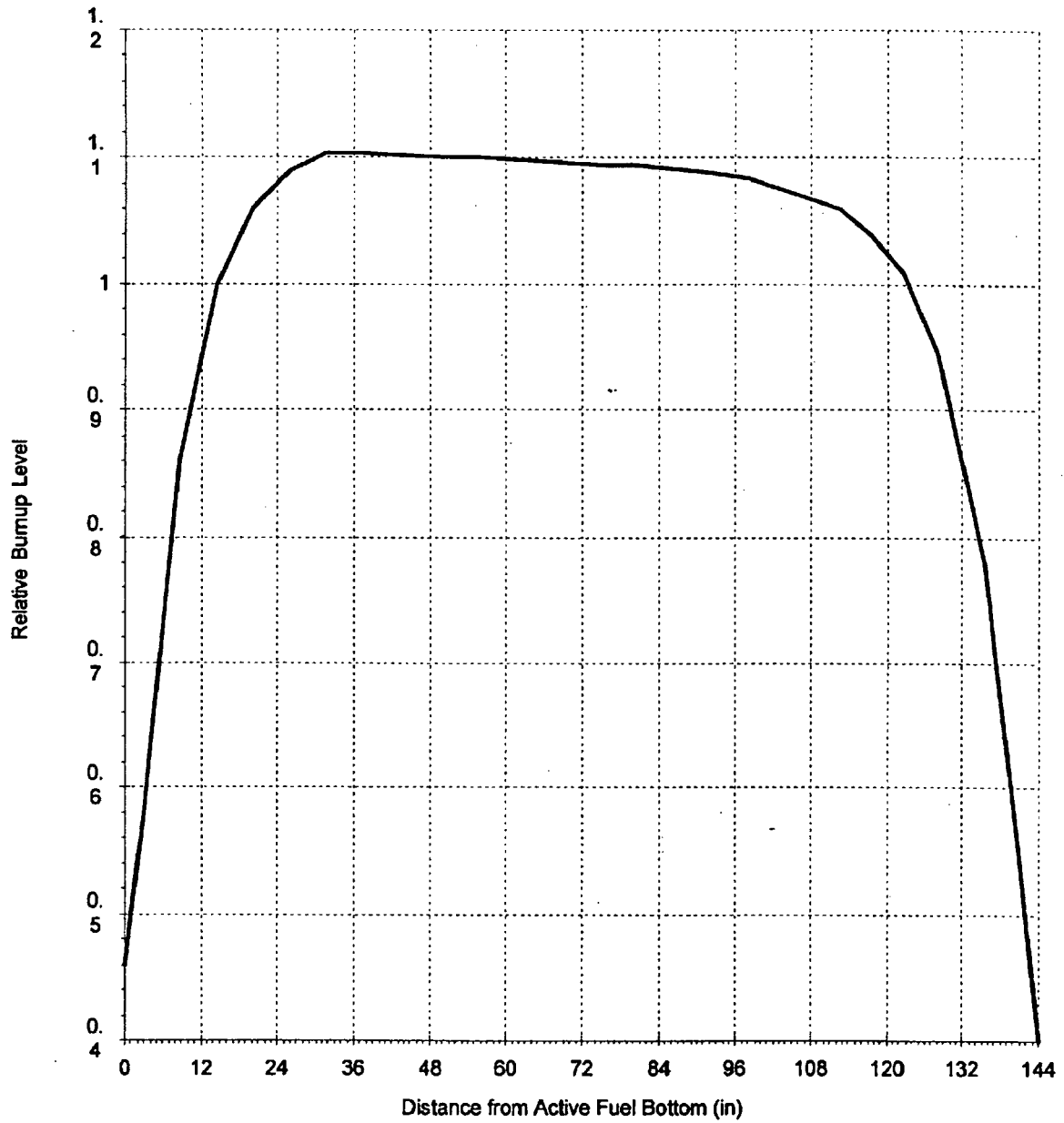


Figure 1.2.13A; Trojan Plant Fuel Axial Burnup Distribution Profile

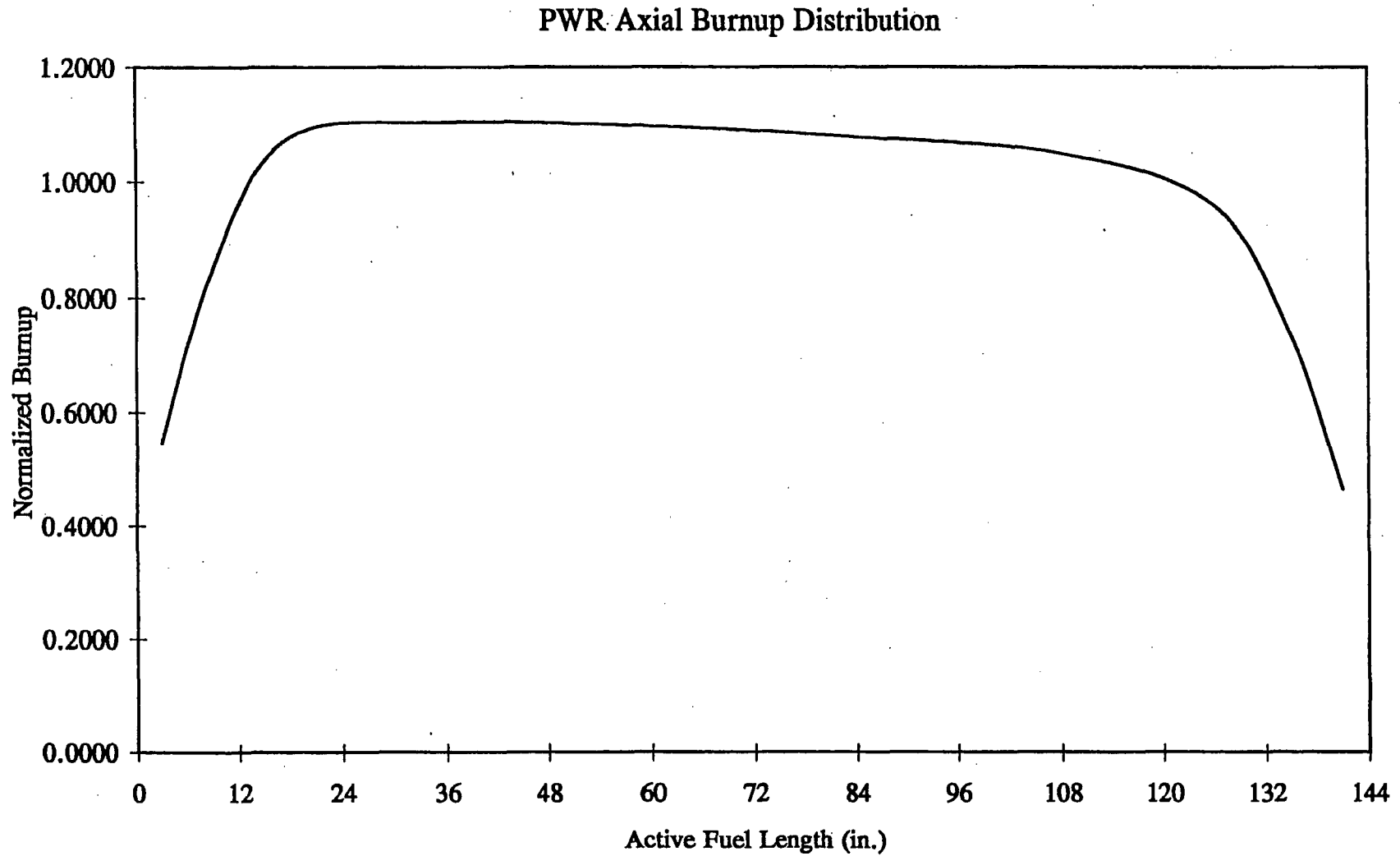


Figure 1.2.13; PWR Axial Burnup Profile with Normalized Distribution

### BWR Axial Burnup Distribution

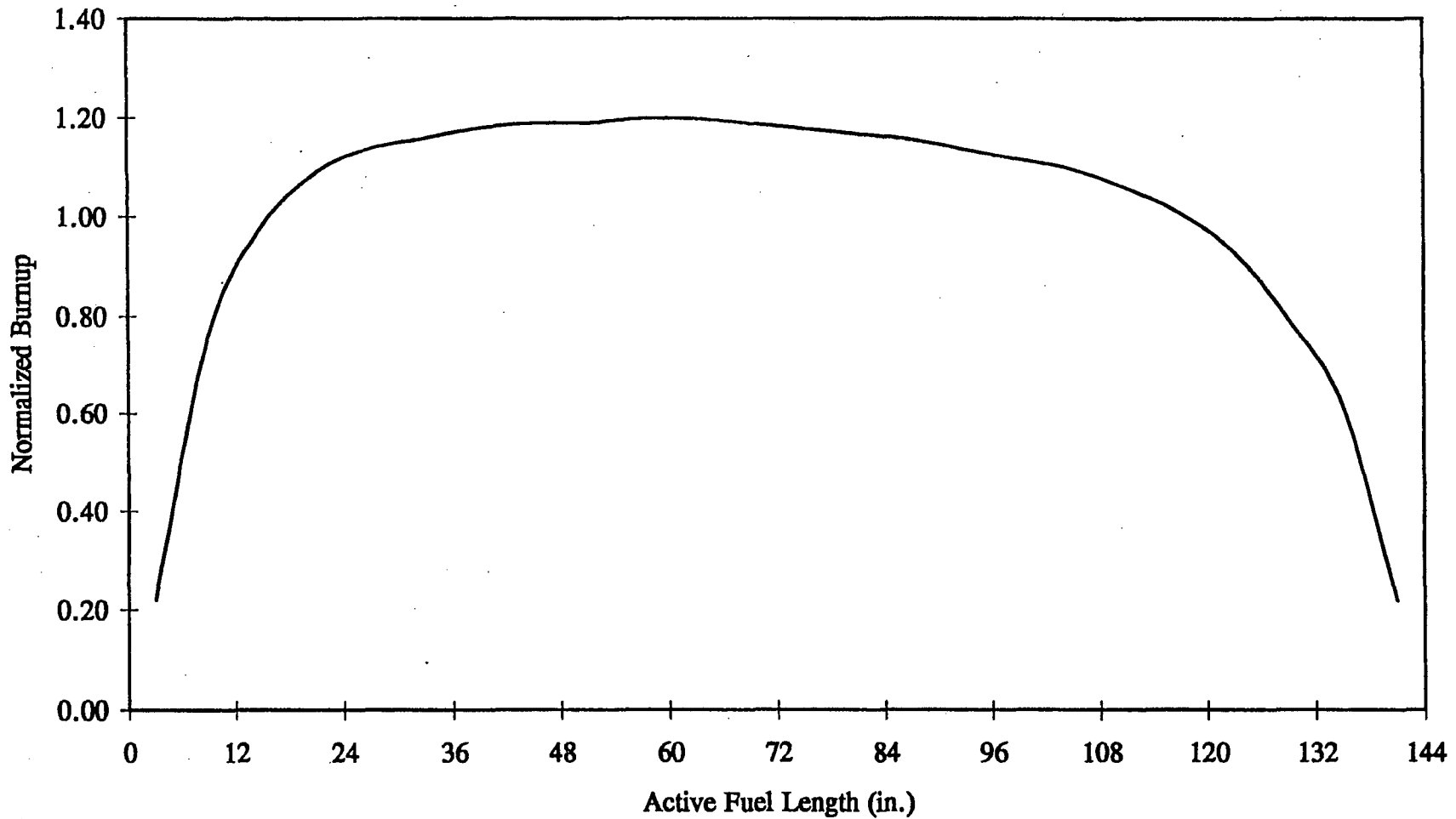


Figure 1.2.14; BWR Axial Burnup Profile with Normalized Distribution

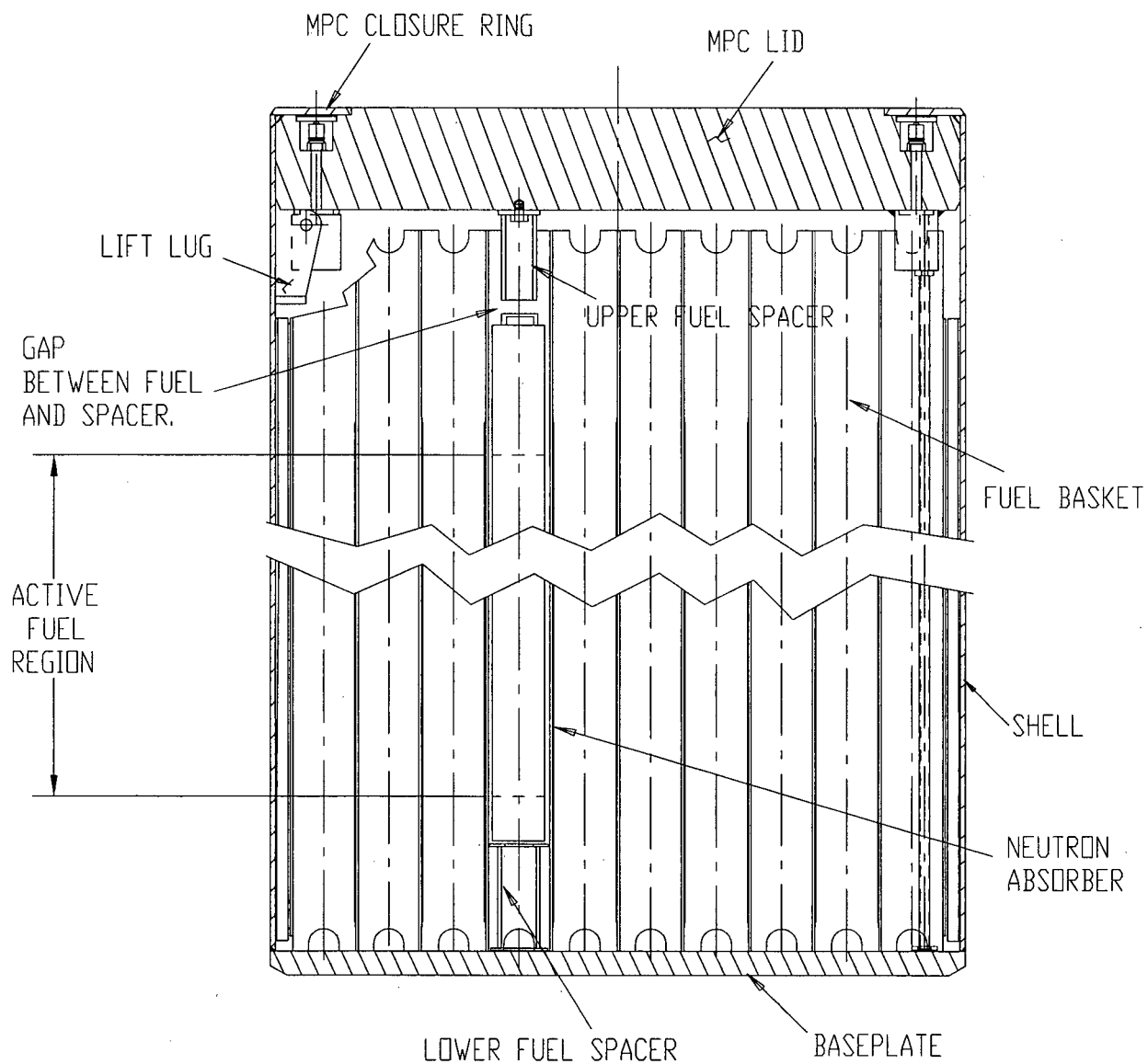


FIGURE 1.2.15; HI-STAR 100 MPC WITH UPPER AND LOWER FUEL SPACERS

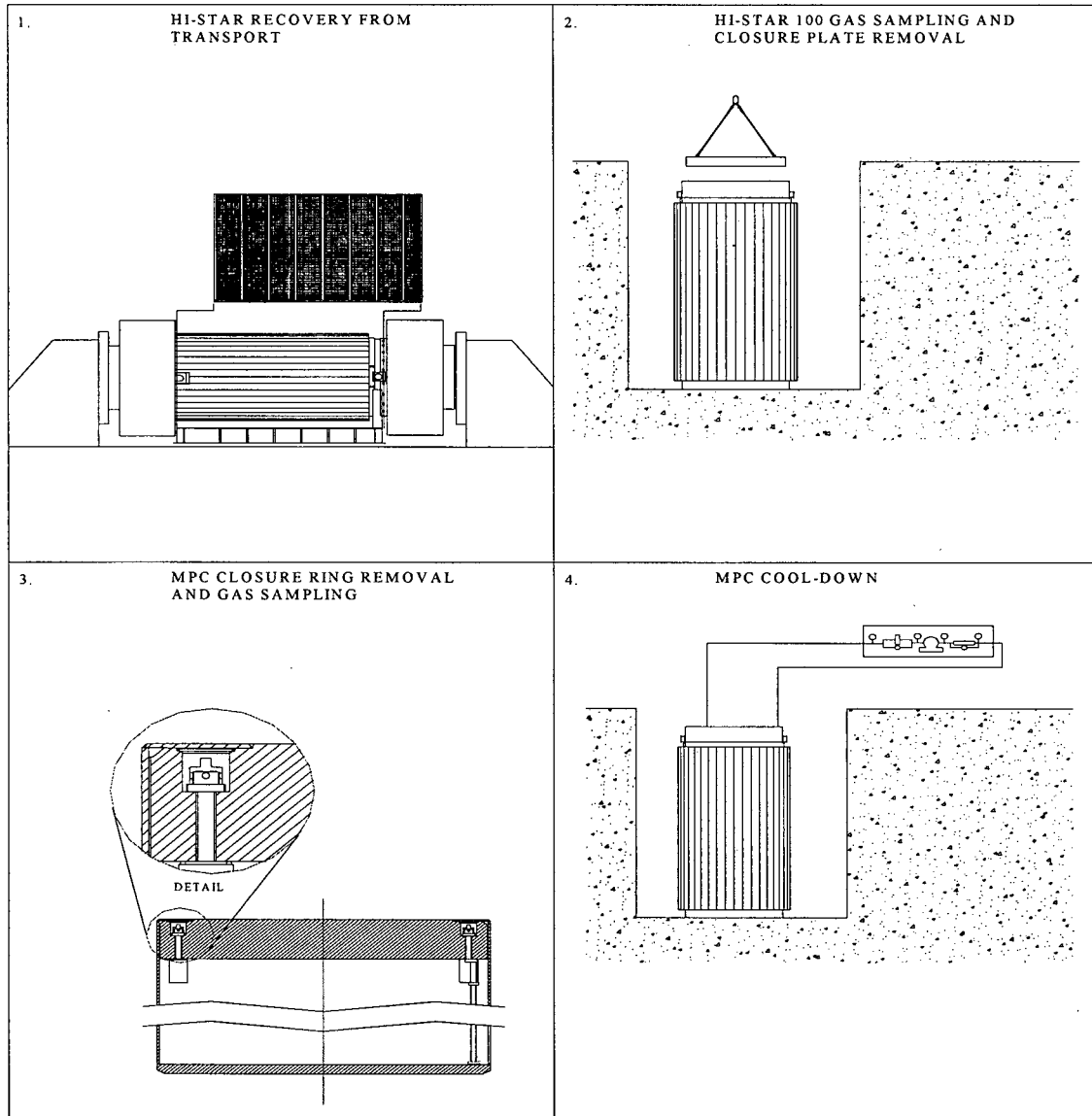
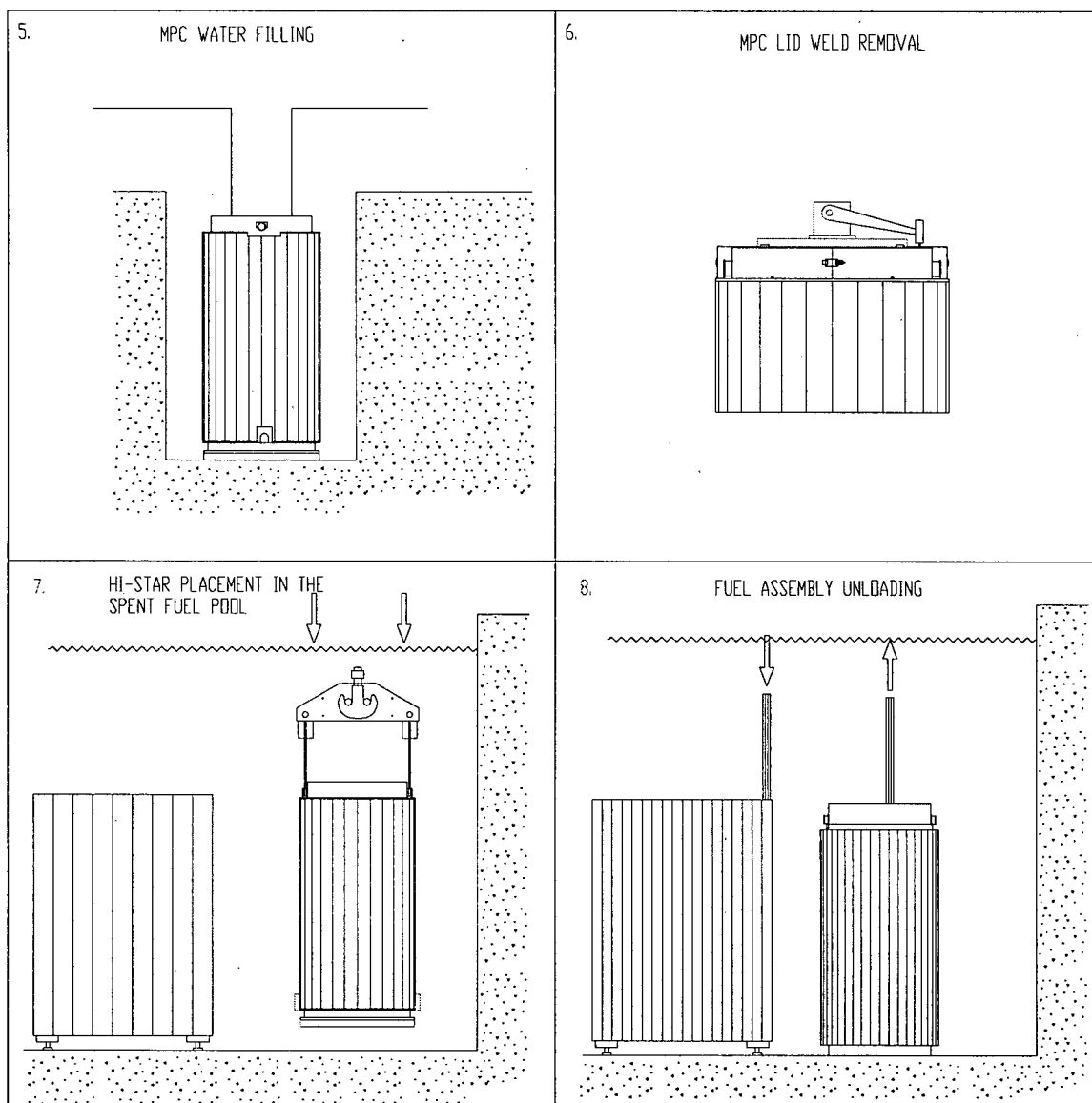
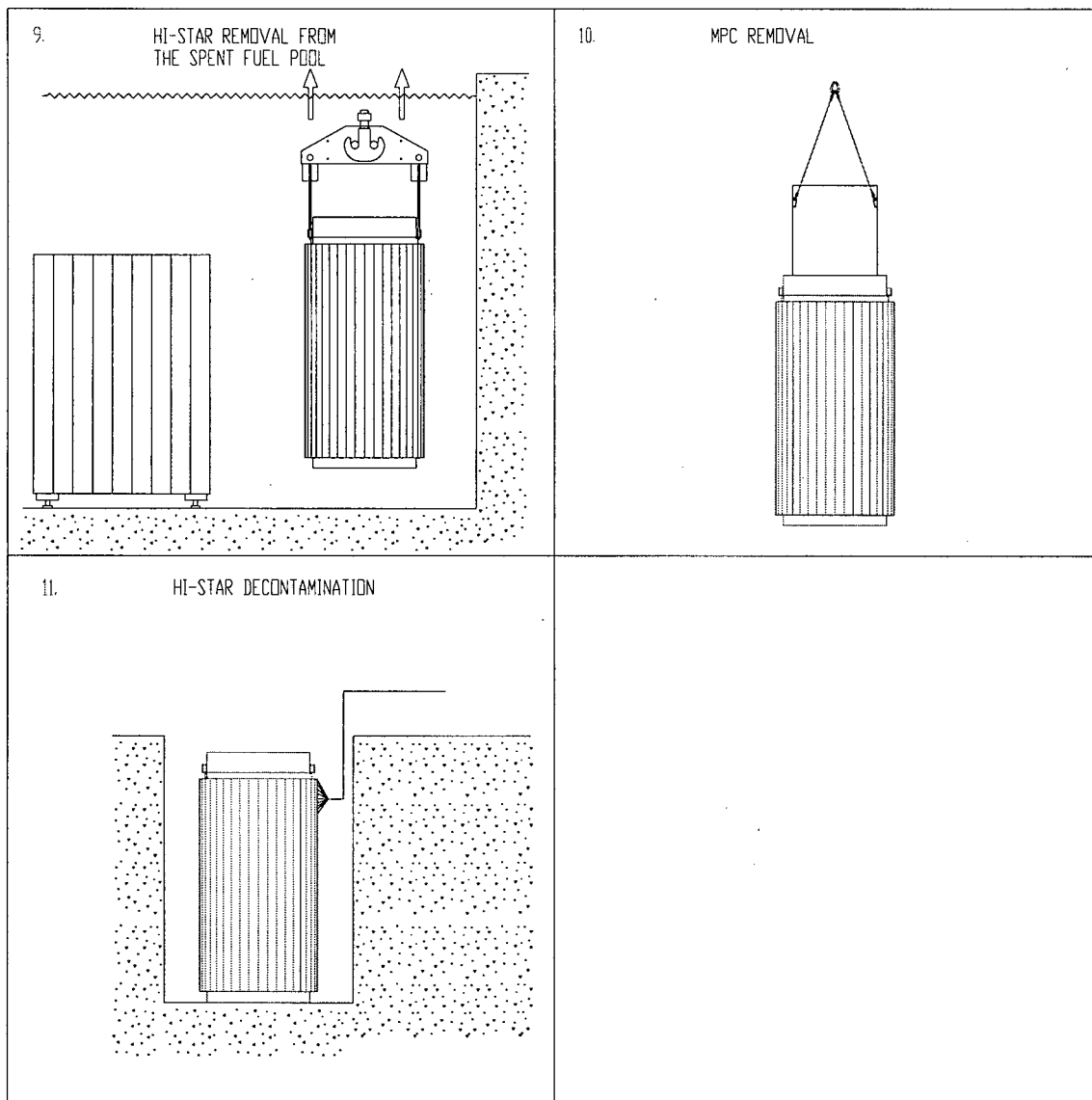


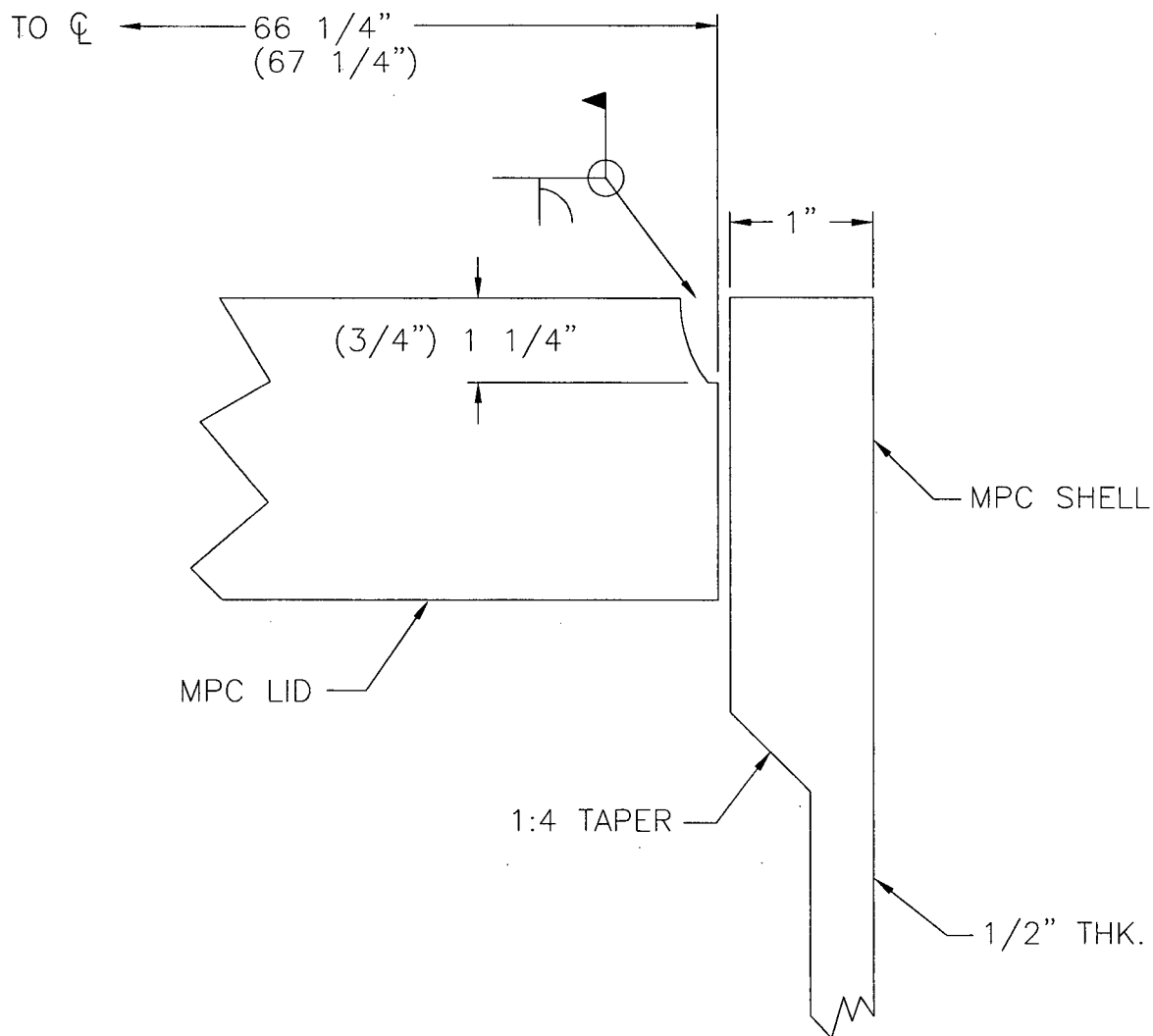
Figure 1.2.16; Major HI-STAR 100 Unloading Operations (Sheet 1 of 3)



**Figure 1.2.16; Major HI-STAR 100 Unloading Operations (Sheet 2 of 3)**



**Figure 1.2.16; Major HI-STAR 100 Unloading Operations (Sheet 3 of 3)**



- NOTES: 1. Standard MPC dimensions in parentheses.  
 2. Standard MPC shell thickness is 1/2" along its entire length.  
 3. Figure is not to scale.  
 4. All dimensions are nominal.

Figure 1.2.17; Fuel Debris MPC ("F" Model)

### Combined Curves B&W 15x15 Assemblies

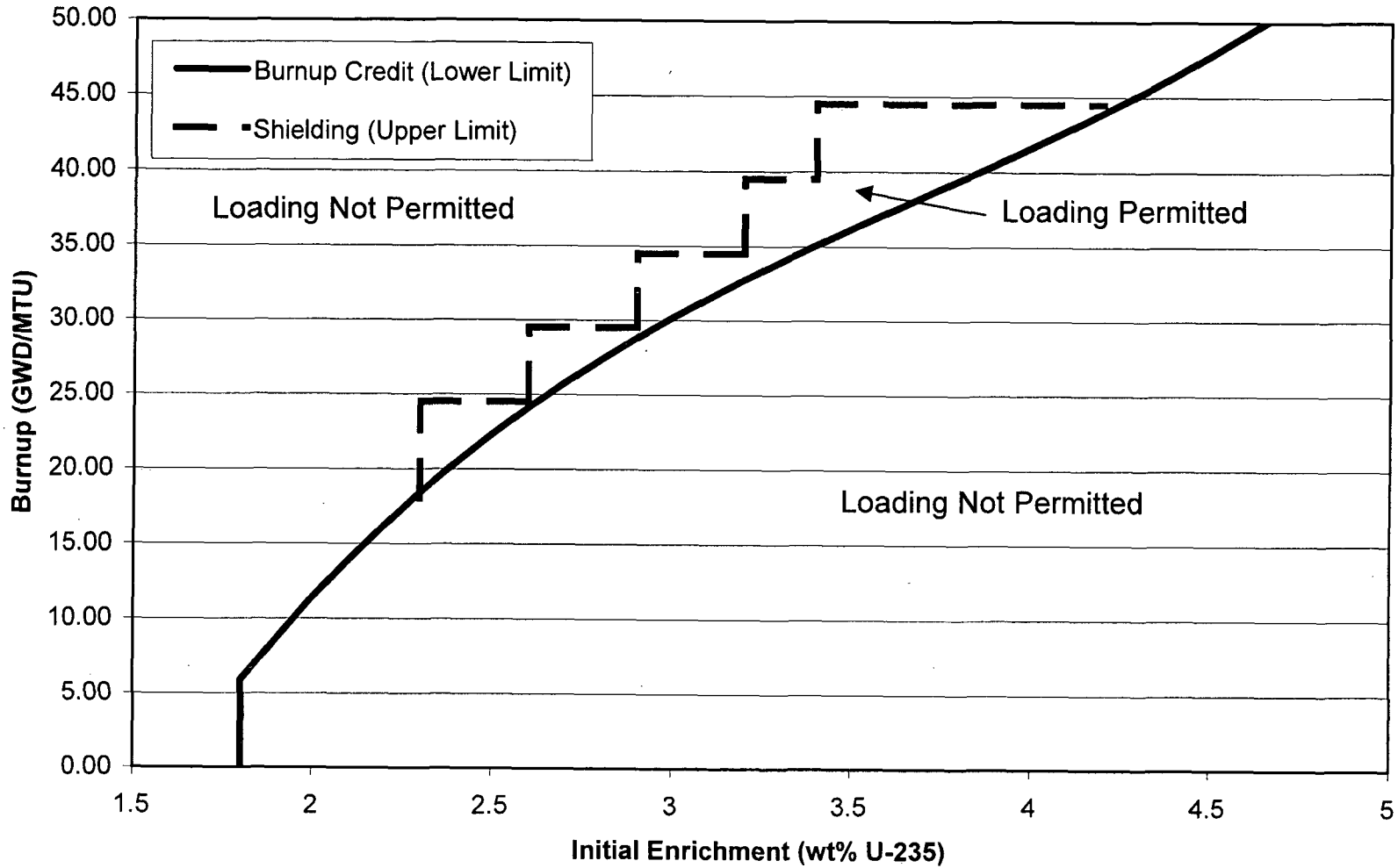


Figure 1.2.18; Combined Burnup and Enrichment Requirements for B&W 15x15 Fuel in the MPC-32

### 1.3 DESIGN CODE APPLICABILITY

The ASME Boiler and Pressure Vessel Code (ASME Code), 1995 Edition with Addenda through 1997 [1.3.1], is the governing code for the construction of the HI-STAR 100 System, as clarified in Table 1.3.2. The ASME Code is applied to each component consistent with the function of the component. Table 1.3.3 lists each structure, system and component (SSC) of the HI-STAR 100 System that are labeled Important to Safety (ITS), along with its function and governing Code. Some components perform multiple functions and in those cases, the most restrictive Code is applied. In accordance with NUREG/CR-6407, "Classification of Transportation Packaging and Dry Spent Fuel Storage System Components" [1.3.2] and according to importance to safety, components of the HI-STAR 100 System are classified as A, B, C, or NITS (not important to safety) in Table 1.3.3. Table 1.3.3 may not include all NITS items associated with the HI-STAR 100 Package.

Table 1.3.1 lists the applicable ASME Code section and paragraph for material procurement, design, fabrication and inspection of the components of the HI-STAR 100 System that are governed by the ASME Code. The ASME Code section listed in the design column is the section used to define allowable stresses for structural analyses.

Table 1.3.2 lists the alternatives to the ASME Code for the HI-STAR 100 System and the justification for those alternatives.

The MPC is classified as important to safety. The MPC structural components include the internal fuel basket and the enclosure vessel. The fuel basket is designed and fabricated as a core support structure, in accordance with the applicable requirements of Section III, Subsection NG of the ASME Code, with certain NRC-approved alternatives, as discussed in Table 1.3.2. The enclosure vessel is designed and fabricated as a Class 1 component pressure vessel in accordance with Section III, Subsection NB of the ASME Code, with certain NRC-approved alternatives, as discussed in Table 1.3.2. The principal exceptions are the MPC lid, vent and drain cover plates, and closure ring welds to the MPC lid and shell, as discussed in Table 1.3.2. In addition, the threaded holes in the MPC lid are designed in accordance with the requirements of ANSI N14.6 [1.3.3] for critical lifts to facilitate vertical MPC transfer.

The MPC closure welds are partial penetration welds that are structurally qualified by analysis, as presented in Chapter 2. The MPC closure ring welds are inspected by performing a liquid penetrant examination of the root pass (if more than one weld pass is required) and final weld surface, in accordance with the requirements contained in Section 8.1. The MPC lid weld may be examined by either volumetric or multi-layer liquid penetrant examination. If volumetric examination is used, it shall be the ultrasonic method and shall include a liquid penetrant examination of the root and final weld layers. If multi-layer liquid penetrant examination is used alone, at a minimum, it must include the root and final weld layers and each approximately 3/8 inch of weld to detect critical weld flaws. The integrity of the MPC lid weld is further verified by performing a pressure test (hydrostatic or pneumatic) in accordance with the requirements contained in Section 8.1.

The structural analysis of the MPC, in conjunction with the redundant closures and nondestructive examination, and pressure testing performed during MPC fabrication and MPC closure, provides assurance of canister closure integrity in lieu of the specific weld joint requirements of the ASME Code, Section III, Subsection NB.

The HI-STAR overpack is classified as important to safety. The HI-STAR overpack top flange, closure plate, inner shell, and bottom plate are designed and fabricated in accordance with the requirements of ASME Code, Section III, Subsection NB, to the maximum extent practical (see Table 1.3.2). The remainder of the HI-STAR overpack steel structure is designed and fabricated in accordance with the requirements of ASME Code, Section III, Subsection NF, to the maximum extent practical (see Table 1.3.2).

Table 1.3.1

## HI-STAR 100 ASME BOILER AND PRESSURE VESSEL CODE APPLICABILITY

HI-STAR 100 Component	Material Procurement	Design	Fabrication	Inspection
Overpack containment boundary	Section II; and Section III, Subsection NB, NB-2000	Section III, Subsection NB, NB-3200	Section III, Subsection NB, NB-4000	Section III, Subsection NB, NB-5000 and Section V
Overpack intermediate shells, radial channels, outer enclosure	Section II; and Section III, Subsection NF	Section III, Subsection NF, NF-3300	Section III, Subsection NF, NF-4000	Section III, Subsection NF, NF-5360 and Section V
MPC helium retention boundary	Section II; and Section III, Subsection NB, NB-2000	Section III, Subsection NB, NB-3200	Section III, Subsection NB, NB-4000	Section III, Subsection NB, NB-5000 and Section V
MPC fuel basket	Section II; and Section III, Subsection NG, NG-2000 for core support structures (NG-1121)	Section III, Subsection NG, NG-3300 and NG-3200 for core support structures (NG-1121)	Section III, Subsection NG, NG-4000 for core support structures (NG-1121)	Section III, Subsection NG, NG-5000 and Section V for core support structures (NG-1121)
Lifting Trunnions	Section II; and Section III, Subsection NF, NF-2000	ANSI N14.6	Section III, Subsection NF, NF-4000	ANSI 14.6 See Chapter 8
MPC Basket Supports (Angled Plates)	Section II, and Section III, Subsection NG, NG-2000 for internal structures (NG-1122)	Section III, Subsection NG, NG-3300 and NG-3200 for internal structures (NG-1122)	Section III, Subsection NG, NG-4000 for internal structures (NG-1122)	Section III, Subsection NG, NG-5000 and Section V for internal structures (NG-1122)
Damaged Fuel Container	Section II, and Section III, Subsection NG, NG-2000	Section III, Subsection NG, NG-3300 and NG-3200	Section III, Subsection NG, NG-4000	Section III, Subsection NG, NG-5000 and Section V

Table 1.3.2

LIST OF ASME CODE ALTERNATIVES FOR HI-STAR 100 SYSTEM

Component	Reference ASME Code Section/Article	Code Requirement	Alternative, Justification & Compensatory Measures
MPC, MPC basket assembly, and HI-STAR overpack steel structure.	Subsection NCA	General Requirements. Requires preparation of a Design Specification, Design Report, Overpressure Protection Report, Certification of Construction Report, Data Report, and other administrative controls for an ASME Code stamped vessel.	<p>Because the MPC and overpack are not ASME Code stamped vessels, none of the specifications, reports, certificates, or other general requirements specified by NCA are required. In lieu of a Design Specification and Design Report, the HI-STAR SAR includes the design criteria, service conditions, and load combinations for the design and operation of the HI-STAR 100 System as well as the results of the stress analyses to demonstrate that applicable Code stress limits are met. Additionally, the fabricator is not required to have an ASME-certified QA program. All important-to-safety activities are governed by the NRC-approved Holtec QA program.</p> <p>Because the cask components are not certified to the Code, the terms "Certificate Holder" and "Inspector" are not germane to the manufacturing of NRC-certified cask components. To eliminate ambiguity, the responsibilities assigned to the Certificate Holder in the various articles of Subsections NB, NG, and NF of the Code, as applicable, shall be interpreted to apply to the NRC Certificate of Compliance (CoC) holder (and by extension, to the component fabricator) if the requirement must be fulfilled. The Code term "Inspector" means the QA/QC personnel of the CoC holder and its vendors assigned to oversee and inspect the manufacturing process.</p>
MPC	NB-1100	Statement of requirements for Code stamping of components.	MPC vessel is designed and will be fabricated in accordance with ASME Code, Section III, Subsection NB to the maximum practical extent, but Code stamping is not required.
MPC	NB-2000	Requires materials to be supplied by ASME-approved material supplier.	Materials will be supplied by Holtec approved suppliers with Certified Material Test Reports (CMTRs) in accordance with NB-2000 requirements.

Table 1.3.2 (continued)

## LIST OF ASME CODE ALTERNATIVES FOR HI-STAR 100 SYSTEM

Component	Reference ASME Code Section/Article	Code Requirement	Alternative, Justification & Compensatory Measures
MPC basket supports and lift lugs	NB-1130	<p>NB-1132.2(d) requires that the first connecting weld of a nonpressure-retaining structural attachment to a component shall be considered part of the component unless the weld is more than <math>2t</math> from the pressure-retaining portion of the component, where <math>t</math> is the nominal thickness of the pressure-retaining material.</p> <p>NB-1132.2(e) requires that the first connecting weld of a welded nonstructural attachment to a component shall conform to NB-4430 if the connecting weld is within <math>2t</math> from the pressure-retaining portion of the component.</p>	<p>The MPC basket supports (nonpressure-retaining structural attachments) and lift lugs (nonstructural attachments used exclusively for lifting an empty MPC) are welded to the inside of the pressure-retaining MPC shell, but are not designed in accordance with Subsection NB. The basket supports and associated attachment welds are designed to satisfy the stress limits of Subsection NG and the lift lugs and associated attachment welds are designed to satisfy the stress limits of Subsection NF, as a minimum. These attachments and their welds are shown by analysis to meet the respective stress limits for their service conditions. Likewise, non-structural items, such as shield plugs, spacers, etc. if used, can be attached to pressure-retaining parts in the same manner.</p>
MPC, MPC basket assembly, and HI-STAR overpack steel structure.	NB-3100 NG-3100 NF-3100	Provides requirements for determining design loading conditions, such as pressure, temperature, and mechanical loads.	These requirements are not applicable. The HI-STAR SAR, serving as the Design Specification, establishes the service conditions and load combinations for the storage system.

Table 1.3.2 (continued)

## LIST OF ASME CODE ALTERNATIVES FOR HI-STAR 100 SYSTEM

Component	Reference ASME Code Section/Article	Code Requirement	Alternative, Justification & Compensatory Measures
MPC	NB-3350	NB-3352.3 requires, for Category C joints, that the minimum dimensions of the welds and throat thickness shall be as shown in Figure NB-4243-1.	<p>The MPC shell-to-baseplate weld joint design (designated Category C) may not include a reinforcing fillet weld or a bevel in the MPC baseplate, which makes it different than any of the representative configurations depicted in Figure NB-4243-1. The transverse thickness of this weld is equal to the thickness of the adjoining shell (1/2 inch). The weld is designed as a full penetration weld that receives VT and RT or UT, as well as final surface PT examinations. Because the MPC shell design thickness is considerably larger than the minimum thickness required by the Code, a reinforcing fillet weld that would intrude into the MPC cavity space is not included. Not including this fillet weld provides for a higher quality radiographic examination of the full penetration weld.</p> <p>From the standpoint of stress analysis, the fillet weld serves to reduce the local bending stress (secondary stress) produced by the gross structural discontinuity defined by the flat plate/shell junction. In the MPC design, the shell and baseplate thicknesses are well beyond that required to meet their respective membrane stress intensity limits.</p>
MPC, MPC basket assembly, and HI-STAR overpack steel structure	NB-4120 NG-4120 NF-4120	NB-4121.2, NG-4121.2, and NF-4121.2 provide requirements for repetition of tensile or impact tests for material subjected to heat treatment during fabrication or installation.	<p>In-shop operations of short duration that apply heat to a component, such as plasma cutting of plate stock, welding, machining, coating, and pouring of Holtite are not, unless explicitly stated by the Code, defined as heat treatment operations.</p> <p>For the steel parts in the HI-STAR 100 System components, the duration for which a part exceeds the off-normal temperature limit shall be limited to 24 hours in a particular manufacturing process (such as the Holtite pouring process).</p>

Table 1.3.2 (continued)

## LIST OF ASME CODE ALTERNATIVES FOR HI-STAR 100 SYSTEM

Component	Reference ASME Code Section/Article	Code Requirement	Alternative, Justification & Compensatory Measures
MPC and HI-STAR overpack steel structure	NB-4220 NF-4220	Requires certain forming tolerances to be met for cylindrical, conical, or spherical shells of a vessel.	The cylindricity measurements on the rolled shells are not specifically recorded in the shop travelers, as would be the case for a Code-stamped pressure vessel. Rather, the requirements on inter-component clearances (such as the MPC-to-overpack) are guaranteed through fixture-controlled manufacturing. The fabrication specification and shop procedures ensure that all dimensional design objectives, including inter-component annular clearances are satisfied. The dimensions required to be met in fabrication are chosen to meet the functional requirements of the dry storage components. Thus, although the post-forming Code cylindricity requirements are not evaluated for compliance directly, they are indirectly satisfied (actually exceeded) in the final manufactured components.
MPC Lid and Closure Ring Welds	NB-4243	Full penetration welds required for Category C Joints (flat head to main shell per NB-3352.3)	MPC lid and closure ring are not full penetration welds. They are welded independently to provide a redundant seal. Additionally, a weld efficiency factor of 0.45 has been applied to the analyses of these welds.
MPC Lid-to-Shell Weld	NB-5230	Radiographic (RT) or ultrasonic (UT) examination required.	Only UT or multi-layer liquid penetrant (PT) examination is permitted. If PT alone is used, at a minimum, it will include the root and final weld layers and each approximately 3/8 inch of weld depth.
MPC Closure Ring, Vent and Drain Cover Plate Welds	NB-5230	Radiographic (RT) or ultrasonic (UT) examination required.	Root (if more than one weld pass is required) and final liquid penetrant examination to be performed in accordance with NB-5245. The closure ring provides independent redundant closure for vent and drain cover plates.

Table 1.3.2 (continued)

LIST OF ASME CODE ALTERNATIVES FOR HI-STAR 100 SYSTEM

Component	Reference ASME Code Section/Article	Code Requirement	Alternative, Justification & Compensatory Measures
MPC Enclosure Vessel and Lid	NB-6111	All completed pressure retaining systems shall be pressure tested.	The MPC vessel is seal welded in the field following fuel assembly loading. The MPC vessel shall then be pressure tested as defined in Chapter 8. Accessibility for leakage inspections precludes a Code compliant pressure test. All MPC vessel welds (except closure ring and vent/drain cover plate) are inspected by volumetric examination, except that the MPC lid-to-shell weld shall be verified by volumetric or multi-layer PT examination. If PT alone is used, at a minimum, it must include the root and final layers and each approximately 3/8 inch of weld depth. For either UT or PT, the maximum undetectable flaw size must be demonstrated to be less than the critical flaw size. The critical flaw size must be determined in accordance with ASME Section XI methods. The critical flaw size shall not cause the primary stress limits of NB-3000 to be exceeded. The inspection results, including relevant findings (indications) shall be made a permanent part of the user's records by video, photographic, or other means which provide an equivalent retrievable record of weld integrity. The video or photographic records should be taken during the final interpretation period described in ASME Section V, Article 6, T-676. The vent/drain cover plate welds are confirmed by liquid penetrant examination and the closure ring weld is confirmed by liquid penetrant examination. The inspection of the weld must be performed by qualified personnel and shall meet the acceptance requirements of ASME Code Section III, NB-5350 for PT or NB-5332 for UT.
MPC Enclosure Vessel	NB-7000	Vessels are required to have overpressure protection.	No overpressure protection is provided. The function of MPC vessel is as a helium retention boundary. MPC vessel is designed to withstand maximum internal pressure considering 100% fuel rod failure and maximum accident temperatures.

Table 1.3.2 (continued)

## LIST OF ASME CODE ALTERNATIVES FOR HI-STAR 100 SYSTEM

Component	Reference ASME Code Section/Article	Code Requirement	Alternative, Justification & Compensatory Measures
MPC Enclosure Vessel	NB-8000	States requirements for nameplates, stamping and reports per NCA-8000.	HI-STAR 100 System to be marked and identified in accordance with 10CFR71 and 10CFR72 requirements. Code stamping is not required. QA data package to be in accordance with Holtec approved QA program.
Overpack Containment Boundary	NB-1100	Statement of requirements for Code stamping of components.	Overpack containment boundary is designed, and will be fabricated in accordance with ASME Code, Section III, Subsection NB to the maximum practical extent, but Code stamping is not required.
Overpack Containment Boundary	NB-2000	Requires materials to be supplied by ASME-approved material supplier.	Materials will be supplied by Holtec approved suppliers with CMTRs per NB-2000.
Overpack Containment Boundary	NB-7000	Vessels are required to have overpressure protection.	No overpressure protection is provided. Function of overpack vessel is as a radionuclide containment boundary under normal and hypothetical accident conditions. Overpack vessel is designed to withstand maximum internal pressure and maximum accident temperatures.
Overpack Containment Boundary	NB-8000	States requirements for nameplates, stamping and reports per NCA-8000.	HI-STAR 100 System to be marked and identified in accordance with 10CFR71 and 10CFR72 requirements. Code stamping is not required. QA data package to be in accordance with Holtec's approved QA program.
MPC Basket Assembly	NG-2000	Requires materials to be supplied by ASME-approved material supplier.	Materials will be supplied by Holtec approved supplier with CMTRs in accordance with NG-2000 requirements.

Table 1.3.2 (continued)

## LIST OF ASME CODE ALTERNATIVES FOR HI-STAR 100 SYSTEM

Component	Reference ASME Code Section/Article	Code Requirement	Alternative, Justification & Compensatory Measures
MPC Basket Assembly	NG-4420	NG-4427(a) allows a fillet weld in any single continuous weld to be less than the specified fillet weld dimension by not more than 1/16 inch, provided that the total undersize portion of the weld does not exceed 10 percent of the length of the weld. Individual undersize weld portions shall not exceed 2 inches in length.	<p>Modify the Code requirement (intended for core support structures) with the following text prepared to accord with the geometry and stress analysis imperatives for the fuel basket: For the longitudinal MPC basket fillet welds, the following criteria apply: 1) The specified fillet weld throat dimension must be maintained over at least 92 percent of the total weld length. All regions of undersized weld must be less than 3 inches long and separated from each other by at least 9 inches. 2) Areas of undercuts and porosity beyond that allowed by the applicable ASME Code shall not exceed 1/2 inch in weld length. The total length of undercut and porosity over any 1-foot length shall not exceed 2 inches. 3) The total weld length in which items (1) and (2) apply shall not exceed a total of 10 percent of the overall weld length. The limited access of the MPC basket panel longitudinal fillet welds makes it difficult to perform effective repairs of these welds and creates the potential for causing additional damage to the basket assembly (e.g., to the neutron absorber and its sheathing) if repairs are attempted. The acceptance criteria provided in the foregoing have been established to comport with the objectives of the basket design and preserve the margins demonstrated in the supporting stress analysis.</p> <p>From the structural standpoint, the weld acceptance criteria are established to ensure that any departure from the ideal, continuous fillet weld seam would not alter the primary bending stresses on which the design of the fuel baskets is predicated. Stated differently, the permitted weld discontinuities are limited in size to ensure that they remain classifiable as local stress elevators ("peak stress", F, in the ASME Code for which specific stress intensity limits do not apply).</p>
MPC Basket Assembly	NG-8000	States requirements for nameplates, stamping and reports per NCA-8000.	The HI-STAR 100 System will be marked and identified in accordance with 10CFR71 and 10CFR72 requirements. No Code stamping is required. The MPC basket data package will be in conformance with Holtec's QA program.
Overpack Intermediate Shells	NF-2000	Requires materials to be supplied by ASME-approved material supplier.	Materials will be supplied by Holtec approved supplier with CMTRs in accordance with NF-2000 requirements.

Table 1.3.2 (continued)

LIST OF ASME CODE ALTERNATIVES FOR HI-STAR 100 SYSTEM

Component	Reference ASME Code Section/Article	Code Requirement	Alternative, Justification & Compensatory Measures
Overpack Containment Boundary	NB-2330	Defines the methods for determining the $T_{NDT}$ for impact testing of materials.	$T_{NDT}$ shall be defined in accordance with Regulatory Guides 7.11 and 7.12 for the containment boundary components.
Overpack Containment Boundary	NF-3320 NF-4720	NF-3324.6 and NF-4720 provide requirements for bolting.	<p>These Code requirements are applicable to linear structures wherein bolted joints carry axial, shear, as well as rotational (torsional) loads. The overpack bolted connections in the structural load path are qualified by design based on the design loadings defined in the SAR. Bolted joints in these components see no shear or torsional loads under normal storage conditions. Larger clearances between bolts and holes may be necessary to ensure shear interfaces located elsewhere in the structure engage prior to the bolts experiencing shear loadings (which occur only during side impact scenarios).</p> <p>Bolted joints that are subject to shear loads in accident conditions are qualified by appropriate stress analysis. Larger bolt-to-hole clearances help ensure more efficient operations in making these bolted connections, thereby minimizing time spent by operations personnel in a radiation area. Additionally, larger bolt-to-hole clearances allow interchangeability of the lids from one particular fabricated cask to another.</p>

Table 1.3.2 (continued)

LIST OF ASME CODE ALTERNATIVES FOR HI-STAR 100 SYSTEM

Component	Reference ASME Code Section/Article	Code Requirement	Alternative, Justification & Compensatory Measures
MPC-68 Serial #1021-023, 036, 037 Closure Rings	NB-2531	Requires UT inspection of plate.	The sole deviation of the 3/8" thick austenitic stainless steel material used for the MPC closure ring is the omission of a straight beam UT inspection as required by NB-2531. The ASME Code required straight beam inspection for vessels because the predominant indication in plates is laminations. Straight beam inspection cannot detect indications perpendicular to the surface of the plate. With respect to maintaining confinement, an indication perpendicular to the surface of the plate is the most critical. Laminations in the plate parallel to the surface of the plate cannot cause leakage through the plate. Therefore, the straight beam UT inspection does not add any value for detecting a defect in the thin closure ring with respect to its confinement function.

Table 1.3.3

## MATERIALS AND COMPONENTS OF THE HI-STAR 100 SYSTEM

OVERPACK <sup>(1,2)</sup>

Primary Function	Component <sup>(3)</sup>	Safety Class <sup>(4)</sup>	Codes/Standards (as applicable to component)	Material	Strength (ksi)	Special Surface Finish/Coating	Contact Matl. (if dissimilar)
Containment	Inner Shell	A	ASME Section III; Subsection NB	SA203-E or SA350-LF3	Table 2.3.4	Paint inside surface with Thermaline 450 (Note 5). External surface to be coated with a surface preservative.	NA
Containment	Bottom Plate	A	ASME Section III; Subsection NB	SA350-LF3	Table 2.3.4	Paint inside surface with Thermaline 450 (Note 5).	NA
Containment	Top Flange	A	ASME Section III; Subsection NB	SA350-LF3	Table 2.3.4	Paint inside surface with Thermaline 450. Paint outside surface with Carboline 890 (Note 5).	NA
Containment	Closure Plate	A	ASME Section III; Subsection NB	SA350-LF3	Table 2.3.4	Paint inside surface with Thermaline 450. Paint outside surface with Carboline 890 (Note 5).	NA
Containment	Closure Plate Bolts	A	ASME Section III; Subsection NB	SB637-N07718	Table 2.3.5	NA	NA
Containment	Port Plug	A	Non-code	SA193-B8	Not required	NA	NA
Containment	Port Plug Seal	A	Non-code	Alloy X750	Not required	NA	NA
Containment	Closure Plate Seal	A	Non-code	Alloy X750	Not required	NA	NA
Containment	Port Cover Seal	B	Non-code	Alloy X750	Not required	NA	NA

Notes: 1) There are no known residuals on finished component surfaces.

2) All welding processes used in welding the components shall be qualified in accordance with the requirements of ASME Section IX. All welds shall be made using welders qualified in accordance with ASME Section IX. Weld material shall meet the requirements of ASME Section II and the applicable Subsection of ASME Section III. For parts beyond the purview of ASME Section III, compliance with Section IX and Section II of the Code shall be observed to the extent practicable.

3) Component nomenclature taken from drawings in Chapter 1.

4) A,B and C denote important to safety classifications as described in NUREG/CR-6407. NITS stands for Not Important To Safety.

5) Thermaline 450 and Carboline 890 were the product names at the time of initial licensing. Chemically identical products with different names are permitted. For example, Carboline 890 was re-named Carboguard 890 in 2000, with no change to the coating material and is, therefore, acceptable for use where Carboline 890 is specified.

TABLE 1.3.3 (continued)

## MATERIALS AND COMPONENTS OF THE HI-STAR 100 SYSTEM

OVERPACK <sup>(1,2)</sup>

Primary Function	Component <sup>(3)</sup>	Safety Class <sup>(4)</sup>	Codes/Standards (as applicable to component)	Material	Strength (ksi)	Special Surface Finish/Coating	Contact Matl. (if dissimilar)
Shielding	Intermediate Shells	B	ASME Section III; Subsection NF	SA516-70	Table 2.3.2	Internal surfaces to be coated with a silicone encapsulant (Dow-Corning SYLGARD 567 or equivalent) for surface preservation, except for HI-STAR HB. Exposed areas of fifth intermediate shell to be painted with Carboline 890 (Note 5).	NA
Shielding	Neutron Shield	B	Non-code	Holtite-A	Not required	NA	Holtite/CS
Shielding	Plugs for Drilled Holes	NITS	Non-code	SA193-B7	Not required	NA	NA
Shielding	Removable Shear Ring	B	ASME Section III; Subsection NF	Carbon Steel	Not required	Paint external surface with Carboline 890 (Note 5).	NA
Shielding	Pocket Trunnion Plug Plate	C	Non-code	SA240-304	Not required	NA	NA
Heat Transfer	Radial Channels (not used on the HI-STAR HB)	B	ASME Section III; Subsection NF	SA515-70	Table 2.3.3	Paint outside surface with Carboline 890 (Note 5).	NA

Notes: 1) There are no known residuals on finished component surfaces.

2) All welding processes used in welding the components shall be qualified in accordance with the requirements of ASME Section IX. All welds shall be made using welders qualified in accordance with ASME Section IX. Weld material shall meet the requirements of ASME Section II and the applicable Subsection of ASME Section III. For parts beyond the purview of ASME Section III, compliance with Section IX and Section II of the Code shall be observed to the extent practicable.

3) Component nomenclature taken from drawings in Chapter 1.

4) A,B and C denote important to safety classifications as described in NUREG/CR-6407. NITS stands for Not Important To Safety.

5) Thermaline 450 and Carboline 890 were the product names at the time of initial licensing. Chemically identical products with different names are permitted. For example, Carboline 890 was re-named Carboguard 890 in 2000, with no change to the coating material and is, therefore, acceptable for use where Carboline 890 is specified.

TABLE 1.3.3 (continued)

## MATERIALS AND COMPONENTS OF THE HI-STAR 100 SYSTEM

OVERPACK <sup>(1,2)</sup>

Primary Function	Component <sup>(3)</sup>	Safety Class <sup>(4)</sup>	Codes/Standards (as applicable to component)	Material	Strength (ksi)	Special Surface Finish/Coating	Contact Matl. (if dissimilar)
Rotation Pivot and Shielding	Pocket Trunnion	B	Non-Code	SA705-630 17-4 PH or SA564-630 17-4 PH	Table 2.3.5	NA	NA
Structural Integrity	Lifting Trunnion	A	ANSI N14.6	SB637- N07718	Table 2.3.5	NA	NA
Structural Integrity	Relief Device	C	Non-code	Commercial	Not required	NA	Brass-C/S
Structural Integrity	Relief Device Plate	C	Non-code	SA 516 Grade 70 or A569	Not required	NA	NA
Structural Integrity	Removable Shear Ring Bolt	C	Non-code	SA193-B7	Not required	NA	NA
Structural Integrity	Thermal Expansion Foam	NITS	Non-code	Silicone Foam	Not required	NA	Silicone with CS, brass, and Holtite
Structural Integrity	Closure Bolt Washer	NITS	Non-code	ASTM A564, 17-7 PH	Not required	NA	NA
Structural Integrity	Enclosure Shell Panels	B	ASME Section III; Subsection NF	SA515-70	Table 2.3.3	Paint outside surface with Carboline 890 (Note 5).	NA

Notes: 1) There are no known residuals on finished component surfaces.

2) All welding processes used in welding the components shall be qualified in accordance with the requirements of ASME Section IX. All welds shall be made using welders qualified in accordance with ASME Section IX. Weld material shall meet the requirements of ASME Section II and the applicable Subsection of ASME Section III. For parts beyond the purview of ASME Section III, compliance with Section IX and Section II of the Code shall be observed to the extent practicable.

3) Component nomenclature taken from drawings in Chapter 1.

4) A,B and C denote important to safety classifications as described in NUREG/CR-6407. NITS stands for Not Important To Safety.

5) Thermaline 450 and Carboline 890 were the product names at the time of initial licensing. Chemically identical products with different names are permitted. For example, Carboline 890 was re-named Carboguard 890 in 2000, with no change to the coating material and is, therefore, acceptable for use where Carboline 890 is specified.

TABLE 1.3.3 (continued)

## MATERIALS AND COMPONENTS OF THE HI-STAR 100 SYSTEM

OVERPACK <sup>(1,2)</sup>

Primary Function	Component <sup>(3)</sup>	Safety Class <sup>(4)</sup>	Codes/Standards (as applicable to component)	Material	Strength (ksi)	Special Surface Finish/Coating	Contact Matl. (if dissimilar)
Structural Integrity	Enclosure Shell Return	B	ASME Section III; Subsection NF	SA515-70	Table 2.3.3	Paint outside surface with Carboline 890 (Note 5).	NA
Structural Integrity	Port Cover	B	ASME Section III; Subsection NF	SA203E or SA350-LF3	Table 2.3.4	Paint outside surface with Carboline 890 (Note 5).	NA
Structural Integrity	Port Cover Bolt	C	Non-code	SA193-B7	Not required	NA	NA
Operations	Trunnion Locking Pad and End Cap Bolt	C	Non-code	SA193-B7	Not required	NA	NA
Operations	Lifting Trunnion End Cap	C	Non-code	SA516-70 or SA515 Gr. 70	Table 2.3.2	Paint exposed surfaces with Carboline 890 (Note 5).	NA
Operations	Lifting Trunnion Locking Pad	C	Non-code	SA516-70	Table 2.3.2	Paint exposed surfaces with Carboline 890 (Note 5).	NA
Operations	Nameplate	NITS	Non-code	S/S	Not required	NA	NA

Notes: 1) There are no known residuals on finished component surfaces.

2) All welding processes used in welding the components shall be qualified in accordance with the requirements of ASME Section IX. All welds shall be made using welders qualified in accordance with ASME Section IX. Weld material shall meet the requirements of ASME Section II and the applicable Subsection of ASME Section III. For parts beyond the purview of ASME Section III, compliance with Section IX and Section II of the Code shall be observed to the extent practicable.

3) Component nomenclature taken from drawings in Chapter 1.

4) A,B and C denote important to safety classifications as described in NUREG/CR-6407. NITS stands for Not Important To Safety.

5) Thermaline 450 and Carboline 890 were the product names at the time of initial licensing. Chemically identical products with different names are permitted. For example, Carboline 890 was re-named Carboguard 890 in 2000, with no change to the coating material and is, therefore, acceptable for use where Carboline 890 is specified.

Table 1.3.3 (cont'd)

## MATERIALS AND COMPONENTS OF THE HI-STAR 100 SYSTEM

MPC <sup>(1,2)</sup>

Primary Function	Component <sup>(3)</sup>	Safety Class <sup>(4)</sup>	Codes/Standards (as applicable to component)	Material	Strength (ksi)	Special Surface Finish/Coating	Contact Matl. (if dissimilar)
Helium Retention	Shell	A	ASME Section III; Subsection NB	Alloy X <sup>(5)</sup>	See Appendix 1.A	NA	NA
Helium Retention	Baseplate	A	ASME Section III; Subsection NB	Alloy X	See Appendix 1.A	NA	NA
Helium Retention	Lid (One-piece design and top portion of optional two-piece design)	A	ASME Section III; Subsection NB	Alloy X	See Appendix 1.A	NA	NA
Helium Retention	Closure Ring	A	ASME Section III; Subsection NB	Alloy X	See Appendix 1.A	NA	NA
Helium Retention	Port Cover Plates	A	ASME Section III; Subsection NB	Alloy X	See Appendix 1.A	NA	NA
Criticality Control	Basket Cell Plates	A	ASME Section III; Subsection NG; core support structures (NG-1121)	Alloy X	See Appendix 1.A	NA	NA
Criticality Control	Boral	A	Non-code	NA	NA	NA	Aluminum/SS
Shielding	Drain and Vent Shield Block	C	Non-code	Alloy X	See Appendix 1.A	NA	NA
Shielding	Plugs for Drilled Holes	NITS	Non-code	Alloy X	See Appendix 1.A	NA	NA
Shielding	Bottom portion of optional two-piece MPC lid design	B	Non-code	Alloy X	See Appendix 1.A	NA	NA
Heat Transfer	Optional Heat Conduction Elements	B	Non-code	Aluminum; Alloy 1100	NA	Sandblast Specified	Aluminum/SS

Notes: 1) There are no known residuals on finished component surfaces.

2) All welding processes used in welding the components shall be qualified in accordance with the requirements of ASME Section IX. All welds shall be made using welders qualified in accordance with ASME Section IX. Weld material shall meet the requirements of ASME Section II and the applicable Subsection of ASME Section III. For parts beyond the purview of ASME Section III, compliance with Section IX and Section II of the Code shall be observed to the extent practicable.

3) Component nomenclature taken from Bill of Materials in Chapter 1.

4) A,B and C denote important to safety classifications as described in NUREG/CR-6407. NITS stands for Not Important To Safety.

5) For details on Alloy X material, see Appendix 1.A.

TABLE 1.3.3 (continued)

MATERIALS AND COMPONENTS OF THE HI-STAR 100 SYSTEM

MPC<sup>(1,2)</sup>

Primary Function	Component <sup>(3)</sup>	Safety Class <sup>(4)</sup>	Codes/Standards (as applicable to component)	Material	Strength (ksi)	Special Surface Finish/Coating	Contact Matl. (if dissimilar)
						Surfaces	
Structural Integrity	Upper Fuel Spacer Column	B	ASME Section III; Subsection NG (only for stress analysis)	Alloy X	See Appendix 1.A	NA	NA
Structural Integrity	Sheathing	A	Non-code	Alloy X	See Appendix 1.A	Aluminum/SS	NA
Structural Integrity	Shims	NITS	Non-code	Alloy X	See Appendix 1.A	NA	NA
Structural Integrity	Basket Supports (Angled Plates)	A	ASME Section III; Subsection NG; internal structures (NG-1122)	Alloy X	See Appendix 1.A	NA	NA
Structural Form	Basket Supports (Flat Plates)	NITS	Non-code	Alloy X	See Appendix 1.A	NA	NA
Structural Integrity	Upper Fuel Spacer Bolt	NITS	Non-code	A193-B8	Per ASME Section II	NA	NA
Structural Integrity	Upper Fuel Spacer End Plate	B	Non-code	Alloy X	See Appendix 1.A	NA	NA
Structural Integrity	Lower Fuel Spacer Column	B	ASME Section III; Subsection NG (only for stress analysis)	S/S	See Appendix 1.A	NA	NA
Structural Integrity	Lower Fuel Spacer End Plate	B	Non-code	Alloy X	See Appendix 1.A	NA	NA

Notes: 1) There are no known residuals on finished component surfaces.

2) All welding processes used in welding the components shall be qualified in accordance with the requirements of ASME Section IX. All welds shall be made using welders qualified in accordance with ASME Section IX. Weld material shall meet the requirements of ASME Section II and the applicable Subsection of ASME Section III. For parts beyond the purview of ASME Section III, compliance with Section IX and Section II of the Code shall be observed to the extent practicable.

3) Component nomenclature taken from Bill of Materials in Chapter 1.

4) A,B and C denote important to safety classifications as described in NUREG/CR-6407. NITS stands for Not Important To Safety.

5) For details on Alloy X material, see Appendix 1.A.

TABLE 1.3.3 (continued)

## MATERIALS AND COMPONENTS OF THE HI-STAR 100 SYSTEM

MPC<sup>(1,2)</sup>

Primary Function	Component <sup>(3)</sup>	Safety Class <sup>(4)</sup>	Codes/Standards (as applicable to component)	Material	Strength (ksi)	Special Surface Finish/Coating	Contact Matl. (if dissimilar)
Structural Integrity	Vent Shield Block Spacer	C	Non-code	Alloy X	See Appendix 1.A	NA	NA
Structural Integrity	Trojan MPC Spacer	B	Non-code	304 S/S	Per ASME Section II	NA	NA
Structural Integrity	Trojan Failed Fuel Can Spacer	B	ASME Section III, Subsection NF	304 or 304LN S/S	Per ASME Section II	NA	NA
Operations	Vent and Drain Tube	C	Non-code	S/S	Per ASME Section II	Thread area surface hardened	NA
Operations	Vent & Drain Cap	C	Non-code	S/S	Per ASME Section II	NA	NA
Operations	Vent & Drain Cap Seal Washer	NITS	Non-code	Aluminum	NA	NA	Aluminum/SS
Operations	Vent & Drain Cap Seal Washer Bolt	NITS	Non-code	Aluminum	NA	NA	NA
Operations	Reducer	NITS	Non-code	Alloy X	See Appendix 1.A	NA	NA
Operations	Drain Line	NITS	Non-code	Alloy X	See Appendix 1.A	NA	NA
Operations	Damaged Fuel Container	C	ASME Section III; Subsection NG	Primarily 304 S/S	See Appendix 1.A	NA	NA
Operations	Trojan Failed Fuel Can	C	ASME Section III; Subsection NG	304 S/S	Per ASME Section II	NA	NA
Operations	Drain Line Guide Tube	NITS	Non-code	S/S	NA	NA	NA

Notes: 1) There are no known residuals on finished component surfaces.

2) All welding processes used in welding the components shall be qualified in accordance with the requirements of ASME Section IX. All welds shall be made using welders qualified in accordance with ASME Section IX. Weld material shall meet the requirements of ASME Section II and the applicable Subsection of ASME Section III. For parts beyond the purview of ASME Section III, compliance with Section IX and Section II of the Code shall be observed to the extent practicable.

3) Component nomenclature taken from Bill of Materials in Chapter 1.

4) A, B and C denote important to safety classifications as described in NUREG/CR-6407. NITS stands for Not Important To Safety.

5) For details on Alloy X material, see Appendix 1.A.

1.4 DRAWINGS

The following drawings provide sufficient detail to describe the HI-STAR 100 packaging. Refer to Supplement 1.I for drawings related to the HI-STAR HB.

The classification of all components important to safety in accordance with Regulatory Guide 7.10 and NUREG/CR-6407 is provided in Table 1.3.3. Operational information, such as bolt torque and pressure-relief specifications are provided in Chapters 7 and 8. The maximum weight of the package and the maximum weight of the contents is provided in Table 2.2.1.

The following HI-STAR 100 System design drawings are provided in this section.

Drawing Number/Sheet	Description	Rev.
3913	Licensing Drawing for HI-STAR 100 Overpack Assembly	10
3923	Licensing Drawing for MPC Enclosure Vessel	25
3925	Licensing Drawing for MPC-24E/EF Fuel Basket Assembly	9
3926	Licensing Drawing for MPC-24 Fuel Basket Assembly	11
3927	Licensing Drawing for MPC-32 Fuel Basket Assembly	16
3928	Licensing Drawing for MPC-68/68F/68FF Fuel Basket Assembly	14
5014-C1765 Sht 1/7 <sup>†</sup>	HI-STAR 100 Impact Limiter	6
5014-C1765 Sht 2/7 <sup>†</sup>	HI-STAR 100 Bottom Impact Limiter	4
5014-C1765 Sht 3/7 <sup>†</sup>	HI-STAR 100 Top Impact Limiter	5
5014-C1765 Sht 4/7 <sup>†</sup>	HI-STAR 100 Top Impact Limiter	5
5014-C1765 Sht 5/7 <sup>†</sup>	HI-STAR 100 Top Impact Limiter Detail of Item #6	2
5014-C1765 Sht 6/7 <sup>†</sup>	HI-STAR 100 Impact Limiter Honeycomb Details	5
5014-C1765 Sht 7/7 <sup>†</sup>	HI-STAR 100 Bottom Impact Limiter	1
3930	HI-STAR 100 Assembly For Transport	2
4111	Licensing Drawing for Trojan MPC Spacer Ring	0
4119	Licensing Drawing for Holtec Damaged Fuel Container for Trojan Plant Fuel	1

<sup>†</sup> These drawing titles include the term "CoC No. 9261, Appendix B." Rather than appending the drawings directly to the CoC, they are incorporated into the CoC by reference. The "Appendix B" will be removed from each drawing as part of its next normal revision.

<b>Drawing Number/Sheet</b>	<b>Description</b>	<b>Rev.</b>
4122	Licensing Drawing for Trojan FFC Spacer	0
PFFC-001	Failed Fuel Can Assembly	8
PFFC-002	Failed Fuel Can Shell and Lid Assembly	7

DRAWINGS WITHHELD IN ACCORDANCE WITH 10CFR2.390

## 1.5 Compliance with 10CFR71

The HI-STAR 100 packaging complies with the requirements of 10CFR71 for a Type B(U)F-96 package. Analyses which demonstrate that the HI-STAR 100 packaging complies with the requirements of Subparts E and F of 10CFR71 are provided in this SAR. Specific reference to each section of the SAR that is used to specifically address compliance is provided in Table 1.0.2. The HI-STAR 100 packaging complies with the general standards for all packages, 10CFR71.43, as demonstrated in Section 2.4. Under the tests specified in 10CFR71.71 (normal conditions of transport) the HI-STAR 100 packaging is demonstrated to sustain no degradation in its safety function allowing the HI-STAR 100 packaging to meet the requirements of 10CFR71, Paragraphs 71.45, 71.51, and 71.55. Under the tests specified in 10CFR71.73 (hypothetical accident conditions) and 10CFR71.61 (special requirement for irradiated nuclear fuel shipments), the degradation sustained by the HI-STAR 100 packaging is shown not to cause the HI-STAR 100 packaging to exceed the requirements of 10CFR71, Paragraphs 71.51, 71.55, and 71.63.

The HI-STAR 100 packaging meets the structural, thermal, containment, shielding and criticality requirements of 10CFR71, as described in Chapters 2 through 6. The operational procedures and acceptance tests and maintenance program provided in Chapters 7 and 8 ensure compliance with the requirements of 10CFR71.

The following is a summary of the information provided in Chapter 1 that is directly applicable to verifying compliance with 10CFR71:

- The HI-STAR 100 packaging has been described in sufficient detail to provide an adequate basis for its evaluation.
- Drawings provided in Section 1.4 contain information that provides an adequate basis for evaluation of the HI-STAR 100 packaging against the 10CFR71 requirements. Each drawing is identified, consistent with the text of the SAR, and contains keys or annotation to explain and clarify information on the drawing.
- Section 1.0 includes a reference to the NRC-approved Holtec International quality assurance program for the HI-STAR 100 packaging.
- Section 1.3 identifies the applicable codes and standards for the HI-STAR 100 packaging design, fabrication, assembly, and testing.
- The HI-STAR 100 packaging meets the general requirements of 10CFR71.43(a) and 10CFR71.43(b), as demonstrated by the drawings provided in Section 1.4 and the discussion provided in Subsection 1.2.1.9, respectively.
- The drawings provided in Section 1.4 provide a detailed packaging description that can be evaluated for compliance with 10CFR71 for each technical discipline.

- Any restrictions on the use of the HI-STAR 100 packaging are specified in Subsection 1.2.3 and Chapter 7.

1.6 REFERENCES

- [1.0.1] 10CFR Part 71, "Packaging and Transportation of Radioactive Materials", Title 10 of the Code of Federal Regulations, Office of the Federal Register, Washington, D.C.
- [1.0.2] 49CFR173, "Shippers - General Requirements For Shipments and Packagings", Title 49 of the Code of Federal Regulations, Office of the Federal Register, Washington, D.C.
- [1.0.3] Regulatory Guide 7.9, "Standard Format and Content of Part 71 Applications for Approval of Packaging for Radioactive Material", Proposed Revision 2, USNRC, May 1986.
- [1.0.4] 10CFR Part 72, "Licensing Requirements for the Storage of Spent Fuel in an Independent Spent Fuel Storage Installation", Title 10 of the Code of Federal Regulations, Office of the Federal Register, Washington, D.C.
- [1.0.5] NUREG-1617, "Standard Review Plan for Transportation Packages for Spent Nuclear Fuel", , U.S. Nuclear Regulatory Commission, March 2000.
- [1.0.6] HI-STAR 100 Final Safety Analysis Report, Holtec Report No. HI-2012610, Revision 1, Docket No. 72-1008.
- [1.0.7] HI-STORM 100 Final Safety Analysis Report, Holtec Report No. HI-2002444, Revision 1, Docket No. 72-1014.
- [1.0.8] Pacific Gas & Electric Company HIL-06-001, "Humboldt Bay ISFSI Final Safety Analysis Report", Revision 0, January 2006, USNRC Docket 72-27.
- [1.1.1] U.S. Department of Energy, "Multi-Purpose Canister (MPC) Subsystem Design Procurement Specification", Document No. DBG000000-01717-6300-00001, Rev. 5, January 11, 1996.
- [1.1.2] U.S. Department of Energy, "MPC Transportation Cask Subsystem Design Procurement Specification", Document No. DBF 000000-01717-6300-00001, Rev. 5, January 11, 1996.
- [1.2.1] U.S. NRC Information Notice 96-34, "Hydrogen Gas Ignition During Closure Welding of a VSC-24 Multi-Assembly Scale Basket".
- [1.2.2] Directory of Nuclear Reactors, Vol. II, Research, Test & Experimental Reactors, International Atomic Energy Agency, Vienna, 1959.
- [1.2.3] V.L. McKinney and T. Rockwell III, Boral: A New Thermal-Neutron Shield,

USAEC Report AECD-3625, August 29, 1949.

- [1.2.4] Reactor Shielding Design Manual, USAEC Report TID-7004, March 1956.
- [1.2.5] Deleted.
- [1.2.6] ORNL/TM-10902, "Physical Characteristics of GE BWR Fuel Assemblies", by R.S. Moore and K.J. Notz, Martin Marietta (1989).
- [1.2.7] U.S. DOE SRC/CNEAF/95-01, Spent Nuclear Fuel Discharges from U.S. Reactors 1993, Feb. 1995.
- [1.2.8] S.E. Turner, "Uncertainty Analysis - Axial Burnup Distribution Effects," presented in "Proceedings of a Workshop on the Use of Burnup Credit in Spent Fuel Transport Casks", SAND-89-0018, Sandia National Laboratory, Oct., 1989.
- [1.2.9] Commonwealth Edison Company, Report No. NFS-BND-95-083, Chicago, Illinois.
- [1.2.10] Regulatory Guide 7.11, "Fracture Toughness Criteria of Base Material for Ferritic Steel Shipping Cask Containment Vessels with a Maximum Wall Thickness of 4 Inches (0.1m)", U.S. Nuclear Regulatory Commission, Washington, D.C., June 1991.
- [1.2.11] NUREG-0612, "Control of Heavy Loads at Nuclear Power Plants", U.S. Nuclear Regulatory Commission, Washington, D.C., July 1980.
- [1.2.12] Trojan ISFSI Safety Analysis Report, Revision 3, USNRC Docket 72-0017.
- [1.2.13] NRC Interim Staff Guidance Document No. 8, "Burnup Credit in the Criticality Safety Analyses of PWR Spent Fuel in Transportation and Storage Casks", Revision 2.
- [1.2.14] NRC Interim Staff Guidance Document No. 11, "Cladding Considerations for the Transportation and Storage of Spent Fuel", Revision 3.
- [1.2.15] DOE/RW-0184, Volume 3, "Characteristics of Spent Fuel, High Level Waste, and Other Radioactive Wastes Which May Require Long-Term Isolation," Appendix 2.A, "Physical Descriptions of LWR Fuel Assemblies," U.S. Department of Energy, Office of Civilian Radioactive Waste Management, December 1987.
- [1.2.16] PGE Letter ISFSI-004-04L, dated June 17, 2004, "Change to the Definition of Damaged Fuel – Detailed Trojan Fuel Assembly Damage", from S. B.

Nichols (PGE) to Eric G. Lewis (Holtec)

- [1.2.17] "Qualification of METAMIC® for Spent Fuel Storage Application," EPRI, 1003137, Final Report, October 2001.
- [1.2.18] "Safety Evaluation by the Office of Nuclear Reactor Regulation Related to Holtec International Report HI-2022871 Regarding Use of Metamic in Fuel Pool Applications," Facility Operating License Nos. DPR-51 and NPF-6, Entergy Operations, Inc., Docket No. 50-313 and 50-368, USNRC, June 2003.
- [1.2.19] "Metamic 6061+40% Boron Carbide Metal Matrix Composite Test", California Consolidated Tech. Inc. Report dated August 21, 2001 to NAC International.
- [1.2.20] "Recommendations for Preparing the Criticality Safety Evaluation for Transportation Packages", NUREG/CR-5661, USNRC, Dyer and Parks, ORNL.
- [1.2.21] Holtec Proprietary Report HI-2043215, "Sourcebook for Metamic Performance Assessment", Revision 2.
- [1.3.1] American Society of Mechanical Engineers, "Boiler and Pressure Vessel Code", 1995 with Addenda through 1997.
- [1.3.2] NUREG/CR-6407, "Classification of Transportation Packaging and Dry Spent Fuel Storage System Components According to Importance to Safety", U.S. Nuclear Regulatory Commission, Washington D.C., February 1996.
- [1.3.3] ANSIN14.6-1993, "Special Lifting Devices for Shipping Containers Weighing 10,000 Pounds (4500 Kg) or More", June 1993.

**APPENDIX 1.A: ALLOY X DESCRIPTION****1.A ALLOY X DESCRIPTION****1.A.1 Alloy X Introduction**

Alloy X is used within this licensing application to designate a group of stainless steel alloys. Alloy X can be any one of the following alloys:

- Type 316
- Type 316LN
- Type 304
- Type 304LN

Qualification of structures made of Alloy X is accomplished by using the least favorable mechanical and thermal properties of the entire group for all MPC mechanical, structural, neutronic, radiological, and thermal conditions. The Alloy X approach is conservative because no matter which material is ultimately utilized, the Alloy X approach guarantees that the performance of the MPC will meet or exceed the analytical predictions.

This appendix defines the least favorable material properties of Alloy X.

**1.A.2 Alloy X Common Material Properties**

Several material properties do not vary significantly from one Alloy X constituent to the next. These common material properties are as follows:

- density
- specific heat
- Young's Modulus (Modulus of Elasticity)
- Poisson's Ratio

The values utilized for this licensing application are provided in their appropriate chapters.

**1.A.3 Alloy X Least Favorable Material Properties**

The following material properties vary between the Alloy X constituents:

- Design Stress Intensity ( $S_m$ )
- Tensile (Ultimate) Strength ( $S_u$ )
- Yield Strength ( $S_y$ )
- Coefficient of Thermal Expansion ( $\alpha$ )
- Coefficient of Thermal Conductivity ( $k$ )

Each of these material properties are provided in the ASME Code Section II [1.A.1]. Tables 1.A.1 through 1.A.5 provide the ASME Code values for each constituent of Alloy X along with the least favorable value utilized in this licensing application. The ASME Code only provides values to -20°F. The design temperature of the MPC is -40°F to 725°F as stated in Table 1.2.3. Most of the above-mentioned properties become increasingly favorable as the temperature drops. Conservatively, the values at the lowest design temperature for the HI-STAR 100 System have been assumed to be equal to the lowest value stated in the ASME Code. The lone exception is the thermal conductivity. The thermal conductivity decreases with the decreasing temperature. The thermal conductivity value for -40°F is linearly extrapolated from the 70°F value using the difference from 70°F to 100°F.

The Alloy X material properties are the minimum values of the group for the design stress intensity, tensile strength, yield strength, and coefficient of thermal conductivity. Using minimum values of design stress intensity is conservative because lower design stress intensities lead to lower allowables that are based on design stress intensity. Similarly, using minimum values of tensile strength and yield strength is conservative because lower values of tensile strength and yield strength lead to lower allowables that are based on tensile strength and yield strength. When compared to calculated values, these lower allowables result in factors of safety that are conservative for any of the constituent materials of Alloy X. Further discussion of the justification for using the minimum values of coefficient of thermal conductivity is given in Chapter 3. The maximum and minimum values are used for the coefficient of thermal expansion of Alloy X. The maximum and minimum coefficients of thermal expansion are used as appropriate in this submittal. Figures 1.A.1-1.A.5 provide a graphical representation of the varying material properties with temperature for the Alloy X materials.

#### 1.A.4 References

[1.A.1] ASME Boiler & Pressure Vessel Code Section II, 1995 ed. with Addenda through 1997.

Table 1.A.1

ALLOY X AND CONSTITUENT DESIGN STRESS INTENSITY ( $S_m$ ) vs. TEMPERATURE

Temp. ( $^{\circ}$ F)	Type 304	Type 304LN	Type 316	Type 316LN	Alloy X (minimum of constituent values)
-40	20.0	20.0	20.0	20.0	20.0
100	20.0	20.0	20.0	20.0	20.0
200	20.0	20.0	20.0	20.0	20.0
300	20.0	20.0	20.0	20.0	20.0
400	18.7	18.7	19.3	18.9	18.7
500	17.5	17.5	18.0	17.5	17.5
600	16.4	16.4	17.0	16.5	16.4
650	16.2	16.2	16.7	16.0	16.0
700	16.0	16.0	16.3	15.6	15.6
750	15.6	15.6	16.1	15.2	15.2
800	15.2	15.2	15.9	14.9	14.9

## Notes:

1. Source: Table 2A on pages 314, 318, 326, and 330 of [1.A.1].
2. Units of design stress intensity values are ksi.

Table 1.A.2

ALLOY X AND CONSTITUENT TENSILE STRENGTH ( $S_u$ ) vs. TEMPERATURE

Temp. (°F)	Type 304	Type 304LN	Type 316	Type 316LN	Alloy X (minimum of constituent values)
-40	75.0 (70.0)	75.0 (70.0)	75.0 (70.0)	75.0 (70.0)	75.0 (70.0)
100	75.0 (70.0)	75.0 (70.0)	75.0 (70.0)	75.0 (70.0)	75.0 (70.0)
200	71.0 (66.2)	71.0 (66.2)	75.0 (70.0)	75.0 (70.0)	71.0 (66.2)
300	66.0 (61.5)	66.0 (61.5)	73.4 (68.5)	70.9 (66.0)	66.0 (61.5)
400	64.4 (60.0)	64.4 (60.0)	71.8 (67.0)	67.1 (62.6)	64.4 (60.0)
500	63.5 (59.3)	63.5 (59.3)	71.8 (67.0)	64.6 (60.3)	63.5 (59.3)
600	63.5 (59.3)	63.5 (59.3)	71.8 (67.0)	63.1 (58.9)	63.1 (58.9)
650	63.5 (59.3)	63.5 (59.3)	71.8 (67.0)	62.8 (58.6)	62.8 (58.6)
700	63.5 (59.3)	63.5 (59.3)	71.8 (67.0)	62.5 (58.4)	62.5 (58.4)
750	63.1 (58.9)	63.1 (58.9)	71.4 (66.5)	62.2 (58.1)	62.2 (58.1)
800	62.7 (58.5)	62.7 (58.5)	70.9 (66.2)	61.7 (57.6)	61.7 (57.6)

## Notes:

1. Source: Table U on pages 437, 439, 441, and 443 of [1.A.1].
2. Units of tensile strength are ksi.
3. Values in parentheses are for SA-336 forging material (Types F304, F304LN, F316, and F316LN) that are used solely for the one-piece MPC lids. Other values correspond to SA-240 plate material.

Table 1.A.3

ALLOY X AND CONSTITUENT YIELD STRESSES ( $S_y$ ) vs. TEMPERATURE

Temp. (°F)	Type 304	Type 304LN	Type 316	Type 316LN	Alloy X (minimum of constituent values)
-40	30.0	30.0	30.0	30.0	30.0
100	30.0	30.0	30.0	30.0	30.0
200	25.0	25.0	25.8	25.5	25.0
300	22.5	22.5	23.3	22.9	22.5
400	20.7	20.7	21.4	21.0	20.7
500	19.4	19.4	19.9	19.4	19.4
600	18.2	18.2	18.8	18.3	18.2
650	17.9	17.9	18.5	17.8	17.8
700	17.7	17.7	18.1	17.3	17.3
750	17.3	17.3	17.8	16.9	16.9
800	16.8	16.8	17.6	16.6	16.6

## Notes:

1. Source: Table Y-1 on pages 518, 519, 522, 523, 530, 531, 534, and 535 of [1.A.1].
2. Units of yield stress are ksi.

Table 1.A.4

ALLOY X AND CONSTITUENT COEFFICIENT OF THERMAL EXPANSION  
vs. TEMPERATURE

Temp. (°F)	Type 304 and Type 304LN	Type 316 and Type 316LN	Alloy X Maximum	Alloy X Minimum
-40	8.55	8.54	8.55	8.54
100	8.55	8.54	8.55	8.54
150	8.67	8.64	8.67	8.64
200	8.79	8.76	8.79	8.76
250	8.90	8.88	8.90	8.88
300	9.00	8.97	9.00	8.97
350	9.10	9.11	9.11	9.10
400	9.19	9.21	9.21	9.19
450	9.28	9.32	9.32	9.28
500	9.37	9.42	9.42	9.37
550	9.45	9.50	9.50	9.45
600	9.53	9.60	9.60	9.53
650	9.61	9.69	9.69	9.61
700	9.69	9.76	9.76	9.69
750	9.76	9.81	9.81	9.76
800	9.82	9.90	9.90	9.82

## Notes:

1. Source: Table TE-1 on pages 590 and 591 of [1.A.1].
2. Units of coefficient of thermal expansion are in./in.-°F x 10<sup>-6</sup>.

Table 1.A.5

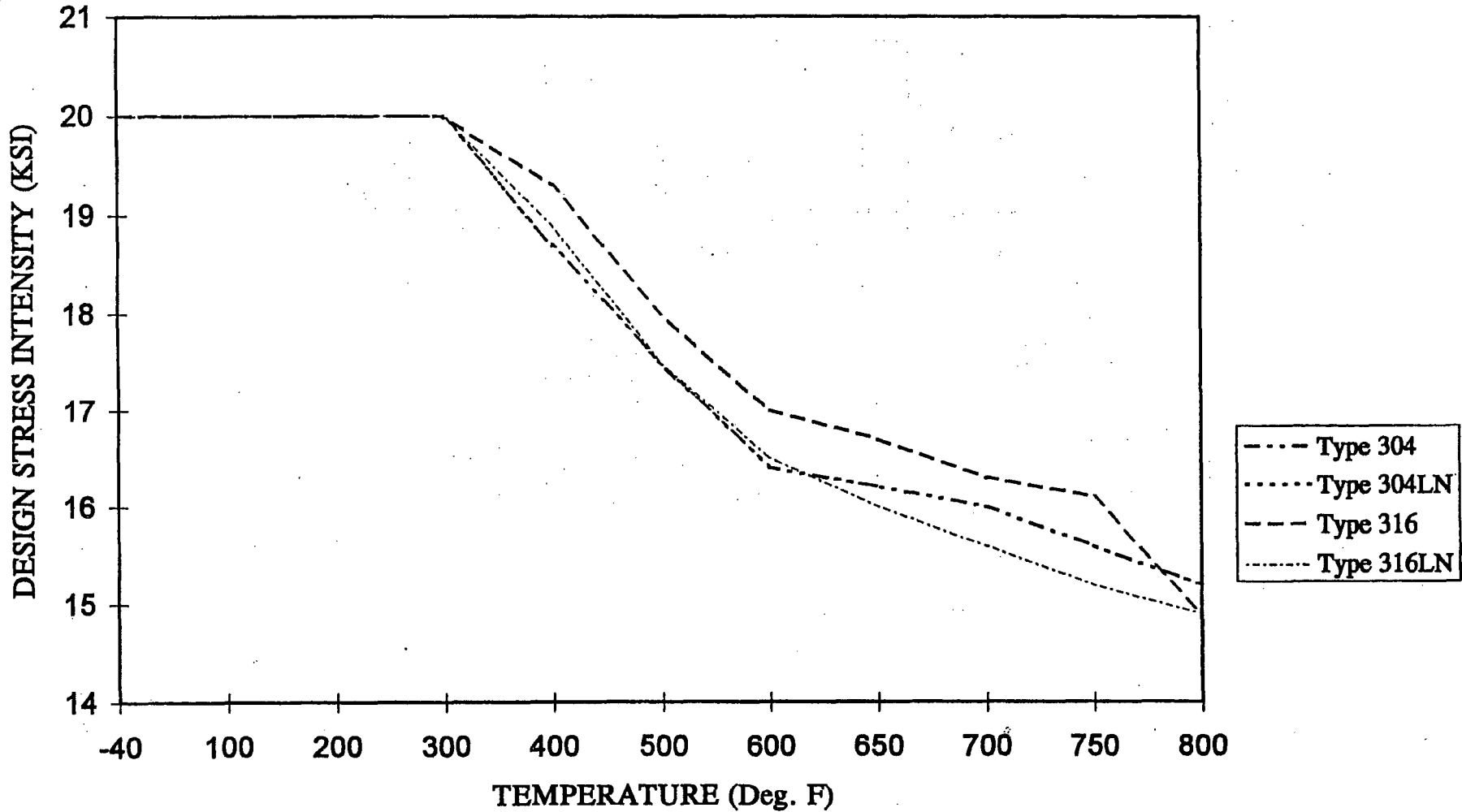
## ALLOY X AND CONSTITUENT THERMAL CONDUCTIVITY vs. TEMPERATURE

Temp. (°F)	Type 304 and Type 304LN	Type 316 and Type 316LN	Alloy X (minimum of constituent values)
-40	8.23	6.96	6.96
70	8.6	7.7	7.7
100	8.7	7.9	7.9
150	9.0	8.2	8.2
200	9.3	8.4	8.4
250	9.6	8.7	8.7
300	9.8	9.0	9.0
350	10.1	9.2	9.2
400	10.4	9.5	9.5
450	10.6	9.8	9.8
500	10.9	10.0	10.0
550	11.1	10.3	10.3
600	11.3	10.5	10.5
650	11.6	10.7	10.7
700	11.8	11.0	11.0
750	12.0	11.2	11.2
800	12.2	11.5	11.5

## Notes:

1. Source: Table TCD on page 606 of [1.A.1].
2. Units of thermal conductivity are Btu/hr-ft-°F.

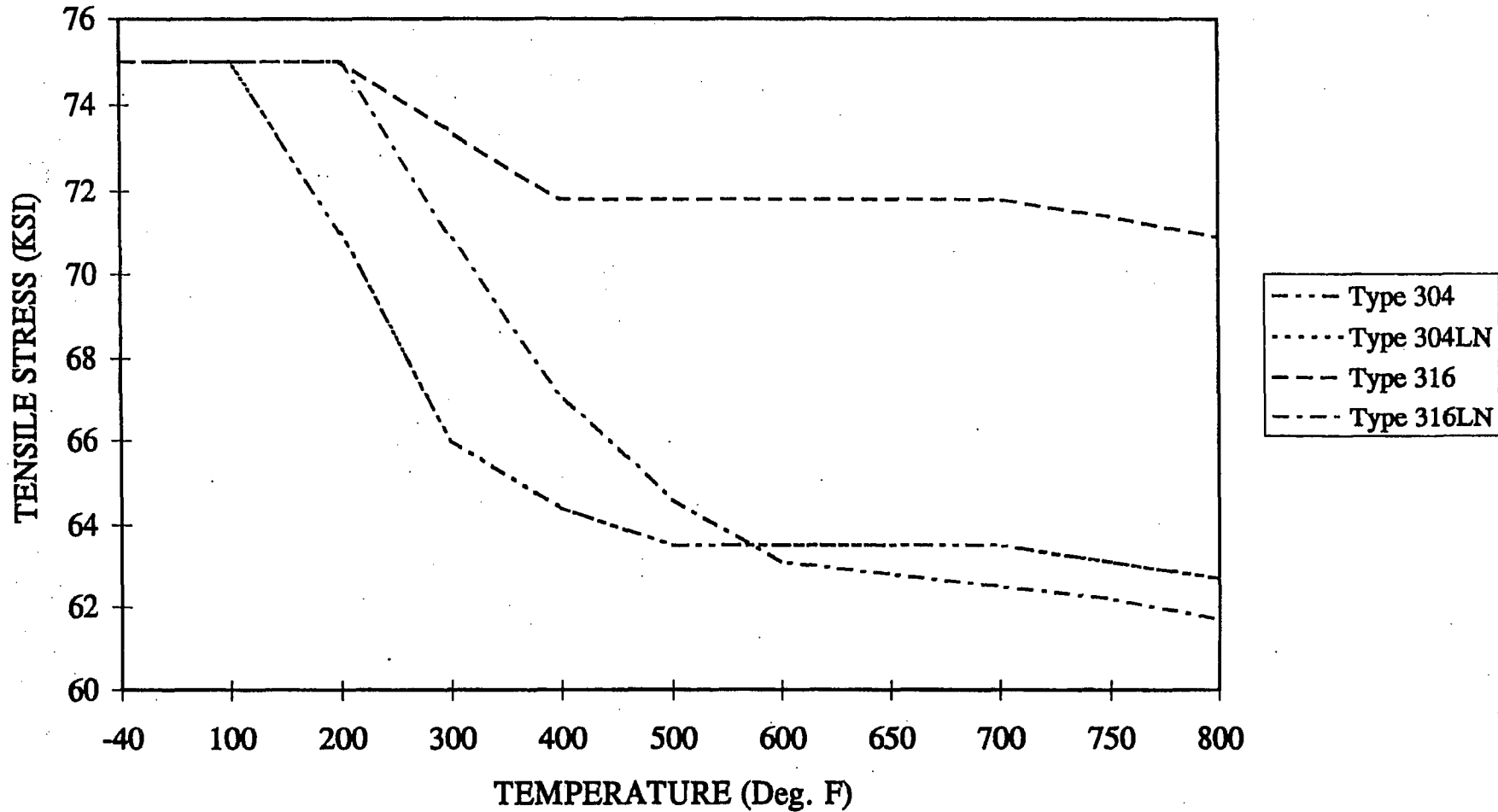
### DESIGN STRESS INTENSITY VS. TEMPERATURE



SOURCE: TABLE 1.A.1

FIGURE 1.A.1; DESIGN STRESS INTENSITY VS. TEMPERATURE

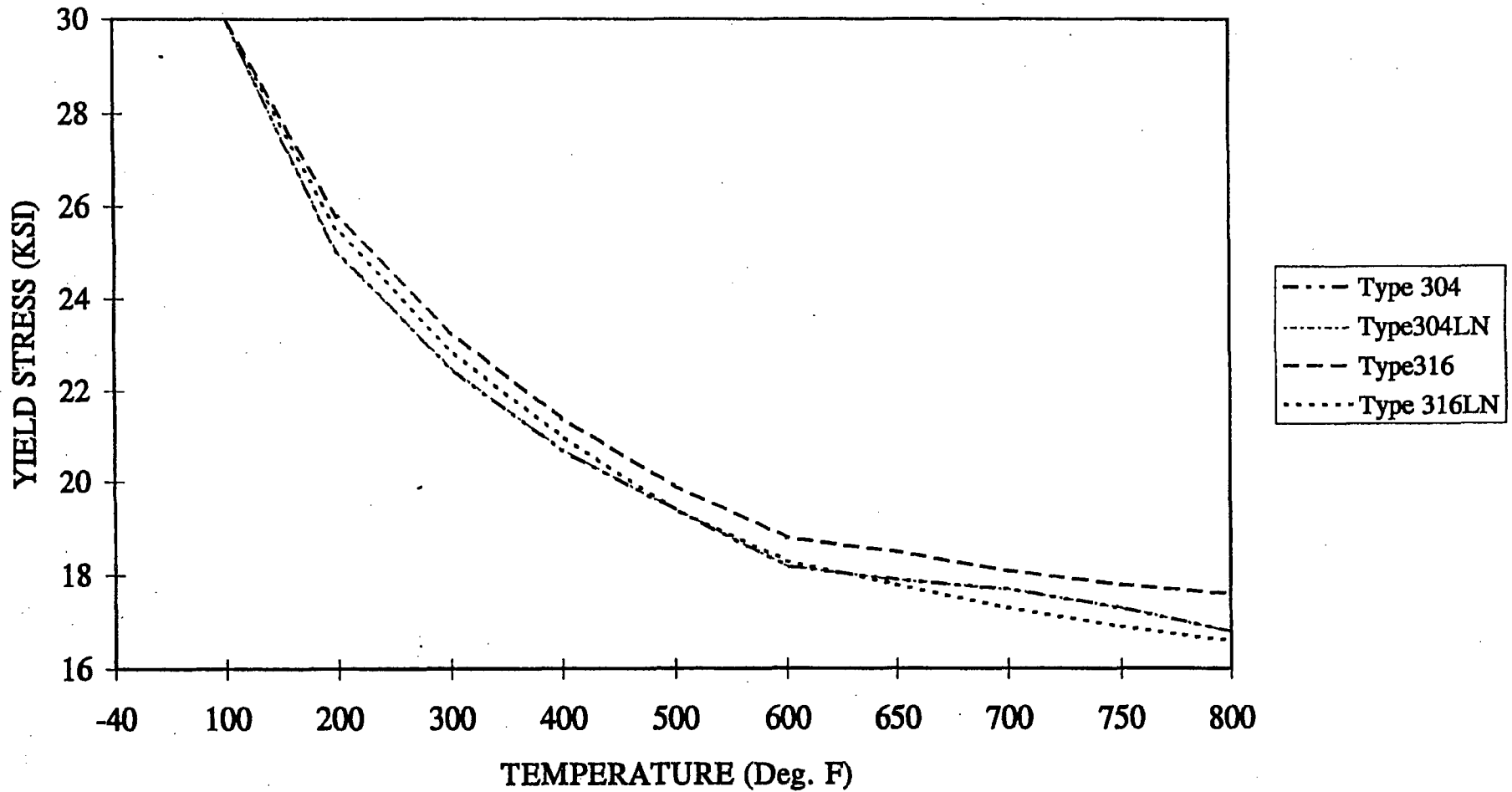
### TENSILE STRENGTH VS. TEMPERATURE



SOURCE: TABLE 1.A.2

FIGURE 1.A.2; TENSILE STRENGTH VS. TEMPERATURE

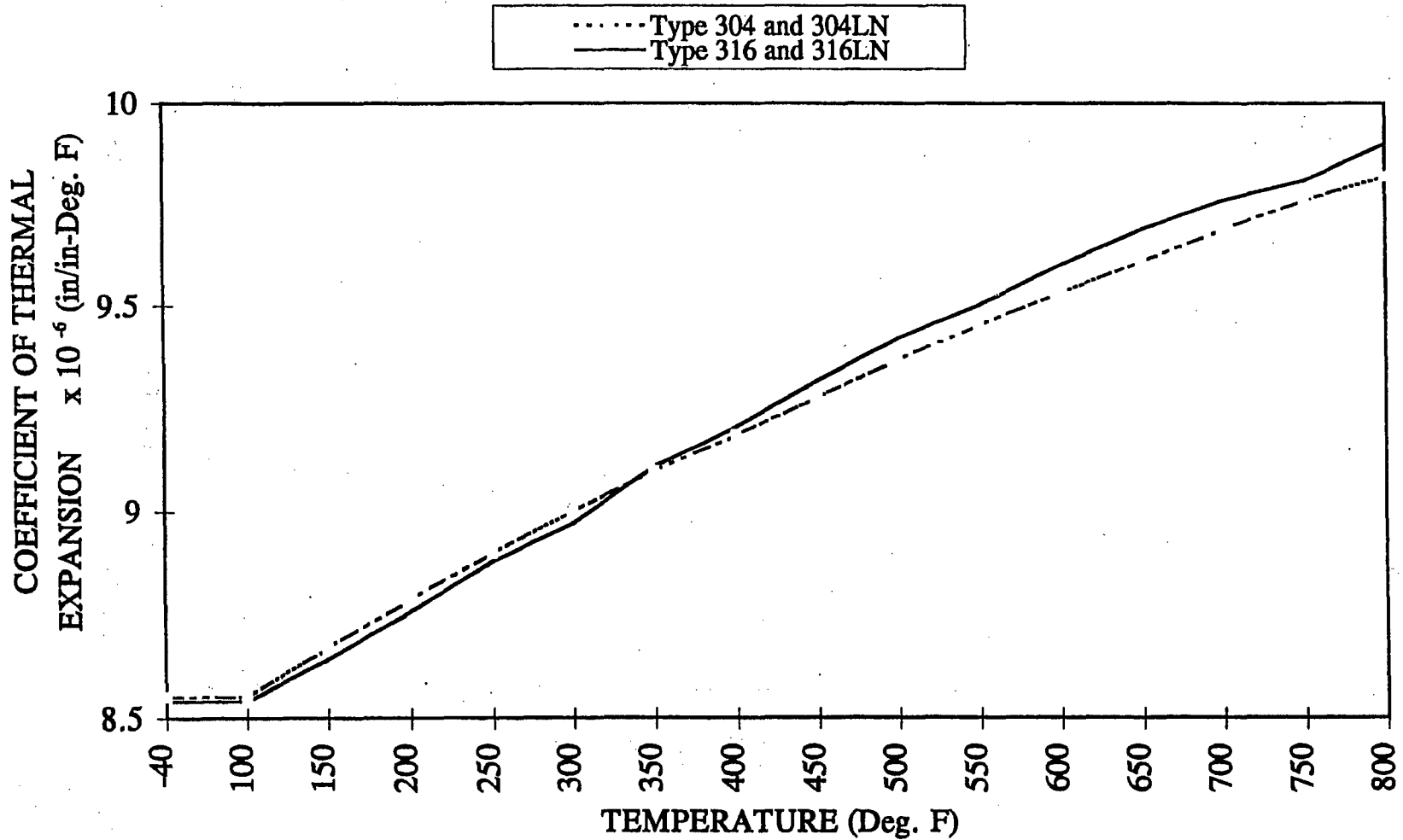
### YIELD STRESS VS. TEMPERATURE



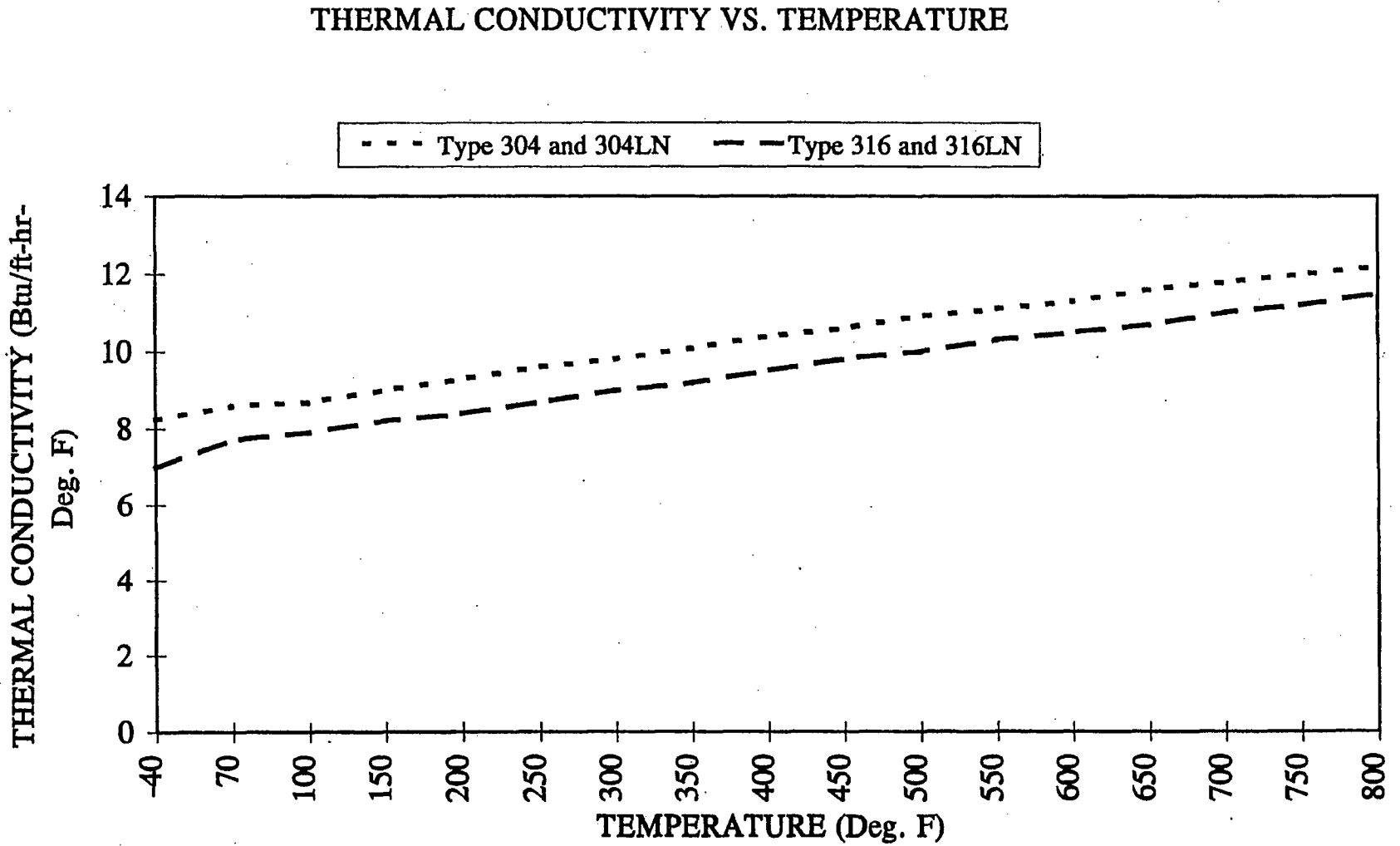
SOURCE: TABLE 1.A.3

FIGURE 1.A.3; YIELD STRESS VS. TEMPERATURE

### COEFFICIENT OF THERMAL EXPANSION VS. TEMPERATURE



SOURCE: TABLE 1.A.4      FIGURE 1.A.4; COEFFICIENT OF THERMAL EXPANSION VS. TEMPERATURE



SOURCE: TABLE 1.A.5

FIGURE 1.A.5; THERMAL CONDUCTIVITY VS. TEMPERATURE

**APPENDIX 1.B: HOLTITE™ MATERIAL DATA**

The information provided in this appendix describes the neutron absorber material, Holtite-A for the purpose of confirming its suitability for use as a neutron shield material in spent fuel storage casks. Holtite-A is one of a family of Holtite neutron shield materials denoted by the generic name Holtite™. It is currently the only neutron shield material approved for installation in the HI-STAR 100 cask. It is chemically identical to NS-4-FR which was originally developed by Bisco, Inc. and used for many years as a shield material with B<sub>4</sub>C or Pb added.

Holtite-A contains aluminum hydroxide (Al(OH)<sub>3</sub>) in an epoxy resin binder. Aluminum hydroxide is also known by the industrial trade name of aluminum tri-hydrate or ATH. ATH is often used commercially as a fire-retardant. Holtite-A contains approximately 62% ATH supported in a typical 2-part epoxy resin as a binder. Holtite-A contains 1% (nominal) by weight B<sub>4</sub>C, a chemically inert material added to enhance the neutron absorption property. Pertinent properties of Holtite-A are listed in Table 1.B.1.

The essential properties of Holtite-A are:

1. the hydrogen density (needed to thermalize neutrons),
2. thermal stability of the hydrogen density, and
3. the uniformity in distribution of B<sub>4</sub>C needed to absorb the thermalized neutrons.

ATH and the resin binder contain nearly the same hydrogen density so that the hydrogen density of the mixture is not sensitive to the proportion of ATH and resin in the Holtite-A mixture. B<sub>4</sub>C is added as a finely divided powder and does not settle out during the resin curing process. Once the resin is cured (polymerized), the ATH and B<sub>4</sub>C are physically retained in the hardened resin. Qualification testing for B<sub>4</sub>C throughout a column of Holtite-A has confirmed that the B<sub>4</sub>C is uniformly distributed with no evidence of settling or non-uniformity. Furthermore, an excess of B<sub>4</sub>C is specified in the Holtite-A mixing and pouring procedure as a precaution to assure that the B<sub>4</sub>C concentration is always adequate throughout the mixture.

The specific gravity specified in Table 1.B.1 does not include an allowance for weight loss. The specific gravity assumed in the shielding analysis includes a 4% reduction to conservatively account for potential weight loss at the design temperature of 300°F or an inability to reach theoretical density. Tests on the stability of Holtite-A were performed by Holtec International. The results of the tests are summarized in Holtec Proprietary Reports HI-2002396, "Holtite-A Development History and Thermal Performance Data" and HI-2002420, "Results of Pre- and Post-irradiation Test Measurements." The information provided in these reports demonstrates that Holtite-A possesses the necessary thermal and radiation stability characteristics to function as a reliable shielding material in the HI-STAR 100 overpack.

The Holtite-A is encapsulated in the HI-STAR 100 overpack and therefore should experience a very small weight reduction during the design life of the HI-STAR 100 System.

The data and test results confirm that Holtite-A remains stable under design thermal and radiation conditions, the material properties meet or exceed that assumed in the shielding analysis, and the B<sub>4</sub>C remains uniformly distributed with no evidence of settling or non-uniformity.

Based on the information described above, Holtite-A meets all of the requirements for an acceptable neutron shield material.

Table 1.B.1

## REFERENCE PROPERTIES OF HOLTITE-A NEUTRON SHIELD MATERIAL

<b>PHYSICAL PROPERTIES</b>	
% ATH	62 (nominal)
Specific Gravity	1.68 g/cc (nominal)
Max. Continuous Operating Temperature	300°F
Hydrogen Density	0.096 g/cc minimum
Radiation Resistance	Excellent
<b>CHEMICAL PROPERTIES (Nominal)</b>	
wt% Aluminum	21.5
wt% Hydrogen	6.0 (nominal)
wt% Carbon	27.7
wt% Oxygen	42.8
wt% Nitrogen	2.0
wt% B <sub>4</sub> C	1.0 (nominal)

**APPENDIX 1.C: MISCELLANEOUS MATERIAL DATA**

The information provided in this appendix specifies the thermal expansion foam (silicone sponge), paint, and anti-seize lubricant properties and demonstrates their suitability for use in spent nuclear fuel storage casks. The following is a listing of the information provided.

- HT-800 Series, Silicone Sponge, Bisco Products Technical Data Sheet
- Thermaline 450, Carboline, Product Data Sheet and Application Instructions
- Carboline 890, Carboline, Product Data Sheet and Application Instructions
- FEL-PRO Technical Bulletin, N-5000 Nickel Based-Nuclear Grade Anti-Seize Lubricant

HT-870 silicone sponge is specified as a thermal expansion foam to be placed in the overpack outer enclosure with the neutron shield. Due to differing thermal expansion of the neutron shield and outer enclosure carbon steel, the silicone sponge is provided to compress and allow the neutron shield material to expand. The compression-deflection physical properties are provided for the silicone sponge.

Silicone has a long and proven history in the nuclear industry. Silicone is highly resistant to degradation as a result of radiation at the levels required for the HI-STAR 100 System. Silicone is inherently inert and stable and will not react with the metal surfaces or neutron shield material. Additionally, typical operating temperatures for silicone sponges range from -50° F to 400° F.

Thermaline 450 is specified to coat the inner cavity of the overpack and Carboline 890 is specified to coat the external surfaces of the overpack. As can be seen from the product data sheets, the paints are suitable for the design temperatures (see Table 2.2.3) and chemical environment. Chemically identical substitutes are permitted (i.e., Carboguard 890 in lieu of Carboline 890).

Nuclear grade anti-seize lubricant, N-5000, from FEL-PRO is specified as the lubricant for the overpack closure bolts. The lubricant is formulated to have the lowest practical levels of halogens, sulfur, and heavy metals. NEVER-SEEZ NGBT provides equivalent properties to FEL-PRO N-5000 and is also acceptable for use on the HI-STAR 100 System.

## HT-800 SERIES

Specification Grade  
Silicone Sponge

### PHYSICAL PROPERTIES

PROPERTY	SPECIFICATION			TEST METHOD
	HT-870 (Soft)	HT-800 (Medium)	HT-820 (Firm)	
Density	12 - 24 pcf	16 - 28 pcf	20 - 32 pcf	ASTM D-3574
Compression Force @ 25% Deflection	2 - 7 psi	6 - 14 psi	12 - 20 psi	ASTM D-1056
Compression Set (Maximum)	10%	10%	10%	ASTM D-1056 (Compressed 50% for 22 hrs. @ 100°C)
Water Absorption (Maximum)	10%	5%	5%	ASTM D-1056

#### Available Industry Specifications:

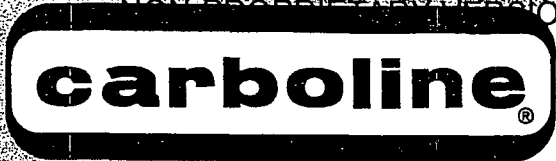
AMS-3195 (HT-800)

AMS-3196 (HT-820)

UL-94 (Limited to specific classes, densities, thicknesses and colors)

DATA is based on laboratory tests and should not be used for writing specifications. Each user should run independent tests to confirm material suitability for each specific application.

Bisco Products and Dow Corning neither represent nor use this material for medical device applications or for pharmaceutical end-use.



# THERMALINE 450



## SELECTION DATA

**GENERIC TYPE:** A glass flake filled, phenolic modified, amine cured epoxy novalac.

**GENERAL PROPERTIES:** A dense cross-linked polymer which exhibits outstanding barrier protection against a variety of chemical exposures. Excellent resistance to wet/dry cycling conditions at elevated temperatures. Designed to coat the exterior of insulated piping. It is also suitable for coating non-insulated piping and equipment exposed to chemical attack. The glass flakes help provide excellent abrasion resistance, permeation resistance and internal reinforcement.

- Temperature resistance to 450°F
- Excellent abrasion resistance
- Excellent overall chemical resistance
- Excellent thermal shock resistance

**RECOMMENDED USES:** Typically used as a one coat system to coat pipes and tanks that will be insulated. May also be used to coat non-insulated pipe, structural steel, equipment or concrete that may be subjected to severe chemical attack, abrasion or other abuse typical of a chemical plant environment.

### TYPICAL CHEMICAL RESISTANCE:

<u>Exposure</u>	<u>Splash &amp; Spillage</u>	<u>Fumes</u>
Acids	Excellent	Excellent
Alkalies	Excellent	Excellent
Solvents	Excellent	Excellent
Salt	Excellent	Excellent
Water	Excellent	Excellent

### TEMPERATURE RESISTANCE (Under insulation):

Continuous: 425°F (218°C)  
Excursions to: 450°F (232°C)

At 200°F (93°C) coating discoloration may be observed without loss of film integrity.

**SUBSTRATES:** Apply over properly prepared steel.

**COMPATIBLE COATINGS:** Normally applied directly to substrate. May be applied over epoxies and phenolics as recommended. May be topcoated with epoxies, polyurethanes or other finish coats as recommended.

July 96 Replaces September 95

## SPECIFICATION DATA

### THEORETICAL SOLIDS CONTENT OF MIXED MATERIAL:

THERMALINE 450 By Volume  
70 ± 2%

### VOLATILE ORGANIC CONTENT (VOC):

The following are nominal values:  
As supplied: 2.13 lbs./gal. (255 gm./liter).

<u>Thinner</u>	<u>Fluid</u> <u>Ounces/Gal.</u>	<u>Pounds/</u> <u>Gallon</u>	<u>Grams/</u> <u>Liter</u>
213	13	2.56	307

### RECOMMENDED DRY FILM THICKNESS:

8-10 mils (200-250 microns) to be achieved in 1 or 2 coats.

### THEORETICAL COVERAGE PER MIXED GALLON\*:

1,117 sq. ft. (27.9 sq.m/l at 25 microns)  
139 sq. ft at 8 mils (3.5 sq. m/l at 200 microns)  
111 sq. ft at 10 mils (2.8 sq.m/l at 250 microns)

\*Mixing and application losses will vary and must be taken into consideration when estimating job requirements.

### STORAGE CONDITIONS:

Store indoors.  
Temperature: 40-110°F (4-43°C) Humidity: 0-90%

**SHELF LIFE:** 24 months when stored indoors at 75°F (24°C)

**COLOR:** Red (0500) and Gray (5742)

**GLOSS:** Low (Epoxies lose gloss, discolor and eventually chalk in sunlight exposure.)

## ORDERING INFORMATION

Prices may be obtained from your Carboline Sales Representative or Carboline Customer Service Department.

### APPROXIMATE SHIPPING WEIGHT:

	<u>1's</u>	<u>5's</u>
THERMALINE 450	12 lbs. (5.5 kg)	58 lbs. (26.3 kg)
Thinner 213	8.4 lbs. (3.8 kg)	41 lbs. (18.6 kg)

### FLASH POINT: (Setaflash)

THERMALINE 450 Part A:	53°F	( 12°C)
THERMALINE 450 Part B:	>200°F	(>93°C)
Thinner 213	22°F	( -6°C)

0928

To the best of our knowledge the technical data contained herein are true and accurate at the date of issuance and are subject to change without prior notice. User must contact Carboline Company to verify correctness before specifying or ordering. No guarantee of accuracy is given or implied. We guarantee our products to conform to Carboline quality control. We assume no responsibility for coverage, performance or injuries resulting from use. Liability, if any, is limited to replacement of products. Prices and cost data, if shown, are subject to change without prior notice. NO OTHER WARRANTY OR GUARANTEE OF ANY KIND IS MADE BY CARBOLINE, EXPRESS OR IMPLIED, STATUTORY, BY OPERATION OF LAW, OR OTHERWISE, INCLUDING MERCHANTABILITY AND FITNESS FOR A PARTICULAR PURPOSE.

# APPLICATION INSTRUCTIONS

## THERMALINE 450

These instructions are not intended to show product recommendations for specific service. They are issued as an aid in determining correct surface preparation, mixing instructions and application procedure. It is assumed that the proper product recommendations have been made. These instructions should be followed closely to obtain the maximum service from the materials.

0928

**SURFACE PREPARATION:** Remove all oil or grease from surface to be coated with Thinner 2 or Surface Cleaner 3 (refer to Surface Cleaner 3 instructions) in accordance with SSPC-SP 1.

### STEEL:

**Not Insulated:** Abrasive blast to a Commercial Finish in accordance with SSPC-SP 6 and obtain a 2-3 mil (50-75 micron) blast profile.

**Under Insulation:** Abrasive blast to a Near White Finish in accordance with SSPC-SP 10 and obtain a 2-3 (50-75 micron) blast profile.

**MIXING:** Power mix each component separately, then combine and power mix in the following proportions.

Allow 30 minutes induction time at 75°F (24°C) prior to use.

	1 Gal. Kit	5 Gal. Kit
THERMALINE 450 Part A:	0.8 gals.	4.0 gals.
THERMALINE 450 Part B:	0.2 gals.	1.0 gals.

**THINNING:** May be thinned up to 13 oz/gal with Thinner 213.

Use of thinners other than those supplied or approved by Carboline may adversely affect product performance and void product warranty, whether express or implied.

**POT LIFE:** Three hours at 75°F (24°C) and less at higher temperatures. Pot life ends when coating loses body and begins to sag.

### APPLICATION CONDITIONS:

	Material	Surfaces	Ambient	Humidity
Normal	65-85°F (18-29°C)	65-85°F (18-29°C)	65-85°F (18-29°C)	30-60%
Minimum	55°F (13°C)	50°F (10°C)	50°F (10°C)	0%
Maximum	90°F (32°C)	110°F (43°C)	100°F (38°C)	85%

Do not apply when the surface temperature is less than 5°F or 3°C above the dew point.

Special thinning and application techniques may be required above or below normal conditions.

**SPRAY:** The following spray equipment has been found suitable and is available from manufacturers such as Binks, DeVilbiss and Graco.

**Conventional:** Pressure pot equipped with dual regulators, 1/2" I.D. minimum material hose, .110" I.D. fluid tip and appropriate air cap.

July 96 Replaces September 95

### Airless:

Pump Ratio:	30:1 (min)*
GPM Output:	3.0 (min)
Material Hose:	1/2" I.D. (min)
Tip Size:	.035"-.041"
Output psi:	2200-2500

\*Teflon packings are recommended and are available from the pump manufacturer.

**BRUSH:** For striping of welds, touch-up of small areas only. Use a natural bristle brush, applying full strokes. Avoid rebrushing.

**ROLLER:** Not recommended.

**DRYING TIMES:** These times are based on a dry film thickness of 10 mils (250 microns). Higher film thickness, insufficient ventilation or cooler temperatures will require longer cure times and could result in solvent entrapment and premature failure.

Surface Temperature	Dry To Handle	Dry to Topcoat	Final Cure
50°F (10°C)	18 hours	48 hours	21 days
60°F (16°C)	12 hours	32 hours	14 days
75°F (24°C)	6 hours	16 hours	7 days
90°F (32°C)	3 hours	8 hours	4 days

If the final cure time has been exceeded, the surface must be abraded by sweep blasting prior to the application of any additional coats.

**EXCESSIVE HUMIDITY OR CONDENSATION ON THE SURFACE DURING CURING MAY RESULT IN A SURFACE HAZE OR BLUSH; ANY HAZE OR BLUSH MUST BE REMOVED BY WATER WASHING BEFORE RE-COATING.**

**VENTILATION & SAFETY: WARNING: VAPORS MAY CAUSE EXPLOSION.** When used in enclosed areas, thorough air circulation must be used during and after application until the coating is cured. The ventilation system should be capable of preventing the solvent vapor concentration from reaching the lower explosion limit for the solvents used. In addition to insuring proper ventilation, fresh air respirators or fresh air hoods must be used by all application personnel. Where flammable solvents exist, explosion-proof lighting must be used. Hypersensitive persons should wear clean, protective clothing, gloves and/or protective cream on face, hands and all exposed areas.

**CLEANUP:** Use Thinner 2.

**CAUTION: READ AND FOLLOW ALL CAUTION STATEMENTS ON THIS PRODUCT DATA SHEET AND ON THE MATERIAL SAFETY DATA SHEET FOR THIS PRODUCT.**

**CAUTION: CONTAINS FLAMMABLE SOLVENTS. KEEP AWAY FROM SPARKS AND OPEN FLAMES. WORKMEN IN CONFINED AREAS MUST WEAR FRESH AIRLINE RESPIRATORS. HYPERSENSITIVE PERSONS SHOULD WEAR GLOVES OR USE PROTECTIVE CREAM. ALL ELECTRICAL EQUIPMENT AND INSTALLATIONS SHOULD BE MADE IN ACCORDANCE WITH THE NATIONAL ELECTRICAL CODE. IN AREAS WHERE EXPLOSION HAZARDS EXIST, WORKMEN SHOULD BE REQUIRED TO USE NONFERROUS TOOLS AND TO WEAR CONDUCTIVE AND NONSPARKING SHOES.**



Revision 1.0-4 Issued October 11, 2010

350 Hanley Industrial Ct. • St. Louis, MO 63144-1599

**SELECTION DATA****GENERIC TYPE:** Cross-linked epoxy.**GENERAL PROPERTIES:** CARBOLINE 890 is a self priming, high solids, high gloss, high build epoxy mastic. It can be applied by spray, brush, or roller over hand or power tool cleaned steel and is compatible with most existing coatings and tightly adhered rust. The cured film provides a tough, cleanable surface and is available in a wide variety of colors.

- Single coat corrosion protection.
- Excellent chemical resistance.
- Good flexibility and lower stress upon curing than most epoxy coatings.
- Excellent tolerance of damp (not wet) substrates.
- Very good abrasion resistance.
- Suitable replacement for Carbomastic 801.

**RECOMMENDED USES:** Recommended where a high performance, chemically resistant epoxy coating is desired. Offers outstanding protection for interior floors, walls, piping, equipment and structural steel or as an exterior coating for railcars, structural steel and equipment in various corrosive environments. Industrial environments include Chemical Processing, Offshore Oil and Gas, Food Processing, Pharmaceutical, Water and Waste Water Treatment, Pulp and Paper and Power Generation among others. May be used as a two coat system direct to metal or concrete for Water and Municipal Waste Water immersion. Acceptable for use in incidental food contact areas and as a lining for hopper cars carrying food grade plastic pellets when processed according to FDA criteria (ref: FDA 21 CFR 175.300). Consult Carboline Technical Service Department for other specific uses.**NOT RECOMMENDED FOR:** Strong acid or solvent exposures, immersion service other than water, exterior weathering where color retention is desired, such as a finish for tank exteriors or over chlorinated rubber and latex coatings.**TYPICAL CHEMICAL RESISTANCE:**

<u>Exposure</u>	<u>Immersion</u>	<u>Splash &amp; Spillage</u>	<u>Fumes</u>
Acids	NR	Very Good	Very Good
Alkalies	NR	Excellent	Excellent
Solvents	NR	Very Good	Excellent
Salt Solutions	Excellent	Excellent	Excellent
Water	Excellent	Excellent	Excellent

**TEMPERATURE RESISTANCE:** (Non-Immersion)

Continuous: 250°F (121°C)

Non-continuous: 300°F (149°C)

At temperatures above 225°F, coating discoloration and loss of gloss can be observed, without loss of film integrity.

**SUBSTRATES:** Apply over suitably prepared metal, concrete, or other surfaces as recommended.**COMPATIBLE COATINGS:** May be applied directly over inorganic zincs, weathered galvanizing, epoxies, phenolics or other coatings as recommended. A test patch is recommended before use over existing coatings. A mist coat of CARBOLINE 890 is required when applied over inorganic zincs to minimize bubbling. May be topcoated with polyurethanes or acrylics to upgrade weathering resistance. Not recommended over chlorinated rubber or latex coatings. Consult Carboline Technical Service Department for specific recommendations.

June 96 Replaces December 95

To the best of our knowledge the technical data contained herein are true and accurate at the date of issuance and are subject to change without prior notice. User must contact Carboline Company to verify correctness before specifying or ordering. No guarantee of accuracy is given or implied. We guarantee our products to conform to Carboline quality control. We assume no responsibility for coverage, performance or injuries resulting from use. Liability, if any, is limited to replacement of products. Prices and cost data, if shown, are subject to change without prior notice. NO OTHER WARRANTY OR GUARANTEE OF ANY KIND IS MADE BY CARBOLINE, EXPRESS OR IMPLIED, STATUTORY, BY OPERATION OF LAW, OR OTHERWISE, INCLUDING MERCHANTABILITY AND FITNESS FOR A PARTICULAR PURPOSE.

**SPECIFICATION DATA****THEORETICAL SOLIDS CONTENT OF MIXED MATERIAL:\***

CARBOLINE 890

By Volume  
75% ± 2%**VOLATILE ORGANIC CONTENT:\***

As Supplied: 1.78 lbs./gal. (214 grams/liter)

Thinned:

<u>Thinner</u>	<u>Fluid Ounces/Gal.</u>	<u>Pounds/Gallon</u>	<u>Grams/Liter</u>
2	8	2.08	250
2	13	2.26	271
33	16	2.38	285

\*Varies with color

**RECOMMENDED DRY FILM THICKNESS PER COAT:**

4-6 mils (100-150 microns).

6-8 mils (150-200 microns) DFT for a more uniform gloss over inorganic zincs, or for use over light rust.

In more severe environments a second coat of 4-6 mils (100-150 microns) is recommended.

Dry film thickness in excess of 10 mils (250 microns) per coat is not recommended. Excessive film thickness over inorganic zinc may increase damage during shipping or erection.

**THEORETICAL COVERAGE PER MIXED GALLON:**

1203 mil sq. ft. (30 sq. m/l at 25 microns)

241 sq. ft. at 5 mils (6.0 sq. m/l at 125 microns)

Mixing and application losses will vary and must be taken into consideration when estimating job requirements.

**STORAGE CONDITIONS:** Store indoors

Temperature: 40-110°F (4-43°C)

Humidity: 0-100%

**SHELF LIFE:** 36 months when stored at 75°F (24°C).**COLORS:** Available in Carboline Color Chart colors. Some colors may require two coats for adequate hiding.**GLOSS:** High gloss (Epoxies lose gloss, discolor and eventually chalk in sunlight exposure).**ORDERING INFORMATION**

Prices may be obtained from your Carboline Sales Representative or Carboline Customer Service Department.

**APPROXIMATE SHIPPING WEIGHT:**

	<u>2 Gal. Kit</u>	<u>10 Gal. Kit</u>
CARBOLINE 890	29 lbs. (13 kg)	145 lbs. (66 kg)

	<u>1's</u>	<u>5's</u>
THINNER #2	8 lbs. (4 kg)	39 lbs. (18 kg)
THINNER #33	9 lbs. (4 kg)	45 lbs. (20 kg)

**FLASH POINT:** (Setaflash)

CARBOLINE 890 Part A

89°F (32°C)

CARBOLINE 890 Part B

71°F (22°C)

THINNER #2

24°F (-5°C)

THINNER #33

89°F (32°C)

# APPLICATIONS INSTRUCTIONS NON-PROPRIETARY VERSION CARBOLINE® 890

These instructions are not intended to show product recommendations for specific service. They are issued as an aid in determining correct surface preparation, mixing instructions and application procedure. It is assumed that the proper product recommendations have been made. These instructions should be followed closely to obtain the maximum service from the materials.

**SURFACE PREPARATION:** Remove all oil or grease from surface to be coated with Thinner #2 or Surface Cleaner #3 (refer to Surface Cleaner #3 instructions) in accordance with SSPC-SP 1.

**Steel:** For mild environments Hand Tool or Power Tool Clean in accordance with SSPC-SP 2, SSPC-SP 3 or SSPC-SP 11 to produce a rust-scale free surface.

For more severe environments, abrasive blast to a Commercial Finish in accordance with SSPC-SP 6 and obtain a 1½ - 3 mil (40-75 micron) blast profile.

For immersion service, abrasive blast to a Near White Metal Finish in accordance with SSPC-SP10 and obtain a 1½ - 3 mil (40-75 micron) blast profile.

**Concrete:** Must be cured at least 28 days at 70°F (21°C) and 50% R.H. or equivalent time. Remove fins and other protrusions by stoning, sanding or grinding. Abrasive blast to open all surface voids and remove all form oils, incompatible curing agents, hardeners, laitance and other foreign matter and produce a surface texture similar to that of a medium grit sandpaper. Voids in the concrete may require surfacing. Blow or vacuum off sand and dust.

**MIXING:** Power mix separately, then combine and power mix in the following proportions:

	<u>2 Gal. Kit</u>	<u>10 Gal. Kit</u>
CARBOLINE 890 Part A	1 gallon	5 gallons
CARBOLINE 890 Part B	1 gallon	5 gallons

**THINNING:** For spray applications, may be thinned up to 13 oz./gal. with Thinner #2. For hot and windy conditions, or for brush and roller application, may be thinned up to 16 oz./gal. with Thinner #33.

Use of thinners other than those supplied or approved by Carboline may adversely affect product performance and void product warranty, whether express or implied.

**POT LIFE:** Three hours at 75°F (24°C) and less at higher temperatures. Pot life ends when material loses film build.

**APPLICATION CONDITIONS:**

	<u>Material</u>	<u>Surfaces</u>	<u>Ambient</u>	<u>Humidity</u>
Normal	60-85°F (16-29°C)	60-85°F (16-29°C)	60-90°F (16-32°C)	0-80%
Minimum	50°F (10°C)	50°F (10°C)	50°F (10°C)	0%
Maximum	90°F (32°C)	125°F (52°C)	110°F (43°C)	90%

Do not apply or cure the material when the surface temperature is less than 5°F or 3°C above the dew point.

Special thinning and application techniques may be required above or below normal conditions.

**SPRAY:** This is a high solids coating and may require slight adjustments in spray techniques. Wet film thicknesses are easily and quickly achieved. The following spray equipment has been found suitable and is available from manufacturers such as Binks, DeVilbiss and Graco.

**Conventional:** Pressure pot equipped with dual regulators, 3/8" I.D. minimum material hose, .070" I.D. fluid tip and appropriate air cap.

June 96 Replaces December 95

**Airless:**  
**Pump Ratio:** 30:1 (min.)\*  
**GPM Output:** 3.0 (min.)  
**Material Hose:** 3/8" I.D. (min.)  
**Tip Size:** .017-.021"  
**Output psi:** 2100-2300  
**Filter Size:** 60 mesh

\*Teflon packings are recommended and are available from the pump manufacturer.

**BRUSH OR ROLLER:** Use medium bristle brush, or good quality short nap roller. Avoid excessive rebrushing and rerolling. Two coats may be required to obtain desired appearance, hiding and recommended DFT. For best results, tie-in within 10 minutes at 75°F (24°C).

**DRYING TIMES:** These times are based on a 5 mils (125 microns) dry film thickness. Higher film thicknesses, insufficient ventilation or cooler temperatures will require longer cure times and could result in solvent entrapment and premature failure.

Dry to Touch 2 1/2 hours at 75°F (24°C)  
 Dry to Handle 6 1/2 hours at 75°F (24°C)

<u>Surface Temperature</u>	<u>Recoating With Itself</u>	<u>Dry to Topcoat</u>	<u>Final Cure</u>
50°F (10°C)	12 hours	24 hours	3 days
60°F (16°C)	8 hours	16 hours	2 days
75°F (24°C)	4 hours	8 hours	1 day
90°F (32°C)	2 hours	4 hours	16 hours

Excessive humidity or condensation on the surface during curing can interfere with the cure, can cause discoloration and may result in a surface haze or blush. Any haze or blush must be removed by water washing before recoating. During high humidity conditions, it is recommended that the application be done while temperatures are increasing. For best results over "damp" surfaces, apply by brush or roller.

**Maximum Recoat or Topcoat Times at 75°F (24°C):**

With Epoxies - 30 days  
 With Polyurethanes - 90 days

If the maximum recoat time has been exceeded, surface must be abraded by sweep blasting prior to the application of any additional coats.

Minimum cure time before immersion service is 5 days at 75°F (24°C) surface temperature. Cure at temperatures below 60°F (16°C) is not recommended for immersion service.

**VENTILATION & SAFETY: WARNING: VAPORS MAY CAUSE EXPLOSION.** When used as a tank lining or in enclosed areas, thorough air circulation must be used during and after application until the coating is cured. The ventilation system should be capable of preventing the solvent vapor concentration from reaching the lower explosion limit for the solvents used. In addition to ensuring proper ventilation, fresh air respirators or fresh air hoods must be used by all application personnel. Where flammable solvents exist, explosion-proof lighting must be used. Hypersensitive persons should wear clean, protective clothing, gloves and/or protective cream on face, hands and all exposed areas.

**CLEANUP:** Use Thinner # 2.

**CAUTION: READ AND FOLLOW ALL CAUTION STATEMENTS ON THIS PRODUCT DATA SHEET AND ON THE MATERIAL SAFETY DATA SHEET FOR THIS PRODUCT.**

**CAUTION: CONTAINS FLAMMABLE SOLVENTS. KEEP AWAY FROM SPARKS AND OPEN FLAMES. IN CONFINED AREAS, WORKMEN MUST WEAR FRESH AIRLINE RESPIRATORS. HYPERSENSITIVE PERSONS SHOULD WEAR GLOVES OR USE PROTECTIVE CREAM. ALL ELECTRIC EQUIPMENT AND INSTALLATIONS SHOULD BE MADE AND GROUNDED IN ACCORDANCE WITH THE NATIONAL ELECTRICAL CODE. IN AREAS WHERE EXPLOSION HAZARDS EXIST, WORKMEN SHOULD BE REQUIRED TO USE NONFERROUS TOOLS AND TO WEAR CONDUCTIVE AND NONSPARKING SHOES.**



350 Hanley Industrial Ct. • St. Louis, MO 63144-1599  
 In (F&P) Company • 314-844-1000

0986

# FELPRO®

## Technical Bulletin

### N-5000 NICKEL BASED - NUCLEAR GRADE ANTI-SEIZE LUBRICANT

N-5000 is a nickel based nuclear grade anti-seize lubricant produced under 100% controlled conditions for highest purity and traceability. It is formulated to have the lowest practical levels of halogens, sulfur, and heavy metals, including copper. N-5000 has a general composition of nickel and graphite flake in petroleum carrier. All ingredients are selected for extreme purity. It meets or exceeds the following specifications, appendix A of NEDE-31295P, "BWR Operator's Manual for Materials and Processes", Westinghouse Material Specification 53701WQ, and 10CFR Ch1, Part 21, and Part 50, appendix B.

#### Special Features:

- High purity- made from highest purity ingredients.
- Traceability- each can marked.
- Free from copper- less than 50 ppm copper.
- Testing- each batch tested before packaging.
- Certifications- 3 copies with each case.

#### Recommended applications:

- Bolts, studs, valves, pipe fittings, slip fits and press fits in electric power generating plants, chemical plants, pharmaceutical plants, paper mills, and other locations where stainless steel fasteners are used.

#### Operational Benefits:

- Before assembly - certifications and traceability.
- During assembly - prevents high friction, galling, and seizing. Promotes uniform and predictable clamping.
- During operation - high purity prevents stress corrosion.
- Disassembly - prevents seizing, galling, destruction of threads.

#### Typical Physical Properties:

Composition	Nickel and Graphite in Petroleum Oil
Appearance	Silver-Gray paste
Specific gravity	1.12
Flash point (ASTM D 92-85)	424°F/218°C
Torque coefficient, K (Steel nuts and Bolts) (Type 304 Stainless)	0.15 0.18
Maximum use temperature	1800°F/982°C

#### Quality Control Physical Properties:

Weight per gallon (ASTM D 1475-85)	Range 9.5 - 10.4
Penetration (ASTM D 217-88 unworked)	300 - 380

#### Purity:

Impurities - Elemental and Combined	Test Method Type	References ASTM OR (SM16)	Controlled Maximum	Average Values
Halogens: Chlorine, Bromine, Iodine	Parr Bomb, Turbidimetric	D808-87, G699-79	50 ppm	18 ppm
Fluorine	Parr Bomb, Specific ION Electrode	D3761-84	200 ppm	7 ppm
Sulfur	Parr Bomb, Turbidimetric	D129-64, D1266-87	100 ppm	9 ppm
Lead	Wet Digestion, AAS	(302D), D3559-84	25 ppm	1 ppm
Cadmium	Wet Digestion, AAS	(302D), D3557-84	2 ppm	0.2 ppm
Tin	Wet Digestion, AAS	(302D), E37-76	25 ppm	9 ppm
Zinc	Wet Digestion, AAS	(302D), D1691-84	25 ppm	1 ppm
Copper	Wet Digestion, AAS	(302D), D1688-84	50 ppm	12 ppm
Mercury	Wet Digestion, Cold Vapor AAS	(302D), D3223-80	2 ppm	0.04 ppm

**Directions for use:**

- Before or during assembly, wipe brush onto threads and other joint surfaces needing protection.
- Do not overuse, as excess will be pushed off.
- Use full strength, do not thin.

**Packaging:**

Part Number	Net Contents	Type Container	Units/Case	Shipping Wt./Case
51243	8 oz. (227 g)	Can-brush top	12	9 lb. (4. Kg.)
51245	8 lb. (3.6 kg)	Can	2	18 lb. (8. Kg.)
51246	2 lb. (908 g)	Can	12	29 lb. (13. Kg.)
51269	1 lb. (454 g)	Can-brush top	12	16 lb. (7. Kg.)
51346	1 oz. (28 g)	Tube	48	6 lb. (2.7 Kg.)

N-5000 has an unlimited shelf life when stored at room temperature in the original unopened container.

**FOR INDUSTRIAL USE ONLY.**

**WASH THOROUGHLY AFTER HANDLING.**

**KEEP OUT OF REACH OF CHILDREN.**

**SEE MATERIAL SAFETY DATA** For immediate answers to your technical questions, in the United States or Canada call the **Technical Support Line at 1-800-992-9799.**

International customers call (303) 289-5651, or fax (303) 289-5283

For a Material Safety Data Sheet or Technical Bulletin on this or any Fel-Pro product call our toll-free **FAX FOR THE INFO** line 24 hours a day, 7 days a week, in the United States or Canada call **800-583-3069**. International customers call (303) 289-5651, or fax (303) 289-5283.

Except as expressly stipulated, Fel-Pro's liability, expressed or implied, is limited to the stated selling price of any defective goods.

N-5000 8/97

**FEL-PRO CHEMICAL PRODUCTS, L.P.**

Fel-Pro  
3412 W. Touhy Ave.  
Lincolnwood, IL  
60645 U.S.A.  
847-568-2820  
Fax 847-674-0019

Fel-Pro  
6120 E. 58th Ave  
Commerce City, CO  
80022 U.S.A.  
800-992-9799  
Fax 303-289-5283

Fel-Pro of Canada, Ltd  
6105 Kastrel Road  
Mississauga, Ontario  
L5T 1Y8 Canada  
905-564-1530  
Fax 905-564-1534

Fel-Pro Ltd.  
4 Arkwright Way  
North Newmoor, Irvine  
KA11 4JU Scotland  
44-1294-216094  
Fax 44-1294-218157

Fel-Pro Chemical Products Latin America L.P.  
Bodega No. 12, Zona Franca Palmaseca  
Aeropuerto Internacional Bonilla Aragon  
Cali, Colombia  
57-2-651-1168  
Fax 57-2-651-1179

Fel-Pro Chemical Products, Chile S.A.  
Av. Pdte. Eduardo Frei M. 9231 Quilicura  
Casilla (P.O. Box) 14325  
Santiago, Chile  
56-2-623-9216  
Fax 56-2-623-2569

## SUPPLEMENT 1.I

## GENERAL DESCRIPTION OF THE HI-STAR 100 SYSTEM FOR HUMBOLDT BAY

1.I.0 GENERAL INFORMATION

The HI-STAR 100 System has been expanded to include options specific for use at PG&E's Humboldt Bay (HB) plant for dry storage and future transportation of spent nuclear fuel (SNF)[1.0.8]. HB fuel assemblies are considerably shorter in length than the typical BWR fuel assemblies. As a result, the HI-STAR 100 system now includes an overpack assembly and MPC for use at HB; the HI-STAR 100 Version HB (also called HI-STAR HB) and the MPC-HB. Note that the HB fuel has a cooling time of more than 25 years and relatively low burnup. The heat load and nuclear source terms of this fuel are therefore substantially lower than the design basis fuel described in the main part of this chapter. Consequently, peak cladding temperatures and dose rates are below the regulatory limits with a substantial margin. Nevertheless, all major dimensions and features, such as diameter, wall thickness, flange design, top and bottom thicknesses, are maintained identical to the standard design. Therefore, from a structural perspective, the HI-STAR HB will be even more robust than the standard overpack, due to its shorter length. Information pertaining to the HI-STAR HB System is generally contained in the "I" supplements to each chapter of this SAR. Certain sections of the main SAR are also affected and are appropriately modified for continuity with the "I" supplements. Unless superseded or specifically modified by information in the "I" supplements, the information in the main SAR is applicable to the HI-STAR System for use at HB.

1.I.0.1 Engineering Change Orders

The changes authorized by Holtec Engineering Change Orders (ECOs) for the following licensed components are reflected in this revision of this SAR.

MPC-HB Basket: 1125-28.

HI-STAR HB overpack: 1125-15, 20 and 28

MPC-HB Enclosure Vessel: None.

Ancillary Equipment: Damaged Fuel Container HB – see drawing for engineering change (ECO N/A)

1.I.1 INTRODUCTION

The HI-STAR 100 System as deployed at Humboldt Bay will consist of a HI-STAR HB overpack, an MPC-HB that includes a fuel basket assembly and enclosure vessel specific to HB, and impact limiters. The HB specific components are described below and key parameters for HI-STAR HB are presented in Table 1.I.1. Section 1.I.3 provides the HI-STAR HB design code applicability and details any alternatives to the ASME Code if different than HI-STAR 100. All discussion is supplemented by a set of drawings in Section 1.I.4.

## 1.1.2 PACKAGE DESCRIPTION

### 1.1.2.1 Packaging

#### 1.1.2.1.1 Gross Weight

Table 2.1.2.1 summarizes the maximum calculated weights for the HI-STAR HB overpack, impact limiters, and each MPC loaded to maximum capacity with design basis SNF. Table 2.1.2.1 also provides the location of the center of gravity of the fully loaded package.

#### 1.1.2.1.2 Materials of Construction, Dimensions, and Fabrication

Humboldt Bay specific materials of construction along with outline dimensions for important-to-safety items are provided in the drawings in Section 1.1.4.

##### 1.1.2.1.2.1 HI-STAR HB Overpack

The HI-STAR HB overpack is a heavy-walled, steel cylindrical vessel identical to the standard HI-STAR, except that the outer and inner heights are approximately 128 and 115 inches, respectively. Unlike the HI-STAR 100, the HI-STAR HB overpack does not contain radial channels vertically welded to the outside surface of the outermost intermediate shell.

##### 1.1.2.1.2.2 MPC-HB

MPC-HB is similar to the MPC-68F except it is approximately 114 inches high. Key parameters of the MPC-HB are given in Table 1.1.2. The MPC-HB is designed to transport up to 80 Humboldt Bay BWR spent nuclear fuel assemblies meeting the specifications in Table 1.1.4. Damaged SNF and fuel debris must be placed into a Holtec damaged fuel container or other authorized canister for transportation inside the MPC-HB and the HI-STAR HB overpack. Figure 1.1.1 provides a sketch of the container authorized for transportation of damaged fuel and fuel debris in the HI-STAR HB System.

### 1.1.2.2 Operational Features

The sequence of basic operations necessary to load fuel and prepare the HI-STAR HB system for transport is identical to that of HI-STAR 100. The supporting drawings for HB can be found in Section 1.1.4.

### 1.1.2.3 Contents of Package

This section delineates the authorized contents permitted for shipment in the HI-STAR HB System, including fuel assembly types; non-fuel hardware; neutron sources; physical parameter limits for fuel assemblies and sub-components; enrichment, burnup, cooling time, and decay heat limits; location requirements; and requirements for canning the material, as applicable.

#### 1.I.2.3.1 Determination of Design Basis Fuel

The HI-STAR HB package is designed to transport Humboldt Bay fuel assemblies. The HB fuel assembly designs evaluated are listed in Table 1.I.3. Table 1.I.4 provides the fuel characteristics determined to be acceptable for transport in the HI-STAR HB System. Each “array/class” listed in this table represents a bounding set of parameters for one or more fuel assembly types. The array/classes are defined for HB in Section 6.I.2. Table 1.I.5 lists the fuel assembly designs that are found to govern for the qualification criteria. Tables 1.I.4 and 1.I.7 provide the specific limits for all material authorized to be transported in the HI-STAR HB System.

#### 1.I.2.3.2 Design Payload for Intact and/or Undamaged Fuel

The fuel characteristics specified in Table 1.I.4 have been evaluated in this SAR and are acceptable for transport in the HI-STAR HB System. Holtec considers that almost all of the Humboldt Bay fuel assemblies not classified as damaged are intact, however the inspection records of the Humboldt Bay fuel assemblies precludes classifying the assemblies as intact fuel since the interior rods of the assembly are in an unknown condition. This fuel is therefore classified as undamaged and can still perform all fuel specific and system related functions, even with possible breaches or defects. Except where specifically noted, throughout this document references to Humboldt Bay fuel as intact or undamaged are equivalent.

#### 1.I.2.3.3 Design Payload for Damaged Fuel and Fuel Debris

Limits for transporting HB damaged fuel and fuel debris are given in Table 1.I.7. Damaged HB fuel and fuel debris must be transported in the Holtec designed Humboldt Bay Damaged Fuel Container (DFC) as shown in Figure 1.I.1.

#### 1.I.2.3.4 Structural Payload Parameters

The main physical parameters of an SNF assembly applicable to the structural evaluation are the fuel assembly length, envelope (cross sectional dimensions), and weight. In order to qualify for transport in the HI-STAR HB MPC, the SNF must satisfy the physical parameters listed in Table 1.I.7. The center of gravity for HB, reported in Chapter 2.I, is based on the maximum fuel assembly weight. Upper fuel spacers (as appropriate) in the form of welded I-beams, approximately 4 inches high, maintain the axial position of the fuel assembly within the MPC basket and, therefore, the location of the center of gravity. The upper spacers are designed to withstand normal and accident conditions of transport. An axial clearance of approximately 2 inches is provided to account for the irradiation and thermal growth of the fuel assemblies.

#### 1.I.2.3.5 Thermal Payload Parameters

Table 1.I.7 provides the maximum heat generation for all fuel assemblies authorized for transportation in the HI-STAR HB System.

1.I.2.3.6 Radiological Payload Parameters

The design basis dose rates are met by the burnup level, cooling time, and minimum enrichment presented in Table 1.I.6 for HI-STAR HB.

1.I.2.3.7 Criticality Payload Parameters

The neutron absorber's minimum <sup>10</sup>B areal density loading for MPC-HB is specified in Table 1.I.2.

1.I.2.3.8 Non-Fuel Hardware and Neutron Sources

None.

1.I.2.3.9 Summary of Authorized Contents

Table 1.I.1 summarizes the key system data for the HI-STAR HB. Table 1.I.2 summarizes the key parameters and limits for the MPC-HB. Tables 1.I.4 and 1.I.7 and other tables referenced from these tables provide the limiting conditions for all material to be transported in the HI-STAR HB.

1.I.3 DESIGN CODE APPLICABILITY

Design code applicability for the HI-STAR HB is identical to HI-STAR 100 as presented in Section 1.3, except that the internal surfaces of the intermediate shells will not be coated with a silicone encapsulant due to its lower heat loads.

1.I.4 DRAWINGS

Drawing Number/Sheet	Description	Rev.
4082	Licensing Drawing for HI-STAR HB Overpack Assembly	7
4102	Licensing Drawing for MPC HB Enclosure Vessel	1
4103	Licensing Drawing for MPC HB Fuel Basket Assembly	6
4113	Licensing Drawing for Damaged Fuel Container	2

DRAWINGS WITHHELD IN ACCORDANCE WITH 10CFR2.390

1.I.5 COMPLIANCE WITH 10CFR71

Same as in Section 1.5.

1.I.6        REFERENCES

Same as in Section 1.6.

Table 1.I.1

SUMMARY OF KEY SYSTEM DATA FOR HI-STAR HB

PARAMETER	VALUE (Nominal)	
Types of MPCs in this Supplement	1	MPC HB
MPC capacity	MPC HB	- Up to 80 intact and/or undamaged ZR Humboldt Bay fuel assemblies. - Up to 28 Damaged Fuel Assemblies/Fuel Debris in DFCs located in the peripheral basket cells, remaining cells loaded with intact and/or undamaged ZR Humboldt Bay fuel assemblies; or, - Up to 40 Damaged Fuel Assemblies/Fuel Debris in DFCs arranged in a checkerboard pattern with 40 intact and/or undamaged ZR Humboldt Bay fuel assemblies

Table 1.I.2  
KEY PARAMETERS FOR MPC-HB

PARAMETER	VALUE (Nominal)
Unloaded MPC weight (lb)	See Table 2.I.2.1
Fixed neutron absorber (Metamic) <sup>10</sup> B loading density (g/cm <sup>2</sup> )	0.01
Pre-disposal service life (years)	40
Design temperature, max. /min. (°F)	725°/-40°
Design Internal pressure (psig)	
Normal Conditions	100
Off-normal Conditions	100
Accident Conditions	200
Total heat load, max. (kW)	2
Maximum permissible peak fuel cladding temperature (°F)	752 (Normal conditions) 1058 (Accident conditions)
MPC internal environment Helium filled (psig)	≥ 0 and ≤ 48.8 psig at a reference temperature of 70°F
MPC external environment/overpack internal environment Helium filled initial pressure (psig, at STP)	≥ 10 and ≤ 14
Maximum permissible reactivity including all uncertainty and biases	<0.95
End closure(s)	Welded
Fuel handling	Opening compatible with standard grapples
Heat dissipation	Passive

Table 1.I.3

## HUMBOLDT BAY FUEL ASSEMBLIES EVALUATED TO DETERMINE DESIGN BASIS SNF

Assembly Class	Array Type	
Humboldt Bay	All 6x6	All 7x7

Table 1.I.4

## HUMBOLDT BAY FUEL ASSEMBLY CHARACTERISTICS

Fuel Assembly Array/Class	6x6D	7x7C
Clad Material	ZR	ZR
Design Initial U (kg/assy.)	$\leq 78$	$\leq 78$
Initial Maximum Rod Enrichment (wt.% <sup>235</sup> U)	$\leq 4.0$ (see Note 1)	$\leq 4.0$
Maximum planar-average initial enrichment (wt.% <sup>235</sup> U)	$\leq 2.6$	$\leq 2.6$
No. of Fuel Rod Locations	36	49
Fuel Clad O.D. (in.)	$\geq 0.5585$	$\geq 0.4860$
Fuel Clad I.D. (in.)	$\leq 0.5050$	$\leq 0.426$
Fuel Pellet Dia. (in.)	$\leq 0.4880$	$\leq 0.4110$
Fuel Rod Pitch (in.)	$\leq 0.740$	$\leq 0.631$
Active Fuel Length (in.)	$\leq 80$	$\leq 80$
No. of Water Rods	0	0
Channel Thickness (in.)	$\leq 0.060$	$\leq 0.060$

Note 1: Two 6x6D assemblies contain one high power test rod with an initial enrichment of 5.5%.

Table 1.I.5

## DESIGN BASIS FUEL ASSEMBLY FOR EACH DESIGN CRITERION

<b>Criterion</b>	<b>MPC-HB</b>
Reactivity	6x6D and 7x7C
Shielding (Source Term)	6x6D
Fuel Assembly Effective Planar Thermal Conductivity	7x7C
Fuel Basket Effective Axial Thermal Conductivity	6x6D

Table 1.I.6

## HUMBOLDT BAY FUEL ASSEMBLY COOLING, AVERAGE BURNUP, AND MINIMUM ENRICHMENT LIMITS

<b>Post-irradiation Cooling Time (years)</b>	<b>Assembly Burnup (MWD/MTU)</b>	<b>Assembly Minimum Enrichment (wt. % <sup>235</sup>U)</b>
≥ 29	≤ 23,000	≥ 2.09

Table 1.I.7  
LIMITS FOR MATERIAL TO BE TRANSPORTED IN MPC-HB

PARAMETER	VALUE (Note 1)	
Fuel Type (Note 2)	Uranium oxide, HB BWR intact and/or undamaged fuel assemblies meeting the limits in Table 1.I.4 for the applicable array/class, with or without Zircaloy channels	Uranium oxide, HB BWR damaged fuel assemblies or fuel debris meeting the limits in Table 1.I.4 for array/class 6x6D or 7x7C with or without Zircaloy channels, placed in HB Damaged Fuel Containers (DFCs)
Cladding Type	ZR	ZR
Maximum Initial Enrichment	As specified in Table 1.I.4 for the applicable array/class	As specified in Table 1.I.4 for the applicable array/class
Post-irradiation Cooling Time, Average Burnup, and Minimum Initial Enrichment per Assembly	As specified in Table 1.I.6.	As specified in Table 1.I.6.
Decay Heat Per Assembly	$\leq 50$ Watts	Fuel debris up to a maximum of one equivalent fuel assembly is allowed (Note 4)
Fuel Assembly Length	$\leq 96.91$ in. (nominal design)	$\leq 96.91$ in. (nominal design)
Fuel Assembly Width	$\leq 4.70$ in. (nominal design)	$\leq 4.70$ in. (nominal design)
Fuel Assembly Weight	$\leq 400$ lbs (including channels)	$\leq 400$ lbs, (including channels and DFC)(Note 3)
Quantity per MPC	Up to 80 HB BWR intact and/or undamaged fuel assemblies	Up to 28 DFCs loaded in the peripheral cells of the basket with 52 intact and/or undamaged assemblies in the remainder (figure 6.I.3) <u>or</u> Up to 40 DFCs with 40 intact and/or undamaged assemblies loaded in a checkerboard pattern (figure 6.I.4)
Other Limitations	Stainless steel channels are not permitted.	

Table 1.I.7 (cont.)

LIMITS FOR MATERIAL TO BE TRANSPORTED IN MPC-HB

Notes:

1. A fuel assembly must meet the requirements of any one column and the other limitations to be authorized for transportation.
2. Fuel assemblies with channels may be stored in any fuel cell location.
3. The total quantity of damaged fuel permitted in a single DAMAGED FUEL CONTAINER is limited to the equivalent weight and special nuclear material quantity of one intact or undamaged assembly.
4. Fuel debris in the form of loose debris consisting of zirconium clad pellets, stainless steel clad pellets, unclad pellets or rod segments up to a maximum of one equivalent fuel assembly is allowed. A maximum of 1.5 kg of stainless steel clad is allowed per cask.

NON-PROPRIETARY VERSION

NOTES:

1. ALL DIMENSIONS ARE IN INCHES AND ARE NOMINAL.
2. ALL MATERIAL IS STAINLESS STEEL.

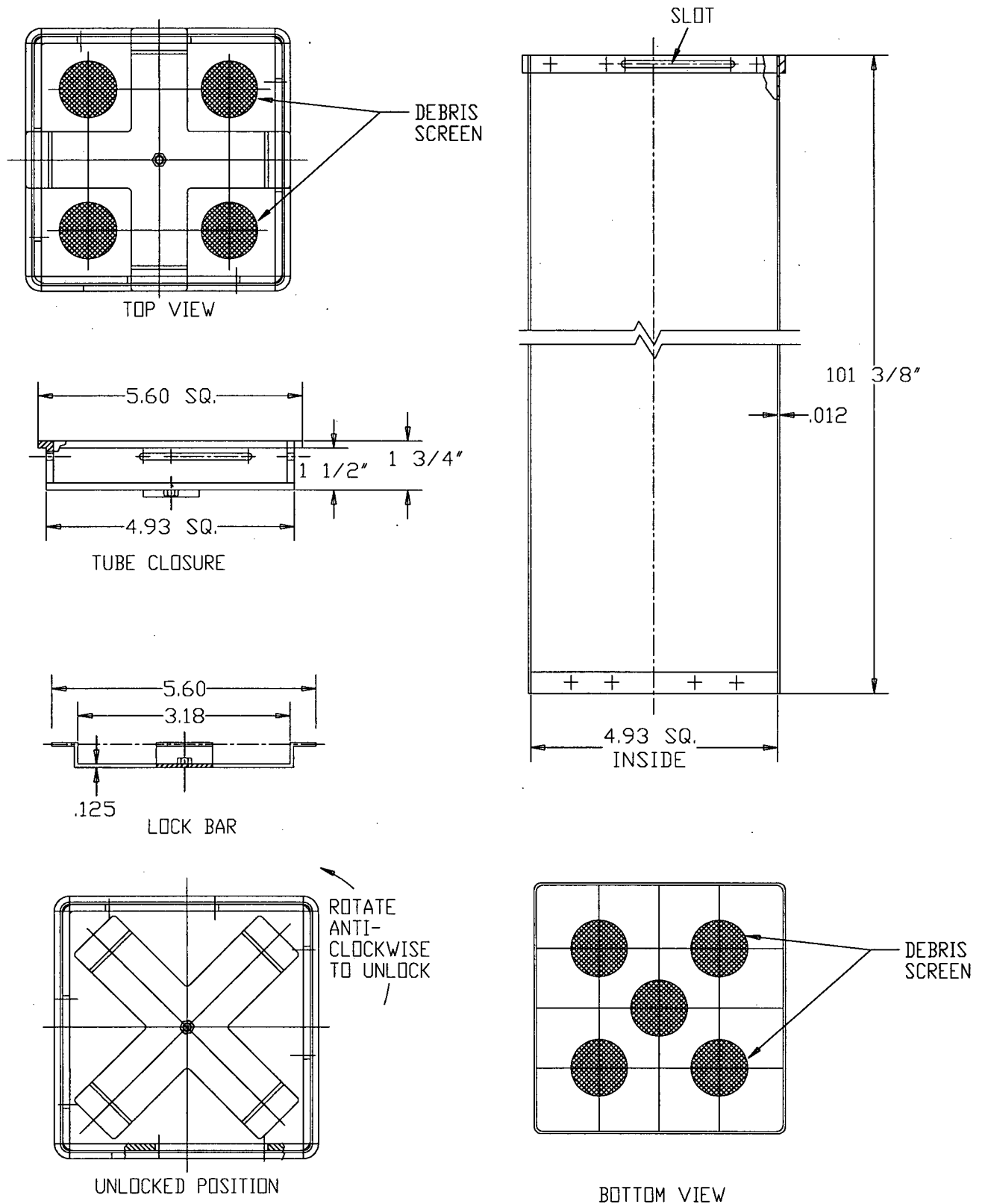


FIGURE 1.I.1; HOLTEC DAMAGED FUEL CONTAINER FOR HUMBOLDT BAY SNF IN MPC-HB

## CHAPTER 2: STRUCTURAL EVALUATION

This chapter presents a synopsis of the evaluations carried out to establish the mechanical and structural characteristics of the HI-STAR 100 package as they pertain to demonstrating compliance with the provisions of 10CFR71. All required structural design analyses of the packaging, components, and systems Important to Safety (ITS) pursuant to the provisions of 10CFR71 are documented in this chapter. The objectives of this chapter are twofold:

- a. To demonstrate that the structural performance of the HI-STAR 100 package has been adequately evaluated for the conditions specified under normal conditions of transport and hypothetical accident conditions.
- b. To demonstrate that the HI-STAR 100 package design has adequate structural integrity to meet the regulatory requirements of 10CFR71 [2.1.1].

To facilitate regulatory review, the assumptions and conservatism inherent in the analyses are identified along with a complete description of the analytical methods, models, and acceptance criteria. A summary of other considerations germane to satisfactory structural performance, such as corrosion and material fracture toughness is also provided.

This SAR is written to conform to the requirements of NUREG-1617 and 10CFR71 and follows the format of Regulatory Guide 7.9 [1.0.3]. It is noted that the areas of NRC staff technical inquiries with respect to 10CFR71 structural compliance span a wide array of technical topics within and beyond the material in this chapter. To facilitate the staff's review, Table 2.0.1 "Matrix of NUREG-1617/10CFR71 Compliance - Structural Review", is included in this chapter. A comprehensive cross-reference of the topical areas set forth in Section 2.3.2 (Regulatory Requirements) of the draft Regulatory Guide 1617, along with the sponsoring paragraphs in 10CFR71, and the location of the required compliance information, within this SAR, is contained in Table 2.0.1.

Section 2.10.2 contains a summary of the evaluation findings derived from the technical information presented in this chapter.

TABLE 2.0.1- MATRIX OF NUREG-1617/10CFR71 COMPLIANCE – STRUCTURAL REVIEW†

SECTION IN NUREG-1617 AND APPLICABLE 10CFR71/REG.GUIDE (R.G.) SECTIONS	NUREG-1617/10CFR71 COMPLIANCE ITEM	LOCATION IN SAR CHAPTER 2	LOCATION OUTSIDE OF SAR CHAPTER
<b>2.3.1 Description of Structural Design</b>			
10CFR71.31(a)(1); 10CFR71.33	Description of Structural Design	2.1	1.2.3
10CFR71.33	Drawings		1.4
10CFR71.33	Weights and Center of Gravity	2.2	
10CFR71.31(c)	Applicable Codes/Standards		1.3
<b>2.3.2 Material Properties</b>			
10CFR71.33	Materials and Material Specifications	2.3	
10CFR71.33	Prevention of Chemical, Galvanic, or Other Reactions	2.4	
10CFR71.43(d)	Effects of Radiation on Materials	2.4.4	

TABLE 2.0.1- MATRIX OF NUREG-1617/10CFR71 COMPLIANCE – STRUCTURAL REVIEW (Continued)

SECTION IN NUREG-1617 AND APPLICABLE 10CFR71/REG.GUIDE (R.G.) SECTIONS	NUREG-1617/10CFR71 COMPLIANCE ITEM	LOCATION IN SAR CHAPTER 2	LOCATION OUTSIDE OF SAR CHAPTER
R.G 7.11, 7.12	Brittle Fracture	2.1.2.3	
<b>2.3.3 Lifting and Tie Down Standards for All Packages</b>			
10CFR71.45(a)	Lifting Devices	2.5	1.4
10CFR71.45(b)	Tie-Down Devices	2.5	1.4
<b>2.3.4 General Considerations for Structural Evaluation of Packaging</b>			
10CFR71, Subpart E,F	Evaluation by Analysis		
10CFR71.35(a), 71.41(a)	• Models, Methods, and Results	2.6, 2.7.1,2.7.2	
10CFR71, Subpart E,F	• Material Properties	2.3	
“	• Boundary Conditions	2.6	
“	• Dynamic Amplifiers	2.6, 2.7	
“	• Load Combinations	2.1	
“	• Margins of Safety	2.5, 2.6, 2.7	

TABLE 2.0.1- MATRIX OF NUREG-1617/10CFR71 COMPLIANCE – STRUCTURAL REVIEW (Continued)

SECTION IN NUREG-1617 AND APPLICABLE 10CFR71/REG.GUIDE (R.G.) SECTIONS	NUREG-1617/10CFR71 COMPLIANCE ITEM	LOCATION IN SAR CHAPTER 2	LOCATION OUTSIDE OF SAR CHAPTER
10CFR71, Subparts E,F	Evaluation by Test		
10CFR71.73(a)	• Procedures for Impact Testing	2.7.1 2.A	
“	• Test Specimens	2.7.1 2.A	
10CFR71.73(c)(1)	• Drop Orientations	2.7.1 2.A	
“	• Conclusions	2.7.1 2.A	
<b>2.3.5 Normal Conditions of Transport</b>			
10CFR71.71 with reference to 10CFR71 sections 71.35(a), 71.43(f), 71.51(a)(1), 71.55(d)(4)	Heat	2.6.1	
“	Cold	2.6.2	
“	Reduced External Pressure	2.6.3	
“	Increased External Pressure	2.6.4	
“	Vibration	2.6.5	
“	Water Spray	2.6.6	
“	Free Drop	2.6.1; 2.6.2; 2.6.7	
“	Corner Drop	NA	NA
“	Compression	NA	NA
“	Penetration	NA	NA

TABLE 2.0.1- MATRIX OF 10CFR71 COMPLIANCE – STRUCTURAL REVIEW (Continued)

SECTION IN NUREG-1617 AND APPLICABLE 10CFR71/REG.GUIDE (R.G.) SECTIONS	NUREG-1617/10CFR71 COMPLIANCE ITEM	LOCATION IN SAR CHAPTER 2	LOCATION OUTSIDE OF SAR CHAPTER
<b>2.3.6 Hypothetical Accident Conditions</b>			
10CFR71.73(c)(1)	Free Drop	2.7.1, 2.A	
10CFR71.73(c)(2)	Crush	NA	NA
10CFR71.73(c)(3)	Puncture	2.7.2	
10CFR71.73(c)(4)	Thermal	2.7.3	
10CFR71.73(c)(5)	Immersion-Fissile Material	2.7.4	NA
10CFR71.73(c)(6)	Immersion – All Material	2.7.5	
<b>2.3.7 Special Requirements for Irradiated Nuclear Fuel Shipments</b>			
10CFR71.61	Elastic Stability of Containment	2.7.5	
“	Closure Seal Region Below Yield Stress	2.7.1	
<b>2.3.8 Internal Pressure Test</b>			
10CFR71.85(b)	Internal Pressure Test – All stresses below yield	2.6.1.4.3	8.1

TABLE 2.0.1- MATRIX OF 10CFR71 COMPLIANCE – STRUCTURAL REVIEW (Continued)

SECTION IN 10CFR71	10CFR71 COMPLIANCE ITEM	LOCATION IN SAR CHAPTER 2	LOCATION OUTSIDE OF SAR CHAPTER
<b>Appendices</b>			
	Supplemental Information	2.10	

† Legend for Table 2.0.1

Per the nomenclature defined in Chapter 1, the first digit refers to the chapter number, the second digit is the section number within the chapter; an alphabetic character in the second place means it is an appendix to the chapter.

NA Not Applicable for this item

## 2.1 STRUCTURAL DESIGN

### 2.1.1 Discussion

The HI-STAR 100 System (also designated as the HI-STAR 100 Package) consists of three principal components: the multi-purpose canister (MPC), the overpack assembly, and a set of impact limiters. The overpack confines the MPC and provides the containment boundary for transport conditions. The MPC is a hermetically sealed, welded structure of cylindrical profile with flat ends and an internal honeycomb fuel basket for SNF. A complete description of the HI-STAR MPC is provided in Section 1.2.1.2.2 wherein its design and fabrication details are presented with the aid of figures. A discussion of the HI-STAR 100 overpack is presented in Subsection 1.2.1.2.1. Drawings for the HI-STAR 100 System are provided in Section 1.4. In this section, the discussion is directed to characterizing and establishing the structural features of the MPC and the transport overpack.

The design of the HI-STAR 100 MPC seeks to attain three objectives that are central to its functional adequacy, namely;

- **Ability to Dissipate Heat:** The thermal energy produced by the spent fuel must be transported to the outside surface of the MPC such that the prescribed temperature limits for the fuel cladding and the fuel basket metal walls are not exceeded.
- **Ability to Withstand Large Impact Loads:** The MPC with its payload of nuclear fuel must be sufficiently robust to withstand large impact loads associated with the hypothetical accident conditions during transportation of the system. Furthermore, the strength of the MPC must be sufficiently isotropic to assure structural qualification under a wide variety of drop orientations.
- **Restraint of Free End Expansion:** The membrane and bending stresses produced by restraint of free end expansion of the fuel basket are conservatively categorized as primary stresses. In view of the concentration of heat generation in the fuel basket, it is necessary to ensure that structural constraints to its external expansion do not exist.

Where the first two criteria call for extensive inter-cell connections, the last criterion requires the opposite. The design of the HI-STAR 100 MPC seeks to realize all of the above three criteria in an optimal manner.

As the description presented in Chapter 1 indicates, the MPC enclosure vessel is a spent nuclear fuel (SNF) pressure vessel designed to meet ASME Code, Section III, Subsection NB stress limits. The enveloping canister shell, the MPC baseplate, and the closure lid system form a complete closed pressure vessel referred to as the "enclosure vessel". This enclosure vessel serves as the helium retention boundary when the HI-STAR 100 is within the purview of 10CFR71. Within this cylindrical vessel is an integrally welded assemblage of cells of square cross sectional openings, referred to herein as the "fuel basket". The fuel basket is analyzed under the provisions of Subsection NG of Section III of the ASME Code. There are different multi-purpose canisters that are exactly alike in their external dimensions. The essential difference between the MPCs lies in the fuel baskets. Each fuel storage MPC is designed to house fuel assemblies with different characteristics.

Although all HI-STAR 100 MPC fuel baskets are configured to maximize structural ruggedness through extensive inter-cell connectivity, they are sufficiently dissimilar in structural details to warrant separate evaluations. Therefore, analyses for the different MPC types are presented, as appropriate, throughout this chapter.

The HI-STAR 100 overpack provides the containment function for the stored SNF. There is an undivided reliance on the structural integrity of this containment vessel to maintain complete isolation of its contained radioactive contents from the environment under all postulated accident scenarios, even though the MPC is a completely autonomous, ASME Section III Class 1 pressure vessel which provides an unbreachable enclosure for the fuel. The containment boundary is made up of the inner shell, the bottom plate, the top flange, and the closure plate.

Components of the HI-STAR 100 System that are important to safety and their applicable design codes are defined in Chapter 1.

The structural function of the MPC in the transport mode is:

1. To maintain position of the fuel in a sub-critical configuration.
2. To maintain a helium confinement boundary.

The structural function of the overpack in the transport mode is:

1. To serve as a penetration and puncture barrier for the MPC.
2. To provide a containment boundary.
3. To provide a structurally robust support for the radiation shielding.

The structural function of the impact limiters in the transport mode is:

1. To cushion the HI-STAR 100 overpack and the contained MPC with fuel during normal transport handling and in the event of a hypothetical drop accident during transport.

Some structural features of the MPCs that allow the system to perform their structural functions are summarized below:

- There are no external or gasketed ports or openings in the MPC. The MPC does not rely on any sealing arrangement except welding. The absence of any gasketed or flanged joints precludes joint leaks. The MPC enclosure vessel contains no valves or other pressure relief devices.

- The closure system for the MPCs consists of two components, namely, the MPC lid and the closure ring. The MPC lid is a thick circular plate continuously welded to the MPC shell along its circumference. The MPC closure system is shown in the drawings in Section 1.4. The MPC lid-to-MPC shell weld is a J-groove weld that is subject to root and final pass liquid penetrant examinations and finally, a volumetric examination to ensure the absence of unacceptable flaws and indications. The MPC lid is equipped with vent and drain ports which are utilized for evacuating moisture and air from the MPC following fuel loading and subsequent backfilling with an inert gas (helium) in a specified quantity. The vent and drain ports are covered by a cover plate and welded before the closure ring is installed. The closure ring is a thin circular annular plate edge-welded to the MPC shell and to the MPC lid. Lift points for the MPC are provided in the MPC lid.
- The MPC fuel basket consists of an array of interconnecting plates. The number of storage cells formed by this interconnection process varies depending on the type of fuel being transported. Basket designs for different PWR and BWR cell configurations have been designed and are explained in detail in Subsection 1.2. All baskets are designed to fit into the same MPC shell. Welding the plates along their edges essentially renders the fuel basket into a multi-flange beam. For example, Figure 2.1.1 provides an isometric illustration of a fuel basket for the MPC-68 design.
- The MPC basket is separated from the longitudinal supports installed in the enclosure vessel by a small gap. The gap size decreases as a result of thermal expansion (depending on the magnitude of internal heat generation from the stored spent fuel). The provision of a small gap between the basket and the basket support structure is consistent with the natural thermal characteristics of the MPC. The planar temperature distribution across the basket, as shown in Chapter 3, approximates a shallow parabolic profile. This profile will create high thermal stresses unless structural constraints at the interface between the basket and the basket support structure are removed.

The MPCs will be loaded with fuel assemblies with widely varying heat generation rates. The basket/basket support structure gap tends to be reduced for higher heat generation rates due to increased thermal expansion rates. The basket/basket support structure gap tends to be reduced due to thermal expansion from decay heat generation. Gaps between the fuel basket and the basket support structure are specified to be sufficiently large such that a gap exists around the periphery under all normal or accident conditions of transport.

A small number of optional flexible thermal conduction elements (thin aluminum tubes) may be interposed between the basket and the MPC shell. The elements are designed to be resilient. They do not provide structural support for the basket, and thus their resistance to thermal growth is negligible.

Structural features of the overpack that allow the HI-STAR 100 package to perform its safety function are summarized below:

- The overpack features a thick inner shell welded to a bottom plate which forms a load bearing surface for the HI-STAR 100 System. A solid metal top flange welded at the top of the inner shell provides the attachment location for the lifting trunnions. The top flange is designed to provide a recessed ledge for the closure plate to protect the bolts from direct shear loading resulting from an impulsive load at the top edge of the overpack (Figure 2.1.2). In the transport mode the overpack inner shell, bottom plate, top flange, and closure plate with metallic seals constitute the containment boundary for the HI-STAR 100 System. The HI-STAR 100 overpack is subject to the stress limits of the ASME Code, Section III, Subsection NB [2.1.5].
- The inner shell (containment boundary) is reinforced by multi-layered intermediate shells. The multi-layer approach eliminates the potential for a crack in any one layer, developed by any postulated mechanical loading or material flaw, to travel uninterrupted through the vessel wall. The intermediate shells also buttress the overpack inner shell against buckling. The intermediate shells of the HI-STAR 100 overpack are subject to the stress limits of the ASME Code, Section III, Subsection NF, Class 3 [2.1.7].
- To facilitate handling of the loaded package, the HI-STAR 100 overpack is equipped with two lifting trunnions at the top of the overpack. The initial seven HI-STAR 100 overpacks are also equipped with pocket trunnions, embedded in the overpack intermediate shells, just above the bottom plate. HI-STAR 100 overpacks fabricated after the initial seven do not have pocket trunnions (see Subsection 2.5 for further discussion). Lifting trunnions are conservatively designed to meet the design safety factor requirements of NUREG-0612 [2.1.9] and ANSI N14.6-1993 [2.1.10] for single failure proof lifting equipment.
- A circular recess is incorporated on the inner surface of the overpack closure plate. The purpose of this recess is to reduce the moment applied to the flanged joint from MPC impact during a hypothetical top end drop accident. During a hypothetical drop accident where the top end of the overpack impacts first, the MPC contacts the inner surface of the overpack closure plate. Because of the recess, the MPC will only contact an annular region of the inner surface of the overpack closure plate. Thus, the load on the overpack closure plate from the MPC is located closer to the bolt circle, and the moment on the flanged joint is reduced.
- A small circular gap between the MPC external surface and the inside surface of the overpack is provided to allow insertion and removal of the MPC. This gap diminishes monotonically with the increase in the heat generation rate in the MPC, but is sized to avoid metal-to-metal contact between the MPC and the overpack cylindrical surface as a result of thermal expansion under the most adverse thermal conditions.
- There are no valves in the HI-STAR 100 overpack containment boundary. The vent and drain ports used during HI-STAR 100 overpack loading and unloading operations are closed with port plugs and metallic seals. The port plugs are recessed and are suitably protected with a cover plate with seal. These small penetrations equipped with dual seals are not deemed to be particularly vulnerable locations in the HI-STAR 100 System.

The HI-STAR 100 System is equipped with a set of impact limiters (AL-STAR) attached to the top and bottom ends of the overpack. The structural function of the impact limiters is to cushion the HI-STAR 100 overpack and the contained MPC with fuel in the event of a hypothetical drop accident during transport, and to provide the necessary resistance to the longitudinal decelerations experienced during normal rail transport. The design of the impact limiter is independent of the design of the MPC and overpack. This is achieved by establishing design basis deceleration limits for normal transport and for the hypothetical 30-foot drop accident and demonstrating that impact limiter performance limits the deceleration levels imposed on the cask.

Table 1.3.3 provides a listing of the applicable design codes for all structures, systems, and components that are designated as Important to Safety (ITS).

2.1.2 Design Criteria

Regulatory Guide 7.6 provides design criteria for the structural analysis of shipping casks [2.1.4]. Loading conditions and load combinations that must be considered for transport are defined in 10CFR71 [2.1.1] and in USNRC Regulatory Guide 7.8 [2.1.2]. Consistent with the provisions of these documents, the central objective of the structural analysis presented in this chapter is to ensure that the HI-STAR 100 System possesses sufficient structural capability to meet the demands of normal conditions and hypothetical accident conditions of transport.

The following table provides a synoptic matrix to demonstrate our explicit compliance with the seven regulatory positions stated in Regulatory Guide 7.6.

<b>REGULATORY GUIDE 7.6 COMPLIANCE</b>	
<b>Regulatory Position</b>	<b>Compliance in HI-STAR 100 SAR</b>
1. Material properties, design stress intensities, and fatigue curves are obtained from the ASME Code	Tables 2.1.12-2.1.20 for allowable stresses/stress intensities and Tables 2.3.1-2.3.5 for material properties are obtained from the ASME Code (the 1995 Code tables are used). Section 2.6.1.3.3 uses the appropriate fatigue data from the Code.
2. Under normal conditions of transport, the limits on stress intensity are those limits defined by the ASME Code for primary membrane and for primary membrane plus bending for Level A conditions.	Tables 2.1.3-2.1.5 define the correct stress intensity limits for normal conditions of transport as stated in the ASME Code for Level A conditions.
3. Perform fatigue analysis for normal conditions of transport using ASME Code Section III methodology (NB) and appropriate fatigue curves.	Section 2.6.1.3.3 considers the potential for fatigue using accepted ASME Code methodology and fatigue data from the ASME Code.
4. The stress intensity $S_n$ associated with the range of primary plus secondary stresses under normal conditions should be less than $3S_m$ where $S_m$ is the primary membrane stress intensity from the Code.	Section 2.6.1.3.3 considers the fatigue potential of the HI-STAR 100 Package based on the $3S_m$ limit.
5. Buckling of the containment vessel should not occur under normal or accident conditions.	The methodology used is Code Case N-284; this has been accepted by the NRC as an appropriate vehicle to evaluate buckling of the containment.

<b>REGULATORY GUIDE 7.6 COMPLIANCE</b>	
<b>Regulatory Position</b>	<b>Compliance in HI-STAR 100 SAR</b>
6. Under accident conditions, the values of primary membrane stress intensity should not exceed the lesser of $2.4S_m$ and $0.7S_u$ (ultimate strength), and primary membrane plus bending stress intensity should not exceed the lesser of $3.6S_m$ and $S_u$ .	Tables 2.1.3-2.1.5 of the SAR state these requirements.
7. The extreme total stress intensity range should be less than $S_a$ at 10 cycles as given by the appropriate fatigue curves.	Subsection 2.6.1.3.3 demonstrates compliance by conservatively bounding the total stress intensity range and demonstrating that the bounding value is less than $S_a$ at 10 cycles as given by the appropriate fatigue curves.

Note that Regulatory Guide 7.6 references ASME Code Sections in the 1977 code year. This SAR has been prepared using the identical information on allowable stress intensities and fatigue data as listed in the 1995 ASME Code.

Table 1.3.1, in Chapter 1, summarizes the ASME pressure vessel code applicability to HI-STAR 100 components. Table 1.3.2 in Chapter 1 provides a statement of exceptions taken to the ASME Code requirements.

Stresses arise in the components of the HI-STAR 100 System due to various loads that originate under normal and hypothetical accident conditions of transport. These individual loads are combined to form load combinations. Stresses and stress intensities resulting from the load combinations are compared to allowable stresses and stress intensities. The following subsections present loads, load combinations, and allowable strengths for use in the structural analyses of the MPC and the HI-STAR 100 overpack.

2.1.2.1 Loading and Load Combinations

10CFR71 and Regulatory Guide 7.6 define two conditions that must be considered for qualification of a transport package. These are defined as "Normal Conditions of Transport" and "Hypothetical Accident Conditions", which are related herein to the ASME Code Service Levels for the purposes of quantifying allowable stress limits. In terms of the ASME terminology, the following parallels are applicable.

Normal Conditions of Transport = ASME Design Condition and ASME Level A or B Service Condition

Hypothetical Accident Condition = ASME Level D Service Condition

To establish the appropriate loadings and load combinations that require evaluation, the pressure and temperatures used for the design analyses must be defined. Table 2.1.1 establishes the design pressures for the two transport conditions that must be evaluated. Table 2.1.2 establishes reference hot temperature limits for the two conditions of transport. The ASME Code does not prescribe a metal temperature limit for Level D (also called "faulted") conditions. Under the provisions of the ASME Code, large strains (such as deformations resulting from a thermal shock) are acceptable if

the post-event structural configuration of the component is within the limits prescribed for it subsequent to the faulted event (ASME Code Section III, Subsection NCA-2142.4). In the case of the cask, it is required that the containment boundary continues to perform its function and that the outer skin continues to provide an enclosure for the radiation shielding. For conservatism, the peak metal bulk temperature during and after the fire transient in the overpack containment structure is required to be limited to the maximum temperature limit prescribed in the ASME Section II Part D allowable stress /stress intensity tables. That is, the maximum bulk metal temperature is equal to the maximum temperature for which the allowable stress intensity,  $S_m$ , is listed in the Code for the applicable Code Class. For the external skin of the overpack that is directly exposed to the fire no specific temperature limits are enforced by the governing documents. The performance expectation of the HI-STAR 100 package, however, is that the skin does not melt, slump, or sever from the overpack structure. This performance objective is considered to be fulfilled with adequate margin if the metal temperature of the enclosure shell at any section does not exceed 50% of the melting point of the shell material. Tables 2.1.3 and 2.1.4 set forth the allowable strength bases for the two conditions of transport based on their designation as Level A, B, or D.

For its qualification as an acceptable packaging component, the following types of loads are defined for the HI-STAR 100 MPC.

- Dead load (lb.),  $D$ ;
- Internal design pressure (psi),  $P_i$ ;
- External design pressure (psi),  $P_o$ ;
- Accident internal pressure (psi),  $P_i^*$ ;
- Accident external pressure (psi),  $P_o^*$ ;
- Thermal load due to design basis heat generation in the MPC,  $T$ , and under most adverse external environmental conditions,  $T'$ ;
- Side drop at  $0^\circ$  basket circumferential orientation under normal conditions of transport,  $H$ ;
- Side drop at  $45^\circ$  basket circumferential orientation under normal conditions of transport,  $H$ ;
- Drop at  $0^\circ$  fuel basket circumferential orientation under design basis deceleration for hypothetical accident conditions,  $H'$  (angle of inclination that the package longitudinal axis makes with the horizontal plane varies);
- Drop at  $45^\circ$  fuel basket circumferential orientation under design basis deceleration for hypothetical accidental conditions,  $H'$  (angle of inclination that the package longitudinal axis makes with the horizontal plane varies);
- Vertical drop under design basis deceleration for hypothetical accident conditions,  $H'$ .

Insofar as the fuel basket is not radially symmetric, the orientation of the basket cross section with respect to the direction of side drop will affect the state of stress induced by the deceleration produced by the impact. Heretofore, two horizontal drop circumferential orientations are considered which are referred to as the 0 degree drop and 45 degree drop, respectively. Figures 2.1.3 and 2.1.4, showing an MPC-68 fuel basket, illustrate the two orientations. In the 0-degree drop, the basket drops with its two sets of panels, respectively; parallel and normal to the vertical (Figure 2.1.3). The 45-degree drop implies that the basket's honeycomb section is rotated meridionally by 45 degrees (Figure 2.1.4).

For the above loads, a series of load combinations for the fuel baskets and the enclosure vessel are compiled in Tables 2.1.6 and 2.1.7, respectively. These load combinations represent both normal conditions of transport and the hypothetical accident conditions.

The loadings and load combinations applicable to the overpack are more numerous, because all external loads directly bear on it and several potentially limiting oblique drop orientations exist. In the following, each individual overpack loading which enters in subsequent load combinations is explained.

- **Internal Design Pressure,  $P_i$ :** An internal design pressure is defined for the containment cavity of the overpack pressure vessel (Figure 2.1.5). The coincident external pressure is assumed to be atmospheric (0 psig) (Table 2.1.1). For conservatism, the design value is set equal to the MPC internal pressure under normal conditions of transport.
- **External Design Pressure,  $P_o$ :** An external design pressure with the cavity depressurized (0 psig) is defined for the overpack pressure vessel as the second design condition loading (Figure 2.1.6),(Table 2.1.1).
- **Accident External Pressure,  $P_o^*$ :** An external accident design pressure with cavity depressurized (Figure 2.1.6) (Table 2.1.1). This loading in conjunction with the buckling analysis of the overpack inner shell, is intended to demonstrate that the containment boundary is in compliance with the requirements of 10CFR71.61. This loading condition bounds the external pressure specified by 10CFR71.73(c) (5) and (6).
- **Accident Internal Pressure,  $P_i^*$ :** An internal accident design pressure is defined for the containment cavity of the overpack pressure vessel (Figure 2.1.5). The coincident external pressure is assumed to be atmospheric (0 psig) (Table 2.1.1). The design value is based on conservatively assuming that the MPC enclosure vessel is breached.
- **Thermal Conditions:** Thermal conditions pertain to the stresses that develop due to thermal gradient in the overpack. The temperature field in the overpack under the maximum heat generation scenario is developed in Chapter 3. The effect of this temperature field,  $T_h$ , is included in all load cases, as appropriate.

The condition where the overpack is subject to a  $-40^{\circ}\text{F}$  ambient environment and maximum decay heat is labeled as  $T_s$ . Likewise, the condition when the overpack is subject to a  $-20^{\circ}\text{F}$  ambient environment is denoted by  $T_c$ . Finally, the thermal load during and after 30 minutes of exposure to a  $1475^{\circ}\text{F}$  enveloping fire is referred to as  $T_f$ .

- **Overpack Joint Sealing Load,  $W_s$ :** The pre-load applied to the overpack closure plate bolts seat the metallic seals and create a contact pressure on the inside land which serves to protect the joint from leakage under postulated impact loading events. The bolt pre-load, however, produces a state of stress in the overpack top closure plate, the overpack top flange, and the overpack inner and intermediate shell region adjacent to the flange. The pre-load,  $W_s$ , is, therefore, treated as a distinct loading type.
- **Fabrication Loads,  $F$ :** The internal loads induced due to the method of fabrication employed in building the overpack are included in the load combinations.
- **Bottom End Drop,  $D_{ba}$ :** This is the first of six drop accident scenarios, wherein the packaging is assumed to drop vertically with its overpack bottom plate sustaining the impulsive load transmitted through the bottom impact limiter. The weight of the package is included in all drop load cases. A schematic of the external forces working on the overpack under this drop scenario is illustrated in Figure 2.1.7. The deceleration load under the 30 ft drop event (accident event) is labeled  $D_{ba}$ . (The design basis deceleration is given in Table 2.1.10).
- **Top End Drop,  $D_{ta}$ :** This drop condition is the opposite of the preceding case. The top closure plate withstands the impact load transmitted through the impact limiter. This loading is illustrated in Figure 2.1.8. The design basis deceleration is given in Table 2.1.10.
- **Side Drop,  $D_{sn}$  and  $D_{sa}$ :** The overpack along with its contents drops with its longitudinal axis horizontal. The loaded MPC bears down on the overpack as it decelerates under the resistance offered by the two impact limiters pressing against an essentially unyielding surface (Figure 2.1.9). The subscripts “n” and “a” denote normal transport and hypothetical accident conditions, respectively. The design basis deceleration is given in Table 2.1.10.
- **Bottom C.G.-Over-the-Corner Drop,  $D_{ca}$ :** In this drop scenario, the HI-STAR 100 System is assumed to impact an essentially unyielding surface with its center-of-gravity directly above its bottom corner (Figure 2.1.10) under the hypothetical drop accident condition. The design basis deceleration is given in Table 2.1.10.
- **Top Center-of-Gravity Over-the-Corner Drop,  $D_{ga}$ :** This loading case is identical to the preceding case, except that the package is assumed to be dropping with its top end down and its center-of-gravity is aligned with the corner of the top closure plate (Figure 2.1.11). The design basis deceleration is given in Table 2.1.10.

- **Side Puncture Force Event,  $P_s$ :** This event consists of a free drop of the packaging for 1 meter (40 in.) on to a stationary and vertical mild steel bar of 6 in. diameter with its leading edge (top edge) rounded to 1/4 in. radius. The bar is assumed to be of such a length as to cause maximum damage to the overpack. The package is assumed to be dropping horizontally with the penetrant force being applied at the mid-length of the cask (Figure 2.1.12).
- **Top End Puncture Force,  $P_t$ :** This event is similar to the preceding case except the penetrant force is assumed to act at the center of the top closure plate (Figure 2.1.13).
- **Bottom End Puncture Force,  $P_b$ :** This is the third of the bar puncture events configured to create a condition of maximum damage to the package. The loading event is identical to the preceding two cases, except that the puncture load acts on the center of the bottom plate of the overpack (Figure 2.1.14).
- **Vibration and Shock,  $V$ :** Vibration and shock loads arise during transport of the packaging. The vibratory loads transmitted to the HI-STAR 100 System will produce negligibly small stresses in comparison with stresses that will be produced by the loadings described previously. Therefore, this loading is neglected in the analyses performed herein.

The foregoing loadings are combined in the manner of Table 1 of Regulatory Guide 7.8 to form four (4) distinct load combinations for the normal condition of transport and nineteen (19) load combinations for the hypothetical accident conditions. These load combinations are summarized in Tables 2.1.8 and 2.1.9.

Two concluding observations are relevant with respect to a Flange Seating Condition and to the External Pressure Condition:

- **Flange Seating Condition:** The stress field in the overpack under the bolt pre-stress load condition is evaluated with the elastic constants of the finite element gridwork in the overpack set at its coincident hot environment condition (100°F ambient). The bolt pre-load and material elastic constants under the cold environment condition (-20°F) will be different, resulting in a slightly different stress field. However, the consequence of this refinement is considered to be a second order effect and is, therefore, neglected.
- **External Pressure Condition:** The condition of 20 psia external pressure in Table 1 of Regulatory Guide 7.8 is conservatively bounded by the deep submergence pressure under 200 meters of water. Likewise, the internal design pressure of 100 psig with outside at ambient is assumed to conservatively bound the minimum external pressure (3.5 psia) service condition.

In the load cases considered (Tables 2.1.6-2.1.9), material behavior is always considered to be linearly elastic. To facilitate review, the following matrix is provided to relate the load combinations specifically addressed in Table 1 of Regulatory Guide 7.8 to the load combinations defined in this SAR by Tables 2.1.6-2.1.9. Also included in the matrix are locations in the SAR where particular results are presented that are germane to demonstrating compliance with the intent of Regulatory Guide 7.8.

Compliance of HI-STAR 100 SAR With Regulatory Guide 7.8 Load Combinations		
Reg. Guide Load Combination	HI-STAR 100 Explicit Load Combination (Tables 2.1.6-2.1.9)	Location in SAR for Results
<b>NORMAL CONDITIONS</b>		
Hot Environment	Table 2.1.7(Case E1.c) Table 2.1.8(Case 1)	2.6.1.3.1.2; Tables 2.6.6,2.6.7 Table 2.6.5; Table 2.6.9
Cold Environment	Table 2.1.8(Case 2)	Table 2.6.12
Increased External Pressure	Table 2.1.9 (Case 18 bounds)	2.6.4
Minimum External Pressure	---	2.6.3
Vibration and Shock	---	2.6.5
One-Foot Free Drop	Table 2.1.6(Case F2) Table 2.1.7(Case E2) Table 2.1.8(Cases 3,4)	Tables 2.6.2,2.6.8 Table 2.6.3 Tables 2.6.9,2.6.12
<b>ACCIDENT CONDITIONS</b>		
Thirty-Foot Free Drop	Table 2.1.6(Case F3) Table 2.1.7(Case E3) Table 2.1.9(Cases 1-5;9-13)	Tables 2.7.1,2.7.4,2.7.7 Tables 2.7.2,2.7.4,2.7.7 Tables 2.7.3,2.7.5,2.7.6-2.7.8
Puncture by Bar	Table 2.1.9(Cases 6-8;14-16)	Tables 2.7.3,2.7.5,2.7.6-2.7.8
Fire Accident	Table 2.1.9(Cases 17,19)	Tables 2.7.3,2.7.8

2.1.2.2 Allowables

Components of the HI-STAR 100 System Important to Safety (ITS) are listed in Table 1.3.3. Allowable stresses are tabulated for these components for all applicable service levels. The applicable service level from the ASME Code for determination of allowables is listed in Subsection 2.1.2.1.

Allowable stress limits for the overpack containment structure and for the MPC enclosure vessel are obtained from the ASME Code, Section III, Division 1, Subsection NB [2.1.5]. The MPC fuel basket is subject to the stress limits of ASME Section III, Division 1, Subsection NG [2.1.6].

All non-containment parts of the overpack (e.g., intermediate shells, outer enclosure shells, radial channels), are subject to the stress limits of ASME Section III, Subsection NF [2.1.7] for mechanical loadings. The overpack containment boundary and the MPC enclosure vessel are also evaluated for stability in accordance with ASME Code Case N-284 [2.1.8]. Overpack closure bolts are subject to the stress limits of ASME Section III, Subsection NB. Finally, lifting trunnions and other lifting components are subject to the stress limits of NUREG-0612 [2.1.9], which references ANSI N14.6 [2.1.10].

Allowable stresses and stress intensities are calculated using the data provided in the ASME Code, Section II, Part D [2.1.11] and Tables 2.1.3 through 2.1.5. Tables 2.1.11 through 2.1.20 contain numerical values of the allowable stresses/stress intensities for all MPC and overpack load-bearing materials as a function of temperature.

In all tables, the terms  $S_m$ ,  $S_y$ , and  $S_u$ , respectively, denote the design stress intensity, minimum yield strength, and the ultimate strength. Property values at intermediate temperatures that are not reported in the ASME Code are obtained by linear interpolation as allowed by paragraph NB-3229. Property values are not extrapolated beyond the limits of the Code in any structural analysis.

Additional terms relevant to the analyses are extracted from the ASME Code (Figure NB-3222-1) as follows.

<u>Symbol</u>	<u>Description</u>	<u>Notes</u>
$P_m$	Average primary stress across a solid section.	Excludes effects of discontinuities and concentrations. Produced by pressure and mechanical loads.
$P_L$	Average stress across any solid section.	Considers effects of discontinuities but not concentrations. Produced by pressure and mechanical loads, including inertia earthquake effects.
$P_b$	Primary bending stress.	Component of primary stress proportional to the distance from the centroid of a solid section. Excludes the effects of discontinuities and concentrations. Produced by pressure and mechanical loads, including inertia earthquake effects.
$P_e$	Secondary expansion stress.	Stresses which result from the constraint of free-end displacement. Considers effects of discontinuities but not local stress concentration. (Not applicable to vessels.)
$Q$	Secondary membrane plus bending stress.	Self-equilibrating stress necessary to satisfy continuity of structure. Occurs at structural discontinuities. Can be caused by pressure, mechanical loads, or differential thermal expansion.
$F$	Peak stress.	Increment added to primary or secondary stress by a concentration (notch), or, certain thermal stresses that may cause fatigue but not distortion. This value is not used in the tables.

It is shown in this report that there is no interference between component parts due to free thermal expansion. Therefore,  $P_e$  does not develop within any HI-STAR 100 component. A summary of the allowable limits for normal conditions of transport and for the hypothetical accident conditions as they apply to various components of the package is presented in Table 2.1.3 for the overpack and MPC enclosure vessel (shell, lid, and baseplate), in Table 2.1.4 for the MPC fuel basket, and in Table 2.1.5 for the non-containment parts of the overpack.

It is recognized that the planar temperature distribution in the fuel basket and the overpack under the maximum heat load condition is the highest at the cask center and drops monotonically, reaching its lowest value at the outside surface. Strictly speaking, the allowable stresses/stress intensities at any location in the basket, the enclosure vessel, or the overpack should be based on the coincident metal temperature under the specific operating condition. However, in the interest of conservatism, reference temperatures may be established for each component that are upper bounds on the metal temperature for each situational condition. Table 2.1.21 provides the reference temperatures for the MPC and the overpack and, utilizing Tables 2.1.11 through 2.1.20, provides conservative numerical limits for the stresses and stress intensities for all loading cases.

Summarizing the previous discussions, in accordance with the Regulatory Guide 7.6 and with ASME Code Section III, Subsection NB, the allowable stress limits for the overpack containment boundary are based on design stress intensities ( $S_m$ ), yield strengths ( $S_y$ ) and ultimate strengths ( $S_u$ ). These limits govern the design of the overpack (including the inner shell, the top flange, the bottom plate, and the closure plate), and also govern the design of the MPC enclosure vessel. The stress limits for the MPC fuel basket are based on stress intensities as set forth in ASME, Section III, Subsection NG. For applicable accident conditions, Appendix F of the ASME Code applies [2.1.12]. Stress limits for closure bolts conform to those given in Table 2.1.24.

The lifting devices in the HI-STAR 100 overpack and the multi-purpose canisters, collectively referred to as "trunnions", are subject to specific limits set forth by NUREG-0612: the primary stresses in a trunnion must be less than the smaller of 1/10 of the material ultimate strength and 1/6 of the material yield strength while loaded by the lifted load that includes an appropriate dynamic load amplifier.

The region around the trunnion is part of the NF structure in HI-STAR 100 and an NB pressure boundary in the MPC, and as such, must satisfy the applicable stress (or stress intensity) limits for the load combination. In addition to meeting the applicable Code limits, it is further required that the local primary stresses at the trunnion/mother structure interface must not exceed the material yield stress at three times the handling condition load. This criterion eliminates the potential of local yielding at the trunnion/structure interface.

Impact limiters are not designed to any stress or deformation criteria. Rather, their function is solely to absorb the impact energy by plastic deformation. The impact limiter must perform its energy absorption function over the range of environmental temperatures.

Allowable stresses derived from other authoritative sources are summarized in Table 2.1.24.

### 2.1.2.3 Brittle Fracture Failure

The MPC canister and basket are constructed from a series of stainless steels termed Alloy X. These stainless steel materials do not undergo a ductile-to-brittle transition in the minimum temperature range of the HI-STAR 100 System. Therefore, brittle fracture is not a concern for the MPC components. However, the HI-STAR 100 overpack is composed of ferritic steel materials, which will be subject to impact loading in a cold environment and, therefore, must be evaluated and/or subjected to impact testing in accordance with the ASME Code to ensure protection against brittle fracture.

Tables 2.1.22 and 2.1.23 provide the fracture toughness test criteria for the HI-STAR 100 overpack components in accordance with the applicable ASME Codes and Regulatory Guide requirements for prevention of brittle fracture. Regulatory Guides 7.11 [2.1.13] and 7.12 [2.1.14] are used to determine drop test requirements for the containment boundary components, as discussed below.

All containment boundary materials subject to impact loading in a cold environment must be evaluated and/or tested for their propensity for brittle fracture. The overpack baseplate, top flange, and closure plate have thicknesses greater than four inches. Table 1 of Regulatory Guide 7.12 requires that the Nil Ductility Transition temperature,  $T_{NDT}$  (for the lowest service temperature of  $-20^{\circ}\text{F}$ ), be  $-129^{\circ}\text{F}$  for 6-inch thick material, and linear interpolation of the table shows that for 7-inch thick material, the  $T_{NDT}$  is  $-132^{\circ}\text{F}$ . SA350-LF3 has been selected as the material for these overpack components based on the material's capability to perform at low temperatures with excellent ductility properties.

The overpack inner shell has a thickness of 2.5 inches. SA203-E has been selected as the material for this item due to its capability to perform at low temperatures (Table A1.15 of ASME Section IIA. Regulatory Guide 7.11 requires that the  $T_{NDT}$  for this material be less than  $-70^{\circ}\text{F}$  (at the lowest service temperature of  $-20^{\circ}\text{F}$ ).

The overpack closure plate bolts are fabricated from SB-637 Grade N07718, a high strength nickel alloy material. Section 5 of NUREG/CR-1815 [2.1.15] indicates that bolts are generally not considered a fracture critical component. Nevertheless, this material has a high resistance to fracture at low temperatures, as can be shown by calculating the transition temperature of the material and assessing its performance as indicated in NUREG/CR-1815.

The Aerospace Structural Metals Handbook [2.1.16] shows that minimum impact absorption energy for SB-637 Grade N07718 at  $-320^{\circ}\text{F}$  is 18.5 ft-lb. This may be transferred into a fracture toughness value by using the relationship (presented in Section 4.2 of NUREG/CR-1815) between Charpy impact measurement,  $C_v$  (ft-lb), and dynamic fracture toughness,  $K_{ID}$  (psi  $\sqrt{\text{in.}}$ )

$$K_{ID} = (5 E C_v)^{1/2}$$

where  $E = 31 \times 10^6$  psi at  $-320^{\circ}\text{F}$  and  $C_v$  (minimum) = 18.5 ft-lb.

Therefore,

$$K_{ID} = 53.5 \text{ ksi}\sqrt{\text{in.}}$$

Using Figure 2 of NUREG/CR-1815 yields

$$(T - T_{NDT}) = 32 \text{ degrees F}$$

Since the data used is for  $T = -320^{\circ}\text{F}$ , then  $T_{NDT} = -320^{\circ}\text{F} - 32^{\circ}\text{F} = -352^{\circ}\text{F}$

Using Figure 3 of NUREG/CR-1815 where thickness is defined as the bolt diameter (1.5 inch), and  $\sigma/\sigma_{yd} = 1$  per Regulatory Guide 7.11, A (degrees F) is found to be 60 degrees F. Therefore, the required maximum nil ductility transition temperature per NUREG/CR-1815 for the closure bolts is:

$$\begin{aligned} T_{NDT} &= T_{LT} - A \\ &= -40^{\circ} - 60^{\circ} = -100^{\circ}\text{F} \end{aligned}$$

where  $T_{LT}$  = lowest temperature of  $-40^{\circ}\text{F}$  (conservatively below the lowest service temperature).

The large margin between the calculated  $T_{NDT}$  and the required maximum Nil Ductility Transition temperature leads to the conclusion that SB-637 Grade N07718 possesses appropriate fracture toughness for use as closure lid bolting.

ASME Code Section III, Subsection NF requires Charpy V-notch tests for materials of certain noncontainment components of the overpack. The intermediate shells used for gamma shielding are fabricated from normalized SA516-70. Table A1.15 of ASME Section IIA shows that normalized SA516-70 should have minimum energy absorption of 12 ft-lb at  $-40^{\circ}\text{F}$  for a Charpy V-notch test. The lowest anticipated temperature the overpack is to experience is conservatively set at  $-40^{\circ}\text{F}$ . Therefore, these tests on the normalized SA516-70 materials of the intermediate shells will confirm the minimum energy absorption of 12 ft-lb at  $-40^{\circ}\text{F}$  and the ability of the intermediate shells to perform their intended function at the lowest service temperature.

The pocket trunnions in the initial seven HI-STAR 100 overpacks are fabricated from 17-4PH (or equivalent) material that is precipitation hardened to condition H1150. ARMCO Product Data Bulletin S-22 [2.1.17] shows that Charpy V-notch testing of 17-4PH H1150 material at  $-110^{\circ}\text{F}$  gives energy absorption values of approximately 48 ft-lbs. Using the same methodology as used for the closure bolts,

$$K_{ID} = 83 \text{ ksi}\sqrt{\text{in.}}$$

where  $E = 28.7 \times 10^6$  psi and  $C_v = 48$  ft-lbs.

Using Figure 2 of NUREG/CR-1815 yields

$$T - T_{NDT} = 65^{\circ}\text{F}$$

and therefore

$$T_{\text{NDT}} = -110^{\circ}\text{F} - 65^{\circ}\text{F} = -175^{\circ}\text{F}$$

While the optional pocket trunnions are not part of the containment for the overpack, Regulatory Guide 7.12 is used to define the required  $T_{\text{NDT}}$  for the trunnion pocket thickness ( $T_{\text{NDT}} = -140^{\circ}\text{F}$ ). The  $35^{\circ}\text{F}$  margin between the calculated  $T_{\text{NDT}}$  and the  $T_{\text{NDT}}$  defined in Regulatory Guide 7.12 provides assurance that brittle fracture failure of the 17-4 material will not occur at the lowest service temperature.

#### 2.1.2.4 Impact Limiter

The impact limiters are designed as energy absorbers to ensure that the maximum impact deceleration applied to the package is limited to values less than the design basis deceleration, as applicable.

#### 2.1.2.5 Buckling

Certain load combinations subject structural sections with relatively large slenderness ratios (such as the MPC enclosure vessel shell) to compressive stresses that may actuate buckling instability before the allowable stress is reached. Tables 2.1.7 and 2.1.9 list load combinations for the MPC enclosure vessel and the HI-STAR 100 overpack structure; the cases that warrant stability (buckling) check are listed therein.

Table 2.1.1

## DESIGN PRESSURES

Pressure Location	Condition	Pressure (psig)
MPC Internal Pressure	Normal Condition of Transport	100
	Hypothetical Accident	200 <sup>†</sup>
MPC External Pressure	Normal Condition of Transport	40
	Hypothetical Accident	60 <sup>††</sup>
Overpack External Pressure	Normal Condition of Transport	(0) Ambient
	Hypothetical Accident	300
Overpack Internal Pressure	Normal Condition of Transport	-Same as MPC Internal Pressure
	Hypothetical Accident	Same as MPC Internal Pressure
Overpack Enclosure Shell Internal Pressure	Normal Condition of Transport	30
	Hypothetical Accident	30

<sup>†</sup> This pressure is only associated with the hypothetical accident where 100% rod rupture is assumed to occur. For all other accident events, such as a 30-ft drop, the applicable MPC internal pressure is the design pressure under normal conditions of transport.

<sup>††</sup> For transport, this represents the differential pressure limit for elastic/plastic stability calculations.

Table 2.1.2

NORMAL REFERENCE TEMPERATURES AND ACCIDENT BULK METAL  
TEMPERATURE LIMITS

HI-STAR 100 Component	Normal Operating Condition Reference Temp. Limits <sup>†</sup> (Deg.F)	Hypothetical Accident Condition Metal Bulk Temp. Limits <sup>††</sup> (Deg.F)
MPC shell	450	550
MPC basket	725	950
MPC lid	550	775
MPC closure ring	400	775
MPC baseplate	400	775
MPC neutron absorber	800	950
MPC heat conduction elements	725	950
Overpack inner shell	400	500
Overpack bottom plate	350	700
Overpack closure plate	400	700
Overpack top flange	400	700
Overpack closure plate seals	400	1200
Overpack closure plate bolts	350	600
Port plug seals (vent and drain)	400	1600
Port cover seals (vent and drain)	400	932
Neutron shielding	300	†††
Overpack Intermediate Shells	350	700
Overpack Outer Enclosure Shell	350	1350
Optional Pocket Trunnion	200	700
Impact Limiter	150	1105

<sup>†</sup> These temperatures are maximum possible temperatures for the normal operating condition. They bound the actual calculated temperatures.

<sup>††</sup> These temperatures are maximum possible temperatures for the postulated fire accident. They must bound the actual calculated temperatures.

<sup>†††</sup> For shielding analysis, the neutron shield is conservatively assumed to be lost during the fire accident.

Table 2.1.3

OVERPACK CONTAINMENT STRUCTURE AND MPC ENCLOSURE VESSEL STRESS INTENSITY LIMITS FOR DIFFERENT LOADING CONDITIONS (ELASTIC ANALYSIS PER NB-3220)<sup>†</sup>

STRESS CATEGORY	NORMAL CONDITIONS OF TRANSPORT	HYPOTHETICAL ACCIDENT <sup>††</sup>
Primary Membrane, $P_m$	$S_m$	AMIN ( $2.4S_m, .7S_u$ )
Local Membrane, $P_L$	$1.5S_m$	150% of $P_m$ Limit
Membrane plus Primary Bending	$1.5S_m$	150% of $P_m$ Limit
Primary Membrane plus Primary Bending	$1.5S_m$	150% of $P_m$ Limit
Membrane plus Primary Bending plus Secondary	$3S_m$	N/A
Average <sup>†††</sup> Primary Shear (Section in Pure Shear)	$0.6S_m$	$0.42S_u$

<sup>†</sup> Stress combinations including F (peak stress) apply to fatigue evaluations only.

<sup>††</sup> Governed by Appendix F, Paragraph F-1331 of the ASME Code, Section III. Stress limited to  $S_u$

<sup>†††</sup> Governed by NB-3227.2 or F-1331.1(d) of the ASME Code, Section III (NB or Appendix F)

Table 2.1.4

**MPC BASKET STRESS INTENSITY LIMITS  
FOR DIFFERENT LOADING CONDITIONS (ELASTIC ANALYSIS PER NG-3220)**

<b>STRESS CATEGORY</b>	<b>NORMAL CONDITIONS OF TRANSPORT</b>	<b>HYPOTHETICAL ACCIDENT<sup>†</sup></b>
Primary Membrane, $P_m$	$S_m$	AMIN ( $2.4S_m, .7S_u$ ) <sup>††</sup>
Primary Membrane plus Primary Bending	$1.5S_m$	150% of $P_m$ Limit (Limited to $S_u$ )
Primary Membrane plus Primary Bending plus Secondary	$3S_m$	N/A

<sup>†</sup> Governed by Appendix F, Paragraph F-1331 of the ASME Code, Section III.

<sup>††</sup> Average primary shear stress across a section loaded in pure shear shall not exceed  $0.42S_u$ .

Table 2.1.5

STRESS INTENSITY LIMITS FOR DIFFERENT  
LOADING CONDITIONS FOR THE EXTERNAL STRUCTURALS IN THE HI-STAR OVERPACK  
(ELASTIC ANALYSIS PER NF-3260 - CLASS 3)  
(ELASTIC ANALYSIS PER NF-3220 - CLASS 1)

STRESS CATEGORY	NORMAL CONDITION OF TRANSPORT <sup>†</sup>	HYPOTHETICAL ACCIDENT <sup>††</sup>
Primary Membrane, $P_m$	S (Class 3) $S_m$ (Class 1)	AMAX ( $1.2S_y$ , $1.5S_m$ ) but $< .7S_u$
Primary Membrane, $P_m$ , plus Primary Bending, $P_b$	$1.5S$ (Class 3) $1.5S_m$ (Class 1)	150% of $P_m$ (Limited to $S_u$ )
Shear Stress	N/A (Class 3) $.6S_m$ (Class 1)	$< 0.42S_u$

## Definitions:

- S = Allowable Stress Value for Table 1A, ASME Section II, Part D  
 $S_m$  = Allowable Stress Intensity Value from Table 2A, ASME Section II, Part D  
 $S_u$  = Ultimate Strength

<sup>†</sup> Limits for Normal Condition of Transport are on stress for Class 3 and on stress intensity for Class 1, upper value in column is for Class 3; lower value in column is for Class 1.

<sup>††</sup> Governed by Appendix F, Paragraph F-1332 of the ASME Code, Section III. Class 1 and Class 3 use same stress intensity limits.

Table 2.1.6

## LOADING CASES FOR THE MPC FUEL BASKET

Case Number	Load Combination <sup>†</sup>	Notes
F1	T or T'	Demonstrate that the most adverse of the temperature distributions in the basket will not cause fuel basket to expand and contact the enclosure vessel wall. Compute the stress intensity and show that it is less than allowable.
F2		
F2.a	D+H	1 ft. side drop, 0 degrees circumferential orientation (Figure 2.1.3)
F2.b	D+H	1 ft. side drop, 45 degrees circumferential orientation (Figure 2.1.4)
F3		
F3.a	D + H'	30 ft. vertical axis drop
F3.b	D + H'	30 ft. side Drop, 0 degrees circumferential orientation (Figure 2.1.3)
F3.c	D + H'	30 ft. side Drop, 45 degrees circumferential orientation (Figure 2.1.4)

<sup>†</sup> The symbols used for loads are defined in Subsection 2.1.2.1.

Table 2.1.7

## LOADING CASES FOR THE MPC ENCLOSURE VESSEL

Case Number	Load Combination <sup>†</sup>	Notes
E1		
E1.a	Design internal pressure, $P_i$	Primary Stress intensity
E1.b	Design external pressure, $P_o$	Primary stress intensity limits, buckling stability
E1.c	Design internal pressure plus Temperature, $P_i + T$	Primary plus secondary stress intensity under Level A condition
E2		
E2.a	$(P_i, P_o) + D + H$	1 ft. side drop, $0^\circ$ circumferential orientation (Figure 2.1.3)
E2.b	$(P_i, P_o) + D + H$	1 ft. side drop, $45^\circ$ circumferential orientation (Figure 2.1.4)

<sup>†</sup> The symbols used for loads are defined in Subsection 2.1.2.1. Note that in the analyses, the bounding pressure ( $P_i, P_o$ ) is applied, e.g., in stability calculations  $P_o$  is bounding, whereas in stress calculations both  $P_o$  and  $P_i$  are appropriate.

Table 2.1.7 (continued)

Case Number	Load Combination <sup>†</sup>	Notes
E3 E3.a	D + H' + P <sub>o</sub> (Stability of the shell considers internal pressure plus drop deceleration)	30 ft. vertical axis drop
E3.b	D + H' + P <sub>i</sub>	30 ft. side drop, 0° circumferential orientation (Figure 2.1.3)
E3.c	D + H' + P <sub>i</sub>	30 ft. side drop, 45° circumferential orientation (Figure 2.1.4)
E4	T or T'	Demonstrate that interference with the overpack will not develop for T
E5	(P <sub>i</sub> <sup>*</sup> , P <sub>o</sub> <sup>*</sup> ) + D + T'	Demonstrate compliance with level D stress limits - buckling stability

<sup>†</sup> The symbols used for loads are defined in Subsection 2.1.2.1. Note that in the analyses, the bounding pressure (P<sub>i</sub>, P<sub>o</sub>) is applied, e.g., in stability calculations P<sub>o</sub> is bounding, whereas in stress calculations both P<sub>o</sub> and P<sub>i</sub> are appropriate.

Table 2.1.8

## OVERPACK LOAD CASES FOR NORMAL CONDITION OF TRANSPORT

Case Number	Load Combination <sup>†</sup>	Notes
1	$T_h + P_i + F + W_s$	Hot Environment
2	$T_s + P_o + F + W_s$	Super-Cold Environment
3	$T_h + D_{sn} + P_i + F + W_s$	Free One Foot Side Drop - Hot Environment
4	$T_c + D_{sn} + P_o + F + W_s$	Free One Foot Side Drop - Cold Environment
5	$T_c$ and $T_h + P_i + V$	Rapid Ambient Temperature Change

Note that load case 5 is outside of the load combinations of Reg. Guide 7.8

<sup>†</sup> The symbols used here are defined in Subsection 2.1.2.1.

Table 2.1.9

## OVERPACK LOAD CASES FOR HYPOTHETICAL ACCIDENT CONDITIONS OF TRANSPORT

Case Number	Load Combination <sup>†</sup>	Notes
1	$T_h + D_{ba} + P_i + F + W_s$	Bottom End 30 ft. Drop - Hot
2	$T_h + D_{ta} + P_i + F + W_s$	Top End 30 ft Drop - Hot
3	$T_h + D_{sa} + P_i + F + W_s$	Side 30 ft Drop - Hot
4	$T_h + D_{ca} + P_i + F + W_s$	30 ft C.G. Over-the-Bottom-Corner Drop - Hot
5	$T_h + D_{ga} + P_i + F + W_s$	30 ft C.G. Over-the-Top-Corner Drop Hot
6	$T_h + P_s + P_i + F + W_s$	Side Puncture - Hot
7	$T_h + P_t + P_i + F + W_s$	Top End Puncture - Hot
8	$T_h + P_b + P_i + F + W_s$	Bottom End Puncture - Hot
9	$T_c + D_{ba} + P_o + F + W_s$	Case 1 - Cold
10	$T_c + D_{ta} + P_o + F + W_s$	Case 2 - Cold
11	$T_c + D_{sa} + P_o + F + W_s$	Case 3 - Cold
12	$T_c + D_{ca} + P_o + F + W_s$	Case 4 - Cold
13	$T_c + D_{ga} + P_o + F + W_s$	Case 5 - Cold
14	$T_c + P_s + P_o + F + W_s$	Case 6 - Cold
15	$T_c + P_t + P_o + F + W_s$	Case 7 - Cold
16	$T_c + P_b + P_o + F + W_s$	Case 8 - Cold
17	$T_f + P_i + F + W_s$	Fire Event (Bolt unloading)
18	$P_o^*$	Containment Stability - Hot Deep Submergence
19	$P_i^* + T_f + F + W_s$	Fire Accident Internal Pressure - Hot
20	$T_h + D_{ga} + P_i + F + W_s$	30 ft C.G. Oblique Drop (30 Degree) on Top Forging - Hot
21	$T_c + D_{ga} + P_i + F + W_s$	30 ft C.G. Oblique Drop (30 Degree) on Top Forging - Cold
22	$T_c + D_{ga} + P_i + F + W_s$	30 ft Drop -Slapdown Secondary Impact Limiter at Top Forging - Hot

<sup>†</sup> The symbols used here are defined in Subsection 2.1.2.1.

Table 2.1.10  
BOUNDING DECELERATIONS FOR DROP EVENTS

<b>Event</b>	<b>Deceleration Value (in multiples of acceleration due to gravity)</b>
Normal conditions of transport, drop from 1 ft. height (any circumferential orientations)	17
Transport hypothetical accident conditions; drop from 30 ft. height (any axial and circumferential orientations)	60

Table 2.1.11

## DESIGN, LEVELS A AND B: STRESS INTENSITY

Code: ASME NB  
 Material: SA203-E  
 Service Conditions: Normal Conditions of Transport  
 Item: Stress Intensity

Temp. (degree F)	Classification and Value (ksi)					
	$S_m$	$P_m^\dagger$	$P_L^\dagger$	$P_L + P_b^\dagger$	$P_L + P_b + Q$	$P_e^{**}$
-20 to 100	23.3	23.3	35.0	35.0	69.9	69.9
200	23.3	23.3	35.0	35.0	69.9	69.9
300	23.3	23.3	35.0	35.0	69.9	69.9
400	22.9	22.9	34.4	34.4	68.7	68.7
500	21.6	21.6	32.4	32.4	64.8	64.8

## Definitions:

- $S_m$  = Stress intensity values per ASME Code  
 $P_m$  = Primary membrane stress intensity  
 $P_L$  = Local membrane stress intensity  
 $P_b$  = Primary bending stress intensity  
 $P_e$  = Expansion stress  
 $Q$  = Secondary stress  
 $P_L + P_b$  = Either primary or local membrane plus primary bending

Definitions for Table 2.1.11 apply to all following tables unless modified.

† Evaluation required for Design condition only.

\*\*  $P_e$  not applicable to vessels.

Table 2.1.12

## LEVEL D: STRESS INTENSITY

Code: ASME NB  
 Material: SA203-E  
 Service Condition: Hypothetical Accident  
 Item: Stress Intensity

Temp. (degree F)	Classification and Value (ksi)		
	$P_m$	$P_L$	$P_L + P_b$
-20 to 100	49.0	70.0	70.0
200	49.0	70.0	70.0
300	49.0	70.0	70.0
400	48.2	68.8	68.8
500	45.4	64.9	64.9

## Notes:

1. Level D allowables per NB-3225 and Appendix F, Paragraph F-1331.
2. Average primary shear stress across a section loaded in pure shear may not exceed  $0.42 S_u$ .
3. Limits on values are presented in Table 2.1.3.

Table 2.1.13

## DESIGN, LEVELS A AND B: STRESS INTENSITY

Code: ASME NB  
 Material: SA350-LF3  
 Service Conditions: Normal Conditions of Transport  
 Item: Stress Intensity

Temp. (degree F)	Classification and Value (ksi)					
	$S_m$	$P_m^\dagger$	$P_L^\dagger$	$P_L + P_b^\dagger$	$P_L + P_b + Q$	$P_e^{\dagger\dagger}$
-20 to 100	23.3	23.3	35.0	35.0	69.9	69.9
200	22.8	22.8	34.2	34.2	68.4	68.4
300	22.2	22.2	33.3	33.3	66.6	66.6
400	21.5	21.5	32.3	32.3	64.5	64.5
500	20.2	20.2	30.3	30.3	60.6	60.6
600	18.5	18.5	27.75	27.75	55.5	55.5
700	16.8	16.8	25.2	25.2	50.4	50.4

## Notes:

1. Source for  $S_m$  is ASME Code.
2. Limits on values are presented in Table 2.1.3.

† Evaluation required for Design condition only.

††  $P_e$  not applicable to vessels.

Table 2.1.14

## LEVEL D, STRESS INTENSITY

Code: ASME NB  
 Material: SA350-LF3  
 Service Conditions: Hypothetical Accident  
 Item: Stress Intensity

Temp. (degree F)	Classification and Value (ksi)		
	$P_m$	$P_L$	$P_L + P_b$
-20 to 100	49.0	70.0	70.0
200	48.0	68.5	68.5
300	46.7	66.7	66.7
400	45.2	64.6	64.6
500	42.5	60.7	60.7
600	38.9	58.4	58.4
700	35.3	53.1	53.1

## Notes:

1. Level D allowables per NB-3225 and Appendix F, Paragraph F-1331.
2. Average primary shear stress across a section loaded in pure shear may not exceed  $0.42 S_u$ .
3. Limits on values are presented in Table 2.1.3.

Table 2.1.15

## DESIGN AND LEVEL A: STRESS AND STRESS INTENSITY

Code:	ASME NF (Class 3)	ASME NF (Class 1)
Material:	SA515, Grade 70	SA515, Grade 70
	SA516, Grade 70	SA516, Grade 70
Service Conditions:	Normal Conditions of Transport	Normal Conditions of Transport
Item:	Stress	Stress Intensity

Temp. (degree F)	Classification and Value (ksi)					
	S (Class 3)	S <sub>m</sub> (Class 1)	Membrane Stress (Class 3)	P <sub>m</sub> (Class 1)	Membrane plus Bending Stress (Class 3)	P <sub>m</sub> +P <sub>b</sub> (Class 1)
-20 to 100	17.5	23.3	17.5	23.3	26.3	34.95
200	17.5	23.1	17.5	23.1	26.3	34.65
300	17.5	22.5	17.5	22.5	26.3	33.75
400	17.5	21.7	17.5	21.7	26.3	32.55
500	17.5	20.5	17.5	20.5	26.3	30.75
600	17.5	18.7	17.5	18.7	26.3	28.05
650	17.5	18.4	17.5	18.4	26.3	27.6
700	16.6	18.3	16.6	18.3	24.9	27.45

## Notes:

1. S = Maximum allowable stress values from Table 1A of ASME Code, Section II, Part D.
2. Stress classification per Paragraph NF-3260.
3. Limits on values are presented in Table 2.1.5.
4. Level A allowable stress intensities per NF.3221.1.
5. S<sub>m</sub> = Stress intensity values per Table 2A of ASME, Section II, Part D.

Table 2.1.16

## LEVEL D: STRESS INTENSITY

Code: ASME NF  
 Material: SA515, Grade 70  
 SA516, Grade 70  
 Service Conditions: Hypothetical Accident  
 Item: Stress Intensity

Temp. (degree F)	Classification and Value (ksi)		
	$S_m$	$P_m$	$P_m + P_b$
-20 to 100	23.3	45.6	68.4
200	23.1	41.5	62.3
300	22.5	40.4	60.6
400	21.7	39.1	58.7
500	20.5	36.8	55.3
600	18.7	33.7	50.6
650	18.4	33.1	49.7
700	18.3	32.9	49.3

## Notes:

1. Level D allowable stress intensities per Appendix F, Paragraph F-1332.
2.  $S_m$  = Stress intensity values per Table 2A of ASME, Section II, Part D.
3. Limits on values are presented in Table 2.1.5.

Table 2.1.17

## DESIGN, LEVELS A AND B: STRESS INTENSITY

Code: ASME NB  
 Material: Alloy X  
 Service Conditions: Normal Conditions of Transport  
 Item: Stress Intensity

Temp. (degree F)	Classification and Numerical Value					
	$S_m$	$P_m^\dagger$	$P_L^\dagger$	$P_L + P_b^\dagger$	$P_L + P_b + Q$	$P_e^{\dagger\dagger}$
-20 to 100	20.0	20.0	30.0	30.0	60.0	60.0
200	20.0	20.0	30.0	30.0	60.0	60.0
300	20.0	20.0	30.0	30.0	60.0	60.0
400	18.7	18.7	28.1	28.1	56.1	56.1
500	17.5	17.5	26.3	26.3	52.5	52.5
600	16.4	16.4	24.6	24.6	49.2	49.2
650	16.0	16.0	24.0	24.0	48.0	48.0
700	15.6	15.6	23.4	23.4	46.8	46.8
750	15.2	15.2	22.8	22.8	45.6	45.6
800	14.9	14.9	22.4	22.4	44.7	44.7

## Notes:

1.  $S_m$  = Stress intensity values per Table 2A of ASME II, Part D.
2. Alloy X  $S_m$  values are the lowest values for each of the candidate materials at temperature.
3. Stress classification per NB-3220.
4. Limits on values are presented in Table 2.1.3.

† Evaluation required for Design condition only.

††  $P_e$  not applicable to vessels.

Table 2.1.18

## LEVEL D: STRESS INTENSITY

Code: ASME NB  
 Material: Alloy X  
 Service Conditions: Hypothetical Accident  
 Item: Stress Intensity

Temp. (degree F)	Classification and Value (ksi) <sup>†</sup>		
	P <sub>m</sub>	P <sub>L</sub>	P <sub>L</sub> + P <sub>b</sub>
-20 to 100	48.0 (48.0)	72.0 (72.0)	72.0 (72.0)
200	48.0 (46.3)	72.0 (69.5)	72.0 (69.5)
300	46.2 (43.1)	69.3 (64.7)	69.3 (64.7)
400	44.9 (42.0)	67.4 (63.0)	67.4 (63.0)
500	42.0 (41.5)	63.0 (62.3)	63.0 (62.3)
600	39.4 (39.4)	59.1 (59.1)	59.1 (59.1)
650	38.4 (38.4)	57.6 (57.6)	57.6 (57.6)
700	37.4 (37.4)	56.1 (56.1)	56.1 (56.1)
750	36.5 (36.5)	54.8 (54.8)	54.8 (54.8)
800	35.8 (35.8)	53.7 (53.7)	53.7 (53.7)

## Notes:

1. Level D stress intensities per ASME NB-3225 and Appendix F, Paragraph F-1331.
2. The average primary shear strength across a section loaded in pure shear may not exceed 0.42 S<sub>u</sub>.
3. Limits on values are presented in Table 2.1.3.

<sup>†</sup> Values in parentheses apply strictly to the one-piece construction MPC lids, which are made from SA-336 forging material rather than SA-240 plate material.

Table 2.1.19

## DESIGN, LEVELS A AND B: STRESS INTENSITY

Code: ASME NG  
 Material: Alloy X  
 Service Conditions: Normal Conditions of Transport  
 Item: Stress Intensity

Temp. (degree F)	Classification and Value (ksi)				
	$S_m$	$P_m$	$P_m+P_B$	$P_m+P_b+Q$	$P_c$
-20 to 100	20.0	20.0	30.0	60.0	60.0
200	20.0	20.0	30.0	60.0	60.0
300	20.0	20.0	30.0	60.0	60.0
400	18.7	18.7	28.1	56.1	56.1
500	17.5	17.5	26.3	52.5	52.5
600	16.4	16.4	24.6	49.2	49.2
650	16.0	16.0	24.0	48.0	48.0
700	15.6	15.6	23.4	46.8	46.8
750	15.2	15.2	22.8	45.6	45.6
800	14.9	14.9	22.4	44.7	44.7

## Notes:

1.  $S_m$  = Stress intensity values per Table 2A of ASME, Section II, Part D.
2. Alloy X  $S_m$  values are the lowest values for each of the candidate materials at temperature.
3. Classifications per NG-3220.
4. Limits on values are presented in Table 2.1.4.

Table 2.1.20

## LEVEL D: STRESS INTENSITY

Code: ASME NG  
 Material: Alloy X  
 Service Conditions: Hypothetical Accident  
 Item: Stress Intensity

Temp. (degrees F)	Classification and Value (ksi)		
	$P_m$	$P_L$	$P_L + P_b$
-20 to 100	48.0	72.0	72.0
200	48.0	72.0	72.0
300	46.2	69.3	69.3
400	44.9	67.4	67.4
500	42.0	63.0	63.0
600	39.4	59.1	59.1
650	38.4	57.6	57.6
700	37.4	56.1	56.1
750	36.5	54.8	54.8
800	35.8	53.7	53.7

## Notes:

1. Level D stress intensities per ASME NG-3225 and Appendix F, Paragraph F-1331.
2. The average primary shear strength across a section loaded in pure shear may not exceed  $0.42 S_u$ .
3. Limits on values are presented in Table 2.1.4.

Table 2.1.21

REFERENCE TEMPERATURES AND STRESS LIMITS  
FOR THE VARIOUS LOAD CASES

Load Case Number	Material	Reference Temperature <sup>†</sup> , (°F)	Stress Intensity Allowables, ksi		
			P <sub>m</sub>	P <sub>L</sub> + P <sub>b</sub>	P <sub>L</sub> + P <sub>b</sub> + Q
F1	Alloy X	725	15.4	23.1	46.2
F2	Alloy X	725	15.4	23.1	46.2
F3	Alloy X	725	36.9	55.4	NL <sup>††</sup>
E1	Alloy X	450 <sup>†††</sup>	18.1	27.2	NL
E2	Alloy X	450 <sup>†††</sup>	18.1	27.2	54.3
E3	Alloy X	450 <sup>†††</sup>	43.4	65.2	NL
E4	Alloy X	450 <sup>†††</sup>	18.1	27.2	54.3
E5	Alloy X	775 <sup>†††</sup>	36.15	54.25	NL

<sup>†</sup> Values for reference temperatures are taken as the design temperatures (Table 2.1.2).

<sup>††</sup> NL: No specific limit in the Code.

<sup>†††</sup> Levels used for enclosure vessel top closure and baseplate only.

Table 2.1.21 (continued)

REFERENCE TEMPERATURES AND STRESS LIMITS  
FOR THE VARIOUS LOAD CASES

Condition	Material	Reference Temperature, (°F)	Stress Intensity Allowables, ksi		
			$P_m$	$P_L + P_b$	$P_L + P_b + Q$
Normal	SA203-E	400 <sup>†</sup>	22.9	34.4	68.7
	SA350-LF3	400 <sup>†</sup>	21.5	32.3	64.5
	SA516 Gr. 70 SA515 Gr. 70	400 <sup>†</sup>	17.5	26.3	52.5
	SA203-E	-20	23.3	35.0	69.9
	SA350-LF3	-20	23.3	35.0	69.9
	SA516 Gr. 70 SA515 Gr. 70	-20	17.5	26.3	52.5
Hypothetical Accident - Mechanical Loads	SA203-E	400 <sup>†</sup>	48.2	68.8	NL <sup>††</sup>
	SA350-LF3	400 <sup>†</sup>	45.2	64.6	NL
	SA516 Gr. 70 SA515 Gr. 70	400 <sup>†</sup>	39.1	58.7	NL
	SA203-E	-20	49.0	70.0	NL
	SA350-LF3	-20	49.0	70.0	NL
	SA516 Gr. 70 SA515 Gr. 70	-20	45.6	68.4	NL
Fire	SA203-E	500	45.4	64.9	NL
	SA350-LF3	700	35.3	53.1	NL
	SA516 Gr. 70	700	32.9	49.3	NL

<sup>†</sup> Values for reference temperatures are taken as the design temperatures (Table 2.1.2).

<sup>††</sup> NL: No limit specified in the Code.

Table 2.1.22

## FRACTURE TOUGHNESS TEST CRITERIA: CONTAINMENT BOUNDARY

Item	Material	Thickness (in.)	Charpy V-Notch Temperature <sup>†</sup>	Drop Test Temperature <sup>††</sup>
Weld Metal for NB Welds	As required	NA	As required per ASME Section III, Subsection NB, Article NB-2430 and Article NB-2330 Min. test temperature = -40°F	As required per ASME Section III, Subsection NB, Articles NB-2430 and Article NB-2330
Shell	SA203E or SA350-LF3	2-1/2	$T_{NDT} \leq -70^{\circ}\text{F}$ with testing and acceptance criteria per ASME Section III, Subsection NB, Article NB-2330	$T_{NDT} \leq -70^{\circ}\text{F}$ per Reg. Guide 7.11
Top Flange	SA350-LF3	8-3/4	$T_{NDT} \leq -136^{\circ}\text{F}$ with testing and acceptance criteria per ASME Section III, Subsection NB, Article NB-2330	$T_{NDT} \leq -136^{\circ}\text{F}$ per Reg. Guide 7.12

<sup>†</sup> Temperature is  $T_{NDT}$  unless noted.

<sup>††</sup> Materials to be tested in accordance with ASTM E208-87a.

Table 2.1.22 (Continued)

## FRACTURE TOUGHNESS TEST CRITERIA: CONTAINMENT BOUNDARY

Item	Material	Thickness (in.)	Charpy V-Notch Temperature <sup>†</sup>	Drop Test Temperature <sup>††</sup>
Bottom Plate	SA350-LF3	6	$T_{NDT} \leq -129^{\circ}\text{F}$ with testing and acceptance criteria per ASME Section III, Subsection NB, Article NB-2330	$T_{NDT} \leq -129^{\circ}\text{F}$ per Reg. Guide 7.12
Closure Plate	SA350-LF3	6	$T_{NDT} \leq -129^{\circ}\text{F}$ with testing and acceptance criteria per ASME Section III, Subsection NB, Article NB-2330	$T_{NDT} \leq -129^{\circ}\text{F}$ per Reg. Guide 7.12

<sup>†</sup> Temperature is  $T_{NDT}$  unless noted.

<sup>††</sup> Materials to be tested in accordance with ASTM E208-87a.

Table 2.1.23

## FRACTURE TOUGHNESS TEST CRITERIA: MISCELLANEOUS ITEMS

Item	Material	Thickness (in.)	Charpy V-Notch Temperature <sup>†</sup>	Drop Test Temperature
Intermediate Shells	SA516 Grade 70	1-1/4 and 1	Test temperature = -40 Deg. F with acceptance criteria per ASME Section III, Subsection NF, Table NF-2331(a)-3 and Figure NF-2331(a)-2, except BOM items 15 & 16 shall meet Table NF-2331(a)-1 and NF-2331 (a)-4	Not Required
Port Cover Plates	SA203E or SA350-LF3	1-1/2	Test temperature = -40 Deg. F with acceptance criteria per ASME Section III, Subsection NF, Table NF-2331(a)-3 and Figure NF-2331(a)-2	Not Required
Weld Metal for NF Welds	As required	NA	As required per ASME Section III, Subsection NF, Article NF-2430 and Article NF-2330 Test temperature = -40 Deg. F	Not Required

<sup>†</sup> Temperature is T<sub>NDT</sub> unless noted.

Table 2.1.24

ALLOWABLE STRESS CRITERIA FROM OTHER SOURCES

OVERPACK CLOSURE BOLTS<sup>†</sup>:

STRESS CATEGORY	NORMAL CONDITIONS OF TRANSPORT	HYPOTHETICAL ACCIDENT
Average Tensile Stress	$2/3 S_y$	AMIN( $S_y$ , $0.7 S_u$ )
Average Shear Stress	$0.6 (2/3 S_y)$	AMIN( $0.6 S_y$ , $0.42 S_u$ )
Combined Tensile and Shear Stress <sup>††</sup>	$R_t^2 + R_s^2 < 1.0$	$R_t^2 + R_s^2 < 1.0$

IMPACT LIMITER ATTACHMENT BOLTS:

STRESS CATEGORY	NORMAL CONDITIONS OF TRANSPORT	HYPOTHETICAL ACCIDENT
Average Tensile Stress	$2/3 S_y$	$S_u$
Average Shear Stress	$0.6 (2/3 S_y)$	$S_u$
Combined Tensile and Shear Stress	$R_t^2 + R_s^2 < 1.0$	$R_t^2 + R_s^2 < 1.0$

LIFTING TRUNNIONS AND LIFTING BOLTS:

The lifting trunnions and the lifting bolts, for the overpack closure plate and for the MPC lid, are designed in accordance with NUREG-0612 and ANSI N14.6. Specifically, the design must meet factors of safety of six based on the material yield stress and ten based on the material ultimate stress for non-redundant lifting devices.

<sup>†</sup> The overpack closure bolts are designed in accordance with NUREG/CR-6007, "Stress Analysis of Closure Bolts for Shipping Casks".

<sup>††</sup>  $R_t$  and  $R_s$  are the ratios of actual stress to shear stress, respectively.

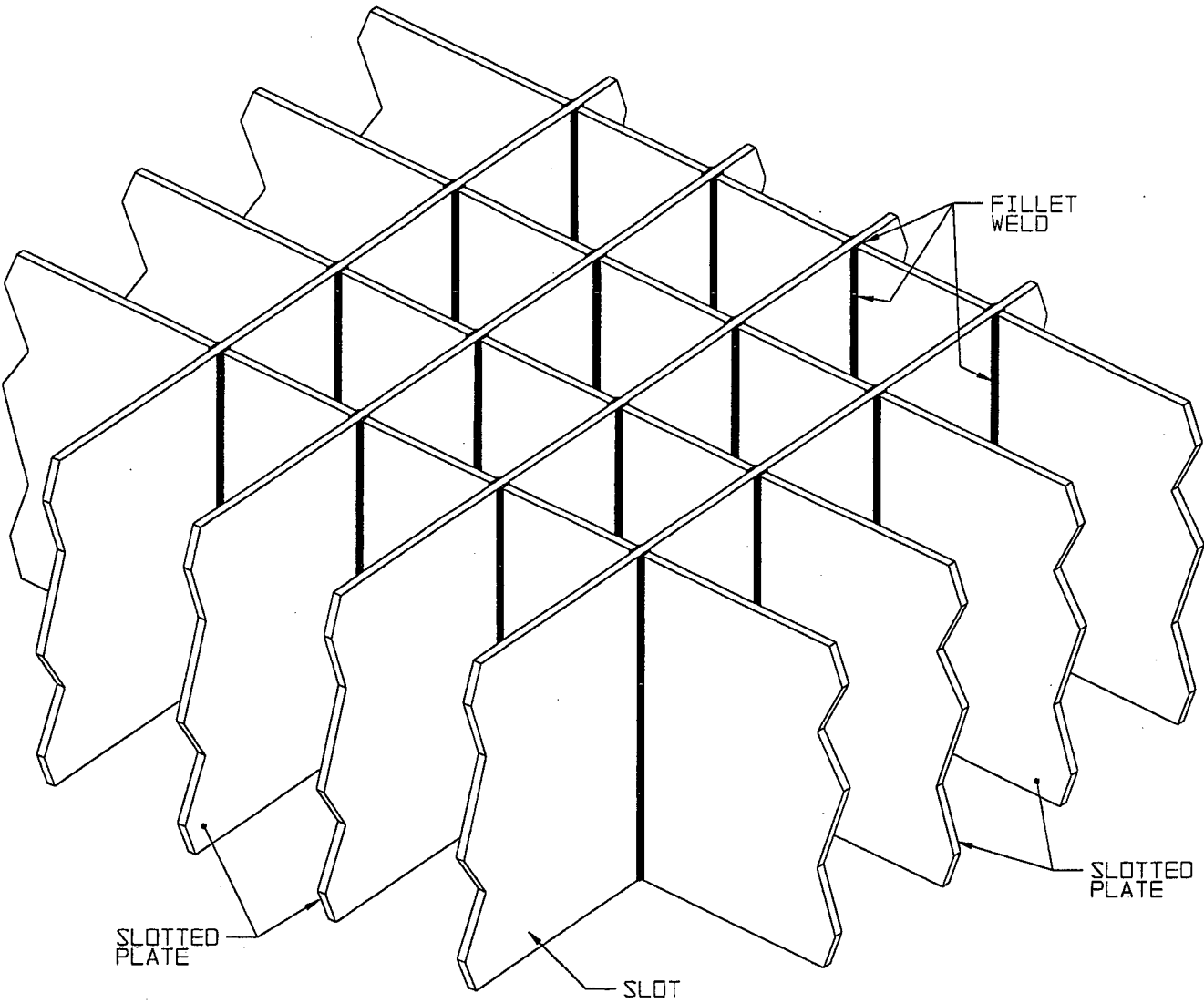
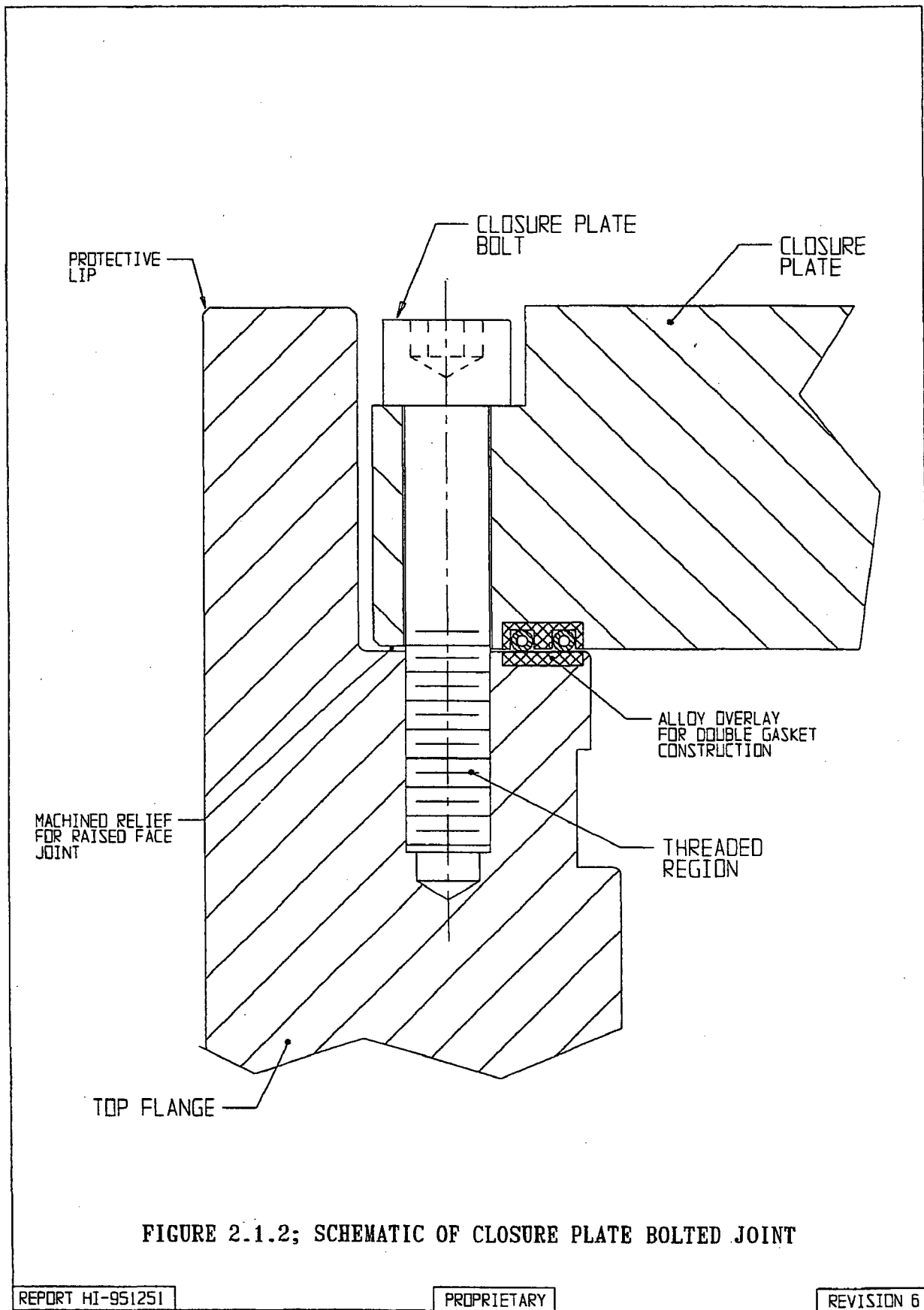
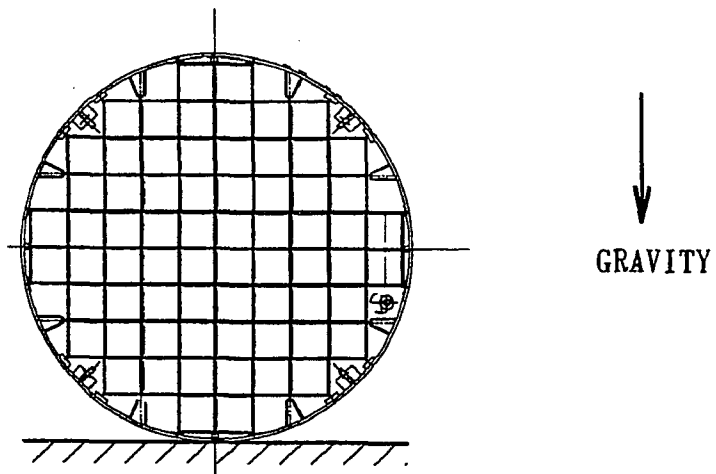


FIGURE 2.1.1; MPC FUEL BASKET GEOMETRY





*FIGURE 2.1.3; 0° DROP ORIENTATION FOR THE MPCs*

REPORT HI-951251

REV. 10

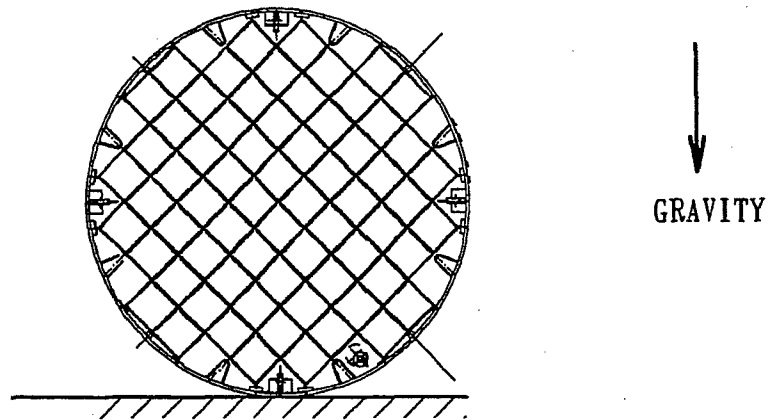


*FIGURE 2.1.4; 45° DROP ORIENTATION FOR THE MPCs*

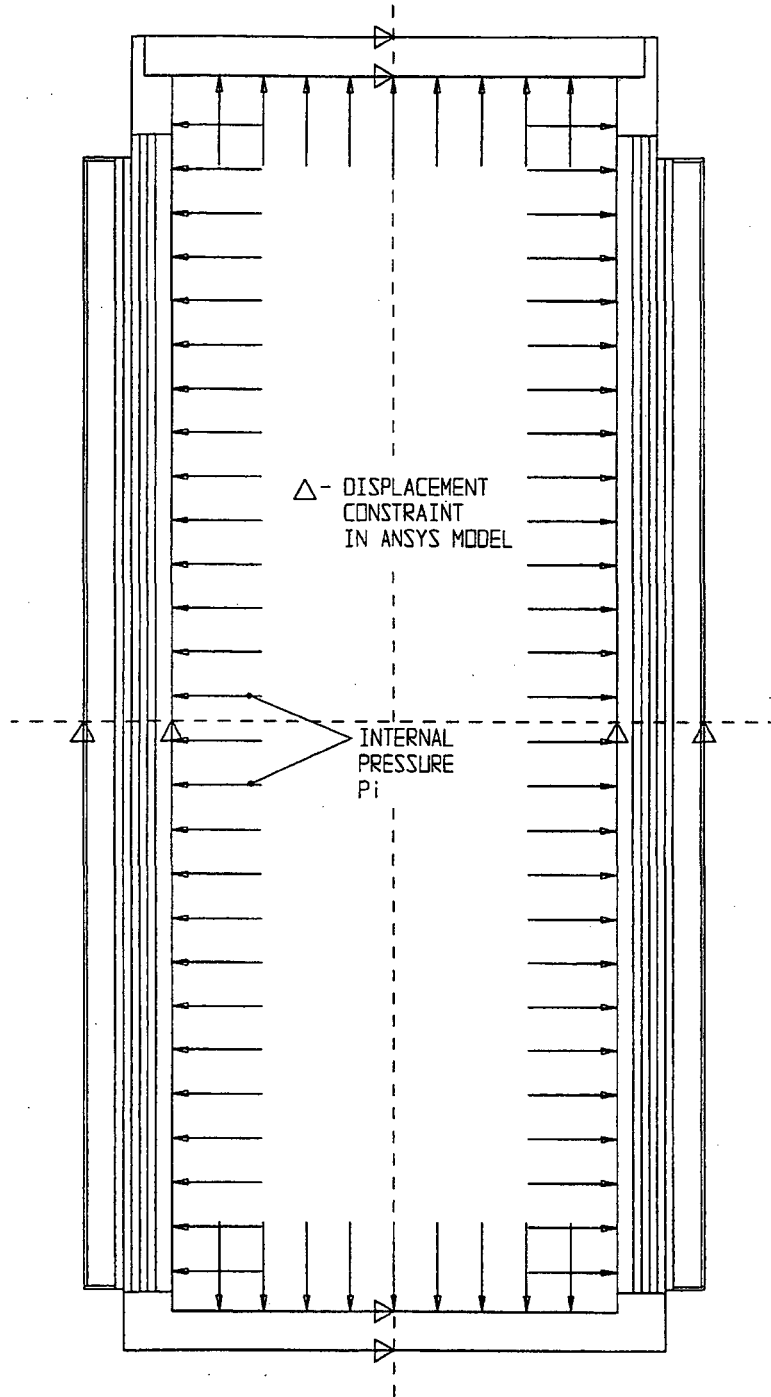


FIGURE 2.1.5; FREE BODY DIAGRAM OF OVERPACK - INTERNAL PRESSURE

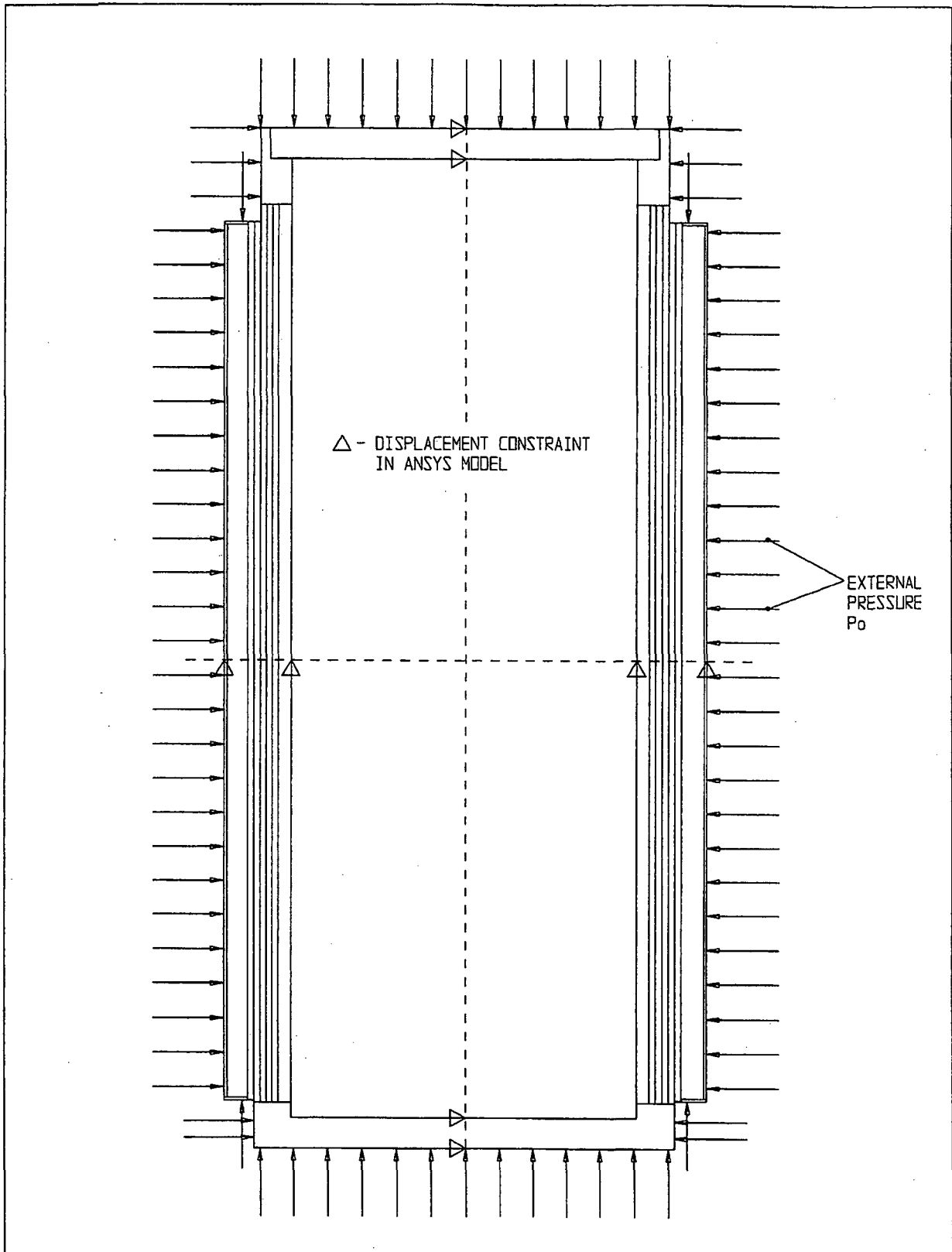


FIGURE 2.1.6; FREE BODY DIAGRAM OF OVERPACK - EXTERNAL PRESSURE

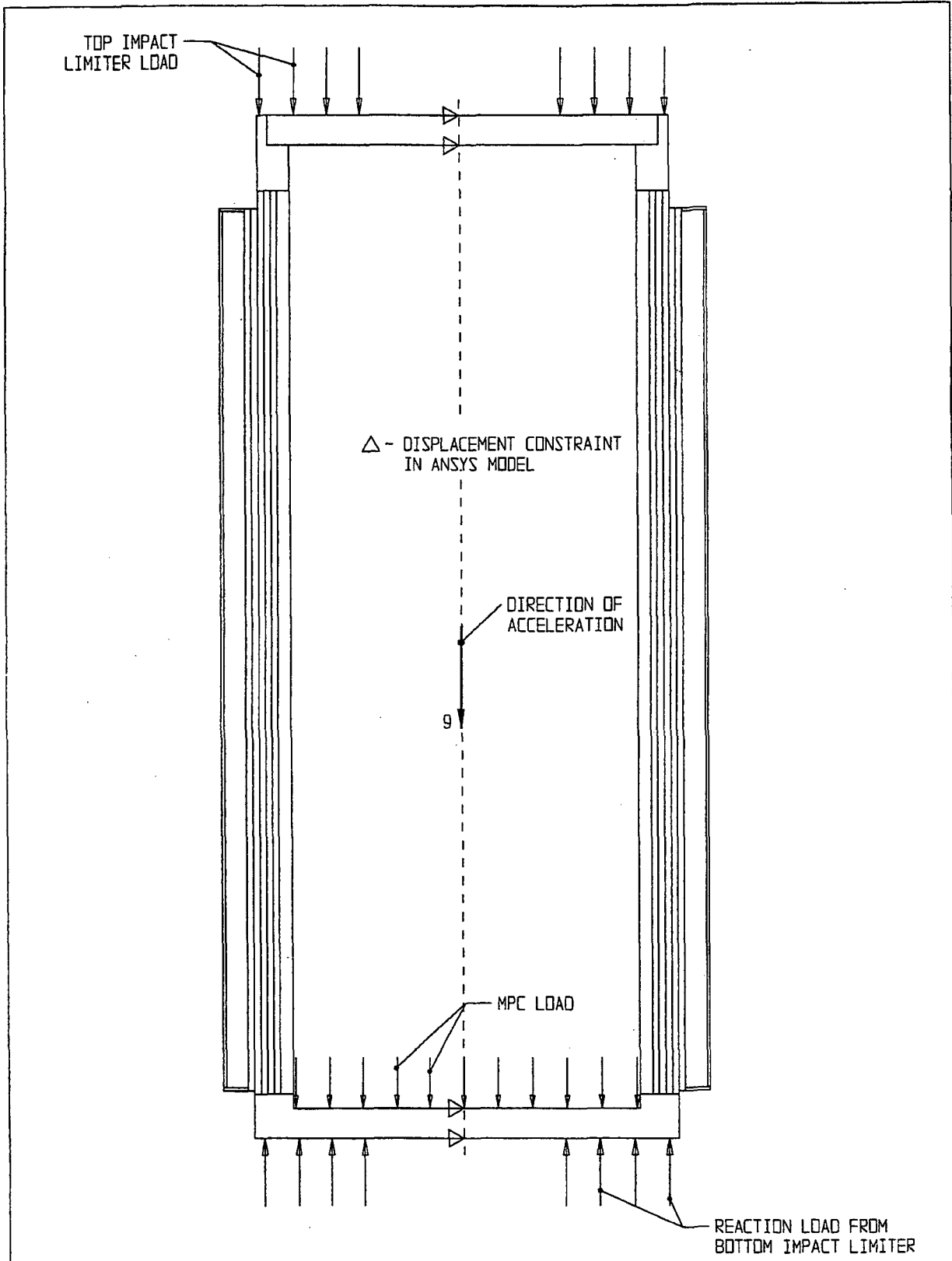


FIGURE 2.1.7; FREE BODY DIAGRAM OF OVERPACK - BOTTOM END DROP

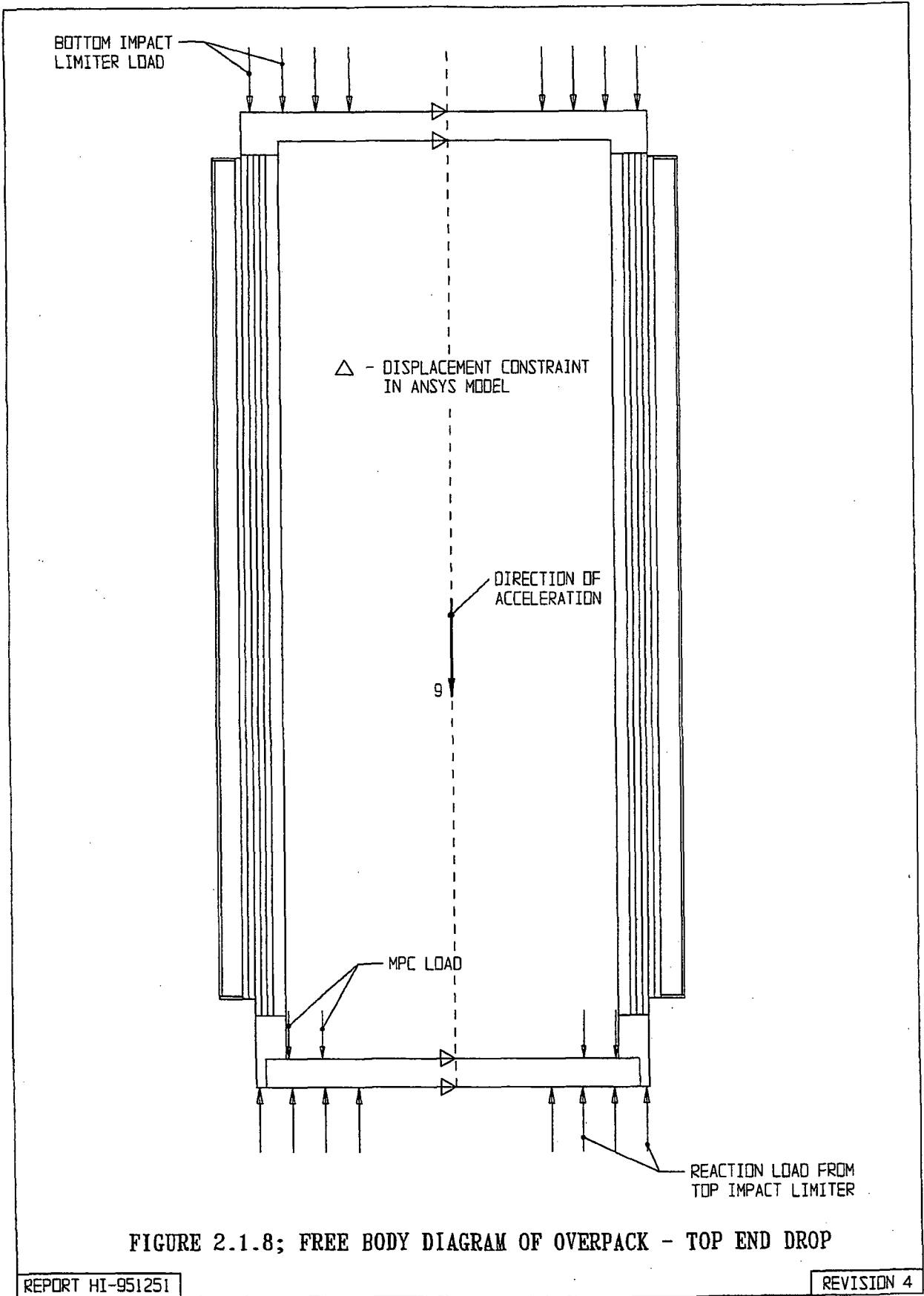


FIGURE 2.1.8; FREE BODY DIAGRAM OF OVERPACK - TOP END DROP

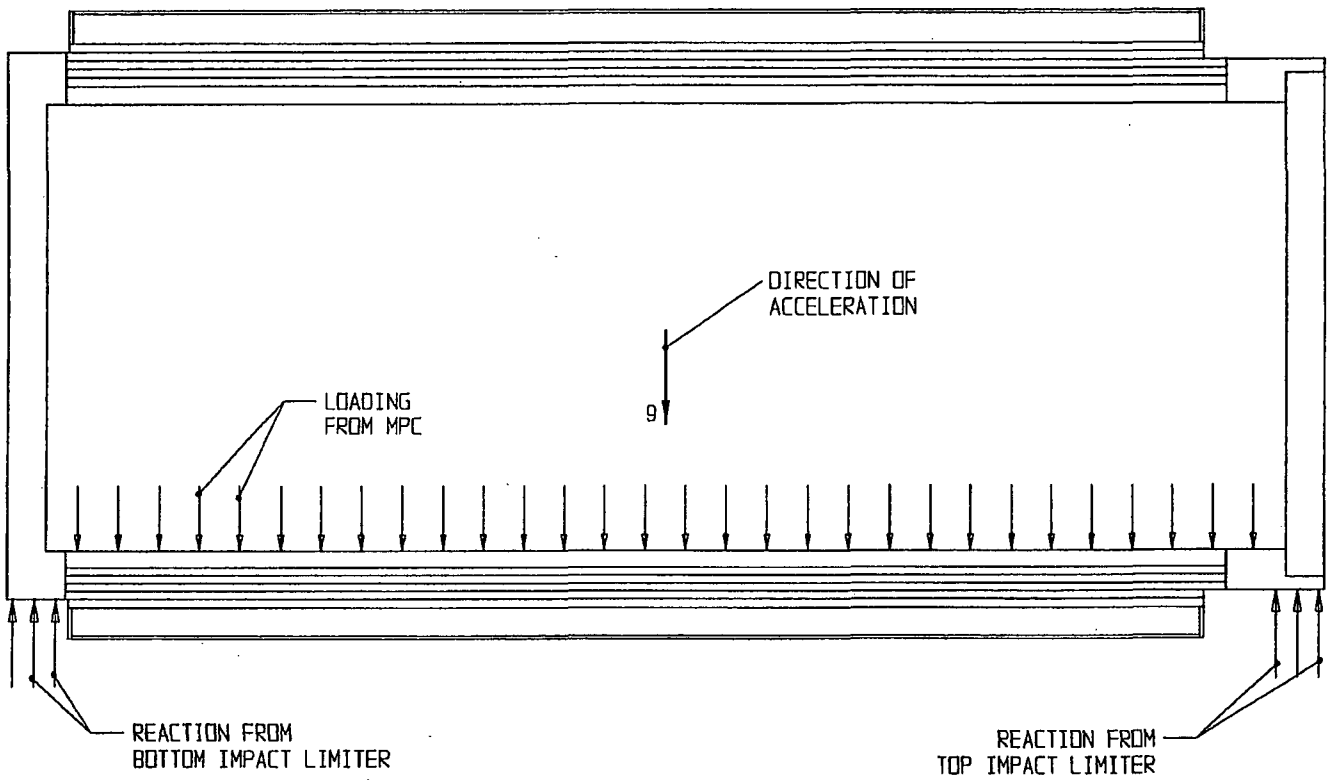


FIGURE 2.1.9; FREE BODY DIAGRAM OF OVERPACK - SIDE DROP

REPORT HI-951251

REVISION 4

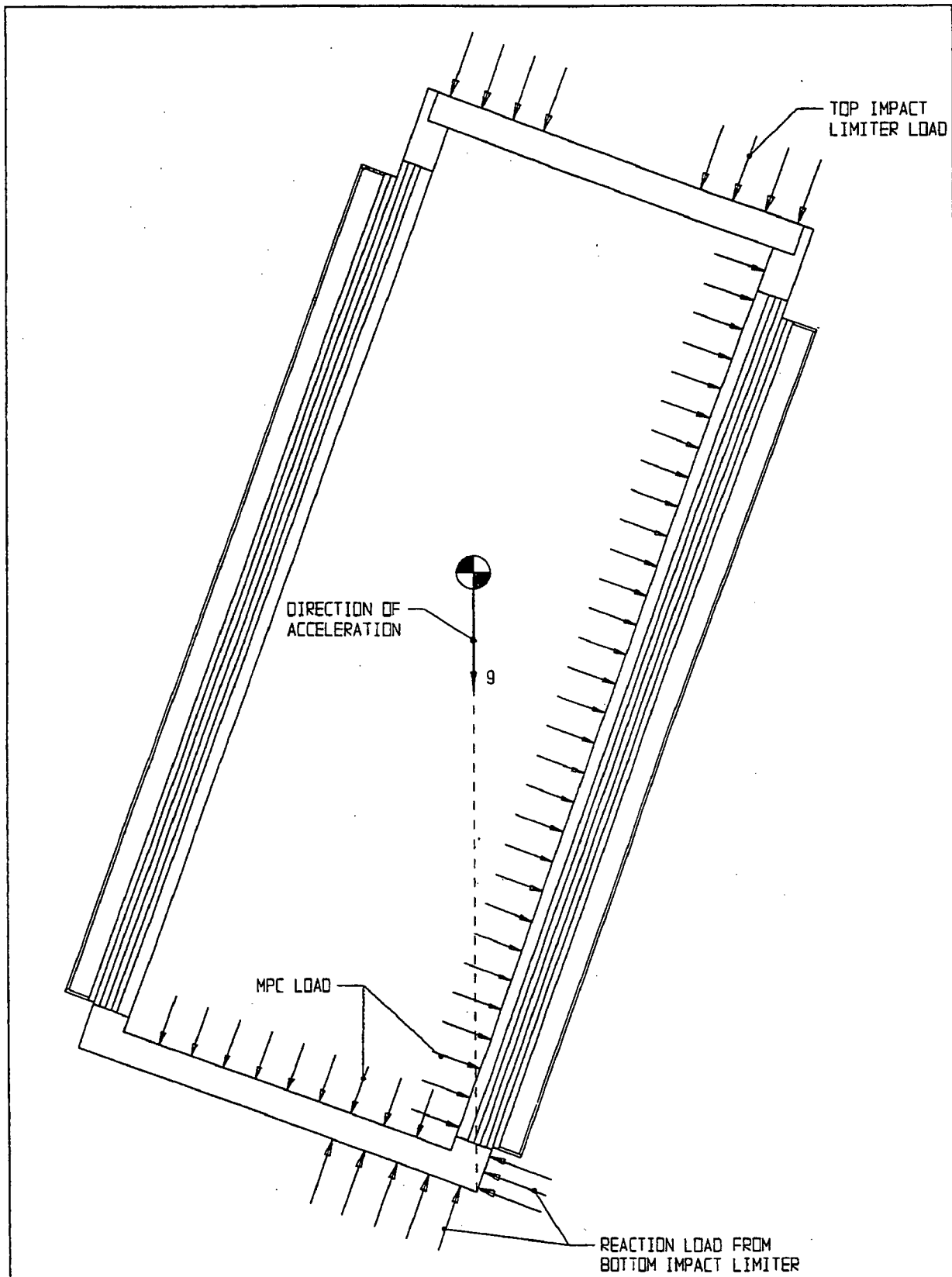
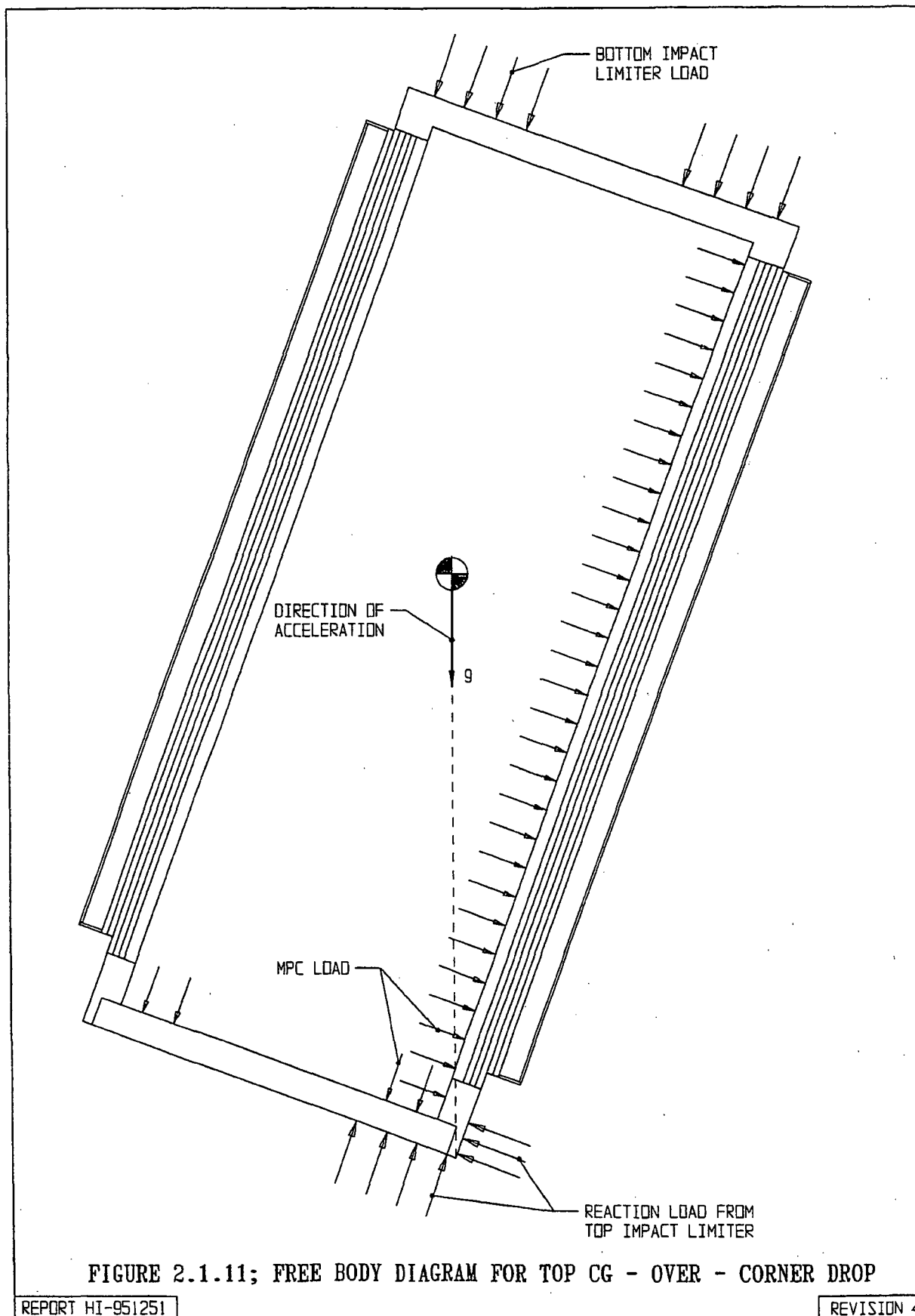


FIGURE 2.110 ; FREE BODY DIAGRAM FOR BOTTOM CG - OVER - CORNER DROP

REPORT HI-951251

REVISION 6



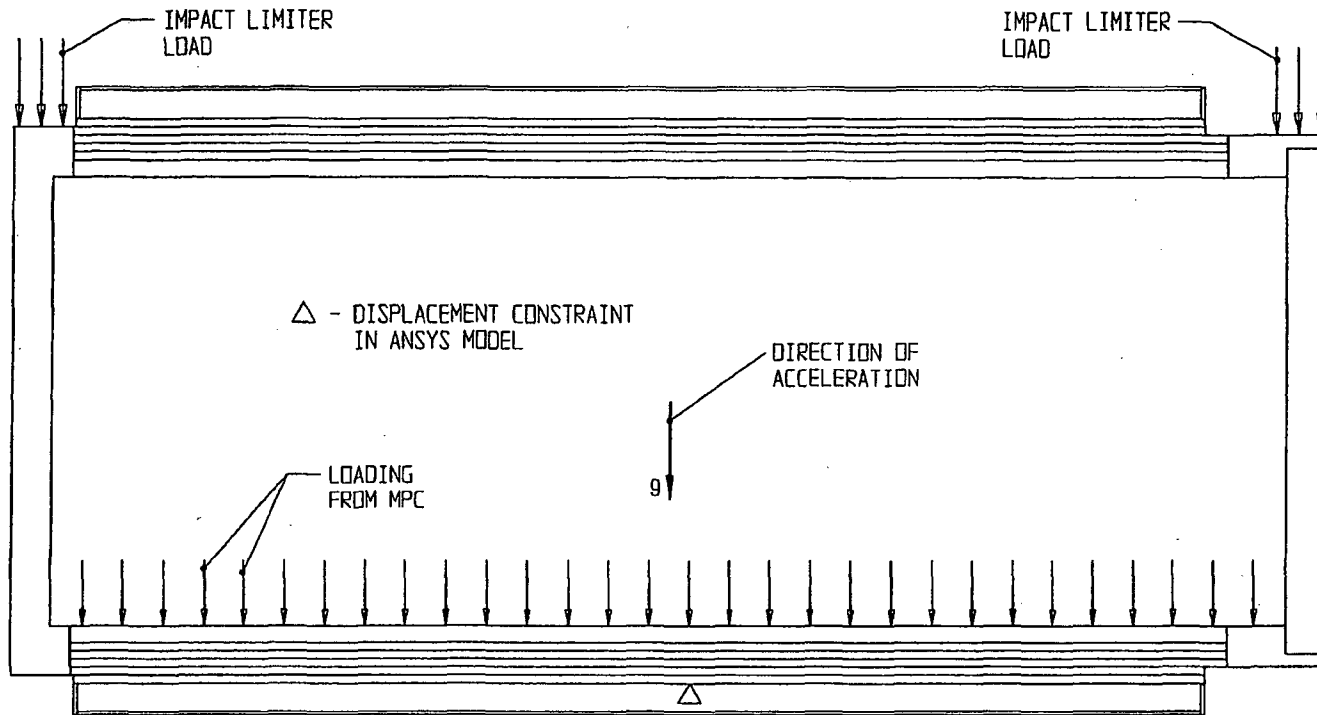


FIGURE 2.1.12; FREE BODY DIAGRAM FOR PUNCTURE DROP ONTO BAR - SIDE

REPORT HI-951251

REVISION 4

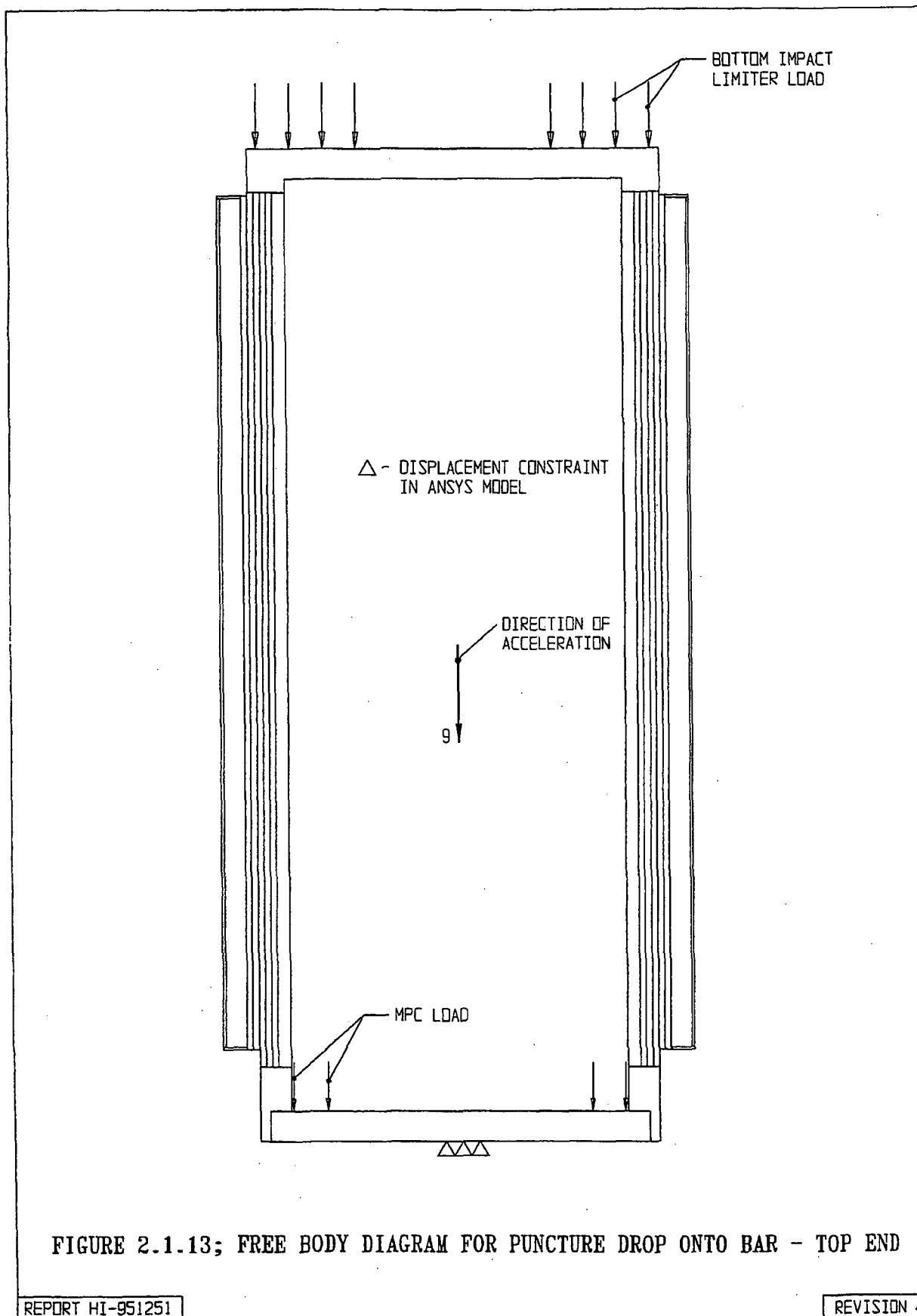


FIGURE 2.1.13; FREE BODY DIAGRAM FOR PUNCTURE DROP ONTO BAR - TOP END

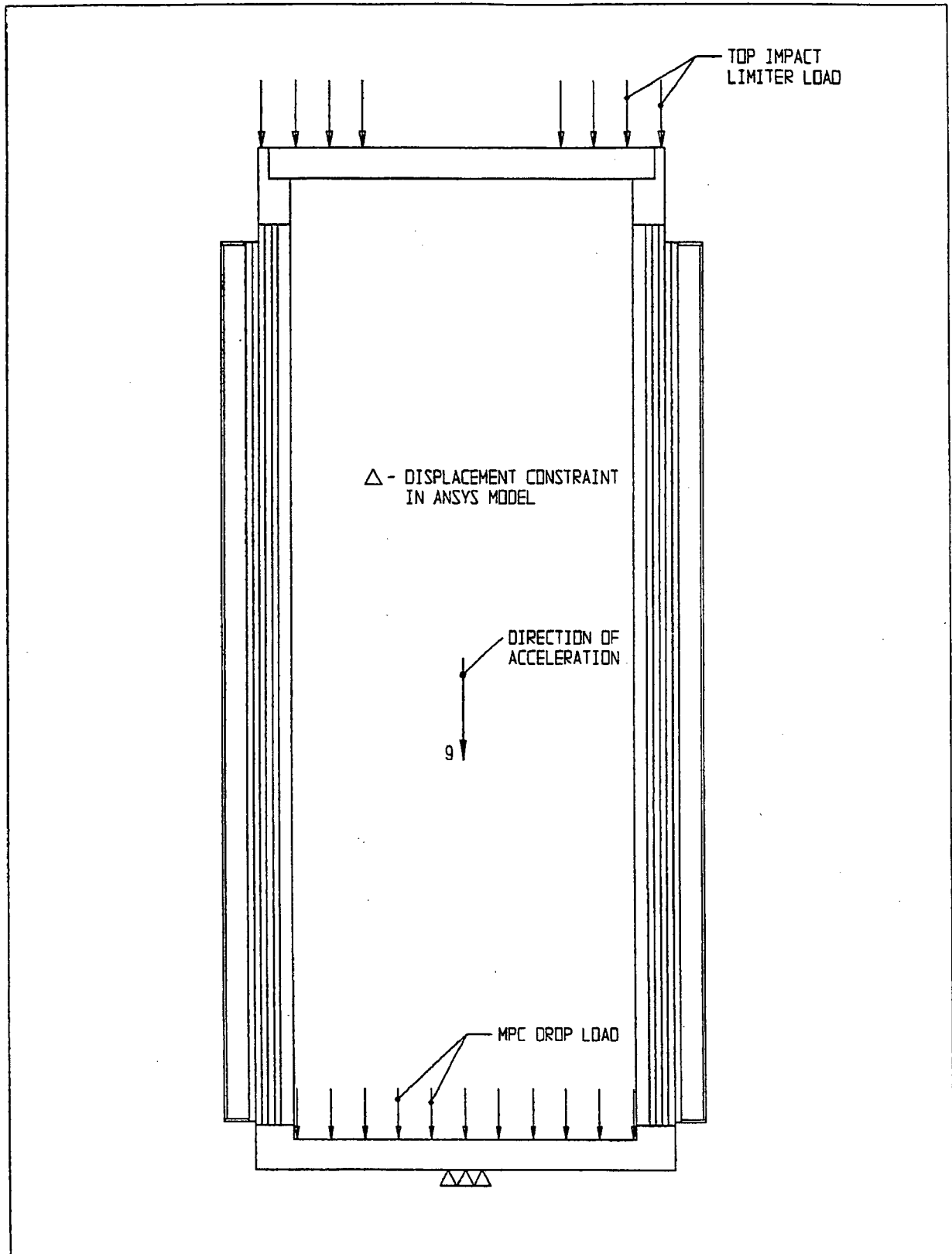


FIGURE 2.114; FREE BODY DIAGRAM FOR PUNCTURE DROP ONTO BAR - BOTTOM END

## 2.2 WEIGHTS AND CENTERS OF GRAVITY

Table 2.2.1 provides the weights of the individual HI-STAR 100 components as well as the total system weights. The weight of the impact limiter is also provided.

The locations of the calculated centers of gravity (CGs) are presented in Table 2.2.2 per the locations described in Figure 2.2.1. All centers of gravity are located on the cask centerline since the non-axisymmetry effects of the cask system plus contents are negligible.

Table 2.2.3 provides the lift weight for the HI-STAR 100 System when the heaviest fully loaded MPC is lifted from the fuel pool. The effect of buoyancy is neglected, and the weight of rigging is set at a conservative value.

Table 2.2.4 provides a table of bounding weights that may be used in calculations where additional conservatism is introduced by increasing the weight.

Table 2.2.1

HI-STAR 100 CALCULATED WEIGHT DATA<sup>†</sup>

Item	Component Weight (lb)	Component Weight (lb)	Total Weight (lb)
Overpack <sup>††</sup> Overpack closure plate	-	7,984	153,710
Bottom impact limiter			17,231
Top impact limiter			19,187
MPC Weights <sup>†††</sup>	<b>Fuel Basket</b>	<b>Basket + Shell Without SNF</b>	<b>Fully Loaded with SNF and Fuel Spacers</b>
MPC-68	16,240	37,591	87,171
MPC-24	20,842	40,868	82,494
MPC-32	12,340	34,507	89,765
MPC-24E/EF	23,535	43,561	85,188
Trojan MPC-24E/EF <sup>††††</sup>	21,284	40,643	80,963
Overpack with loaded MPC-68/68F			240,881
Overpack with loaded MPC-24			236,204
Overpack with loaded MPC-32			243,745
Overpack with loaded MPC-24E/EF			238,898
Overpack with loaded MPC-24E/EF (Trojan)			235,283
Overpack with minimum weight MPC without SNF		187,500	
Total weight of transport package			
With MPC-68/68F	277,299		
With MPC-24	272,622		
With MPC-32	279,893		
With MPC-24E/EF	275,316		
With Trojan MPC-24E/EF	271,701		

<sup>†</sup> All calculated weights are rounded up to the nearest whole number.

<sup>††</sup> Including overpack closure plate.

<sup>†††</sup> MPC vessel (shell, baseplate, and lid) weights include a 4% upward adjustment; fuel weight is design basis, including all non-fuel components and DFC (i.e., 1680 lbs for PWR and 700 lbs for BWR).

<sup>††††</sup> MPC vessel weight used is for MPC-24, which bounds shell weight for Trojan MPC-24E/EF due to height difference. Trojan MPC weight includes MPC spacer.

Table 2.2.2

## CENTERS OF GRAVITY OF HI-STAR 100 CONFIGURATIONS

Component	Height of CG Above Datum, inches
Overpack empty	99.7
MPC-68 empty	111.5
MPC-24 empty	109.0
MPC-32 empty	113.2
MPC-24E/EF empty	107.8
Trojan MPC-24E/EF	104.2
MPC-68 with fuel in overpack	102.5
MPC-24 with fuel in overpack	102.3
MPC-32 with fuel in overpack	102.1
MPC-24E/EF with fuel in overpack	102.2
Trojan MPC-24E/EF with fuel in overpack	101.0

Note: The datum used for calculations involving the overpack is the bottom of the overpack bottom plate. The datum used for calculations involving the MPC only is the bottom of MPC baseplate (Figure 2.2.1). The location of the loaded Trojan centroid includes top spacer ring above MPC top lid.

Table 2.2.3

## CALCULATED MAXIMUM LIFT WEIGHT ON CRANE HOOK ABOVE POOL

Item	Weight (lb)
Total weight of overpack	153,710
Total weight of MPC(upper bound) + fuel	89,765 <sup>†</sup>
Overpack closure plate	-7,984
Water in MPC and overpack	16,384
Lift yoke	3,600
Inflatable annulus seal	50
<b>TOTAL</b>	<b>255,525<sup>††</sup></b>

---

<sup>†</sup> Includes MPC closure rings.

<sup>††</sup> Trunnions are rated to lift 250,000 lbs. For weight exceeding 250,000 lbs, weight can be reduced by partial draining of the MPC. See Chapter 7 for operational controls.

Table 2.2.4

## COMPONENT WEIGHTS AND DIMENSIONS FOR ANALYTIC CALCULATIONS\*

<b>Component</b>	<b>Weight (lbs)</b>
MPC baseplate	3,000
MPC closure lid	10,400
MPC shell	5,900
MPC miscellaneous parts	3,700
Fuel basket	24,000/16,400 (PWR/BWR)
Fuel	54,000
Total MPC	90,000
Overpack baseplate	10,000
Overpack closure plate	8,000
Overpack shell	137,000
Total overpack	158,000
Total HI-STAR 100 lift weight	250,000
Impact limiters	37,000
HI-STAR with limiters	282,000
<b>Item</b>	<b>Dimension (inch)</b>
Overpack Outer Diameter	96
Overpack Length	203.125
MPC Outer Diameter	68.375
MPC Length	190.5
Overpack Inner Diameter	68.75

Note: Analytical calculations may use weights and dimensions in Table 2.2.4 or actual weights and dimensions for conservatism in calculation of safety factors. Finite element analyses may use weights calculated based on input weight densities.

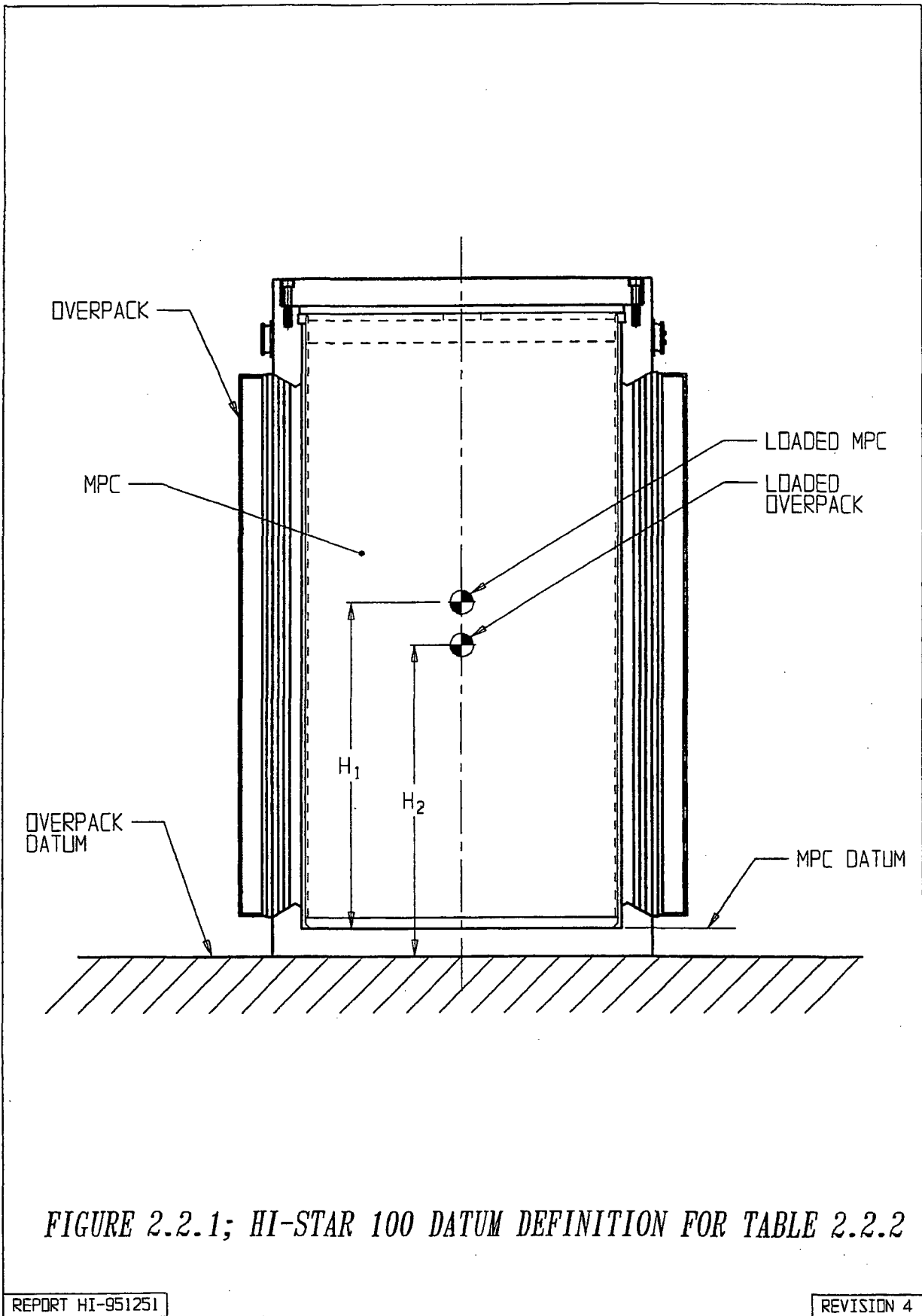


FIGURE 2.2.1; HI-STAR 100 DATUM DEFINITION FOR TABLE 2.2.2

## 2.3 MECHANICAL PROPERTIES OF MATERIALS

This section provides the mechanical properties used in the structural evaluation. The properties include yield stress, ultimate stress, modulus of elasticity, Poisson's ratio, weight density, and coefficient of thermal expansion. The property values are presented for a range of temperatures for which structural calculations are performed.

The materials selected for use in the HI-STAR 100 MPC and overpack are presented in the Bills-of-Materials in Chapter 1, Section 1.4. In this chapter, the materials are divided into two categories, structural and nonstructural. Structural materials are those that serve a load bearing function. Materials that do not support mechanical loads are considered nonstructural. For example, the overpack inner shell is a structural material, while Holtite-A (neutron shield) is a nonstructural material.

### 2.3.1 Structural Materials

#### 2.3.1.1 Alloy X

A hypothetical material termed Alloy X is defined for all MPC structural components. The material properties of Alloy X are the least favorable values from the set of candidate stainless alloys. The purpose of a 'least favorable' material definition is to ensure that all structural analyses are conservative, regardless of the actual MPC material. For example, when evaluating the stresses in the MPC, it is conservative to work with the minimum values for yield strength and ultimate strength. This guarantees that the material used for fabrication of the MPC is of equal or greater strength than the hypothetical material used in the analysis. In the structural evaluation, the only property for which it is not always conservative to use the minimum values is the coefficient of thermal expansion. Two sets of values for the coefficient of thermal expansion are specified, a minimum set and a maximum set. For each analysis, the set of coefficients, minimum or maximum that causes the more severe load on the cask system is used. Table 2.3.1 lists the numerical values for the material properties of Alloy X versus temperature. These values, taken from the ASME Code, Section II, Part D [2.1.11], are used to complete all structural analyses. The maximum temperatures in MPC components may exceed the allowable limits of temperature during short time duration events. However, under no scenario does the maximum temperature of Alloy X material used in the helium confinement boundary exceed 1000°F. As shown in ASME Code Case N-47-33 (Class 1 Components in Elevated Temperature Service, 1995 Code Cases, Nuclear Components), the strength properties of austenitic stainless steels do not change due to exposure to 1000 °F temperature for up to 10,000 hours. Therefore, there is no significant effect on mechanical properties of the helium confinement boundary or fuel basket material during the short time duration loading. Further description of Alloy X, including the materials from which it is derived, is provided in Appendix 1.A.

Two properties of Alloy X which are not included in Table 2.3.1 are weight density and Poisson's ratio. These properties are assumed constant for all structural analyses, regardless of the temperature. The values used are shown in the table below.

PROPERTY	VALUE
Weight Density (lb./in <sup>3</sup> )	0.290
Poisson's Ratio	0.30

#### 2.3.1.2 Carbon Steel, Low-Alloy, and Nickel Alloy Steel

The carbon steels used in the HI-STAR 100 System are SA516 Grade 70, SA515 Grade 70. These steels are not constituents of Alloy X. The material properties of SA516 Grade 70 and SA515 Grade 70 are shown in Tables 2.3.2 and 2.3.3, respectively. The nickel alloy and low-alloy steels are SA203-E and SA350-LF3, respectively. The material properties of SA203-E and SA350-LF3 are given in Table 2.3.4.

Two properties of these steels which are not included in Tables 2.3.2 through 2.3.4 are weight density and Poisson's ratio. These properties are assumed constant for all structural analyses. The values used are shown in the table below.

PROPERTY	VALUE
Weight Density (lb./in <sup>3</sup> )	0.283
Poisson's Ratio	0.30

#### 2.3.1.3 Bolting Materials

Material properties of the bolting materials used in the HI-STAR System are given in Table 2.3.5.

#### 2.3.1.4 Weld Material

All weld filler materials utilized in the welding of the Code components will comply with the provisions of the appropriate ASME subsection (e.g., Subsection NB for the overpack and enclosure vessel) and Section IX. All non-Code welds shall also be made using weld procedures that meet Section IX of the ASME Code. All non-code welds shall also be made using weld procedures that meet Section IX of the ASME Code. The minimum tensile strength of the weld wire and filler material (where applicable) will be equal to or greater than the tensile strength of the base metal listed in the ASME Code.

#### 2.3.1.5 Impact Limiter

The Impact Limiter for the HI-STAR 100 System has been named AL-STAR™. The original design of AL-STAR for the HI-STAR 100 package is composed of cross core (i.e., bi-directional) and uni-directional aluminum honeycomb made by layering corrugated sheets of aluminum (Alloy 5052). With appropriately adjusted crush strengths of aluminum honeycomb, AL-STAR is also used for HI-STAR HB (see Supplement 2.I), which is a shorter and lighter

version of HI-STAR 100. An improved design of AL-STAR, which is evaluated in Appendix 2.C for use with the HI-STAR 100 cask only, uses just one type of cross core aluminum honeycomb material and no uni-directional material. For the cross core material, alternate layers of corrugated aluminum sheets are laid in orthogonal direction to each other (Figure 2.3.1). The layers are bonded together by a high-temperature epoxy. The Holtec drawing in Section 1.4 illustrates the arrangement of the cross core and uni-directional honeycomb sectors in AL-STAR to realize adequate crush moduli in all potential impact modes. The external surface of AL-STAR consists of a stainless steel skin to provide long-term protection against weather and environmental conditions.

Rail transport considerations limit the maximum diameter of the impact limiter to 128 inches. The axial dimension of AL-STAR is limited by the considerations of maximum permissible packaging weight for rail transport. Within the limitations of space and weight, AL-STAR must possess sufficient energy absorption capacity so as to meet the design basis rigid body deceleration limits (Table 2.1.10) under all postulated drop orientations. The sizing of the AL-STAR internal structure is principally guided by the above considerations. For example, in order to ensure that a sufficient portion of the honeycomb structure participates in lateral impacts, a thick carbon steel shell buttressed with gussets provides a hard backing surface for the aluminum honeycomb to crush against.

Two properties of the cross core honeycomb germane to its function are the crush strength and the nominal density. The crush strength of AL-STAR is the more important of the two properties; the density is significant in establishing the total weight of the package. The crush strength increases monotonically with density. For example, the cross core honeycomb of 2500 psi crush strength has a nominal density of 27 lb. per cubic foot. At 2,000 psi crush strength, the change in aluminum honeycomb parameters lowers the density to approximately 22 lb. per cubic foot. The crush strength of the honeycomb can be varied within a rather wide range by adjusting the aluminum foil thickness and corrugation size. Table 2.3.7 lists the required crush strengths of the honeycomb section types (see drawings in Section 1.4) in the various regions of AL-STAR for use with the HI-STAR 100 and HI-STAR HB transport casks.

Like all manufactured materials, the crush strength and density of the honeycomb material are subject to slight variation within a manufactured lot. For all aluminum honeycomb materials used in AL-STAR, the crush strength will be held to the tolerance specified in Table 2.3.7.

Hexcel Corporation's publication TSB 120, "Mechanical Properties of Hexcel Honeycomb Materials", [2.3.1] provides detailed information on the mechanical characteristics of aluminum honeycomb materials. Hexcel's experimental data shows that the load-deflection curve of aluminum honeycomb simulates the shape of elastic-perfectly plastic materials. The honeycomb crushes at a nearly uniform load (slowly applied) until solidity in the range of 30 to 40% is reached. It is the crushing at constant load characteristic of aluminum honeycomb along with its excellent crush strength-to-weight ratio that makes it an ideal energy absorption material. The cross layered honeycomb (cross-core) has an identical crush strength in two orthogonal directions. In other words, from a load-deflection standpoint, the cross-layered honeycomb is a transversely isotropic material.

A typical honeycomb pressure-strain curve is illustrated in Figure 2.A.2.1 in Appendix 2.A wherein additional discussion on the crush properties of the honeycomb material is provided.

However, three key properties of the honeycomb material which are central to its function as a near-ideal impact limiter crush material are summarized below.

- i. The honeycomb material can be used in the "un-crushed" or "pre-crushed" condition. The difference is in the initial "bump" in the pressure-strain curve shown in Figure 2.A.2.1. By pre-crushing the honeycomb, its pressure-strain relationship simulates that of an ideal elastic-perfectly-plastic material, which is most desirable in limiting abrupt peaks in the deceleration of the package under drop events.
- ii. Irrespective of the crush strength, under quasi-static loading, all honeycomb materials begin to strain harden at about 60% strain and lock up at about 70%. Thus, a 10-inch thick honeycomb column will crush down to a thickness of 4 inches at near constant force; crushing further will require progressively greater compression force. The six inches of available crush distance is referred to as the available "stroke" in the lexicon of impact limiter design technology.
- iii. Because the crush material is made entirely out of one of the most cryogenically competent industrial metals available, aluminum, the pressure-crush behavior of the AL-STAR honeycomb material is insensitive to the environmental temperature range germane to Part 71 transport (-20 degrees F to 100 degrees F). Table Y-1 of the ASME Code [2.1.11] lists the yield strength of the material (Alloy 5052) to be constant in the range -20 degrees F to 350 degrees F.

Independent confirmation of the invariance of the ALSTAR's crush properties with temperature in the range of temperatures applicable to the HI-STAR 100 packaging was provided by experiments conducted by Holtec International in June 1998 [2.3.2] using sample material obtained from Hexcell. The test objective was to evaluate the temperature sensitivity, if any, of the static compression strength of the honeycomb material. To that end, test specimens were cut from the sample material and were subject to static compression testing using a Q.A. validated procedure.

A series of specimens of two different strengths were tested at three different temperatures. The specimens were tested at -29 degrees C, 23 degrees C and 80 degrees C which represent "Cold", "Ambient", and "Heat" environmental conditions. Ten specimens were prepared for each crush strength, to allow for multiple data points at each test temperature. The specimens were not pre-crushed so the static compression-crush curves exhibited an initial peak. After discounting the initial peaks in the static force-crush curve, the constant force range for each specimen could be identified from the test data and a crush pressure for the specimen defined by dividing this constant force by the measured specimen loaded area.

The computed crush pressures showed no significant trending that could be ascribed to environmental effects. Figure 2.3.2 is a plot of the test results and plots the average of the calculated test crush pressures from the series of specimens at each of the three temperatures.

The results for individual test samples at any given temperature were within manufacturing tolerance. It is clear from the plotted results that the effect of temperature is well within the data scatter due to manufacturing tolerance. Therefore, within the temperature range germane to the ALSTAR impact limiter, the force-crush characteristic is expected to be essentially unaffected by the coincident honeycomb metal temperature. This leads to the conclusion that environmental temperature effects will not influence impact limiter performance predictions.

Appendix 2.A contains further information on the AL-STAR honeycomb and its performance characteristics. The sensitivity of the package performance to variations in compression strength of the aluminum honeycomb is evaluated in Appendix 2.C for the latest HI-STAR 100 impact limiter design and in Supplement 2.I for the HI-STAR HB impact limiter design, respectively.

In summary, the AL-STAR impact limiter is composed of a carbon steel inner shell structure, an assemblage of cross core and uni-directional aluminum honeycombs and a stainless steel external sheathing.

None of the structural materials has a low melting point or is flammable. A Holtite-A layer is situated deep in the honeycomb in such a manner that it does not participate in the crushing process, but provides neutron shielding in the axial direction.

### 2.3.2 Nonstructural Materials

#### 2.3.2.1 Neutron Shield

The neutron shield in the overpack is not considered as a structural member of the HI-STAR 100 System. Its load carrying capacity is neglected in all structural analyses except where such omission would be nonconservative. The only material property of the neutron shield which is important to the structural evaluation is weight density ( $1.63 \text{ g/cm}^2$ ).

#### 2.3.2.2 Solid Neutron Absorber

The fuel basket solid neutron absorber is not a structural member of the HI-STAR 100 System. Its load carrying capacity is neglected in all structural analyses. The only material property of solid neutron absorber that is important to the structural evaluation is weight density. As the MPC fuel baskets can be constructed with neutron absorber panels of variable areal density, the weight that produces the most severe cask load is assumed in each analysis. (Density  $2.644 \text{ g/cm}^3$ ).

#### 2.3.2.3 Aluminum Heat Conduction Elements

The aluminum heat conduction elements are located between the fuel basket and MPC vessel in several of the early vintage MPC-68s and MPC-68Fs. They have since been removed from the MPC design and none were installed in the PWR MPCs. They are thin, flexible elements whose sole function is to transmit heat from the basket. They are not credited with any structural load capacity and are shaped to provide negligible resistance to basket thermal expansion. The total weight of the aluminum heat conduction elements is less than 1,000 lb. per MPC.

Table 2.3.1

## ALLOY X MATERIAL PROPERTIES

Temp. (°F)	Alloy X				
	$S_y$	$S_u^\dagger$	$\alpha_{\min}$	$\alpha_{\max}$	E
-40	30.0	75.0 (70.0)	8.54	8.55	28.82
100	30.0	75.0 (70.0)	8.54	8.55	28.14
150	27.5	73.0 (68.1)	8.64	8.67	27.87
200	25.0	71.0 (66.2)	8.76	8.79	27.6
250	23.75	68.5 (63.85)	8.88	8.9	27.3
300	22.5	66.0 (61.5)	8.97	9.0	27.0
350	21.6	65.2 (60.75)	9.10	9.11	26.75
400	20.7	64.4 (60.0)	9.19	9.21	26.5
450	20.05	64.0 (59.65)	9.28	9.32	26.15
500	19.4	63.5 (59.3)	9.37	9.42	25.8
550	18.8	63.3 (59.1)	9.45	9.50	25.55
600	18.2	63.1 (58.9)	9.53	9.6	25.3
650	17.8	62.8 (58.6)	9.61	9.69	25.05
700	17.3	62.5 (58.4)	9.69	9.76	24.8
750	16.9	62.2 (58.1)	9.76	9.81	24.45
800	16.6	61.7 (57.6)	9.82	9.90	24.1

## Definitions:

$S_y$  = Yield Stress (ksi)

$\alpha$  = Mean Coefficient of thermal expansion (in./in. per degree F x  $10^{-6}$ )

$S_u$  = Ultimate Stress (ksi)

E = Young's Modulus (psi x  $10^6$ )

## Notes:

1. Source for  $S_y$  values is Table Y-1 of [2.1.11].
2. Source for  $S_u$  values is Table U of [2.1.11].
3. Source for  $\alpha_{\min}$  and  $\alpha_{\max}$  values is Table TE-1 of [2.1.11].
4. Source for E values is material group G in Table TM-1 of [2.1.11].

<sup>†</sup> The ultimate stress of Alloy X is dependent on the product form of the material (i.e., forgings vs. plate). Values in parentheses are based on SA-336 forging materials (Type F304, F304LN, F316, and F316LN), which are used solely for the one-piece construction MPC lids. All other values correspond to SA-240 plate material.

Table 2.3.2

## SA516, GRADE 70 MATERIAL PROPERTIES

Temp. (°F)	SA516, Grade 70			
	S <sub>y</sub>	S <sub>u</sub>	α	E
-40	38.0	70.0	5.53	29.34
100	38.0	70.0	5.53	29.34
150	36.3	70.0	5.71	29.1
200	34.6	70.0	5.89	28.8
250	34.15	70.0	6.09	28.6
300	33.7	70.0	6.26	28.3
350	33.15	70.0	6.43	28.0
400	32.6	70.0	6.61	27.7
450	31.65	70.0	6.77	27.5
500	30.7	70.0	6.91	27.3
550	29.4	70.0	7.06	27.0
600	28.1	70.0	7.17	26.7
650	27.6	70.0	7.30	26.1
700	27.4	70.0	7.41	25.5
750	26.5	69.3	7.50	24.85

## Definitions:

S<sub>y</sub> = Yield Stress (ksi)

α = Mean Coefficient of thermal expansion (in./in. per degree F x 10<sup>-6</sup>)

S<sub>u</sub> = Ultimate Stress (ksi)

E = Young's Modulus (psi x 10<sup>6</sup>)

## Notes:

1. Source for S<sub>y</sub> values is Table Y-1 of [2.1.11].
2. Source for S<sub>u</sub> values is Table U of [2.1.11].
3. Source for α values is material group C in Table TE-1 of [2.1.11].
4. Source for E values is "Carbon steels with C ≤ 0.30%" in Table TM-1 of [2.1.11].

Table 2.3.3

## SA515, GRADE 70 MATERIAL PROPERTIES

Temp. (°F)	SA515, Grade 70			
	$S_y$	$S_u$	$\alpha$	E
-40	38.0	70.0	5.53	29.34
100	38.0	70.0	5.53	29.34
150	36.3	70.0	5.71	29.1
200	34.6	70.0	5.89	28.8
250	34.15	70.0	6.09	28.6
300	33.7	70.0	6.26	28.3
350	33.15	70.0	6.43	28.0
400	32.6	70.0	6.61	27.7
450	31.65	70.0	6.77	27.5
500	30.7	70.0	6.91	27.3
550	29.4	70.0	7.06	27.0
600	28.1	70.0	7.17	26.7
650	27.6	70.0	7.30	26.1
700	27.4	70.0	7.41	25.5
750	26.5	69.3	7.50	24.85

## Definitions:

 $S_y$  = Yield Stress (ksi) $\alpha$  = Mean Coefficient of thermal expansion (in./in. per degree F x  $10^{-6}$ ) $S_u$  = Ultimate Stress (ksi)E = Young's Modulus (psi x  $10^6$ )

## Notes:

1. Source for  $S_y$  values is Table Y-1 of [2.1.11].
2. Source for  $S_u$  values is Table U of [2.1.11].
3. Source for  $\alpha$  values is material group C in Table TE-1 of [2.1.11].
4. Source for E values is "Carbon steels with C  $\leq$  0.30%" in Table TM-1 of [2.1.11].

Table 2.3.4

## SA350-LF3 AND SA203-E MATERIAL PROPERTIES

Temp. (°F)	SA350-LF3			SA350-LF3/SA203-E		SA203-E		
	S <sub>m</sub>	S <sub>y</sub>	S <sub>u</sub>	E	α	S <sub>m</sub>	S <sub>y</sub>	S <sub>u</sub>
-100	23.3	37.5	70.0	28.5	6.20	23.3	40.0	70.0
100	23.3	37.5	70.0	27.6	6.27	23.3	40.0	70.0
200	22.8	34.2	68.5	27.1	6.54	23.3	36.5	70.0
300	22.2	33.2	66.7	26.7	6.78	23.3	35.4	70.0
400	21.5	32.2	64.6	26.1	6.98	22.9	34.3	68.8
500	20.2	30.3	60.7	25.7	7.16	21.6	32.4	64.9
600	18.5	-	-	-	-	-	-	-
700	16.8	-	-	-	-	-	-	-

## Definitions:

- S<sub>m</sub> = Design Stress Intensity (ksi)  
 S<sub>y</sub> = Yield Stress (ksi)  
 S<sub>u</sub> = Ultimate Stress (ksi)  
 α = Coefficient of Thermal Expansion (in./in. per degree F x 10<sup>-6</sup>)  
 E = Young's Modulus (psi x 10<sup>6</sup>)

## Notes:

1. Source for S<sub>m</sub> values is Table 2A of [2.1.11].
2. Source for S<sub>y</sub> values is Table Y-1 of [2.1.11].
3. Source for S<sub>u</sub> values is ratioing S<sub>m</sub> values.
4. Source for α values is material group E in Table TE-1 of [2.1.11].
5. Source for E values is material group B in Table TM-1 of [2.1.11].

Table 2.3.5

SB637-N07718, SA564-630, AND SA705-630 MATERIAL PROPERTIES

Temp. (°F)	SB637-N07718				
	S <sub>y</sub>	S <sub>u</sub>	E	α	S <sub>m</sub>
-100	150.0	185.0	29.9	---	50.0
-20	150.0	185.0	---	---	50.0
70	150.0	185.0	29.0	7.05	50.0
100	150.0	185.0	---	7.08	50.0
200	144.0	177.6	28.3	7.22	48.0
300	140.7	173.5	27.8	7.33	46.9
400	138.3	170.6	27.6	7.45	46.1
500	136.8	168.7	27.1	7.57	45.6
600	135.3	166.9	26.8	7.67	45.1
SA705-630/SA564-630 (Age Hardened at 1075°F)					
Temp. (°F)	S <sub>y</sub>	S <sub>u</sub>	E	α	-
200	115.6	145.0	28.5	5.9	-
300	110.7	145.0	27.9	5.9	-
400	106.7	141	-	-	-
500	103.5	140	-	-	-
SA705-630/SA564-630 (Age Hardened at 1150°F)					
200	97.1	135.0	28.5	5.9	-
300	93.0	135.0	27.9	5.9	-
400	89.8	131.4	-	-	-
500	87	128.5	-	-	-

Definitions:

- S<sub>m</sub> = Design Stress Intensity (ksi)
- S<sub>y</sub> = Yield Stress (ksi)
- α = Mean Coefficient of thermal expansion (in./in. per degree F x 10<sup>-6</sup>)
- S<sub>u</sub> = Ultimate Stress (ksi)
- E = Young's Modulus (psi x 10<sup>6</sup>)

Notes:

1. Source for S<sub>m</sub> values is Table 4 of [2.1.11].
2. Source for S<sub>y</sub>, S<sub>u</sub> values is ratioing design stress intensity values.
3. Source for α values is Tables TE-1 and TE-4 of [2.1.11], as applicable.
4. Source for E values is Table TM-1 of [2.1.11].

Table 2.3.6

YIELD STRENGTH OF SA-193-B8S IMPACT LIMITER ATTACHMENT BOLTS

Yield Stress for Attachment Bolt Calculations <sup>†</sup>	
Item	Yield Stress (psi)
Yield Stress	50,000

<sup>†</sup> Source for stress is Table 3 of [2.1.11].

Table 2.3.7

CRUSH STRENGTHS OF AL-STAR IMPACT LIMITER ALUMINUM HONEYCOMB  
MATERIALS

**THIS TABLE IS PROPRIETARY IN ITS ENTIRETY**

## 2.4 GENERAL STANDARDS FOR ALL PACKAGES

The compliance of the HI-STAR 100 System to the general standards for all packaging, specified in 10CFR71.43, is demonstrated in the following paragraphs.

### 2.4.1 Minimum Package Size

The HI-STAR 100 package meets the requirements of 10CFR71.43(a); the outer diameter of the overpack is approximately 96" and its length is approximately 203".

### 2.4.2 Tamperproof Feature

During transport operations, a wire tamper seal with a stamped identifier will be attached between the lower base of the upper impact limiter shell and the head of one of the impact limiter attachment bolts for the purpose of indicating possible tampering. In order to access the radioactive contents of the overpack, the upper impact limiter is required to be removed to access the closure plate bolting. This tamper seal satisfies the requirements of 10CFR71.43(b). A second wire tamper seal will be attached between the lower impact limiter and an attachment bolt head to indicate tampering. This seal will prevent access to the drain port. The assembly drawing in Section 1.4 depicts the security seals.

### 2.4.3 Positive Closure

There are no quick-connect/disconnect valves in the containment boundary of the HI-STAR 100 packaging. The only access to the overpack internals is through the closure plate on the overpack, which weighs over 7000 pounds, and the overpack vent and drain ports which are sealed and protected by bolted cover plates. This closure plate is fastened to the overpack flange with heavy bolts, which are torqued to closure values in Table 7.1.1. Opening of the overpack vent and drain port would require removal of the bolted cover plate and unthreading of the port plug. Inadvertent opening of the overpack is not feasible; opening an overpack requires mobilization of special tools and a source of power. The overpack containment boundary is analyzed for normal and accident condition internal pressure and demonstrates integrity under both conditions.

### 2.4.4 Chemical and Galvanic Reactions

There is no credible mechanism for significant chemical or galvanic reactions in the HI-STAR 100 System during loading operations.

The MPC, which is filled with helium, provides a nonaqueous and inert environment. Insofar as corrosion is a long-term time-dependent phenomenon, the inert gas environment in the MPC precludes the incidence of corrosion during transport. Furthermore, the only dissimilar material groups in the MPC are: (1) the neutron absorber material and stainless steel and (2) aluminum and stainless steel. Neutron absorber materials and stainless steel have been used in close

proximity in wet storage for over 30 years. Many spent fuel pools at nuclear plants contain fuel racks, which are fabricated from neutron absorber materials and stainless steel materials, with geometries similar to the HI-STAR 100 MPC. Not one case of chemical or galvanic degradation has been found in fuel racks built by Holtec. This experience provides a sound basis to conclude that corrosion will not occur in these materials. Additionally, the aluminum heat conduction elements and stainless steel basket are very close on the galvanic series chart. Aluminum, like other metals of its genre (e.g., titanium and magnesium) rapidly passivates in an aqueous environment, leading to a thin ceramic ( $Al_2O_3$ ) barrier, which renders the material essentially inert and corrosion-free over long periods of application. The physical properties of the material, e.g., thermal expansion coefficient, diffusivity, and thermal conductivity, are essentially unaltered by the exposure of the aluminum metal stock to an aqueous environment.

The aluminum in the optional heat conduction elements will quickly passivate in air and in water to form a protective oxide layer that prevents any significant hydrogen production during MPC cask loading and unloading operations. The aluminum in neutron absorber material may also react with water to generate hydrogen gas. The exact rate of generation and total amount of hydrogen generated is a function of a number of variables (see Section 1.2.1.4.1) and cannot be predicted with any certainty. Therefore, to preclude the potential for hydrogen ignition during lid welding or cutting, the operating procedures in Chapter 7 describe steps to monitor and mitigate combustible gas accumulation space beneath the MPC lid. Once the MPC cavity is drained, dried, and backfilled with helium, the source of hydrogen gas (the aluminum-water reaction) is eliminated.

The HI-STAR 100 overpack combines low-alloy and nickel alloy steels, carbon steels, neutron and gamma shielding, thermal expansion foam, and bolting materials. All of these materials have a long history of nongalvanic behavior within close proximity of each other. The internal and external carbon steel surfaces of the overpack and closure plates are sandblasted and coated to preclude surface oxidation. The coating does not chemically react with borated water. Therefore, chemical or galvanic reactions involving the overpack materials are highly unlikely and are not expected.

The interfacing seating surfaces of the closure plate metallic seals are clad with stainless steel to assure long-term sealing performance and to eliminate the potential for localized corrosion of the seal seating surfaces.

In accordance with NRC Bulletin 96-04, a review of the potential for chemical, galvanic, or other reactions among the materials of the HI-STAR 100 System, its contents and the operating environment, which may produce adverse reactions, has been performed. Table 2.4.1 provides a listing of the materials of fabrication for the HI-STAR 100 System and evaluates the performance of the material in the expected operating environments during short-term loading/unloading operations and transport operations. As a result of this review, no operations were identified which could produce adverse reactions beyond those conditions already analyzed in this SAR.

The HI-STAR 100 System is composed of materials with a long proven history of use in the nuclear industry. The materials are not affected by the radiation levels caused by the spent nuclear fuel. Gamma radiation damage to metals (e.g., aluminum, stainless steel, and carbon steel) does not occur until the dose reaches  $10^{18}$  rads or more. The gamma dose from the spent nuclear fuel transported in the HI-STAR 100 System is on the order of  $10^{10}$  rads. Moreover, significant radiation damage due to neutron exposure does not occur for neutron fluences below approximately  $10^{19}$  n/cm<sup>2</sup> [2.4.1, 2.4.2], which is far greater than the neutron fluence for which components of the HI-STAR 100 System will be exposed.

Table 2.4.1

HI-STAR 100 SYSTEM MATERIAL COMPATIBILITY  
WITH OPERATING ENVIRONMENTS

Material/Component	Fuel Pool (Borated and Unborated Water) <sup>1</sup>	Transport (Open to Environment)
Alloy X: -MPC Fuel Basket -MPC Baseplate -MPC Shell -MPC Lid -MPC Fuel Spacers	Stainless steels have been extensively used in spent fuel storage pools with both borated and unborated water with no adverse reactions or interactions with spent fuel.	The MPC internal and external environment will be inert (helium) atmosphere. No adverse interactions identified.
Aluminum -Conduction Inserts	Aluminum and stainless steels form a galvanic couple. However, they are very close on the galvanic series chart and aluminum rapidly passivates in an aqueous environment forming a thin ceramic (Al <sub>2</sub> O <sub>3</sub> ) barrier. The aluminum will be installed in a passivated condition. Therefore, during the short time they are exposed to fuel pool water, corrosion is not expected.	In a non-aqueous atmosphere galvanic corrosion is not expected.
Neutron Absorber Material:	Extensive in-pool experience on spent fuel racks with no adverse reactions. See Chapter 7 for additional requirements for combustible gas monitoring and required actions for control of combustible gas accumulation under the MPC lid.	No adverse reactions identified.

<sup>1</sup> HI-STAR 100 System short-term operating environment during loading and unloading.

Table 2.4.1 (continued)

HI-STAR 100 SYSTEM MATERIAL COMPATIBILITY  
WITH OPERATING ENVIRONMENTS

Material/Component	Fuel Pool (Borated and Unborated Water) <sup>2</sup>	Transport (Open to Environment)
<p>Steels:</p> <ul style="list-style-type: none"> <li>-SA350-LF3</li> <li>-SA203-E</li> <li>-SA515 Grade 70</li> <li>-SA516 Grade 70</li> <li>-SA750 630 17-4 PH</li> <li>-SA564 630 17-4 PH</li> <li>-SA106</li> <li>-SA193-B7</li> </ul> <p>Overpack Body</p>	<p>All exposed steel surfaces (except seal areas, pocket trunnions, and bolt locations) will be coated with paint specifically selected for performance in the operating environments. Even without coating, no adverse reactions (other than nominal corrosion) have been identified.</p>	<p>Internal surfaces of the overpack will be painted and maintained in an inert atmosphere. Exposed external surfaces (except those listed in fuel pool column) will be painted and will be maintained with a fully painted surface. No adverse reactions identified.</p>
<p>Stainless Steels:</p> <ul style="list-style-type: none"> <li>-SA240 304</li> <li>-SA193 Grade B8</li> <li>-18-8 S/S</li> </ul> <p>Miscellaneous Components</p>	<p>Stainless steels have been extensively used in spent fuel storage pools with both borated and unborated water with no adverse reactions.</p>	<p>Stainless steel has a long proven history of corrosion resistance when exposed to the atmosphere. These materials are used for bolts and threaded inserts. No adverse reactions with steel have been identified. No impact on performance.</p>

<sup>2</sup> HI-STAR 100 System short-term operating environment during loading and unloading.

Table 2.4.1 (continued)

HI-STAR 100 SYSTEM MATERIAL COMPATIBILITY  
WITH OPERATING ENVIRONMENTS

Material/Component	Fuel Pool (Borated and Unborated Water) <sup>3</sup>	Transport (Open to Environment)
Nickel Alloy: -SB637-NO7718 Bolting	Bolts are not used in pool.	Exposed to weathering effects. No adverse reactions with overpack closure plate. No impact on performance.
Brass: -Rupture Disk	Small surface of rupture disk will be exposed. No significant adverse impact identified.	Exposed to external weathering. No loss of function expected. Disks inspected prior to transport.
Holtite-A: -Neutron Shield	The neutron shield is fully enclosed by the outer enclosure. No adverse reaction identified. No adverse reactions with thermal expansion foam or steel.	The neutron shield is fully enclosed in the outer enclosure. No adverse reaction identified. No adverse reactions with thermal expansion foam or steel.
Silicone Foam: -Thermal Expansion Foam	Fully enclosed in the outer enclosure. No adverse reaction identified. No adverse reactions with neutron shield or steel.	Foam is fully enclosed in outer enclosure. No adverse reaction identified. No adverse reactions with neutron shield or steel.

<sup>3</sup> HI-STAR 100 System short-term operating environment during loading and unloading.

Table 2.4.1 (continued)

HI-STAR 100 SYSTEM MATERIAL COMPATIBILITY  
WITH OPERATING ENVIRONMENTS

Material/Component	Fuel Pool (Borated and Unborated Water) <sup>4</sup>	Transport (Open to Environment)
<p><u>Paint:</u></p> <ul style="list-style-type: none"> <li>- Carboline 890</li> <li>- Thermaline 450</li> </ul>	<p>Carboline 890 used for exterior surfaces. Acceptable performance for short-term exposure in mild borated pool water.</p> <p>Thermaline 450 selected for excellent high temperature resistance properties. Will only be exposed to demineralized water during in-pool operations as annulus is filled prior to placement in the spent fuel pool and the inflatable seal prevents fuel pool water in-leakage. No adverse interaction identified which could affect MPC/fuel assembly performance.</p>	<p>Good performance on exterior surfaces. Discoloration is not a concern.</p> <p>During transport, internal overpack surfaces will operate in an inert (helium) atmosphere. No adverse reaction identified.</p>
<p><u>Metallic Seals:</u></p> <ul style="list-style-type: none"> <li>- Alloy X750</li> <li>- 304 S/S</li> </ul>	<p>Not installed or exposed during in-pool handling.</p>	<p>Seals enclosed by closure plate or port cover plates.</p> <p>Closure plate seals seat against stainless steel overlay surfaces. No degradation of seal integrity due to corrosion is expected.</p>

<sup>4</sup> HI-STAR 100 System short-term operating environment during loading and unloading.

## 2.5 LIFTING AND TIE-DOWN STANDARDS

### 2.5.1 Lifting Devices

As required by Reg. Guide 7.9, in this subsection, analyses for all lifting operations applicable to the transport of a HI-STAR 100 package are presented to demonstrate compliance with the requirements of paragraph 71.45(a) of 10CFR71.

The HI-STAR 100 System has the following types of lifting devices: lifting trunnions located on the overpack top flange and threaded holes for eye bolts to lift the overpack closure plate. Lifting devices associated with movement of the MPC are not considered here; MPC lifting is addressed in a companion HI-STORM 100 document (FSAR, Docket 72-1014), and summarized in Subsection 2.5.1.3.

The evaluation of the adequacy of the lifting devices entails careful consideration of the applied loading and associated stress limits. The load combination D+H, where H is the "handling load", is the generic case for all lifting adequacy assessments. The term D denotes the dead load. Quite obviously, D must be taken as the bounding value of the dead load of the component being lifted. Table 2.2.4 gives bounding weights. In all lifting analyses considered in this document, the handling load H is assumed to be equal to 0.15D. In other words, the inertia amplifier during the lifting operation is assumed to be equal to 0.15g. This value is consistent with the guidelines of the Crane Manufacturer's Association of America (CMAA), Specification No. 70, 1988, Section 3.3, which stipulates a dynamic factor equal to 0.15 for slowly executed lifts. Thus, the "apparent dead load" of the component for stress analysis purposes is  $D^* = 1.15D$ . Unless otherwise stated, all lifting analyses in this section use the "apparent dead load",  $D^*$ , in the lifting analysis.

Analysis methodology to evaluate the adequacy of the lifting device may be analytical or numerical. For the analysis of the trunnion, an accepted conservative technique for computing the bending stress is to assume that the lifting force is applied at the tip of the trunnion "cantilever" and that the stress state is fully developed at the base of the cantilever. This conservative technique, recommended in NUREG-1536 for use in a storage FSAR, is applied to the trunnion analyses presented in this SAR.

The lifting trunnions are designed to meet the requirements of 10CFR71.45(a). The lifting attachments that are part of the HI-STAR 100 package also meet the design requirements of NUREG-0612 [2.1.9], which defines specific additional safety margins to ensure safe handling of heavy loads in critical regions of nuclear power plants. Satisfying the more conservative design requirements of NUREG-0612 ensures that the design requirements of 10CFR71.45(a) are met.

In general, the stress analysis to establish safety in lifting, pursuant to NUREG-0612, 10CFR71.45(a), and the ASME Code, requires evaluation of three discrete zones which may be referred to as (i) the trunnion, (ii) the trunnion/component interface, hereinafter referred to as Region A, and (iii) the rest of the component, specifically the stressed metal zone adjacent to Region A, herein referred to as Region B.

Stress limits germane to each of the above three areas are discussed below:

- i. Trunnion: NUREG-0612 requires that under the “apparent dead load”,  $D^*$ , the maximum primary stress in the trunnion be less than 10% of the trunnion material ultimate strength *and* less than 1/6th of the trunnion material yield strength. In other words, the maximum moment and shear force developed in the trunnion cantilever is less than 1/6 of the moment and shear force corresponding to incipient plasticity, and less than 1/10 of the flexural collapse moment or ultimate shear force for the section.
- ii. Region A: Trunnion/Component Interface: Stresses in Region A must meet ASME Code Level A limits under applied load  $D^*$ . Additionally, paragraph 71.45(a) of 10CFR71 requires that the maximum primary stress under  $3D^*$  be less than the yield strength of the weaker of the two materials at the trunnion/component interface. In cases involving section bending, the developed section moment must be compared against the plastic moment at yield. Typically, the stresses in the component in the vicinity of the trunnion/component interface are higher than elsewhere. However, exceptional situations exist. For example, when lifting a loaded MPC, the overpack baseplate, which supports the entire weight of the loaded MPC, is a candidate location for high stress even though it is far removed from the lifting location (which is located in the top lid).
- iii. Region B: This region constitutes the remainder of the component where the stress limits under the concurrent action of the apparent dead load  $D^*$  and other mechanical loads that may be present during handling (e.g. internal pressure) are required to meet Level A Service Limits under normal conditions of transport.

In summary, both Region A and Region B are required to meet the stress limits corresponding to ASME Level A under the load  $D^*$ . Additionally, portions of the component that may experience high stress during the lift are subject to the stress criterion of paragraph 71.45(a) of 10CFR71, which requires satisfaction of yield strength as the limit when the sole applied load is  $3D^*$ . In general, all locations of high stress in the component under  $D^*$  must also be checked for compliance with ASME Code Level A stress limits.

Unless explicitly stated otherwise, all analyses of lifting operations presented in this report follow the load definition and allowable stress provisions of the foregoing. Consistent with the practice adopted throughout this chapter, results are presented in dimensionless form, as safety factors, defined as SF, where

$$SF = (\text{Allowable Stress in the Region Considered})/(\text{Computed Maximum Stress in the Region})$$

It should be emphasized that the safety factor, SF, defined in the foregoing, represents the additional margin that is over and beyond the margin built into NUREG 0612 (e.g. a factor of 10 on ultimate strength or 6 on yield strength).

In the following subsections, each of the lifting analyses performed to demonstrate compliance with regulations is described. Summary results are presented for each of the analyses.

It is recognized from the discussion in the foregoing that stresses in Region A are subject to two distinct criteria, namely Level A stress limits under D\* and any other loading that may be present (such as pressure) and yield strength at 3D\*. The "3D\*" identifier is used whenever the paragraph 71.45(a) load case (the stresses must be bounded by the yield point at 3D\*) is the applied loading.

The HI-STAR 100 System has two types of lifting devices that are used during handling and loading operations. Two lifting trunnions are located on the overpack top flange for vertical package handling operations. There are also four lifting eyeholes for handling of the overpack closure plate. Four lifting eyes are installed in the holes for connection to lifting slings.

The two lifting trunnions on the overpack top flange are spaced at 180-degree intervals. Trunnion analysis results are presented in Subsection 2.5.1.1.

The four threaded holes of the overpack closure plate accommodate lifting eyes that are used only for installation or removal of the overpack closure plate.

#### 2.5.1.1 Overpack Trunnion Analysis

The lifting trunnion for the HI-STAR 100 overpack is presented in the Holtec Drawings (Section 1.4). The two lifting trunnions for HI-STAR 100 are circumferentially spaced at 180 degrees. The trunnions are designed for a two-point lift and are sized to satisfy the aforementioned NUREG-0612 criteria. The trunnion material is SB-637-N07718 bolt material, which is the same high strength material used for the closure plate bolts.

Each trunnion is initially threaded into the outer wall of the overpack top flange and is held in place by a locking pad. During a lifting operation, the moment and shear force are resisted by bearing and shearing stresses in the threaded connection.

The embedded trunnion is analyzed as a cantilever beam subjected to a uniformly distributed load applied over a short span of surface at the outer edge of the trunnion. Calculations demonstrate that the stresses in the trunnions, computed in the manner of the foregoing, comply with NUREG-0612 provisions.

Specifically, the following results are obtained:

Safety Factors from HI-STAR 100 Lifting Trunnion Stress Analysis <sup>†</sup>			
Item	Value (ksi) or (lb) or (lb-in)	Allowable (ksi) or (lb) or (lb-in)	Safety Factor
Bending stress (Comparison with Yield Stress/6)	17.3	24.5	1.41
Shear stress (Comparison with Yield Stress/6)	7.4	14.7	1.99
Bending Moment (Comparison with Ultimate Moment/10)	323,000	574,600	1.78
Shear Force (Comparison with Ultimate Force/10)	144,000	282,000	1.97

<sup>†</sup> The bounding lifted load is 250,000 lb. (per Table 2.2.4).

We note from the above that all safety factors are greater than 1.0. A factor of safety of exactly 1.0 means that the maximum stress, under apparent lift load D\*, is equal to the yield stress in tension or shear divided by 6, or that the section moment or shear force is equal to the ultimate section moment capacity or section force capacity divided by 10.

It is also important to note that safety factors associated with satisfaction of 10CFR71.45(a) are double those reported in the table since 10CFR71.45 only requires a factor of safety of 3 on the yield strength.

#### 2.5.1.2 Stresses in the Overpack Closure Plate, Main Flange, and Baseplate During Lifting

##### 2.5.1.2.1 Analysis of Closure Plate Lifting Holes and Eyes

The closure plate of the HI-STAR 100 overpack is lifted using four wire rope slings. The slings are attached to the closure plate using clevis eyebolts threaded into four holes in the closure plate.

10CFR71.45(a) requires a safety factor of 3 (based on yield strength) for the stress qualification of the clevis eyebolts. Lid lifting will normally be carried out with a lift angle of 90 degrees. However, to be conservative, the analysis assumes a minimum lift angle of 45 degrees.

The eyebolts are sized for a bounding weight of 9,200 lbs. (a value that includes a 15% dynamic amplifier). The working capacity of standard eyebolts is specified with a safety factor of four. Accordingly, its bolt size is selected such that it has a working capacity of approximately 17,000 lb (vertical). This results in a safety factor of greater than 7.0 calculated against the clevis ultimate load capacity. The tapped holes and specified bolts in the closure plate are analyzed and it is demonstrated that adequate thread strength and engagement length exists using allowable stresses in accordance with NUREG-0612 requirements (which are more severe than 10CFR71.45(a) requirements)

Minimum safety factors are summarized in the table below where we note that a safety factor of 1.0 means that the stress is the lessor of yield stress/6 or ultimate stress/10.

Overpack Top Closure B Minimum Safety Factors			
Item	Value (lb.)	Capacity (lb.)	Minimum Safety Factor
Overpack Top Closure Lifting Bolt Shear	9,200	12,080	1.31
Overpack Top Closure Lifting Bolt Tension	9,200	15,390	1.67

#### 2.5.1.2.2 Top Flange

- ASME Service Condition (Region B)

During lifting of a loaded HI-STAR 100, the top flange of the overpack (in which the lift trunnions are located) is identified as a potential location for high stress levels.

The top flange interface with the trunnion under the lifted load D\* is analyzed using simplified strength of materials models that focus on the local stress state in the immediate vicinity of the connection that develops to react the applied trunnion load. The bending moment that is transferred from the trunnion to the top forging is reacted by a shear stress distribution on the threads. Figure 2.5.1 shows a schematic of the distribution used to react the applied moment by thread shear. The top flange is considered a NB component subject to the lifted load and internal pressure. The membrane stress intensity due to both components of load is computed at the interface and compared to the allowable local membrane stress intensity. The interface region is also conservatively considered as subject to the provisions of NUREG-0612 and the thread shear stress and bearing stress are compared to 1/6 of the top forging yield stress in shear or compression. The following table summarizes the results:

Top Flange B Minimum Safety Factors (Interface with Trunnion)			
Item	Value (ksi)	Allowable (ksi)	Safety Factor
Bearing Stress (NUREG-0612 Comparison)	3.808	5.975	1.57
Thread Shear Stress (NUREG-0612 Comparison)	3.376	3.585	1.06
Stress Intensity (NB Comparison)	7.857	34.6	4.4

It is noted from the above that all safety factors are greater than 1.0 and that the safety factors for bearing stress and thread shear stress represent the *additional* margin over the factor of safety inherent in the member by virtue of the load multiplier mandated in NUREG-0612.

- Overpack Top Flange and Baseplate Under 3D\*

Analyses are performed for the components of the HI-STAR 100 structure that are considered as Region A (namely, the top flange region and baseplate) and evaluated for safety under three times the apparent lifted load (3D\*). A one-quarter symmetry finite element model of the top section of the HI-STAR, without the lid has been constructed. The model is assumed constrained at 36" below the top of the top flange. Contact elements are used to model the interface between the trunnion and the top flange and the material behavior is assumed to be elastic-plastic in nature (i.e. a bi-linear stress strain curve is input into the finite element analysis model). The analysis seeks to demonstrate that under 3 times the lifted load, the maximum primary membrane stress across any section in the immediate vicinity of the trunnion is below the material yield strength and the primary membrane plus primary bending stress across any section does not exceed 1.5 times yield. The overpack baseplate is also analyzed using formulas from classical plate theory, conservatively assuming that the allowable strengths are determined at the component design temperature rather than at the lower normal operating conditions.

The results are summarized in the table below:

Overpack Top Flange and Baseplate Minimum Safety Factors (10CFR71.45(a) Loading)			
Item	Value (ksi)	Allowable (ksi)	Safety Factor
Top Flange Membrane Stress Intensity (3D*)	27.44	32.2	1.17
Top Flange Membrane plus Bending Stress Intensity (3D*)	30.0	48.3	1.61
Baseplate Membrane plus Bending Stress Intensity (3D*)	1.452	32.2	22.2

The safety factors are all greater than 1.0 indicating that the requirements of 10CFR71.45(a) are satisfied in the top flange and baseplate of the HI-STAR 100 overpack.

### 2.5.1.3 MPC Lifting Analyses

The MPC can be inserted or removed from an overpack by lifting bolts that are designed for installation into threaded holes in the top lid. In the HI-STORM 100 FSAR (Docket 72-1014), the MPC top closure is examined considering the top lid as "Region B", where satisfaction of ASME Code Level A requirements is demonstrated. The analysis also considers highly stressed regions of the top closure as "region A" where applied load is "3D\*". The MPC baseplate is analyzed under normal handling and subject to the allowable strengths appropriate to a component considered in "Region B". Finally, the baseplate region is further analyzed where loading is "3D\*" consistent with the MPC baseplate being considered as "Region A". The definitions of "Region A", "Region B", and "3D\*" as they apply to lifting analyses have been introduced at the beginning of this subsection.

The lifting analysis for the MPC lid considers both the one-piece and the two-piece lid constructions,

which are shown on the licensing drawings in Section 1.4. In addition, for the two-piece lid construction the analysis assumes that the bottom piece is fabricated from Alloy X material, since it is the weaker of the two material options (i.e., Alloy X or carbon steel covered/coated with stainless steel). The results of the MPC lifting analyses are summarized in Subsection 3.4.3 of the HI-STORM 100 FSAR [2.5.1], which shows that all factors of safety are greater than 1.0 as required.

#### 2.5.1.4.1 Lifting of Damaged Fuel Canisters

All damaged fuel canisters suitable for deployment in the HI-STAR 100 Package are analyzed for structural integrity during a lifting operation. Appendix 2.B describes the analyses undertaken and summarizes the results obtained.

In conclusion, the synopses of lifting device, device/component interface, and component stresses, under all contemplated lifting operations for the HI-STAR 100 overpack and MPC have been presented in the foregoing, and show that all factors of safety are greater than 1.0.

#### 2.5.2 Tie-Down Devices

##### 2.5.2.1 Discussion

The initial design of the HI-STAR 100 Systems envisioned a shear ring located on the top flange and pocket trunnions located near the bottom of the outer enclosure shell to serve as locations for tie-down. Accordingly, previous issues of the SAR included analyses to qualify the shear ring/pocket trunnion components as tie-down devices complying with the requirements of 10CFR71.45(b).

The pair of semi-obround recesses referred to as pocket trunnions were originally incorporated into the HI-STAR design to permit the cask to be upended (or downended) by using circular shafts inserted in the "pockets" to serve as rotation pivots. Recent handling experience with the seven HI-STAR 100 overpacks manufactured thus far (ca. April 2002) and the HI-TRAC transfer casks (which are similar in overall dimensions and weight) has shown that utilizing an L-shaped cradle, designed as an ancillary under Part 72 regulations for the upending and downending operations, is a more robust method of cask handling. The cradle method of handling Holtec's overpacks and MPCs has garnered considerable experience through ISFSI implementation operations at several sites. Because the cradle method of upending and downending does not require the pocket trunnions, and because the recesses to incorporate the pocket trunnions lead to increased local dose, the pocket trunnions are being henceforth eliminated from the HI-STAR design. All HI-STAR 100 overpacks (except the first seven units already manufactured) shall be fabricated without the twin pocket trunnions; even in the first seven units that have the shear ring and pocket trunnions, these locations are no longer designated as tie-down locations.

In lieu of relying on the pocket trunnions for tie-down, the revised tie-down arrangement for HI-STAR 100 secures the overpack to the transport vehicles in such a manner that the longitudinal inertia forces (the most frequent mode of motion-induced loading the package during transport) do not exert an overturning moment on the cask (as is the case with a pocket trunnion-based fastening means). In fact, the revised tie-down device seeks to eliminate or minimize all localized loadings on the body of the overpack, thus incorporating an additional element of safety in the transport package.

The new tie-down configuration, pictorially illustrated in Figure 1.2.8, essentially consists of a near-full-length saddle integral to the bed of the transport vehicle to react the lateral and vertical loads, and a pair of End-Restraints, also integral to the transport vehicle, that save for a small calibrated axial clearance to provide for differential thermal expansion, provide a complete axial confinement to the overpack. The details of the design of the tie-down structure are governed by the reaction forces computed using static equilibrium relationships for inertia loads corresponding to §72.45(b) and reported in this SAR.

To comply with the requirements of 10CFR71.45(b), it must be shown by test or analysis that all devices used for package tie-down are acceptable. Therefore, in this section, we present the load analyses of the HI-STAR 100 tie-down system. The HI-STAR 100 System is shown in a transport orientation in Drawing 3930 and in Figure 1.2.8.

To summarize, HI-STAR 100 is secured to the transport vehicle in a horizontal position by the following components (no additional support structure is permanently attached to the cask for transport tie-down):

- a. A long saddle support, bearing on the overpack outer enclosure shell and enclosure shell panels, over an angle of approximately 140 degrees. Multiple tie-down straps, sized to support uplift loads, secure the HI-STAR 100 to the saddle. The saddle resists lateral loads and vertical downward oriented loads through its extensive interface with the body of the HI-STAR overpack. Vertical upward directed loads are reacted by the tie-down straps.
- b. Longitudinal loads in either direction are transmitted to the End-Restraint by the sacrificial disc on each impact limiter. Because the axial transport loads are bounded by the 10g's in either longitudinal direction, the aluminum honeycomb discs are quite adequate to transmit axial loads without crushing.

In accordance with 10CFR71.45(b), the inertia forces, applied at the center of gravity of the loaded HI-STAR 100, arise from:

- a. a horizontal component along the longitudinal axis of  $\pm 10g$
- b. a vertical component of  $\pm 2g$
- c. a lateral component of  $\pm 5g$

These accelerations are referred to as the first set of load amplifiers. These forces are applied simultaneously in the respective directions with their lines of action selected to maximize the reactions. In the following, "load combinations" are identified by assembling the three loads with appropriate plus or minus signs to reflect the fact that the lateral load can be in either direction, the vertical load can be in either direction, and the longitudinal load is uni-directional.

As required by the governing regulations, the components of the cask that are used for tie-down must be capable of withstanding the force combinations without generating stress in the cask components in excess of the material yield strength.

The saddle support under the enclosure shell, the slings, and the front and rear end structures that resist longitudinal load are not part of the HI-STAR 100 package and therefore, are not part of this submittal. The loads used to design these components are determined using the load amplifiers given by the American Association of Railroads (AAR) Field Manual, Rule 88. These amplifiers, henceforth called the second set of load amplifiers, are:

- $\pm 7.5g$ 's longitudinal
- $\pm 2.0$  g's vertical
- $\pm 2.0$  g's lateral

In what follows, the equations of equilibrium for the packaging subject to three orthogonal inertia loads are set down. Tie-down reactions using either set of load amplifiers are determined from the same equilibrium equations. Numerical results are obtained for both sets of input load amplifiers and presented at the end of this section as Tables 2.5.1 and 2.5.2.

Figure 1.2.8 shows a schematic of the tie-down; Figure 2.5.2 shows a partial free-body diagram of the transport package on the railcar. The following steps to comply with the provisions of 10CFR71.45(b) are carried out:

- Develop the general equilibrium equations to solve for the tie-down forces.
- Apply the equations to develop numerical results for the tie-down forces. Results are provided for the load multipliers specified in 10CFR71.45(b) and for the load multipliers in the AAR Field Manual.

- The tie-down force values with the 10CFR71.45(b) load amplifiers are used to evaluate the structural integrity of the cask components affected by the tie-down devices. Tie-down reactions obtained using the AAR Field Manual amplifiers for are reported for information only (for future use in designing the tie-down members of the railroad car).

#### 2.5.2.2 Equilibrium Equations to Determine the Tie-Down Forces

For longitudinal loading, the applied load, amplified by the imposed deceleration, is reacted directly by either the top or bottom impact limiter. It is shown in Subsection 2.6 that all components of the HI-STAR 100 package in this load path meet ASME Level A stress limits for a bounding deceleration of 17 g's. Therefore, by suitable choice of support structure on the railcar, the HI-STAR 100 Package is assured of meeting regulatory requirements under the mandated longitudinal transport load of 10g's in either direction. Furthermore, the crush strength of the aluminum honeycomb material is sufficiently high to prevent the impact limiters from crushing under the 10g transport load.

For vertical loading, the resultant vertical force on the saddle is reacted by a symmetric bearing pressure, or by developing a reacting tension in the tie-down strap. Figure 2.5.12 shows a free body at a saddle support. The vertical load is conservatively assumed resisted by a radial component only, with no credit assumed for any shear stresses arising from friction at the interface. The radial pressure,  $p_v$ , is assumed to vary with circumferential location using a cosine function, with peak pressure occurring under the overpack centerline.

For lateral loading, the resultant force is conservatively assumed reacted only by a radial bearing pressure,  $p_h$ , distributed on one side of the saddle and varying around the periphery in accordance with a sine function (shear stresses due to frictional effects are conservatively neglected). Figure 2.5.13 shows the appropriate free-body. Since the radial pressure distribution corresponds to both a vertical and lateral force resultant, an opposing vertical force is developed in the tie-down strap. This vertical force is proportional to the applied lateral force, and ensures equilibrium. For the evaluation of lateral force equilibrium, it is also necessary to determine the vertical and horizontal location of the center of pressure of the radial bearing force on the enclosure shell and shell panels. This location is designated by the coordinates  $y_2$  and  $z_2$  in Figure 2.5.2 and in Figure 2.5.13 and ensures that there is no net moment (around the cask centerline longitudinal axis) produced by the bearing pressure.

For the geometry associated with the HI-STAR 100 transport saddles, the induced vertical upward force in the tie-down straps from the application of a lateral load is approximately equal to the magnitude of the lateral load. Thus, for a combination of lateral load and upward vertical load, there are two contributions to the total load in the tie-down sling.

- Equilibrium Equations for Tie-Down

The equilibrium equations necessary to solve for the tie-down forces under the postulated loads will be written using classical vector algebra. There are three loading cases that govern the analysis of the tie-down components: longitudinal (x), vertical (y), and lateral (z). The reaction forces for each loading case are determined by the equations of force and moment equilibrium. The general equations of force and moment equilibrium are developed following the partial free body diagram shown in Figure 2.5.2. Figure 2.5.2 defines the following force vectors:  $\bar{F}_c$ ,  $F_b$ , and  $F_t$  are the applied loads from the cask, and from the bottom and top impact limiters, respectively.  $S_i$  ( $i=1,2,3$ ) are the three reaction forces at the locations on the saddle support where tie-down straps are located. For all tie-down force calculations to determine the restraint forces, the following bounding values (for a 1g load) are ascribed to the cask and to the overpack (Table 2.2.1).

HI-STAR 100 – 250,000 lb.

Top Impact Limiter – 20,000 lb.

Bottom Impact Limiter – 18,000 lb

Results from numerical computations are summarized in tabular form at the end of this section. In the following sub-sections, discussion of the various loads and the method by which they are reacted, is presented

#### 2.5.2.3 Longitudinal Loading

The longitudinal load is directly resisted by the impact limiters at the top and bottom of the cask. The two impact limiters have an annular region with impact limiting material chosen to resist normal transport longitudinal loads without loss of function in the event of a cask drop accident. The HI-STAR overpack is shown in Subsection 2.6 to meet Level A ASME Code stress limits.

#### 2.5.2.4 Vertical Load

The vertical loads, directed either upwards or downwards, are resisted by the tie-down straps or the saddle support at the three locations shown in Figures 1.2.8 and 2.5.2. Planer equilibrium equations for force and moment equilibrium have the form (refer to Figure 2.5.2):

$$\sum_i S_i = G$$

$$\sum_i x_i S_i = M$$

where  $G = F_t + F_c + F_b$  and  $M = F_t x_t + F_c x_c - F_b x_b$

These two equations, coupled with the assumption that the cask is rigid, yields the solution for the three tie-down reactions; the magnitude of the three vertical reactions are determined in the form:

$$S_{i(\text{vertical})} = f_i F + g_i M \quad i = 1,2,3$$

The detailed numerical computations leading to the results reported in tabular form at the end of this subsection conservatively assume that the outermost tie-down straps are located so that their centerlines are approximately 1' from the upper and lower edge of the outer enclosure panels. In the above equation, F is the total vertical applied force and M is the total moment, about a horizontal axis through the base of the cask, from the vertical components of the applied force. The applied forces are the weights of the cask, and the top and bottom impact limiters, amplified by the appropriate "g" value and located at the centroid of the components (per Figure 2.5.2). When the applied load is directed downward, the reactions at the saddle supports are distributed bearing pressures at the saddle/enclosure shell interface, as shown in Figure 2.5.12; when the applied load is directed upward, the reactions are provided by tensile loads in the tie-down straps, which are distributed to the enclosure shell as a radial pressure.

#### 2.5.2.5 Lateral Load

For this load case, lateral loads, in either direction, are distributed to each saddle support location where tie-down straps are present, and are resisted by a radial bearing pressure distribution at the saddle/enclosure shell interface. The radial pressure distribution has a lateral and vertical resultant force. The lateral component of the reaction load at each saddle/enclosure shell interface is computed from force and moment equilibrium and the same form of solution is achieved as given for the vertical loads. In this case, however, since the resultant resisting force is directed through the cask longitudinal centerline, at each of the support locations, there is an induced vertical force in the tie-down strap that develops to balance the vertical component of the force between the overpack and the support at each location. Figure 2.5.13 shows how the forces are distributed so that at each location, the vertical force from the interface pressure is balanced by the induced load in the tie-down strap, while the horizontal net force from the interface pressure balances the lateral reaction force at that location. The location of the resultant force at the saddle/enclosure shell interface ensures that there is no net moment at the support. That is, the relation between the lateral load, the induced vertical load, and the center of pressure coordinates  $y_2$  and  $z_2$  is:

$$F(\text{lateral}) \times (y_2) = F(\text{induced vertical}) \times (z_2)$$

The saddle support angle is chosen to ensure that the resultant force is inclined approximately 45 degrees to the vertical, so that the applied lateral force induces a vertical force of the same magnitude that is resisted by the tie-down straps.

#### 2.5.2.6 Numerical Results for Tie-Down Reactions

The longitudinal load in either direction is reacted by the impact limiters and does not impose any load on the saddle support or the tie-down straps. The lateral load and vertical load results in a bearing pressure between the saddle support and the enclosure shell and a tensile load in the tie-down strap. The only directional effect leading to different results is the direction of the applied vertical load. Therefore, the load combinations to be considered are:

- (1) Longitudinal load, +lateral load, +vertical load upward
- (2) Longitudinal load +lateral load, + vertical load downward

The results for the tie-down reactions due to each individual load and due to the defined load combinations are presented in Table 2.5.1.

As noted earlier, the AAR Field Manual, Rule 88 specifies a set of load amplifiers that are appropriate for designing the saddle and the trunnion support but are not part of the packaging qualification effort. For information purposes only, results for the tie-down reactions are provided for the load case combinations using the load amplifiers (defined earlier as the second set) given by the AAR Field Manual, Rule 88. Results are given in Table 2.5.2.

To comply with the governing requirements (10CFR71.45(b)(1)), it should be demonstrated that under the tie-down loads, no part of the cask experience stresses in excess of the material yield strength. It has been noted earlier that the impact limiters are capable of resisting longitudinal loads in excess of the regulatory requirements for transport. Therefore, only transport loads in the vertical and lateral direction need be assessed for their affect on cask stress. The only loads transmitted to the overpack from lateral and vertical loads are radial pressures on the overpack outer enclosure. The enclosure shell is backed by the Holtite-A material, which, in reality, can resist some compression and transfer the load to the intermediate shells. However, since no structural credit is assumed for Holtite-A, it is conservatively considered that the radial loads from the tie-down forces are transmitted only through the radial channel legs connecting the outer enclosure shell to the overpack intermediate shells. The following simplified analysis serves to ensure that the cask components do not exceed their yield stress under the combined action of lateral and vertical tie-down loads.

An examination of the bounding loads from Table 2.5.1 concludes that the most demand on the cask structure occurs when the tie-down strap load, from both lateral and vertical transport forces, is assumed reacted over 180 degrees and therefore, transmitted to the overpack intermediate shells as a compressive direct load in nineteen (19) radial channel legs (see applicable drawing in Section 1.4 showing the radial channels). This enables the determination of a minimum length of contact between the tie-down straps and the enclosure shell to ensure that the direct stress in the radial channels remains below the yield strength. Conservatively evaluating the yield strength of the radial channels at 400 degrees F per Table 2.1.2, Tables 2.3.2 and 2.3.3 give:

$$S_y = 32,600 \text{ psi}$$

The average direct stress, "St", in a channel is computed by first determining the equivalent uniform radial pressure developed at the interface between the tie-down strap and the enclosure shell. From simple equilibrium, this radial pressure is determined by the formula:

$$p = 2T/DL$$

T is the load in the tie-down strap, D is the outer diameter of the enclosure shell, and L is the length of enclosure shell under pressure.

The pressure,  $p$ , is related to the direct compressive load, “ $G$ ”, in one of the channel legs, by the following equation:

$$G = p \times (sL) \quad \text{where the span between channel legs is approximated as } s = (3.14159 \times (D/2))/19$$

Finally, the stress in the channel leg, “ $St$ ”, is given as:

$$St = G/(tL) \quad \text{where } t \text{ is the channel leg thickness.}$$

$$\text{Setting } St = Sy \text{ and solving for “}L\text{”, gives: } L = (3.14159/19) \times (T/t \times Sy)$$

The minimum length  $L$  is computed using  $T = 647,000 \text{ lb./2}$ , and  $t=0.5$ ”, to obtain:

$$L = 3.282''$$

Since the minimum sling length needed to support the load is 6” (or greater), it is seen that the cask stress developed to resist the lateral and vertical transport loads is much less than the yield stress of the channel legs; therefore, the governing regulatory requirement of 10CFR71.45(b)(1) is satisfied.

#### 2.5.2.7 Structural Integrity of Pocket Trunnions on Applicable HI-STAR 100 Systems

The summary of results provided in tabular form, herein, is applicable only to the units that have been previously manufactured and, therefore, have pocket trunnions. The structural function of the pocket trunnions on applicable HI-STAR 100 Systems is limited to supporting the HI-STAR overpack during upending /downending operations if a separate downending cradle is not employed. If the pocket trunnion recess is utilized as a loaded pivot point during downending, the applied load for this operation is conservatively considered as the loaded weight of the package without impact limiters (250,000 lb.), amplified by a 15% inertia load factor. This load can be applied in any direction as the package is rotated 90 degrees. Results of structural integrity analyses, performed to qualify the rotation trunnion recess on the affected units, are summarized below.

Analyses are performed to evaluate the structural performance of various portions of the pocket trunnion under the stated total load, divided equally between the two trunnions. Since the trunnions are not utilized as tie-down devices, they are not considered as ASME Code items; nevertheless, their performance is evaluated by comparing calculated stresses against yield strengths (to conform to the methodology employed in the HI-STAR 100 FSAR). Analyses for bearing stress levels, primary stress levels in the trunnion recess body, and weld stress in the weld group that attaches the recess forging to the intermediate shells. The methods of analysis include both simple strength of materials evaluation and finite element analysis of the pocket trunnion body. For the bearing stress analysis, the average bearing stress is computed based on the diameter of the male trunnion that would fit the trunnion pocket. For the general primary stress state in the trunnion forging, a finite element model of the trunnion recess is developed. Finally, for the analysis of the weld stress distribution, simple strength of materials equilibrium analysis is used with weld sizes appropriate to the minimum weld configuration in-place on the affected HI-STARs. The maximum weld stress is computed accounting for the weld material between the trunnion recess and the intermediate shells and between the pocket trunnion and the outer enclosure shell.

The results of the pocket trunnion recess analyses for an upending/downending load equal to 125,000 lb. x 1.15, are summarized in the following table:

Structural Integrity Results for HI-STAR Systems Equipped with Pocket Trunnions			
Item	Calculated Stress (ksi)	Allowable Stress (ksi)	Safety Factor = $\frac{\text{Allowable Value}}{\text{Calculated Value}}$
Bearing Stress	6.183	97.1	15.71 (based on material yield strength)
Pocket Recess Primary Membrane + Primary Bending Stress	14.17	32.33	2.282 (based on 1/3 of trunnion material yield strength)
Maximum Weld Stress	2.399	14.533	4.802 (based on 1/3 of base metal yield strength)

### 2.5.3 Failure of Lifting and Tie-Down Devices

10CFR71.45 establishes criteria for minimum safety factors for lifting attachments, and provides input design loads for tie-down devices. 10CFR71.45 also requires that the lifting attachments and tie-down devices permanently attached to the cask, be designed in a manner such that a structural failure during lifting or transport will not impair the ability of the transportation package to meet other requirements of Part 10CFR71. In this section of the SAR, the issues concerning a structural failure during lifting or tie-down during transport are addressed. Specifically, the following issues are considered and resolved below:

#### a. Lifting Attachments:

Analyses are performed, using simple strength of materials concepts and evaluations to demonstrate that the ultimate load carrying capacity of the lifting trunnions is governed by the cross section of the trunnion external to the overpack top forging rather than by any section within the top forging. Detailed calculations that compare the ultimate load capacity of the shank of the lifting trunnion (the external cylindrical portion extending outside of the overpack top forging) to the ultimate load capacity of the top forging are performed. The ultimate load carrying capacity of the trunnion shank is based on an examination of the ultimate capacity of the section in both shear and bending. The ultimate load capacity of the top forging is determined by its capacity to resist moment by thread shear at the trunnion/forging threaded interface and to equilibrate the lifting load by bearing action at the trunnion forging bearing surface interface. It is concluded that the trunnion shank reaches ultimate load capacity limit prior to the top forging reaches its corresponding ultimate load capacity limit. Loss of the external shank of the lifting trunnion will not cause loss of any other structural or shielding function of the HI-STAR 100 overpack; therefore, the requirement imposed by 10CFR71.45(a) is satisfied.

The following safety factors are established:

$$\frac{(\text{Ultimate Bearing Capacity at Trunnion/Top Forging Interface})}{(\text{Ultimate Trunnion Load})} = 1.16$$

$$\frac{(\text{Ultimate Moment Capacity at Trunnion/Top Forging Thread Interface})}{(\text{Ultimate Trunnion Moment Capacity})} = 1.57$$

b. Tie-Down Devices

There are no tie-down devices that are permanently attached to the cask; therefore, no analyses are required to demonstrate that the requirements of 10CFR71.45(b)(3) are satisfied.

2.5.4 Conclusions

Lifting devices have been considered in Subsection 2.5.1 and Tie-Down devices have been considered in Subsection 2.5.2. It is shown that requirements of 10CFR71.45(a)(lifting devices) and 10CFR71.45(b)(tie-down devices) are satisfied. All safety factors exceed 1.0.

No tie-down device is a permanent part of the cask. All tie-down devices (saddle, tie-down straps, and fore and aft impact limiter targets, are part of the rail car and accordingly are not designed in this SAR. The maximum loads imposed on these items are recorded for subsequent design efforts.

Table 2.5.1

TIE-DOWN REACTIONS<sup>†</sup> - 10CFR71 LOAD RESULTS

Item	Component	Load Combination 1 (kips)	Load Combination 2 (kips)
Impact Limiter Target	Longitudinal	2,880	2,880
Top End Saddle -1	Lateral	420.85	420.85
	Vertical – Saddle	420.85	252.51 + 420.85
	Vertical - Tie-Down Strap	84.17 + 420.85	420.85
Intermediate Saddle-2	Lateral	480.15	480.15
	Vertical - Saddle	480.15	288.09 + 480.15
	Vertical - Tie-Down Strap	96.03 + 480.15	480.15
Bottom End Saddle -3	Lateral	539	539
	Vertical – Saddle	539	323.4 + 539
	Vertical - Tie-Down Strap	107.8 + 539	539

<sup>†</sup> See Figure 2.5.2 for definition of the symbols for the reaction loads.

Table 2.5.2

TIE-DOWN REACTIONS<sup>†</sup> - AAR RULE 88 LOAD RESULTS

Item	Component	Load Combination 1 (kips)	Load Combination 2 (kips)
Impact Limiter Target	Longitudinal	2,160	2,160
Top End Saddle -1	Lateral	168.34	168.34
	Vertical - Saddle	168.34	252.51 +168.34
	Vertical - Tie-Down Strap	84.17 + 168.34	168.34
Intermediate Saddle-2	Lateral	192.06	192.06
	Vertical - Saddle	192.06	288.09 +192.06
	Vertical - Tie-Down Strap	96.03 +192.06	192.06
Bottom End Saddle -3	Lateral	215.6	215.6
	Vertical - Saddle	215.6	323.4 + 215.6
	Vertical - Tie-Down Strap	107.8 + 215.6	215.6

<sup>†</sup> See Figure 2.5.2 for definition of the symbols for the reaction loads.

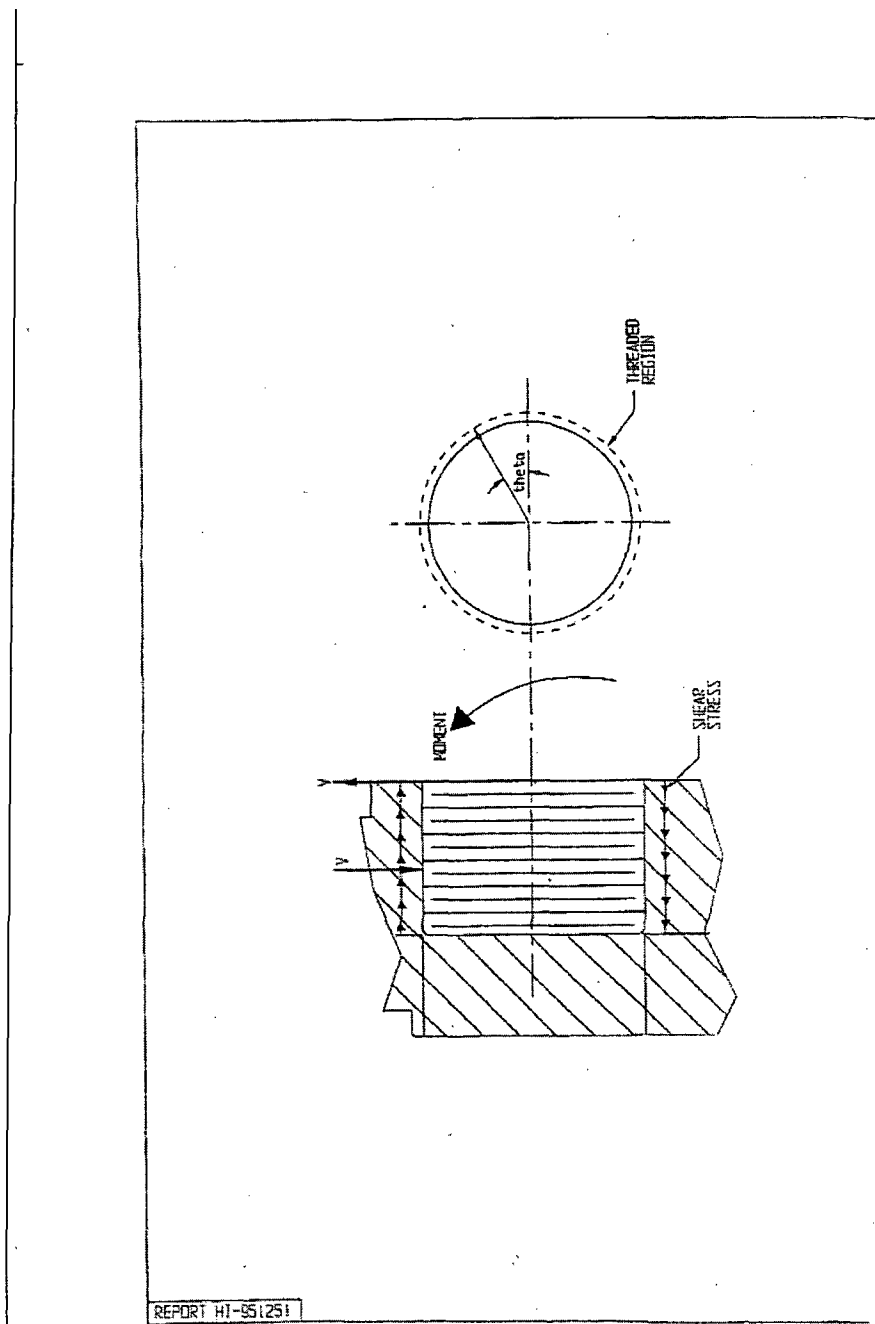


FIGURE 2.5.1; FREE BODY SKETCH OF LIFTING TRUNNION THREADED REGION SHOWING MOMENT BALANCE BY SHEAR STRESS

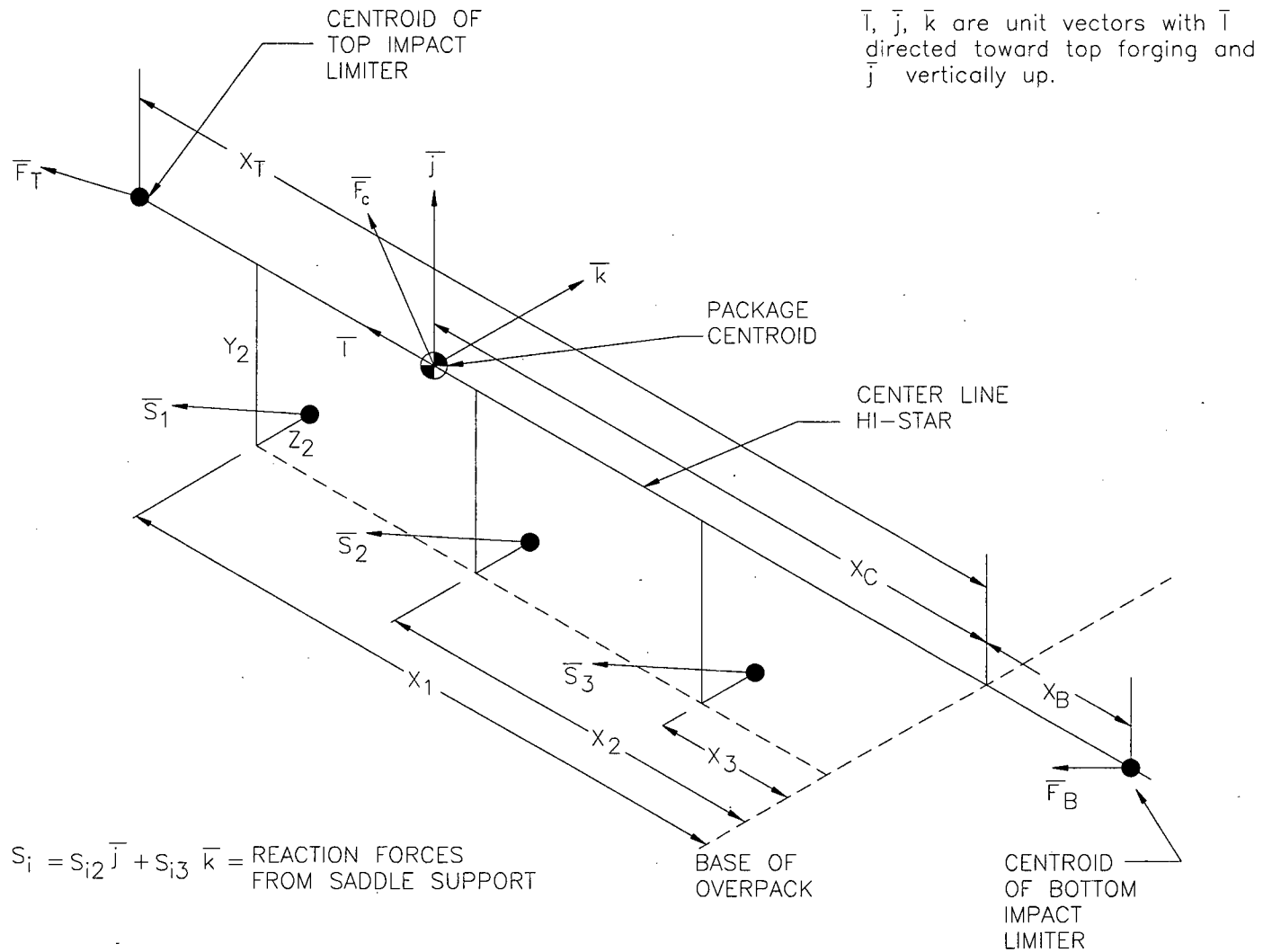


FIGURE 2.5.2; PARTIAL FREE BODY DIAGRAM OF OVERPACK SHOWING APPLIED TRANSPORT LOAD AND TIE-DOWN REACTION VECTORS AT SADDLE SUPPORTS

**Figures 2.5.3 through 2.5.11**  
**INTENTIONALLY DELETED**

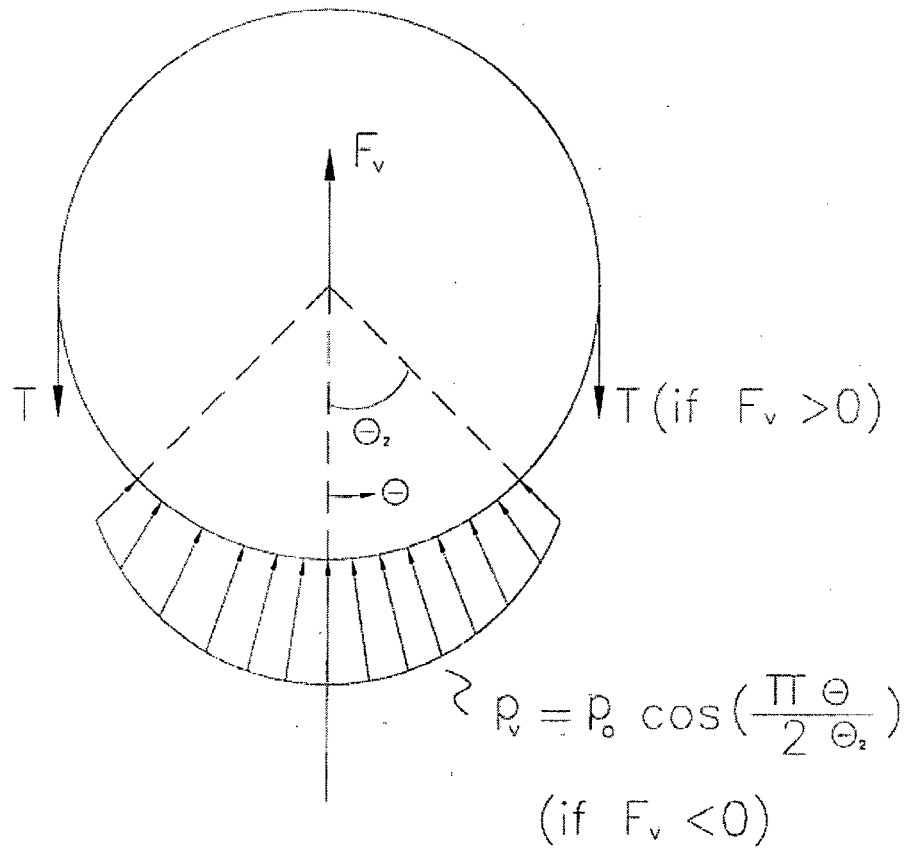
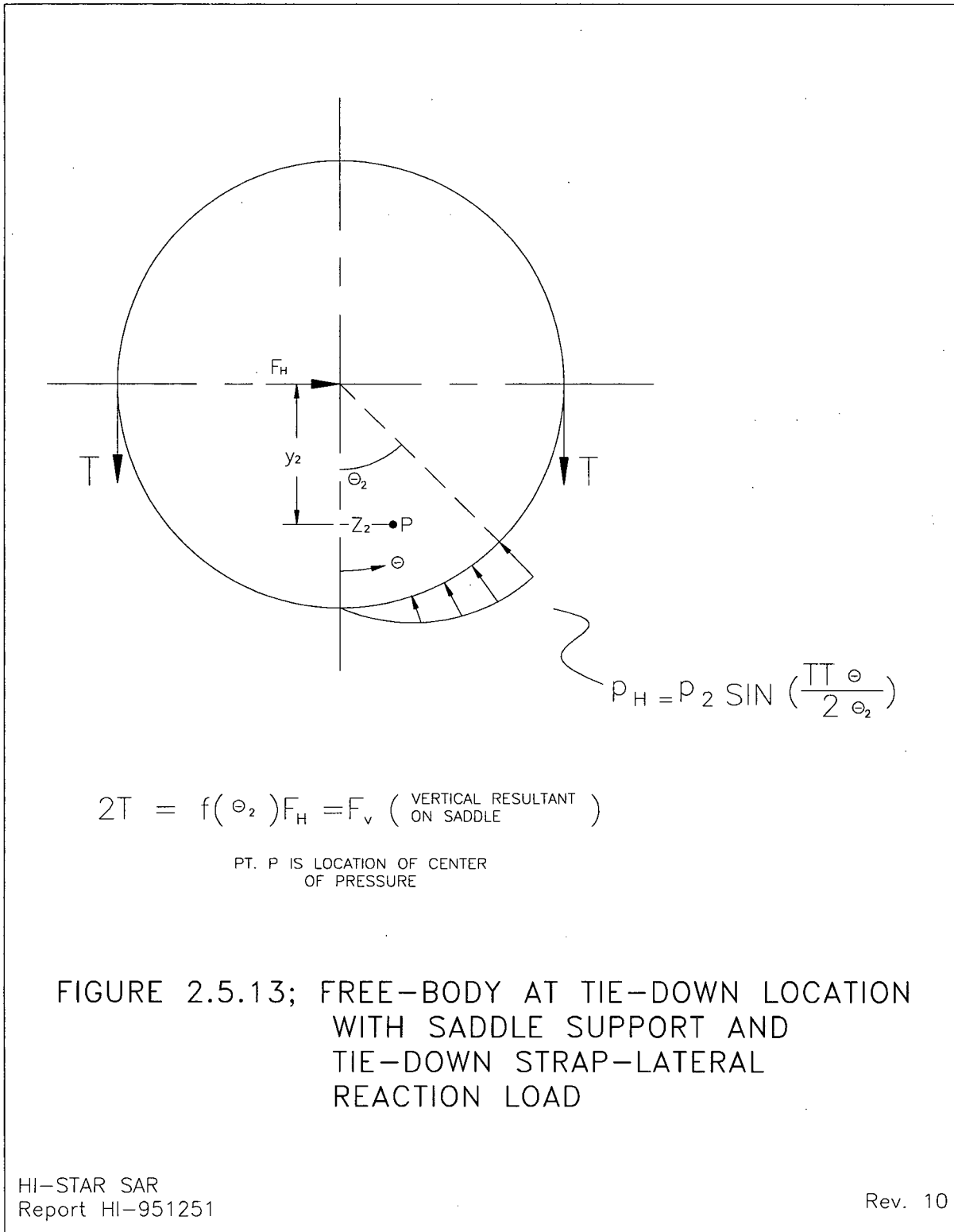


FIGURE 2.5.12; FREE-BODY AT TIE DOWN LOCATION WITH SADDLE SUPPORT AND TIE-DOWN STRAP-VERTICAL REACTION LOAD.



## 2.6 NORMAL CONDITIONS OF TRANSPORT

The HI-STAR 100 package, when subjected to the normal conditions of transport specified in 10CFR71.71, meets the design criteria in Subsection 2.1.2 (derived from the stipulations in 10CFR71.43 and 10CFR71.51) as demonstrated in the following section.

### 2.6.1 Heat

Subsection 2.6.1, labeled “Heat” in Regulatory Guide 7.9, is required to contain information on all structural (including thermoelastic) analyses performed on the cask to demonstrate positive safety margins, except for lifting operations that are covered in the preceding Section 2.5. Accordingly, this subsection contains all necessary information on the applied loadings, differential thermal expansion considerations, stress analysis models, and results for all normal conditions of transport. Assessment of potential malfunction under “Cold” conditions is required to be presented in Subsection 2.6.2.

Consistent with Regulatory Guide 7.9, the thermal evaluation of the HI-STAR 100 Package is reported in Chapter 3. The thermal evaluation also establishes the material temperatures, which are used in the structural evaluations discussed in this section and in Section 2.7.

#### 2.6.1.1 Summary of Pressures and Temperatures

Design pressures and design temperatures for all conditions of transport are listed in Tables 2.1.1 and 2.1.2, respectively.

Load cases F1 (Table 2.1.6) and E4 (Table 2.1.7) are defined to study the effect of differential thermal expansion among the constituent components in the HI-STAR 100 Package. Figures 2.6.1 and 2.6.2 provide the defining bounding temperature distributions used for the MPC and overpack finite element thermal stress calculations to maximize stresses that develop due to temperature gradients. The distribution T is applied conservatively to analyze its effect on the fuel basket, the enclosure vessel (helium retention boundary), and the overpack.

#### 2.6.1.2 Differential Thermal Expansion

In addition to the finite element solutions for free expansion stress (due to temperature gradients), simplified closed form calculations are independently performed to demonstrate that a physical interference will not develop between the overpack and the MPC canister, and between the MPC canister and the fuel basket due to unconstrained thermal expansion of each component during normal conditions of transport. To assess this in the most conservative manner, the thermal solutions computed in Chapter 3 are surveyed for the following information.

- The radial temperature distribution in each of the fuel baskets at the location of peak center metal temperature.
- The highest and lowest mean temperatures of the canister shell for the hot environment condition.

- The inner and outer surface temperature of the overpack shell (inner shell, intermediate shells, neutron shield, and outer closure) at the location of highest and lowest surface temperature (which will produce the lowest mean temperature).

The thermal evaluation is performed in Chapter 3. Tables 3.4.17 and 3.4.18 present the resulting temperatures used in the deflection evaluation.

Using the temperature information in the above-mentioned tables, simplified thermoelastic solutions of equivalent axisymmetric problems are used to obtain conservative estimates of gap closures. The following procedure, which conservatively neglects axial variations in temperature distribution, is utilized.

1. Use the surface temperature information for the fuel basket to define a parabolic distribution in the fuel basket that bounds (from above) the actual temperature distribution. Using this result, generate a conservatively high estimate of the radial and axial growth of the different fuel baskets using classical closed form solutions for thermoelastic deformation in cylindrical bodies.
2. Use the temperatures obtained for the canister to predict an estimate of the radial and axial growth of the canister to check the canister-to-basket gaps.
3. Use the temperatures obtained for the canister to predict an estimate of the radial and axial growth of the canister to check the canister-to-overpack gaps.
4. Use the overpack surface temperatures to construct a logarithmic temperature distribution (characteristic of a thick walled cylinder) at the location used for canister thermal growth calculations; and use this distribution to predict an estimate of overpack radial and axial growth.
5. For given initial clearances, compute the operating clearances.

The results are summarized in the tables given below for normal conditions of transport.

THERMOELASTIC DISPLACEMENTS IN THE MPC AND OVERPACK UNDER HOT TEMPERATURE ENVIRONMENT CONDITION				
CANISTER - FUEL BASKET				
	Radial Direction (in.)		Axial Direction (in.)	
Unit	Initial Clearance	Final Gap	Initial Clearance	Final Gap
All PWR MPCs	0.1875	0.101	2.0	1.57
MPC-68	0.1875	0.104	2.0 (min)	1.586 (min)
CANISTER - OVERPACK				
	Radial Direction (in.)		Axial Direction (in.)	
Unit	Initial Clearance	Final Gap	Initial Clearance	Final Gap
All PWR MPCs	0.09375	0.058	0.625	0.422
MPC-68	0.09375	0.059	0.625	0.429

It can be verified by referring to the Design Drawings provided in Section 1.4 of this report, and the foregoing table, that the clearances between the MPC basket and canister structure, as well as those between the MPC shell and overpack inside surface, are sufficient to preclude a temperature induced interference from the thermal expansions listed above.

It is concluded that the HI-STAR 100 package meets the requirement that there be no restraint of free thermal expansion in any of the constituent components (i.e, the fuel basket, the enclosure vessel, and the overpack structure).

#### 2.6.1.3 Stress Calculations

In this subsection, the normal conditions of transport associated with the thermal environment designated as "Heat" are considered. The stresses due to the combined effect of pressure, mechanical loads, and thermal gradient are evaluated. Within this subsection, the effects of fatigue and structure elastic/plastic stability under compression and lateral loading are also considered. Included in the subsection is a complete description of the finite element models developed to assess package performance under various loads. A two-dimensional finite element model of the fuel basket and the MPC enclosure shell is developed to evaluate the effect of pressure, radial temperature gradients and lateral deceleration induced inertia loads. A three-dimensional model of the overpack is also developed in this section to assess performance of the overpack under all load

cases. Since both of these finite element models are used again in Section 2.7, where hypothetical accident conditions of transport are examined, the explanation of the features of the model is presented herein in a general manner. Included in this description of the features of the model is a discussion of the loads applied, how they are chosen, and the methodology used to insure satisfaction of equilibrium. Where the loads, assumptions, geometry, etc. are common to both normal conditions of transport analyses and to hypothetical accident conditions of transport, the detailed description is presented in this section. Where the descriptions and discussions are relevant only for the hypothetical accident condition of transport, the detailed descriptions required for full understanding of the analysis are presented in Section 2.7.

This subsection presents the methodology for calculation of the stresses in the different components of the HI-STAR 100 Package from the load cases assembled in Section 2.1. Where the results are finite element based the methodology and the model is described in detail in this section. Results of finite element stress analyses are used for the comparison with allowable stresses performed in Subsection 2.6.1.4. Loading cases for the MPC fuel basket, the MPC enclosure vessel, and the HI-STAR 100 storage overpack are listed in Tables 2.1.6 through 2.1.8, respectively, for normal conditions of transport. An abbreviated description of each of the analyses is presented in the body of the chapter.

In general, as required by Regulatory Guide 7.9, the comparison of the calculated stresses with their corresponding allowables is presented in Subsection 2.6.1.4. However, for clarity in the narrative in this subsection (2.6.1.3), unnumbered summary tables are presented within the text. The key stress comparisons are subsequently reproduced in numbered tables in Subsection 2.6.1.4 to provide strict compliance with Regulatory Guide 7.9.

For all stress evaluations, the allowable stresses and stress intensities for the various HI-STAR 100 System components are based on bounding high metal temperatures to provide additional conservatism (Table 2.1.21 for the MPC basket and shell, for example). Elastic behavior is assumed for all stress analyses. Elastic analysis is based on the assumption of a linear relationship between stress and strain.

In Section 2.7, the same analytical models described here for normal conditions of transport are used to assess package performance under the hypothetical accident conditions. Therefore, the description of the models provided below is also applicable to the analysis performed in Section 2.7 except as previously noted.

In addition to the loading cases germane to stress evaluations mentioned above, cases pertaining to the elastic stability of the overpack are also considered.

The specific finite element models and component calculations described and reported in this subsection are:

1. MPC stress and stability calculations
2. HI-STAR 100 overpack stress and stability calculations

MPC stress and elastic stability analyses are considered in Subsection 2.6.1.3.1 wherein load cases from Tables 2.1.6 and 2.1.7 appropriate to normal conditions of transport are considered. The following analyses for the MPC are performed:

- a. Finite element analysis of the MPC fuel basket and MPC helium retention shell under lateral loads from handling loads during normal transport.
- b. Finite element and analytical analysis of the helium retention vessel (enclosure vessel) as an ASME Code pressure vessel.
- c. Analysis of the fuel support spacers under longitudinal inertia compression load appropriate to normal conditions of transport.
- d. Elastic stability and yielding of the MPC enclosure shell under axial and lateral loads arising from normal handling and external pressure.

Overpack stress and elastic stability analyses are considered in Subsection 2.6.1.3.2. Load cases from Table 2.1.8 are considered. The following analyses are performed to establish the structural adequacy of the overpack:

- a. Three-dimensional finite element analysis of the overpack subjected to load cases listed in Table 2.1.8 for normal conditions of transport.
- b. Consideration of fabrication stresses.
- c. Structural analysis of the closure bolting for normal condition of transport.
- d. Stress Analysis of overpack enclosure shell and return.

#### 2.6.1.3.1 MPC Stress Calculations

The structural function of the MPC in the transport mode is stated in Section 2.1. The calculations presented here demonstrate the ability of the MPC to perform its structural function. Analyses are performed for each of the MPC designs. The following subsections describe the model, individual loads, load combinations, and analysis procedures applicable to the MPC.

##### 2.6.1.3.1.1 Analysis of Load Cases F2 (Table 2.1.6) and E2, and E4 (Table 2.1.7)

The load cases considered herein pertain to lateral loading on the MPC components, namely the fuel basket and the enclosure vessel. For this purpose, a finite element model of the MPC is necessary. During normal conditions of transport, a bounding handling load is simulated by applying a deceleration induced inertia load from a 1' drop with impact limiters installed. During hypothetical accident conditions (see Section 2.7), the MPC is subject to the design basis decelerations from a 30' drop. The finite element model used to simulate both load cases is described here and is used for analyses for normal conditions of transport and later in Section 2.7 is used for the hypothetical accident analyses.

- Description of Finite Element Models of the MPCs under Lateral Loading

A finite element model of each MPC is used to assess the effects of normal and accident conditions of transport. The models are constructed using ANSYS [2.6.4], and they are identical to the models used in HI-STAR's 10CFR72 submittal under Docket Number 72-1008. The following model description is common to all MPCs.

The MPC structural model is two-dimensional. It represents a one-inch long cross section of the fuel basket and the MPC canister.

The MPC model includes the fuel basket, the basket support structures, and the MPC shell. A basket support is defined as any structural member that is welded to the inside surface of the MPC shell. A portion of the overpack inner surface is modeled to provide the correct boundary conditions for the MPC. Figures 2.6.3 through 2.6.11 show the MPC models.

The fuel basket support structure shown in the figures here, and in the design drawings in Section 1.4, is a multi-plate structure consisting of solid shims or support members having two separate compressive load supporting members. For conservatism in the finite element model some dual path compression members are simulated as single columns. Therefore, the calculated stress intensities in the fuel basket supports from the finite element solution are conservatively overestimated in some locations. Independent strength of materials calculations for the fuel basket supports (including the standard and optional constructions for the MPC-32 and MPC-68) have also been performed in [2.6.5] to demonstrate that their load bearing members and their attachment welds meet the applicable ASME code stress limits.

The ANSYS model is not intended to resolve the detailed stress distributions in weld areas. Individual welds are not included in the finite element model.

No credit is taken for any load support offered by the neutron absorber panels, sheathing, and the optional aluminum heat conduction elements. Therefore, these so-called non-structural members are not represented in the model. The bounding MPC weight used, however, does include the mass contributions of these non-structural components.

The model is built using five ANSYS element types: BEAM3, PLANE82, CONTAC12, CONTAC26, and COMBIN14. The fuel basket and MPC shell are modeled entirely with two-dimensional beam elements (BEAM3). Plate-type basket supports are also modeled with BEAM3 elements. Eight-noded plane elements (PLANE82) are used for the solid-type basket supports. The gaps between the fuel basket and the basket supports are represented by two-dimensional point-to-point contact elements (CONTAC12). Contact between the MPC shell and the overpack is modeled using two-dimensional point-to-ground contact elements (CONTAC26) with an appropriate clearance gap.

For each MPC type, three variations of the finite element model were prepared. The basic model includes only the fuel basket and the enclosure shell (Figures 2.6.3 through 2.6.5 show representative configurations) and is used only to study the free thermal expansion due to the

temperature field developed in the system. The other two models include a representation of the overpack and are used for the two drop cases considered. Two orientations of the deceleration vector are considered. The 0-degree drop model includes the overpack-MPC interface in the basket orientation illustrated in Figures 2.6.6 through 2.6.8. The 45-degree drop model represents the overpack interface with the basket oriented in the manner shown in Figures 2.6.9 through 2.6.11. Table 2.6.1 lists the element types and number of elements for all three models for all fuel storage MPC types.

A contact surface is provided in the models used for drop analyses to represent the overpack inner shell. As the MPC makes contact with the overpack, the MPC shell deforms to mate with the inside surface of the inner shell. The nodes that define the elements representing the fuel basket and the MPC shell are located along the centerline of the plate material. As a result, the line of nodes that forms the perimeter of the MPC shell is inset from the real boundary by a distance that is equal to half of the shell thickness. In order to maintain the specified MPC shell/overpack gap dimension, the radius of the overpack inner shell is decreased by an equal amount in the model.

Contact is simulated using two-dimensional point-to-ground elements (CONTAC26). The surface is tangent to the MPC shell at the initial point of impact and extends approximately 135 degrees on both sides. This is sufficient to capture the full extent of contact between the MPC and the overpack.

The three discrete components of the HI-STAR System, namely the fuel basket, the MPC shell, and the overpack, are engineered with small diametral clearances that are large enough to permit unconstrained thermal expansion of the three components under the rated (maximum) heat duty condition. A small diametral gap under ambient conditions is also necessary to assemble the system without physical interference between the contiguous surfaces of the three components. The required gap to ensure unrestricted thermal expansion between the basket and the MPC shell is less than 0.1 inch. This gap, too, will decrease under maximum heat load conditions, but will introduce a physical nonlinearity in the structural events involving lateral loadings (such as side drop of the system) under ambient conditions. It is evident from the system design drawings that the fuel basket, which is non-radially symmetric, is in proximate contact with the MPC shell at a discrete number of locations along the circumferences. At these locations, the MPC shell, backed by the massive overpack weldment, provides a virtually rigid support line to the fuel basket during lateral drop events. Because the fuel basket, the MPC shell, and the overpack are all three-dimensional structural weldments, their inter-body clearances may be somewhat uneven at different azimuthal locations. As the lateral loading is increased, clearances close at the support locations, resulting in the activation of the support from the overpack.

The bending stresses in the basket and the MPC shell at low lateral loading levels, which are too small to close the support location clearances, are secondary stresses since further increase in the loading will activate the overpack's support action, mitigating further increase in the stress. Therefore, to compute primary stresses in the basket and the MPC shell under lateral drop events, the gaps should be assumed to be closed. However, for conservatism, it is assumed that an initial gap of 0.1875" exists, in the direction of the applied deceleration, at all support locations between the basket and the shell, and the diametral gap between the shell and the overpack at the support locations is 3/32". All stresses produced by the applied loading on this configuration are compared

with primary stress levels even though the self-limiting stresses should be considered secondary in the strict definition of the ASME Code. Therefore, many of the reported safety factors for conditions of normal transport are conservative in that secondary stress allowables are ignored in the computation of safety factors. Similarly, in Section 2.7, the safety factors reported for the hypothetical accident conditions will also be conservative since the secondary stress is contained in the result.

- Description of Individual Loads and Boundary Conditions Applied to the MPCs

The method of applying each individual load to the MPC model is described in this subsection. The individual loads and the load combinations are shown in Tables 2.1.6 and 2.1.7. As an example, a free-body diagram of the MPC-68 corresponding to each individual load is given in Figures 2.6.12 through 2.6.14. In the following discussion, reference to vertical and horizontal orientations is made. Vertical refers to the direction along the cask axis, and horizontal refers to a radial direction.

Quasi-static structural analysis methods are used. The effect of any dynamic load factors (DLFs) is included in the final evaluation of safety factors. All analyses are carried out using the design basis decelerations in Table 2.1.10.

The MPC models used for side drop evaluations are shown in Figures 2.6.6 through 2.6.11. In each model, the fuel basket and the enclosure vessel are constrained to move only in the direction that is parallel to the acceleration vector. The overpack inner shell, which is defined by three nodes needed to represent the contact surface, is fixed in all degrees of freedom. The fuel basket, enclosure vessel, and overpack inner shell are all connected at one location by linear springs (see Figure 2.6.6, for example).

(a) Accelerations (Load Case F2 (Table 2.1.6) and E2 (Table 2.1.7))

During a side impact event, the stored fuel is directly supported by the cell walls in the fuel basket. Depending on the orientation of the drop, 0 or 45 degrees (see Figures 2.1.3 and 2.1.4), either one or two walls support the fuel. The effect of deceleration on the fuel basket and canister metal structure is accounted for by amplifying the gravity field in the appropriate direction. In the finite element model this load is introduced by applying a uniformly distributed pressure over the full span of the supporting walls. Figure 2.6.15 shows the pressure load on a typical cell for both the 0 degree and the 45 degree drop cases. The magnitude of the pressure is determined by the weight of the fuel assembly (Table 1.2.13), the axial length of the fuel basket support structure, the width of the cell wall, and the impact acceleration. It is assumed that the load is evenly distributed along an axial length of basket equal to the fuel basket support structure. For example, the pressure applied to an impacted cell wall during a 0-degree side drop event is calculated as follows:

$$p = \frac{a_v W}{L \ell}$$

where:

p = pressure

$a_v$  = ratio of the impact acceleration to the gravitational acceleration

$W$  = weight of a stored fuel assembly

$L$  = axial length of the fuel basket support structure

$t$  = width of a cell wall

For the case of a 45-degree side drop the pressure on any cell wall equals  $p$  (defined above) divided by the square root of two. Figures 2.6.13, 2.6.14, and 2.6.15 show the details of the fuel assembly pressure load on the fuel basket.

(b) Internal/External Pressure (Load Case E1 (Table 2.1.7))

Design internal pressure in the MPC model is applied by specifying pressure on the inside surface of the enclosure vessel. The magnitude of the internal pressure applied to the model is taken from Table 2.1.1.

For this load condition, the center of the fuel basket is fixed in all degrees of freedom.

(c) Temperature (Load Cases F1 (Table 2.1.6) and E4 (Table 2.1.7))

Temperature distributions are developed in Chapter 3 and applied as nodal temperatures to the finite element model of the MPC enclosure vessel (confinement boundary). Maximum design heat load has been used to develop the temperature distribution used to demonstrate compliance with ASME Code stress intensity levels. A plot of the applied temperature distribution as a function of radius is shown in Figure 2.6.1. Figure 2.6.12 shows the MPC-68 with the typical boundary conditions for all thermal and pressure load cases.

- Analysis Procedure

The analysis procedure for this set of load cases is as follows:

1. The stress intensity and deformation field due to the combined loads is determined by the finite element solution. Results are then subject to post-processing.
2. The results for each load combination are compared to allowables. The comparison with allowable values is made in Subsection 2.6.1.4.

2.6.1.3.1.2 Analysis of Load Cases E1.a and E1.c (Table 2.1.7)

Load Cases E1.a and E1.c pertain to the performance of the helium retention boundary structure (enclosure vessel) considered as an ASME Section III, Subsection NB pressure vessel.

Since the MPC shell is a pressure vessel, the classical Lamé's calculations should be performed to

demonstrate the shell's performance as a pressure vessel. Note that dead load has an insignificant effect on this stress state. Calculations for the shell under internal pressure are performed initially. Subsequently, a finite element analysis on the entire helium retention boundary as a pressure vessel subject to both internal pressure and temperature gradients is performed. Finally, confirmatory hand calculations are performed to gain confidence in the finite element predictions,

- **Lame's Solution for the MPC Shell**

The stress from internal pressure is found using classical formulas:

Define the following quantities:

P = pressure, r = MPC radius, and t = shell thickness.

Using classical thin shell theory, the circumferential stress,  $\sigma_1 = Pr/t$ , the axial stress  $\sigma_2 = Pr/2t$ , and the radial stress  $\sigma_3 = -P$  are computed for both normal and accident internal pressures. The results are given in the following table:

Classical Shell Theory Results for Normal and Accident Internal Pressures				
Item	$\sigma_1$ (psi)	$\sigma_2$ (psi)	$\sigma_3$ (psi)	$\sigma_1 - \sigma_3$ (psi)
P= 100 psi	6,838	3,419	-100	6,938
P= 200 psi	13,677	6,838	-200	13,877

Table 2.1.21 provides the allowable membrane stress for Load Case E1 for Alloy X under normal conditions of transport. It is seen that a safety factor greater than 1.0 exists

$$FS = \frac{18.1 \text{ ksi}}{6.938 \text{ ksi}} = 2.6$$

Subsection 2.7.3.3.1 develops the corresponding safety factor for the case of accident pressure.

- **Finite Element Analysis (Load Case E1.a and E1.c of Table 2.1.7)**

Having performed the classical "thin shell under pressure" evaluation, a finite element analysis is performed where the interaction between the end closures and the MPC shell is rigorously modeled.

The MPC shell, the top lid, and the baseplate together form the helium retention boundary (enclosure vessel) for storage of spent nuclear fuel. In this section, the operating condition consisting of dead weight, internal pressure, and thermal effects for the normal heat condition of transport is evaluated. The top and bottom plates of the MPC enclosure vessel (EV) are modeled using plane axisymmetric elements, while the shell is modeled using the axisymmetric thin shell element. The thickness of the top lid varies in the MPC types and can be either a single thick lid, or two lids, welded around their common periphery; the minimum thickness top lid is modeled in the finite element analysis. As

applicable, the results for the MPC top lid are modified to account for the fact that in the dual lid configuration, the two lids act independently under mechanical loading. The temperature distributions for all MPC constructions are nearly identical in magnitude and gradient. Temperature differences across the thickness of both the baseplate and the top lid exist during HI-STAR 100's operations. There is also a thermal gradient from the center of the top lid and baseplate out to the shell wall. The metal temperature profile is essentially parabolic from the centerline of the MPC out to the MPC shell. There is also a parabolic temperature profile along the length of the MPC canister. Figure 2.6.20 shows a sketch of the confinement boundary structure with identifiers A-I (also called locating points) where temperature input data is used to represent a continuous temperature distribution for analysis purposes. The overall dimensions of the confinement boundary are also shown in the figure.

Section 3.4 provides the desired temperatures for thermal stress analysis of the helium retention boundary. From the tables (3.4.22 and 3.4.23), it is seen that the distribution from PWRs provides the largest temperature gradients in the baseplate (from centerline to outer edge) and in the shell (from the joint at the baseplate to the half-height of the cask). It will be shown later that stress intensities are greatest in these components of the vessel. Because of the intimate contact between the two lid plates when the MPC lid is a two-piece unit, there is no significant thermal discontinuity through the thickness; thermal stresses arising in the MPC top lid will be bounding when there is only a single lid. Therefore, for thermal stresses, results from the analysis that considers the lid as a one-piece unit are used and are amplified to reflect the increase in stress in the dual lid configuration

Figure 2.6.21 shows details of the finite element model of the top lid (considered as a single piece), canister shell, and baseplate. The top lid is modeled with 40 axisymmetric quadrilateral elements; the weld connecting the lid to the shell is modeled by a single element solely to capture the effect of the top lid attachment to the canister offset from the middle surface of the top lid. The MPC canister is modeled by 50 axisymmetric shell elements, with 20 elements concentrated in a short length of shell appropriate to capture the so-called "bending boundary layer" at both the top and bottom ends of the canister. The remaining 10 shell elements model the MPC canister structure away from the shell ends in the region where stress gradients are lower (from the physics of the problem). The baseplate is modeled by 20 axisymmetric quadrilateral elements. Deformation compatibility at the connections is enforced at the top by the single weld element, and deformation and rotation compatibility at the bottom by additional shell elements between nodes 106-107 and 107-108.

The geometry of the model is listed below (terms are defined in Figure 2.6.21):

$H_t =$	9.5" (the minimum total thickness lid is assumed)
$R_L =$	0.5 x 67.25" (Nominal dimension used for calculation)
$L_{MPC} =$	190.5" (Nominal dimension used for calculation)
$t_s =$	0.5" (MPC drawing in Section 1.4)
$R_S =$	0.5 x 68.375" (Nominal radius)

$$t_{BP} = 2.5" \text{ (MPC drawing in Section 1.4)}$$

$$\beta L = 2\sqrt{R_s t_s} \approx 12" \text{ (The bending boundary layer)}$$

Stress analyses are carried out for two cases as follows:

- a. internal pressure = 100 psi
- b. internal pressure = 100 psi, plus applied temperature field

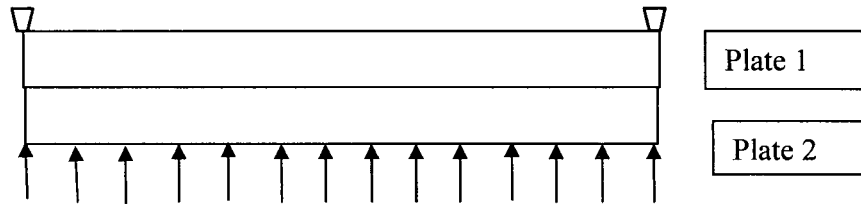
The dead weight of the top lid reduces the stresses due to pressure. For example, the equivalent pressure simulating the effect of the weight of the top lid is an external pressure of 3 psi, which reduces the pressure difference across the top lid to 97 psi. Thus, for conservatism, dead weight of the top lid is neglected to provide additional conservatism in the results. The dead weight of the baseplate, however, adds approximately 0.73 psi to the effective internal pressure acting on the base. The effect of dead weight is still insignificant compared to the 100 psi design pressure, and is therefore neglected. The thermal loading in the confinement vessel is obtained by developing a parabolic temperature profile to the entire length of the MPC canister and to the top lid and baseplate. The temperature data provided at locations A-I in Figures 2.6.20 and 2.6.21 are sufficient to establish the profiles. Through-thickness temperatures are assumed linearly interpolated between top and bottom surfaces of the top lid and baseplate. All material properties and expansion coefficients are considered to be temperature-dependent in the model.

Results for stress intensity are reported for the case of internal pressure alone and for the combined loading of pressure plus temperature (Load Case E1.c in Table 2.1.7). Tables 2.6.6 and 2.6.7 report results at the inside and outside surfaces of the top lid and baseplate at the centerline and at the extreme radius. Canister results are reported in the "bending boundary layer" and at a location near mid-length of the MPC canister. In the tables, the calculated value is the value from the finite element analysis, the categories are  $P_m$  = primary membrane;  $P_L + P_b$  = local membrane plus primary bending; and  $P_L + P_b + Q$  = primary plus secondary stress intensity. The allowable stress intensity value is obtained from the appropriate table in Section 2.1 for Level A conditions, and the safety factor SF is defined as the allowable strength divided by the calculated value. Allowable stresses for Alloy X are taken at 300° F, which bounds the normal heat condition of transport temperatures everywhere except at the mid-length position of the MPC shell (Location I in Figure 2.6.20) during the normal operation. At Location I, the allowable strength is taken at 400°F. The results given in Tables 2.6.6 and 2.6.7 demonstrate the ruggedness of the MPC as a confinement boundary. Since mechanically induced stresses in the top lid are increased when a dual lid configuration is considered, the stress results obtained from an analysis of a single top lid must be corrected to reflect the maximum stress state when a dual lid configuration is considered. The modifications required are based on the following logic:

Consider the case of a simply supported circular plate of thickness  $h$  under uniform lateral pressure "q". Classical strength of materials provides the solution for the maximum stress, which occurs at the center of the plate, in the form:

$$\sigma_s = 1.225q(a/h)^2 \quad \text{where } a \text{ is the radius of the plate and } h \text{ is the plate thickness.}$$

Now consider the MPC simply supported top lid as fabricated from two plates “1” and “2”, of thickness  $h_1$  and  $h_2$ , respectively, where the lower surface of plate 2 is subjected to the internal pressure “ $q$ ”, the upper surface of plate 1 is the outer surface of the helium retention boundary, and the lower surface of plate 1 and the upper surface of plate 2 are in contact. The following sketch shows the dual lid configuration for the purposes of this discussion:



From classical plate theory, if it is assumed that the interface pressure between the two plates is uniform and that both plates deform to the same central deflection, then if

$$h_1+h_2 = h, \text{ and if } h_2/h_1=r$$

the following relations exist between the maximum stress in the two individual plates,  $\sigma_1$ ,  $\sigma_2$  and the maximum stress  $\sigma_s$  in the single plate of thickness “ $h$ ”:

$$\frac{\sigma_1}{\sigma_s} = \frac{(1+r)^2}{(1+r^3)} \qquad \frac{\sigma_2}{\sigma_s} = \frac{(1+r)^2}{(1+r^3)} r$$

Since the two lid thicknesses are the same in the dual lid configuration,  $r = 1.0$  so that the stresses in plates 1 and 2 are both two times larger than the maximum stress computed for the single plate lid having the same total thickness. In Tables 2.6.6 and 2.6.7, bounding results for the dual lid configuration are reported by using these ratios at all locations in the top lid.

The preceding analysis for the dual lid configuration assumes that both lids are made from the same material (i.e., Alloy X). Per the licensing drawings in Section 1.4, there is an option for the bottom lid to be fabricated from carbon steel (covered or coated with stainless steel) in lieu of Alloy X. However, since carbon steel has a higher yield strength and Young’s modulus than Alloy X, all stress calculations for the MPC split lid conservatively assume that the bottom lid is made from the weaker of the two material options (i.e., Alloy X).

- Confirmatory Closed Form Solution

The results in Table 2.6.6 and 2.6.7 also show that the baseplate and the shell connection to the baseplate are the most highly stressed regions under the action of internal pressure. To confirm the

finite element results, an alternate closed form solution is performed using classical plate and shell theory equations that are listed in or developed from the reference Timoshenko and Woinowsky-Krieger, Theory of Plate and Shells, McGraw Hill, Third Edition.

Assuming that the thick baseplate receives little support against rotation from the thin shell, the bending stress at the centerline is evaluated by considering a simply supported plate of radius  $a$ , and thickness  $h$ , subjected to lateral pressure  $p$ . The maximum bending stress is given by

$$\sigma = \frac{3(3 + \nu)}{8} p \left( \frac{a}{h} \right)^2$$

where:

$$a = .5 \times 68.375''$$

$$h = 2.5''$$

$$\nu = 0.3 \text{ (Poisson's Ratio)}$$

$$p = 100 \text{ psi}$$

Calculating the stress in the plate gives  $\sigma = 23,142$  psi.

Now consider the thin MPC shell ( $t = 0.5''$ ) and first assume that the baseplate provides a clamped support to the shell. Under this condition, the bending stress in the thin shell at the connection to the plate is given as:

$$\sigma_{Bp} = 3 p \frac{a}{t} \frac{(1 - \nu/2)}{\sqrt{3(1 - \nu^2)}^{1/2}} = 10,553 \text{ psi}$$

In addition to this stress, there is a component of stress in the shell due to the baseplate rotation that causes the shell to rotate. The joint rotation is essentially driven by the behavior of the baseplate as a simply supported plate; the shell offers little resistance because of the disparity in thickness and will essentially follow the rotation of the thick plate.

Using formulas from thin shell theory, the additional axial bending stress in the shell due to this rotation  $\theta$  can be written in the form

$$\sigma_{B\theta} = 12 \beta D_s \frac{\theta}{t^2}$$

where

$$\theta = \frac{pa^3}{8D(1+\nu)} * \left( \frac{1}{1+\alpha} \right)$$

and

$$D = \frac{E h^3}{12(1-\nu^2)} \quad E = \text{plate Young's Modulus}$$

and

$$\alpha = \frac{2\beta a t^3}{h^3(1+\nu)}$$

$$\beta^2 = \sqrt{3(1-\nu^2)} / a t$$

$$D_s = \frac{E t^3}{12(1-\nu^2)}$$

Substituting the numerical values gives

$$\sigma_{B\_} = 40,563 \text{ psi}$$

Note that the approximate solution is independent of the value chosen for Young's Modulus as long as the material properties for the plate and shell are the same.

Combining the two contributions to the shell bending stress gives the total extreme fiber stress in the longitudinal direction as 51,116 psi. Note that the same confirmatory solution can be obtained from Roark's Formulas for Stress and Strain, McGraw-Hill, 4th Edition, Table XIII. Case 30 in that text contains the solution for the bending moment at the intersection of a long cylinder and a flat plate due to internal pressures. Using the handbook formula, 53,090 psi is obtained.

The baseplate stress value, 23,142 psi, compares well with the finite element result 20,528 psi (Table 2.6.6). The shell joint stress, 51,116 psi, is greater than the finite element result (43,986 psi in Table 2.6.6). This is due to the local effects of the shell-to-baseplate connection offset. That is, the connection between shell and baseplate in the finite element model is at the surface of the baseplate, not at the middle surface of the baseplate. This offset will cause an additional bending moment that will reduce the rotation of the plate and hence, reduce the stress in the shell due to the rotation of the baseplate.

In summary, the approximate closed form solution confirms the accuracy of the finite element analysis in the MPC baseplate region.

#### 2.6.1.3.1.3 Supplementary MPC Calculations

The MPC has been subject to extensive analysis in the companion HI-STAR 100 FSAR (storage) submittal (Docket Number 72-1008). For completeness, certain information from the FSAR has been repeated here and in Section 2.7 where the results are germane to normal conditions of transport and to hypothetical accident conditions of transport, respectively. Because of the different requirements for storage and transport submittals, some of the results presented here may not be directly associated with a load case defined in Tables 2.1.6 and 2.1.7. Nevertheless, their inclusion here is warranted for completeness. In this subsection, results are summarized from these analyses that pertain to normal conditions of transport. In Section 2.7, additional results pertaining to the hypothetical accident conditions of transport are reported.

- Structural Analysis of the Fuel Support Spacers (Load Case F2)

Upper and lower fuel support spacers are utilized to position the active fuel region of the spent nuclear fuel within the poisoned region of the fuel basket. It is necessary to ensure that the spacers will continue to maintain their structural integrity during normal conditions of transport. Ensuring structural integrity implies that the spacer will not buckle under the maximum compressive load, and that the maximum compressive stress will not exceed the compressive strength of the spacer material (Alloy X). Detailed calculations demonstrate that large structural margins in the fuel spacers are available for the entire range of spacer lengths that may be used in HI-STAR 100 applications (for the various acceptable fuel types). The fuel spacers are shown to meet ASME Code Subsection NG stress limits (the spacers are not, however, required to be designed to any ASME Code, however). Standard Code design formulas are used to evaluate elastic stability limits. For normal conditions of transport (Level A Service Condition), a 10g deceleration load is applied and stress and stability issues are considered. The results are summarized below:

Fuel Spacers - Minimum Safety Factors (Load Cases F2)			
Item	Load (lb.)	Capacity (lb.)	Safety Factor
PWR Fuel Spacer - 10 g Axial Load	16,800	46,200	2.75
BWR Fuel Spacer - 10g Axial Load	7,000	19,250	2.75

The safety factor is greater than 1.0, which demonstrates that the fuel spacers meet the requirements of Level A Service Conditions for the normal condition of transport.

The above results are determined based on the original design of the fuel spacers, which consists of a length of square tubing welded between top and bottom end plates. Per the licensing drawing, the lower fuel spacers may also be fabricated using I-beams instead of square tubing. Since the cross-sectional area and moment of inertia of the specified I-beam are greater than the section properties of the square tubing, the above analysis bounds both options.

The above result also represents a conservative minimum safety factor for the Trojan failed fuel can (FFC) spacer under normal conditions of transport. The reasons are (i) the FFC spacer has the same cross sectional area as the PWR lower fuel spacer and (ii) the FFC spacer supports less

weight than the PWR lower fuel spacer. Whereas the PWR lower fuel spacer is designed and licensed to support the design fuel assembly weight of 1680 lb, the maximum weight that the FFC spacer supports is somewhat less than 1680 lb since the total weight of the Trojan FFC plus its contents, which includes the FFC spacer, is restricted to 1680 lb.

- MPC Shell Stability

The MPC shell is examined for elastic/plastic instability due to external pressure or compressive loads introduced as part of the load cases (design external pressure, normal transport). Each load component is examined separately. Design external pressure is applied to the outer surface of the enclosure vessel shell in the MPC model. The magnitude of the external pressure applied to the model is taken from Table 2.1.1. Analysis of the MPC under external pressure is performed using the methodology of ASME Code Case N-284 [2.1.8]. The following stability evaluations are performed for the MPC shell for normal transport conditions:

- Normal Transport Deceleration Load from 10CFR71.45(b).
- Design external pressure plus a 1g compressive dead load.

The following table summarizes the limiting result from the calculations:

MPC Shell - Elastic/Plastic Stability (ASME Code Case N-284) - Minimum Safety Factors			
Item	Value	Allowable	Safety Factor
Load Case 10CFR71.45(b) (Yield)	0.193	2.0	10.36
Load Case E1.b - Table 2.1.7 (Stability Interaction Curve)	0.832	1.0	1.20

Note that for the load case associated with the 10CFR71.45(b) requirement, the yield strength criteria in the Code Case N-284 method governs the “allowable” value. In this event, the safety factor 2.0, built into the Code Case, is included in the tabular result in order to obtain the actual safety factor with respect to the yield strength of the material.

The results demonstrate that the MPC shell meets the requirements of Code Case N-284. Note that the stability results presented above are very conservative. The stability analyses carried out for the MPC shell assumed no axial stiffening from the fuel basket supports that run the full length of the shell. An analysis that included the effect of the stiffening (and therefore, recognized the fact that instability will most likely occur between stiffeners) will give increased safety factors for Load Case E1.b.

#### 2.6.1.3.2 Overpack Stress Calculations

The structural functions of the overpack are stated in Section 2.1. The analyses documented here demonstrate the ability of components of the HI-STAR 100 overpack to perform their structural functions under normal conditions of transport. Load cases applicable to the structural evaluation of

the HI-STAR 100 overpack under these conditions are compiled in Table 2.1.8.

In this subsection, stresses and stress intensities in the HI-STAR 100 overpack due to the combined effects of thermal gradients, pressure, and mechanical loads are presented. The results are obtained from a series of finite element analyses on the complete overpack and separate analyses on overpack components.

#### 2.6.1.3.2.1 Finite Element Analysis - Load Cases 1 to 4 in Table 2.1.8

Load Case 1 pertains to a demonstration of the containment boundary as an ASME “NB component under Design Pressure and Level A Service Condition thermal loading. Other cases pertain to handling inertia loads imposed during normal conditions of transport and an extreme environmental condition. To analyze these load cases, a suitable finite element model of the complete overpack is required. As noted earlier, since the identical finite element model is used in Section 2.7 to analyze the hypothetical accident conditions of transport, the following discussion refers to both sets of analyses to avoid textual repetition.

- Description of Finite Element Model (Normal Conditions and Hypothetical Accident)

The purpose of the HI-STAR 100 overpack model is to calculate stresses and stress intensities resulting from the loadings defined in Subsection 2.1 and compiled into load cases in Table 2.1.8.

A three-dimensional finite element model of the HI-STAR 100 overpack is used to assess the effects of loads associated with normal conditions of transport. The same finite element model is used in Section 2.7 to evaluate the effects of loading due to hypothetical accident scenarios. The overpack is a large structure subject to a variety of complex loads and boundary conditions. The finite element model developed for this analysis allows efficient determination of the stresses in this complex structure.

The finite element model of the overpack is constructed using ANSYS [2.6.4]. This model is duplicated in the HI-STAR 100 FSAR (10CFR72) submittal for storage.

For structural analysis purposes, the overpack is assumed to be symmetric about a diametral mid-plane. This assumption is reasonable because the purpose of the model is to investigate global stresses in the model. The model is not intended to resolve effects due to small penetrations that produce peak stresses (which are significant only in cyclic fatigue conditions).

Element plots of the model are shown in a series of figures (Figures 2.6.16 through 2.6.19C). Figure 2.6.16 shows an overall view of half of the overpack subject to detailed finite element analysis. The view is directed toward the internal cavity and shows the surface of symmetry. To enforce symmetry, displacements normal to the plane of symmetry at all nodes on the plane of symmetry are not permitted. Out-of-plane rotations at the nodes on the plane of symmetry are also set to zero. The basic building blocks of the finite element model are 20-node brick (SOLID95), 8-node brick (SOLID45), and 6-node tetrahedron elements (SOLID45). These are 3-D solid elements with 3 degrees of freedom at each node (three linear displacement degrees of freedom). Element densities are increased towards the top and bottom of the model in order to provide increased resolution of the

stress fields in those regions.

The top flange/closure plate interface is modeled using linear spring elements (COMBIN14). The concentric seals are not modeled explicitly. The model is not intended to resolve the stress field around the grooves for the seals. The status of joint seal is ascertained by “compression springs” that simulate the O-ring gaskets. Contact between the overpack top flange and closure plate is verified by checking the status of these spring elements. If contact between the closure plate and top flange is maintained under an applied loading (indicated by a compressive load in the “compression springs”), then the integrity of the seal is determined to have been maintained under that load.

The overpack closure bolts are modeled with beam elements (BEAM4). The top of the beam elements represent the bolt head and are connected to the overpack closure plate. The bottom of the elements represents the threaded region of the bolt and is connected to nodes of elements representing the top flange. Torsional displacements of the bolts are suppressed to conform to the degrees of freedom permitted at the nodes of the connecting solid elements.

The inner shell of the overpack is modeled with two solid element layers through the thickness of the shell.

Each of the lifting trunnions is modeled as three rigid beam elements (BEAM4) connected to the top forging. The beams extend from the forging and meet at a single node location. Trunnion stress analysis is documented in Subsection 2.5; the inclusion of the trunnion herein is solely to provide the appropriate offset for handling loads. The beam elements representing the trunnions are not shown on any of the figures describing the finite element model.

The neutron shield material is not a load bearing or supporting component in the finite element model. However, the weight of the neutron shield material must be included in the model in order to obtain the proper inertia loads. The neutron shield material is modeled with SOLID45 elements having a weight density that is specified in Subsection 2.3.2.1. In the model herein, the neutron shield material is included as an element set to ensure that proper accounting of total weight (and accompanying deceleration loads) occurs. Therefore, the neutron shield material must be assigned a Young's Modulus in the model. A value approximately equal to 1% of the Modulus of the steel load carrying components is assigned to the neutron shield material to insure that the neutron shield material serves as a load rather than a structural member in the model.

Figure 2.6.17 shows the finite element grid used for the bottom plate.

Figure 2.6.18 provides the details of the solid element grid for the top forging. Also shown in the figure are the line elements that represent the lid bolts. Since the lid is not shown in this figure, the upper part of the line elements is not attached to any node point.

Figure 2.6.19 shows a view from above of the overpack lid and details the element grid around the 180-degree periphery modeled.

Figure 2.6.19A shows the finite element grid for the inner shell and the five intermediate shells. The inner shell is modeled with two layers of solid elements; each of the five intermediate shells is

modeled by a single layer of solid elements to capture a linear stress distribution through the thickness.

Figure 2.6.19B presents the solid element distribution modeling the Holtite-A material. As noted previously, the structural effect of this material is neglected; the elements are included in the model to insure a proper mass distribution for the different analyses.

Finally, Figure 2.6.19C shows the shell element grid used to model the enclosure shell. Thin shell elements are used to simulate all components of the enclosure shell.

It is recognized that the layered shells of the overpack (shown in Figures 2.6.16 and 2.6.19A) are connected to each other and to the inner shell only at their top and bottom extremities. The finite element model must allow for separation between the intermediate shells in the non-connected regions under certain loading. Likewise, the intermediate shells cannot interpenetrate each other or the inner shell structure. To simulate these competing effects without making the model non-linear because of the introduction of contact elements, radial coupling of adjacent intermediate shell nodes is used in appropriate locations of the model. It is necessary to utilize physical reasoning to establish the regions where a nodal coupling is warranted because the shells cannot separate from each other. For example, radial coupling over two 60-degree spans serves to prevent interpenetration where it may occur during an impact simulation. Similarly, where physical reasoning indicates that a separation between the shell layers may occur, the nodes are left uncoupled. For example, when ovalization of the shells may occur under a specified loading, no coupling between shells is assumed. Figure 2.6.22 illustrates the nodal coupling pattern. The intermediate shell nodes that lie in the 60-degree sector between the top and bottom portions of the model remain uncoupled. The intermediate shells, in the uncoupled region, are free to separate from one another as the overpack cross section ovalizes during side impact. This modeling approach ensures that load transfer in a drop with significant lateral deceleration loads is modeled correctly. With respect to the overpack model, "bottom portion" refers to the 60-degree segment of the model closest to the point of impact. Conversely, "top portion" refers to the 60-degree sector farthest from the point of impact. This nodal coupling arrangement conservatively represents the structural behavior of the intermediate shells. In addition, no axial or circumferential nodal coupling has been used between adjacent intermediate shells. Thus, axial bending stiffness of the composite shell structure is conservatively underestimated. This underestimation of stiffness provides additional conservatism to the predicted values for safety factors.

The rotation trunnions present in the first seven HI-STAR 100 units (see Subsection 2.5) are conservatively neglected in the finite element models. Separate calculations, where applicable, are summarized later.

Elements at locations of welds in the modeled components are assumed to have complete connectivity in all directions. Material in the model located at positions where welds exist is assumed to have material properties identical to the base material.

To summarize, the total number of nodes and elements in the overpack model are 11265 and 8642, respectively. The elements used are SOLID45, SOLID95, BEAM4, SHELL63, and COMBIN14.

For all structural analyses, material properties are obtained from the appropriate tables in Section 2.3. Property data for temperatures that are not listed in the material property tables are obtained by linear interpolation. Property values are not extrapolated beyond the limits of the code for any structural analysis.

- Description of Individual Loads and Boundary Conditions

The method of applying each individual load to the overpack model is described in this subsection. The individual loads are defined in Subsection 2.1.2.1 and are listed in Table 2.1.8 for normal conditions of transport. A free-body diagram of the overpack corresponding to each individual load is given in Figures 2.1.5 through 2.1.14. The figures presented in Section 2.1 present a general description of the loading but are lacking in specific details concerning the extent of the area exposed to the load. Therefore, in this subsection, each of the applied loadings for the various cases considered is further discussed and additional details on the specific application of the loads are provided. In the following discussion, reference to vertical and horizontal orientations is made. Vertical refers to the longitudinal direction along the cask axis, and horizontal refers to a lateral direction.

Quasi-static methods of structural analysis are used. The effects of any dynamic load factors (DLF) are discussed in the final evaluation of safety factors. The load combinations are formed from the solution of individual load cases

- (a) Accelerations (Used to Form Load Cases 3 and 4 in Table 2.1.8)

Table 2.1.10 provides the bounding values of the accelerations used for design basis structural evaluation. The loading is imposed by amplifying the gravity vector by the design basis deceleration. The proper distribution of the body forces induced by the accelerations is internally consistent based on the mass distribution associated with the different components of the finite element model. How these acceleration induced loadings are put in equilibrium with reaction loads from the impact limiters is discussed in detail in a later section.

In the following, appropriate boundary conditions for analyses for load cases associated with normal conditions of transport (Table 2.1.8) are discussed. However, since the same finite element model is used to evaluate hypothetical accident conditions of transport (Table 2.1.9) in Section 2.7, boundary conditions for Section 2.7 analyses are discussed here, as well, in the ongoing interest of conciseness of the presentation.

Boundary conditions for the model are as follows:

- i. End drop - In an end drop, displacement fixities are applied to the model on a cross-section through the top flange that is normal to the drop direction. Figures 2.1.7 and 2.1.8 show the free-body diagram for these load events. No reactions or internal body forces are shown. Further discussion is provided in Section 2.7.

- ii. Side drop - In a side drop, the inertia loads are reacted by the impact limiters. The overpack is in equilibrium with essentially end pinned supports. Figure 2.1.9 shows the configuration for this case. Further elaboration is provided in Section 2.7.

(b) Loads on the Overpack from the MPC

Pressures are applied on the inner surfaces of the overpack model to represent loads from the MPC for the drop loads.

- i. End drop - For a bottom end drop (Load Case1, Hypothetical Accident, Table 2.1.9), the pressure load on the inside surface of the overpack bottom plate is assumed to be uniform and represents the load from the heaviest MPC (Figure 2.1.7). Note that this analysis conservatively assumes that the drop angle is not exactly 90° from the horizontal; attention is focussed on the overpack baseplate subject to the deceleration load from the heaviest MPC (applied as a uniform pressure) without the ameliorating effect of opposing distributed reaction from the impacted surface.

The magnitude of the pressure is the weight of the heaviest fully loaded MPC divided by the area of the faces of the elements over which the pressure is applied. The weight of the heaviest fully loaded MPC is taken from the tables in Section 2.2, and is amplified by the design basis deceleration. Amplified loads from the MPC (weight times 60g acceleration) are applied as a pressure load to the entire inner surface of the bottom plate or the lid depending on the drop orientation. Note that for a top end drop, the MPC inertia loads act only on an outer annulus of the lid due to the raised surface deliberately introduced to act as a “landing” area for the MPC and reduce lid stress and deformation. By neglecting this raised annular area on the lid and applying the MPC load as a uniform pressure, stresses in the lid and the bolts are maximized. Further discussion is provided in Section 2.7.

- ii. Side drop - The shape and extent of the pressure distribution is determined from the results of the structural analysis of the MPC under similar orientations. In the MPC structural analysis, the extent of the support conditions of the MPC shell is determined with contact elements. In the analysis of the MPC under amplified inertia loads, the overpack is represented as a rigid circular surface. Based on results from the MPC evaluations, the loaded region is taken as 72 degrees (measured from the vertical). The MPC load on the overpack model is applied uniformly along the axial length of the inner surface of the model. Further discussion is provided in Section 2.7.
- iii. Oblique drop - Figures 2.1.10 and 2.1.11 show the balance loading applied for the oblique drop. A fixed node is defined away from the assumed impact point to insure that the package is in equilibrium under the applied loads. This drop orientation is only considered for the hypothetical accident evaluation. Therefore, a detailed discussion as to the methodology used to apply the loads and insure overall equilibrium is provided in Section 2.7 (specifically 2.7.1.3 and 2.7.1.4).

(c) Temperature (Used to Form Load Case 05 in Table 3.1.5)

Based on the results of the thermal evaluation for the normal hot environment presented in Chapter 3, a temperature distribution with a bounding gradient is applied to the overpack model. The purpose is to determine the stress intensities that develop in the overpack under the applied thermal load. A plot of the applied temperature distribution as a function of radius is shown in Figure 2.6.2.

The temperature distribution is applied to the ANSYS finite element model at discrete nodes using a parabolic curve fit of the computed distribution.

(d) Internal Pressure (Used to Form Load Cases 1 in Table 2.1.8)

Design internal pressure is applied to the overpack model. All interior overpack surfaces, including the inner shell, the bottom of the closure plate, and the top of the bottom plate are loaded with pressure. The magnitude of the internal pressure applied to the model is taken from Table 2.1.1. Figure 2.1.5 shows the displacement constraints for this load case. Figure 2.6.23 is a finite element grid plot showing the surfaces where internal pressure is applied.

(e) External Pressure (Used to Form Load Case 2 in Table 2.1.8)

Design external pressure is applied to the overpack model. External pressure is applied to the model as a uniform pressure on the outer surface of the model. The magnitude of the external pressure applied to the model is taken from Table 2.1.1. Figure 2.1.6 shows the displacement constraints for this load case. External pressures are imposed in the same manner as shown in Figure 2.6.23 except that the surfaces and magnitude are different.

(f) Bolt Pre-load (Used in all load cases in Tables 2.1.8 and 2.1.9)

The overpack closure bolts are torqued to values predicted to preclude separation. This torque generates a pre-load in the bolts and stresses in the closure plate and top flange in the region adjacent to the bolts. The finite element representation of the bolt elements is shown in Figure 2.6.18. The initial preload of the bolts is applied to the overpack model by applying an initial strain to the beam elements representing the bolts. This induces a tensile stress in each of the bolts and a corresponding compression in the seals (represented by spring elements). This load case is present in every load combination.

(g) Fabrication stresses

Fabrication stresses are conservatively computed for the inner shell and all of the intermediate shells. Fabrication effects are not easily introduced into the finite element model unless compression-only contact elements are used. Since the fabrication stresses are circumferential secondary stresses in the shells, the incorporation of this load case is best accomplished outside of the finite element analysis. Therefore, there is no fabrication load case associated with the finite element analyses.

- Finite Element Analysis Solution Procedure

The analysis procedure is as follows:

1. The stress and deformation field due to each individual load is determined.
2. The results from each individual load case are combined in a postprocessor to create each load case. The load cases analyzed are listed in Table 2.1.8 for normal conditions of transport and in Table 2.1.9 for hypothetical accident conditions of transport.
3. The results for each load case are compared to allowables. The calculated values are compared with allowable values in Subsection 2.6.1.4 for normal conditions of transport and in an appropriate subsection of Section 2.7 for hypothetical accident conditions.

#### 2.6.1.3.2.2 Fabrication Stress

The fabrication stresses originate from welding operations to affix the intermediate shells in position. As the molten weld metal solidifies, it shrinks pulling the two parts of the shells together. Adjacent points at the weld location will close together after welding by an amount " $\delta$ " which is a complex function of the root opening, shape of the bevel, type of weld process, etc. The residual stresses generated by the welding process are largely confined to the weld metal and the "heat affected zone". The ASME Code recognizes the presence of residual stresses in the welds, but does not require their calculation. The Code also seeks to minimize fabrication stresses in the welds through controlled weld procedures. Nevertheless, fabrication stresses cannot be eliminated completely.

The computation of fabrication stresses is carried out to comply with the provisions of Regulatory Guide 7.8, Article C-1.5. The Regulatory Guide requires that "Fabrication and installation stresses in evaluating transportation loadings should be consistent with the joining, forming, fitting, and aligning processes employed during the construction of casks...the phrase fabrication stresses includes the stresses caused by interference fits and the shrinkage of bonded lead shielding during solidification but does not include the residual stresses due to plate formation, welding, etc."

A literal interpretation of the above-cited Regulatory Guide text exempts the HI-STAR 100 designer from computing the stresses in the containment and intermediate shells due to welding. However, in the interest of conservatism, an upper bound, on the stresses induced in the containment shell and in the intermediate shells, is computed for the fabrication process.

To calculate the so-called fabrication stresses, it is recalled that in affixing the intermediate shells to the cask body, the design objective does not call for a definite radial surface pressure between the layers. Rather, the objective is to ensure that the shells are not loosely installed. Fortunately, extensive experience in fabricating multi-layer shells has been acquired by the industry over the past half-century. The technology that was developed and has matured for fabrication in older industries (such as oil and chemical) is used in HI-STAR 100 fabrication of the multi-layered shells. Mock-up tests on carbon steel coupons indicate that the total shrinkage after welding can range from 0.010" to 0.0625" for the bevel and fit-up geometry in the HI-STAR 100 design drawings. Therefore, the evaluations are carried out using the upper bound gap of 0.0625". To bound the computed stresses even further, the inter-layer friction coefficient is set equal to zero. It is intuitively apparent that increasing the friction increases the localized stresses near the "point of pull" (i.e., the weld) while mitigating the stresses elsewhere. Since the object is to maximize the distributed (membrane) stress, the friction coefficient is set equal to zero in the analysis.

A two-dimensional finite element analysis of the inner confinement shell and the five intermediate shells is performed to establish the level of fabrication circumferential stress developing during the assembly process. A 180-degree section through the overpack, consisting of six layers of metal, is modeled. The ANSYS finite element code is used to model the fabrication process; each layer is modeled using PLANE42 four node quadrilateral elements. Contact (or lack of contact) is modeled by CONTAC48 point-to-surface elements. Symmetry boundary conditions apply at 90 degrees, and radial movement of the inner node point of the confinement layer is restrained. At -90 degrees, the inner confinement layer is restrained while the remaining layers are subject to a prescribed circumferential displacement  $d$  to stretch the layer and to simulate the shrinkage caused by the weld

process. Although the actual fabrication process locates the longitudinal weld in each layer at different circumferential orientation, in the analytical simulations all layer welds are located together. This is acceptable for analysis since the stress of interest is the primary membrane component. Figure 2.6.24 shows a partial free body of a small section of one of the layers. Normal pressures  $p$  develop between each layer due to the welding process; shear stresses due to friction between the layers also develop since there is relative circumferential movement between the layers. Figure 2.6.25 shows a free body of the forces that develop on each layer.

The fabrication stress distribution is a function of the coefficient-of-friction between the layers. For a large enough coefficient-of-friction the effects of the assembly process are localized near the weld. Localized stresses are not considered as primary stresses. For a coefficient-of-friction = 0.0, the membrane hoop stress in the component shells is non-local in nature. Therefore, the fabrication stress computation conservatively considers only the case coefficient of friction (COF) = 0.0 since this will develop the largest in-plane primary membrane stress in each layer. The simulation is nonlinear in that each of the contact elements is checked for closure during increments of applied loading (the weld displacement).

The results from the analyses are summarized in the table below:

Fabrication Stresses in Overpack Shells - Minimum Safety Factors (Level A Service Condition at Assembly Temperature)			
Item	Value (ksi)	Allowable (ksi) (Note3)	Safety Factor
First Intermediate Shell (Note 1)	11.22	52.5	4.68
Fourth Intermediate Shell (Note 1)	7.79	52.5	6.74
Inner Shell Mid Plane (Note 2)	10.6	69.9	6.59
Inner Shell Outer Surface (Note 2)	16.27	69.9	4.30

Notes:

1. The fabrication stress is a tensile circumferential stress.
2. The fabrication stress is a compressive circumferential stress
3. Fabrication stresses are self-limiting and are therefore classified as "secondary" and are compared to 3 times the allowable membrane stress or stress intensity.

The above table leads to the conclusion that the maximum possible values for stresses resulting from HI-STAR 100 fabrication process are only a fraction of the relevant ASME Code limit.

2.6.1.3.2.3 Structural Analysis of Overpack Closure Bolting (Load Case 1 - Table 2.1.8)

Stresses are developed in the closure bolts due to pre-load, pressure loads, temperature loads, and accident loads. Closure bolts are explored in detail in Reference [2.6.3] prepared for analysis of shipping casks. The analysis herein of the overpack closure bolts under normal conditions of transport and for the hypothetical accident conditions uses the methodology and the procedures defined and explained in Reference [2.6.3]; the sole exception is that some of the formulas in the reference are modified to account for the annulus on the inner surface of the overpack closure lid; this annulus exists for the sole purpose of ensuring that the interface area between the MPC lid and the overpack top closure is a peripheral ring area rather than the entire surface area of the MPC lid. This feature ensures a reduction in the computed bolt stress.

The following combined load case is analyzed for normal conditions of transport.

Normal: Pressure, temperature, and pre-load loads are included (Load Case 1 in Table 2.1.8).

Reference [2.6.3] reports safety factors defined as the calculated stress combination divided by the allowable stress for the load combination. This definition of safety factor is the inverse of the definition consistently used in this SAR. In summarizing the closure bolt analyses performed, results are reported using the safety factor definition of allowable stress divided by calculated stress. The following result for closure lid bolting for normal conditions of transport are obtained:

Overpack Closure Bolt - Safety Factor (Load Case 1 in Table 2.1.8)	
Combined Load Case	Safety Factor on Bolt Tension
Average Tensile Stress	1.44
Combined Tension, Shear, Bending, and Torsion	1.57

It is seen from the above table that the safety factor is greater than 1.0 as required. Note that the magnitude of the safety factors reflect the large preload required for successful performance of the bolts under a hypothetical accident drop event where the demand is more severe.

2.6.1.3.2.4 Stress Analysis of Overpack Enclosure Shell

The overpack enclosure shell and the overpack enclosure return are examined for structural integrity under a bounding internal pressure. Flat beam strips of unit width are employed to simulate the performance of the flat panels and the flat plate return section (see drawings in Subsection 1.4). It is shown that large safety factors exist against overstress due to an internal pressure developing from off-gassing of the neutron absorber material. The minimum safety factors are summarized below:

Location	Calculated Stress (ksi)	Allowable Stress (ksi)	Safety Factor
Enclosure Shell Return (bottom)	2.56	26.3	10.2
Enclosure Shell Return (top)	3.42	26.3	7.68
Enclosure Shell Flat Panels	5.58	26.3	4.71
Weld Shear	0.63	10.52	16.7

### 2.6.1.3.3 Fatigue Considerations

Regulatory Guide 2.9 requires consideration of fatigue due to cyclic loading during normal conditions of transport. Considerations of fatigue associated with long-term exposure to vibratory motions associated with normal conditions of transport are considered below where individual components of the package are assessed for the potential for fatigue.

- Overpack and MPC Fatigue Considerations

The temperature and pressure cycles within the MPC and the inner shell of the overpack are entirely governed by the mechanical and thermal-hydraulic conditions presented by the fuel. The external surfaces of the overpack, however, are in direct contact with the ambient environment. The considerations of cyclic fatigue due to temperature and pressure cycling of the HI-STAR 100 System, therefore, must focus on different locations depending on the source of the cyclic stress.

As shown in the following, the overpack and the MPCs in the HI-STAR 100 System do not require a detailed fatigue analysis because all applicable loadings are well within the range that permits exemption from fatigue analysis per the provisions of Section III of the ASME Code. Paragraph NB-3222.4 (d) of Section III of the ASME Code provides five criteria that are strictly material and design condition dependent to determine whether a component can be exempted from a detailed fatigue analysis. The sixth criterion is applicable only when dissimilar materials are involved, which is not the case in the HI-STAR 100 System.

The Design Fatigue curves for the overpack and MPC materials are given in Appendix I of Section III of the ASME Code. Each of the five criteria is considered in the following:

#### i. Atmospheric to Service Pressure Cycle

The number of permissible cycles,  $n$ , is bounded by  $f(3S_m)$ , where  $f(x)$  means the number of cycles from the appropriate fatigue curve at stress amplitude of  $x$  psi. In other words

$$n < f(3S_m)$$

From Tables 2.1.11 through 2.1.20 for normal conditions, and the fatigue curves, the number of permissible cycles is

$$n(\text{overpack}) \leq 1600 \quad (3S_m = 68,700 \text{ psi}) \quad (\text{Figure I.9-1 of ASME Appendix I})$$

$$n(\text{MPC}) \leq 40,000 \quad (3S_m = 46,200 \text{ psi}) \quad (\text{Figure I.9-2 of ASME Appendix I})$$

The MPC, which is an all-welded component, is unlikely to undergo more than one cycle, indicating that a huge margin of safety with respect to this criterion exists. The overpack, however, is potentially subject to multiple uses. However, 1000 pressurizations in the 40-year life of the overpack is an upper bound estimate. In conclusion, the projected pressurizations of the HI-STAR components do not warrant a usage factor evaluation.

ii. Normal Service Pressure Fluctuation

Fluctuations in the service pressure during normal operation of a component are considered if the total pressure excursion  $\delta_p$  exceeds  $\Delta_p$ .

where

$$\Delta_p = \text{Design pressure} * S / (3S_m)$$

$$S = \text{Value of } S_a \text{ for one million cycles}$$

Using the above mentioned tables and appropriate fatigue curves,

$$(\Delta p)_{\text{overpack}} = \frac{(100)(13000)}{(3)(22,900)} = 18.9 \text{ psi}$$

$$(\Delta p)_{\text{MPC}} = \frac{(100)(26000)}{(3)(16000)} = 54.2 \text{ psi}$$

During normal operation the pressure fields in the MPC and the overpack are steady state. Therefore, normal pressure fluctuations are negligibly small. Normal service pressure oscillations do not warrant a fatigue usage factor evaluation.

iii. Temperature Difference - Startup and Shutdown

Fatigue analysis is not required if the temperature difference  $\Delta T$  between any two adjacent points on the component during normal service does not exceed  $S_a / 2E\alpha$ , where  $S_a$  is the cyclic stress amplitude for the specified number of startup and shutdown cycles.  $E$  and  $\alpha$  are the Young's Modulus and instantaneous coefficients of thermal expansion (at the service temperature). Assuming 1000 startup and shutdown cycles, Tables 2.3.1 and 2.3.4 and the appropriate ASME fatigue curves in Appendix I or Section III of the ASME Code give:

$$(\Delta T)_{\text{overpack}} = \frac{90,000}{(2)(26.1)(6.98)} = 247^{\circ}\text{F}$$

$$(\Delta T)_{\text{MPC}} = \frac{130,000}{(2)(25)(9.69)} = 268^{\circ}\text{F}$$

There are no locations on either the overpack or MPC where  $\Delta T$  between any two adjacent points approach these calculated temperatures. As reported in Tables 3.4.16-18, the maximum  $\Delta T$  that occurs between two components, the MPC shell and the basket periphery, is only 115 degrees F. Therefore, it is evident this temperature criterion is satisfied for 1,000 startup and shutdown cycles.

iv. Temperature Difference - Normal Service

Significant temperature fluctuations that require consideration in this criterion are those in which the range of temperature difference between any two adjacent points under normal service conditions is less than  $S/2E\alpha$  where S corresponds to  $10^6$  cycles. Substituting, gives

$$(\Delta T)_{\text{MPC}} = \frac{26,000}{(2)(25)(9.69)} = 53.7^{\circ}\text{F}$$

$$(\Delta T)_{\text{overpack}} = \frac{13,000}{(2)(26.1)(6.98)} = 35.7^{\circ}\text{F}$$

During normal operation, the temperature fields in the MPC and the overpack are steady state. Therefore, normal temperature fluctuations are negligibly small. Normal temperature fluctuations do not warrant a fatigue usage factor evaluation.

v. Mechanical Loads

Mechanical loadings of appreciable cycling occur in the HI-STAR 100 System only during transportation. The stress cycling under transportation conditions is considered significant if the stress amplitude is greater than  $S_a$  corresponding to  $10^6$  cycles. It, therefore, follows that the stress limits that exempt the overpack and MPC are 13,000 psi and 26,000 psi, respectively.

From Subsection 2.5.2.1, g-loads typically associated with rail transport will produce stress levels in the MPC and overpack which are a small fraction of the above limits. Therefore, no potential for fatigue expenditure in the MPC and overpack materials is found to exist under transportation conditions.

In conclusion, the overpack and the MPC do not require fatigue evaluation under the exemption criteria of the ASME Code.

- Fatigue Analysis of Closure Bolts:

The maximum tensile stress developed in the overpack closure bolts during normal operating conditions is shown by analyses not to exceed 93.0 ksi. The alternating stress in the bolt is equal to 1/2 of the maximum stress due to normal conditions, or 46.5 ksi. The design service temperature for the bolts per Table 2.1.2 is 350 degrees F. Per Table 2.3.5, the Young's Modulus at 350 degrees F is 27,000 ksi. Therefore, the effective stress intensity amplitude for calculating usage factor using

$$S_a = \frac{(46.5)(4)(30e+06)}{27.7e+06} \\ = 201.4 \text{ ksi}$$

Figure I-9.4 (ASME Code, Appendices) is (ratioing the modulus used in the figure to the modulus used here):

Using Figure I-9.4 (NB, loc. cit), the permissible number of cycles is 200.

This result indicates the main closure bolts should *not be torqued and untorqued more than 200 times. After 200 loading cycles, they must be replaced.*

The total shear area of the overpack closure bolt threads is  $A_v = 9.528 \text{ in}^2$ . Therefore, the shear stress in the top closure bolt threads is, (use the limiting bolt load for normal operation and the tensile stress area of a bolt =  $1.680 \text{ in}^2$ ).

$$\sigma_v = \frac{93.0 \text{ ksi} \times 1.68 \text{ in}^2}{9.528 \text{ in}^2} = 16.4 \text{ ksi}$$

The shear stress developed in the threads of the overpack closure bolts is significantly less than the stress developed in the bolt. Therefore, fatigue of the overpack closure bolts is not controlled by shear stress in the bolt threads.

- Fatigue Considerations for Top Flange Closure Bolt Threads:

The shear area of the main flange closure bolt threads is  $12.371 \text{ in}^2$ . Therefore, the shear stress in the flange threads under the limit load on the bolt is:

$$\sigma_v = \frac{93.0 \text{ ksi} \times 1.68 \text{ in}^2}{12.928 \text{ in}^2} = 12.6 \text{ ksi}$$

The primary membrane stress in the main flange threads is equal to twice the maximum shear stress, or 21.1 ksi. The alternating stress in the threads,  $S_a$ , is equal to 1/2 of the total stress range, or 10.56 ksi. At 400 degrees F design temperature (per Table 2.1.2) the Young's Modulus (Table 2.3.4) is  $26.1 \times 10^6$  psi.

The effective stress amplitude accounting for the fatigue strength reduction and Young's Modulus effects is given by

$$S_a = \frac{(12.6)(4)(30)}{26.1} = 57.9 \text{ ksi}$$

Using Figure I-9.4 (of NB, loc. cit), the allowable number of cycles is equal to 1,800.

Therefore, the *maximum service life of the main flange threads is 1,800 cycles* of torquing and untorquing of the overpack closure system.

- MPC Fatigue Analysis

The maximum primary and secondary alternating stress range for normal transport conditions is conservatively assumed to be equal to the allowable alternating stress range of  $0.5 \times 40,000$  psi. Conservatively using a Young's Modulus of  $25 \times 10^6$  psi for the fatigue evaluation, yields

$$S = 20,000 \text{ psi} \times \frac{28.3 \times 10^6 \text{ psi}}{25 \times 10^6 \text{ psi}} = 22,640 \text{ psi}$$

Cyclic life is in excess of  $1 \times 10^6$  cycles per Figure I-9.2.1 of Appendix I of the ASME Code.

- Satisfaction of Regulatory Guide 7.6 Commitment

The minimum alternating stress range,  $S_a$ , at 10 cycles from all appropriate fatigue curves is 600 ksi. All primary stresses under any of the analyses performed in this SAR under the required load combinations are shown to lead to stress intensities that are less than the ultimate strength of the containment vessel material (70 ksi). Fabrication stresses are conservatively evaluated and are summarized in Subsection 2.6.1.3.2.2. Maximum fabrication stress intensities are less than 17 ksi. Conservatively assuming a stress concentration of 4 regardless of specific location produces a stress intensity range below  $4 \times (70 + 17) = 348$  ksi ( $< 600$  ksi). Therefore, satisfaction of the Regulatory Guide 7.6 commitment is assured.

#### 2.6.1.4 Comparison with Allowable Stresses

Consistent with the formatting guidelines of Regulatory Guide 7.9, calculated stresses and stress intensities from the finite element analyses are compared with the allowable stresses and stress intensities defined in Subsection 2.1 (Tables 2.1.11 through 2.1.21) as applicable for conditions of normal transport. The results of these comparisons are presented in the form of factors of safety (SF) defined as:

$$SF = \frac{\text{Allowable Stress}}{\text{Calculated Stress}}$$

Safety factors associated components identified as lifting and tie-down devices have been presented in Section 2.5 as required by Regulatory Guide 7.9.

Major conservatisms are inherent in the finite element models for both the MPC fuel basket and the enclosure vessel, and for the HI-STAR 100 overpack. These conservatisms are elucidated here with additional discussion as needed later in the text associated with each particular issue.

#### Conservative Assumptions in Finite Element Analyses and Evaluation of Safety Factors

1. Comparison with allowable stresses or stress intensities is made using the design temperature of the component rather than the actual operating temperature existing in the metal at that location. As an example, all comparisons with allowables for the Alloy X fuel basket material uses the allowable strength at 725 degrees F (Table 2.1.21). Under the normal heat conditions of transport, temperatures near the periphery of the fuel basket are below 450 degrees F. High stresses in the fuel basket generally occur at the basket periphery. From Table 2.1.19, the allowable stresses for primary membrane plus bending at the two temperatures are compared to evolve the additional margin in the computed safety factor as  $27.2/23.1 = 1.18$ . Therefore, the reported safety factors from the analysis have at least an additional 18% hidden component from this effect. Similar hidden margins from this kind of simplification arise in the various components of the overpack. Depending on the material, these hidden margins, which increase the reported safety factor, may be large or small. From Figures 3.4.17 and 3.4.18 in Chapter 3, it is concluded that the normal heat condition of transport maximum inner shell temperature is less than 300 degrees F. The allowable stresses are uniformly assumed at 400 degrees F per Table 2.1.21. From Table 2.1.11, the additional hidden safety factor multiplier is computed as  $35/34.4 = 1.02$ . In the inner shell of the overpack, the increase in the reported safety factor from this effect is only 2% for normal conditions of transport.

2. Comparisons with primary stress allowables are made with secondary stresses included. This has an adverse effect on the reported safety factor, especially in areas near discontinuities.

3. In the modeling of the HI-STAR 100 overpack, the full structural connectivity of the intermediate shells and the inner containment shell is not included in the finite element model in order to maintain the linear elastic analysis methodology. The neglect of such interaction means that the overall bending stiffness of the overpack is underestimated; this leads to over-prediction of stresses and consequent adverse effects on reported safety factors.

4. In the modeling of the MPC fuel basket, the local reinforcement of the fuel basket panel from the fillet welds is neglected. The increase in the section modulus at the weld location is ignored leading to a decrease in stiffness of the basket panel. Consequently, under mechanical loading, the stress state is overestimated at the basket panel connection.

#### 2.6.1.4.1 MPC Fuel Basket and Enclosure Vessel

It is recalled that the stress analyses have been performed for the load cases applicable to normal conditions of transport as assembled in Tables 2.1.6 and 2.1.7 for the fuel basket and the enclosure vessel, respectively. Detailed analyses, including finite element model details and the necessary explanations to collate and interpret the voluminous numerical results have been archived. A compendium of finite element results for the fuel basket and enclosure vessel for each load case associated with normal conditions of transport has been developed. Tables 2.6.6 and 2.6.7 summarize results obtained from the analyses (for all baskets) of Load Cases E1.a and E1.c defined in Table 2.1.7. Table 2.6.8 contains a synopsis of all safety factors obtained from the results. To further facilitate perusal of results, another level of summarization is performed in Tables 2.6.2 and 2.6.3 where the global minima of safety factor for each load case are presented. Finally, miscellaneous safety factors associated with the fuel basket and the MPC enclosure vessel are reported in Table 2.6.10.

The following element of information is relevant in ascertaining the safety factors under the various load cases presented in the tables.

- In the interest of simplification of presentation and conservatism, the total stress intensities under mechanical loading are considered to be of the primary genre' even though, strictly speaking, a portion can be categorized as secondary (that have much higher stress limits).

A perusal of the results for Tables 2.6.2 and 2.6.3 under different load combinations for the fuel basket and the enclosure vessel reveals that all factors of safety are above 1.0. The relatively modest factor of safety for the fuel basket under side drop events (Load Case F2.a and F2.b) in Table 2.6.2 warrants further explanation.

The wall thickness of the storage cells, which is by far the most significant variable in the fuel basket's structural strength, is significantly greater in the HI-STAR 100 MPCs than in comparable fuel baskets licensed in the past. For example, the cell wall thickness in the TN-32 basket (Docket No. 72-1021, M-56), is 0.1 inch and that in the NAC-STC basket (Docket No. 71-7235) is 0.048 inch. In contrast, the cell wall thickness in the MPC-68 is 0.25 inch. In spite of their relatively high flexural rigidities, computed margins in the HI-STAR 100 fuel baskets are rather modest. This is because of some conservative assumptions in the analysis that lead to an overstatement of the state of stress in the fuel basket. For example:

- i. The section properties of longitudinal fillet welds that attach contiguous cell walls to each other are completely neglected in the finite element model (Figure 2.6.15). The fillet welds strengthen the cell wall section modulus at the very locations where maximum stresses develop.

- ii. The radial gaps at the fuel basket-MPC shell and at the MPC shell-overpack interface are explicitly modeled. As the applied loading is incrementally increased, the MPC shell and fuel basket deform until a "rigid" backing surface of the overpack is contacted, making further unlimited deformation under lateral loading impossible. Therefore, some portion of the fuel basket and enclosure vessel (EV) stress has the characteristics of secondary stresses (which by definition, are self-limited by deformation in the structure to achieve compatibility). For conservativeness in the incremental analysis, no distinction between deformation controlled (secondary) stress and load controlled (primary) stress in the stress categorization is made. All stresses, regardless of their origin, are considered as primary stresses. Such a conservative interpretation of the Code has a direct (adverse) effect on the computed safety factors.

The above remarks can be illustrated simply by a simple closed-form bounding calculation. If all deformation necessary to close the gaps is eliminated from consideration, then the capacity of the fuel basket cell wall under loads which induce primary bending stress can be ascertained by considering a clamped beam (cell wall) subject to a lateral pressure representing the amplified weight of fuel assembly plus self-weight of the cell wall (e.g., see Figure 2.6.15).

Using the cell wall thickness and an appropriate unsupported length for the MPC-68, for example, the fixed edge bending stress is computed as 238.22 psi (using the actual fuel weights, cell wall weights, cell wall thickness and unsupported length). This implies a safety factor of 5.704 for a Level A event (for a 17g deceleration,  $SF = 23,100 / (238.22 \times 17) = 5.704$ ) where the allowable bending stress intensity for Alloy X at 725 degrees F (Table 2.1.21) has been used. The above simple calculation demonstrates that the inherent safety margin under accident loading is considerably greater than is implied by the result in Table 2.6.8 ( $SF=2.42$ ) for the MPC-68 and 0-degree drop orientation. Similar conclusions can be reached for other MPCs by performing scoping calculations in a similar manner.

- iii. The SNF inertia loading on the cell panels is simulated by a uniform pressure, which is a most conservative approach for incorporating the SNF/cell wall structure interaction.

The above assumptions all act to depress the computed values of factors of safety in the fuel basket finite element analysis and render conservative results.

The reported values do not include the effect of dynamic load amplification. Calculations show that, for the duration of impact and the predominant natural frequency of the basket panels under lateral hypothetical accident conditions, the dynamic load factors (DLF) are bounded by 1.05. It is expected that for the normal condition of transport 1' drop, the amplification would be reduced further.

Table 2.6.8 does not report the safety factors associated with Load Case F1 in Table 2.1.6 where it is shown that secondary stresses due to the thermal gradients are below the allowable secondary stress intensity limits. A representative stress intensity level arising from fuel basket thermal gradients is

15.07 ksi. Using the allowable stress intensity limit for primary plus secondary components per Table 2.1.21, the following representative fuel basket safety factor appropriate to Load Case F1 is obtained as "SF", where:

$$SF = 46.2 \text{ ksi}/15.07 \text{ ksi} = 3.06 \quad (\text{Load Case F1 from Table 2.1.6})$$

It is concluded that since all reported factors of safety for the fuel basket panels (based on stress analysis) are greater than the DLF, the MPC fuel basket is structurally adequate for its intended functions during and after a postulated lateral drop event associated with the normal conditions of transport.

Tables 2.6.6 and 2.6.7 report stress intensities and safety factors for the helium retention boundary (enclosure vessel) subject to internal pressure alone and to internal pressure plus the normal operating condition temperature with the most severe thermal gradient (Load Cases E1.a and E1.c in Table 2.1.7). Table 2.6.8 reports safety factors from the finite element analyses of the 1' free drop simulating a normal handling condition of transport. The final values for safety factors in the various locations of the helium retention boundary provide assurance that the MPC enclosure vessel is a robust pressure vessel.

#### 2.6.1.4.2 Overpack

##### 2.6.1.4.2.1 Discussion

The overpack is subject to the load cases listed in Table 2.1.8 for normal conditions of transport. Results from the series of finite element analyses are tabulated for normal heat and cold conditions of transport. The tabular results include contributions from mechanical and thermal loading and are needed to insure satisfaction of primary plus secondary stress limits for normal conditions of transport. Results are also tabulated from analyses that neglect thermal stresses. These tables are used to check primary stress limits.

The following text is a brief description of how the results are presented for evaluation and how the evaluation is organized in final form:

- The stress intensity results are sorted by safety factor in ascending order for each component making up the overpack. In particular, results are sorted separately for locations in the lid, the inner shell, and the bottom plate that together make up the containment boundary.
- The extensive body of results is initially summarized in Table 2.6.9 wherein the minimum safety factor for different components of the overpack for each of the load cases is presented. This table lists minimum safety factors for the load cases associated with the normal heat conditions of transport. All safety factors are conservatively computed using allowable stresses based on the maximum normal operating temperatures (see Tables 2.1.2 and 2.1.21 for temperatures and for allowable stresses).
- The finite element analyses include the stress state induced by bolt preload but do not include the effect of secondary fabrication stresses. Table 2.6.5 presents results of recalculation of the safety factors for the inner containment shell and for the intermediate

shells to include the “fabrication stresses” reported in Subsection 2.6.1.3.2.2. Table 2.6.5 summarizes these recomputed safety factors, based on limits for primary plus secondary stresses, and reports the limiting safety factors for the overpack shells for events subject to normal conditions of transport (Level A Service Conditions). The incorporation of the fabrication stress and the computation of revised safety factors begins with the individual principal stress components for the shells, conservatively adds the circumferential fabrication stress in the inner and intermediate shells to the principal stress having the same sign as the fabrication stress, and then re-computes the stress intensity and the safety factor. For the inner shell, the safety factors including fabrication stress are computed from principal stress data including mechanical and thermal loading. For the intermediate shell, however, the recomputed safety factors are based on principal stresses that only include mechanical loading (no thermal stresses need be evaluated for a component designed in accordance with ASME Code Section III, Subsection NF regardless of Class 1 or Class 3 designation (see paragraph NF-3121.11)).

- Finally, Table 2.6.4 summarizes the minimum values of safety factors (global minima) for the overpack components for the normal conditions of transport.

The modifications summarized in Table 2.6.5 are briefly discussed below for the normal heat conditions of transport. The same series of modifications are also performed for the normal cold conditions of transport.

Case 1 (Pressure) - Safety factors are summarized in Table 2.6.9 prior to inclusion of fabrication stress. Table 2.6.5 shows the modified safety factor resulting from "adding" the fabrication stress for the inner containment shell to the appropriate principal stress that includes the combination of mechanical plus thermal loads. The same conservative methodology is applied to modify the safety factor for the intermediate shell to include fabrication stress. However, since the intermediate shells are designed to ASME Code Section III, Subsection NF, no thermal stresses need be included in the strength evaluation.

Case 3 (1 foot drop): Results are tabulated including both thermal and mechanical loading. Safety factors for the inner containment shell are summarized in Table 2.6.9 prior to inclusion of fabrication stress. Table 2.6.5 shows modified safety factors that are computed in the same manner as reported for Case 1. For the intermediate shell, principal stress results that do not include thermal stress effects are conservatively modified to include fabrication effects.

#### 2.6.1.4.3 Result Summary for the Normal Heat Condition of Transport

- Stress Results from Overall Finite Element Models of the MPC and Overpack

Tables 2.6.6 through 2.6.9 summarize minimum safety factors from load cases analyzed using the finite element models of the MPC fuel basket plus canister and the overpack described in Subsections 2.6.1.3.1 and 2.6.1.3.2. All safety factors are greater than 1.0 and are greater than any credible dynamic amplifier for the location. Table 2.6.5 provides a summary table that includes the effect of fabrication stress on safety factors for the intermediate and inner shells of the overpack. Table 2.6.5 reports safety factors based on primary plus secondary allowable strengths.

- Status of Lid Bolts and Seals on the Overpack

The finite element analysis for the overpack provides results at the lid-to-top flange interface. In particular, tabulated results for seals and lid bolts are examined. The output results for each load combination indicate that all seal springs remain closed (i.e. the loading in the elements representing the seal remains compressive) indicating that the sealworthiness of the bolted joint will not be breached during normal heat conditions of transport.

Each load combination results in a report of the total compressive force on the closure plate-overpack interface as well as the total tangential force ("friction force"). If the ratio "total friction force/total compressive force" is formed for each set of results, the maximum value of the ratio is 0.219. There will be no slip of the closure plate relative to the overpack if the interface coefficient of friction is greater than the value given above. Mark's Handbook for Mechanical Engineers [3.4.9] in Table 3.2.1 shows  $\mu = 0.74-0.79$  for clean and dry steel on steel surfaces. Therefore, it is concluded that there is no propensity for relative movement.

Based on the results of the finite element analysis for normal heat conditions of transport, the following conclusions are reached.

No bolt overstress is indicated under any loading event associated with normal conditions of transport. This confirms the results of alternate closure bolt analyses, performed in accordance with NUREG/CR-6007 UCRL-ID-110637, "Stress Analysis of Closure Bolts for Shipping Casks", by Mok, Fischer, and Hsu, LLL, 1993.

The closure plate seals do not unload under any load combination; therefore, the seals continue to perform their function.

- Stress and Stability Results from Miscellaneous Component Analyses in Subsection 2.6.1.3

Tables 2.6.10 and 2.6.11 repeat summary results from additional analyses described and reported on in Subsection 2.6.1.3 for components of the MPC and the overpack. The safety factors are summarized in this subsection in accordance with the requirements of Regulatory Guide 7.9. The tables report comparisons of calculated values with allowable values for both stress and stability and represent a compilation of miscellaneous analyses.

- Overpack Internal Pressure Test

The overpack is considered as an ASME pressure vessel. A hydrostatic test of the overpack under 1.5 times internal pressure must result in no stresses in excess of the material yield strength at room temperature to meet the requirement of 10CFR71.85(b). In the following, the necessary results to support the conclusion that the HI-STAR 100 transport containment boundary meets the requirement are presented. Table 2.3.4 gives the material yield strengths of SA350 LF3 and SA 203-E as 37.5 ksi and 40.0 ksi, respectively, at 100 degrees F. A survey of the safety factors for the containment boundary reported in Table 2.6.9 gives the following minimum safety factors:

CONTAINMENT BOUNDARY SAFETY FACTORS - Internal Pressure	
Item	Safety Factor
Lid	2.87
Inner Shell	12.1
Baseplate	11.2

These safety factors are determined using allowable stress intensities at the reference temperatures listed in Table 2.1.21 that are less than the yield stress for the corresponding material at room temperature. From the large safety factors in the above table, it is concluded, without further analysis, that an increase in the internal pressure by 50% will not cause stresses in the containment boundary to exceed the material yield stress.

- Summary of Minimum Safety Factors for Normal Heat Conditions of Transport

Tables 2.6.2 through 2.6.4 present a concise summary of safety factors for the fuel basket, the enclosure vessel, and the overpack, respectively. Locations within this SAR from which the summary results are culled are also indicated in the above tables.

Based on the results of all analyses, with results presented or summarized in the text and in tables, it is concluded that:

- All safety factors reported in the text and in the summary tables are greater than 1.0.
- There is no restraint of free thermal expansion between component parts of the HI-STAR 100 System.

Therefore, the HI-STAR 100 System, under the normal heat conditions of transport, has adequate structural integrity to satisfy the subcriticality, containment, shielding, and temperature requirements of 10CFR71.

## 2.6.2 Cold

The Normal Cold Condition of Transport assumes an ambient environmental temperature of -20 degrees Fahrenheit and maximum decay heat. A special condition of extreme cold is also defined where the system and environmental temperature is at -40 degrees F and the system is exposed to increased external pressure with minimum internal pressure. A discussion of the resistance to failure due to brittle fracture is provided in Subsection 2.1.2.3.

The value of the ambient temperature has two principal effects on the HI-STAR 100 storage system, namely:

- i. The steady-state temperature of all material points in the cask system will go up or down by the amount of change in the ambient temperature.
- ii. As the ambient temperature drops, the absolute temperature of the contained helium will drop accordingly, producing a proportional reduction in the internal pressure in accordance with the Ideal Gas Law.

In other words, the temperature gradients in the cask system under steady-state conditions, will remain the same regardless of the value of the ambient temperature. The internal pressure, on the other hand, will decline with the lowering of the ambient temperature. Since the stresses under normal transport condition arise principally from pressure and thermal gradients, it follows that the stress field in the MPC under a bounding "cold" ambient would be smaller than the "heat" condition of normal transport, treated in the preceding subsection. Therefore, the stress margins computed in Section 2.6.1 can be conservatively assumed to apply to the "cold" condition as well. Calculations using the methodology outlined in NUREG/CR-6007 UCRL-ID-110637, "Stress Analysis of Closure Bolts for Shipping Casks", by Mok, Fischer, and Hsu, LLL, 1993 demonstrate that the overpack closure bolts will retain the helium seal under the cold ambient conditions.

In addition, allowable stresses generally increase with decreasing temperatures. Safety factors, therefore, will be greater for an analysis at cold temperatures than at hot temperatures. Therefore, the safety factors reported for the hot conditions in Subsection 2.6.1 provide the limiting margins. The overpack, however, is analyzed under cold conditions to ensure that the integrity of the seals is maintained.

As no liquids are included in the HI-STAR 100 System design, loads due to expansion of freezing liquids are not considered.

#### 2.6.2.1 Differential Thermal Expansion

The methodology for determination of the effects of differential thermal expansion in the normal heat condition of transport has been presented in Subsection 2.6.1.2. The same methodology is applied to evaluate the normal cold condition of transport.

The results are summarized in the tables given below for normal cold condition of transport.

THERMOELASTIC DISPLACEMENTS IN THE MPC AND OVERPACK UNDER COLD TEMPERATURE ENVIRONMENT CONDITION				
CANISTER - FUEL BASKET				
	Radial Direction (in.)		Axial Direction (in.)	
Unit	Initial Clearance	Final Gap	Initial Clearance	Final Gap
All PWRs	0.1875	0.095	2.0	1.524
BWR	0.1875	0.101	2.0(min)	1.554 (min)
CANISTER - OVERPACK				
	Radial Direction (in.)		Axial Direction (in.)	
Unit	Initial Clearance	Final Gap	Initial Clearance	Final Gap
All PWRs	0.09375	0.069	0.625	0.487
BWR	0.09375	0.071	0.625	0.497

It can be verified by referring to the Design Drawings, and the foregoing table, that the clearances between the MPC basket and canister structure, as well as those between the MPC shell and overpack inside surface, are sufficient to preclude a temperature induced interference from the thermal expansions listed above.

It is concluded that the HI-STAR 100 package meets the requirement that there be no restraint of free thermal expansion that would lead to development of primary stresses under normal cold conditions of transport.

2.6.2.2 MPC Stress Analysis

The only significant load on the MPCs under cold conditions arises from the postulated 1-foot side drop. Since the allowable stress intensities are higher under the extreme cold condition, results for the MPCs are bounded by the analysis for heat; no additional solutions need to be considered. Since the MPCs are constructed of austenitic stainless steel, there is no possibility of a brittle fracture occurring in any of the MPCs

2.6.2.3 Overpack Stress Analysis

Table 1 of NRC Regulatory Guide 7.8 [2.1.2] mandates load cases at the extreme cold temperature. The overpack may not be bounded by the results of the heat condition load cases for these following conditions:

- increased external pressure with minimum internal pressure, and extreme cold at - 40 degrees F.
- minimal internal pressure plus 1 foot drop with extreme cold condition at - 20 degrees F.
- rapid ambient temperature change during normal condition of transport (note that this case is not explicitly listed as a load case in Regulatory Guide 7.8).

The first two bulleted items are presented in Table 2.1.8; the results of those analyses are presented here. Structural evaluation for the last bulleted item is performed in this subsection. The structural evaluation uses inputs from thermal transient analyses performed and reported in Chapter 3 subsection 3.4.3.1.

Results of finite element analyses for increased external pressure with minimum internal pressure, and for minimum internal pressure plus 1 foot drop (Load Cases 2 and 4 in Table 2.1.8)

Safety factors for Load Cases 2 and 4 in Table 2.1.8 are computed from the results tabulated from the archived finite element analyses Table 2.6.12 summarizes the safety factors obtained. The finite element analysis does not clearly elucidate the effect of temperature on bolt preload. Separate calculations, using the methodology outlined in NUREG/CR-6007 UCRL-ID-110637, "Stress Analysis of Closure Bolts for Shipping Casks", by Mok, Fischer, and Hsu, LLL, 1993 analyze the closure bolts under extreme cold ambient condition plus pressure and provides the appropriate change in bolt preload expected from operation at the extreme low temperature. A small decrease from the initial preload stress in the bolt results from this operating condition.

The computed change in stress due to the assumption of a severe local low temperature condition is insignificant compared to the initial bolt stress and to the change in the allowable bolt stress because of the lowered temperature. It is concluded that the small change in bolt preload stress has no effect on structural calculations and safety factors.

The overpack load cases for normal conditions of transport described for the hot condition are re-analyzed for the cold condition in accordance with the requirements of Regulatory Guide 7.9. Since higher allowable stresses apply to the overpack components, it is not expected that the re-analyses will result in lower safety factors than have been already reported for the heat condition. The purpose of the analyses is to demonstrate that the overpack seals remain intact under the cold condition. The results of the analyses for normal cold conditions of transport are summarized in Tables 2.6.12 and 2.6.13.

Stress Analysis for Rapid Lowering of Ambient Temperature from 100 degrees F to -40 degrees F (Load Case 5 in Table 2.1.8)

During transportation, the HI-STAR 100 packaging may experience changes in the ambient temperature. Since the HI-STAR 100 packaging is a passive heat rejection device, a change in the ambient temperature has a direct influence on the temperature of its metal parts. In the preceding sub-sections, all structural integrity evaluations have focused on the steady state thermal conditions

using 100°F and -40°F as the limiting upper and lower ambient steady state values. In this sub-section, the structural consequences of a rapid change from the hot (100°F) to cold (-40°F) ambient condition is considered. This scenario is labelled as ASME Code Service Condition A, which requires that the range of primary plus secondary stress intensity must be less than  $3 S_m$  ( $S_m$  = allowable stress intensity at the mean metal temperature). The loadings assumed to exist coincidentally with the thermal stresses from the transient event are: (i) overpack internal design pressure,  $P_i$  and (ii) the inertial deceleration load during transport ( $10g$ 's). The primary plus secondary stress intensity range from the simultaneous action of internal pressure, axial  $g$ -load ( $10 g$ 's), and thermal transient must be shown to be less than  $3S_m$ .

It should be noted that the reverse transient (i.e. rapid change from cold to hot will produce a less severe thermal stress gradient. Therefore, the magnitudes of the results of a "rapid cooldown" event bound the corresponding results for the "rapid heat up" event.

To perform a bounding evaluation, it is necessary to identify the material locations on the overpack where the thermal stresses are apt to be most adverse. The thick top forging, which is directly exposed to the ambient air during transport is clearly a candidate location. The other location is the planar cross section of the overpack at approximately mid-height where the heat emission rate from the SNF is at its maximum. These locations are identified in Figure 3.4.24 and further explained in sub-section 3.4.3.

To evolve thermal gradient results for the postulated rapid ambient temperature change, a transient temperature problem is formulated and solved in Chapter 3. The thermal problem and finite element model are fully articulated in Chapter 3 (Subsection 3.4.3.1) where a three-dimensional thermal transient analysis of the HI-STAR 100 Package is performed under a postulated rapid drop in ambient temperature (100 degree F to -40 degree F in one hour). The design basis decay heat load is imposed throughout the time span of the transient solution. The temperature profiles through the wall of the overpack and the top forging are determined as functions of time and the change in thermal gradient through the wall of the sections are documented in Chapter 3, Figures 3.4.25-3.4.27. These locations are limiting since there is direct exposure to the ambient temperature on the outer surface of these components. It is shown in the figures that the top forging experiences a change in through-wall thermal gradient of less than 2.5 degrees K (4.5 degrees F) and that other sections of the overpack experience an even weaker change in thermal gradient. The finite element analyses for normal conditions of transport report results and safety factors for all locations for the normal heat and cold conditions of storage (under assumed steady state thermal conditions). The following additional calculation provides the stress state due to the maximum through-wall thermal gradient in the top forging. This stress state is then combined with the stresses from other load cases and stress intensities formed.

Based on the results from the thermal solutions, the material properties for this calculation are obtained for a metal temperature of 150 degrees F. For the top forging material, the Young's Modulus,  $E$ , and the coefficient of linear thermal expansion,  $\alpha$ , are (at 150 degrees F):

$$E = 27,400,000 \text{ psi}$$

$$\alpha = 6.405 \times 10^{-6} \text{ inch/inch-degree F}$$

As reported in sub-section 3.4.3.1, the maximum change in temperature difference in the top forging material is bounded by 4.5°F. The ASME Code, (paragraph NB-3222.4(a)(4)) defines a significant temperature change  $\Delta T_s$  as

$$\Delta T_s = S/2E\alpha$$

Where S is the value of  $S_a$  from the applicable design fatigue curve for 1 million cycles. For the forging material, S = 18,900 psi, which yields

$$\Delta T_s = 18,900/(2 \times 27,400,000 \times 0.00000641) = 53.9 \text{ } ^\circ\text{F}$$

It therefore follows that the metal temperature gradient change produced by the rapid cooldown (or heat up event) does not lead to a significant stress adder. Nevertheless, the factor of safety under this loading condition is quantified.

The linear temperature profile gives a linear stress distribution through the wall thickness with compressive stresses at the inside surface of the top forging. The magnitude of the stress due to the maximum thermal gradient is:

$$\Delta\sigma = E\alpha(\Delta T)/(2(1-\nu))$$

For  $\Delta T=(4.5 \text{ degrees F (change)} + 1.5 \text{ degrees F (initial)})$  and  $\nu = 0.3$ , the stress intensity is computed as:

$$\Delta\sigma = 752 \text{ psi}$$

This stress is now combined with transport longitudinal stress from a 10g deceleration plus longitudinal stress from the normal condition internal pressure. These stresses are computed below:

Pressure stress:

$$\begin{aligned} p &= 100 \text{ psi (internal pressure per Table 2.1.1)} \\ \text{inside radius of top forging} &= a = 34.375'' \\ \text{outside radius of top forging} &= b = 41.625'' \end{aligned}$$

The magnitude of the longitudinal and circumferential stresses at the inside surface is

$$\sigma_x = (a^2/(b^2-a^2))p = 2.14 \times p = 214 \text{ psi}$$

$$\sigma_h = ((a^2 + b^2)/(b^2-a^2))p = 5.289 \times p = 529 \text{ psi}$$

Axial stress from deceleration:

The package weight = 282,000 lb. (Table 2.2.4)

The direct stress due to the axial deceleration is

$$\sigma_d = 10g \times 282,000 \text{ lb/Area} \quad \text{where the cross-section area is Area} = 1731 \text{ sq. inch}$$

Therefore,

$$\sigma_d = 1,629 \text{ psi}$$

Adding the absolute values of the stresses (for conservation), the maximum surface stress intensity is

$$SI = (\sigma_d + \sigma_x + \Delta\sigma) + p = 2,695 \text{ psi}$$

This value is compared against 3 x the allowable stress intensity since it involves a secondary thermal stress. From Table 2.1.13, the allowable primary plus secondary stress intensity is

$$SI(\text{allowable}) \quad 3 \times \text{allowable membrane stress intensity} = 69,100 \text{ psi}$$

$$\text{The safety factor is } 69,100/2,695 = 25.64$$

Therefore, the HI-STAR 100 overpack is shown to meet the Level A stress intensity limits under the rapid ambient temperature change event with a large margin of safety.

### Conclusions

Based on the results of the finite element analysis and the calculations carried out within this subsection, the following conclusions are reached for normal cold conditions of transport:

- No bolt yielding is indicated under any loading event.
- The closure plate seal springs do not unload under any load combination; therefore, the seals continue to perform their function.
- The postulated rapid drop in the ambient temperature from hot (100 degrees F) to cold (-40 degrees F) conditions of transport has no appreciable effect on the stress intensities in the transport overpack. The top forging will experience a small increase in through-wall thermal gradient. Calculations show that the change in thermal stress induced by this through-wall thermal gradient is small; large safety factors are calculated when the secondary thermal stress is combined with the pressure stress and the longitudinal transport stress.

Relative movement between the top flange and the top closure lid has been examined for the normal cold condition of transport. Each load combination reported provides the total compressive force on the lands as well as the total tangential force on the lands ("friction force"). If the ratio "total friction force/total compressive force" is formed for each set of results appropriate to the cold condition of normal transport, the maximum value of the ratio is 0.138. There will be no slip of the closure plate

relative to the overpack if the coefficient of friction is greater than the value given above. Mark's Handbook for Mechanical Engineers [2.6.2] shows  $\mu = 0.74-0.79$  for clean and dry steel on steel surfaces. Therefore, it is concluded that there is no propensity for relative movement.

Since the results show that all safety factors are greater than 1.0, it is concluded that the HI-STAR 100 System under the normal cold conditions of transport has adequate structural integrity to satisfy the subcriticality, containment, shielding, and temperature requirements of 10CFR71.

### 2.6.3 Reduced External Pressure

The effects of a reduced external pressure equal to 3.5 psia, which is required by USNRC Regulatory Guide 7.8 [2.1.2], are bounded by the effects of the accident internal pressure for the overpack (Table 2.1.1). This is considered in Subsection 2.7 for the overpack inner shell. This case does not provide any bounding loads for other components of the overpack containment boundary. Therefore, the only additional analysis performed here to demonstrate package performance for this condition is an analysis of the outer enclosure shell panels.

Under this load condition, the outer enclosure shell panels (see Section 1.4, Drawing) deform as long plates under the 3.5 psi pressure that tends to deform the panels away from the neutron absorber material. The stress developed in this situation can be determined by considering the panel as a clamped beam subject to lateral pressure. The appropriate dimensions are:

$L = \text{unsupported width of panel} = 7.875''$

$t = \text{panel thickness} = 0.5''$

$p = \text{differential pressure} = 3.5 \text{ psi}$

The stress is computed from classical strength of materials beam theory as:

$$\sigma = 0.5p \left( \frac{L}{t} \right)^2$$

Substituting the numerical values gives the stress as 434 psi. From Table 2.1.15, the allowable stress is 26.3 ksi for this condition. Therefore, the safety factor is

$$SF = 60.6$$

Clearly, this event is not a safety concern for package performance.

#### 2.6.4 Increased External Pressure

The effects of an external pressure equal to 20 psia on the package, which is required by USNRC Regulatory Guide 7.8 [2.1.2], are bounded by the effects of the large value for the design external pressure specified for the hypothetical accident (Table 2.1.1). Instability of the overpack shells is examined in Section 2.7. Therefore, no additional analyses need be performed here to demonstrate package performance.

#### 2.6.5 Vibration

During transport, vibratory motions occur which could cause low-level stress cycles in the system due to beam-like deformations. If any of the package components have natural frequencies in the flexible range (i.e., below 33 Hz), or near the flexible range, then resonance may amplify the low level input into a significant stress response.

As discussed in Section 2.1, there are no "flexible" beam-like members in the HI-STAR 100 MPC. The MPC is a fully welded, braced construction over its entire length and it is fully supported by the overpack during transport. Since the MPC is supported by the overpack, and is itself a rigid structure, any vibration problems would manifest themselves in the fuel basket walls.

It is shown below that the lowest frequency of the fuel basket walls and the overpack, acting as a beam, are well above 33 Hz. Therefore, additional stresses from vibration are not expected.

The lowest frequency of vibration during normal transport conditions will occur due to vibrations of a fuel basket cell wall. It is demonstrated that the lowest frequency of the component, computed based on the assumption that there is support sufficient to limit vibration to that representative of a clamped beam, is 658 Hz for a PWR basket and 1,200 Hz for a BWR basket.

These frequencies are significantly higher than the 33 Hz transition frequency for rigidity.

When in a horizontal position, the overpack is supported over a considerable length of the enclosure shell. Conservatively considering the HI-STAR as a supported beam at only the two ends of the enclosure shell, and assuming the total mass of the MPC moves with the overpack, an estimate of the lowest material frequency of the structure during transport is in excess of 469 Hz

Based on these frequency calculations, it is concluded that vibration effects are minimal and no new calculations are required.

#### 2.6.6 Water Spray

The condition is not applicable to the HI-STAR 100 System per Reg. Guide 7.8 [2.1.2].

2.6.7 Free Drop

The structural analysis of a 1-foot side drop under heat and cold conditions has been performed in Subsections 2.6.1 and 2.6.2 for heat and cold conditions of normal transport. As demonstrated in Subsections 2.6.1 and 2.6.2, safety factors are well over 1.0.

2.6.8 Corner Drop

This condition is not applicable to the HI-STAR 100 System per [2.1.2].

2.6.9 Compression

The condition is not applicable to the HI-STAR 100 System per [2.1.2].

2.6.10 Penetration

The condition is not applicable to the HI-STAR 100 System per [2.1.2].

Table 2.6.1

## FINITE ELEMENTS IN THE MPC STRUCTURAL MODELS

MPC Type Element Type	Model Type		
	Basic	0 Degree Drop	45 Degree Drop
<b>MPC-24</b>	1068	1179	1178
BEAM3	1028	1028	1028
CONTAC12	40	38	38
CONTAC26	0	110	110
COMBIN14	0	3	2
<b>MPC-32</b>	766	873	872
BEAM3	738	738	738
CONTAC12	28	27	24
CONTAC26	0	106	105
COMBIN14	0	2	5
<b>MPC-68</b>	1234	1347	1344
BEAM3	1174	1174	1174
PLANE82	16	16	16
CONTAC12	44	43	40
CONTAC26	0	112	111
COMBIN14	0	2	3

Table 2.6.1 Continued

FINITE ELEMENTS IN THE MPC STRUCTURAL MODELS

MPC Type Element Type	Model Type		
	Basic	0 Degree Drop	45 Degree Drop
<b>MPC-24E/24EF</b>	1070	1183	1182
BEAM3	1030	1030	1030
CONTAC12	40	38	38
CONTAC26	0	112	112
COMBIN14	0	3	2

Table 2.6.2

MINIMUM SAFETY FACTORS FOR THE MPC FUEL BASKET - NORMAL CONDITIONS OF TRANSPORT

Case Number	Load <sup>1</sup> Combination	Safety Factor	Location in SAR where Details are Provided
F1	T or T'	3.06	2.6.1.4.1
F2			
F2.a	D+H, 1 ft side drop 0°	1.57	Table 2.6.8
F2.b	D+H, 1 ft side drop 45°	1.29	Table 2.6.8

<sup>1</sup> The symbols used for loads are defined in Subsection 2.1.2.1.

Table 2.6.3

MINIMUM SAFETY FACTORS FOR THE MPC ENCLOSURE VESSEL - NORMAL CONDITIONS OF TRANSPORT

Case Number	Load Combination <sup>1</sup>	Safety Factor	Location in SAR where Details are Provided or Safety Factors Extracted
E1	E1.a Design internal pressure, $P_i$	5.06	Lid
		1.5	Baseplate
		1.36	Shell
	E1.b Design external pressure, $P_o$	NA	Lid
		NA	Baseplate
		1.2	Shell
E1.c Design internal pressure plus temperature	8.50	Lid	
	2.67	Base	
	1.5	Shell	
E2	E2.a $(P_i, P_o) + D + H$ , 1 ft side drop, 0 deg.	1.41	Table 2.6.8
	E2.b $(P_i, P_o) + D + H$ , 1 ft. side drop, 45 deg.	1.63	Table 2.6.8
E4	T or T'	Sections show expansion does not result in restraint of free thermal expansion	2.6.1.2

<sup>1</sup> The symbols used for loads are defined in Subsection 2.1.2.1.

Table 2.6.4

## MINIMUM SAFETY FACTORS FOR OVERPACK FOR NORMAL CONDITION OF TRANSPORT

Case Number	Load Combination <sup>1</sup>	Safety Factor	Location in SAR where Details are Provided
1	$T_h + P_i + F + W_s$	1.65	Table 2.6.5
2	$T_s + P_o + F + W_s$	3.38	Table 2.6.13
3	$T_h + D_{sn} + P_i + F + W_s$	1.68	Table 2.6.9
4	$T_c + D_{sn} + P_o + F + W_s$	2.41	Table 2.6.13

---

1 The symbols used here are defined in Subsection 2.1.2.1.

Table 2.6.5

MINIMUM SAFETY FACTORS INCLUDING FABRICATION STRESSES –  
PRIMARY PLUS SECONDARY STRESS INTENSITY, NORMAL HEAT CONDITIONS OF TRANSPORT

Case	Inner Shell Exterior Surface	Intermediate Shell
1 - Internal pressure	1.65*	4.12
3 - 1 ft. Side Drop	1.70*	2.42

\* Applicable to inner shell fabricated from SA203-E material. Safety factor must be multiplied by 0.93 if inner shell is fabricated from optional SA350-LF3 material.

Note: Thermal stresses are included for inner containment shell per ASME Section III, Subsection NB, but excluded in intermediate shell per ASME Code, Section III, Subsection NF.

Table 2.6.6

STRESS INTENSITY RESULTS FOR CONFINEMENT BOUNDARY -  
INTERNAL PRESSURE ONLY (Load Case E1.a in Table 2.1.7)

Component Locations (Per Fig. 2.6.20)	Calculated Value of Stress Intensity (psi)	Category	Table 2.1.19 Allowable Value (psi) <sup>†</sup>	Safety Factor (Allowable/Calculated)
<u>Top Lid<sup>††</sup></u>				
A	3,282	$P_L + P_b$	30,000	9.14
Neutral Axis	40.4	$P_m$	20,000	495
B	3,210	$P_L + P_b$	30,000	9.34
C	1,374	$P_L + P_b$	30,000	21.8
Neutral Axis	1,462	$P_m$	20,000	13.6
D	5,920	$P_L + P_b$	30,000	5.06
<u>Baseplate</u>				
E	19,683	$P_L + P_b$	30,000	1.5
Neutral Axis	412	$P_m$	20,000	48.5
F	20,528	$P_L + P_b$	30,000	1.5
G	9,695	$P_L + P_b$	30,000	3.1
Neutral Axis	2,278	$P_m$	20,000	8.8
H	8,340	$P_L + P_b$	30,000	3.5

<sup>†</sup> Stress intensity taken at 300 degrees F in this comparison.

<sup>††</sup> The stresses in the top lid are reported for the dual lid configuration. The stresses for the single lid configuration are 50% less (see Subsection 2.6.1.3.1.2 for further details).

Table 2.6.6 Continued

STRESS INTENSITY RESULTS FOR CONFINEMENT BOUNDARY -  
INTERNAL PRESSURE ONLY (Load Case E1.a in Table 2.1.7)

Component Locations (Per Fig.2.6.20)	Calculated Value of Stress Intensity (psi)	Category	Table 2.1.19 Allowable Value (psi) <sup>†</sup>	Safety Factor (Allowable/Calculated)
<u>Canister</u>				
I	6,860	P <sub>m</sub>	18,700	2.72
Upper Bending Boundary Layer Region	7,189	P <sub>L</sub> + P <sub>b</sub> + Q	30,000	4.2
	7,044	P <sub>L</sub> + P <sub>b</sub>	20,000	2.8
Lower Bending Boundary Layer Region	43,986	P <sub>L</sub> + P <sub>b</sub> + Q	60,000	1.36
	10,621	P <sub>L</sub> + P <sub>b</sub>	30,000	2.82

<sup>†</sup> Allowable stress intensity based at 300 degrees F except for Location I where allowable stress intensity values are based on 400 degree F.

Table 2.6.7

PRIMARY AND SECONDARY STRESS INTENSITY RESULTS FOR  
HELIUM RETENTION BOUNDARY - PRESSURE PLUS THERMAL LOADING (Load Case E1.c in Table 2.1.7)

Component Locations (Per Fig. 2.6.20)	Calculated Value of Stress Intensity (psi)	Category	Table 2.1.19 Allowable Value (psi) <sup>†</sup>	Safety Factor (Allowable/Calculated)
<u>Top Lid<sup>††</sup></u>				
A	4,634	$P_L + P_b + Q$	60,000	12.9
Neutral Axis	1,464	$P_L$	30,000	20.4
B	2,140	$P_L + P_b + Q$	60,000	28.0
C	1,942	$P_L + P_b + Q$	60,000	30.8
Neutral Axis	3,528	$P_L$	30,000	8.50
D	7,048	$P_L + P_b + Q$	60,000	8.51
<u>Baseplate</u>				
E	22,434	$P_L + P_b + Q$	60,000	2.67
Neutral Axis	1,743	$P_L$	30,000	17.2
F	18,988	$P_L + P_b + Q$	60,000	3.16
G	5,621	$P_m + P_L$	60,000	10.7
Neutral Axis	5,410	$P_L$	30,000	5.55
H	12,128	$P_L + P_b + Q$	60,000	4.95

<sup>†</sup> Allowable stresses based on temperature of 300 degrees F.

<sup>††</sup> The stresses in the top lid are reported for the dual lid configuration. The stresses for the single lid configuration are 50% less (see Subsection 2.6.1.3.1.2 for further details).

Table 2.6.7 Continued

PRIMARY AND SECONDARY STRESS INTENSITY RESULTS FOR  
 HELIUM RETENTION BOUNDARY - PRESSURE PLUS THERMAL LOADING (Load Case E1.c in Table 2.1.7)

Component Locations (Per Fig.2.6.20)	Calculated Value of Stress Intensity (psi)	Category	Table 2.1.19 Allowable Value (psi) <sup>1</sup>	Safety Factor (Allowable/Calculated)
<u>Canister</u>				
I	6,897	P <sub>L</sub>	28,100	4.07
Upper Bending Boundary Layer Region	6,525	P <sub>L</sub> + P <sub>b</sub> + Q	60,000	9.2
	3,351	P <sub>L</sub>	30,000	8.95
Lower Bending Boundary Layer Region	40,070	P <sub>L</sub> + P <sub>b</sub> + Q	60,000	1.5
	6,665	P <sub>L</sub>	30,000	4.5

<sup>1</sup> Allowable stresses based on temperature of 300 degree F except at Location I where the temperatures are based on 400 degrees F.

Table 2.6.8 - FINITE ELEMENT ANALYSIS RESULTS  
 MINIMUM SAFETY FACTORS FOR MPC COMPONENTS UNDER NORMAL CONDITIONS

Component - Stress Result	MPC-24		MPC-68	
	1 Ft. Side Drop, 0 deg Orientation	1 Ft. Side Drop, 45 deg Orientation	1 Ft. Side Drop, 0 deg Orientation	1 Ft. Side Drop, 45 deg Orientation
	Load Case F2.a or E2.a	Load Case F2.b or E2.b	Load Case F2.a or E2.a	Load Case F2.b or E2.b
Fuel Basket – Primary Membrane ( $P_m$ )	4.12	5.64	4.42	6.15
Fuel Basket - Local Membrane Plus Primary Bending ( $P_L + P_b$ )	1.73	1.87	2.42	1.50
Enclosure Vessel - Primary Membrane ( $P_m$ )	2.71	2.71	2.67	2.72
Enclosure Vessel - Local Membrane Plus Primary Bending ( $P_L + P_b$ )	3.30	3.29	2.17	1.80
Basket Supports - Primary Membrane ( $P_m$ )	N/A	N/A	5.32	5.33
Basket Supports - Local Membrane Plus Primary Bending ( $P_L + P_b$ )	N/A	N/A	1.67	2.16

Table 2.6.8 (Continued) - FINITE ELEMENT ANALYSIS RESULTS  
 MINIMUM SAFETY FACTORS FOR MPC COMPONENTS UNDER NORMAL CONDITIONS

Component - Stress Result	MPC-32		MPC-24E/EF	
	1 Ft. Side Drop, 0 deg Orientation	1 Ft. Side Drop, 45 deg Orientation	1 Ft. Side Drop, 0 deg Orientation	1 Ft. Side Drop, 45 deg Orientation
	Load Case F2.a or E2.a	Load Case F2.b or E2.b	Load Case F2.a or E2.a	Load Case F2.b or E2.b
Fuel Basket - Primary Membrane ( $P_m$ )	4.05	5.65	4.04	5.55
Fuel Basket - Local Membrane Plus Primary Bending ( $P_L + P_b$ )	1.57	1.29	1.69	1.83
Enclosure Vessel - Primary Membrane ( $P_m$ )	2.55	2.69	2.70	2.70
Enclosure Vessel - Local Membrane Plus Primary Bending ( $P_L + P_b$ )	1.41	1.63	3.04	3.13
Basket Supports - Primary Membrane ( $P_m$ )	3.96	5.33	N/A	N/A
Basket Supports - Local Membrane Plus Primary Bending ( $P_L + P_b$ )	3.49	3.12	N/A	N/A

Table 2.6.9 - FINITE ELEMENT ANALYSIS RESULTS  
 MINIMUM SAFETY FACTORS FOR OVERPACK COMPONENTS UNDER NORMAL CONDITIONS (Hot Environment)

Component – Stress Result	Hot Environment Load Case 1	1 Ft. Side Drop Load Case 3
Lid - Local Membrane Plus Primary Bending ( $P_L + P_b$ )	2.87	2.14
Inner Shell - Local Membrane Plus Primary Bending ( $P_L + P_b$ )	12.1*	3.24*
Inner Shell - Primary Membrane ( $P_m$ )	13.7*	3.53*
Intermediate Shells - Local Membrane Plus Primary Bending ( $P_L + P_b$ )	17.3	2.51
Baseplate - Local Membrane Plus Primary Bending ( $P_L + P_b$ )	11.2	6.28
Enclosure Shell - Primary Membrane ( $P_m$ )	35.2	3.24

\* Applicable to inner shell fabricated from SA203-E material. Safety factor must be multiplied by 0.93 if inner shell is fabricated from optional SA350-LF3 material.

Table 2.6.9 (Continued) - FINITE ELEMENT ANALYSIS RESULTS

## MINIMUM SAFETY FACTORS FOR OVERPACK COMPONENTS UNDER NORMAL CONDITIONS (Hot Environment)

Component - Stress Result	Hot Environment	1 Ft. Side Drop
	Load Case 1	Load Case 3
Lid - Local Membrane Plus Primary Bending Plus Secondary ( $P_L + P_b + Q$ )	2.14	1.90
Inner Shell - Local Membrane Plus Primary Bending Plus Secondary ( $P_L + P_b + Q$ )	2.69*	2.84*
Intermediate Shells - Local Membrane Plus Primary Bending Plus Secondary ( $P_L + P_b + Q$ excluding thermal stress)	34.5	5.01
Baseplate - Local Membrane Plus Primary Bending Plus Secondary ( $P_L + P_b + Q$ )	1.81	1.68
Enclosure Shell - Local Membrane Plus Primary Bending Plus Secondary ( $P_L + P_b + Q$ )	1.97	1.88

\* Applicable to inner shell fabricated from SA203-E material. Safety factor must be multiplied by 0.93 if inner shell is fabricated from optional SA350-LF3 material.

Table 2.6.10

SAFETY FACTORS FROM MISCELLANEOUS MPC CALCULATIONS -  
NORMAL CONDITIONS OF TRANSPORT - HOT ENVIRONMENT

Item	Loading	Safety Factor	Location in SAR Where Details are Provided
Fuel Support Spacers	1' Drop (Load Case F2 in Table 2.1.6)	2.75	Subsection 2.6.1.3.1.3
MPC Stability	Code Case N-284 (Load Case E1.b in Table 2.1.7)	1.2	Subsection 2.6.1.3.1.3

Table 2.6.11

MINIMUM SAFETY FACTORS FROM MISCELLANEOUS OVERPACK CALCULATIONS  
NORMAL HOT CONDITIONS OF TRANSPORT

Item	Loading	Safety Factor	Location in SAR Where Details are Provided
Fabrication Stress in Inner Shell	Fabrication	4.3	Subsection 2.6.1.3.2.2
Closure Bolt	Average Tensile Stress Including Pre-Load	1.44	Subsection 2.6.1.3.2.3

Table 2.6.12 - FINITE ELEMENT ANALYSIS RESULTS  
 MINIMUM SAFETY FACTORS FOR OVERPACK COMPONENTS UNDER NORMAL CONDITIONS (Cold Environment)

Component - Stress Result	Super-Cold Environment Load Case 2	1 Ft. Side Drop Load Case 4
Lid - Local Membrane Plus Primary Bending ( $P_L + P_b$ )	4.55	2.97
Inner Shell - Local Membrane Plus Primary Bending ( $P_L + P_b$ )	14.4	3.37
Inner Shell - Primary Membrane ( $P_m$ )	16.5	3.53
Intermediate Shells - Local Membrane Plus Primary Bending ( $P_L + P_b$ )	21.7	2.48
Baseplate - Local Membrane Plus Primary Bending ( $P_L + P_b$ )	722.8	7.84
Enclosure Shell - Primary Membrane ( $P_m$ )	50.2	3.21

Table 2.6.12 (Continued)

FINITE ELEMENT ANALYSIS RESULTS  
 MINIMUM SAFETY FACTORS FOR OVERPACK COMPONENTS UNDER NORMAL CONDITIONS (Cold Environment)

Component - Stress Result	Super-Cold Environment	1 Ft. Side Drop
	Load Case 2	Load Case 4
Lid - Local Membrane Plus Primary Bending Plus Secondary ( $P_L + P_b + Q$ )	8.79	5.79
Inner Shell - Local Membrane Plus Primary Bending Plus Secondary ( $P_L + P_b + Q$ )	15.5	6.36
Intermediate Shells - Local Membrane Plus Primary Bending Plus Secondary ( $P_L + P_b + Q$ excluding thermal stress)	43.24	4.95
Baseplate - Local Membrane Plus Primary Bending Plus Secondary ( $P_L + P_b + Q$ )	83.8	15.1
Enclosure Shell - Local Membrane Plus Primary Bending Plus Secondary ( $P_L + P_b + Q$ )	21.4	7.67

Table 2.6.13

MINIMUM SAFETY FACTORS INCLUDING FABRICATION STRESS - PRIMARY PLUS SECONDARY  
STRESS INTENSITY, NORMAL COLD CONDITIONS OF TRANSPORT

Case	Inner Shell Exterior Surface	Intermediate Shell
2 Pressure (Secondary Stress)	3.38	4.22
4 1 ft. Side Drop (Secondary Stress)	2.58	2.41

Note: Thermal stresses are included for inner containment shell per ASME Section III, Subsection NB, but excluded in intermediate shell per ASME Code, Section III, Subsection NF.

Table 2.6.14

MISCELLANEOUS SAFETY FACTOR FOR OVERPACK			
Item	Loading	Safety Factor	Location in SAR Where Details are Provided
Outer Enclosure Panels	Reduced External Pressure	60.6	Subsection 2.6.3

**Temperature Distribution for MPC Thermal Stress Analysis**

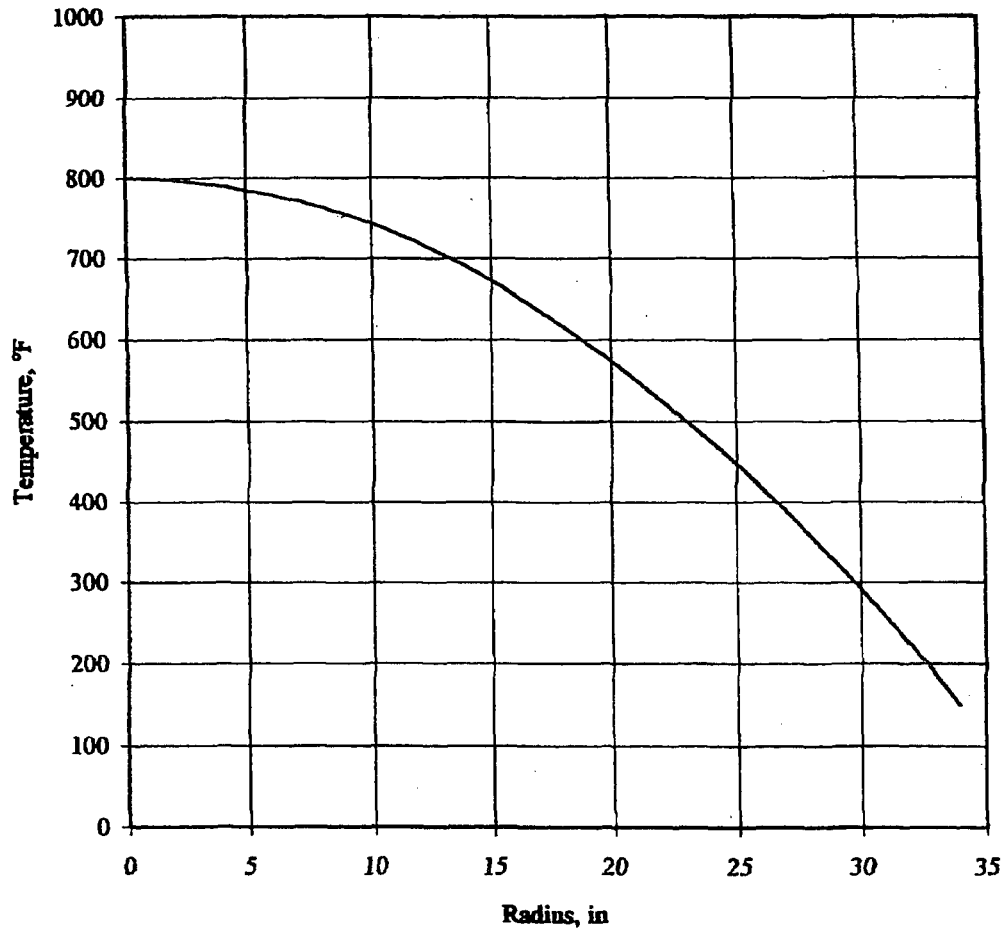


**FIGURE 2.6.1; TEMPERATURE DISTRIBUTION FOR MPC THERMAL STRESS ANALYSIS**

REPORT HI-951251

REVISION 4

**Temperature Distribution for Overpack Thermal Stress Analysis**

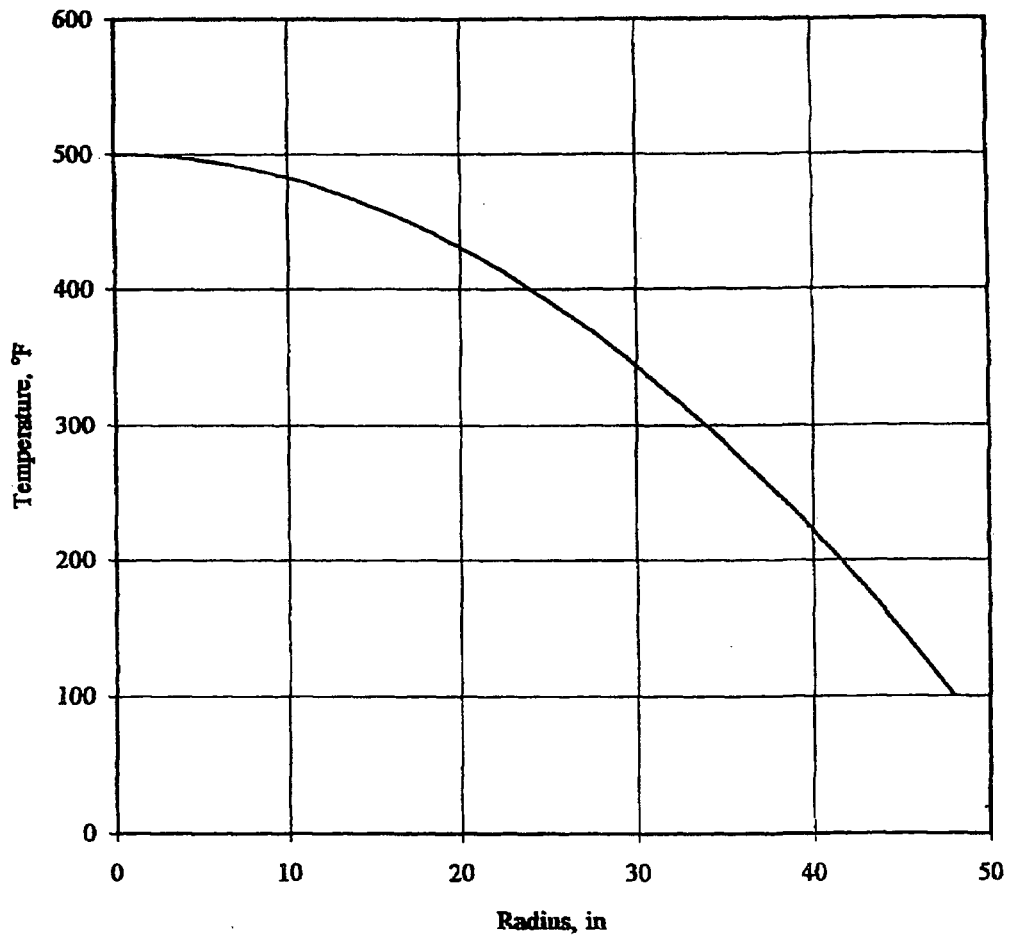
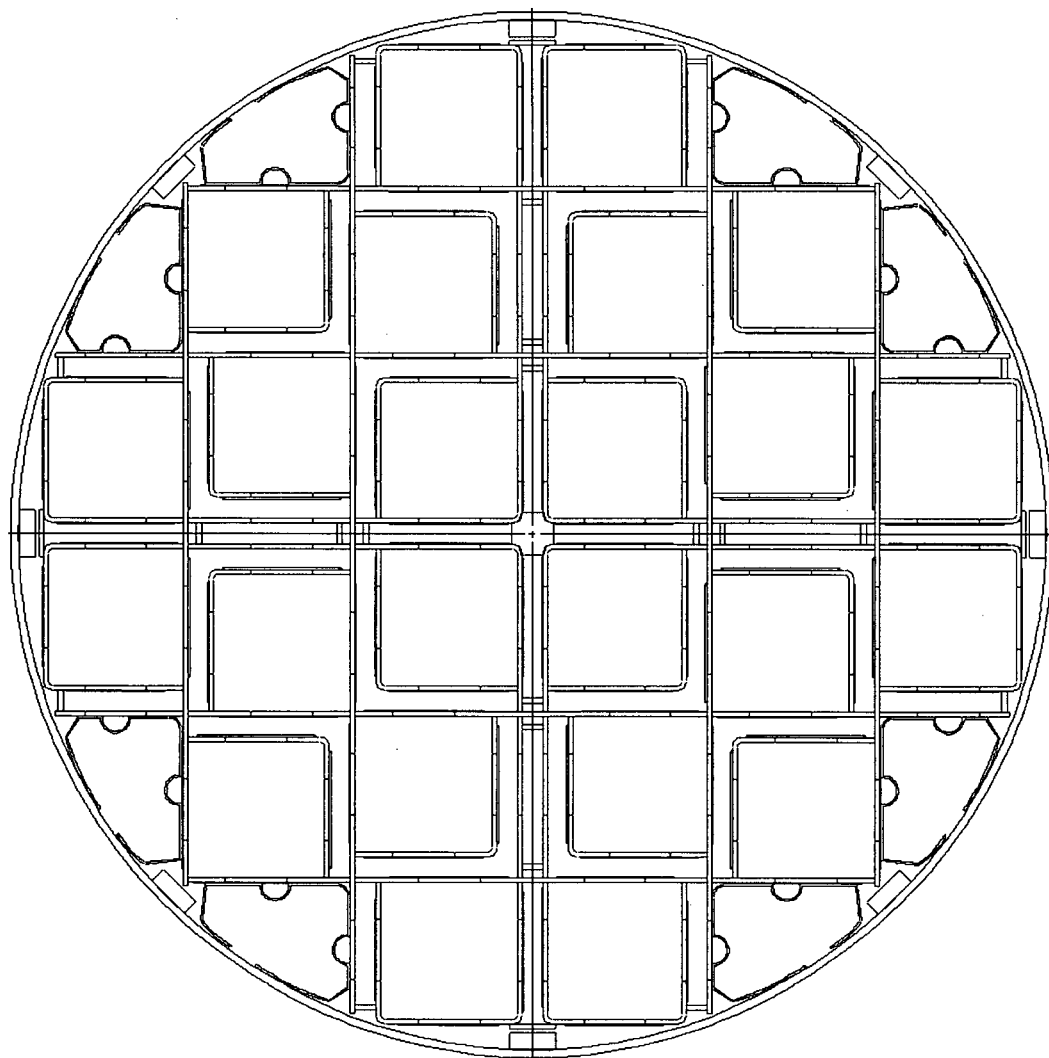


**FIGURE 2.6.2; TEMPERATURE DISTRIBUTION FOR OVERPACK THERMAL STRESS ANALYSIS**



---

Note: Heat conduction elements shown in-place for clarity, but they are not considered in the analysis.

**FIGURE 2.6.3; FINITE ELEMENT MODEL OF MPC24/24E/24EF (BASIC MODEL)**

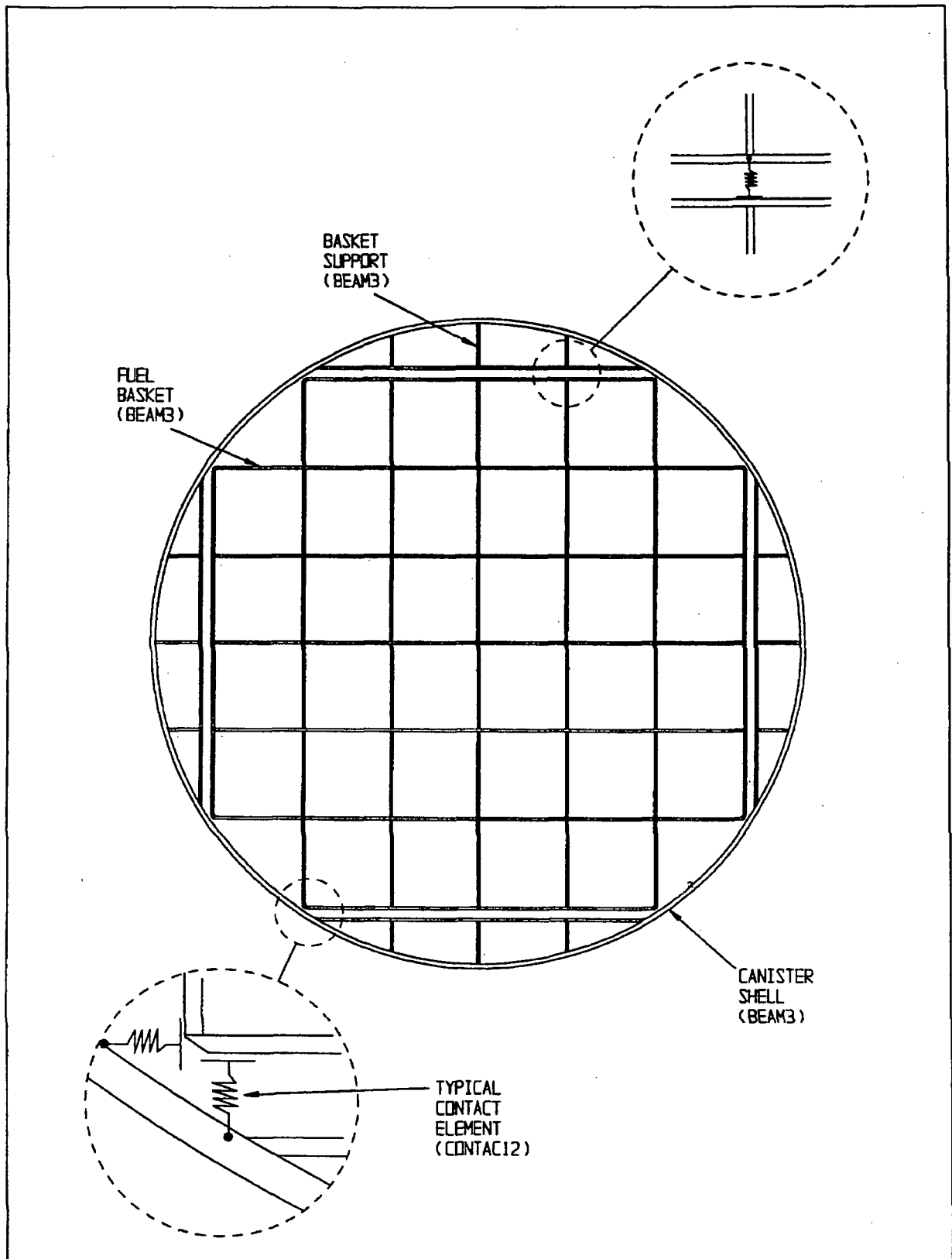


**FIGURE 2.6.4; FINITE ELEMENT MODEL FOR MPC-32  
(BASIC MODEL)**

REPORT HI-951251

REV. 10

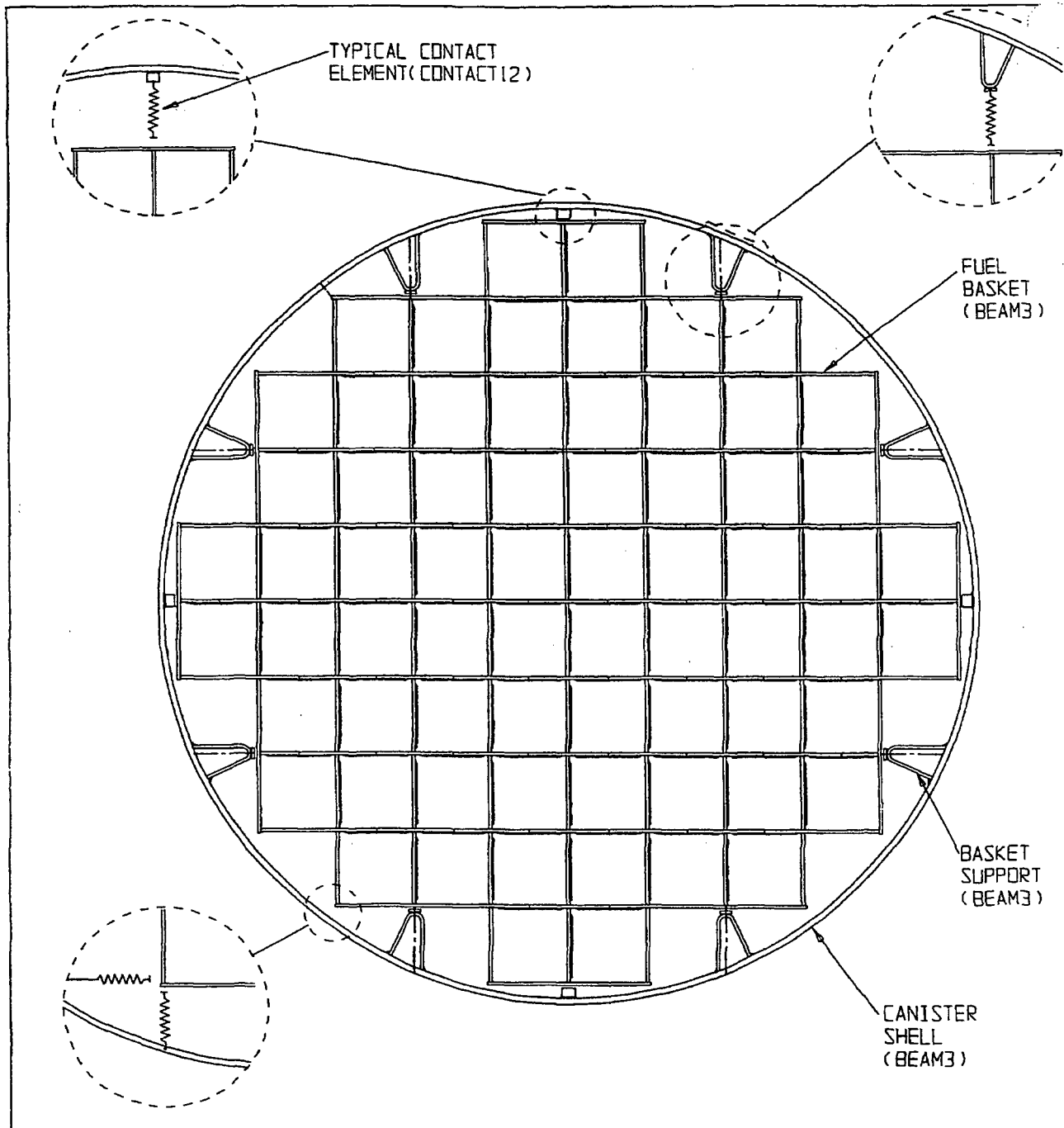


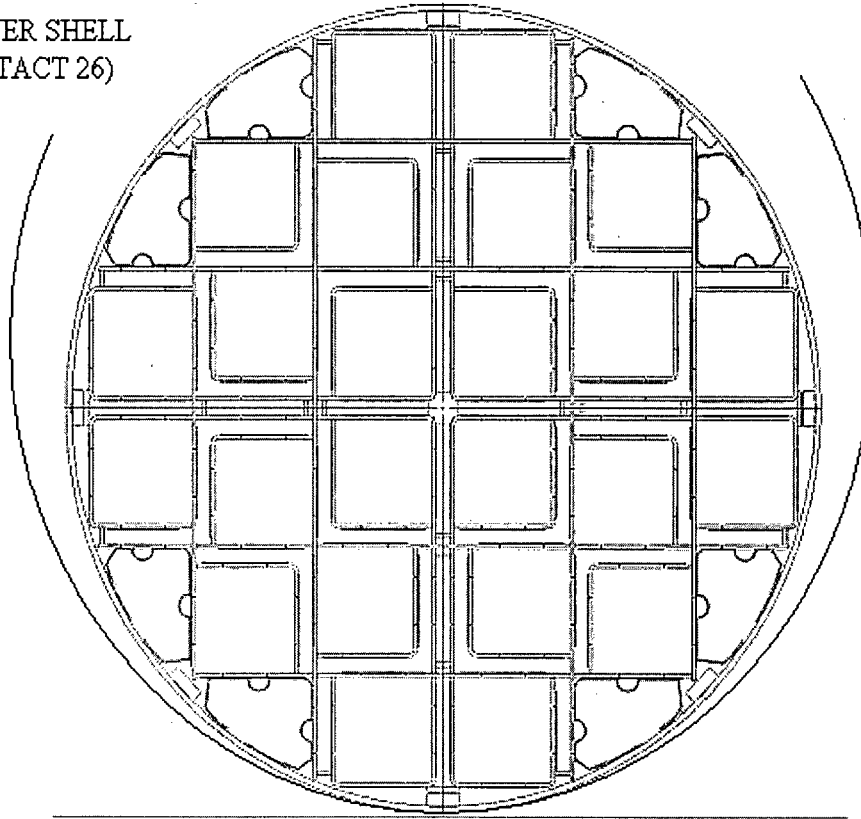
FIGURE 2.6.5; FINITE ELEMENT MODEL OF MPC-68

(BASIC MODEL)

REPORT HI-951251

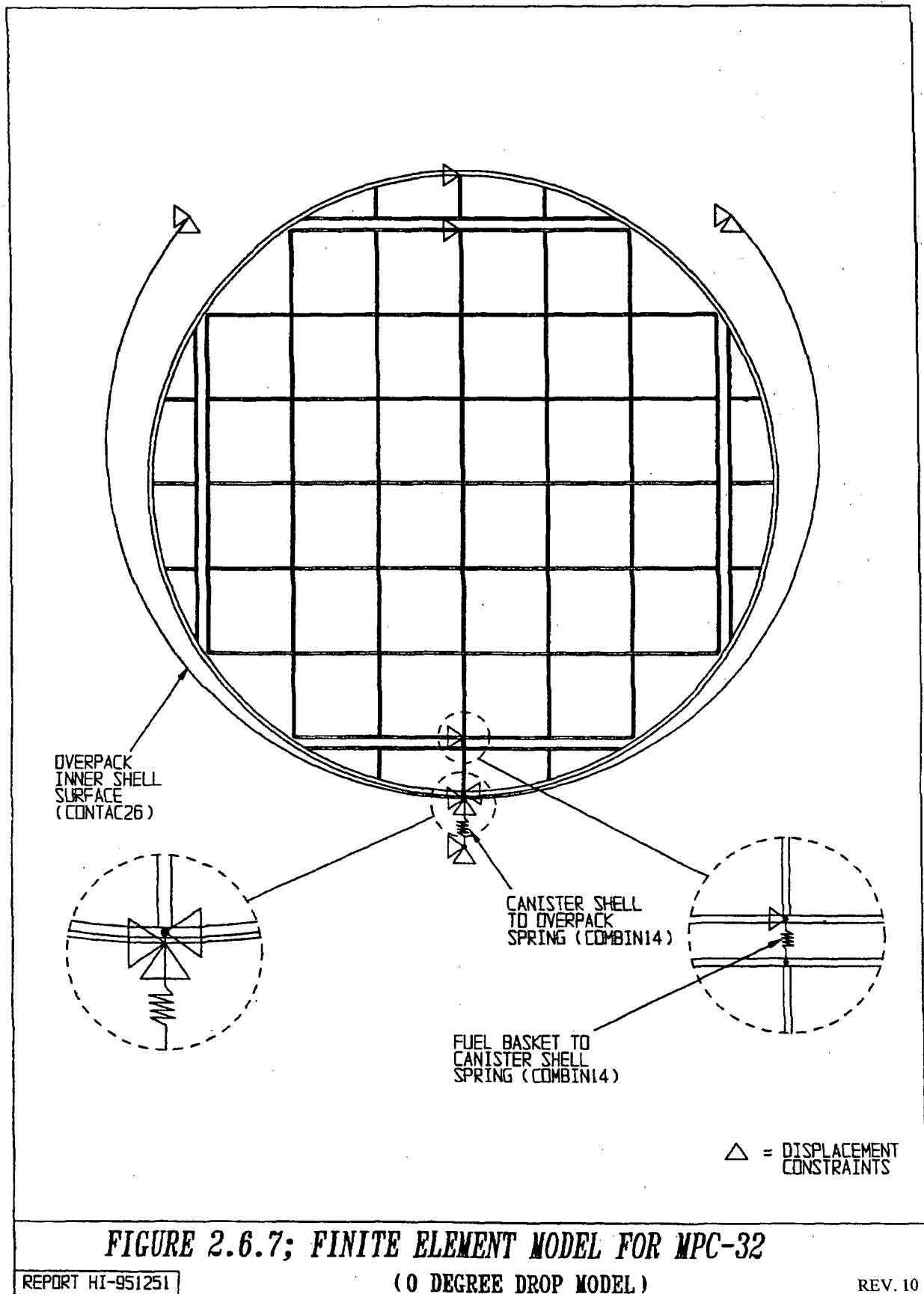
REVISION:

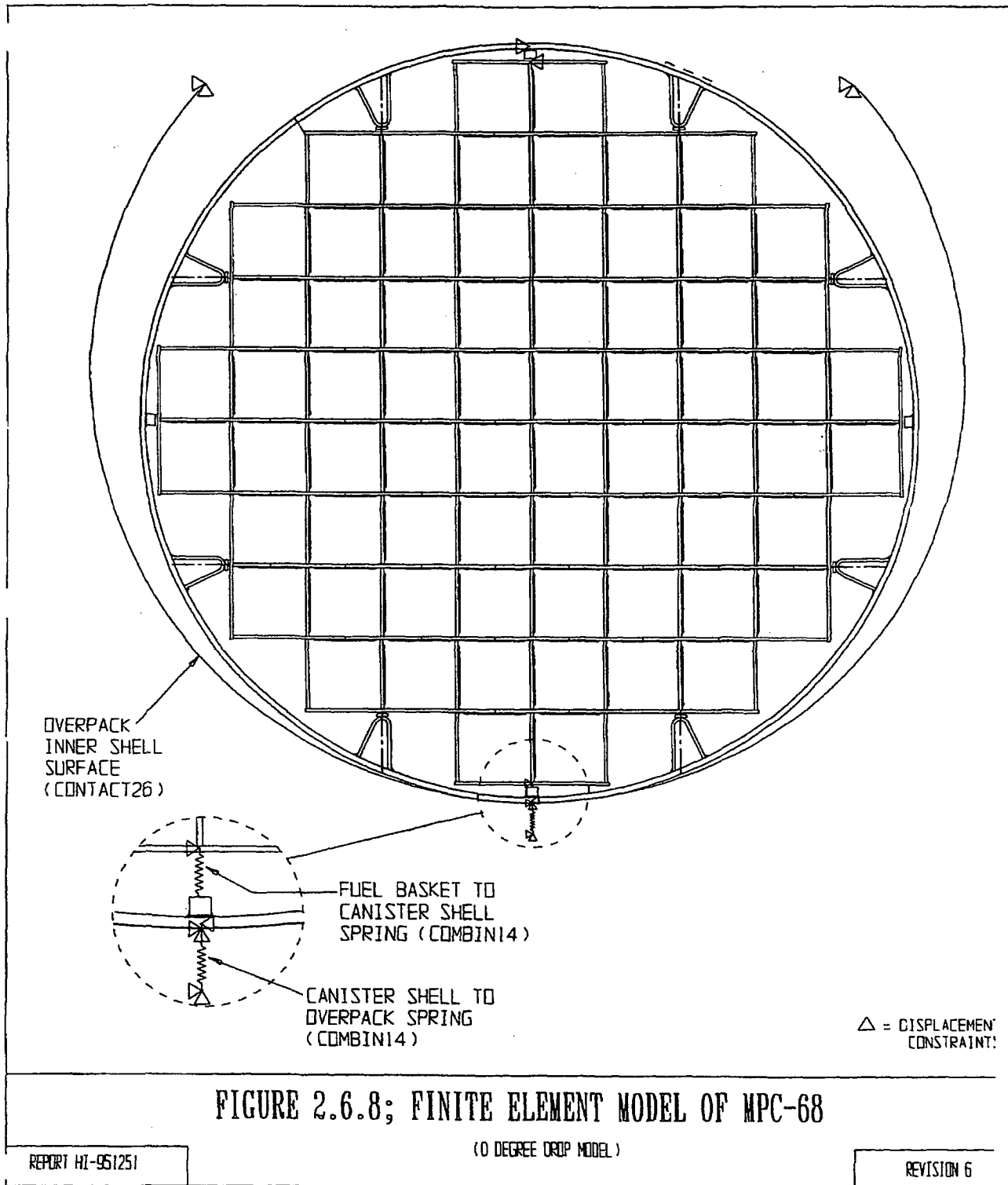
OVERPACK INNER SHELL  
SURFACE (CONTACT 26)



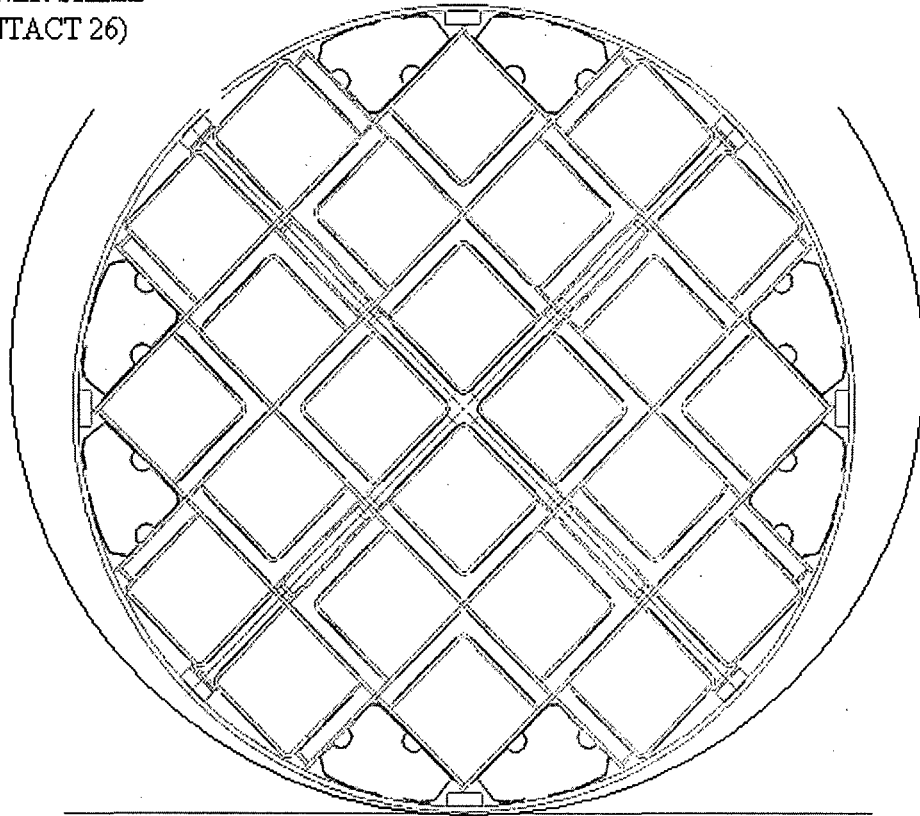
Note: Heat conduction elements shown in-place for clarity, but they are not considered in the analysis.

**FIGURE 2.6.6; FINITE ELEMENT MODEL OF MPC-24/24E/24EF  
(0 DEGREE DROP MODEL)**



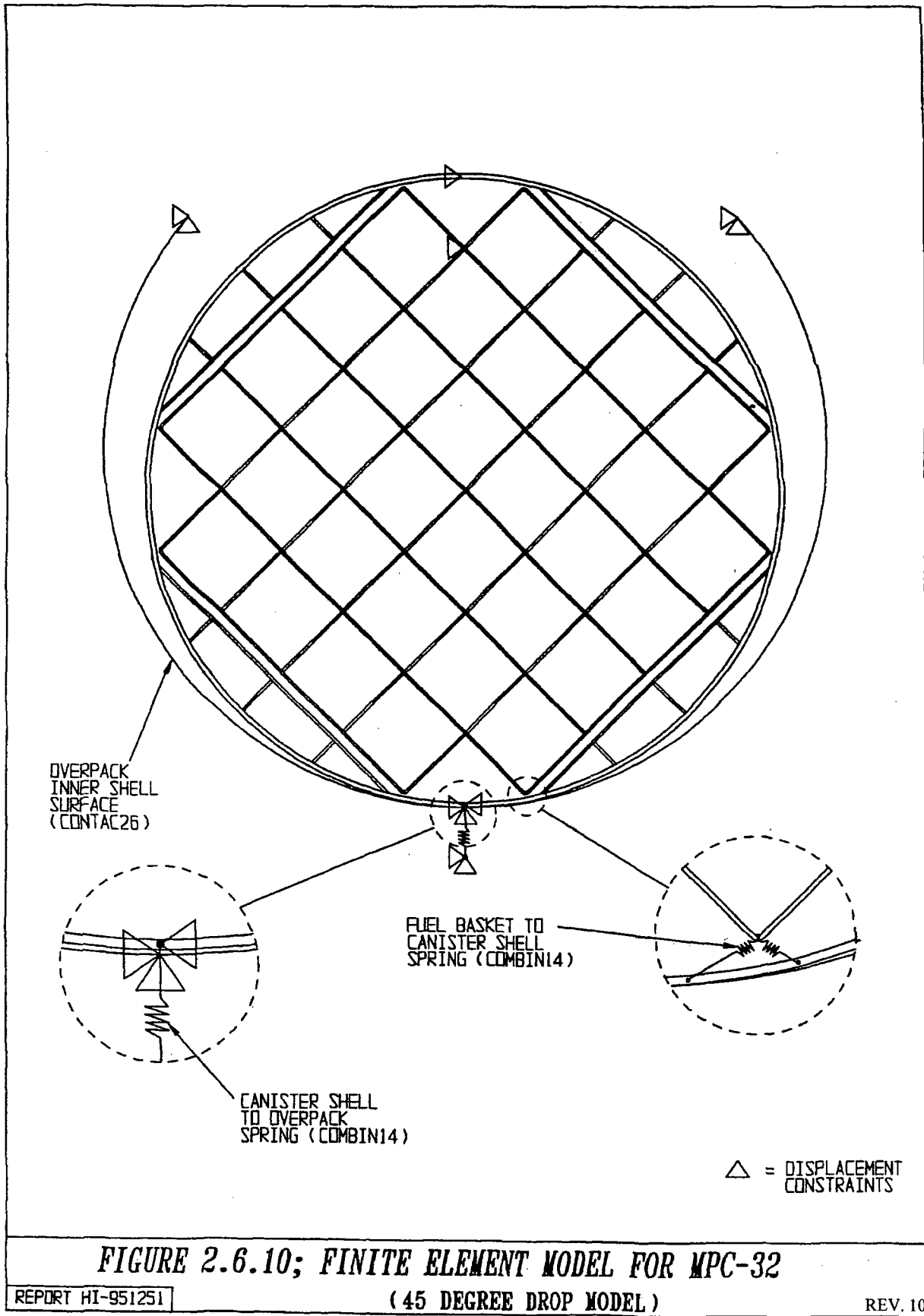


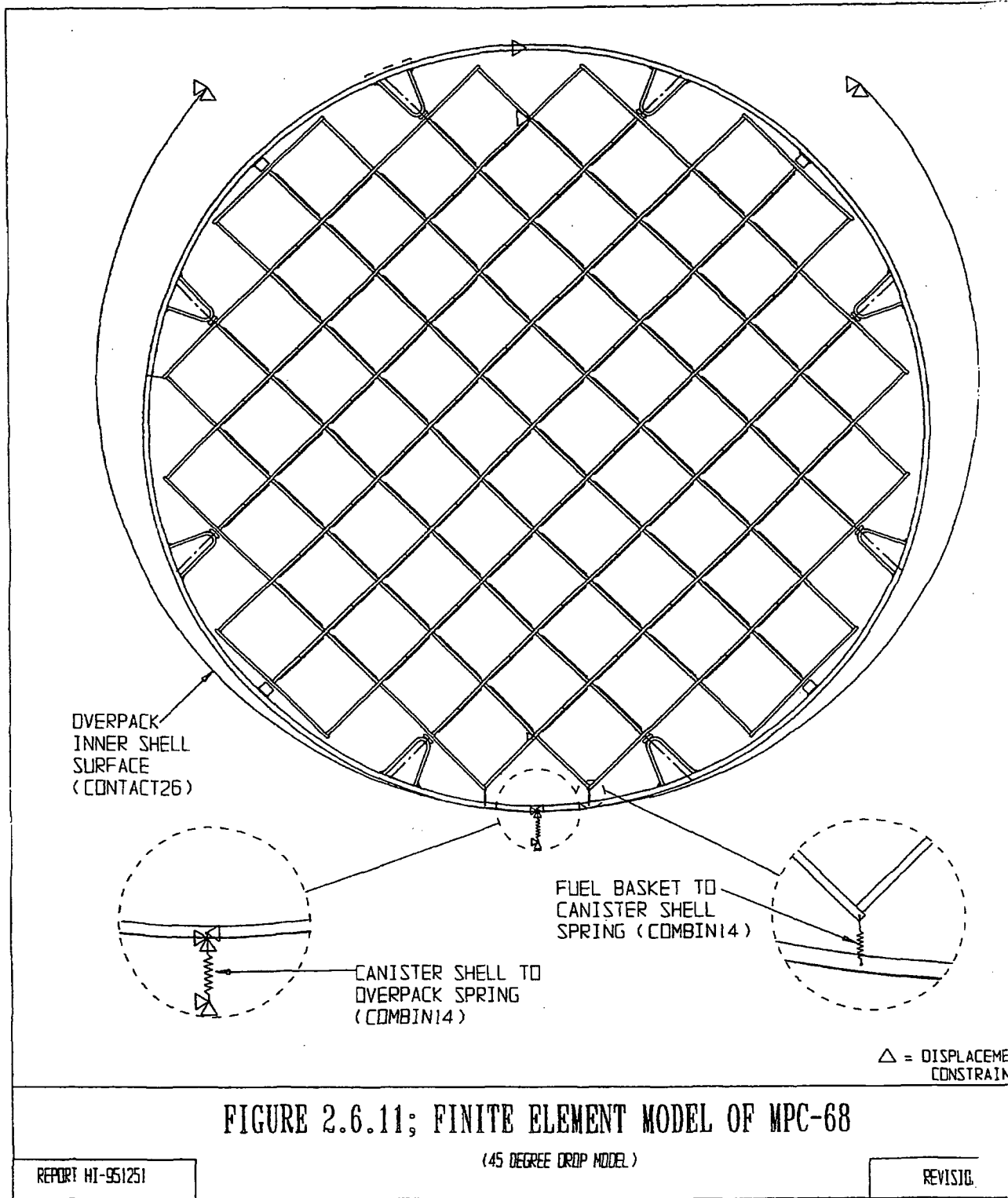
OVERPACK INNER SHELL  
SURFACE (CONTACT 26)



Note: Heat conduction elements shown in-place for clarity, but they are not considered in the analysis.

**FIGURE 2.6.9; FINITE ELEMENT MODEL OF MPC-24/24E/24EF  
(45 DEGREE DROP MODEL)**





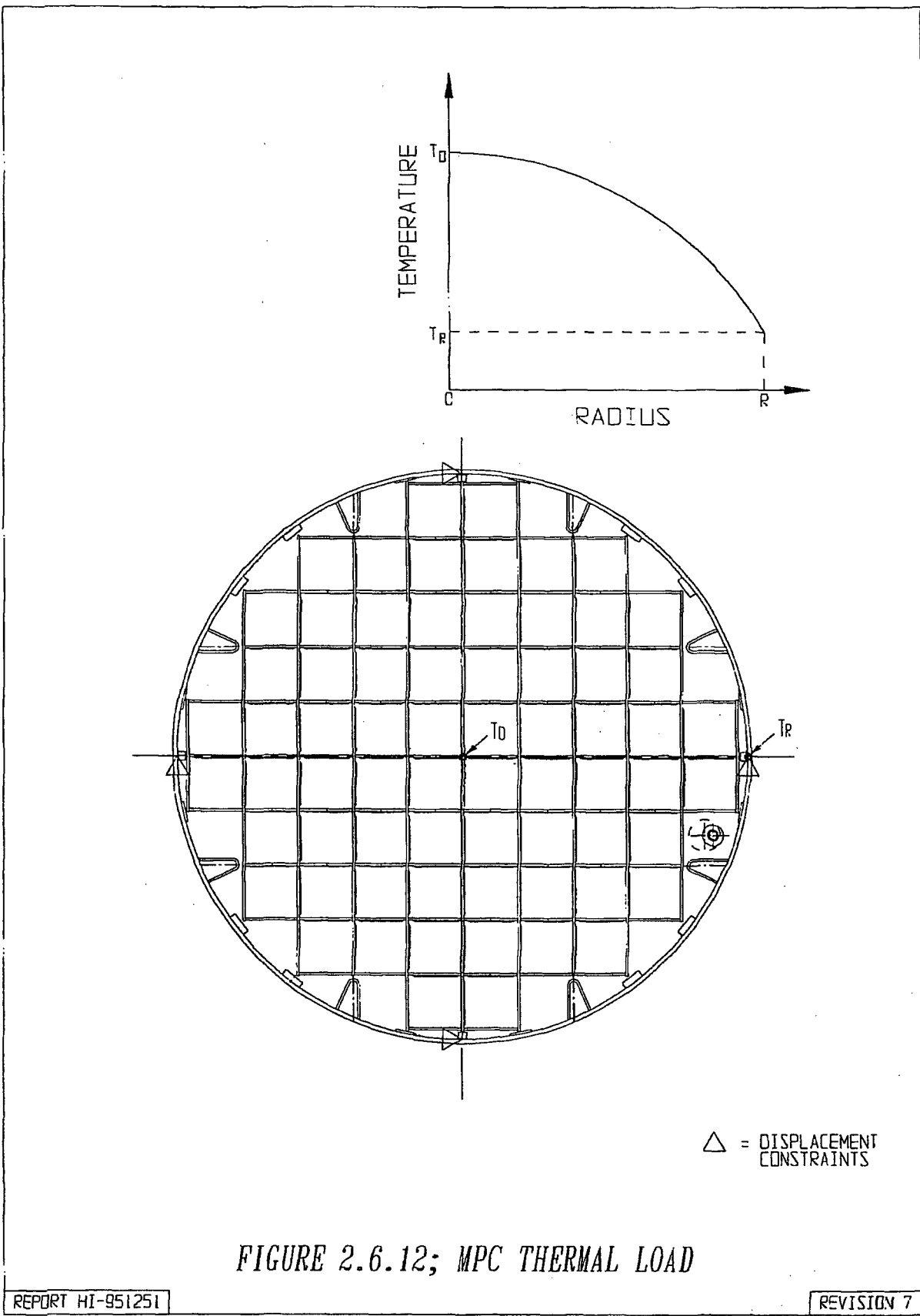


FIGURE 2.6.12; MPC THERMAL LOAD

REPORT HI-951251

REVISION 7

PROJECTS\9514\HI951251\CH\_2\2\_6\_12

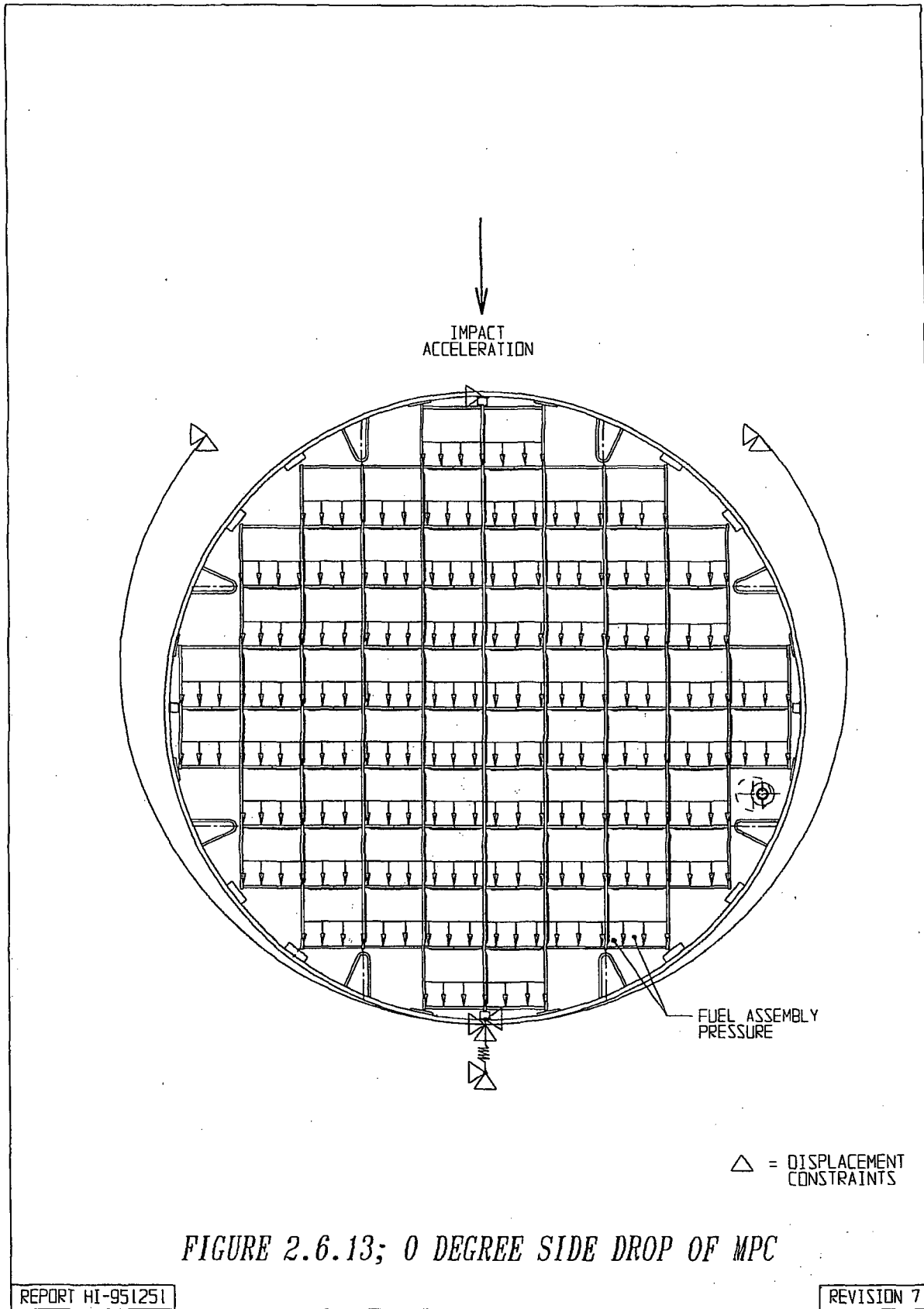
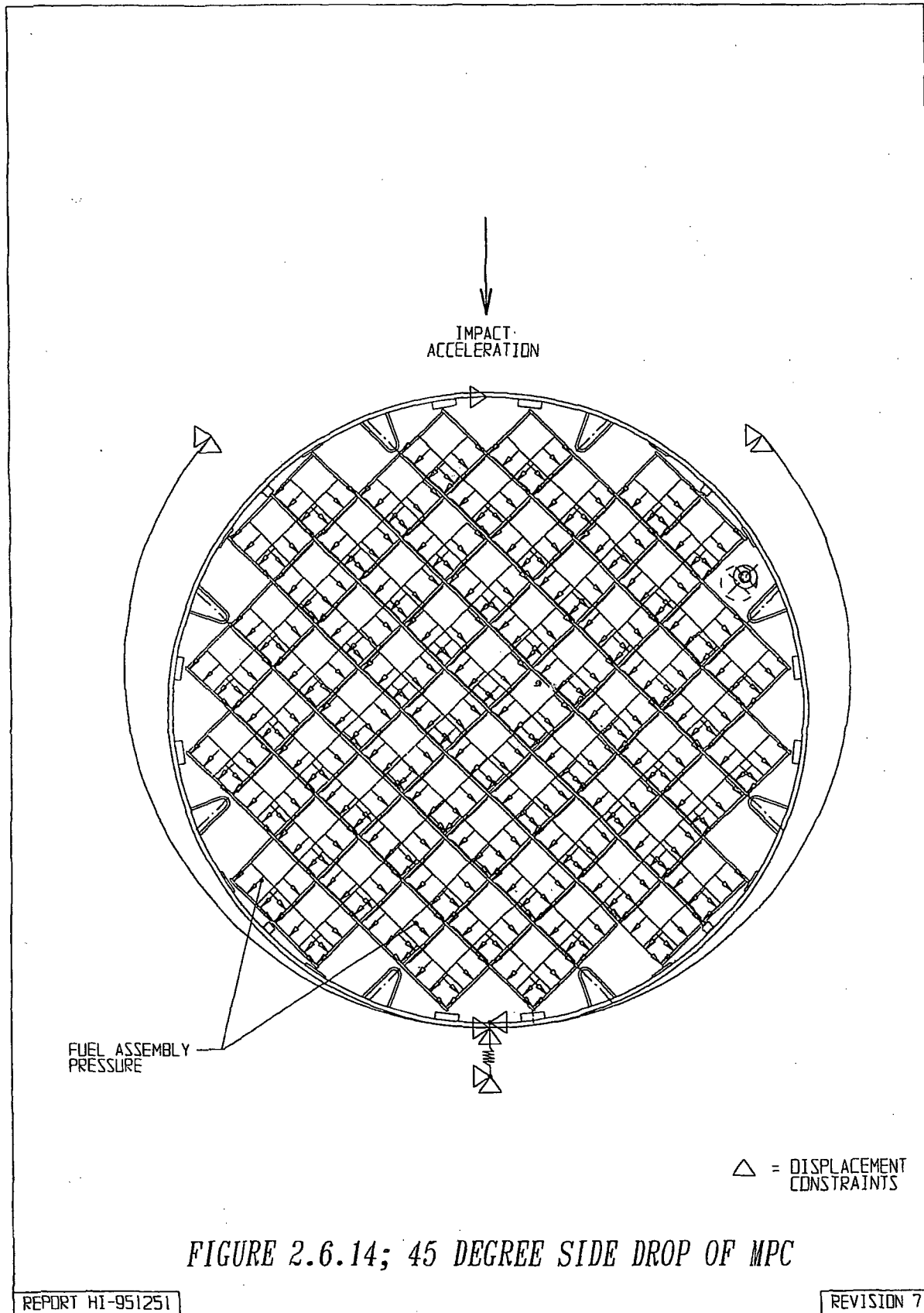


FIGURE 2.6.13; 0 DEGREE SIDE DROP OF MPC

REPORT HI-951251

REVISION 7

\\5014\HI951251\CH\_2\2\_6\_13



\\5014\HI951251\CH 2\2\_6\_14

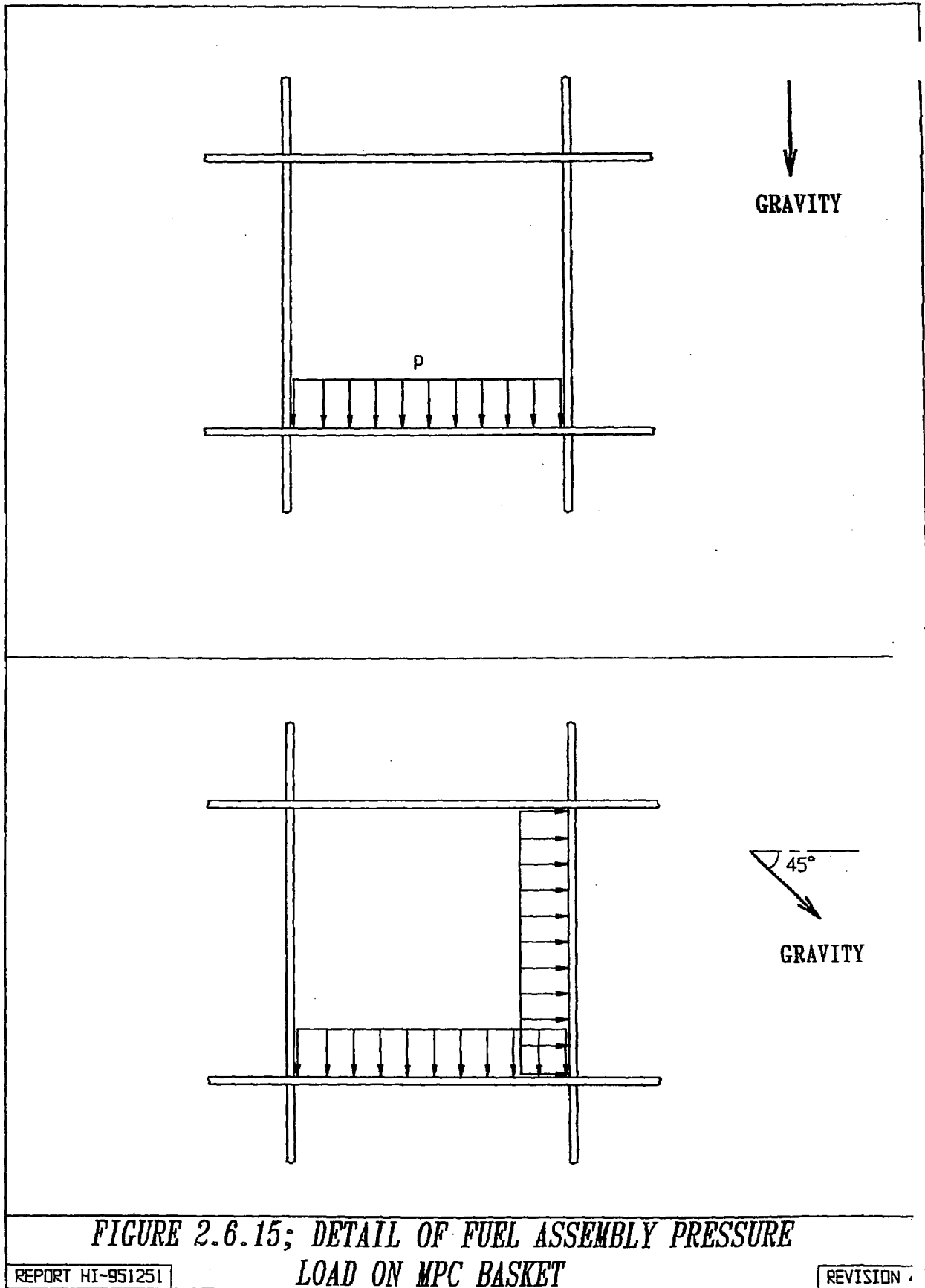


**FIGURE 2.6.15; DETAIL OF FUEL ASSEMBLY PRESSURE  
LOAD ON MPC BASKET**

REPORT HI-951251

REVISION

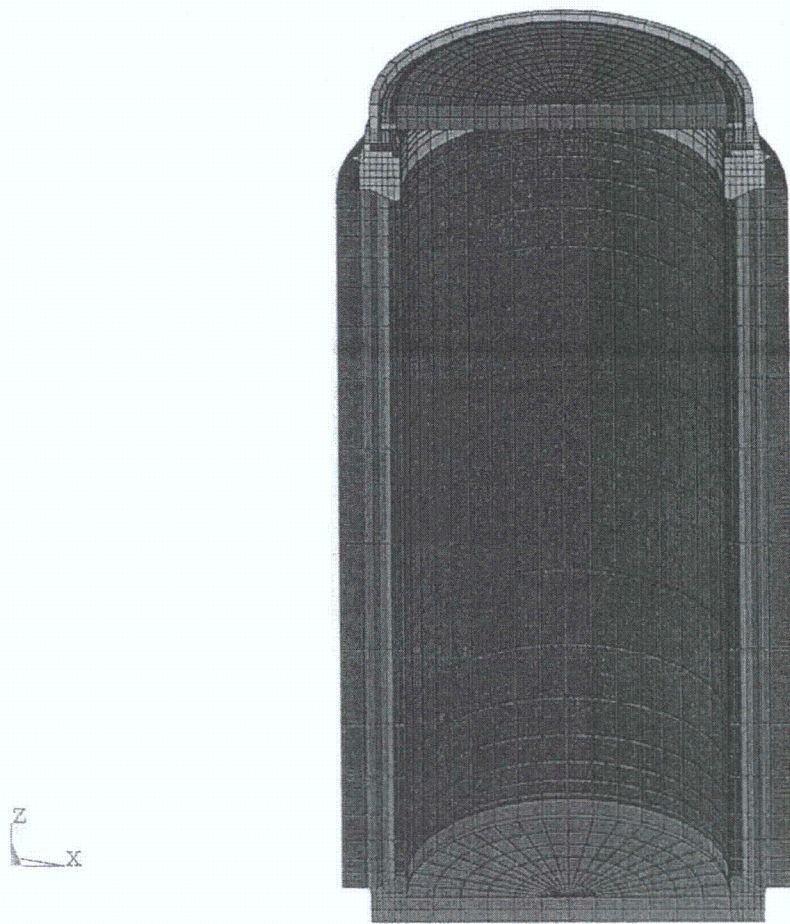


FIGURE 2.6.16 OVERPACK FINITE ELEMENT MODEL

HI-951251

REV. 8

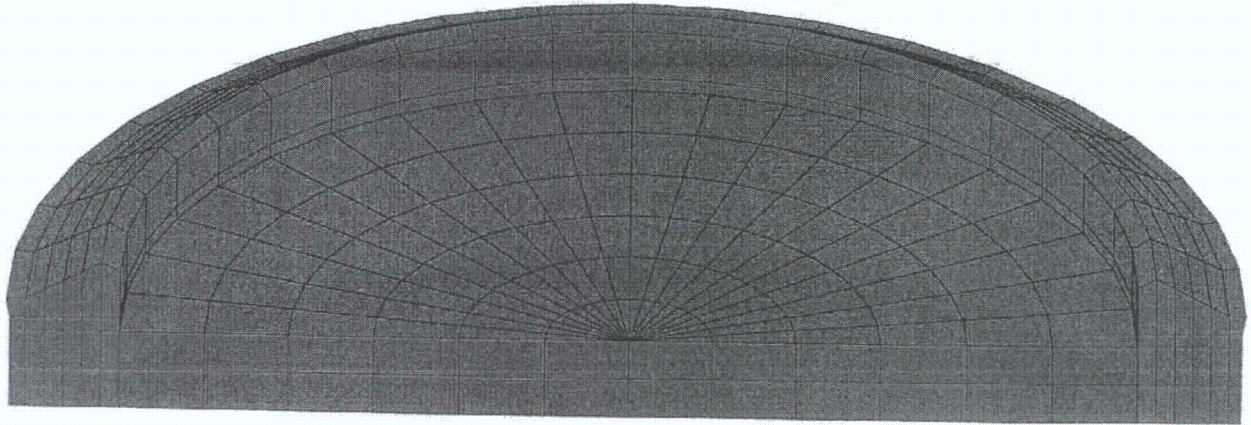


FIGURE 2.6.17 OVERPACK BOTTOM PLATE

HI-951251

REV. 8

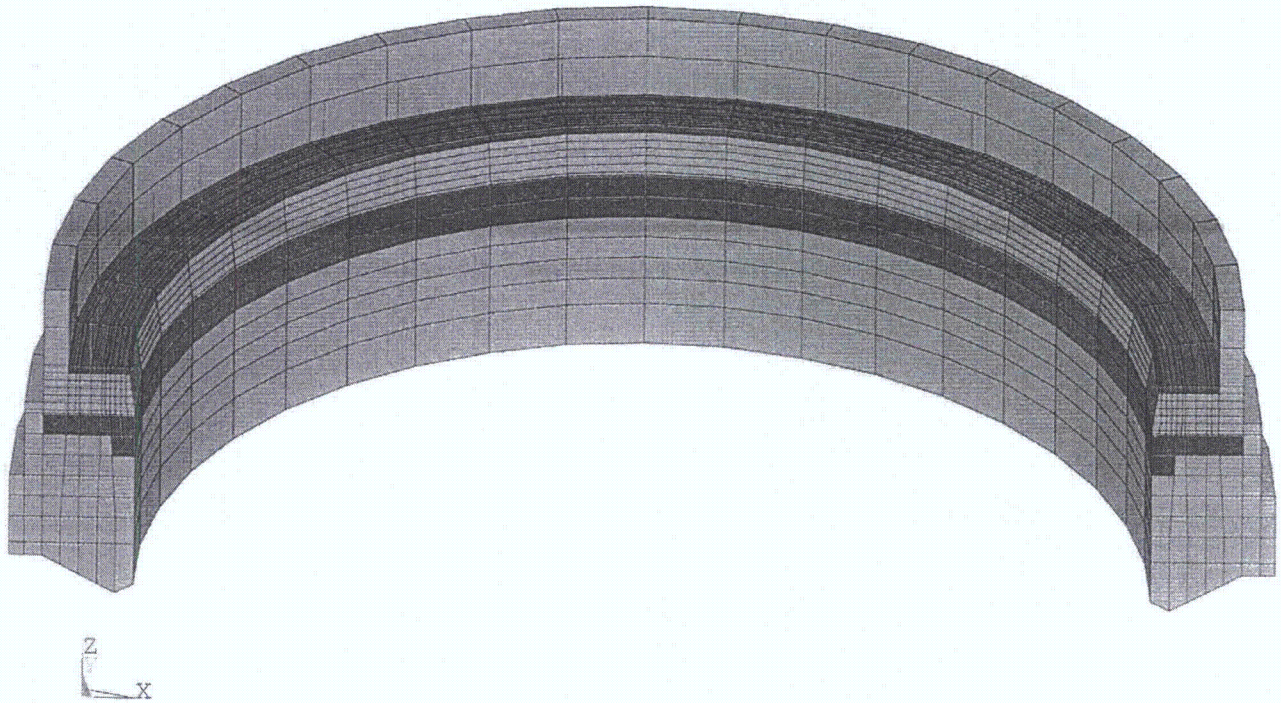


FIGURE 2.6.18 OVERPACK TOP FORGING

HI-951251

REV. 8

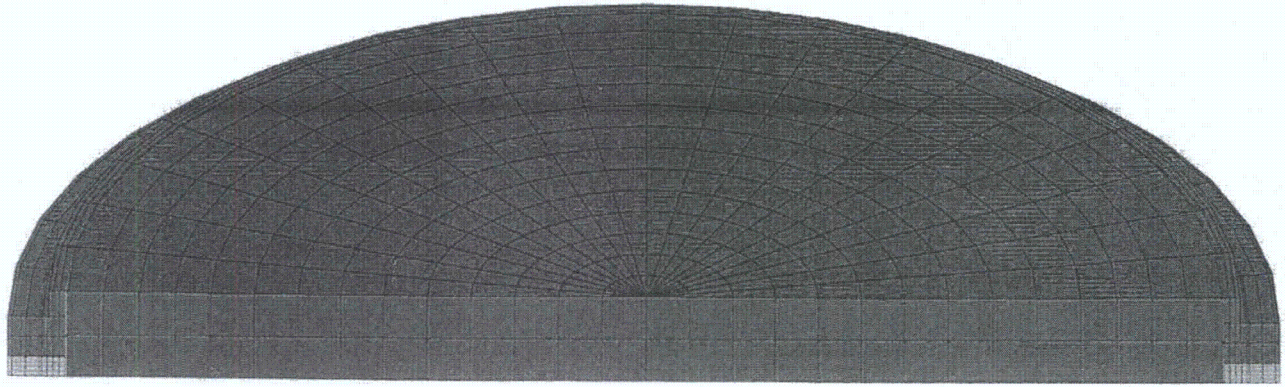


FIGURE 2.6.19 OVERPACK LID

HI-951251

REV. 8

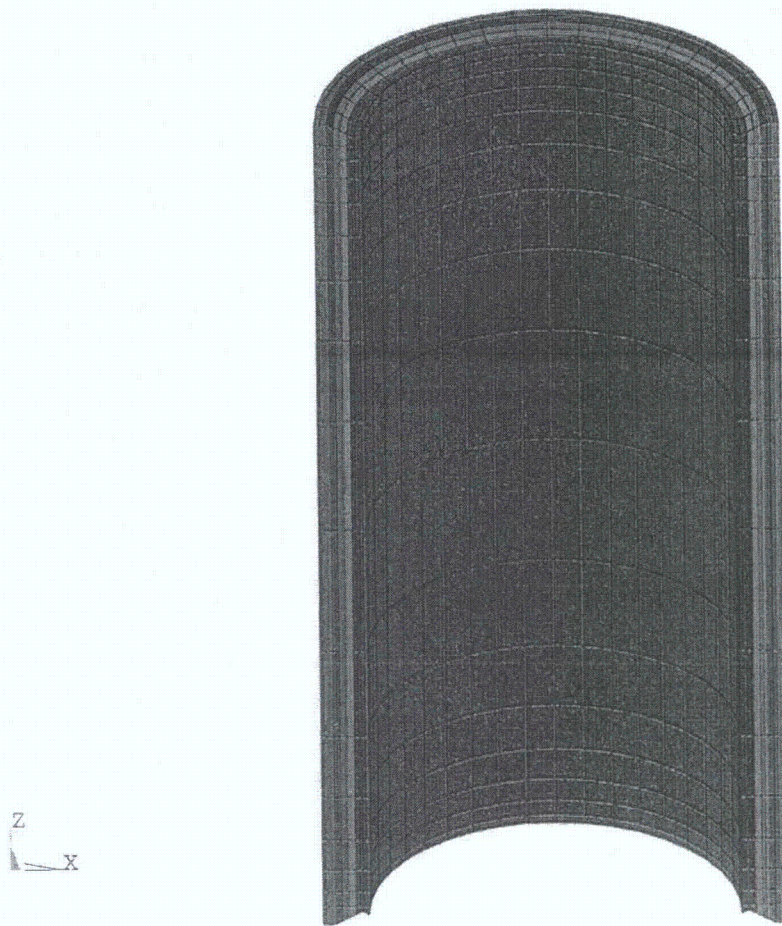


FIGURE 2.6.19A OVERPACK INNER AND INTERMEDIATE SHELLS

HI-951251

REV. 8

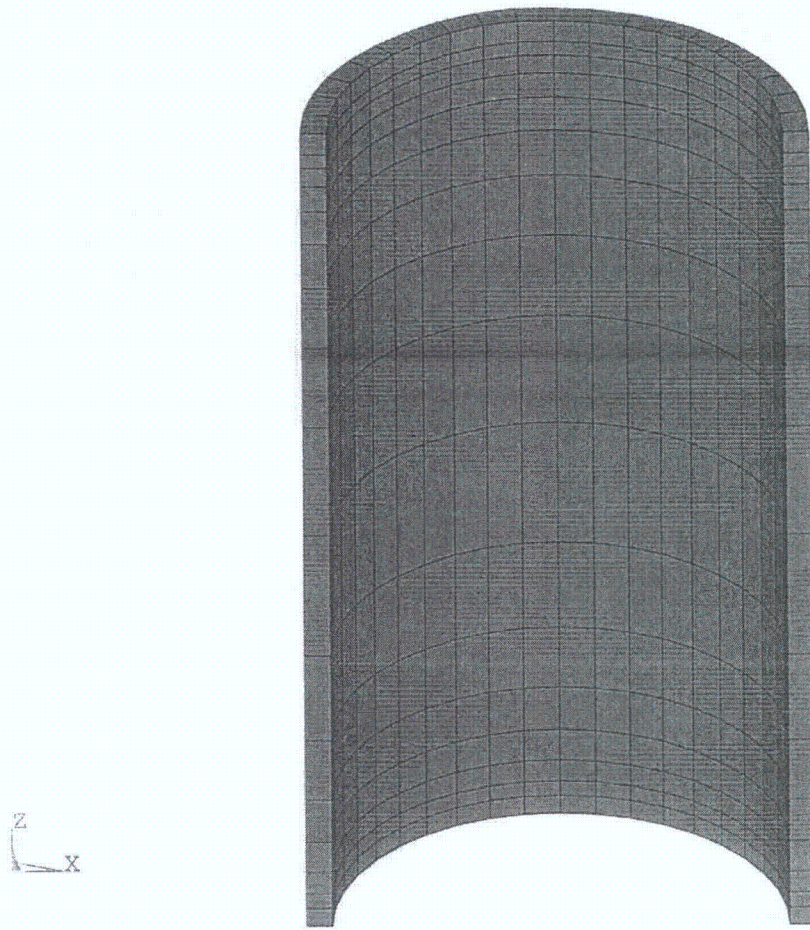


FIGURE 2.6.19B OVERPACK HOLTITE A ELEMENTS

HI-951251

REV. 8

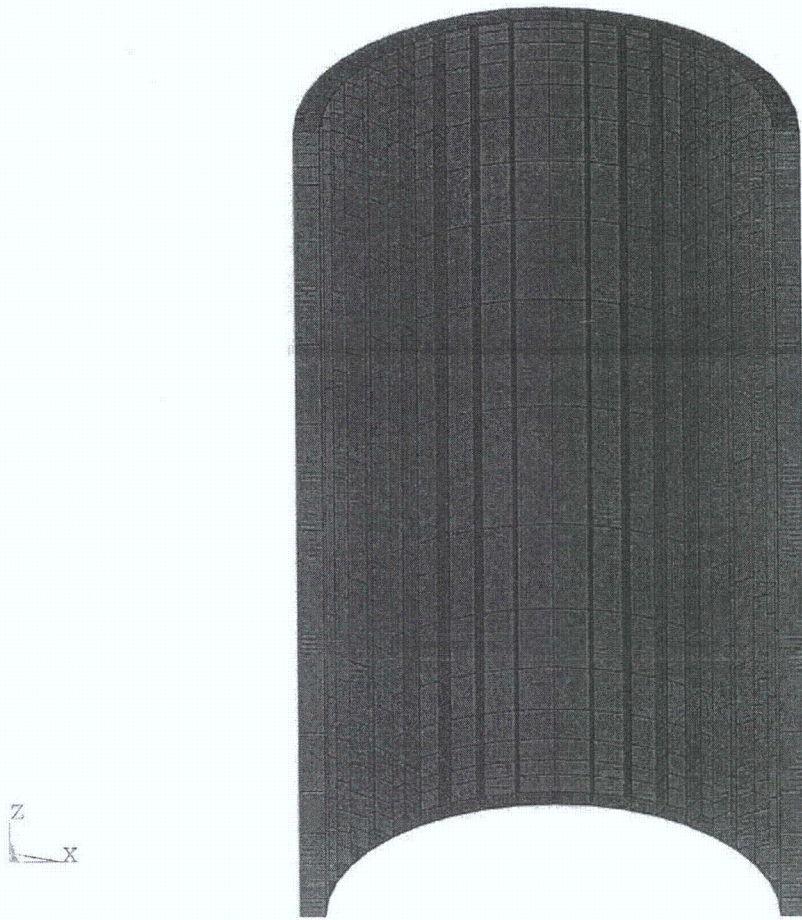
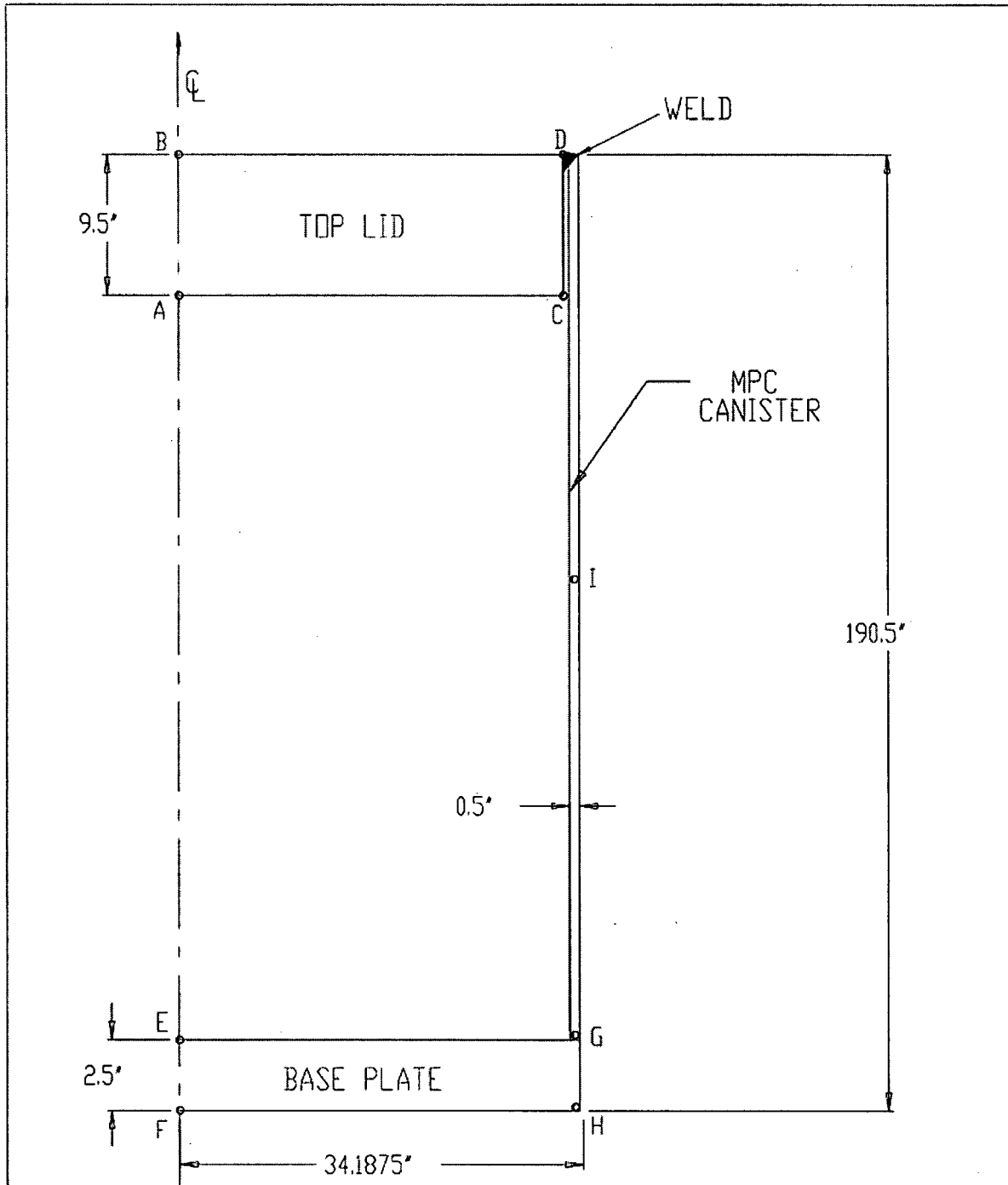


FIGURE 2.6.19C OVERPACK OUTER ENCLOSURE

HI-951251

REV. 8



NOTE: SEE SECTION 2.6.1.3.1.2 FOR VARIOUS LENGTH/THICKNESS SYMBOLS.

FIGURE 2.6.20 CONFINEMENT BOUNDARY MODEL SHOWING TEMPERATURE DATA POINTS

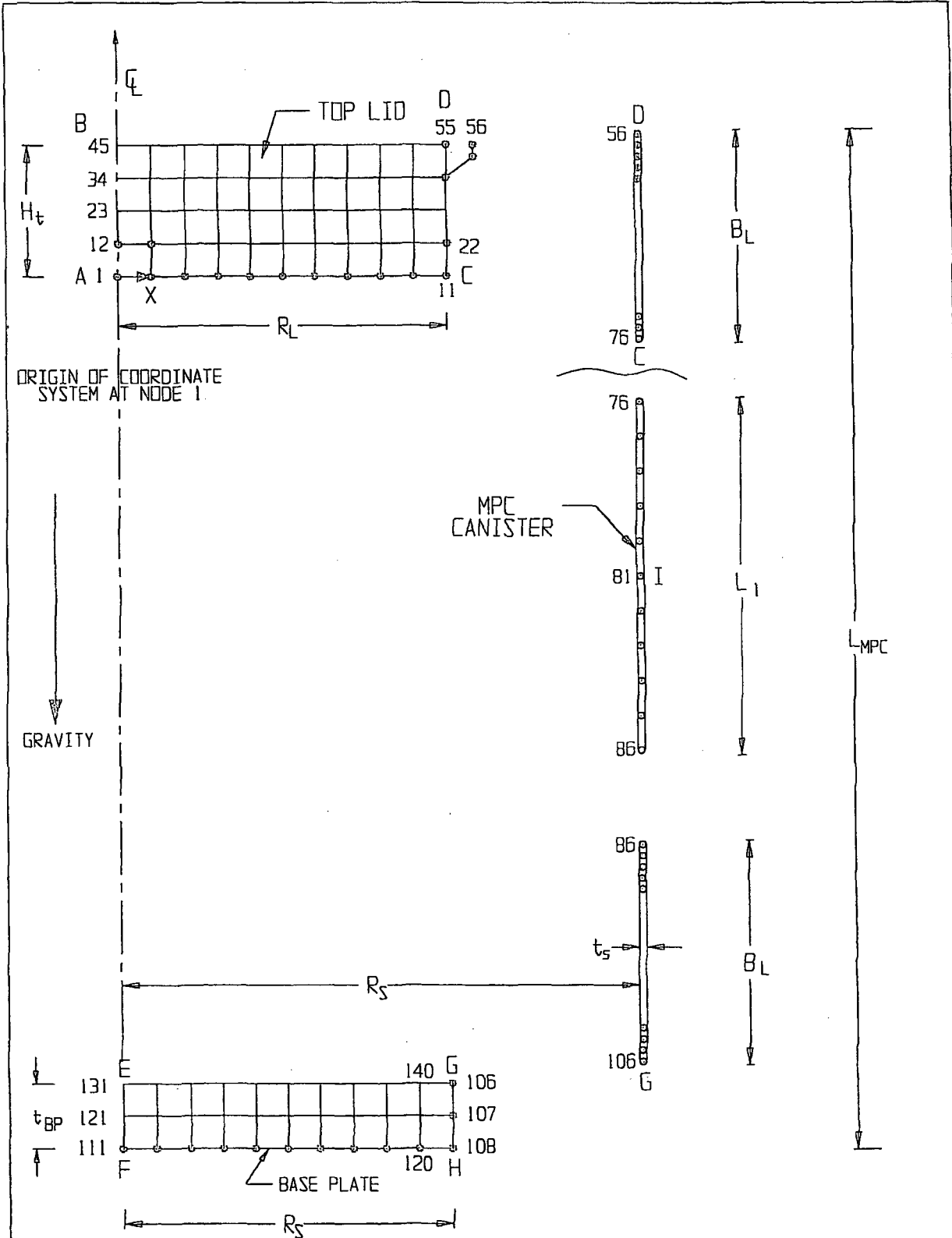


FIGURE 2.6.21 MPC - CONFINEMENT BOUNDARY  
FINITE ELEMENT GRID (EXPLODED VIEW)

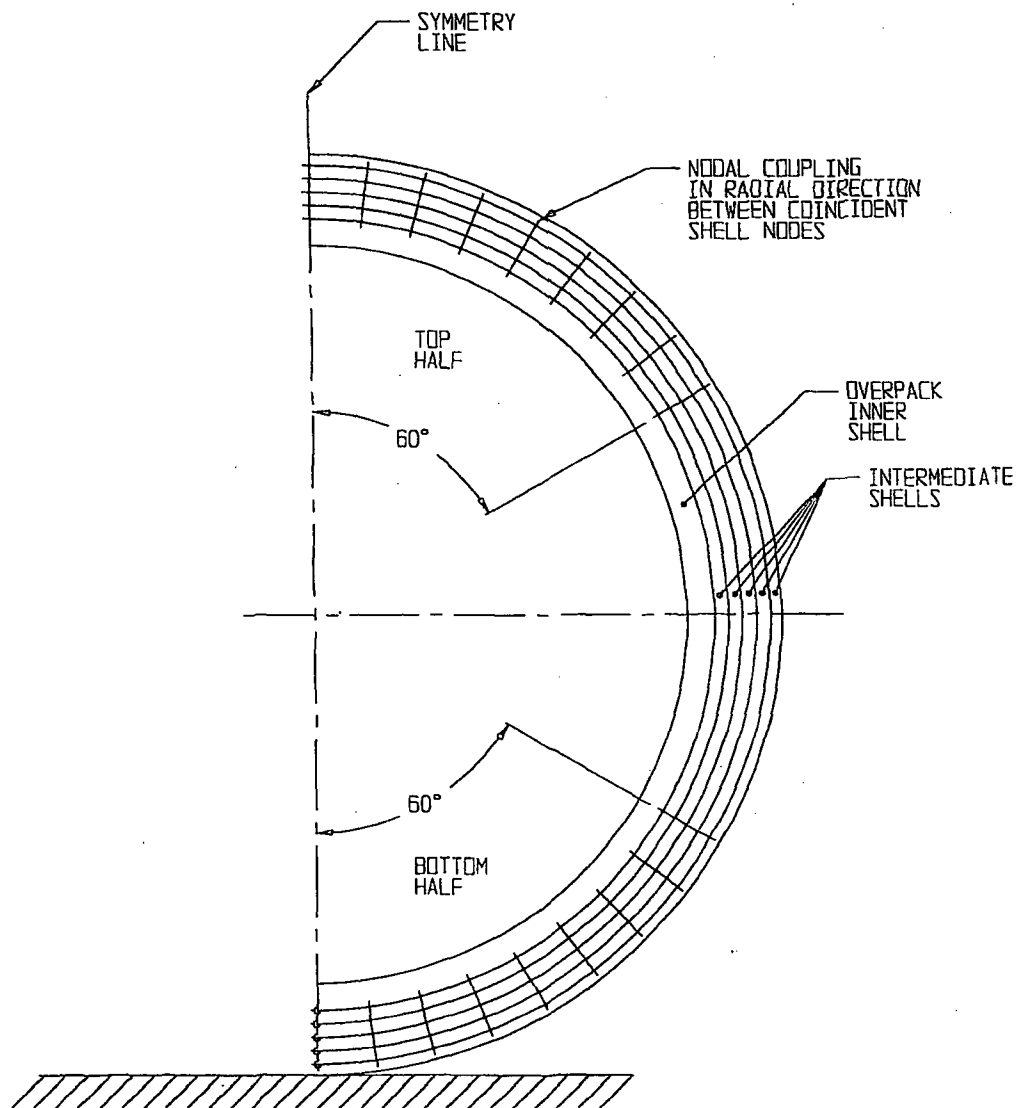


FIGURE 2.6.22; NODAL COUPLING IN OVERPACK FINITE ELEMENT MODEL

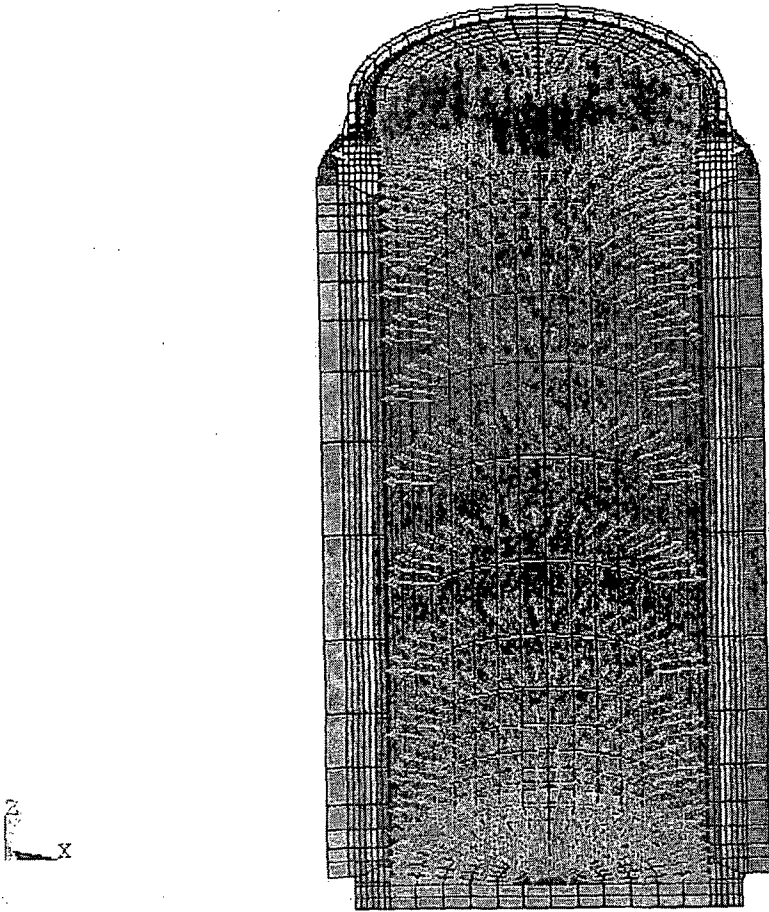


FIGURE 26.23 OVERPACK INTERNAL PRESSURE LOADING

HI-951251

REV. 8

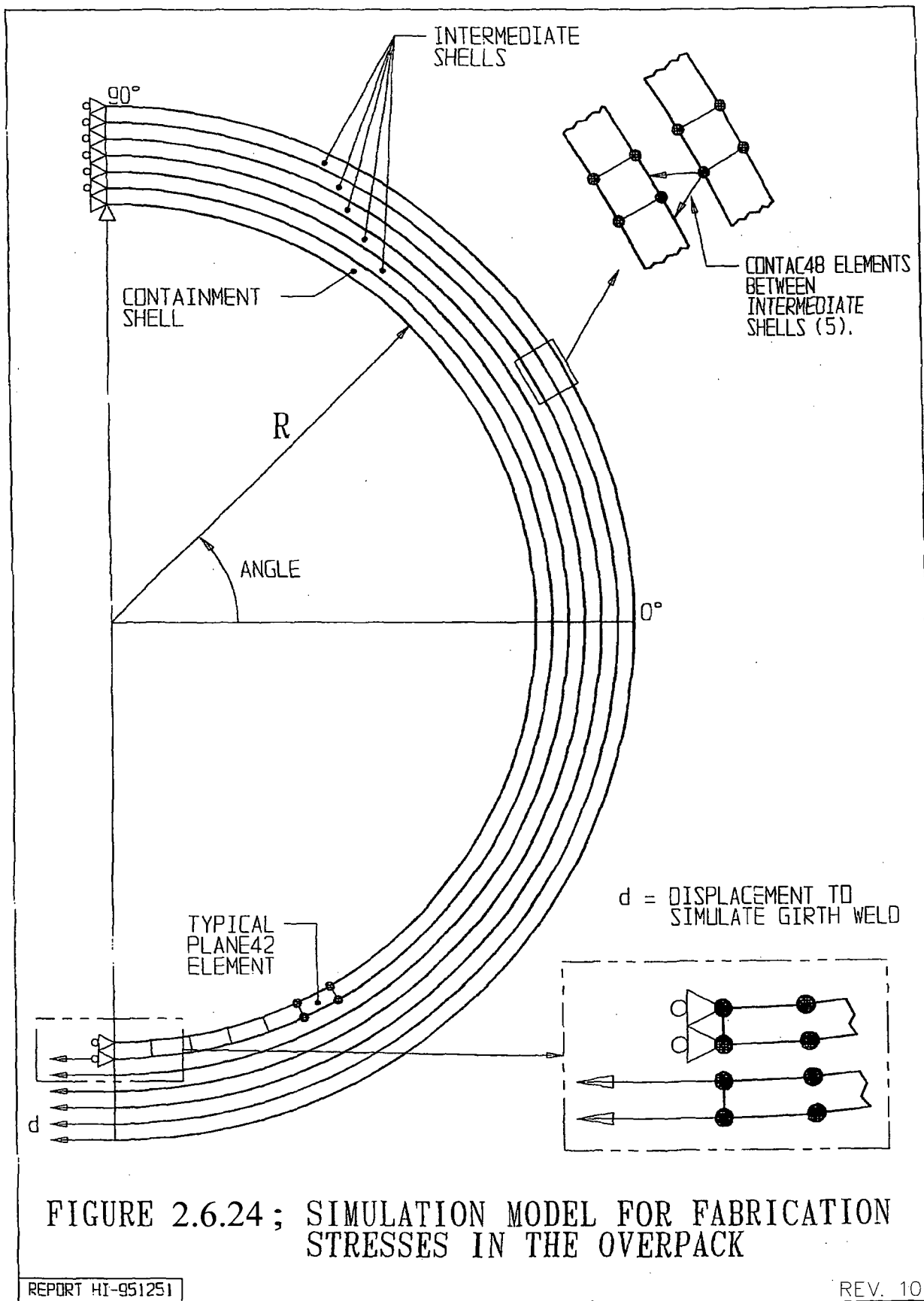
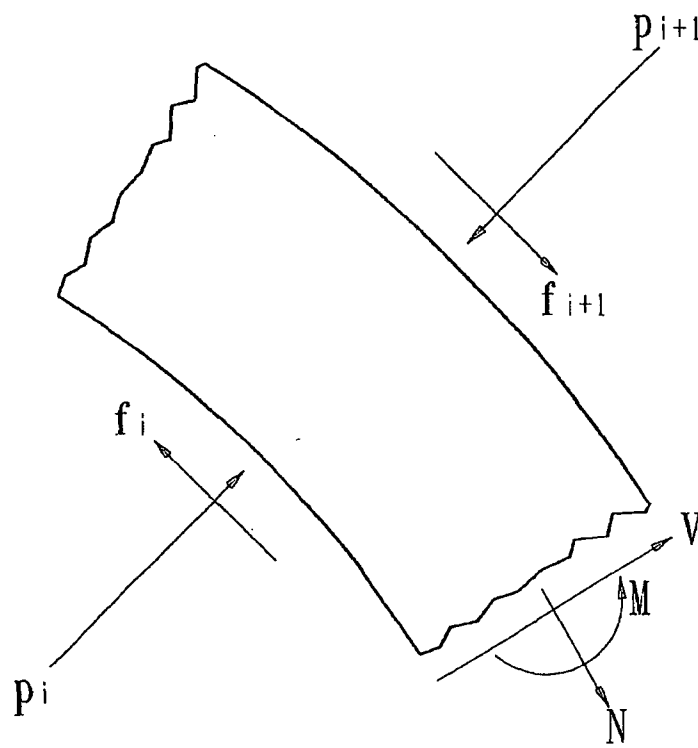


FIGURE 2.6.24 ; SIMULATION MODEL FOR FABRICATION STRESSES IN THE OVERPACK



$$|f_i| \leq \text{COF} * |p_i|$$

COF = COEFFICIENT OF FRICTION

FIGURE 2.6.25; PARTIAL FREE BODY DIAGRAM OF A SHELL SECTION

## 2.7 HYPOTHETICAL ACCIDENT CONDITIONS

It was shown in the preceding section that the load combinations for normal conditions of transport do not induce stresses or stress intensities in excess of allowables. Therefore, it is concluded that the effectiveness of the HI-STAR 100 System is not reduced under normal conditions of transport.

The hypothetical accident conditions, as defined in 10CFR71.73 and Regulatory Guide 7.9, are applied to the HI-STAR 100 System in the required sequence. The system is first subjected to a 9 meter (30 foot) drop in the most damaging orientation, then subject to a 1 meter (40 inch) drop onto a 6 inch diameter mild steel pin (of length sufficient to cause damage to the steel structure), followed by a 1475<sup>o</sup>F temperature fire environment for 30 minutes, and finally to a water immersion test.

The overpack containment boundary is also subjected to deep immersion in accordance with 10CFR71.61.

It is shown in the following subsections that the HI-STAR 100 System meets the standards set forth in 10CFR71, when it is subjected to the hypothetical accident conditions specified in 10CFR71.73. In particular, sufficient analytical and experimental evidence is presented herein to support the conclusion that HI-STAR 100 packaging, when subjected to hypothetical accident conditions, has adequate structural integrity to satisfy the subcriticality, containment, shielding, and temperature requirements of 10CFR71.

### 2.7.1 Free Drop

In this section the performance and structural integrity of the HI-STAR 100 System is evaluated for the most severe drop events. The drop events that are potentially most damaging are the end drops (top or bottom), the side drop, the orientation for which the center of gravity is directly over the point of impact, an oblique drop where the angle of impact is somewhere between center of gravity over corner and a near side drop, and an orientation where package rotation after an impact at one end induces a larger impact deceleration when the other end impacts the target (e.g., slapdown).

The structural assessment of the package is performed in two parts. In the first part, a numerical model to simulate the drop events is prepared and benchmarked against 1/8 scale static tests of the HI-STAR 100 impact limiters, and ¼-scale dynamic drop tests of the HI-STAR 100 Package. This numerical/experimental effort is carried out to confirm that the maximum rigid body decelerations experienced by the package are less than the design basis values set forth in Table 2.1.10. This Classic Dynamics Method (CDM) is discussed in detail in this section and in Appendix 2.A. Note that the scale model test data is also used to benchmark the finite element code LS-DYNA for predicting the dynamic response of the AL-STAR™ impact limiter in a drop event [2.7.4]. The state of the art LS-DYNA analysis method has been employed to perform drop analyses for both HI-STAR 60 [2.7.5] and HI-STAR 180 [2.7.6] transport packages. Appendix 2.C documents the LS-DYNA drop simulations performed to evaluate the improved HI-STAR 100 impact limiter design [2.7.7], which consists of only one type of aluminum honeycomb material, as opposed to four types in the original design. In the second part, the structural integrity of components under the inertia loads due to design basis deceleration levels is evaluated. The deceleration sustained by the internals, such as the fuel basket, are further amplified in recognition of the elasticity of the internal

structures. The dynamic amplifier is considered as an added multiplier on the rigid body deceleration in the structural assessments. Dynamic amplifiers applicable to components of the package have been developed from evaluating the behavior of simplified models.

Part One: Maximum Rigid Body Deceleration Under 10CFR71.73 Free Drop Event

The determination of the AL-STAR impact limiter performance under postulated 10CFR71.73 free drop events was carried out in six phases as summarized below and further elaborated in Appendix 2.A.

- i. Characterize honeycomb material crush behavior: Coupons of both unidirectional and cross-core honeycomb materials at different nominal crush strength values were prepared and tested. A typical pressure vs. deflection curve is shown in Figure 2.A.2.1 in Appendix 2.A. The pressure in the flat portion of the curve denotes the crush pressure.

Mathematical correlation of the data from the population of coupons tested showed that the pressure/crush curve for a honeycomb stock can be represented by one equation wherein the crush pressure,  $p_c$ , is the sole variable. This commonality in the deformation characteristic of the AL-STAR honeycomb materials of different crush strength is extremely helpful in simplifying the dynamic model for the impact limiter.

- ii. AL-STAR Force-Crush Relationship: The AL-STAR impact limiter is a radially symmetric structure whose external and internal diameters are fixed: the I.D. is set by the overpack diameter at its extremities and the O.D. is limited by rail transport considerations to 128". Within this annular space, the arrangement of the aluminum honeycomb material is specified so that the impact limiter can absorb the kinetic energy from a 30' drop event in *any* orientation. The axial dimension of the impact limiter is also limited by considerations of the overall weight of the packaging. To design the impact limiter within the above-mentioned constraints called for a method to predict the force required to crush the impact limiter by a given amount in any given orientation. The mathematical model to define the force-crush (F-d) curve is described in Appendix 2.A. The F-d model was used to establish the nominal crush strengths of the honeycomb sectors used in the various locations of the AL-STAR honeycomb volume to obtain the desired energy absorption characteristics in the equipment.
- iii. Static Scale Model Tests: The static 1/8 scale model tests consisted of preparing 1/8 scale models of the AL-STAR impact limiter and subjecting them to static crush tests in various orientations under normal and abnormal temperature conditions. One object of these tests was to confirm the validity of the theoretical F-d model. Confirming the structural adequacy of the AL-STAR backing structure (which is a thick carbon steel weldment) and the external skin were also objectives of the scale model test. The 1/8 scale static tests, as described in Appendix 2.A, met all project goals: a weakness in the AL-STAR backing structure was identified and corrected in a redesign of the backing structure. The test data also showed that Holtec's F-d model provided a reasonably accurate analytical tool to predict the static crushing behavior of AL-STAR in the various potential crushing orientations. The adequacy of the F-d model to predict static crush behavior was an essential prerequisite for the dynamic test correlation effort that followed.

- iv. Dynamic Scale Model Tests: A 1/4 scale model of the HI-STAR 100 Package, including AL-STAR impact limiters, was used for drop testing. Appendix 2.A herein provides a complete synopsis of the AL-STAR impact limiter design development program, including the 1/4 scale model drop tests which demonstrated the performance of the package. The objectives of the drop tests may be stated as follows:
- i. Select a sufficient number of drop orientations to ensure that under the worst-case orientations, the structural adequacy of the package is demonstrated by testing.
  - ii. Prove that the peak rigid body decelerations experienced by the package in any of the tests is below the Table 2.1.10 design basis value.
  - iii. Demonstrate that the impact limiters prevent the cask from direct contact with the unyielding surface and remain attached through the end of the drop event.

Four drop configurations, namely, vertical (top end), horizontal (side), center-of-gravity-over-corner (CGOC), and slap-down (fully described in Appendix 2.A) were identified as a complete set capable of realizing the aforementioned objectives. The tests were performed in two distinct series as described below.

The first test series, conducted in August 1997, indicated the need to modify the honeycomb material crush strength utilized. The first dynamic test series also helped quantify the dynamic multiplier applicable to the statically determined honeycomb crush strength under impact conditions.

The second test series showed that the peak deceleration in all four drop orientations tested met the Table 2.1.10 limits. Despite meeting deceleration limits, the attachment bolts between the bottom impact limiter and the overpack failed in the side drop test. This required an additional design improvement to the bottom impact limiter-to-overpack attachment design, and re-performance of the side drop test. For the final four tests used for evaluation in Appendix 2.A, no attachment bolts sustained a failure.

- v. AL-STAR Dynamic Response Model: The 1/4 scale tests provided valuable information on the package response which was used to confirm the veracity of Holtec's dynamic simulation model developed for predicting the package response under the other drop conditions. Like all orthotropic materials, the crushing of the honeycomb requires greater force under an impact load than the load necessary to achieve the same extent of crush under static conditions. The conversion of the static "force (F) - crush (d)" model to dynamic conditions simply means applying a dynamic factor to the formula. In other words, under dynamic conditions, the relation between crush force "F" and crush "d" is given as:

$$F = Z f(d)$$

where f(d) is the crush force corresponding to the compression "d" under static conditions

and Z is the dynamic multiplier function. The value of Z was quantified by the first series of 1/4 scale dynamic scale model test, such that a dynamic response simulation model could be developed that satisfied all equilibrium expectations.

In addition to comparing the predicted peak decelerations with the measured value, the duration of crushing and crush depth predicted by the dynamic model were also compared with the measured test data. The comparisons, presented in Appendix 2.A, confirm the ability of the dynamic model to simulate the behavior of the package under a drop event.

- vi. Sensitivity Studies: A significant result from the 1/4 scale model dynamic tests was a complete validation of the dynamic model. For every test performed, the AL-STAR dynamic model was able to simulate the peak accelerations, total crush, *and* crush duration with reasonable agreement. The experimentally benchmarked mathematical model could now be used to simulate drop events for a variety of HI-STAR 100 package weights and honeycomb crush strengths. Results of the simulations to determine the effects of variations in aluminum honeycomb crush strengths and package weights are presented in Appendix 2.A.

The results summarized in Table 2.A.5 of Appendix 2.A, as well as in Appendix 2.C, demonstrates that the maximum rigid body deceleration experienced by the HI-STAR 100 package equipped with the AL-STAR impact limiter will be less than 60g's regardless of the orientation of impact. Therefore, in the balance of analyses performed to evaluate the consequences of "free drop" under the provisions of 10CFR71.73, the package will be assumed to be subject to a rigid body deceleration equal to 60 g's. It is clear from inspection of the geometry of the package that the most vulnerable direction of inertia loading for the HI-STAR fuel basket is the transverse direction wherein the flat panels of the basket are subjected to lateral inertia loading from the contained SNF. As mentioned earlier, the flexibility of basket panel acts to further amplify the package deceleration, which must be considered in the evaluation of results from the stress analysis model. In summary, the net result of the work effort described in the foregoing and further elaborated in Appendix 2.A was to confirm the validity of 60g as the *design basis* rigid body deceleration for the 10CFR71.73 drop event.

In Appendix 2.A, additional supporting technical information requested in Paragraph 2.7 of Reg. Guide 7.9 is provided. Information provided includes free-body diagrams, sketches, governing equations, test method for model testing, scaling factors, discussion of the law of similitude, measurements of crush, impact duration, deceleration histograms, effect of tolerances on package response, and demonstration that the model test will give conservative results for peak g-force and maximum deformation.

Additionally, Reg. Guide 7.9 calls for evaluation of the response of the package in terms of stress and strain to components and structural members, including investigation of structural stability as well as the consequences of the combined effects of temperature gradients, pressure, and other loads. Part Two of the work effort, described in the following, fulfills the above Reg. Guide 7.9 stipulations.

## Part Two: Stress Analysis

The second part of the analysis is performed using the ANSYS finite element software [2.6.4]. The MPC and overpack models used here are identical to those presented in Section 2.6. The loads are applied to the models in accordance with the load combinations defined in Table 2.1.6 (Load Cases F3), Table 2.1.7 (Load Cases E3), and Table 2.1.9 (Load Cases 1-16) for hypothetical accident conditions of transport. The detailed application of each load case is described in the subsections that follow. The presentation and content follows the formatting requirements of Regulatory Guide 7.9. The results from conditions of “Heat” and “Cold” are considered together in the following presentation.

The analysis of the different hypothetical accident conditions of transport are carried out using general finite element models of the MPC and the overpack as well as calculations based on simplified models amenable to strength of materials solutions. The analyses using strength of materials solutions focus on specific loading conditions applied to component parts of the MPC and/or the overpack. The finite element analysis of the overpack involves a complex 3-D model of the overpack to which a series of loads are applied. The results from the solutions are then combined in a post-processing phase to make up the different accident load combination. Given the complexity of the overpack finite element analysis model, some discussion of the stress report is presented to facilitate an understanding of the conclusions. For each of the load combinations, the following components are identified for reporting purposes:

1. Seal
2. Bolts
3. Lid
4. Inner Shell (including the top flange)
5. Intermediate Shells
6. Baseplate
7. Enclosure

The postprocessor collects the nodal stresses from the finite element solution, for each of the components in turn, and reports the principal stresses and the stress intensity at selected locations where physical reasoning suggests that high stresses may occur under the different postulated load combinations. In order to identify the minimum safety factor for each of the above components after the load cases are combined, the collection of nodes is sorted by stress intensity magnitude in descending order. Therefore, since the hypothetical accident condition load combinations involve a comparison of primary stress intensities, a minimum safety factor for each of the defined components in the model may be identified as occurring at the node point with the largest calculated stress intensity. Safety factors are computed using the allowable stress intensities for the material at the reference temperature identified for the component and reported under one of the seven groups identified above. The post-processor collects, sorts, and reports the necessary information to enable documentation of the satisfaction of the applicable requirements. The following items are collected and evaluated for each load combination:

**Seals:** The normal force in each of the springs representing the seal is reported and shown to remain in compression under the load. Maintaining a compressive load in the seal springs assures that there is no separation at the component interfaces.

**Bolts:** The bolts are initially preloaded by applying an initial strain sufficient to result in the desired pre-stress. Subsequent to the application of the different loads to form a specified load combination, the bolts are shown not to unload.

**Lid:** For each load combination, the lid primary membrane plus primary bending stress intensities are compared to the allowable values at the designated reference temperature.

**Inner Shell:** Primary membrane and primary membrane plus bending stress intensity distributions are examined and compared to allowable stress intensity values

**Intermediate Shells:** The five intermediate shells are examined at stress location points and compared to allowable stress intensities at the appropriate reference temperature. Since accident conditions of transport represent a Level D condition (where the comparison of calculated value vs. allowable value is always based on stress intensity), there is no differentiation between intermediate shells considered as Class 1 or Class 3 components.

**Baseplate:** Primary membrane plus bending stress intensities are compared to allowable values at the component reference temperature.

**Enclosure:** The plate and shell elements making up the enclosure for the Holtite-A material are compared to primary membrane stress intensity allowable values.

In the finite element analysis of all load combinations associated with hypothetical accident events, the initial preload case of the bolts and the internal pressure case are included in the final combination. Since no secondary stresses need be evaluated per the ASME Code requirements for an accident level event, the thermal stress load case for the "Heat" condition is not included as a specific load case. However, the allowable stress intensities used for the safety factor evaluation are obtained at the appropriate "Heat" condition reference temperature. In the reporting of safety factors, the variation in allowable stress intensity with temperature is ignored; this introduces an additional measure of conservatism in the reported safety factors since the reference temperatures (Table 2.1.21) are higher than the actual calculated temperatures. For the "Cold" condition, there are no temperature gradients developed. The interaction stresses developed to maintain compatibility under the uniform ambient temperature change are included in the analysis and are treated as primary stresses in the evaluation of the safety factor.

2.7.1.1 End Drop

- Overpack Stress (Load Cases 1,2,9, and 10 in Table 2.1.9)

The overpack is evaluated under both a top end drop and a bottom end drop. In both cases, the impact limiter reaction is assumed to act over the entire area that is backed by structural metal. Given that the total dropped weight is W and that the maximum acceleration is A, the impact

$$|R| = \frac{WA}{g}$$

limiter total reaction load follows from force equilibrium.

This reaction load R is imposed on the appropriate region of the overpack (either lid outer surface or bottom plate outer surface as a uniform pressure load to maximize the bending of the lid or bottom plate.

Since the same finite element model described and used in Section 2.6 for evaluation of loading associated with normal conditions of transport is used here with different applied loads, no further discussion of the model or the analysis methodology is required. Figures 2.1.7 and 2.1.8 show the loading on the overpack in the bottom down and the top down configurations, respectively. The results of the analyses for the top end and bottom end drops are collected and safety factors from the limiting locations in the model are reported in Tables 2.7.5 and 2.7.6 for both heat and cold environments. Table 2.7.5 presents the minimum safety factors for each of the components identified above for the “Heat” condition and Table 2.7.6 presents the safety factors for the “Cold” condition. Within each table, the component is identified, and the minimum safety factor reported.

- Overpack Stability

Structural stability of the overpack containment inner shell under the end drop is assessed. The case of the accident end drop is evaluated for elastic and plastic stability in accordance with the methodology of ASME Code Case N-284 [2.1.8]. All required interaction equation requirements set by [2.1.8] are met. For this event, yield strength limits rather than instability limits govern the minimum safety factor. The minimum safety factor for this case is summarized below:

Code Case N-284 Minimum Safety Factors - (Load Case 1 and 2 in Table 2.1.9)			
Item	Calculated Interaction Value	Allowable Interaction Value <sup>†</sup>	Safety Factor against Yield <sup>†</sup>
Load Case 1 and 2 in Table 2.1.9	0.62*	1.34	2.16*

\* Applicable to inner shell fabricated from SA203-E material. Safety factor must be multiplied by 0.93 if inner shell is fabricated from optional SA350-LF3 material.

† Note that in computing the safety factor against yield for this table, the safety factor implicit in the Code Case N-284 allowable interaction equation is included. Note also that the safety factors given above from the Code Case analysis are all safety factors against the circumferential or longitudinal

stresses reaching the material yield stress. The actual safety factors against instability are larger than the factors reported in the table. In other words, yield strength rather than stability is the limiting condition. Finally, note that fabrication stresses have been included in the stability calculations even though these stresses are self-limiting. Therefore, all results corresponding to the calculated stability interaction equations are very conservative.

The result for the heat environment bound the similar result for the cold environment since yield strengths and elastic modulus are higher. Therefore, no analysis is performed for stability under cold conditions.

- Closure Bolt Analysis

Stresses are developed in the closure bolts due to pre-load, pressure loads, temperature loads, and accident loads. Closure bolts are explored in detail in Reference [2.6.3], which deals with the analysis of shipping casks. The analysis of the overpack closure bolts under normal conditions of transport has been reported in Section 2.6. This subsection presents the results for the analysis for the hypothetical accident end drop. The analysis follows the procedures defined in Reference [2.6.3]. The allowable stresses used for the closure bolts follows that reference. Note that the analyses provide alternative confirmation of the results from the finite element analysis; namely, under any of the identified load combinations, the bolts do not unload.

The following combined load case is for the hypothetical top end drop accident condition of transport. This drop conservatively assumes a nearly vertical orientation with the impact limiter reaction load applied at the outermost location of the lid. This results in the closure bolts resisting the inertial load from the MPC plus contents in addition to the inertia load from the closure lid itself. In reality, the load from the MPC would not load the bolts.

Top End Drop:            Pressure, temperature, and pre-load loads are included.

Reference [2.6.3] reports safety factors defined as the calculated stress divided by the allowable stress for the load combination. This definition of safety factor is the inverse of the definition consistently used in this SAR. In summarizing the closure bolt analyses, results are reported using the safety factor definition of allowable stress divided by calculated stress. The following result for closure lid bolting for the top end drop hypothetical accident condition of transport is obtained.

Overpack Closure Bolt - Safety Factor (Load Case 2 in Table 2.1.9)	
Combined Load Case	Safety Factor on Bolt Tension
Average Tensile Stress	1.30

It is seen from the above table that the safety factor is greater than 1.0 as required. Note that the average tensile stress reflects the preload stress required for successful performance of the bolts as well as the applied load from the hypothetical accident drop event.

- MPC Fuel Basket Stability and Stress (Load Case F3.a in Table 2.1.6)

Under top or bottom end drop in a hypothetical accident condition of transport, the MPC is subject to its own amplified self-weight, causing compressive longitudinal stress in the fuel basket cell walls. The following analysis demonstrates that stability or yield is not a credible safety concern in the fuel basket walls under a hypothetical end drop accident condition of transport.

- MPC Fuel Basket Stability

Stability of the basket panels, under longitudinal deceleration loading (Load Cases F3.a in Table 2.1.6), is demonstrated in the following manner. Table 2.2.1 provides the weight of each fuel basket (including sheathing and neutron absorber panels). The corresponding metal areas of the basket bearing on the MPC baseplate or top lid can be computed for each MPC basket by direct calculation from the appropriate drawings. Dividing weight by bearing area and multiplying by the design basis deceleration for the hypothetical accident from Table 2.1.10 gives the axial stress in the load bearing walls. The results for each basket are compared and the bounding result (maximum weight/area) reported below:

Fuel Basket Compressive Stress For End Drop (Load Case F3.a)			
Item	Weight (lb.)	Bearing Area (sq. inch)	Stress (psi)
Bounding Basket (at 60g's deceleration)	23,535	346.61	4,074

To demonstrate that elastic instability in the basket panels is not credible, the flat panel buckling stress,  $\sigma_{cr}$ , (critical stress level at which elastic buckling may occur) is computed using the formula in reference [2.6.1].

For conservatism, the MPC fuel basket is modeled as a rectangular plate simply supported along two sides and uniformly compressed in the parallel direction. The width of the plate is equal to the maximum unsupported width of a panel from all fuel basket types. Reference [2.6.1] provides the critical stress formula for these conditions as

$$\sigma_{cr} = \frac{2.3 \pi^2 E}{12 (1 - \nu^2)} \left( \frac{T}{W} \right)^2$$

where T is the panel thickness and W is the width of the panel, E is the Young's Modulus at the metal temperature and  $\nu$  is the metal Poisson's Ratio. The following table summarizes the calculation for the critical buckling stress using the formula given above:

Elastic Stability Result for a Flat Panel	
Reference Temperature	725 degrees F
T (bounding thickness)	9/32 inch
W (bounding width)	11.0 inch
E	24,600,000 psi
Critical Axial Stress	33,430 psi

It is noted that the critical axial stress is an order of magnitude greater than the computed basket axial stress reported in the foregoing. Therefore, it is demonstrated that elastic stability under hypothetical accident condition of transport longitudinal deceleration inertia load is not a concern.

- MPC Fuel Basket Stress

The safety factor against yielding of the basket under longitudinal compressive stress from a design basis inertial loading is given by

$$SF = 17,100/4,074 = 4.198$$

where the yield stress of Alloy X has been taken from Table 2.3.1 at 725 degrees F.

Therefore, plastic deformation of the fuel basket under design basis deceleration is not credible.

Analyses of the Damaged Fuel canisters to be transported in the HI-STAR 100 Package are performed to demonstrate structural integrity under an end drop condition. A summary of the methodology and the results for all canisters is provided in Appendix 2.B.

- MPC Enclosure Shell Stability

Structural stability of the MPC enclosure shell under the end drop is evaluated for elastic and plastic/stability in accordance with the ASME Code Case N-284 [2.1.8]. All required interaction equation requirements set by [2.1.8] are met. It is shown that yield strength limits rather than instability limits govern the minimum safety factor. The minimum safety factor for this case is summarized below:

MPC Shell Elastic/Plastic Stability (Load Case E3.a Table 2.1.7)			
Item	Value	Allowable*	Safety Factor
Yield	0.698	1.34	1.92

\* For Load Case E3.a, the yield strength criteria in the Code Case N-284 method govern. In this event, the safety factor 1.34, built into the Code Case, is included in the tabular result in order to obtain the actual safety factor with respect to the yield strength of the material.

- MPC Closure Lid Stress (Load Case E3.a)

The closure lid, the closure lid peripheral weld, and the closure ring are examined for maximum stresses developed during the hypothetical end drop accident event.

The closure lid is modeled as a single simply supported plate and is subject to deceleration from an end drop plus appropriate design pressures. Results are presented for both the single and dual lid configurations (in parentheses) for top end and bottom end drops. For the dual lid configuration, the two plates each support their own amplified weight as simply supported plates under a bottom end drop. The inner lid transfers the total load to the outer plate through the peripheral weld between the two lids. Under a top end drop scenario, the inner lid is partially supported by the outer lid and the amplified load is transmitted by a combination of peripheral support and interface contact pressure. The results for minimum safety factor are reported in the table below:

MPC Top Closure Lid - Minimum Safety Factors - Load Case E3.a in Table 2.1.7			
Item	Stress(ksi) or Load(lb.)	Allowable Stress (ksi) or Load Capacity (lb.)	Safety Factor
Lid Bending Stress - Load Case E3.a (bottom end drop)	3.35/(7.94)	60.7	18.1/(7.65)
Lid Bending Stress* - Load Case E3.a (top end drop)	21.9/(43.8)	60.7	2.77/(1.39)
Lid-to-Shell Peripheral Weld Load - Load Case E3.a	624,000	1,477,000**	2.37
Lid-to-Lid Peripheral Weld Load - Load Case E3.a (bottom end drop)	312,000	443,200***	1.42

\* Stress computation is conservatively based on peripheral support at the outer diameter of the MPC lid. For a top end drop, the actual support diameter is .77 of the outer diameter. Therefore, an analysis based on an overhung plate would provide stresses reduced by a multiplier of 0.59. Consequently, the safety factors would be amplified by the factor 1.69.

\*\* Based on a 0.625” single groove weld and conservatively includes a quality factor of 0.45.

\*\*\* This is a non-Code weld; limit is based on a 0.1875 groove weld and includes a quality factor of 0.45 for additional conservatism

Safety factors are greater than 1.0 as required. The limiting condition for the lid bending evaluation is a top end hypothetical accident end drop because the lid supports the amplified fuel weight as well as the lid amplified self-weight.

- MPC Baseplate and Canister Stress (Load Case E3.a)

Load Case E3.a provides the limiting accident loading on the baseplate wherein the combined effect of a 60g deceleration plus external pressure is considered. The top end hypothetical accident condition is limiting in transport, and here it is conservatively assumed that accident external pressure acts simultaneously, which exceeds the requirements of Table 2.1.7. The results are summarized below:

MPC Baseplate Minimum Safety Factors – Load Cases E3, Table 2.1.7			
Item	Value (ksi)	Allowable (ksi)	Safety Factor
Center of Baseplate - Primary Bending (Load Case E3)	22.12	67.32	3.04
Shell Bending Stress at Connection to Baseplate	31.47	67.32	2.14

Note that all safety factors are greater than 1.0. Also, note that the calculated stress conservatively includes both primary and secondary self-limiting stress components. For the hypothetical transport drop accident, the safety factor computed for the shell bending stress intensity need only consider the effect of primary membrane plus bending stresses that are to be compared against the ultimate stress at temperature for this ASME Code Service Level D event. Since secondary stresses have been included in the evaluation, the reported result for safety factor is conservatively low.

- Trojan MPC Spacer

The Trojan MPC-24E/EF enclosure vessel is 9 inches shorter in length than the generic MPC-24E/EF enclosure vessel. Thus, when the Trojan MPC-24E/EF is transported inside the HI-STAR 100, the axial clearance between the MPC lid and the HI-STAR 100 closure plate is greater than 10 inches. In order to prevent the Trojan MPC from thrusting forward and impacting the closure plate during a top-end drop or a tip-over event (i.e., slapdown), a spacer device is positioned on top of the MPC lid. The Trojan MPC spacer, depicted in Figure 1.1.5, is fabricated from SA240-304 stainless steel in the shape of a circular I-beam. The web of the spacer measures 1-inch thick and has a mean diameter of 60 inches. The total height of the MPC spacer is 9 inches.

During a top end drop, the MPC spacer must support the amplified weight of a fully loaded Trojan MPC-24E/EF. Based on a bounding MPC weight of 90,000 lb (Table 2.2.4) and a bounding deceleration of 60g (Table 2.1.10), the maximum compressive stress in the web is computed as follows.

$$\text{Cross-sectional area of web (A)} = \pi \times D \times t = \pi (60) (1) = 188.5 \text{ in}^2$$

$$\text{Amplified weight of MPC (P)} = G \times W = (60) (90,000) = 5.4 \times 10^6 \text{ lb}$$

$$\text{Compressive stress in web} = P/A = (5.4 \times 10^6) / 188.5 = 28,647 \text{ psi}$$

From Table 2.1.18, the primary membrane stress intensity limit for Alloy X (of which SA240-304 is a member) under Level D conditions is 44.9 ksi at 400°F. Therefore, the safety factor against compressive failure of the Trojan MPC spacer, per ASME Code Subsection NB stress limits, is

$$SF = 44,900 / 28,647 = 1.56$$

#### 2.7.1.2 Side Drop (Load Cases F3 in Table 2.1.6, E3 in Table 2.1.7, and 3 and 11 in Table 2.1.9)

- MPC Fuel Basket and Canister Finite Element Analysis (Load Cases E3.b, E3.c in Table 2.1.7 and Load Cases F3.b, F3.c in Table 2.1.6)

The MPC configurations are assessed for a hypothetical accident condition of transport side drop. All fuel cells are loaded with design basis spent nuclear fuel (SNF). Evaluations are performed for the 0 degree and the 45 degree circumferential orientations of the fuel basket as defined in Figures 2.1.3 and 2.1.4 and are obtained using the finite element model described in Section 2.6.

The results for each MPC configuration for the two different drop orientations are evaluated for each appropriate load case listed in Tables 2.1.6 and 2.1.7. Analyses are performed only for the hot ambient temperature condition since this is the bounding case for the MPC; as noted in Section 2.6, allowable stresses are lower for the “heat” environmental condition.

- Elastic/Plastic Stability of the MPC Fuel Basket

Following the provisions of Appendix F of the ASME Code [2.1.12] for stability analysis of Subsection NG structures, (F1331.5(a)(1)), a comprehensive buckling analysis is performed using ANSYS. For this analysis, ANSYS's large deformation capabilities are used. This feature allows ANSYS to account for large nodal rotations in the fuel basket, which are characteristic of column buckling. The large deflection option is “turned on” so that equilibrium equations for each load increment are computed based on the current deformed shape. The interaction between compressive and lateral loading, caused by the deformation, is included in a rigorous manner. Subsequent to the large deformation analysis, the basket panel that is most susceptible to buckling failure is identified by a review of the results. The lateral displacement of a node located at the mid-span of the panel is measured for the range of impact decelerations. The buckling or collapse load is defined as the impact deceleration for which a slight increase in its magnitude results in a disproportionate increase in the lateral displacement.

The stability requirement for the MPC fuel basket under lateral loading is satisfied if two-thirds of the collapse deceleration load is greater than the design basis horizontal acceleration (Table 2.1.10). Figures 2.7.1, through 2.7.6 are plots of lateral displacement versus impact deceleration for representative fuel baskets. It should be noted that the displacements in Figures 2.7.1, 2.7.2, 2.7.3, 2.7.4, and 2.7.5 are expressed in  $1 \times 10^{-1}$  inch and Figure 2.7.6 is expressed in  $1 \times 10^{-2}$  inch. The plots clearly show that the large deflection collapse load of the MPC fuel basket is greater than 1.5 times the inertia load corresponding to the design basis deceleration for all baskets in all orientations. Thus, the requirements of Appendix F are met for lateral deceleration loading under Subsection NG stress limits for faulted conditions. Therefore, it is concluded that stability of the spent fuel basket cell walls is assured under the hypothetical accident side drop (from 30') condition of transport.

An alternative solution for the stability of the fuel basket panel is obtained using the methodology espoused in NUREG/CR-6322 [2.7.3]. In particular, the fuel basket panels are considered as wide plates in accordance with Section 5 of NUREG/CR-6322. Eq.(19) in that section is utilized with the “K” factor set to the value appropriate to a clamped panel. Material properties are selected corresponding to a metal temperature of 500 degrees F which bounds computed metal temperatures at the periphery of the basket. The critical buckling stress is:

$$\sigma_{cr} = \left(\frac{\pi}{K}\right)^2 \frac{E}{12(1-\nu^2)} \left(\frac{h}{a}\right)^2$$

where h is the panel thickness, a is the unsupported panel length, E is the Young’s Modulus of Alloy X at 500 degrees F (Table 2.3.1),  $\nu$  is Poisson’s Ratio, and  $K=0.65$  (per Figure 6 of NUREG/CR-6322).

Parameters appropriate to a MPC-24E basket are used; the following table shows the results from the finite element stress analysis and from the stability calculation.

Panel Buckling Results From NUREG/CR-6322			
Item	Finite Element Stress (ksi)	Critical Buckling Stress (ksi)	Factor of Safety
Stress	13.339	49.826	3.74

For a stainless steel member under an accident condition load, the recommended safety factor is 2.12. It is seen that the calculated safety factor exceeds this value; therefore, an independent confirmation of the stability predictions of the large deflection analysis is obtained based on classical plate stability analysis.

- Overpack Stress Analysis (Load Cases 3 and 11 in Table 2.1.9)

The overpack is assumed to be subject to a 60g side drop in the manner of the load combinations of Table 2.1.9 for both heat and cold environmental conditions as prescribed by Regulatory Guide 7.9. Reaction loads provided by the impact limiters are imposed as vertical pressures at each end of the overpack on areas of the structure that serve as backing. The applied mechanical loading is internal pressure, inertia load from the MPC and inertia load from the overpack self-weight. Figure 2.1.9 shows the assumed loading for this simulation. Figures 2.7.7, and Figures 2.7.11-2.7.13 are useful to aid in understanding the methodology used to apply the MPC loads and the balancing impact limiter reactions. Figure 2.7.7 shows a view of the overpack looking along the longitudinal axis for the general case of an oblique drop. While the intent of the figure is to describe the reaction loads from the impact limiter under a general oblique drop orientation, only the features necessary to elaborate on the side drop reaction load are discussed here. A region defined by the angle  $\theta$  supports the applied loading in a side drop.

This angle is 18 degrees for the side drop and is chosen based on two considerations. First, the predictions from the theoretical model at the time of maximum “g” loading are examined and a projected loaded area on the top forging and bottom plate estimated. Second, the post-drop evaluation of the tested impact limiters from the one-eighth scale static test and the one-quarter scale dynamic test were visually examined and provided insight into the extent of the loaded region of the overpack at the impact limiter-hard surface interface. From these two evaluations, a conservatively low angle estimate is made for the finite element analysis. Figure 2.7.12 shows the extent around the periphery of the loading imposed by the MPC. From Section 2.6, the angle over which the MPC load is applied to the inner shell of the overpack is 72 degrees from the vertical on each half of the overpack. This angle is determined from the detailed analysis of the MPC enclosure shell and the fuel basket under 60g loading. The inertia load from overpack self-weight is applied by imposing an amplified value for the gravitational constant. Details of the finite element model have been discussed in Section 2.6. The results of the finite element analyses for load cases 3 and 11 in Table 2.1.9, for the overpack, are post-processed as previously discussed; Tables 2.7.5 and 2.7.6 summarize the results for each overpack component and identify the minimum safety factors.

### 2.7.1.3 Corner Drop

Figures 2.1.10 and 2.1.11 show the assumed loading for the bottom center of gravity over corner (CGOC) drop and the top CGOC drop, respectively. The impact limiter reaction load is applied as a pressure loading acting on two surfaces. From the geometry of the cask, with impact limiters in place, the angle of impact is 67.5 degrees from the horizontal plane. Although the theoretical and tested deceleration levels are below 60g's, the design basis 60g-deceleration load is used as the input loading and applied vertically. Therefore, a 55g load is applied along the longitudinal axis of the cask, and a 23g load is applied perpendicular to the cask longitudinal axis.

The lateral inertia load from the MPC, amplified by the appropriate multiplier corresponding to 23g's, is applied in the manner shown in Figures 2.7.11 and 2.7.12. The longitudinal component of the load from the MPC, amplified by 55g, is applied as a pressure over the inside surface of the lid as shown in Figure 2.7.8. In reality, the load would be applied over a narrow annulus near the outside radius of the lid because of the raised “landing region”. To maximize lid and bolt stress, however, the load is applied as a uniform pressure in the finite element model. The corresponding lateral and longitudinal loads from the overpack self-weight are applied by imposing amplified gravitational accelerations in the appropriate directions.

The loading from the impact limiter at the other end of the overpack, not involved in the impact, is applied as a uniform pressure over the surface of the backed area at the other impact limiter. Figure 2.7.10 shows the loading on the outside surface of the bottom plate that arises from the bottom end impact limiter during simulation of a top end drop. The total bottom impact limiter weight is amplified by 55g's and applied as a pressure load. At the top end, where the impact limiter provides the distributed crush force to balance the inertia forces, the balancing reaction loads from the impact limiter are applied as a distributed side pressure loading and a distributed end surface pressure. The extent of the loaded region for this drop orientation is defined by the angle  $\theta$  in Figure 2.7.7. For this case, the angle is approximately 68 degrees since a large “backed” area of the impact limiter is involved in resisting the crush. The angle is consistent with the predictions from the intersection geometry analysis used to develop the force-deformation data used in Appendix 2.A. That force-

crush model has been successfully used to predict maximum decelerations and extent of crush. Static finite element models require setting a fixed origin to insure satisfaction of all equilibrium equations. The center of gravity-over-corner orientation, in theory, provides automatic satisfaction of moment equilibrium so that all forces and moments at such a fixed origin location should be zero.

In this analysis and in the general oblique drop analysis, the fixed point is assumed at a location at the end of the overpack not impacted. The results from the finite element simulation confirm that the computed reactions are negligibly small compared to the applied loads. The loads from internal pressure are self-balancing and do not alter the calculation of equilibrium reactions. Tables 2.7.5 and 2.7.6 summarize the results from these analyses.

Results for the MPC and its internals have been discussed in Subsections 2.7.1.1 and 2.7.1.2 for the end and side drops, respectively, under the action of 60g deceleration and appropriate pressure loading. Under an oblique drop at an angle  $\theta$  with respect to the target plane ( $\theta = 0$  degrees equals the side drop), the MPC and its internals experience deceleration loads parallel and perpendicular to the MPC longitudinal axis. Each of these deceleration components, however, is less than the 60g design basis deceleration used in the end and side drop analyses. For the pure end drop, all stresses in the fuel basket and in the MPC canister (enclosure vessel) are axial. For the pure side drop, the conservative analysis of a 2-D section of the fuel basket and enclosure vessel gives rise to stresses in a plane perpendicular to the longitudinal axis of the MPC/fuel basket.

The results for any oblique drop can be obtained by a linear combination of the results for pure end drop and pure side drop. That is, the combined stress intensity is formed from the results of the two individual cases, after adjustment for the actual lateral and longitudinal “g” levels experienced by the components.

The MPC lid and baseplate are thick plate components; as such, the stress intensities experienced in the end drop orientation (which loads the lid and/or the baseplate in flexure) bound all other cases. Therefore, in what follows; only the enclosure vessel and the fuel basket need be considered. For each of these structures, the result “ $R_\theta$ ”, at a general oblique drop angle  $\theta$ , is expressed in terms of the result for an end drop “ $R_{90}$ ” and the result obtained for a pure side drop “ $R_0$ ” as:

$$R_\theta = R_{90} \left( \frac{g_E}{60} \right) + R_0 \left( \frac{g_S}{60} \right)$$

where  $g_E$  and  $g_S$  are the axial and lateral decelerations imposed on the MPC canister and fuel basket during the oblique drop at angle  $\theta$ .

Since  $g_E = 60 \sin \theta$ , and  $g_S = 60 \cos \theta$ ,

for a design basis oblique drop where the vertical deceleration is 60 g’s, the result for the oblique drop is always expressed in the form,

$$R_\theta = R_{90} \sin \theta + R_0 \cos \theta$$

The following results are obtained for the end drop and side drop analyses:

End Drop:

Fuel Basket – maximum longitudinal membrane stress = 4,074 psi

Enclosure Vessel – maximum longitudinal compressive stress = 11,260 psi

The enclosure vessel result is obtained from the Code Case N-284 evaluation for a bottom end drop and conservatively bounds the result for a top end drop. The longitudinal compressive stress in the enclosure vessel includes the effect of external pressure.

Side Drop:

Stress intensity results for the fuel basket and enclosure vessel are summarized in Table 2.7.4. From Table 2.7.4, for the pure side drop, the minimum safety factor for the fuel basket is 1.17 (primary membrane plus primary bending). The corresponding minimum safety factor for the enclosure vessel is 2.64 (again, for primary membrane plus primary bending). The preceding results are obtained by surveying the summary of minimum safety factors in Table 2.7.4 for all MPC's and both fuel basket orientations within the MPC.

For the pure side drop orientation, the stress intensities (SI) associated with the minimum safety factors are:

Fuel Basket SI = 47,060 psi

Enclosure Vessel SI = 24,650 psi

The stress intensities at the most limiting location for the general oblique drop orientation are then computed as:

Fuel Basket SI =  $4,074 \sin \theta + 47,060 \cos \theta$

Enclosure Vessel SI =  $11,260 \sin \theta + 24,650 \cos \theta$

For the corner drop,  $\theta = 67.5^\circ$  leading to the following final results:

C.G. OVER CORNER DROP MPC SAFETY FACTORS			
Item	Calculated S.I.	Allowable S.I.	Safety Factor
Fuel Basket	21,773 psi	55,450 psi <sup>†</sup>	2.55
Enclosure Vessel	19,836 psi	65,200 psi <sup>††</sup>	3.29

<sup>†</sup> at 725°F

<sup>††</sup> at 450°F

As expected, the safety factors obtained for the corner drop are larger than the corresponding values obtained for the side drop.

Results for general oblique drop angles are now considered for the overpack. In particular, a 30-degree oblique drop is deemed to be most representative of a scenario where only a primary impact is involved. The general formula utilized in the preceding for the specific case of center-of-gravity-over-corner can also be used for a 30-degree drop angle. The following results are reported for the fuel basket and enclosure vessel.

30 DEGREE OBLIQUE DROP MPC SAFETY FACTORS			
Item	Calculated S.I. (psi)	Allowable S.I. (psi)	Safety Factor
Fuel Basket	42,792	55,450 <sup>†</sup>	1.30
Enclosure Vessel	26,978	65,200 <sup>††</sup>	2.42

<sup>†</sup> at 725°F

<sup>††</sup> at 450°F

#### 2.7.1.3.1 MPC "F Class" Enclosure Vessel Lid-to-Shell Weld

The Holtec MPCs labeled with the suffix "F" (designated as "F Class" in this subsection) are intended to store non-intact fuel (defined as damaged fuel in the latest revision of ISG-1 and "failed fuel and fuel debris" in this SAR).

To be certified to store loose fuel debris, the MPC must fulfill the function of the "secondary containment" required by 10CFR71.63(b). To qualify as a "secondary containment", the MPC Enclosure Vessel must be able to withstand the accident condition loading without releasing its contents. The accident condition mechanical loading for the secondary containment is identical to those for the primary containment, namely the inertia forces produced by a 60g deceleration. From Table 2.1.7, the pressure loads applicable to the MPC Enclosure Vessel during a hypothetical vertical end drop (Load Case E3.a) are the normal condition pressures. Therefore, per Table 2.1.1, the maximum pressure differential that exists across the MPC shell when a drop occurs is 60 psig. For conservatism, however, the accident condition internal pressure of 200 psig is used to qualify the MPC Enclosure Vessel as a secondary containment. All candidate vulnerable locations in the MPC Enclosure Vessel must be analyzed to ensure that a thru-wall breach in the pressure-retaining boundary does not occur under the loading combination defined above. In the case of the primary containment (the HI-STAR 100 overpack), the location of containment vulnerability is the cask lid-to-body forging bolted joint; the evaluation of the lid-to-body closure bolt has been analyzed to demonstrate containment integrity and the results of the evaluation summarized in Subsection 2.7.1.1 of the SAR. For the MPC "F Class", considered as secondary containment, the corresponding locations of vulnerability are the two extremities of the Enclosure Vessel where the vessel shell is joined to flat (plate-like) members.

The top lid-to-shell joint, a J-groove (partial penetration) joint made at the plant after fuel loading, is one candidate location, as this weld cannot be volumetrically examined even though the top lid is relatively thick. The MPC baseplate to the shell weld, on the other hand, is a shop-fabricated and volumetrically examined junction. However, because the baseplate is thinner than

the top lid, it may experience greater flexural action under the accident condition mechanical loading, resulting in somewhat greater junction region stresses. Therefore, the weld joints at both extremities of the MPC Enclosure Vessel are denoted as candidate locations whose structural integrity under the load combination appropriate to the MPC's secondary containment function must be demonstrated.

a. Top lid-to-shell joint

For MPCs with the "F" designation, this joint has been buttressed with a thick tapered shell and deeper J-groove weld than that utilized in the standard MPC Enclosure Vessel. A Holtec proprietary position paper, DS-213, "Acceptable Flaw Size in MPC Lid-to-Shell Welds", submitted to the NRC in support of the original certification of HI-STAR 100 in 1999 demonstrates that the largest postulated flaw in the most adverse orientation in the lid-to-shell joint in the "F" canister will not propagate under the impulsive inertia loading arising from a 60g axial deceleration of the MPC's contents.

An elastic stress analysis in the spirit of the ASME Code documented below likewise shows a large margin of safety against joint failure. For conservatism, the following assumptions are made.

- i. The closure ring (the structural member present to provide a second welded barrier against leakage of the contents) is assumed to be absent.
- ii. Even though a thru-wall failure of the joint is the appropriate failure criterion for the joint, non-exceedance of the ASME Code Section III Subsection NB stress intensity limits appropriate to Level D limits, which will occur at a much lower loading level, is set down as the acceptance limit. However, no weld efficiency factor is applied to the lid-to-shell weld since it is not required by Subsection NB.
- iii. The MPC model with the heaviest contents (MPC-32) is used in the analysis to bound the results for all "Type F" MPC models.

The MPC top lid may be fabricated as a single thick circular plate, or may be fabricated as a dual lid with the outer lid attached to the shell with the "J" groove weld, and the inner lid attached to the outer lid around the common periphery. The dual lid configuration has been analyzed for both Normal Conditions of Transport and Hypothetical Accident Conditions of Transport for MPC's carrying intact fuel; the results are documented in Subsection 2.6.1.3.1.2, and 2.7.1.1, respectively. The evaluation for the "F Class" MPC to provide secondary containment capability utilizes the same analytical model but introduces additional assumptions into the analysis to direct load to the lid-to-shell weld. In particular, a top end drop is postulated with the dual lids subjected to a 60g deceleration loading from the fuel, fuel basket, and lid weight, together with the accident internal pressure of the MPC. During a top end drop, the MPC cannot rotate relative to the HI-STAR overpack because of close clearances between the vessel shell and the inner surface of the overpack cavity. Therefore, regardless of the angle of impact, the reaction load from the HI-STAR to equilibrate the applied loads on the lid is uniformly distributed around the circumference. A bounding condition for this analysis for secondary containment is presumed to

be a top end drop where the Enclosure Vessel shell is assumed to contact the support (the HI-STAR lid) before the Enclosure Vessel lid; with this conservative assumption, the peripheral weld is subject to the entire applied load. The key results from the analyses (the case of dual lids bounds the analysis assuming a single thick lid) to support qualification of the MPC "F Class" as secondary containment are summarized in the table below:

KEY RESULTS FOR SECONDARY CONTAINMENT QUALIFICATION OF F CLASS MPC's – Load Case E3.a in Table 2.1.7 (Top End Drop)			
Item	Stress Intensity (ksi) or Load (lb)	Allowable Stress Intensity @ 550 Degrees F (ksi) or Load Capacity (lb)	Safety Factor
Structural Lid Bending Stress Intensity	46.05	60.7	1.32
Shield Plug Bending Stress Intensity	46.65	60.7	1.30
Lid-to-Shell Weld Load	5,268,000	6,627,000	1.26
Primary Local Axial Membrane Stress Intensity at Shell Contact Interface	24.53	40.45	1.65

b. Baseplate-to-Shell Joint

Because the baseplate-to-shell connection is a volumetrically examined, full penetration joint, flaw propagation under the accident condition inertia loads is not a concern for this location. As in the case of the top lid-to-shell junction, the baseplate-to-shell joint is established to be sufficiently robust if the stress intensity limits under the above load combination (appropriate for §71.63(b)) are below their corresponding limits for level D condition for Section III Class 1 (NB) components. Since the baseplate-to-shell joint in the MPC "F Class" units is identical to the joint in the MPC's used for intact fuel, no new analyses are required. The results of evaluation of this joint are reported in Subsection 2.7.1.1 and demonstrate substantial safety factors.

The above analyses demonstrate that the Enclosure Vessel for "Type F" MPCs is capable of serving as a "secondary containment" as required by §71.63(b).

2.7.1.4 Oblique Drops

Appendix 2.A contains results of analytical simulations for various orientations of the cask at impact. In Appendix 2.A, it is shown that lateral decelerations are large for the near side drop (slapdown) and decrease as the angle of orientation, with respect to the horizontal plane, increases. Therefore, it is likely that results presented in Subsections 2.7.1.1 through 2.7.1.3 are bounding for all orientations other than the near side drop (slapdown) in that at any other angle, the resulting g-loads in each direction (longitudinal and lateral) are smaller than the bounding deceleration loads applied in the end, side, and corner drops. Nevertheless, based on the results obtained in Appendix 2.A, the case of an oblique drop with primary impact at 30 degrees from the horizontal is analyzed in detail. This case covers all orientations where the maximum deceleration load occurs and is reacted by the primary impact limiter. For this case, moment equilibrium includes inertia loads from overpack rotation as well as linear deceleration. For the 30-degree drop orientation at the primary impact location, the design basis deceleration load is applied with 52g lateral component and 30g longitudinal component. The loads are applied in the same manner as discussed in Subsection 2.7.1.3 with one additional complication. In contrast to the center of gravity over corner orientation where moment equilibrium is automatically satisfied when the loads are correctly applied, the applied loads and the reaction loads from the impact limiter are not initially in moment equilibrium. No inertial loading due to overpack rotational motion at the instant being considered is included. Without an additional inertial moment loading component, a large reaction force would develop at the far-removed arbitrary fixed reference point because the impact limiter reaction loads are offset from the overpack and MPC inertia loads from the linear decelerations. Figure 2.7.14 shows the overpack in a general oblique orientation. Appropriate arrows show the impact limiter reaction forces and the components of the applied linear decelerations. The loads from the MPC are not shown on the figure but they are applied as previously described for the corner drop. It is clear that moment equilibrium is not satisfied unless reaction loads develop at the arbitrarily chosen fixed support location far removed from the impact point. In the real drop scenario, since there is only a primary impact reaction, the cask must have angular accelerations imposed to insure moment equilibrium since the fixed point is an artifact to meet the requirements of the finite element analysis. To zero this reaction load at the point far-removed from the impact location, an additional load case with a unit angular velocity imposed at the mass center of the system and no other loads is developed. An angular acceleration is internally generated by ANSYS for this load case. The solution to this load case provides a reaction at the hypothetical fixed point assumed at the end of the overpack far removed from the impact location to balance the imposed inertial moment. The addition of this load case, with proper magnitude and sign ascribed to the input angular velocity, serves to eliminate all reactions at the far-removed fixed point. By adding this inertia moment load case, both force and moment equilibrium equations are satisfied for the oblique drop case where there is only a single impact limiter providing external forces to react the cask motion. With reference to Figure 2.7.7, the extent of the impact limiter loaded region on the overpack for this case is  $\theta = 63$  degrees. This angle is estimated from the projected geometry from the theoretical analysis in Appendix 2.A. Figure 2.7.9 shows a side view of the top forging with the end loading from the impact limiter applied as a pressure over the loaded region.

The finite element solution provides stress intensity results for the hot and cold conditions. The safety factors are summarized in Tables 2.7.5 and 2.7.6 (identified as Load Cases 20 and 21 corresponding to the “heat” and “cold” environmental conditions).

The near side drop with impact at the secondary impact limiter (slapdown) is a special case that also merits detailed analysis. For this case, the angle of the cask with the target is near zero degrees, similar to that used for the side drop analysis. The nature of the equilibrium equations is quite different, however. For the side drop, Figure 2.7.17 shows that equilibrium is satisfied by impact limiter reaction pressures at both impact locations. The reaction lateral pressure distribution at each impact limiter is distributed in the manner described by Figure 2.7.7. For the side drop evaluation, no introduction of a rotational component to the overpack is required to insure moment equilibrium. For the analysis of the near side drop secondary impact case, all of the reaction force required to insure that force equilibrium is maintained under the inertia induced loads, is imposed at the location of the secondary impact limiter. Figure 2.7.18 shows a side view of the overpack with the reaction load applied over a specified arc in the same manner as described by Figure 2.7.7. At the time of peak secondary impact deceleration, the theoretical analysis predicted minimal axial deceleration. Therefore, to perform the stress analysis using the finite element model, no axial deceleration is imposed. Referring to Figure 2.7.7, the angle  $\theta$  for this evaluation is chosen on the basis of observed experimental results and theoretical prediction. The angle is related to the angle associated with the observed crush depth of the impact limiter itself. For a near side drop, the outer diameter of the impact limiter is known, and if the crush depth is observed, calculated, or measured, the angular extent of impact limiter crushed material is easily determined. The outer radius, "Ri" of the impact limiter, and the observed and calculated crush depth (see results in Appendix 2.A for a full scale impact limiter), "d", are:

$$R_i = 64"; \quad d = 15"$$

Therefore, the angle " $\phi$ " (on either side of a vertical diameter through the impact limiter) that is associated with the extent of loaded crushed surface of the impact limiter is obtained from simple geometry as:

$$\cos(\phi) = 1 - d/R_i$$

The angle over which the load is applied at the crushed surface of the impact limiter is calculated to be:

$$\phi = 40 \text{ degrees (measured from the vertical, on both sides of the vertical centerline).}$$

The angle of significant reaction loads on the interface surface of the top forging, is greater than this angle. However, it is conservative to perform the finite element analysis of the "slapdown" secondary impact event, using the load angle

$$\theta = \phi = 40 \text{ degrees.}$$

Note that this angle used for the "slapdown" evaluation is larger than the conservative value used to evaluate the side drop. This reflects the increased crush imparted to the impact limiter since the entire amplified load is reacted at the top end. The load from the MPC is imposed on the appropriate inside surface of the inner shell as a uniform load in the same manner as for the side drop analysis. Moment equilibrium is provided by imposing the additional pure rotation on the overpack sufficient to generate opposite reaction forces that zero out the combined reactions at the "balance point" from

the applied inertia decelerations plus the pure rotation case. Because the MPC is constrained within the overpack, no departure from a uniform load transfer to the overpack is anticipated. Therefore, the enforcement of moment equilibrium for this condition is ensured solely by the determination of a proper balancing moment by determining an appropriate angular acceleration for the overpack. This assumption has little effect on the computation of the primary stress intensity distribution that results from the impact.

The results of the analysis are tabulated and combined with other load conditions, and the combined load case is designated as "Load Case 22". Bolt preload, internal pressure, and the inertia loads are combined to form this "slapdown" simulation. The top-end secondary impact analysis reported herein bounds a similar analysis of the bottom end secondary impact case. Summary results for minimum safety factors are reported in Table 2.7.5 only for the "Heat" environmental condition as previous results have demonstrated that this case produces the minimum safety factors. Only primary stress intensities are surveyed and reported in accordance with ASME requirements. Also evaluated is the bolt stress, the net friction force, and the state of the seals and lands. From the post-processed results, it is concluded that no bolts are overstressed, no portion of the seals suffer unloading, and that there is sufficient frictional force to insure that the lid is maintained in position.

The preceding discussion focussed on the transport overpack analyses. The minimum safety factors for the MPC fuel basket and enclosure vessel, for arbitrary drop orientation, are obtained from the general formulation in the preceding subsection 2.7.1.3. The angle that provides the maximum combined stress intensity (S.I.) can be determined by classical means, and the minimum safety factor established. The results are summarized in the table below:

GENERAL OBLIQUE DROP ORIENTATION MPC – SAFETY FACTORS				
Item	Drop Orientation Angle (Degrees)	Calculated S.I. (psi)	Allowable S.I. (psi)	Safety Factor
Fuel Basket	4.54	47,208	55,450	1.17
Enclosure Vessel	24.55	27,100	65,200	2.41

2.7.1.5 Comparison with Allowable Stresses

Tables 2.7.4 through 2.7.8 summarize the limiting safety factor obtained for each hypothetical free drop accident condition of transport defined by the requirements of Regulatory Guide 7.9. In particular, Table 2.7.4 is a summary of safety factors from the analyses of the MPC fuel basket and enclosure vessel, and Tables 2.7.5 and 2.7.6 report safety factors from the overpack analyses. Finally, Tables 2.7.7 and 2.7.8 contain safety factor summary results from miscellaneous evaluations reported within the text. From these results, tables are constructed that summarize limiting safety factors for all of the hypothetical accident conditions of transport that are associated with drop events. Tables 2.7.1 through Tables 2.7.3 present the overall summary of the most limiting safety factor for each of the components of interest for all hypothetical accident conditions of transport. It is concluded from these tables that large factors of safety exist in the fuel basket, in the MPC shell, and in the various components of the overpack under all hypothetical accident conditions of

transport associated with free drop events.

It is noted that the overpack finite element results are developed using a 3-D model of the overpack. Even though symmetry conditions reduce the size of the model, there are over 8000 elements and 11000 nodes.

The postulated accident conditions all tend to load localized regions of the overpack. As an illustration, consider Load Case 20, the 30-degree oblique top-end impact with the target. The limiting results for safety factors are reported in Table 2.7.5. Figures 2.7.15 and 2.7.16 show stress intensity distributions for the inner shell and for the assemblage of intermediate shells, respectively. As expected, the regions of highest stress intensity are naturally concentrated near the impacted region.

## 2.7.2 Puncture

- Overpack Structural Components

10CFR71 mandates that a puncture event be considered as a hypothetical accident condition. For this event, it is postulated that the package falls freely through a distance of 1 meter and impacts a 6 inch diameter mild steel bar. The effects of the puncture drop are most severe when the steel bar is perpendicular to the impact surface. Therefore, all puncture analyses assume that the bar is perpendicular to the impact surface. It is assumed that the steel bar has a flow stress equal to 48,000 psi, which is representative of mild steel. The maximum resisting force can then be calculated as

$$F_R = \frac{\pi D^2}{4} \times 48,000 \text{ psi} = 1.357 \times 10^6 \text{ lb}$$

where D equals the diameter of the steel bar.

$$|A_p| = \frac{F_R g}{W}$$

Since the maximum force applied to the cask is limited to the above value, the average deceleration of the cask can be computed assuming it to be rigid. The average deceleration of the cask (plus contents) (weight = W) is determined as:

For a bounding (low) weight of 230,000 lb. (Table 2.2.1), for example, the rigid body average deceleration over the time duration of impact, is 5.9g.

Candidate locations for impact that have the potential to cause the most severe damage are near the center of the closure plate (top-end puncture), the center of the bottom plate (bottom puncture), and the center height of the overpack shells (side puncture). In accordance with Regulatory Guide 7.9, local damage near the point of impact and the overall effect on the package must be assessed.

An estimate of local puncture resistance is obtained by using Nelms' equation [2.7.1] that is

generally applicable only for lead backed shells. Nevertheless, it is useful to obtain an indication as to whether a potential problem exists in the HI-STAR 100 System. The equation is applied using an ultimate strength of 70,000 psi that is appropriate for the selected impact regions. Nelms' equation predicts a minimum thickness of material necessary to preclude significant puncture damage. For the HI-STAR 100 System,

$$t_m = \left( \frac{W}{S_u} \right)^{0.71} = 2.65 \quad \text{inch}$$

Inasmuch as the HI-STAR 100 overpack has substantially more material thickness in the baseplate, the closure plate, the top flange and the inner plus the initial intermediate shell, the overpack meets local puncture requirements as required by Nelms' equation.

The global effects of puncture are calculated using the overpack model described in Section 2.6, which is the same model that is used for the drop assessments. Figures 2.1.12 through 2.1.14 show free body diagrams of the overpack for the side, top, and bottom puncture events, respectively. In each case, the nodes on the surface of the overpack that directly impact the steel bar are fixed in all degrees of freedom. By then applying acceleration,  $A_p$ , a reaction force develops at those nodes equal in magnitude with  $F_R$ . Tables 2.7.5 and 2.7.6 summarize the safety factors for the overpack components obtained for the puncture acceleration computed above for both heat and cold environmental conditions. Note that for the stress intensities in the lid and baseplate, the highest stresses are exactly under the impact point. The results include the effect of the interface contact stress between the puncture pin and the plate surface. This local effect is not required to be included in the stress intensity comparison with allowable values for the hypothetical accident. Therefore, in the reporting of safety factors, the effect of local surface pressure is not included; rather, the radial and tangential stresses at the load point are used to form the stress intensity and set the lateral surface stress to zero. Tables 2.7.5 and 2.7.6 specifically identify this item by a note. Figure 2.7.17 shows the stress intensity distribution in the lid resulting from a top-end puncture analysis. The localized nature of the stress intensity distribution is clearly evident. The reported safety factors in the summary tables are adjusted to eliminate the effect of non-primary stress components.

- Closure Bolts

The methodology to analyze closure bolts is provided in reference [2.6.3] prepared for analysis of shipping casks. The analysis of the overpack closure bolts under normal conditions of transport, in accordance with the provisions of [2.6.3], has been reported in Section 2.6. In this subsection, the similar analysis for the hypothetical puncture accident is summarized. The analysis follows the procedures defined in Reference [2.6.3] and uses the allowable stresses for the closure bolts in that reference.

The following combined load case is analyzed for the hypothetical pin puncture accident condition of transport.

Puncture: Pressure, temperature, and pre-load loads are included.

Reference [2.6.3] reports safety factors defined as the calculated stress combination divided by the allowable stress for the load combination. This definition of safety factor is the inverse of the definition consistently used in this SAR. In summarizing the closure bolt analysis, results are reported using the SAR safety factor definition of allowable stress divided by calculated stress. The following result for closure lid bolting for the top end drop hypothetical accident condition of transport is obtained.

Overpack Closure Bolt - Safety Factor (Load Case 7 in Table 2.1.9)	
Item	Safety Factor on Bolt Tension
Average Tensile Stress in Bolt	1.86

2.7.3 Thermal

In this subsection, the structural consequences of the thirty-minute fire event are evaluated using the metal temperature data from Section 3.5 where a detailed analysis of the fire and post-fire condition is presented. Specifically, it desired to establish that:

1. The metal temperature, averaged across any section of the containment boundary, remains below the maximum permissible temperature for the Level A condition in the ASME Code for NB components. Strictly speaking, the fire event is a Level D condition for which Subsection NB of the ASME Code, Section III does not prescribe a specific metal temperature limit. The Level A limit is imposed herein for convenience because it obviates the need for creep considerations to ascertain post-fire containment integrity.
2. The external skin of the overpack, directly exposed to the fire will not slump (i.e., suffer rapid primary creep). This condition is readily ruled out for steel components if the metal temperature remains below 50% of the metal melting point.
3. Internal interferences among the constituents of the HI-STAR 100 System do not develop due to their differential thermal expansion during and after the fire transient.
4. Overpack closure bolts will not unload during a transport fire.
5. The helium retention boundary and the containment boundary both continue to perform their function as ASME "NB" pressure vessels.

2.7.3.1 Summary of Pressures and Temperatures

The following peak temperatures (per Tables 3.5.4 and 3.4.11) and pressures are used in Subsections 2.7.3.2, 2.7.3.3, and 2.7.3.4.

Overpack closure plate/bolts	514 degrees F (post-fire)
Overpack bottom plate	662 degrees F (post-fire)

Overpack outer closure	226 degrees F (initial pre-fire cold temperature); 1348 degrees F (maximum)
Overpack containment shell	395 degrees F (MPC –Shell post-fire temp. - increment of 24 degrees F (from data in Table 3.4.11))
MPC-Shell	419 degrees F (post-fire)
Basket (center)	751 degrees F (post-fire)
Basket (periphery)	478 degrees F (MPC-Shell post fire + 59 degrees F - (from data in Table 3.4.11))

It should be noted that the overpack containment shell, closure plate, and bottom plate temperatures are not specifically reported in Table 3.5.4. The temperatures listed above are based on the closest temperature report location. The overpack containment shell temperature is the lowest temperature that occurs prior to the fire accident and is used for the differential thermal expansion analysis. The overpack containment shell temperature falls (post-fire) below the outside basket temperature and subsequently lags the basket temperature by 24 degrees F. The 24 degree F lag is the same lag that occurs in the normal heat condition listed in Table 3.4.11 (i.e., 306 degrees F for the MPC outer shell surface - 282 degrees F for the overpack inner surface). This will maximize the potential for interference between the overpack and the MPC. Similarly, the temperature difference between the MPC shell and the fuel basket periphery will be essentially the same exists in the normal heat conditions of transport. Therefore, from Table 3.4.11, the basket peripheral temperature for the fire event analyses is set as the MPC shell temperature plus the maximum difference (365-306) degrees F from the table.

Subsection 3.5.3 contains a discussion of the peak bulk temperatures occurring during and after the fire transient. It is concluded in that section that:

1. The containment boundary protected by the intermediate shells remains below 500 degrees F (SA-203-E material).
2. The containment boundary that is within the confines of the impact limiters remains below 700 degrees F (SA-350 LF3 material).
3. The portion of the containment boundary directly exposed to the fire may have local outer surface temperatures in excess of 700 degrees F, but the bulk metal temperature of the material volume remains under 700 degrees F (SA-350 LF3 material).

The conclusions in Subsection 3.5.3 enable the statement that the containment boundary metal bulk temperatures remain at or below the upper limits permitted by the ASME Code. Therefore, stress evaluations that make comparisons to allowable stresses to demonstrate that the containment boundary continues to perform as a viable pressure vessel use allowable stresses that are given in the ASME Code (i.e., there is no extrapolation of allowable stresses beyond the recognized code limits). For the helium retention boundary stress calculations, however, allowable stresses for a conservatively high temperature (see Table 2.1.2 and 2.1.21) are used when pressure vessel code compliance is demonstrated.

From Table 3.5.4 in Subsection 3.5.4 of Chapter 3, it is concluded that:

The maximum temperature of the ferritic steel material in the body of the HI-STAR 100 overpack (the outer enclosure and the intermediate shells outside of the containment boundary is well below 50% of the material melting point. (The melting point of carbon and low alloy steels is approximately 2750 degrees F, per Mark's Standard Handbook, Ninth Edition, pp 6-11.)

The shielding experiences temperatures above its stated limit for effectiveness. This means that a limited loss of shielding effectiveness may occur. The shielding analysis in Chapter 5 (Subsection 5.1.2) recognizes this and conservatively assumes that all shielding is lost in post-fire shielding analyses.

Pressures during the fire transient are bounded by the internal and the external design pressures for accident conditions for the MPC shell as stated in Section 2.1. For internal pressure, Table 3.5.3 supports this conclusion. The following calculation is presented to support the conclusion for MPC external pressure.

The overpack annulus initial fill pressure is 14 psig (max.) per the specification in Chapter 7. The overpack annulus lower bound fill temperature is 70 degrees F. The fire condition MPC shell peak temperature is 419 degrees F per Table 3.5.4 and the use of this as the average gas temperature in the annulus is conservative.

Using the above data, the fire condition peak pressure in the annulus between the overpack and the MPC shell is calculated by using the ideal gas law with constant volume assumed in the gap as:

$$p_{\text{fire}} = (14 + 14.7) \times (419 + 460) / (70 + 460) = 47.6 \text{ psia} = 32.9 \text{ psig.}$$

2.7.3.2 Differential Thermal Expansion

The methodology for establishing that there will be no restraint of free thermal expansion has been presented in Subsection 2.6.1.2 for normal conditions of transport. The same methodology is applied in this subsection to evaluate the potential for component interference during and after the postulated hypothetical fire. For conservatism, use the temperatures in the overpack and the MPC temperatures that will maximize the potential for interference between the overpack and the MPC regardless of at what point in time the temperatures occurred. It is shown that there is no structural restraint of free-end expansion in the axial or radial directions under the most limiting temperature difference between the hot basket and the colder overpack/enclosure vessel. Thus, the ability to remove fuel by normal means is not inhibited by structural constraint of free-end expansion. The table below summarizes the results obtained for the limiting MPC temperature distributions assumed.

THERMOELASTIC DISPLACEMENTS IN THE MPC AND OVERPACK UNDER FIRE CONDITION				
CANISTER - FUEL BASKET				
	Radial Direction(in.)		Axial Direction (in.)	
Worst Case Unit	Initial Clearance	Final Gap	Initial Clearance	Final Gap
Bounding MPC	0.1875	0.117	2.0	1.672

CANISTER – OVERPACK				
	Radial Direction (in.)		Axial Direction (in.)	
Worst Case Unit	Initial Clearance	Final Gap	Initial Clearance	Final Gap
Bounding MPC	0.09375	0.004	0.625	0.291

Using the most conservative assumptions (i.e., do not consider a real “snapshot” in time during and after the fire, but rather assume the most detrimental temperature distribution occurs at the same instant in time) that maximize the potential for interference, it is demonstrated that no restraint of free thermal expansion in either the radial or axial directions occurs.

2.7.3.3 Stress Calculations

Under the fire accident, pressures in the MPC and overpack increase simultaneously, while the allowable strengths of the material may decrease from their values under normal conditions of transport. The MPC and overpack stresses are shown below (allowables are taken from Tables 2.1.21). It is required that both the helium retention boundary and the containment boundary meet Level D Service Limits of the ASME Code and continue to function as pressure vessels.

2.7.3.3.1 MPC

- Top Closure

The MPC Top Closure analysis for the fire condition is Load Case E5 in Table 2.1.7. The top closure is conservatively modeled as a simply supported plate considered to be loaded by the accident internal pressure plus self-weight acting in the same direction. For determination of the safety factor, the value of allowable stress from Table 2.1.20 appropriate to the fire temperature is used. The table below summarizes the result (where a multiplier of 2.0 has been incorporated to reflect the bounding dual lid design):

MPC Top Closure Safety Factor for Load Case E5 in Table 2.1.7			
Item	Value (ksi)	Allowable (ksi)	Safety Factor
Bending Stress	3.158 x 2	54.23	8.59

- Baseplate

Under the fire accident condition, the baseplate is subject to accident internal pressure (200 psi). If the HI-STAR 100 is assumed to be in the vertical position, then the baseplate also may support the weight of the fuel basket and the fuel loading. If the HI-STAR 100 is assumed to be oriented in the horizontal position, then the baseplate supports only internal pressure. For a conservative analysis, it is assumed that the internal pressure stress and the stress from basket weight and from fuel weight add. This Load Case E5 is summarized below. The second row is the result that is obtained if the basket and fuel weight is neglected.

MPC Baseplate Safety Factor under Hypothetical Fire Accident			
Item	Value (ksi)	Allowable (ksi)	Safety Factor
Baseplate Bending Stress (Including Basket and Fuel Weight)	46.32	54.23	1.17
Baseplate Bending Stress (Neglecting Basket, Fuel, and Self Weight)	42.28	54.23	1.28

- Shell

The MPC shell is examined for elastic/plastic stability under the fire accident external pressure using the ASME Code Case N-284 analysis method. The result from the stability analysis for Load Case E5 in Table 2.1.7 is summarized below:

MPC Canister Safety Factor - Stability under External Accident Pressure			
Item	Calculated Interaction Factor	Allowable Interaction Factor	Safety Factor
Elastic Stability	0.845	1.00	1.18

The shell is also analyzed for stress under the accident internal pressure by using the Lamé' solution previously used in Section 2.6. The stress due to the internal accident pressure of 200 psi is ( $P$  = pressure,  $r$  = MPC radius,  $t$  = shell thickness):

$$\sigma_1 = \frac{Pr}{t} = \frac{(200 \text{ psi})(68.375 \text{ in}/2)}{0.5 \text{ in}} = 13,675 \text{ psi}$$

$$\sigma_2 = \frac{Pr}{2t} = 6,838 \text{ psi}$$

$$\sigma_3 = -P = -200 \text{ psi}$$

The maximum stress intensity is  $\sigma_1 - \sigma_3 = 13,875 \text{ psi}$

The safety factor is,

$$SF = \frac{36.15 \text{ ksi}}{13.875 \text{ ksi}} = 2.61$$

#### 2.7.3.3.2 Overpack

The overpack stresses for normal heat conditions of transport are reported in Section 2.6. Since these stress solutions are based on linear elasticity, the stresses reported can be scaled up to account for the accident internal pressure and the safety factor computed based on the allowable stress for the fire temperature.

Generally, in the fire accident case, only primary stresses are of interest to demonstrate continued containment. Secondary stresses may be included in the evaluation, but they merely demonstrate additional levels of conservatism. Table 2.6.4 gives the minimum safety factor for the primary stress case of  $T_h + P_i + F + W_s$ .

The highest stress occurs in the inner shell, and has the value 2,832 psi.

The ratio of the accident pressure to normal pressure is (see Table 2.1.1)  $\frac{200}{100} = 2.00$ .

Using this factor, the safety factor is computed as follows:

For the inner shell at 500 degree F fire temperature per Table 2.1.14, the allowable membrane stress intensity under the fire condition is compared to the amplified mean stress and the safety factor computed as

$$SF = \frac{42.5 \text{ ksi}}{(5.664 + 0.200) \text{ ksi}} = 7.25$$

2.7.3.3.3 Closure Bolts

Under the fire transient, it is required to demonstrate that the stresses in the closure bolts do not exceed allowable limits and the bolted joint does not unload to the extent that the pressure boundary is breached. To that end, an analysis of the fire condition is carried out with the purpose of determining the bolt stresses under the applied loading. The methodology employed for this analysis is that presented in the report, "Stress Analysis for Closure Bolts for Shipping Casks" [2.6.3]. The loadings applied are fire temperature, bolt preload, and accident internal pressure. The following result for closure lid bolting for the hypothetical fire accident is obtained.

Overpack Closure Bolt - Safety Factor (Load Case 19 in Table 2.1.9)	
Combined Load Case	Safety Factor on Bolt Tension
Average Tensile Stress	1.69

The average bolt tensile stress under the conditions of pressure, preload, and thermal effects appropriate to the hypothetical fire accident condition of transport is 8.5% greater than the average bolt tensile stress computed under the normal heat condition of transport. Therefore, it is concluded that there will be only minor unloading of the bolted joint and no breach of containment.

2.7.3.3.4 Bounding Thermal Stresses During the Fire Transient

Regulatory Guide 7.6, Section C.7 states that the extreme total stress intensity range between the initial state and accident conditions should be less than twice the adjusted value of the alternating stress intensity at 10 cycles given by the appropriate fatigue curves. It is demonstrated here that under very conservative assumptions on the calculation of thermal stresses, this regulatory requirement is met by the HI-STAR 100 System.

Under the fire transient, thermal gradients can lead to secondary or peak stresses due to local constraint by adjacent material that is at a lower temperature. The ASME Code does not require that secondary stresses be held to any limit for Level D Service Conditions. Nevertheless, bounding calculations are performed here to estimate the magnitude of the thermal stress. The most limiting secondary stress intensity state arises by conservatively assuming complete restraint of material by surrounding cooler material and has the solution:

$$|\sigma| = E \alpha \Delta T$$

where

E = Young's Modulus at temperature  
 $\alpha$  = coefficient of linear thermal expansion  
 $\Delta T$  = temperature change from 70 degrees F, the assumed assembly temperature

For the fuel basket,  $\Delta T = 775 - 70 = 705$  degrees F. The use of 775 degrees F is justified as follows:

The peak temperature of the fuel basket is 950 degrees F during the fire per Table 2.1.2. For a conservative estimate of the temperature between *two adjacent points* on the fuel basket, use the bounding hypothetical accident temperature limit for the enclosure vessel lid or baseplate from Table 2.1.2 as representative of the change between *two adjacent points* on the fuel basket. Therefore, no extrapolation of data is required for the calculations to follow.

From the material property table for Alloy X,

$$\begin{aligned} E &= 24.282 \times 10^6 \text{ psi} \\ \alpha &= 9.853 \times 10^{-6} \text{ inch/inch-degree F} \end{aligned}$$

Therefore,

$$\sigma = 24.282 \times 9.853 \times 705 = 168,672 \text{ psi}$$

The conservative assumption is made that the maximum peak stress intensity due to mechanical loading plus thermal constraint occur at the same point at the same instant in time and reaches the value of  $S_u$  at room temperature. Thus, the total stress intensity range from assembly to this hypothetical conservative state is

$$S_R = 168,672 + 75,000 = 243,672 \text{ psi}$$

The alternating stress intensity range, after accounting for temperature effects of Young's Modulus, is

$$\begin{aligned} S_a &= \frac{S_R}{2} \times \frac{\text{Young's Modulus (70° F)}}{\text{Young's Modulus (775° F)}} \\ &= 121,836 \text{ psi} \times \frac{28.14}{24.282} = 141,194 \text{ psi} \end{aligned}$$

For the overpack, the most severely constrained material is at the bottom plate. Material properties for this calculation are the values available at 700 degrees F and the peak temperature is conservatively set at 700 degrees F.

$$\text{Young's Modulus} = E = 24.9 \times 10^6 \text{ psi (at 700 degrees F)}$$

$$\text{Coefficient of linear thermal expansion} = \alpha = 7.52 \times 10^{-6} \text{ inch/inch-degrees F (Estimated)}$$

Therefore, the secondary stress intensity due to fully constrained thermal growth is

$$\sigma = 24.9 \times 7.52 \times (700-70) = 117,966 \text{ psi}$$

Conservatively, assuming that the membrane plus primary bending stress intensity achieves the ultimate strength at room temperature, at the same location in space and at the same instant in time, gives the total stress intensity range at this hypothetical location as

$$S_R = 117,966 + 75,000 = 192,966 \text{ psi}$$

The alternating stress intensity range, after accounting for temperature effects of Young's Modulus, is

$$S_a = \frac{192,966}{2} \times \frac{28.14}{24.9} = 109,037 \text{ psi}$$

These computed values for bounding alternating stress intensities are used in the next subsection for comparisons with allowable values.

#### 2.7.3.4 Comparison of Fire Accident Results with Allowable Stresses

##### Stress

The safety factors for the MPC and overpack during a fire are addressed in Section 2.7.3.3. The lowest safety factors are 1.18 and 7.74 for the MPC and overpack, respectively.

##### Bounding Fire Transient

In accordance with Regulatory Position C.7 of the Regulatory Guide 7.6, Figure I-9.2.1 of ASME, Section III, Appendix I, gives the 10-cycle alternating stress intensity range as

$$S_{ALT} (\text{Alloy X}) = 700,000 \text{ psi}$$

Using the calculated stress intensity range from Subsection 2.7.3.3, the safety factor for the MPC basket is

$$SF = \frac{700,000}{141,194} = 4.96$$

Figure I-9.1 of ASME Section III, Appendix I is used for the overpack even though the temperature is limited to below 700 degrees F. It is conservative to use this curve for this short time event since increased temperatures will improve the material ductility. From that table, the 10-cycle alternating stress intensity range is given as 400,000 psi. Therefore using the aforementioned calculated results for stress intensity range from Subsection 2.7.3.3, the safety factor is computed as:

$$SF = \frac{400,000}{109,037} = 3.67$$

An analysis of the threaded holes in the top closure has been performed to assess the length of

engagement and stress requirements imposed on the connection by the transport loads. The methodology used to evaluate the connection is that set forth in Machinery's Handbook and uses the specific characteristics of the threaded joint. As part of the calculation, it is demonstrated that the bolt force required to maintain the seal (seal seating load plus pressure force) is only 27% of the total bolt preload force that must be applied to ensure bolt performance under the various drop scenarios. That is, there is 73% excess capacity. Therefore, the momentary joint decompression due to the hypothetical fire accident is not sufficient to unload the seal.

The above calculations demonstrate that the requirements of Paragraph C.7 of Regulatory Guide 7.6 are satisfied.

#### 2.7.4 Immersion - Fissile Material

In order for the spent nuclear fuel in the HI-STAR 100 System to become flooded with water, a leak must develop in both the overpack containment structure and the MPC enclosure vessel. The analysis provided demonstrates that both the overpack containment boundary and the MPC enclosure vessel meet the applicable stress and stress intensity allowables for normal conditions of transport and hypothetical accident conditions. Therefore, no leak will develop.

10CFR71.73(c)(5) specifies that fissile material packages, in those cases where water inleakage has not been assumed for criticality analysis, must be evaluated for immersion under a head of water of at least 0.9 m (3 ft.) in the attitude for which maximum leakage is expected. The criticality analyses presented in Chapter 6 conservatively assumes flooding with water at optimum moderation. Therefore, this paragraph is not applicable. However, analysis is presented to demonstrate that there is no water inleakage and verify that the flooded assumption made in the criticality analysis is conservative.

A head of water at a depth of 0.9 m (3 ft.) is equal to 1.3 psi. This pressure is bounded by the MPC enclosure vessel normal condition of transport and hypothetical accident condition external pressures listed in Table 2.1.1. The head of water (1.3 psi) is also bounded by the hypothetical accident condition external pressure for the overpack. Analysis provided in this chapter demonstrates that both the overpack containment boundary and the MPC enclosure vessel meet the applicable stress and stress intensity allowables for normal conditions of transport and hypothetical accident conditions. Therefore, there is no in-leakage of water into the overpack or MPC under a head of water at a depth of 0.9 m (3 ft.).

#### 2.7.5 Immersion - All Packages

Deep submergence of the HI-STAR 100 System in 200 meters (656 ft.) of water creates an external pressure load equal to 284 psi, which is less than the external design pressure of 300 psi. This condition is established as Load Case 18 in Table 2.1.9. Since the containment boundary is not punctured, stability of the package can be evaluated considering an undamaged package. The results for an external pressure of 300 psi bound the results for 21.7 psi gauge pressure that is established in 10CFR71.73(c)(6) as the applicable external pressure for this evaluation. The elastic/plastic stability of the overpack has been examined using the methodology of ASME Code Case N-284. In the analysis, all structural resistance to the external pressure is conservatively concentrated in the inner

containment shell. No credit is given to any structural support by the intermediate shells. The external pressure is assumed to act directly on the outer surface of the inner containment shell and the secondary fabrication stress is assumed to add to the stress due to the deep submergence pressure. The results for this case are summarized below:

Overpack Stability using ASME Code Case N-284 - Load Case 18 in Table 2.1.9			
Item	Value from Interaction Curve	Allowable Interaction Curve Value	Safety Factor
Yield Stress Limit	0.577*	1.34	2.32*
Elastic Stability	0.253	1.0	3.95

\* Applicable to inner shell fabricated from SA203-E material. Safety factor must be multiplied by 0.93 if inner shell is fabricated from optional SA350-LF3 material.

It is noted that Code Case N-284 imposes limits on both stress and stability and includes a built-in safety factor of 1.34 for the Level D Service Limit. Therefore, the first row in the table above reports the true safety factor existing against exceeding the yield stress in the inner containment shell; the second row in the table provides the safety factor against elastic instability of the inner shell. The large values for the safety factors that are obtained, even with the conservative assumptions, attests to the ruggedness of the inner containment shell.

The analysis performed above for a 300 psi external pressure also confirms that the package meets the requirements of 10CFR71.61 that a 290 psi external pressure can be supported without any instability.

#### 2.7.6 Summary of Damage

The results presented in Subsections 2.7.1 through 2.7.5 show that the HI-STAR 100 System meets the requirements of 10CFR71.61 and 10CFR71.73. All safety factors are greater than 1.0 for the hypothetical accident conditions of transport. Therefore, the HI-STAR 100 package, under the hypothetical accident conditions of transport, has adequate structural integrity to satisfy the subcriticality, containment, shielding, and temperature requirements of 10CFR71.

Table 2.7.1

MINIMUM SAFETY FACTORS FOR THE MPC FUEL BASKET UNDER HYPOTHETICAL ACCIDENT CONDITIONS OF TRANSPORT

Load Case Number	Load Combination <sup>†</sup>	Safety Factor	Location in SAR where Calculations or Results are Presented
F3			
F3.a	D + H', end drop	4.19	Subsection 2.7.1.1; Table 2.7.7
F3.b	D + H', 0° side drop	1.16	Table 2.7.4
F3.c	D + H', 45° side drop	1.28	Table 2.7.4

<sup>†</sup> The symbols used for loads are defined in Subsection 2.1.2.1.

Table 2.7.2

MINIMUM SAFETY FACTORS FOR THE MPC ENCLOSURE VESSEL  
FOR HYPOTHETICAL CONDITIONS OF TRANSPORT

Load Case Number	Load Combination <sup>†</sup>	Safety Factor	Location in SAR where Calculations or Results are Presented
E3			
E3.a	D + H' + P <sub>o</sub> , end drop	1.4 3.04 1.92	Lid Table 2.7.7 Baseplate Table 2.7.7 Shell Table 2.7.7
E3.b	D + H' + P <sub>i</sub> , 0 deg. side drop	2.14 1.16	Shell Table 2.7.4 Supports Table 2.7.4
E3.c	D + H' + P <sub>i</sub> , 45 deg. side drop	2.74 1.51	Shell Table 2.7.4 Supports Table 2.7.4
E5	P <sub>i</sub> <sup>*</sup> or P <sub>o</sub> <sup>*</sup>	8.59 1.17 1.18 (buckling) 4.16 (mean stress)	Lid Table 2.7.7 Baseplate Table 2.7.7 Shell Table 2.7.7 Subsection 2.7.3.3.1

<sup>†</sup> The symbols used for loads are defined in Subsection 2.1.2.1.

Table 2.7.3

**MINIMUM SAFETY FACTORS FOR THE OVERPACK  
FOR HYPOTHETICAL ACCIDENT CONDITIONS OF TRANSPORT**

Load Case Number	Load Combination <sup>†</sup>	Safety Factor	Location in SAR where Calculations or Results are Presented
1	$T_h + D_{ba} + P_i + F + W_s$	2.16	Table 2.7.8
2	$T_h + D_{ta} + P_i + F + W_s$	1.75	Table 2.7.5
3	$T_h + D_{sa} + P_i + F + W_s$	2.19 (see note 2)	Table 2.7.5
4	$T_h + D_{ea} + P_i + F + W_s$	1.49	Table 2.7.5
5	$T_h + D_{ga} + P_i + F + W_s$	2.60 (see note 2)	Table 2.7.5
6	$T_h + P_s + P_i + F + W_s$	2.80 (see note 2)	Table 2.7.5
7	$T_h + P_t + P_i + F + W_s$	2.03 (see note 1)	Table 2.7.5
8	$T_h + P_b + P_i + F + W_s$	1.46	Table 2.7.5
9	$T_c + D_{ba} + P_o + F + W_s$	4.17	Table 2.7.6
10	$T_c + D_{ta} + P_o + F + W_s$	1.87	Table 2.7.6
11	$T_c + D_{sa} + P_o + F + W_s$	2.19	Table 2.7.6
12	$T_c + D_{ea} + P_o + F + W_s$	1.73	Table 2.7.6
13	$T_c + D_{ga} + P_o + F + W_s$	2.65	Table 2.7.6
14	$T_c + P_s + P_o + F + W_s$	3.05	Table 2.7.6
15	$T_c + P_t + P_o + F + W_s$	2.09 (see note 1)	Table 2.7.6
16	$T_c + P_b + P_o + F + W_s$	1.46	Table 2.7.6
17	$T_f + P_i + F + W_s$	pre-load maintained	Subsection 2.7.3.4
18	$P_o^*$	2.32	Table 2.7.8
19	$P_i^* + T_f + F + W_s$	7.25	Subsection 2.7.3.3.2
20	$T_h + D_{ga} + P_i + F + W_s$	1.77	Table 2.7.5
21	$T_c + D_{ga} + P_i + F + W_s$	1.84	Table 2.7.6
22	$T_c + D_{ra} + P_i + F + W_s$	2.14 (see note 2)	Table 2.7.5

- Note: 1. This reported stress is directly under the point of impact. Therefore, the calculated value does not represent a primary stress; however, primary stress levels are met by this peak stress intensity.  
2. Applicable to inner shell fabricated from SA203-E material. Safety factor must be multiplied by 0.93 if inner shell is fabricated from optional SA350-LF3 material.

<sup>†</sup> The symbols used here are defined in Subsection 2.1.2.1.

Table 2.7.4 - FINITE ELEMENT ANALYSIS RESULTS  
 MINIMUM SAFETY FACTORS FOR MPC COMPONENTS UNDER ACCIDENT CONDITIONS

Component - Stress Result	MPC-24		MPC-32		MPC-68	
	30 Ft. Side Drop, 0° Orientation Load Case F3.b or E3.b	30 Ft. Side Drop, 45° Orientation Load Case F3.c or E3.c	30 Ft. Side Drop, 0° Orientation Load Case F3.b or E3.b	30 Ft. Side Drop, 45° Orientation Load Case F3.c or E3.c	30 Ft. Side Drop, 0° Orientation Load Case F3.b or E3.b	30 Ft. Side Drop, 45° Orientation Load Case F3.c or E3.c
Fuel Basket - Primary Membrane ( $P_m$ )	2.80	3.85	2.78	3.90	3.07	4.30
Fuel Basket - Local Membrane Plus Primary Bending ( $P_L + P_b$ )	1.19	1.29	1.19	1.28	2.64	1.56
Enclosure Vessel - Primary Membrane ( $P_m$ )	6.43	6.88	5.77	6.95	5.64	7.12
Enclosure Vessel - Local Membrane Plus Primary Bending ( $P_L + P_b$ )	4.24	4.28	2.14	3.56	3.07	2.74
Basket Supports - Primary Membrane ( $P_m$ )	N/A	N/A	2.72	3.83	6.67	8.67
Basket Supports - Local Membrane Plus Primary Bending ( $P_L + P_b$ )	N/A	N/A	3.89	4.75	1.16	1.51

Table 2.7.4 (Continued) - FINITE ELEMENT ANALYSIS RESULTS  
 MINIMUM SAFETY FACTORS FOR MPC COMPONENTS UNDER ACCIDENT CONDITIONS

Component - Stress Result	MPC-24E/EF	
	30 Ft. Side Drop, 0 deg Orientation Load Case F3.b or E3.b	30 Ft. Side Drop, 45 deg Orientation Load Case F3.c or E3.c
Fuel Basket – Primary Membrane ( $P_m$ )	2.74	3.79
Fuel Basket - Local Membrane Plus Primary Bending ( $P_L + P_b$ )	1.16	1.28
Enclosure Vessel - Primary Membrane ( $P_m$ )	6.39	6.86
Enclosure Vessel - Local Membrane Plus Primary Bending ( $P_L + P_b$ )	3.14	4.13

Table 2.7.5 - FINITE ELEMENT ANALYSIS RESULTS  
 MINIMUM SAFETY FACTORS FOR OVERPACK COMPONENTS UNDER ACCIDENT CONDITIONS (Hot Environment)

Component – Stress Result	30 Ft. Bottom End Drop Load Case 1	30 Ft. Top End Drop Load Case 2	30 Ft. Side Drop Load Case 3	30 Ft. C.G. Over-the- Bottom-Corner Drop Load Case 4
Lid – Local Membrane Plus Primary Bending ( $P_L + P_b$ )	34.04	1.75	2.60	7.76
Inner Shell – Local Membrane Plus Primary Bending ( $P_L + P_b$ )	4.35 (Note 2)	10.02 (Note 2)	2.19 (Note 2)	2.93 (Note 2)
Inner Shell – Primary Membrane ( $P_m$ )	4.48 (Note 2)	7.39 (Note 2)	2.45 (Note 2)	2.33 (Note 2)
Intermediate Shells - Local Membrane Plus Primary Bending ( $P_L + P_b$ )	6.63	7.95	2.33	1.49
Baseplate - Local Membrane Plus Primary Bending ( $P_L + P_b$ )	7.05	21.6	4.71	2.78
Enclosure Shell - Primary Membrane ( $P_m$ )	16.44	12.23	2.19	5.48

- Notes:
1. Load cases are defined in Table 2.1.9.
  2. Applicable to inner shell fabricated from SA203-E material. Safety factor must be multiplied by 0.93 if inner shell is fabricated from optional SA350-LF3 material.

Table 2.7.5 (Continued) - FINITE ELEMENT ANALYSIS RESULTS  
 MINIMUM SAFETY FACTORS FOR OVERPACK COMPONENTS UNDER ACCIDENT CONDITIONS (Hot Environment)

Component - Stress Result	30 Ft. C.G. Over- the-Top-Corner Drop Load Case 5	Side Puncture Load Case 6	Top End Puncture Load Case 7	Bottom End Puncture Load Case 8	30 Ft. – 30 degree Drop Load Case 20	30 Ft. – Slapdown Load Case 22
Lid – Local Membrane Plus Primary Bending ( $P_L + P_b$ )	3.69	5.70	2.03 (See Note 2)	6.29	1.77	2.22
Inner Shell – Local Membrane Plus Primary Bending ( $P_L + P_b$ )	3.16 (Note 3)	2.80 (Note 3)	29.29 (Note 3)	9.52 (Note 3)	2.78 (Note 3)	2.73 (Note 3)
Inner Shell – Primary Membrane ( $P_m$ )	2.60 (Note 3)	5.95 (Note 3)	26.5 (Note 3)	10.61 (Note 3)	2.45 (Note 3)	2.14 (Note 3)
Intermediate Shells - Local Membrane Plus Primary Bending ( $P_L + P_b$ )	3.52	6.19	32.52	15.12	3.28	2.88
Baseplate - Local Membrane Plus Primary Bending ( $P_L + P_b$ )	6.95	21.62	28.62	1.46	27.32	17.9
Enclosure Shell - Primary Membrane ( $P_m$ )	3.56	4.53	51.32	29.9	8.02	2.40

- Notes: 1. Load cases are defined in Table 2.1.9.  
 2. Stress Intensity computed just outboard of the loaded area since surface stress is not a primary stress component.  
 3. Applicable to inner shell fabricated from SA203-E material. Safety factor must be multiplied by 0.93 if inner shell is fabricated from optional SA350-LF3 material.

Table 2.7.6 - FINITE ELEMENT ANALYSIS RESULTS  
 MINIMUM SAFETY FACTORS FOR OVERPACK COMPONENTS UNDER ACCIDENT CONDITIONS (Cold Environment)

Component – Stress Result	30 Ft. Bottom End Drop Load Case 9	30 Ft. Top End Drop Load Case 10	30 Ft. Side Drop Load Case 11	30 Ft. C.G. Over-the- Bottom-Corner Drop Load Case 12
Lid – Local Membrane Plus Primary Bending ( $P_L + P_b$ )	30.29	1.87	2.73	8.00
Inner Shell – Local Membrane Plus Primary Bending ( $P_L + P_b$ )	4.17	9.69	2.19	2.94
Inner Shell – Primary Membrane ( $P_m$ )	4.37	7.33	2.47	2.36
Intermediate Shells - Local Membrane Plus Primary Bending ( $P_L + P_b$ )	4.95	8.66	2.61	1.73
Baseplate - Local Membrane Plus Primary Bending ( $P_L + P_b$ )	7.73	17.07	4.80	2.73
Enclosure Shell - Primary Membrane ( $P_m$ )	20.08	18.4	2.45	5.71

Notes: 1. Load cases are defined in Table 2.1.9.

Table 2.7.6 (Continued) - FINITE ELEMENT ANALYSIS RESULTS  
 MINIMUM SAFETY FACTORS FOR OVERPACK COMPONENTS UNDER ACCIDENT CONDITIONS (Cold Environment)

Component – Stress Result	30 Ft. C.G. Over- the-Top-Corner Drop Load Case 13	Side Puncture Load Case 14	Top End Puncture Load Case 15	Bottom End Puncture Load Case 16	30 Ft.. – 30 degree Drop Load Case 21
Lid – Local Membrane Plus Primary Bending ( $P_L + P_b$ )	3.91	5.91	2.09 (See Note 2)	6.64	1.84
Inner Shell – Local Membrane Plus Primary Bending ( $P_L + P_b$ )	3.21	3.05	24.97	8.54	2.78
Inner Shell – Primary Membrane ( $P_m$ )	2.65	7.60	17.03	9.59	2.48
Intermediate Shells - Local Membrane Plus Primary Bending ( $P_L + P_b$ )	4.10	7.06	27.55	14.9	3.81
Baseplate - Local Membrane Plus Primary Bending ( $P_L + P_b$ )	7.08	29.69	47.25	1.46	21.91
Enclosure Shell - Primary Membrane ( $P_m$ )	4.13	5.17	57.21	76.5	9.64

- Notes: 1. Load cases are defined in Table 2.1.9.  
 2. Surface pressure not included in safety factor evaluation since it is not a primary stress.

Table 2.7.7

MINIMUM SAFETY FACTORS FOR MISCELLANEOUS ITEMS - MPC FUEL BASKET/CANISTER - HYPOTHETICAL  
ACCIDENT CONDITIONS OF TRANSFER

Item	Loading	Safety Factor	Location in SAR Where Calculations or Results are Presented
Fuel Basket Axial Stress	End Drop	4.19	Subsection 2.7.1.1
Fuel Basket Axial Stress	Fire Transient (Regulatory Position C.7 of Regulatory Guide 7.6)	4.96	Subsection 2.7.3.4
MPC Canister Stability	30' End Drop (Load Case E3.a, Table 2.1.7)	1.92	Subsection 2.7.1.1
MPC Top Closure Lid Bending Stress	30' End Drop (Load Case E3.a in Table 2.1.7)	2.8 (single lid) 1.4 (dual lid)	Subsection 2.7.1.1
MPC Top Closure Lid – Loading in Peripheral Weld	30' End Drop (Load Case E3.a in Table 2.1.7)	2.37	Subsection 2.7.1.1
MPC Baseplate Bending Stress	30' End Drop (Load Case E3.a in Table 2.1.7)	3.04	Subsection 2.7.1.1
MPC Canister at Connection to Baseplate	30' End Drop (Load Case E3.a in Table 2.1.7)	2.14	Subsection 2.7.1.1
MPC Top Closure Lid Bending Stress	Fire accident (Load Case E5 in Table 2.1.7)	8.59	Subsection 2.7.3.3.1
MPC Baseplate Bending Stress	Fire accident (Load Case E5 in Table 2.1.7)	1.17	Subsection 2.7.3.3.1
MPC Canister Stability	Fire accident (Load Case E5 in Table 2.1.7)	1.18	Subsection 2.7.3.3.1
MPC Shell Mean Stress	Fire accident (Load Case E5 in Table 2.1.7)	4.16	Subsection 2.7.3.3.1

Table 2.7.8

MINIMUM SAFETY FACTORS FOR MISCELLANEOUS ITEMS - OVERPACK -  
HYPOTHETICAL ACCIDENT CONDITIONS OF TRANSPORT

Item	Loading	Safety Factor	Location in SAR Where Calculations or Results are Presented
Overpack Stability	30' End Drop (Load Cases 1 and 2 in Table 2.1.9)	2.16*	Subsection 2.7.1.1
Closure Bolts	30' End Drop (Load Case 2 in Table 2.1.9)	1.30	Subsection 2.7.1.1
Closure Bolts	Top End Puncture	1.86	Subsection 2.7.2
Overpack Inner Shell Mean Stress	Fire Transient	7.25	Subsection 2.7.3.3.2
Closure Bolts	Fire Transient	1.69	Subsection 2.7.3.3.3
Overpack Stress	Fire Transient (Regulatory Position C.7 of Regulatory Guide 7.6)	3.67	Subsection 2.7.3.4
Overpack Stability (Yield Stress Criteria)	Immersion (Load Case 18 in Table 2.1.9)	2.32*	Subsection 2.7.5
Overpack Stability (Stability Criteria)	Immersion (Load Case 18 in Table 2.1.9)	3.95	Subsection 2.7.5

\* Applicable to inner shell fabricated from SA203-E material. Safety factor must be multiplied by 0.93 if inner shell is fabricated from optional SA350-LF3 material.

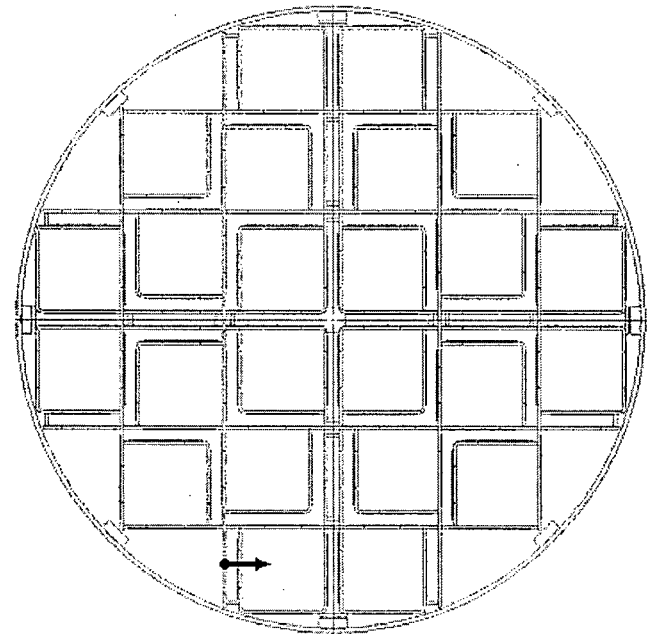
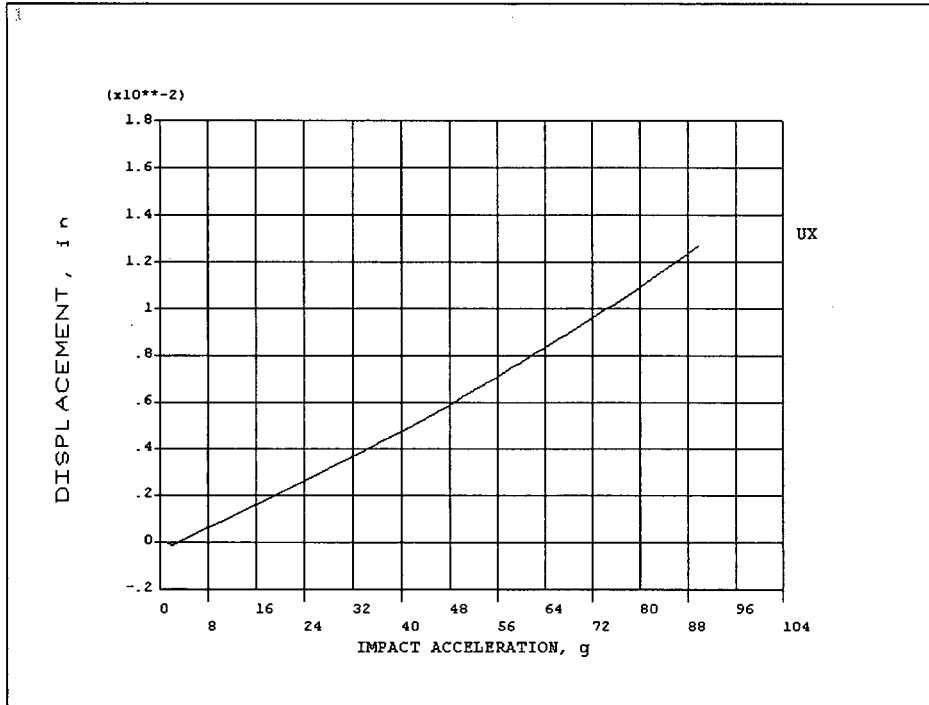


FIGURE 2.7.1; NON-LINEAR BUCKLING ANALYSIS FOR MPC-24  
DISPLACEMENT vs. IMPACT ACCELERATION (0° DROP)

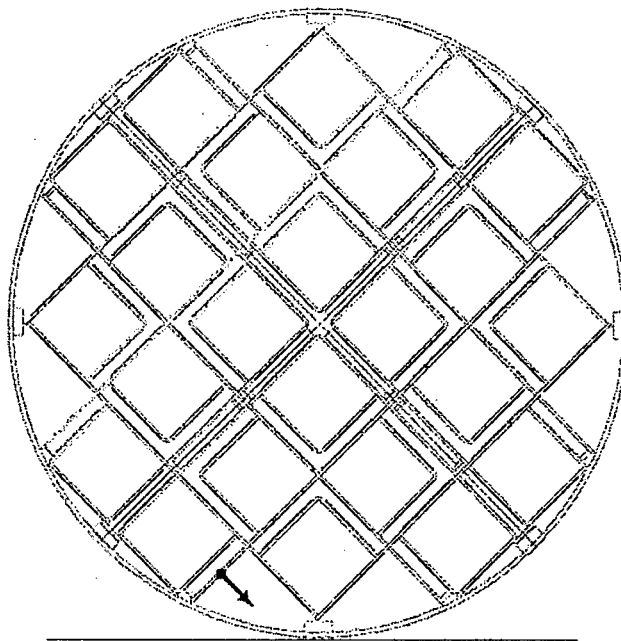
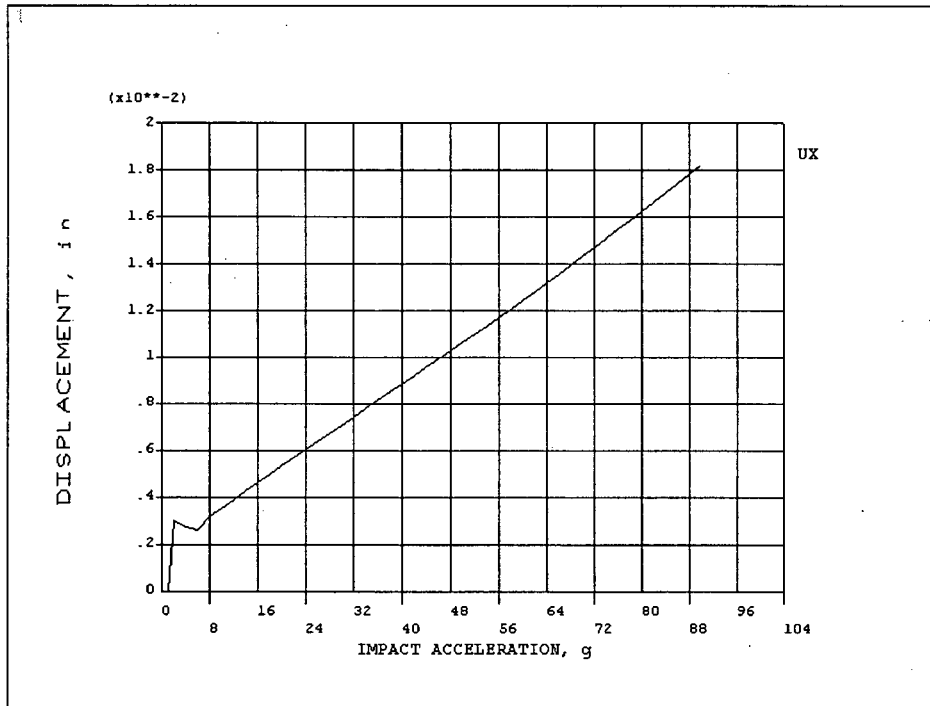


FIGURE 2.7.2; NON-LINEAR BUCKLING ANALYSIS FOR MPC-24  
DISPLACEMENT vs. IMPACT ACCELERATION (45° DROP)

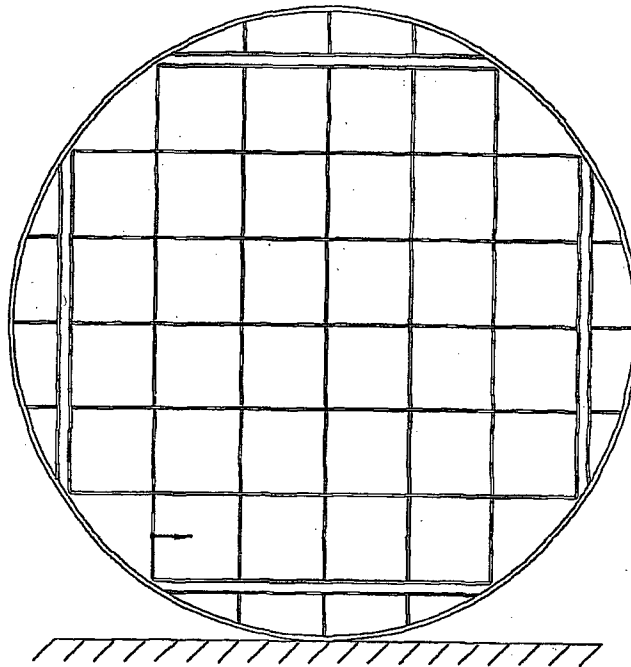
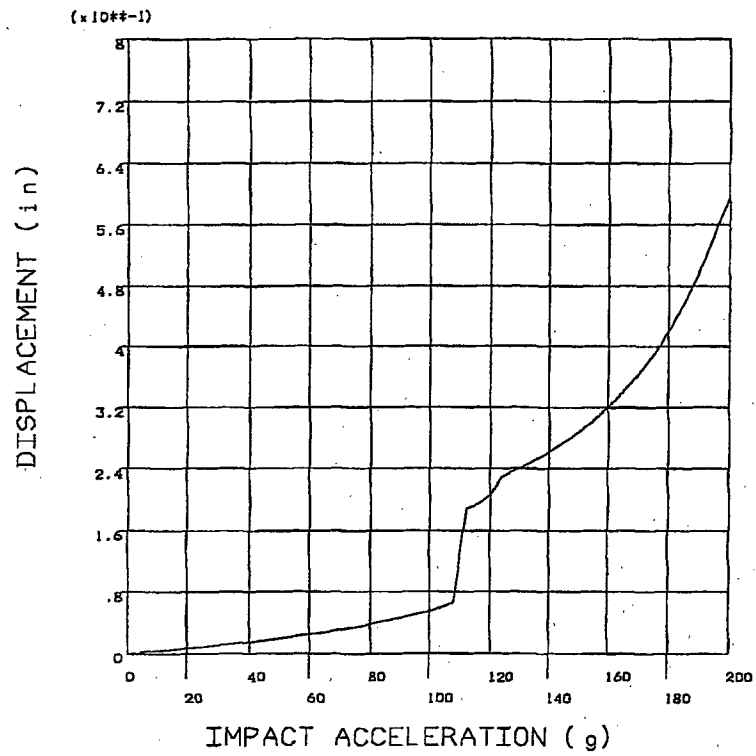


FIGURE 2.7.3 ; NON-LINEAR BUCKLING ANALYSIS FOR MPC-32  
DISPLACEMENT Vs. IMPACT ACCELERATION (0° DROP)

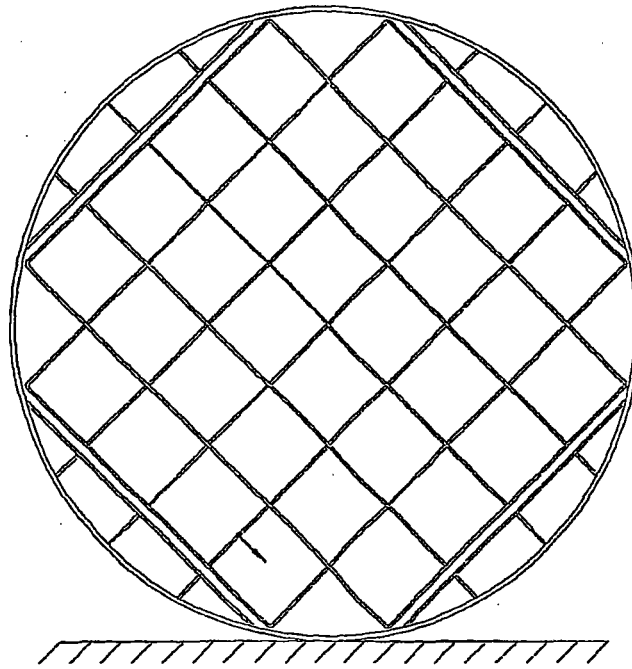
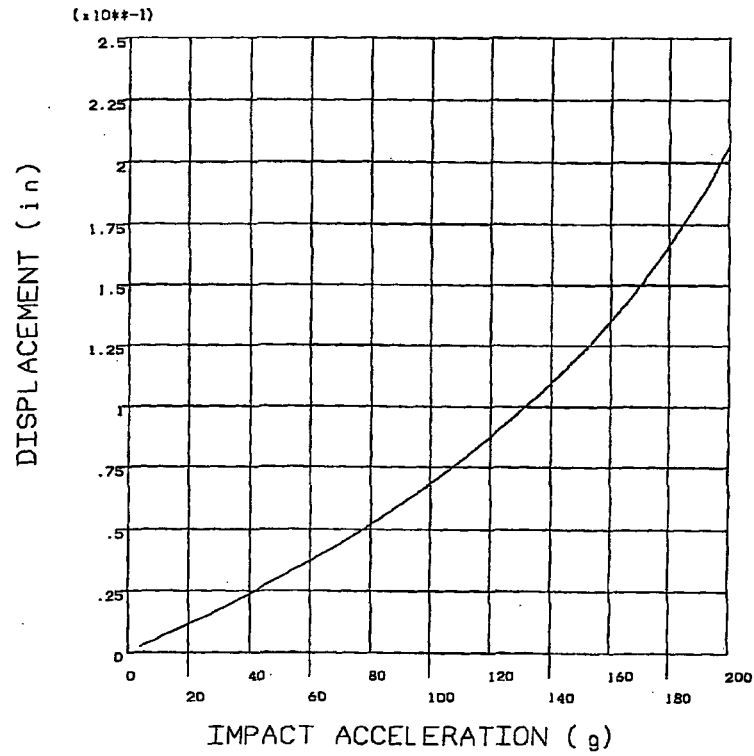


FIGURE 2.7.4 ; NON-LINEAR BUCKLING ANALYSIS FOR MPC-32  
DISPLACEMENT Vs. IMPACT ACCELERATION (45° DROP)

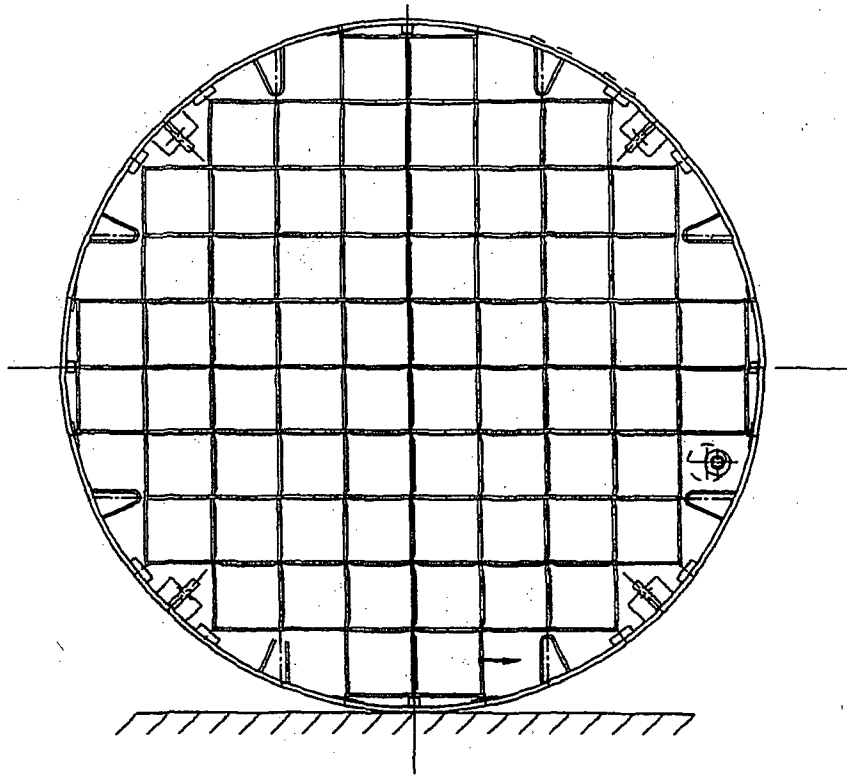
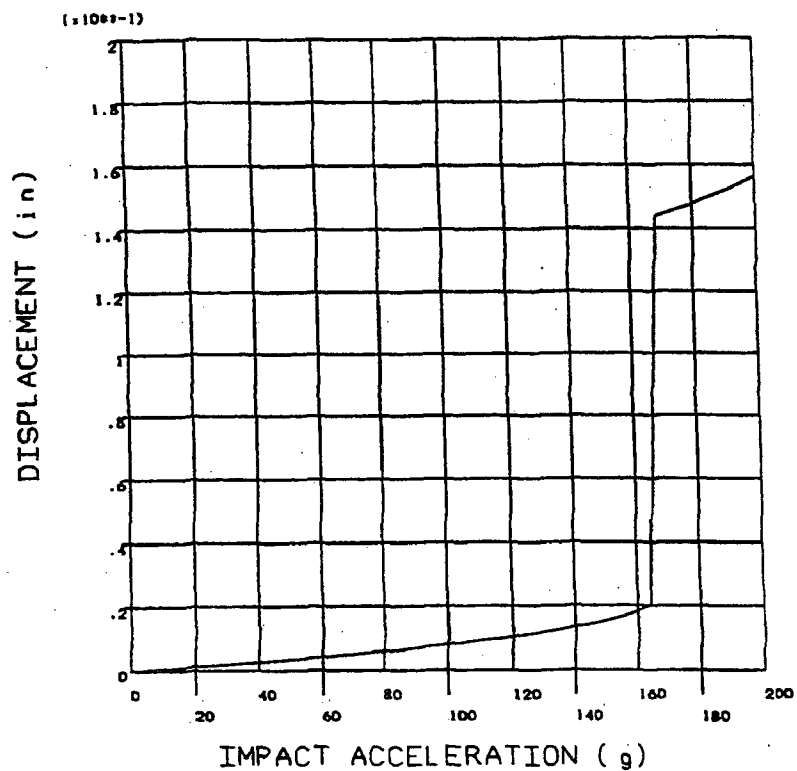


FIGURE 2.7.5; NON-LINEAR BUCKLING ANALYSIS FOR MPC-68  
DISPLACEMENT Vs. IMPACT ACCELERATION (0° DROP)

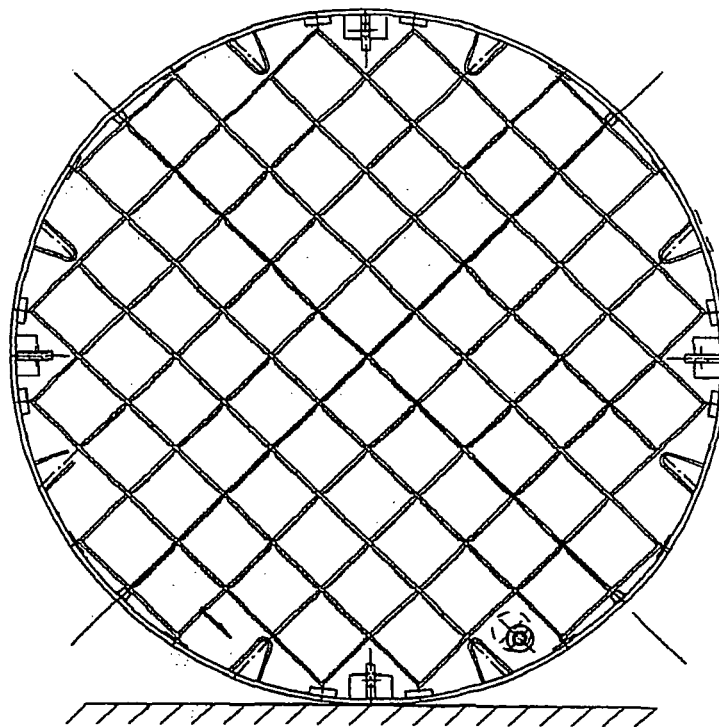
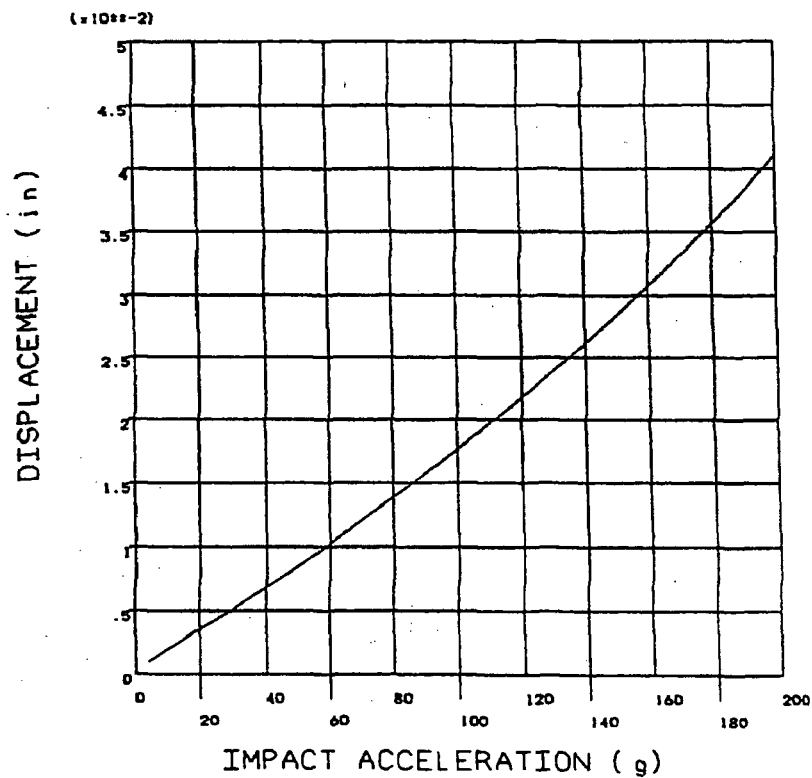


FIGURE 2.7.6: NON-LINEAR BUCKLING ANALYSIS FOR MPC-68  
DISPLACEMENT Vs. IMPACT ACCELERATION (45° DROP)

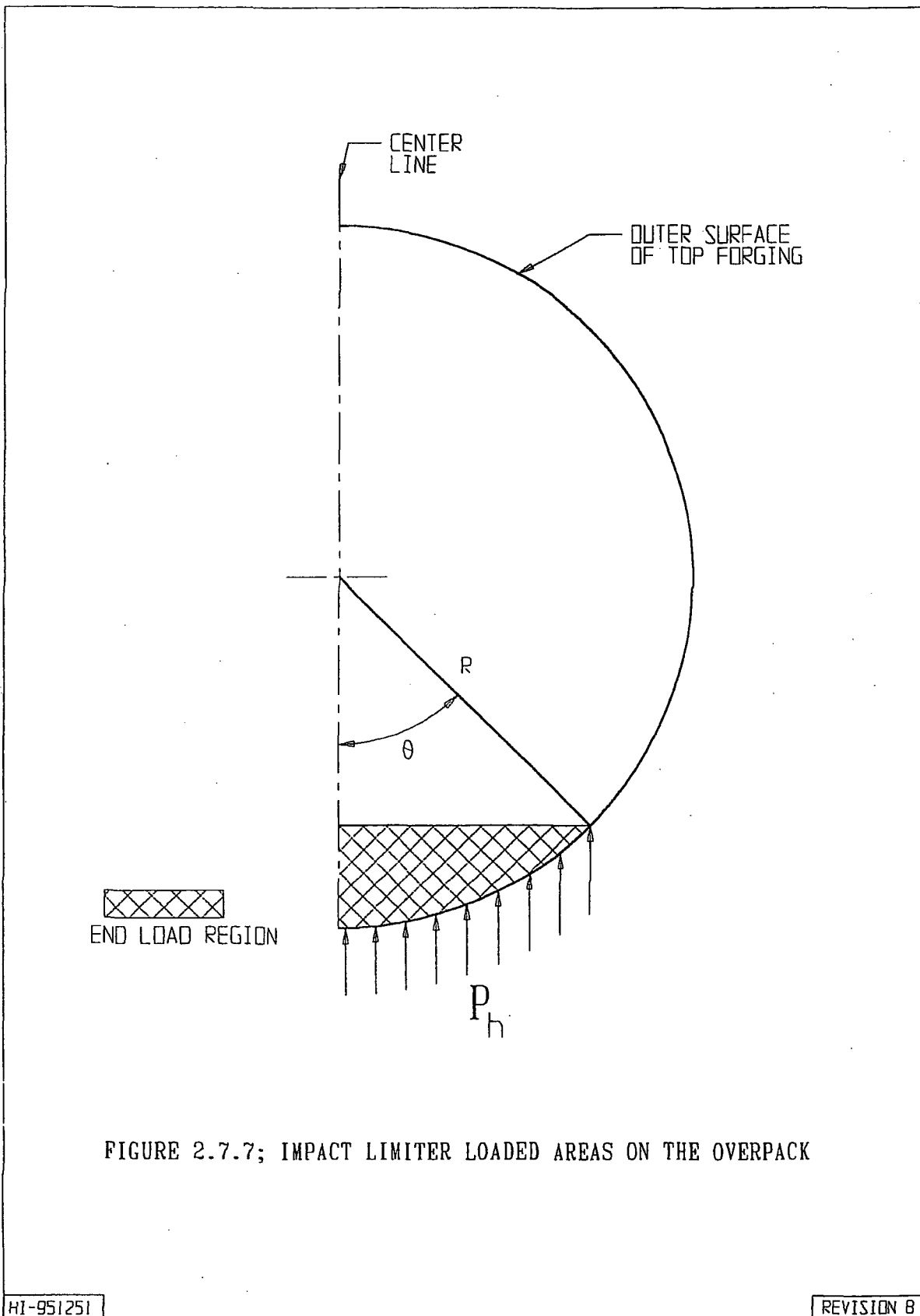


FIGURE 2.7.7; IMPACT LIMITER LOADED AREAS ON THE OVERPACK

HI-951251

REVISION B

PROJECTS\5014\HI951251\CH\_2\2\_7\_7

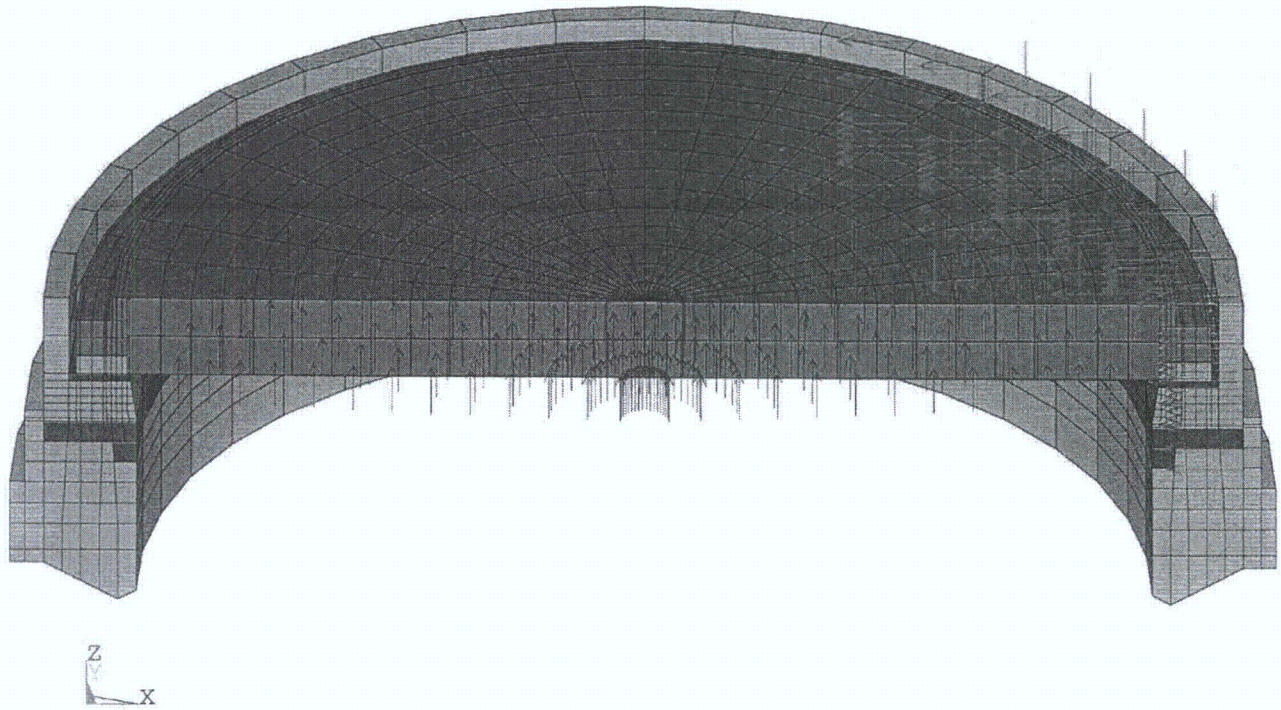


FIGURE 2.7.8 TOP LID LOADING - DROP ANALYSIS

HI-951251

REV. 8

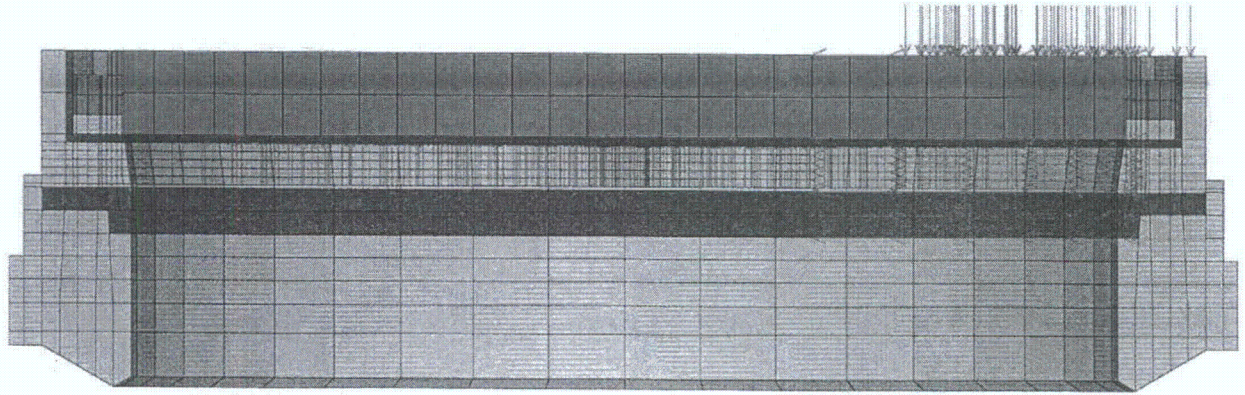


FIGURE 2.7.9 SIDE VIEW OF TOP FORGING SHOWING END LOADS

HI-951251

REV. 8

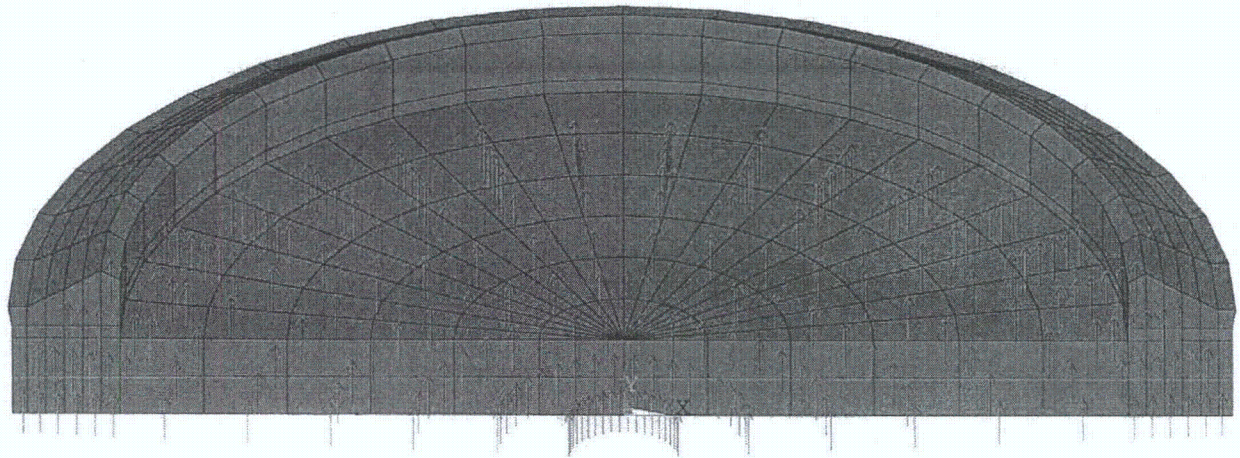


FIGURE 2.7.10 BASEPLATE LOADING FROM IMPACT LIMITER - TOP END DROP

HI-951251

REV. 8

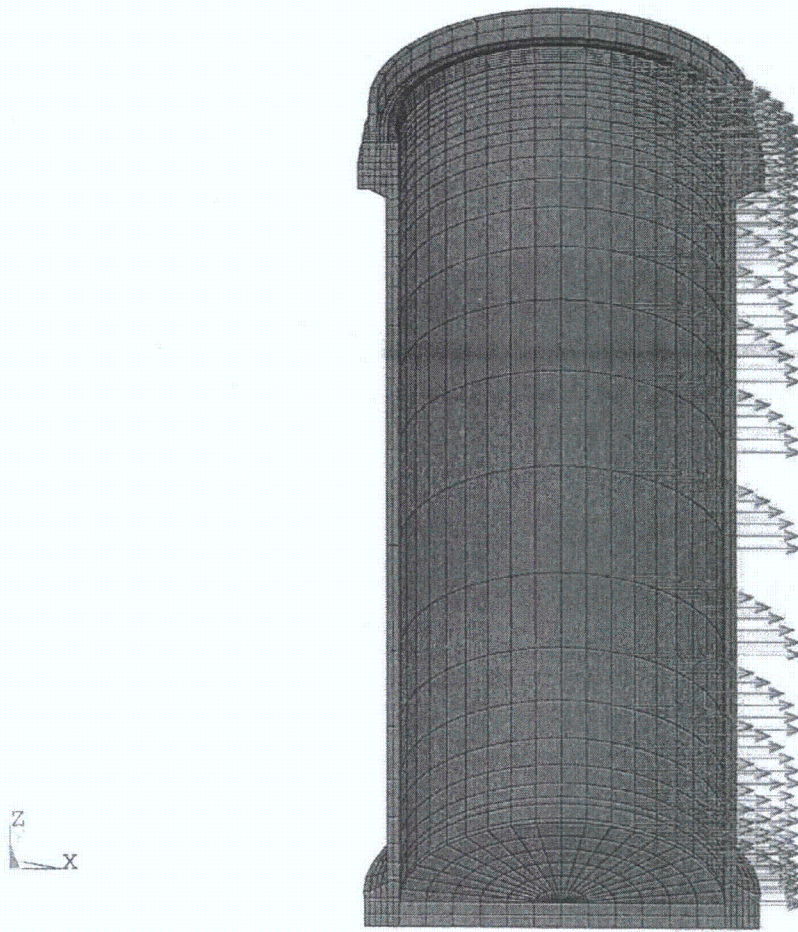
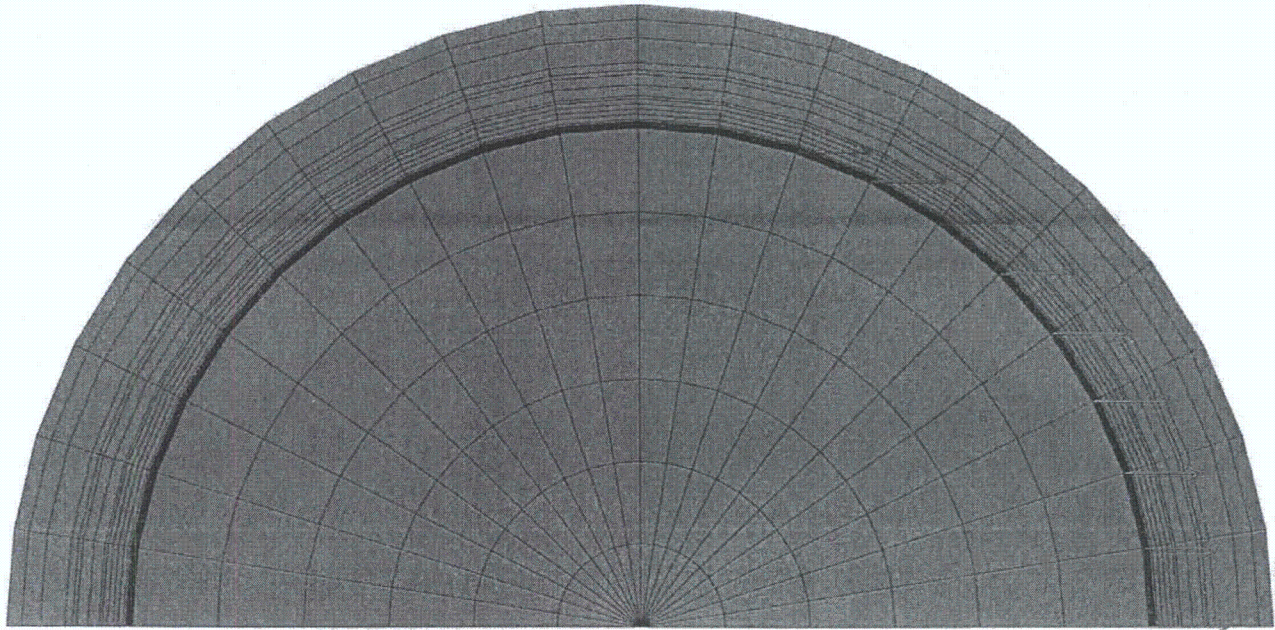


FIGURE 2.7.II LOADING FROM MPC ON INNER SHELL



Z X

FIGURE 2.7.12 END VIEW SHOWING MPC LOADING ON INNER SHELL

HI-951251

REV. 8

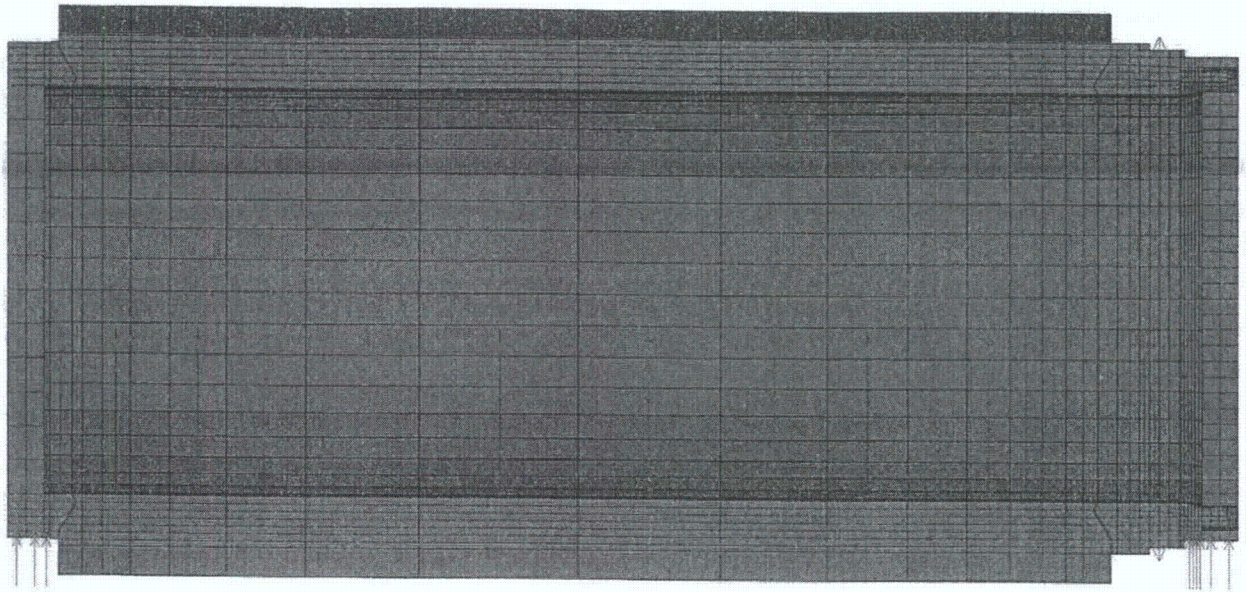
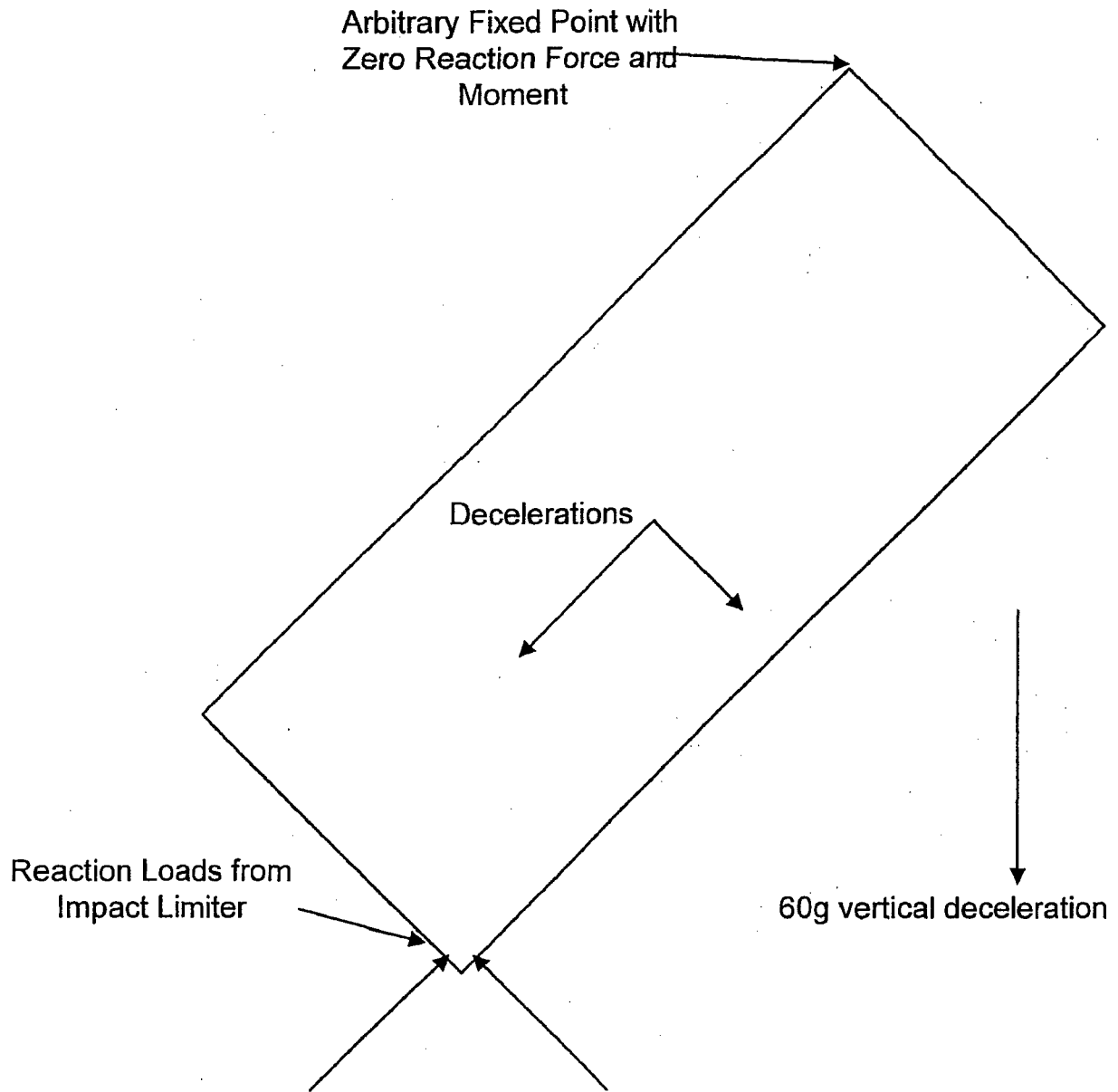


FIGURE 2.7.13 LOAD FROM IMPACT LIMITER AT SUPPORT LOCATIONS – SIDE DROP

HI-951251

REV. 8

Revision 15 issued October 11, 2010



**FIGURE 2.7.14 OBLIQUE DROP SHOWING OFFSET OF IMPACT LIMITER REACTION LOAD FROM APPLIED INERTIA LOADS**

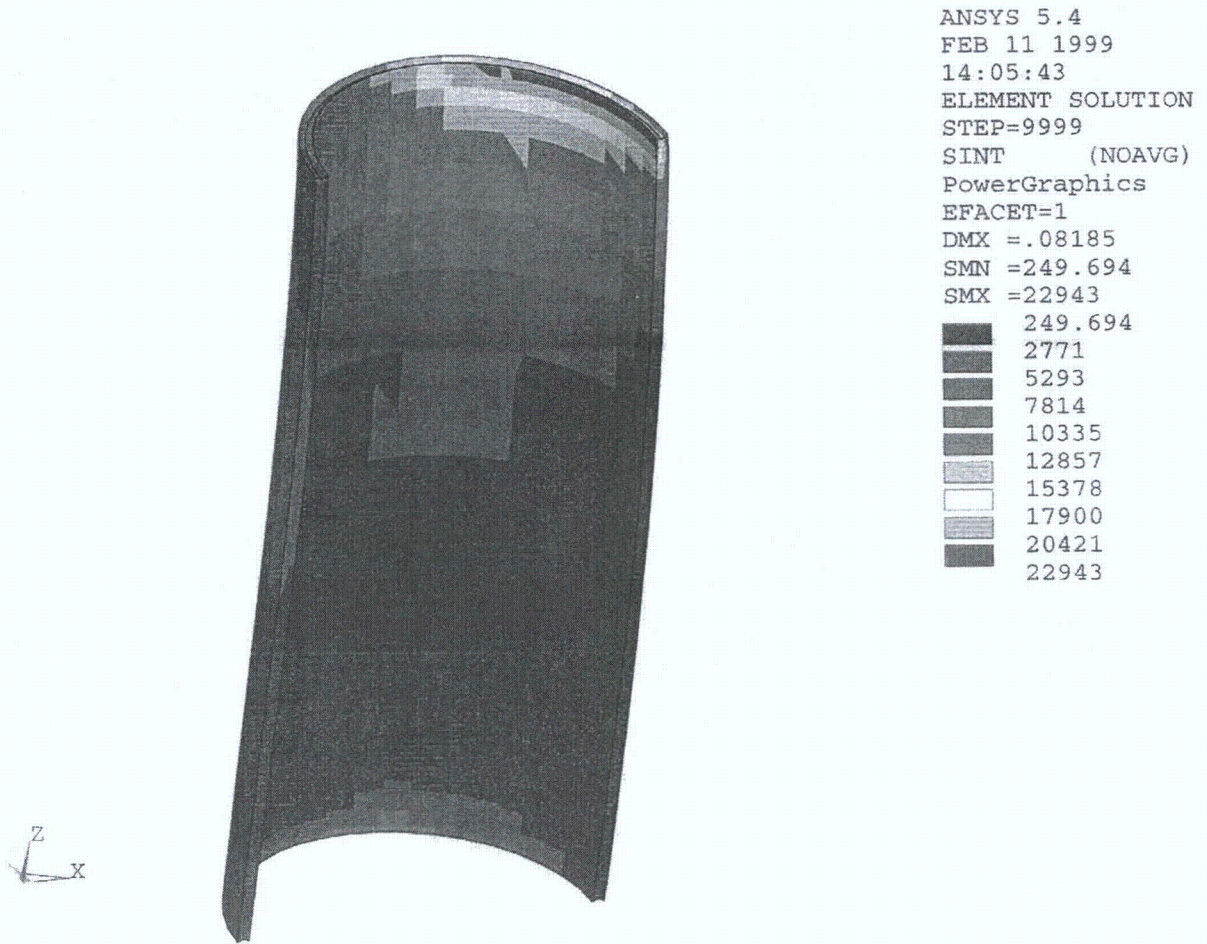


FIGURE 2.7.15 – INNER SHELL STRESS INTENSITY DISTRIBUTION –  
"HEAT" CONDITION – 30 DEGREE – TOP END IMPACT

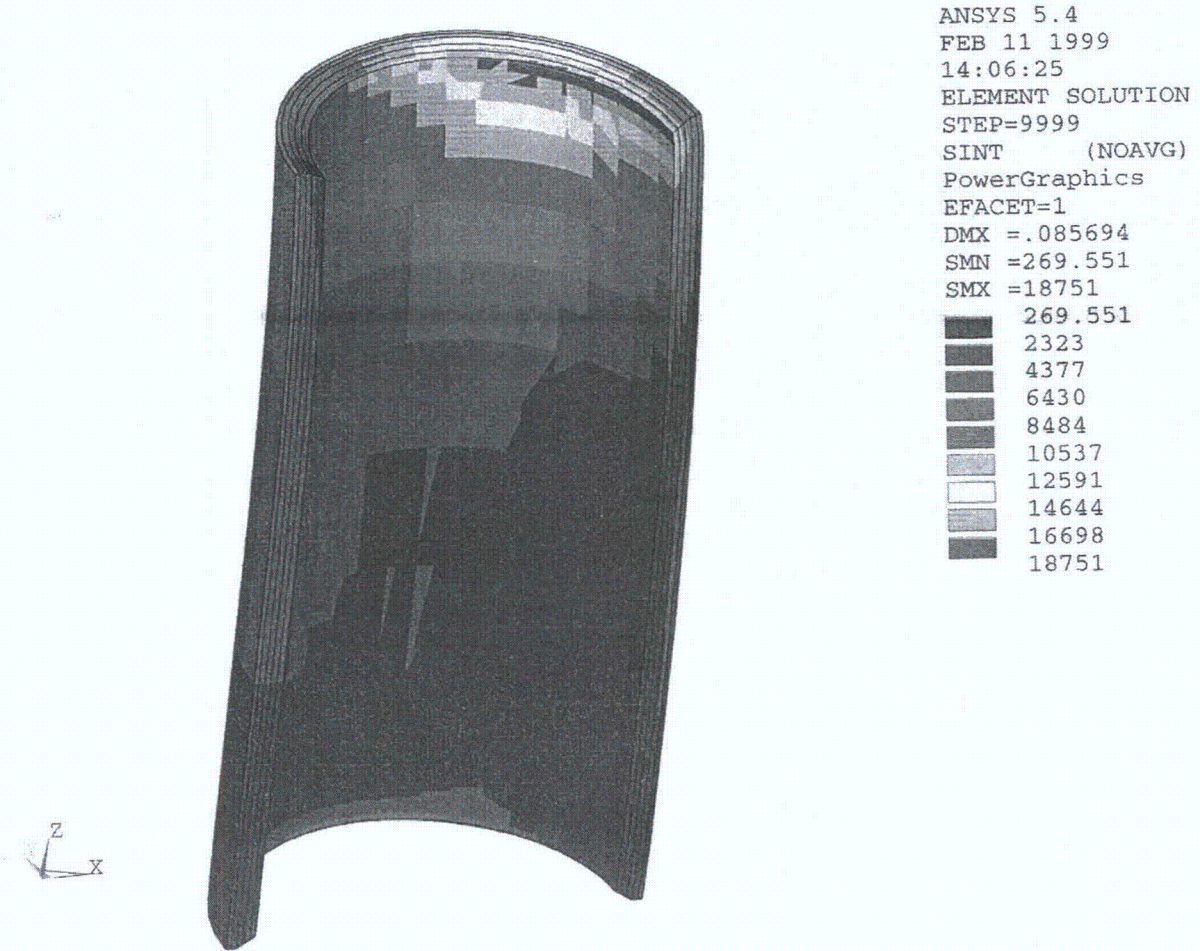


FIGURE 2.7.16 - INTERMEDIATE SHELL-STRESS INTENSITY DISTRIBUTION -  
"HEAT" CONDITION - 30 DEGREE - TOP - END IMPACT

ANSYS 5.4  
FEB 12 1999  
09:32:41  
ELEMENT SOLUTION  
STEP=1  
SUB =1  
TIME=1  
SINT (NOAVG)  
PowerGraphics  
EFACET=1  
DMX =.118  
SMN =685.712  
SMX =74759  
685.712  
8916  
17146  
25377  
33607  
41838  
50068  
58298  
66529  
74759

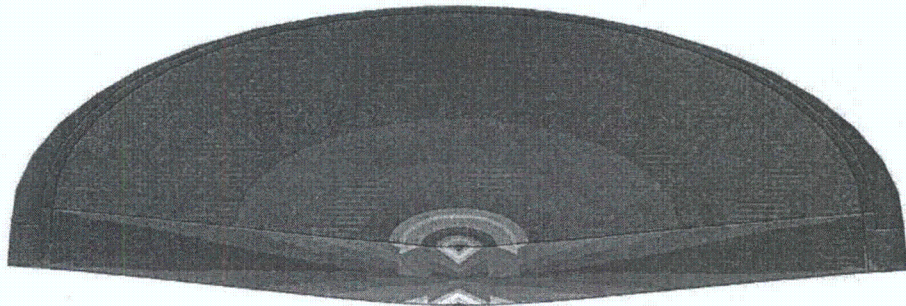


FIGURE 2.7.17 - LOCALIZED STRESS INTENSITY DISTRIBUTION IN LID -  
TOP END PUNCTURE (DEFORMED SHAPE EXPANDED FOR CLARITY)

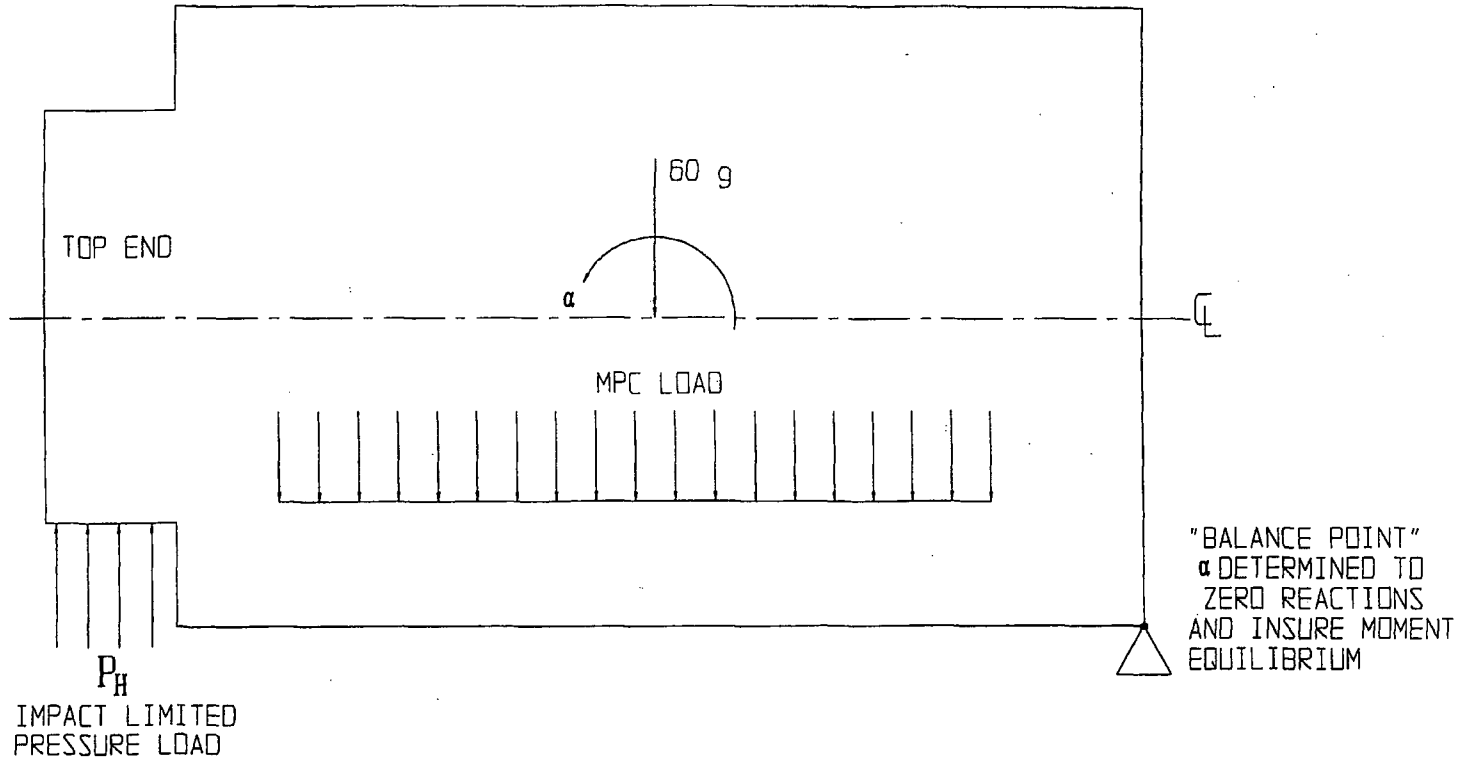


FIGURE 2.7.18; IMPACT LOADS FOR SLAPDOWN FINITE ELEMENT ANALYSIS

2.8 SPECIAL FORM

This section is not applicable to the HI-STAR 100 System. This application does not seek approval for transport of special form radioactive material as defined in 10CFR71.4.

## 2.9 FUEL RODS

The cladding of the fuel rods is the initial confinement boundary in the HI-STAR 100 System. Analyses have been performed in Chapter 3 to ensure that the maximum temperature of the fuel cladding is below the Pacific Northwest Laboratory's threshold values for various cooling times. These temperature limits ensure that the fuel cladding will not degrade in an inert helium environment. Additional details on the fuel rod cladding temperature analyses for the spent fuel to be loaded into the HI-STAR 100 System are provided in Chapter 3.

The dimensions of the storage cell openings in the MPC are equal to or greater than those used in spent fuel racks supplied by Holtec International. Thousands of fuel assemblies have been shuffled in and out of these cells over the years without a single instance of cladding failure. The vast body of physical evidence from prior spent fuel handling operations provides confirmation that the fuel handling and loading operations with the HI-STAR 100 MPC will not endanger or compromise the integrity of the cladding or the structural integrity of the assembly.

The HI-STAR 100 System is designed and evaluated for a maximum deceleration of 60g's. Studies of the capability of spent fuel rods to resist impact loads [2.9.1] indicate that the most vulnerable fuel can withstand greater than 60 g's in the side impact orientation. Therefore, limiting the HI-STAR 100 System to a maximum deceleration of 60 g's (perpendicular to the longitudinal axis of the overpack during all normal and hypothetical accident conditions) ensures that fuel rod cladding integrity is maintained. In [2.9.1], it is assumed that the fuel rod cladding provides the only structural resistance to bending and buckling of the rod. For accidents where the predominate deceleration is directed along the longitudinal axis of the overpack, [2.9.1] also demonstrates that no elastic instability or yielding of the cladding will occur until the deceleration level is well above the HI-STAR 100 limit of 60g's. The solutions presented in [2.9.1], however, assume that the fuel pellets are not intimately attached to the cladding when subjected to an axial deceleration load that may cause an elastic instability of the fuel rod cladding.

The limit based on classical Euler buckling analyses performed by Lawrence Livermore National Laboratory in [2.9.1] is 82 g's. In the LLNL report, the limiting axial load to ensure fuel rod stability is obtained by modeling the fuel rod as a simply supported beam with unsupported length equal to the grid strap spacing. The limiting load under this condition is:

$$F = \pi^2 EI/L^2$$

In the preceding formula, E = Young's Modulus of the cladding, I = area moment of inertia of the cladding, and L = spacing of the grid straps.

Assuming that  $F = W \times A/g$  with W being the weight of a fuel rod, and A = the deceleration, the Euler buckling formula can be expressed as

$$A/g = \pi^2 (ER^3 t_n / W_f a L^2) = \pi^2 \beta$$

In the preceding formula,  $g$  = gravity,  $n$  = number of fuel rods in the fuel assembly,  $W_{fa}$  = the total weight of the fuel assembly,  $t$  = cladding wall thickness, and  $R$  = cladding mean radius.

Using the preceding formula, a survey of a large variety of fuel assembly types in [2.9.1] concluded that a 17 x 17 PWR assembly resulted in the minimum value for deceleration and results in the lower bound limit of:

$$A/g = 82$$

The fuel pellet weight was omitted from the analysis in [2.9.1] by virtue of the assumption that under axial load, the cladding did not support the fuel pellet mass. Since the results may not be conservative because of the assumption concerning the behavior of the fuel pellet mass, a new analysis of the structural response of the fuel cladding is presented here... It is demonstrated that the maximum axially oriented deceleration that can be applied to the fuel cladding is in excess of the design basis deceleration specified in this SAR. Therefore, the initial confinement boundary remains intact during a hypothetical accident of transport where large axially directed decelerations are experienced by the HI-STAR 100 package.

The analysis reported here considers the most limiting fuel rod in the fuel assembly. Most limiting is defined as the fuel rod that may undergo the largest bending (lateral) deformations in the event of a loss of elastic stability. The fuel rod is modeled as a thin-walled elastic tube capable of undergoing large lateral displacements in the event that high axial loads cause a loss of stability (i.e., the non-linear interaction of axial and bending behavior of the elastic tube is included in the problem formulation). The fuel rod and the fuel pellet mass is included in the analysis with the fuel pellet mass assumed to contribute only its mass to the analysis. In the HI-STAR 100 spent fuel basket, continuous support to limit lateral movement is provided to the fuel assembly along its entire length. The extent of lateral movement of any fuel rod in a fuel assembly is limited to: (1) the clearance gap between the grid straps and the fuel basket cell wall at the grid strap locations; and, (2) the maximum available gap between the fuel basket cell wall and the fuel rod in the region between the grid straps. Note that the grid straps act as fuel rod spacers at the strap locations; away from the grid straps, however, there is no restraint against fuel rod-to-rod contact under a loading giving rise to large lateral motion of the individual rods. Under the incremental application of axial deceleration to the fuel rod, the fuel rod compresses and displaces from the axially oriented inertial loads experienced. The non-linear numerical analysis proceeds to track the behavior of the fuel rod up to and beyond contact with the rigid confining walls of the HI-STAR 100 fuel basket.

The analysis is carried out for the "most limiting" spent fuel assembly. The "most limiting" criteria used herein is based on the simple elastic stability formula assuming buckling occurs only between grid straps. This is identical to the methodology employed in [2.9.1] to identify the fuel assembly that limits design basis axial deceleration loading. Table 2.9.1 presents tabular data for a wide variety of fuel assemblies. Considerable data was obtained using the tables in [2.9.2]. The configuration with the lowest value of "Beta" is the most limiting for simple elastic Euler buckling between grid straps; the Westinghouse 14x14 Vantage, "W14V", PWR configuration is used to obtain results.

The material properties used in the non-linear analysis are those for irradiated Zircalloy and are obtained from [2.9.1]. The Young's Modulus and the cladding dynamic yield stress are set as:

$$E = 10,400,000 \text{ psi}$$

$$\sigma_y = 80,500 \text{ psi}$$

The fuel cladding material is assumed to have no tensile or compressive stress capacity beyond the material yield strength.

Calculations are performed for two limiting assumptions on the magnitude of resisting moment at the grid straps. Figures 2.9.1 through 2.9.9 aid in understanding the calculation. It is shown in the detailed calculations that the maximum stress in the fuel rod cladding occurs subsequent to the cladding deflecting and contacting the fuel basket cell wall. Two limiting analyses are carried out. The initial analysis assumes that the large deflection of the cladding between two grid straps occurs without any resisting moment at the grid strap supports. This maximizes the stress in the free span of the cladding, but eliminates all cladding stress at the grid strap supports. It is shown that this analysis provides a conservative lower bound on the limiting deceleration. The second analysis assumes a reasonable level of moment resistance to develop at the grid straps; the level developed is based on an assumed deflection shape for the cladding spans adjacent to the span subject to detailed analysis. For this second analysis, the limiting decelerations are much larger with the limit stress level occurring in the free span and at the grid strap support locations.

It is concluded that the most conservative set of assumptions on structural response still lead to the conclusion that the fuel rod cladding remains intact under the design basis deceleration levels set for the HI-STAR 100.

Table 2.9.1 FUEL ASSEMBLY DIMENSIONAL DATA

Array ID	Array Name	Rod O.D. (in.)	Clad Thk. (in.)	R <sub>mean</sub> (in.)	# of Rods	Assy Wt. (lb.)	Rod Length (in.)	# of Spans	Average Span (in.)	Material Modulus	BETA
						PWR					
14x14A01	W14OFA	0.4000	0.0243	0.20608	179	1177	151.85	6	25.30833	10400000	0.525127806
14x14A02	W14OFA	0.4000	0.0243	0.20608	179	1177	151.85	6	25.30833	10400000	0.525127806
14x14A03	W14V	0.4000	0.0243	0.20608	179	1177	151.85	6	25.30833	10400000	0.525127806
14x14B01	W14STD	0.4220	0.0243	0.21708	179	1302	152.4	6	25.4	10400000	0.550863067
14x14B02	XX14TR	0.4170	0.0295	0.21588	179	1215	152	6	25.33333	10400000	0.708523868
14x14B03	XX14STD	0.4240	0.0300	0.21950	179	1271.2	149.1	8	18.6375	10400000	1.337586884
14x14C01	CE14	0.4400	0.0280	0.22700	176	1270	147	8	18.375	10400000	1.398051576
14x14C02	CE14	0.4400	0.0280	0.22700	176	1220	137	8	17.125	10400000	1.67556245
14x14D01	W14SS	0.4220	0.0165	0.21513	180	1247	126.68	6	21.11333	24700000	1.31385062
15x15A01	CE15P	0.4180	0.0260	0.21550	204	1360	140	9	15.55556	10400000	1.677523904
15x15B01	W15OFA	0.4220	0.0245	0.21713	204	1459	151.85	6	25.30833	10400000	0.569346561
15x15B02	W15V5H	0.4220	0.0245	0.21713	204	1459	151.85	6	25.30833	10400000	0.569346561
15x15B03	W15	0.4220	0.0243	0.21708	204	1440	151.83	6	25.305	10400000	0.571905185
15x15B04	W15	0.4220	0.0243	0.21708	204	1443	151.83	6	25.305	10400000	0.570716193
15x15B05	15(2a-319)	0.4220	0.0242	0.21705	204	1472	151.88	6	25.31333	10400000	0.556610964
15x15C01	SPC15	0.4240	0.0300	0.21950	204	1425	152	6	25.33333	10400000	0.73601861
15x15C02	SPC15	0.4240	0.0300	0.21950	204	1425	152	6	25.33333	10400000	0.73601861
15x15C03	XX15	0.4240	0.0300	0.21950	204	1432.8	152.065	6	25.34417	10400000	0.731386148
15x15C04	XX15	0.4170	0.0300	0.21600	204	1338.6	139.423	9	15.49144	10400000	1.996693327
15x15D01	BW15	0.4300	0.0265	0.22163	208	1515	153.68	7	21.95429	10400000	0.854569793
15x15D02	BW15	0.4300	0.0265	0.22163	208	1515	153.68	7	21.95429	10400000	0.854569793
15x15D03	BW15	0.4300	0.0265	0.22163	208	1515	153.68	7	21.95429	10400000	0.854569793
15x15G01	HN15SS	0.4220	0.0165	0.21513	204	1421	126.72	6	21.12	24700000	1.305875606
16x16A01	CE16	0.3820	0.0250	0.19725	236	1430	161	10	16.1	10400000	1.270423729

Table 2.9.1 FUEL ASSEMBLY DIMENSIONAL DATA (continued)

Array ID	Array Name	Rod O.D. (in.)	Clad Thk. (in.)	R <sub>mean</sub> (in.)	# of Rods	Assy Wt. (lb)	Rod Length (in.)	# of Spans	Average Span (in.)	Material Modulus	BETA
16x16A02	CE16	0.3820	0.0250	0.19725	236	1300	146.499	9	16.27767	10400000	1.367126598
17x17A01	W17OFA	0.3600	0.0225	0.18563	264	1373	151.635	7	21.66214	10400000	0.613275783
17x17A02	W17OFA	0.3600	0.0225	0.18563	264	1365	152.3	7	21.75714	10400000	0.611494853
17x17B01	W17STD	0.3740	0.0225	0.19263	264	1482	151.635	7	21.66214	10400000	0.634902014
17x17B02	W17P+	0.3740	0.0225	0.19263	264	1482	151.635	7	21.66214	10400000	0.634902014
17x17C01	BW17	0.3790	0.0240	0.19550	264	1505	152.688	7	21.81257	10400000	0.687604262
BWR											
6x6A02	XX/ANF6	0.5645	0.0360	0.29125	36	328.4	116.65	4	29.1625	10400000	1.192294364
6x6C01	HB6	0.5630	0.0320	0.28950	36	270	83	3	20.75	10400000	2.500527046
7x7A01	HB7	0.4860	0.0330	0.25125	49	276	83.2	3	20.8	10400000	2.233705011
7x7B01	GE-7	0.5630	0.0320	0.28950	49	682.5	159	7	19.875	10400000	1.467601583
7x7B02	GE-7	0.5630	0.0370	0.29075	49	681	164	7	20.5	10400000	1.619330439
7x7B03	GE-7	0.5630	0.0370	0.29075	49	674.4	164	7	20.5	10400000	1.635177979
7x7B04	GE-7	0.5700	0.0355	0.29388	49	600	161.1	7	20.1375	10400000	1.887049713
7x7B05	GE-7	0.5630	0.0340	0.29000	49	600	161.1	7	20.1375	10400000	1.736760659
8x8B03	GE-8	0.4930	0.0340	0.25500	63	681	164	7	20.5	10400000	1.2906798
8x8C02	GE-8R	0.4830	0.0320	0.24950	62	600	159	7	19.875	10400000	1.352138354
8x8C03	GE-8R	0.4830	0.0320	0.24950	62	600	163.71	7	20.46375	10400000	1.275454448
9x9D01	XX/ANF9	0.4240	0.0300	0.21950	79	575.3	163.84	8	18.20444	10400000	1.367212516
10x10E01	XX10SS	0.3940	0.0220	0.20250	96	376.6	89.98	4	17.996	24700000	3.551678654

Array ID, Rod OD, Clad Thk and # of Rods from Tables 6.2.1 and 6.2.2.

R<sub>mean</sub>, Average Span and THETA are Calculated.

Zircaloy Modulus from LLNL Report [2.9.1].

Stainless Steel (348H) Modulus from ASME Code, Section III, Part D.

Table 2.9.1 FUEL ASSEMBLY DIMENSIONAL DATA (continued)

PWR Assy. Wt., Rod Len. and # of Spans (exc. as noted below) from DOE/RW-0184, Vol. 3, UC-70, -71 and -85, Dec. 1987.  
Assy. Wt., Rod Len. and # of Spans for 15x15B03, 15x15B04, 15x15C01 and 15x15C02 from ORNL/TM-9591/V1-R1.  
BWR Assy. Wt., Rod Len. and # of Spans (exc. as noted below) from ORNL/TM-10902.  
Assy. Wt., Rod Len. and # of Spans for 6x6A02, 9x9D01 and 10x10E01 from DOE/RW-0184, Vol. 3, UC-70, -71 and -85, Dec. 1987.  
Assy. Wt., Rod Len. and # of Spans for 7x7B04 and 7x7B05 from ORNL/TM-9591/V1-R1.  
Assy. Wt. for 8x8C02 and 8x8C03 from ORNL/TM-9591/V1-R1.

In the following, a physical description of the structural instability problem is provided with the aid of Figures 2.9.1 to 2.9.9. A stored fuel assembly consists of a square grid of fuel rods. Each fuel rod consists of a thin-walled cylinder surrounding and containing the fuel pellets. The majority of the total weight of a fuel rod is in the fuel pellets; however, the entire structural resistance of the fuel rod to lateral and longitudinal loads is provided by the cladding. Hereinafter, the use of the words "fuel rod", "fuel rod cladding", or just "cladding" means the structural thin cylinder. The weight of the fuel pellets is conservatively assumed to be attached to the cladding for all discussions and evaluations.

Figure 2.9.1 shows a typical fuel rod in a fuel assembly. Also shown in Figure 2.9.1 are the grid straps and the surrounding walls of the spent fuel basket cell walls. The grid straps serve to maintain the fuel rods in a square array at a certain number of locations along the length of the fuel assembly. When the fuel rod is subject to a loading causing a lateral deformation, the grid strap locations are the first locations along the length of the rod where contact with the fuel basket cell walls occurs. The fuel basket cell walls are assumed to be rigid surfaces. The fuel rod is assumed to be subjected to some axial load and has some slightly initially deformed shape. For the purposes of the analysis, it is assumed that displacement under load occurs in a 2-D plane and that the ends of the fuel rod cladding have a specified boundary condition to restrain lateral deflection. The ends of the fuel rod cladding are assumed to be simply supported and the grid straps along the length of the fuel assembly are assumed to have gap " $g_1$ " relative to the cell walls of the fuel basket. The figure shows a typical fuel rod in the assembly that is located by gaps " $g_2$ " and " $g_3$ " with respect to the fuel basket walls. Because the individual fuel rod is long and slender and is not perfectly straight, it will deform under a small axial load into the position shown in Figure 2.9.2. The actual axial load is due to the distributed weight subject to a deceleration from a hypothetical accident of transport. For the purposes of this discussion, it is assumed that some equivalent axial load is applied to one end of the fuel rod cladding. Because of the distributed weight and the fact that a deceleration load is not likely to be exactly axially oriented, the predominately axial load will induce a lateral displacement of the fuel rod cladding between the two end supports. The displacement will not be symmetric but will be larger toward the end of the cladding where support against the axial deceleration is provided. Depending on the number of grid straps, either one or two grid straps will initially make contact with the fuel basket cell wall and the contact will not be exactly centered along the length of the cell. Figure 2.9.3 illustrates the position of the fuel rod after the axial load has increased beyond the value when initial contact occurred and additional grid straps are now in contact with the cell wall. The maximum stress in the fuel rod will occur at the location of maximum curvature and will be a function of the bending moment ( $F_2 \times (g_2 - g_1)$ ).

At some load  $F_3 > F_2$ , either the limiting stress in the fuel rod cladding is achieved or the rod begins to experience large lateral movements between grid plates because of the coupling between axial and lateral load and deformation. Figure 2.9.4 shows the deformation mode experienced by the fuel rod cladding caused by the onset of an instability between two grid straps that are in contact with the fuel basket cell wall.

Once the lateral displacement initiates, the rod displaces until contact with the cell wall occurs at the mid point "A" ( see Figure 2.9.5) or the cladding stress exceeds the cladding material yield strength. Depending on the particular location of the fuel rod in the fuel assembly, the highest stressed portion

of the fuel rod will occur in the segment with the larger of the two gaps " $g_2$ " and " $g_3$ ". For the discussion to follow, assume that  $g_2 > g_3$ . The boundary condition at the grid strap is conservatively assumed as simply-supported so that the analysis need not consider what happens in adjacent spans between grid straps. At this point in the loading process, the maximum bending moment occurs at the contact point and has the value  $F_4 \times (g_2 - g_1)$ . Figure 2.9.5 shows the displaced configuration at the load level where initial contact occurs with the fuel cell wall. If the maximum fuel rod stress (from the bending moment and from the axial load) equals the yield stress of the fuel rod cladding, it is assumed that  $F_3 = F_4$  is the maximum axial load that can be supported. The maximum stress in the fuel rod cladding occurs at point "A" in Figure 2.9.5 since that location has the maximum bending moment. If the cladding stress is still below yield, additional load can be supported. As the load is further increased, the bending moment is decreased and replaced by reaction loads, "V", at the grid strap and the contact point. These reaction loads V are shown in Figure 2.9.7 and are normal to the cell wall surface. Figure 2.9.6 shows the configuration after the load has been further increased from the value at initial contact. There are two distinct regions that need to be considered subsequent to initial contact with the fuel basket cell wall. During the additional loading phase, the point "A" becomes two "traveling" points, A, and A'. Since the bending moment at A' and A is zero, the moment  $F_5 \times (g_2 - g_1)$  is balanced by forces V at the grid strap and at point A or A'. This is shown in Figure 2.9.7 where the unsupported length current "a" is shown with the balancing load. At this point in the process, two "failure" modes are possible for the fuel rod cladding.

The axial load that develops in the unsupported region between the grid strap and point A' causes increased deformation and stress in that segment, or,

The straight region of the rod, between A and A', begins to experience a lateral deformation away from the cell wall.

Note that in this latter scenario, the slope at A or A' remains zero so this should never govern unless the flat region becomes large. The final limiting load occurs when the maximum stress in either portion of the rod exceeds the yield stress of the tube. In what follows, the most limiting fuel assembly from the array of fuel types considered is subject to detailed analysis and the limiting load established. This limit axial load is considered as the product of the fuel rod weight times the deceleration. Therefore, establishing the limiting load to reach cladding material yield establishes the limiting axial deceleration that can be imposed.

The preceding discussion has assumed end conditions of simple support for conservatism. The location of the fuel rod determines the actual free gap between grid straps. For example, a fuel rod furthest from the cell wall that resists lateral movement of the assembly moves to close up all of the clearances that exist between it and the resisting cell wall. The clearance between rods is the rod pitch minus the rod diameter. In a 14 x 14 assembly, there are 13 clearance gaps plus an additional clearance  $g_3$  between the nearest rod and the cell wall. Therefore, the gap  $g_2$  is given as

$$g_2 = 13(\text{pitch-diameter}) + g_3$$

Figure 2.9.9 provides an illustration of the fuel rod deformation for a case of 5 fuel rods in a column. Clearly for this case, the available lateral movement can be considerable for the "furthest" fuel rod. On the other hand, for this fuel rod, there will be considerable moment resistance at the grid strap from the adjacent section of the fuel rod. The situation is different when the rod being analyzed is assumed to be the closest to the cell wall. In this case, the clearance gap is much smaller, but the moment resistance provided by adjacent sections of the rod is reduced. For calculation purposes, we assume that a moment resistance is provided as  $M = f \times K$  for the fuel rod under analysis where

$$K = 3EI/L, \quad L = \text{span between grid straps, and "f" is an assumed fraction of K}$$

The preceding result for the rotational spring constant assumes a simple support at each end of the span with an end moment "M" applied. Classical strength of materials gives the result for the spring constant. The arbitrary assumption of a constant reduction in the spring constant is to account for undetermined interactions between axial force in the rod and the calculated spring constant. As the compressive force in the adjacent members increases, the spring constant will be reduced. On the other hand, as the adjacent span contacts its near cell wall, the spring constant increases. On balance, it should be conservative to assume a considerable reduction in the spring constant available to the span being analyzed in detail. As a further conservatism, the angle defined by the geometry is used without including any additional elastic displacement shape. This will further reduce the value of the resisting moment at any stage of the solution. In the detailed calculations, two limiting cases are examined. To limit the analysis to a single rod, it is assumed that after "stack-up" of the rods (see Figure 2.9.9), the lateral support provided by the cell wall supports all of the rods. That is, the rods are considered to have non-deforming cross-section.

Numerical Analysis - Based on the tabular results in Table 2.9.1, the fuel assembly with the smallest value for the deceleration based on the classical Euler buckling formula is analyzed in detail. The following input data is specified for the limiting 14 x 14 assembly [2.9.2]:

Inside dimension of a HI-STAR 100 fuel basket cell

$$s := 8.75 \cdot \text{in}$$

Outside envelope dimension of grid plate

$$gp := 7.763 \cdot \text{in}$$

Outer diameter of fuel rod cladding

$$D := .4 \cdot \text{in}$$

Wall thickness of cladding

$$t := .0243 \cdot \text{in}$$

Weight of fuel assembly (including end fittings)

$$W := 1177 \cdot \text{lbf}$$

Number of fuel rods + guide/instrument tubes in a column or row

$$n := 14$$

Overall length of fuel rod between assumed end support

$$L_t := 151 \cdot \text{in}$$

Length of fuel rod between grid straps

$$L_s := 25.3 \cdot \text{in}$$

Average clearance to cell wall at a grid strap location  
assuming a straight and centered fuel assembly

$$g_1 := .5 \cdot (s - gp)$$

$$g_1 = 0.494 \text{ in}$$

Rod pitch

$$\text{pitch} := 0.556 \cdot \text{in}$$

$$\text{Clearance} := (n - 1) \cdot (\text{pitch} - D)$$

$$\text{Clearance} = 2.028 \text{ in}$$

Minimum available clearance for lateral movement of a fuel  
rod between grid straps

$$g_3 := g_1 + .5 \cdot [gp - (n \cdot D + \text{Clearance})]$$

$$g_3 = 0.561 \text{ in}$$

Maximum available clearances for lateral movement of a  
fuel rod between grid straps

$$g_2 := g_3 + \text{Clearance}$$

$$g_2 = 2.589 \text{ in}$$

Young's Modulus of Zircalloy [2.9.1]

$$E := 10400000 \cdot \text{psi}$$

Dynamic Yield Strength of Zircalloy [2.9.1]

$$\sigma_y := 80500 \cdot \text{psi}$$

## Geometry Calculations:

Compute the metal cross section area  $A$ , the metal area moment of inertia  $I$ , and the total weight of a single fuel rod (conservatively assume that end fittings are only supported by fuel rods in the loading scenario of interest).

$$A := \frac{\pi}{4} \cdot [D^2 - (D - 2 \cdot t)^2]$$

$$I := \frac{\pi}{64} \cdot [D^4 - (D - 2 \cdot t)^4]$$

$$A = 0.029 \text{ in}^2$$

$$I = 5.082 \times 10^{-4} \text{ in}^4$$

$$W_r := \frac{W}{n^2}$$

$$W_r = 6.005 \text{ lbf}$$

As an initial lower bound calculation, assume no rotational support from adjacent spans and define a multiplying factor

$$f := 0.0$$

Compute the rotational spring constant available from adjacent sections of the rod.

$$K := 3 \cdot E \cdot \frac{I}{L_s} \cdot f$$

$$K = 0 \text{ lbf} \cdot \text{in}$$

Now compute the limiting load, if applied at one end of the fuel rod cladding, which causes an overall elastic instability and contact with the cell wall. Assume buckling in a symmetric mode for a conservatively low result. The purpose of this calculation is solely to demonstrate the flexibility of the single fuel rod. No resisting moment capacity is assumed to be present at the fittings.

$$P_0 := \pi^2 \cdot E \cdot \frac{I}{L_t^2}$$

$$P_0 = 2.288 \text{ lbf}$$

Note that this is less than the weight of the rod itself. This demonstrates that in the absence of any additional axial support, the fuel rod will bow and be supported by the cell walls under a very small axial load. In reality, however, there is additional axial support that would increase this initial buckling load. The stress induced in the rod by this overall deflected shape is small.

$$\text{Stress}_1 := \frac{P_0 \cdot g_1 \cdot D}{2 \cdot I}$$

$$\text{Stress}_1 = 444.32 \text{ psi}$$

$$\text{Stress}_d := \frac{P_0}{A}$$

$$\text{Stress}_d = 79.76 \text{ psi}$$

The conclusion of this initial calculation is that grid straps come in contact; consideration of what happens between a grid strap is the only region that requires further investigation. First calculate the classical Euler buckling load based on a pin-ended rod and assume conservatively that the entire weight of the rod is providing the axial driving force. This gives a conservatively low estimate of the limiting deceleration that can be resisted before a perfectly straight rod buckles.

$$a_{\text{lim}1} := \pi^2 \cdot E \cdot \frac{I}{L_s^2 \cdot W_r}$$

$$a_{\text{lim}1} = 13.57$$

The rigid body angle of rotation at the grid strap under this load that causes contact is:

$$\theta_1 := \text{atan} \left[ 2 \cdot \frac{(g_2 - g_1)}{L_s} \right]$$

$$\theta_1 = 9.406 \text{ deg}$$

Conservatively assume resisting moment at the grid is proportional to this "rigid body" angle:

$$M_r := K \cdot \theta_1$$

$$M_r = 0 \text{ in}\cdot\text{lbf}$$

(in this first analysis, no resisting moment is assumed)

The total stress at the grid strap due to the axial force and the resisting moment is

$$\sigma_{\text{gs}} := \frac{W_r \cdot a_{\text{lim}1}}{A} + \frac{M_r \cdot D}{2 \cdot I}$$

$$\sigma_{\text{gs}} = 2841.172 \text{ psi}$$

The total stress at the contact location is

$$\text{Stress}_2 := \frac{[W_r \cdot a_{\text{lim}1} \cdot (g_2 - g_1) - M_r] \cdot D}{2 \cdot I}$$

$$\text{Stress}_2 = 6.721 \times 10^4 \text{ psi}$$

$$\text{Stress}_{2d} := \frac{W_r \cdot a_{lim1}}{A}$$

$$\text{Stress}_{2d} = 2841.172 \text{ psi}$$

$$\text{Stress}_{2t} := \text{Stress}_2 + \text{Stress}_{2d}$$

$$\text{Stress}_{2t} = 7.005 \times 10^4 \text{ psi}$$

This is the maximum value of the stress at this location since, for further increase in axial load, the moment will decrease with consequent large decrease in the total stress.

The safety factor is

$$\frac{\sigma_y}{\text{Stress}_{2t}} = 1.149$$

The axial load in the unsupported portion of the beam at this instant is

$$P_{ax} := \frac{(W_r \cdot a_{lim1})}{\cos(\theta_1)}$$

$$P_{ax} = 82.599 \text{ lbf}$$

At this point in the load process, a certain axial load exists in the unsupported span on either side of the contact point. However, since the unsupported span is approximately 50% of the original span, the allowable deceleration limit is larger. As the axial load is incrementally increased, the moment at the contact point is reduced to zero with consequent increases in the lateral force V at the grid strap and at the contact points A and A'. Figure 2.9.8 provides the necessary information to determine the elastic deformation that occurs in the unsupported span as the axial load increases and the contact points separate (and, therefore, decreasing the free span).

From geometry, coupled with the assumption that the deflected shape is a half "sin" function with peak value  $\delta$ , the following relations are developed:

Assume "a" is a fraction of 50% of the span (the following calculations show only the final iterated assumption for the fraction

$$\varepsilon := .9$$

$$a := \varepsilon \cdot \left( \frac{L_s}{2} \right)$$

$$a = 11.385 \text{ in}$$

Calculate "b" in Figure 2.9.8

$$b := \left[ (a)^2 + (g_2 - g_1)^2 \right]^{.5}$$

$$b = 11.576 \text{ in}$$

An equation for  $\delta$  can be developed from the geometric relation

$$\frac{(g_2 - g_1)}{a} := \frac{b}{2(R - \delta)} \quad \blacksquare$$

(please note that the above equation is imported from the electronic spreadsheet program MathCad. The solid rectangle appearing after the equation is a MathCad symbol designating that no computations are performed on that line)

The inverse of the radius of curvature, R, at the point of peak elastic deflection of the free span, is computed as the second derivative of the assumed sin wave deflection shape. Based on the geometry in Figure 2.9.8, the peak deflection is:

$$\delta := .5 \cdot \left[ \left[ a \cdot \frac{b}{2 \cdot (g_2 - g_1)} \right]^2 + 4 \cdot \left( \frac{b}{\pi} \right)^2 \right]^{.5} - a \cdot \frac{b}{4 \cdot (g_2 - g_1)}$$

$$\delta = 0.426 \text{ in}$$

For the assumed "a", the limiting axial load capacity in the unsupported region is conservatively estimated as:

$$a_{\text{lim}2} := \pi^2 \cdot E \cdot \frac{I}{(b)^2 \cdot W_r}$$

$$a_{\text{lim}2} = 64.816$$

The corresponding rigid body angle is:

$$\theta_2 := \text{atan} \left[ 1 \cdot \frac{(g_2 - g_1)}{a} \right]$$

$$\theta_2 = 10.429 \text{ deg}$$

The axial load in the unsupported portion of the beam at this instant is

$$P_{\text{ax}} := \frac{(W_r \cdot a_{\text{lim}2})}{\cos(\theta_2)}$$

$$P_{\text{ax}} = 395.763 \text{ lbf}$$

The resisting moment is

$$M_r := K \cdot \theta_2$$

$$M_r = 0 \text{ in}\cdot\text{lbf}$$

The total stress in the middle of the unsupported section of free span "b" is

$$\text{stress}_3 := \frac{(P_{ax} \cdot \delta - M_r) \cdot D}{2 \cdot I}$$

$$\text{stress}_3 = 6.635 \times 10^4 \text{ psi}$$

$$\text{stress}_{3d} := \frac{P_{ax}}{A}$$

$$\text{stress}_{3d} = 1.38 \times 10^4 \text{ psi}$$

$$\text{stress}_{3t} := \text{stress}_3 + \text{stress}_{3d}$$

$$\text{stress}_{3t} = 8.015 \times 10^4 \text{ psi}$$

The safety factor is

$$\frac{\sigma_y}{\text{stress}_{3t}} = 1.004$$

The total stress at the grid strap due to the axial force and the resisting moment is

$$\sigma_{gs} := \frac{W_r \cdot a_{lim2}}{A} + \frac{M_r \cdot D}{2 \cdot I}$$

$$\sigma_{gs} = 1.357 \times 10^4 \text{ psi}$$

The safety factor is

$$\frac{\sigma_y}{\sigma_{gs}} = 5.932$$

For this set of assumptions, the stress capacity of the rod cladding has been achieved, so that the limiting deceleration is:

$$A_{limit} := a_{lim2}$$

$$A_{limit} = 64.816$$

This exceeds the design basis for the HI-STAR 100 package.

If there is any restraining moment from the adjacent span, there is a possibility of exceeding the rod structural limits at that location due to the induced stress. Therefore, the above calculations are repeated for an assumed moment capacity at the grid strap.

$$f := 1.$$

$$K := 3 \cdot E \cdot \frac{I}{L_s} \cdot f$$

The rigid body angle of rotation at the grid strap under this load that causes contact is:

$$\theta_1 := \text{atan} \left[ 2 \cdot \frac{(g_2 - g_1)}{L_s} \right]$$

$$\theta_1 = 9.406 \text{ deg}$$

Conservatively assume resisting moment at the grid is a function of this angle,

$$M_r := K \cdot \theta_1$$

$$M_r = 102.875 \text{ in-lbf}$$

The total stress at the grid strap due to the axial force and the resisting moment is

$$\sigma_{gs} := \frac{W_r \cdot a_{lim1}}{A} + \frac{M_r \cdot D}{2 \cdot I}$$

$$\sigma_{gs} = 4.333 \times 10^4 \text{ psi}$$

The total stress at the contact location is

$$\text{Stress}_2 := \frac{[W_r \cdot a_{lim1} \cdot (g_2 - g_1) - M_r] \cdot D}{2 \cdot I}$$

$$\text{Stress}_2 = 2.672 \times 10^4 \text{ psi}$$

$$\text{Stress}_{2d} := \frac{W_r \cdot a_{lim1}}{A}$$

$$\text{Stress}_{2d} = 2841.172 \text{ psi}$$

$$\text{Stress}_{2t} := \text{Stress}_2 + \text{Stress}_{2d}$$

$$\text{Stress}_{2t} = 2.956 \times 10^4 \text{ psi}$$

This is the maximum value of the stress at this location since, for further increase in axial load, the moment will decrease with consequent large decrease in the total stress.

The axial load in the unsupported portion of the beam at this instant is

$$P_{ax} := \frac{(W_r \cdot a_{lim1})}{\cos(\theta_1)}$$

$$P_{ax} = 82.599 \text{ lbf}$$

At this point in the load process, a certain axial load exists in the unsupported span on either side of the contact point. However, since the unsupported span is approximately 50% of the original span, the allowable deceleration limit is larger. As the axial load is incrementally increased, the moment at the contact point is reduced to zero with consequent increases in the lateral force V at the grid strap and at the contact points A and A'. Figure 2.9.8 provides the necessary information to determine the elastic deformation that occurs in the unsupported span as the axial load increases and the contact points separate (and, therefore, decreasing the free span).

From geometry, coupled with the assumption that the deflected shape is a half "sine" function with peak value " $\delta$ ", the following relations are developed:

Assume "a" is a fraction of 50% of the span (the following calculations show only the final iterated assumption for the fraction

$$\varepsilon := .7$$

$$a := \varepsilon \cdot \left( \frac{L_s}{2} \right)$$

$$a = 8.855 \text{ in}$$

Calculate "b" in Figure 2.9.8

$$b := \left[ (a)^2 + (g_2 - g_1)^2 \right]^{.5}$$

$$b = 9.1 \text{ in}$$

The inverse of the radius of curvature, R, at the point of peak elastic deflection of the free span, is computed as the second derivative of the assumed sin wave deflection shape. Based on the geometry in Figure 2.9.8, the peak deflection is:

$$\delta := .5 \cdot \left[ \left[ a \cdot \frac{b}{2 \cdot (g_2 - g_1)} \right]^2 + 4 \cdot \left( \frac{b}{\pi} \right)^2 \right]^{.5} - a \cdot \frac{b}{4 \cdot (g_2 - g_1)}$$

$$\delta = 0.427 \text{ in}$$

For the assumed "a", the limiting axial load capacity in the unsupported region is conservatively estimated as:

$$a_{lim2} := \pi^2 \cdot E \cdot \frac{I}{(b)^2 \cdot W_r}$$

$$a_{lim2} = 104.9$$

The corresponding rigid body angle is:

$$\theta_2 := \text{atan} \left[ 1 \cdot \frac{(g_2 - g_1)}{a} \right]$$

$$\theta_2 = 13.314 \text{ deg}$$

The axial load in the unsupported portion of the beam at this instant is

$$P_{ax} := \frac{(W_r \cdot a_{lim2})}{\cos(\theta_2)}$$

$$P_{ax} = 647.331 \text{ lbf}$$

The resisting moment is

$$M_r := K \cdot \theta_2$$

$$M_r = 145.619 \text{ in-lbf}$$

The total stress in the middle of the unsupported section of free span "b" is

$$\text{stress}_3 := \frac{(P_{ax} \cdot \delta - M_r) \cdot D}{2 \cdot I}$$

$$\text{stress}_3 = 5.145 \times 10^4 \text{ psi}$$

$$\text{stress}_{3d} := \frac{P_{ax}}{A}$$

$$\text{stress}_{3d} = 2.257 \times 10^4 \text{ psi}$$

$$\text{stress}_{3t} := \text{stress}_3 + \text{stress}_{3d}$$

$$\text{stress}_{3t} = 7.402 \times 10^4 \text{ psi}$$

The safety factor is

$$\frac{\sigma_y}{\text{stress}_{3t}} = 1.088$$

The total stress at the grid strap due to the axial force and the resisting moment is

$$\sigma_{gs} := \frac{W_r \cdot a_{lim2}}{A} + \frac{M_r \cdot D}{2 \cdot I}$$

$$\sigma_{gs} = 7.928 \times 10^4 \text{ psi}$$

The safety factor is

$$\frac{\sigma_y}{\sigma_{gs}} = 1.015$$

For this set of assumptions, the stress capacity of the rod cladding has been achieved, so that the limit deceleration is:

$$A_{limit} := a_{lim2}$$

$$A_{limit} = 104.9$$

#### Conclusions

An analysis has demonstrated that for the most limiting PWR fuel assembly stored in the HI-STAR 100 fuel basket, a conservative lower bound limit on acceptable axial decelerations exceeds the 60g design basis of the cask. For a reasonable assumption of moment resisting capacity at the grid straps, the axial deceleration limit exceeds the design basis by a large margin.

It is concluded that fuel rod integrity is maintained in the event of a hypothetical accident condition leading to a 60g design basis deceleration in the direction normal to the target.

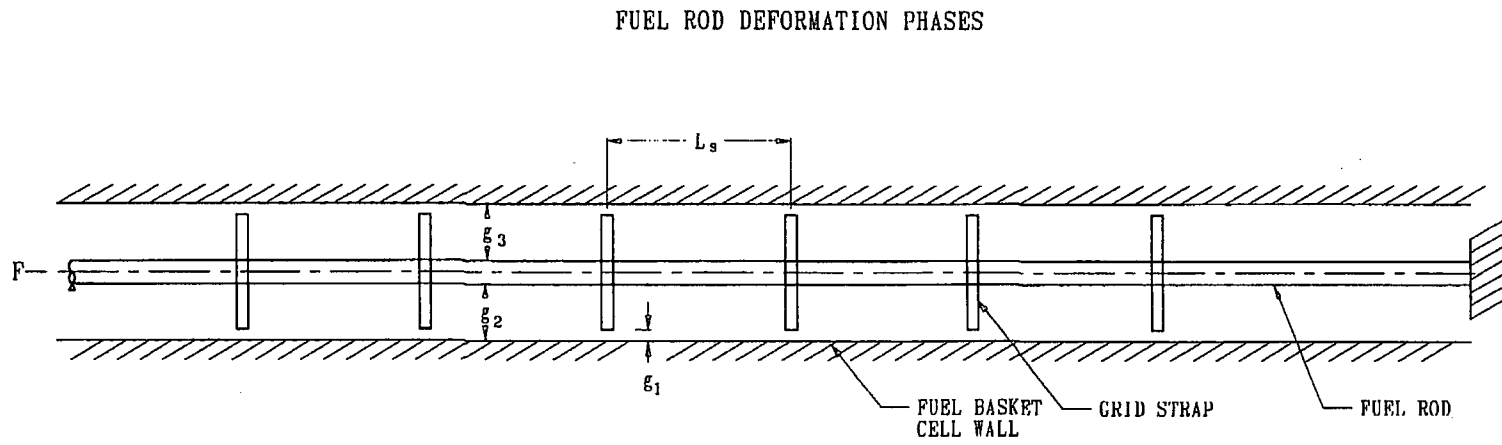


FIGURE 2.9.1;  $g_1 > 0$

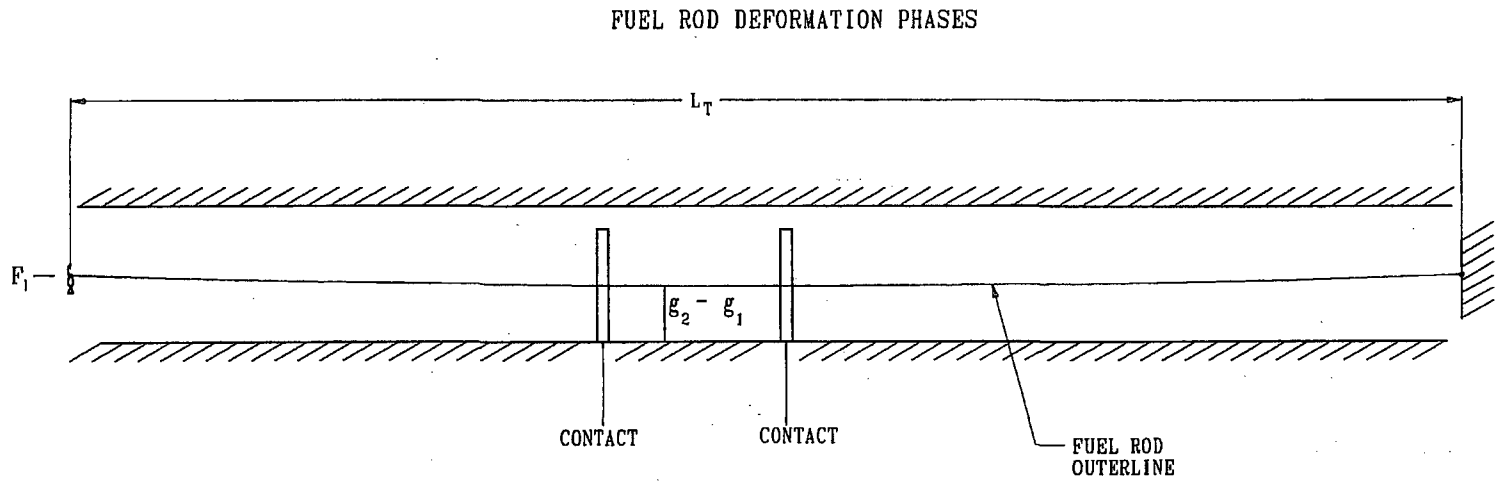


FIGURE 2.9.2;  $g_1 = 0$

FUEL ROD DEFORMATION PHASES

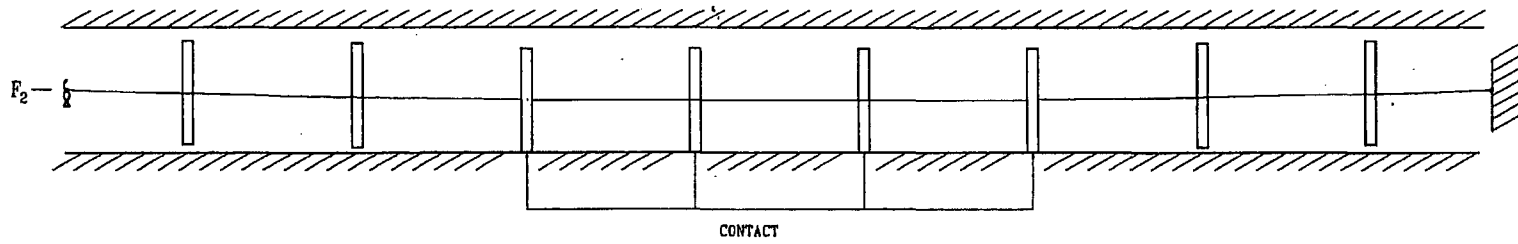


FIGURE 2.9.3;  $g_1 = 0, F_2 > F_1$

### FUEL ROD DEFORMATION PHASES

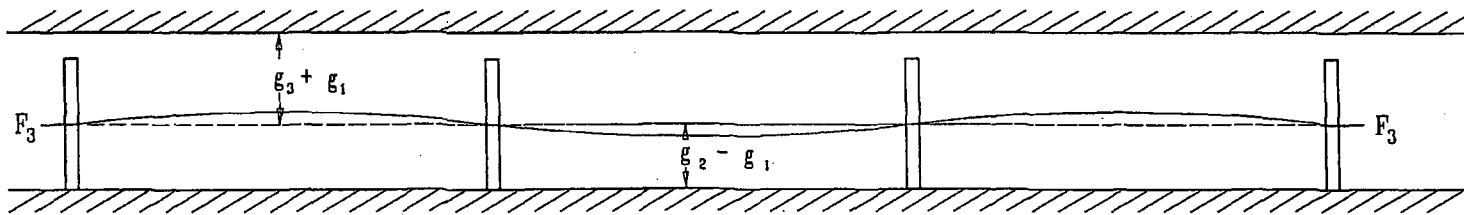


FIGURE 2.9.4; INTER-GRID STRAP DEFORMATION  $F_3 > F_2$

FUEL ROD DEFORMATION PHASES

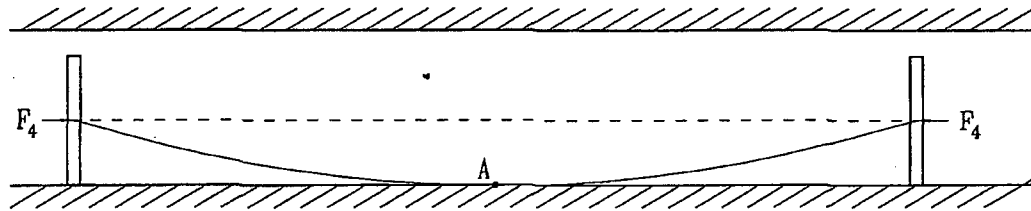


FIGURE 2.9.5; POINT CONTACT AT LOAD  $F_4$   
MAXIMUM BENDING MOMENT AT A

FUEL ROD DEFORMATION PHASES

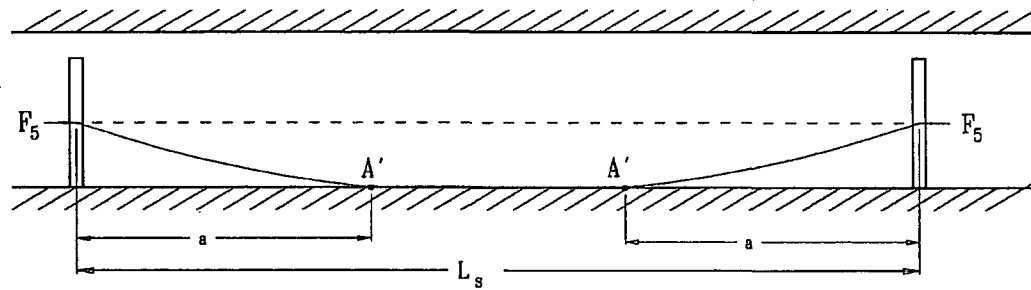


FIGURE 2.9.6; EXTENDED REGION OF CONTACT  
 $F_5 > F_4$  , ZERO BENDING MOMENT AT  $A'$

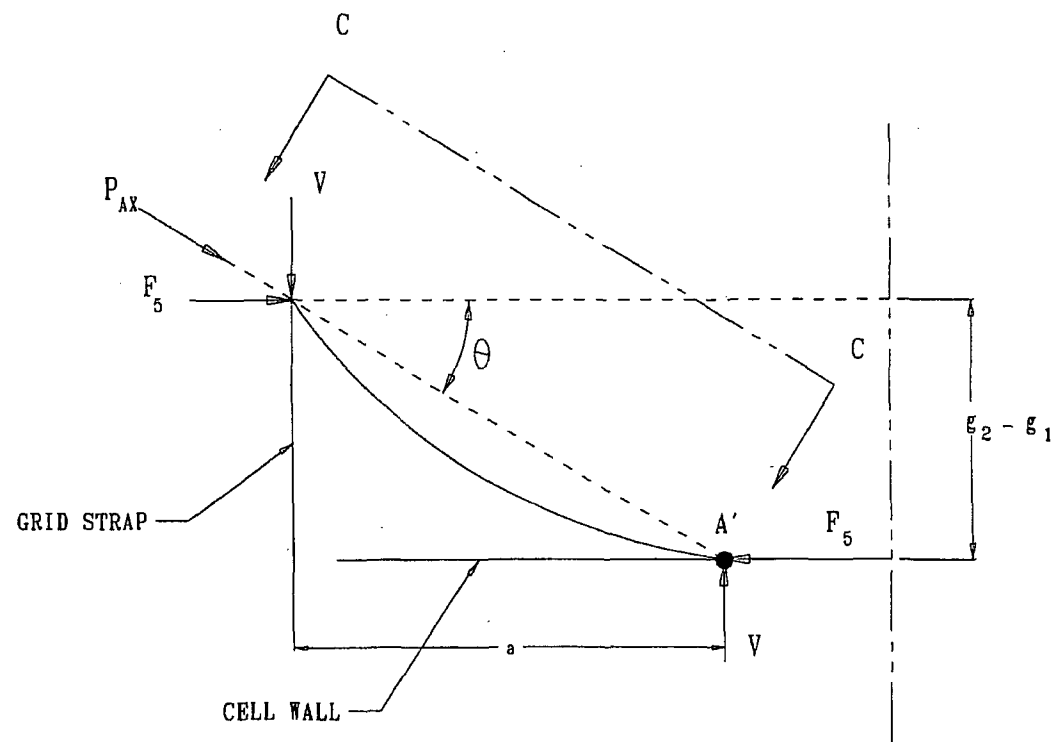
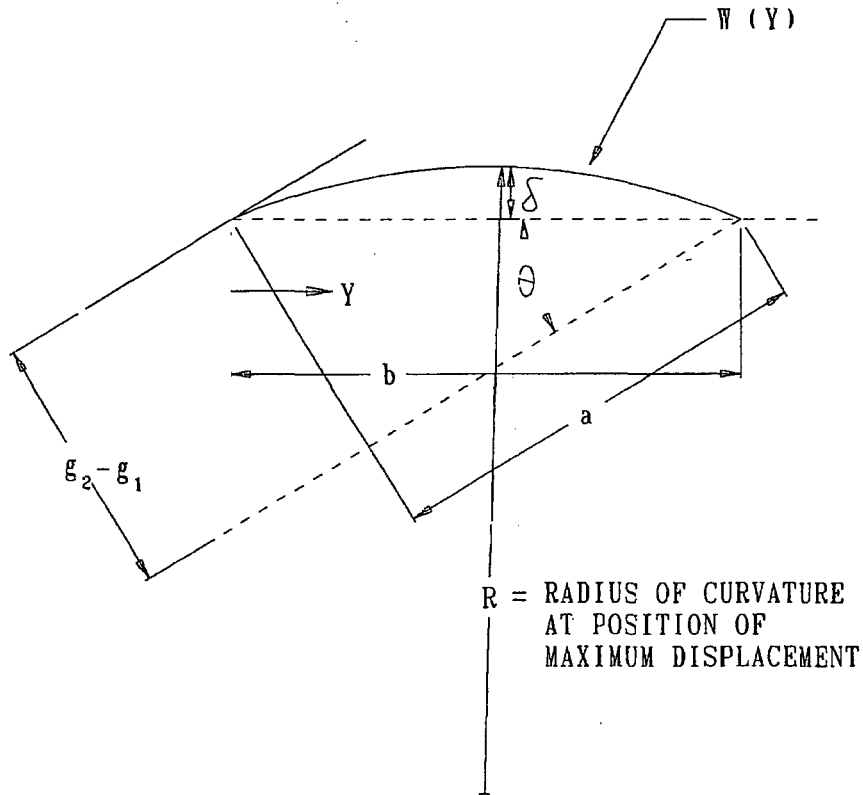


FIGURE 2.9.7; FREE BODY DIAGRAM WHEN MOMENT AT A' = 0  
 $P_{AX} = F_5 / \cos(\theta)$ . RESISTING MOMENT  $M_R$   
 AT GRID STRAP NOT SHOWN



$R$  = RADIUS OF CURVATURE  
AT POSITION OF  
MAXIMUM DISPLACEMENT

$$Z = R - \delta$$

$$W(Y) = \delta \sin(\pi Y/b)$$

FIGURE 2.9.8; VIEW C - C

HI951251

REVISION 8

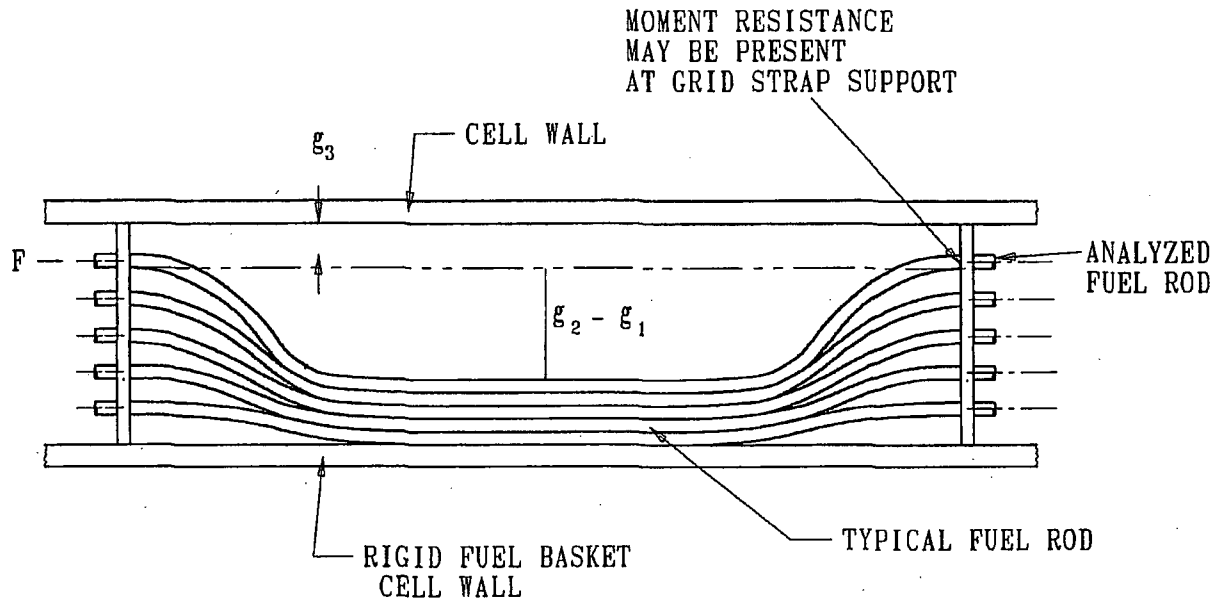


FIGURE 2.9.9; EXAGGERATED DETAIL SHOWING MULTIPLE FUEL RODS SUBJECT TO LATERAL DEFLECTION WITH FINAL STACKING OF ROD COLUMN

2.10 MISCELLANEOUS ITEMS

2.10.1 Appendices

The following appendices are included as supplementary material for Chapter 2 of the SAR.

APPENDIX 2.A: IMPACT LIMITER CHARACTERISTICS, DYNAMIC SIMULATION OF HYPOTHETICAL ACCIDENT EVENT, AND SCALE MODEL TESTS  
(This appendix was 2.H in previous SAR revisions; it has been renumbered reflecting the removal of other appendices from the SAR)

APPENDIX 2.B: SUMMARY OF RESULTS FOR STRUCTURAL INTEGRITY OF DAMAGED FUEL CANISTERS

APPENDIX 2.C: EVALUATION OF AN IMPROVED HI-STAR 100 IMPACT LIMITER DESIGN BASED ON LS-DYNA DROP SIMULATIONS

ALL OTHER APPENDICES (2.D through 2.AO) - DELETED

2.10.2 Summary of NUREG -1617/10CFR71 Compliance

This subsection provides a “road map” of technical information to demonstrate that the SAR in compliance with the provisions of NUREG-1617 and associated referenced sections of 10CFR71 necessary to certify the HI-STAR 100 package for transport.

**Description of Structural Design**

The package structural design description and the contents of the application meet the requirements of 10CFR 71.31 and Regulatory Guide 7.9. Applicable sections where this is demonstrated are 1.2.1; 1.3; 1.4; and 2.1.

The codes and standards used in the package design are listed in 1.3. The use of the ASME Boiler and Pressure Vessel Code is in compliance with NUREG/CR-6407, “Classification of Transportation Packaging and Dry Spent Fuel Storage Components”.

**Material Properties**

There are no significant chemical, galvanic or other reactions among the packaging components, among package contents, or between the packaging components and the contents in dry or wet environment conditions. The applicable subsection where this is demonstrated is 2.4.4.

The effects of radiation on materials are considered and package containment is constructed from materials that meet the requirements of Reg. Guides 7.11 and 7.12. Applicable subsections where this is demonstrated are: 1.2.1; 2.1.2; and, 2.4.4.

### **Lifting and Tie-Down Standards for All Packages**

Lifting and Tie-Down systems meet 10CFR 71.45 standards. The applicable section where this is demonstrated is 2.5.

### **General Considerations for Structural Evaluation of Packaging**

The packaging structural evaluation meets the requirements of 10CFR 71.35. Applicable chapters and/or sections where this is demonstrated are: 2.5; 2.6; 2.7

### **Normal Conditions of Transport**

The packaging structural performance under normal conditions of transport demonstrate that there will be no substantial reduction in the effectiveness of the packaging. The applicable section where this is demonstrated is 2.6.

### **Hypothetical Accident Conditions**

The packaging structural performance under the hypothetical accident conditions demonstrates that the packaging has adequate structural integrity to satisfy the subcriticality, containment, shielding, and temperature requirements of 10CFR Part 71. The applicable section where this is demonstrated is 2.7.

### **Special Requirement for Irradiated Nuclear Fuel Shipments**

The containment structure meets the 10CFR 71.61 requirements for irradiated nuclear fuel shipments. The applicable section where this is demonstrated is 2.7.

### **Internal Pressure Test**

The containment structure meets the 10CFR 71.85(b) requirements for pressure test without yielding. The applicable subsection where this is demonstrated is 2.6.1.4.3.

2.11 REFERENCES

- [2.1.1] 10CFR Part 71, "Packaging and Transportation of Radioactive Materials", Title 10 of the Code of Federal Regulations, Office of the Federal Register, Washington, D.C.
- [2.1.2] Regulatory Guide 7.8, "Load Combinations for the Structural Analysis of Shipping Casks for Radioactive Material", Revision 1, March, 1989, U.S. Nuclear Regulatory Commission.
- [2.1.3] 10CFR Part 72, "Licensing Requirements for the Storage of Spent Fuel in an Independent Spent Fuel Storage Installation", Title 10 of the Code of Federal Regulations, Office of the Federal Register, Washington, D.C.
- [2.1.4] Regulatory Guide 7.6, "Design Criteria for the Structural Analysis of Shipping Cask Containment Vessels", Revision 1, March, 1978, U.S. Nuclear Regulatory Commission.
- [2.1.5] ASME Boiler & Pressure Vessel Code, Section III, Subsection NB, American Society of Mechanical Engineers, 1995.
- [2.1.6] ASME Boiler & Pressure Vessel Code, Section III, Subsection NG, American Society of Mechanical Engineers, 1995.
- [2.1.7] ASME Boiler & Pressure Vessel Code, Section III, Subsection NF, American Society of Mechanical Engineers, 1995.
- [2.1.8] Code Case N-284, "Metal Containment Shell Buckling Design Methods", Section III, Division 1, Class MC, Approval Date 8/25/80.
- [2.1.9] NUREG-0612, "Control of Heavy Loads at Nuclear Power Plants," United States Nuclear Regulatory Commission, July, 1980.
- [2.1.10] ANSI N14.6-1993, "American National Standard for Special Lifting Devices for Shipping Containers Weighing 10,000 Pounds (4,500 kg) or More for Nuclear Materials," American National Standards Institute, Inc.
- [2.1.11] ASME Boiler & Pressure Vessel Code, Section II, Part D, American Society of Mechanical Engineers, 1995.
- [2.1.12] ASME Boiler & Pressure Vessel Code, Section III, Appendices, American Society of Mechanical Engineers, 1995.

- [2.1.13] Regulatory Guide 7.11, "Fracture Toughness Criteria of Base Material for Ferritic Steel Shipping Cask Containment Vessels with a Maximum Wall Thickness of 4 Inches", United States Nuclear Regulatory Commission, June, 1991.
- [2.1.14] Regulatory Guide 7.12, "Fracture Toughness Criteria of Base Material for Ferritic Steel Shipping Cask Containment Vessels with a Wall Thickness Greater Than 4 Inches But Not Exceeding 12 Inches", United States Regulatory Commission, June, 1991.
- [2.1.15] NUREG/CR-1815, "Recommendations for Protecting Against Failure by Brittle Fracture in Ferritic Steel Shipping Containers Up to Four Inches Thick."
- [2.1.16] Aerospace Structural Metals Handbook, Manson.
- [2.1.17] ARMCO Product Data Bulletin S-22
- [2.1.18] NUREG-1617 Standard Review Plan for Transportation Packages for Spent Nuclear Fuel (Draft Report, March 1998).
- [2.3.1] Hexcel Corporation Publication TSB 120, "Mechanical Properties of Hexcel Honeycomb Materials".
- [2.3.2] Test Report For Aluminum Honeycomb Static Compression Testing Under Different Temperatures, Holtec Proprietary Report HI-981979, June 1998.
- [2.4.1] NRC Bulletin 96-04: Chemical, Galvanic or Other Reactions in Spent Fuel Storage and Transportation Casks, July 5, 1996.
- [2.4.2] L.W. Ricketts, Fundamentals of Nuclear Hardening of Electronic Equipment, Robert E. Krieger Publishing Company, Malabar, FL, 1986.
- [2.4.3] D.R. Olander, "Fundamental Aspects of Nuclear Reactor Fuel Elements," TID-26711-P1, 1976.
- [2.6.1] Theory of Elastic Stability, S.P. Timoshenko and J. Gere, McGraw Hill.
- [2.6.2] Mark's Standard Handbook for Mechanical Engineering, 9th ed.
- [2.6.3] Mok, Fischer, and Hsu, "Stress Analysis of Closure Bolts for Shipping Casks" (NUREG/CR-6007-UCRL-ID-110637), Lawrence Livermore National Laboratory/Kaiser Engineering, 1993.

- [2.6.4] ANSYS Finite Element Code, Version 5.2, ANSYS Inc., 1995.
- [2.6.5] "Structural Calculation Package for MPC," Holtec Proprietary Report HI-2012787, Revision 12.
- [2.7.1] Shappert, L.B., "Cask Designer's Guide: A Guide for Design, Fabrication, and Operation of Shipping Casks for Nuclear Applications," ORNL-RSIC-68, Oak Ridge National Laboratories, Feb. 1970.
- [2.7.2] American Society of Civil Engineers, Structural Analysis and Design of Nuclear Power Plants, ASCE No. 58.
- [2.7.3] NUREG/CR-6322, "Buckling Analysis of Spent Fuel Basket", Lawrence Livermore National Laboratory, May, 1995.
- [2.7.4] "Benchmarking of the LS-DYNA Impact Response Prediction Model for the HI-STAR Transport Package Using the AL-STAR Impact Limiter Test Data," Holtec Proprietary Report HI-2073743, Revision 1.
- [2.7.5] HI-STAR 60 (Docket 71-9336) Safety Analysis Report, Holtec Report HI-2073710, Revision 2.
- [2.7.6] HI-STAR 180 (Docket 71-9325) Safety Analysis Report, Holtec Report HI-2073681, Revision 3.
- [2.7.7] Holtec Proprietary Licensing Drawing C1765 (Sht. 1, Rev. 5 and Sht. 6, Rev. 4).
- [2.9.1] Chun, Witte, Schwartz, "Dynamic Impact Effects on Spent Fuel Assemblies", UCID-21246, Lawrence Livermore National Laboratory, October 20, 1987.
- [2.9.2] Physical and Decay Characteristics of Commercial LWR Spent Fuel, Oak Ridge National Laboratory Report, J. Roddy, H. Claiborne, R. Ashline, P. Johnson, and B. Rhyne, ORNL/TM-9591/V1-R1, 1/86.

APPENDIX 2.A:  
DESIGN, TESTING, AND COMPUTER SIMULATION OF THE AL-STAR™  
IMPACT LIMITER

2.A.1 INTRODUCTION

As stated in Subsection 2.7, the central purpose of the AL-STAR™ impact limiter is to limit the package maximum deceleration,  $\alpha_{\max}$ , under a postulated drop event to a specified design value. For the regulatory 9-meter hypothetical free drop event, the AL-STAR design is engineered to limit the maximum rigid body deceleration to 60 times the acceleration due to gravity (Table 2.1.10). The HI-STAR packaging, consisting of the loaded overpack and top and bottom impact limiters (illustrated in Figure 2.A.1.1) is essentially a cylindrical body with a rigid interior (namely, the overpack) surrounded by a pair of relatively soft crushable structures. The crushable structure (impact limiter) must deform and absorb the kinetic energy of impact without detaching itself from the overpack, disintegrating, or otherwise malfunctioning. A falling cylindrical body may theoretically impact the target surface in an infinite number of orientations; the impact limiter must limit the HI-STAR 100 decelerations to below 60g's and preserve the limiter-to-overpack connection regardless of the impact orientation. Figure 2.A.1.2 presents the side drop event. In general, a drop event orientation is defined by the angle of the HI-STAR 100 longitudinal axis,  $\theta$ , with the impact surface. In this notation,  $\theta = 0$  means a side drop and  $\theta = 90^\circ$  implies a vertical or end drop scenario. Inasmuch as the top and bottom impact limiter are made of identical crush material, the top or bottom vertical drop events are mathematically and physically equivalent as far as the impact limiter design is concerned. In any orientation, the drop height is measured from the lowest point on the package.

An intermediate value of  $\theta$ ,  $\theta = 67.5^\circ$ , warrants special mention. At  $\theta = 67.5$  degrees, the point of impact is directly below the center of gravity (C.G.) of the HI-STAR 100 package. This drop orientation is traditionally called the C.G.-over-corner (CGOC) configuration. The CGOC orientation is the demarcation line between single and dual impact events. At  $90^\circ > \theta > 67.5^\circ$ , the leading end of the packaging (denoted as the "primary" impact limiter) is the sole participant in absorbing the incident kinetic energy. At  $\theta < 67.5^\circ$  drop orientations, the initial impact and crush of the leading (primary) impact limiter is followed by the downward rotation of the system with the initial impact surface acting as the pivot, culminating in the impact of the opposite (secondary) impact limiter on the target surface. In the dual impact scenarios, the first and second impact limiter crush events are referred to as the "primary" and "secondary" impacts, respectively. It is reasonable to speculate that for certain values of  $\theta$ , the secondary impact may be the more severe of the two. As stated earlier, the design of AL-STAR must ensure that  $\alpha_{\max} \leq 60$ , regardless of the value of  $\theta$ .

The AL-STAR attachment design must ensure that both impact limiters remain attached to the cask during and after the impact event. The impact limiters are also required to prevent cask body-to-unyielding target contact.

Finally, the package design must satisfy all criteria in ambient temperature conditions ranging from -20° to 100°F, and with humidity ranging from 0 to 100%. Therefore, the impact limiter design must be functionally insensitive to temperature and environmental conditions.

An aluminum honeycomb-based impact limiter design was selected as the preferred material for development. The detailed design of the AL-STAR impact limiters is presented in Holtec Drawing C1765 located in Section 1.4. A pictorial view of AL-STAR is presented in Figure 2.A.1.3.

Figure 2.A.1.3 indicates that in addition to the crushable honeycomb, the AL-STAR contains two internal cylindrical shells (also denoted as “rings”), which are stiffened with radial gussets. These carbon steel shells are sized to behave as undeformable surfaces during impact events. They are essentially the “backbone” of the impact limiter, lending a predictability to the impact limiter crush behavior and forcing the energy absorption to occur in the honeycomb metal mass. The design of this backbone structure was a subject of in-depth computer and experimental 1/8 scale static testing, as documented in Holtec Report HI-962501 [2.A.4] and summarized in Section 2.A.4 herein.

Another noteworthy aspect of the AL-STAR impact limiter design is the arrangement of uniaxial and cross core (biaxial) honeycombs. Regions of the honeycomb space that experience impact loading in only one direction are equipped with unidirectional honeycomb sectors. The regions where the direction of the impact loads can vary have cross-core (bi-directional) honeycomb material, as detailed in Subsection 2.3.1.5.

To summarize, the design objectives of the AL-STAR impact limiter are set down as five discrete items, namely:

- i. Limit peak deceleration ( $\alpha_{max}$ ) to 60g's under all potential drop orientations.
- ii. Impact limiter must not detach from the cask under a 9-meter drop event, under any impact orientation.
- iii. The impact limiters must bring the cask body to a complete stop, such that the overpack does not come in physical contact with the target surface.
- iv. Crush material must be equally effective at ambient temperature conditions ranging from -20° to 100°F, with humidity ranging from 0 to 100%.
- v. All external surfaces must be corrosion-resistant.

The last two objectives are realized by utilizing aluminum honeycomb (Type 5052) as crush material and stainless steel (Type 304), for the external skin enclosure. As shown in the ASME Code (Section II, Part D, Table Y-1), the essential property of the constituent material for the honeycomb and the external skin, namely the yield strength remains constant in the -20° F to

100° F range. The surface of the carbon steel impact limiter backbone is painted to limit corrosion.

The remaining design objectives, namely, limiting of the maximum rigid body deceleration,  $\alpha_{max}$ , to 60 g's under a 9-meter drop event, maintaining positive attachment of the AL-STAR impact limiters to the overpack, and preventing contact of the overpack with the unyielding surface, are demonstrated by a combination of numerical simulations and scale model static and dynamic testing. This was accomplished through a research and development effort that is broadly subdivided into six phases, as follows:

- Phase 1: Characterize the honeycomb pressure-deflection relationship.
- Phase 2: Propose a force (static) vs. crush (F vs. d) model for AL-STAR.
- Phase 3: Perform 1/8 scale model static compression tests to validate the force-crush model and to establish the adequacy of the AL-STAR backbone structure.
- Phase 4: Conduct 9-meter quarter-scale model dynamic drop tests in selected limiting drop configurations and obtain test data.
- Phase 5: Simulate the experimental drop tests with a suitable “dynamic model” and establish that the dynamic model predictions of deceleration, crush and event time duration reasonably match the experimentally measured values. A reasonable prediction of the peak decelerations of each drop event is the minimum for the dynamic model to be acceptable.
- Phase 6: Utilize the experimentally confirmed dynamic model to evaluate the effects of tolerances on crush properties and on package weight, and to confirm the adequacy of the full-scale impact limiter design.

It is of crucial importance that the dynamic model benchmarked in Phase 5 be of high reliability, since it becomes the analytical model for the accident-event response prediction of the packaging when tolerances on material behavior and package mass are considered (Phase 6).

In this appendix, a description of the overall program and results for each of the six phases is presented.

#### 2.A.2 Phase 1: Material Pressure-Crush Relationship

The extent of deflection,  $\Delta$ , sustained by a honeycomb material when subjected to a uniform pressure,  $p$ , is an essential element of information in the impact limiter design. Towards this end, coupon specimens of uniaxial and cross-core honeycomb of various nominal crush strengths and densities were compression-tested by the material manufacturer. The results showed that all honeycomb coupons shared some common load-deflection characteristics, namely:

The initial pressure-deflection curve resembled an elastic material (pressure roughly proportional to deflection).

Upon reaching a limiting pressure, the material crushed at near constant pressure until the crush reached approximately 60-70 percent of the initial thickness. The required crush force had to increase rapidly to achieve small incremental crushing for strains beyond approximately 60-70 percent.

Figure 2.A.2.1 shows a typical static pressure-deflection curve for a 1"-thick honeycomb specimen. The curve with the initial peak is that of an un-precrushed honeycomb specimen; the curve without the peak (shown as a dashed line only where a difference occurs) corresponds to a pre-crushed specimen. Dynamic testing subsequently showed that removal of the initial peak by pre-crushing the material was a desired feature whenever a large flat area of honeycomb material experienced a crush force (such as in a 90 degree end drop).

Curve fitting of data from all tested coupons indicated that a single mathematical relationship between the applied pressure and compression strain could be developed. The mathematical relationship can provide a reasonable fit for coupons of all crush strengths (crush strength defined as the pressure corresponding to the flat portion of the curve in Figure 2.A.2.1; i.e., it is the constant pressure at which the honeycomb undergoes near-perfect plastic deformation). In other words, the pressure,  $p$ , for a given strain,  $\epsilon$ , is represented by a unique function of the crush pressure,  $p_c$ , i.e.

$$p = f(p_c, \epsilon)$$

The relationship between  $p$  and compression strain was used in the subsequent mathematical efforts to simulate AL-STAR crush behavior. The above mathematical relation was developed to simulate material behavior for a honeycomb material under both non-pre-crushed and pre-crushed conditions.

### 2.A.3 Phase 2: Static Force-Crush Prediction Model

An essential step towards the development of a reliable dynamic model to simulate the impact of a dropped HI-STAR 100 package is to develop a static force-crush model that can subsequently be validated by scale model tests. The force-crush model should reliably duplicate the resistance provided by an impact limiter for a range of crush orientations for the full range of crush depths.

The required force-crush model for AL-STAR is developed using the concept of interpenetration, which is explained using the case of the side drop ( $\theta = 0$ ) as an example (Figure 2.A.3.1(a)).

The condition existing in all impact limiter drop scenarios is that the relatively soft honeycomb material lies between two "hard" surfaces that are advancing towards each other during the impact. One of these two rigid surfaces is the essentially unyielding target (Rigid Body 1) and

the other is the structural backbone of the impact limiter (Rigid Body 2). While the target surface is flat, the backbone structure is cylindrical in profile. When squeezed between the two surfaces, the honeycomb material (at each instant in time) will crush at one or both interface locations. To determine which interface surface will undergo crushing at a given point during the impact event, the concept of interpenetration area is utilized as explained below.

In this concept, two separate crush scenarios, one assuming that the crush occurs at the external interface (target-to-impact limiter), and the other assuming that the crushing is at the internal interface (structural backbone/overpack-to-impact limiter), are compared at each instant during a simulated compression of the impact limiter. A metal honeycomb impact limiter, in general, may have multiple honeycomb material sections crushing at each interface. For simplicity in explaining the concept of interpenetration, we assume that each of the interfaces is characterized by a uniform distribution of honeycomb having crush pressures  $p_1$  and  $p_2$ , respectively. To determine the resistive force developed to crush the impact limiter by a small amount,  $d$ , against the external target, the impact limiter is assumed to penetrate the target by the amount “ $d$ ” without deformation. The resulting area  $A_1$  for the case of side drop, illustrated in Figure 2.A.3.1(b), can be computed as an algebraic expression in the amount of approach,  $d$ . (For oblique drop events, ANSYS [2.A.1] or CADKEY [2.A.2] are used to compute interpenetration area as a function of incremental interpenetration.) The pressure-compression relationship for the honeycomb stock at the external interface provides the crush pressure  $p_1$  that develops due to deformation “ $d$ ”. The total force required for crush “ $d$ ”, at the external interface, is therefore equal to  $p_1A_1$ .

In the second (independent) scenario, the impact limiter external surface is assumed to undergo no movement; rather, the backbone structure (along with the overpack) advances towards the target by an amount  $d$  (Figure 2.A.3.1(c)). Once again, assuming that the cylindrical rigid body moves through an amount “ $d$ ”, the resistance pressure developed in the honeycomb material lying in the path of penetration is available from the appropriate material pressure-compression curve. If the pressure corresponding to the deformation is  $p_2$  and the projected area at the internal interface is  $A_2$ , then the total resistive force encountered in realizing an approach equal to “ $d$ ” between the overpack-backbone assemblage and the target under this latter scenario is  $p_2A_2$ . In an actual drop event, at each instant during the event, incremental crush occurs at one of the two interfaces. If  $p_1A_1 < p_2A_2$  at a given instant then crushing will occur at the external interface. Likewise,  $p_1A_1 > p_2A_2$  will imply that crushing will occur internal to the impact limiter. The smaller of  $p_1A_1$  and  $p_2A_2$  is the required crush force and the corresponding location of crush is where the honeycomb material will compress to realize the approach equal to  $d$ . This “inequality test” to determine where crushing occurs is performed at every increment of crush during the simulation of the event. The appropriate value of the crush force is used in the equilibrium equations at that instant. The concept of interpenetration at two interfaces has been confirmed during testing of the impact limiters; the total crush is observed to be a sum of compression at each of the two interfaces.

To construct a mathematical force-deformation relationship for AL-STAR in any given orientation, the above process is repeated as the crush “ $d$ ” is increased in small increments starting with the beginning of compression ( $d = 0$ ). It is quite clear that the development of the

force-deflection model (F-d model) for AL-STAR in any orientation is a straightforward analysis in 3-D geometry. The F-d curve for AL-STAR for any given value of  $\theta$  can be developed where, other than the geometry of the impact limiter, the crush strengths  $p$  of the honeycomb materials utilized in the impact limiter are the only other required inputs.

The force (F) vs. crush (d) relationship developed using the foregoing method is referred to as the F-d model that is subject to validation by appropriate 1/8 scale model compression tests described in the following section.

#### 2.A.4 Phase 3: One-Eighth Scale Model Static Compression Tests

The 1/8 scale model tests consist of subjecting scaled replicas of the full-size AL-STAR to static compression tests in an engineered fixture such that the force-compression curve for the scaled model can be obtained in various orientations of compression. The scale model is made by making the diameters and length of the model one-eighth of the full-size AL-STAR. The thicknesses of the backbone components (i.e., the inner and outer shells and gussets), and the external skin (see Figure 2.A.1.3) are also scaled to one-eighth times the corresponding dimensions (to the nearest sheet metal gage, where applicable) in the full-size AL-STAR. In the one-eighth model, the performance of the attachment system is not assessed nor is the cask body modeled. However, the interface between overpack and impact limiter where the compression load is resisted is properly simulated. The crush pressure is a material property of the energy absorbing material; therefore, the material (and its density) is not scaled. The 1/8 scale model, therefore, has approximately  $(1/8)^3$  or 1/512 the volume and weight of the full-size unit. Holtec documents [2.A.3, 2.A.4] provide complete details on the 1/8 scale model geometry and fabrication. The static compression behavior of such a 1/8-scale model is correlated with that of a full-size unit using the geometric scaling information. For example, under an axial compression test the area under crush in the scale model will be 1/64 of the full-size AL-STAR (recall that the diameter is scaled down by a factor of 8). Therefore, the crush force (which is crush force pressure times the area under crush) will be 1/64 of the full-size unit. On the other hand, the crush stroke (extent of deformation before "lock up") will be 1/8 of the full-size AL-STAR because the axial length of the scale model (which corresponds to the height of the crush column in axial compression) is one-eighth of the full-size hardware. Thus, the total energy absorbed (force times compression) will be  $(1/8)^3$  of the full-size unit. The same scaling factor can be shown to apply in all directions of crush.

In summary, the 1/8 scale model scales the geometric dimensions of AL-STAR. The previously discussed F-d model is required to translate the force-crush relationship from the 1/8 scale replica to the full-size unit. In order to use the analytical F-d model as a valid vehicle for predicting the force-crush of the full-size (or quarter-scale) AL-STAR, it is necessary to check its prediction ability against actual test data from 1/8-scale model static compression tests.

The objectives of static scale model tests are twofold:

- i. Determine whether the static force-crush relationship predicted by the F-d model appropriately simulates the actual relationship determined by test;
- ii. Determine whether the backbone structure of the AL-STAR impact limiter is sufficiently rigid to withstand and transmit the large loads associated with the postulated accident scenarios.

2.A.4.1 Static Compression Tests on Initial Candidate Crush Material

To assess compression performance, a QA validated AL-STAR static test procedure was prepared [2.A.3] for the one-eighth scale model static compression tests and a series of cold and hot static compression tests performed on an impact limiter configuration with the initial candidate crush material. Holtec calculation package HI-961501 [2.A.4] contains a comprehensive documentation of the 1/8 scale static test program and results for the impact limiter configuration. A summary of the complete test program and test results is presented below.

Four 1/8-scale models were fabricated with details of the impact limiter carefully scaled, including the stiffening cylinders and the stainless steel skin. No impact limiter attachment bolts were incorporated in the model.

Aluminum honeycomb segments provided for the 1/8-scale models were manufactured utilizing the same procedures and processes as for the full-scale impact limiter. As stated earlier, the crush strengths were not scaled because they are considered as material properties.

An adjustable 1/8 scale static test fixture was designed, analyzed, and fabricated. The test fixture interfaced with the impact limiter and simulated the overpack hard surface. The test fixture could be adjusted to simulate any crush orientation. Figure 2.A.4.1 shows the test fixture and the 1/8 scale impact limiter being loaded in the heavy-load testing machine.

The following static one-eighth scale test series were carried out:

Test No.	Orientation, degrees	Temperature
1	0 (side)	+120°F
2	30 (oblique)	Ambient
3	60 (oblique)	Ambient
4	90 (end)	-30°F

For all tests except the end compression (where the orientation is immaterial), the circumferential orientation of the impact limiter was selected so that the initial point of contact between the impact limiter and the test machine was at the interface of two aluminum honeycomb sections. After each test, the impact limiters were cut open and examined.

Observations Based on 1/8 Scale Model Testing

- Effect of Ambient Temperature:

The end compression test was performed with the impact limiter cold (-30°F), the side compression test was performed with the impact limiter hot (+120°F), and the two oblique tests performed at ambient temperature. The material behavior showed no influence of test temperature. This confirms the expected result since the aluminum honeycomb and stainless steel skin yield strengths are insensitive to temperature in the range of interest (-20° F to 100° F) as prescribed in Table Y-1 of the ASME Code.

- Side compression orientation - 0 degree:

The inner stiffening cylinder experienced considerable permanent deformation. The gussets which buttress the inner cylinder buckled. The outer stiffening cylinder performed elastically.

- Oblique compression orientation:

Two oblique orientation static tests were performed. The 30-degree oblique test again showed the need to thicken the inner stiffening cylinder and to rearrange the stiffening gussets.

The 60-degree oblique test was a complete success; no plastic deformation of the backbone structure was indicated.

As would be expected, in those cases where the hard region (backbone structure) of the impact limiter sustained deformations, the scale model exhibited greater flexibility in the physical testing than the analytical prediction (the flexibility of the backbone structure added to the crush of the honeycomb resulting in a greater total measured deflection).

- End compression orientation - 90 degree:

The end-compression orientation is, structurally speaking, the least complicated of the four test configurations. The loading of the AL-STAR scale model in this test is purely axisymmetric. The initial peak in the pressure/deformation curve seen in the coupon tests (Figure 2.A.2.1) was clearly evident in the axial (end) compression test (Figure 2.A.4.3). The backbone structure performed without sustaining plastic deformation.

- Comparison of experimental and analytical predictions

Out of the four static 1/8-scale model tests, two tests (side compression and 30-degree oblique) were unsatisfactory because the backbone structure of the impact limiter did not remain elastic. These tests served to identify the need to reinforce the AL-STAR backbone structure. The other tests, namely end-compression (90 degree) and 60-degree oblique, wherein the backbone structure performed as designed, showed close agreement with the numerical model. Figures 2.A.4.3 and 2.A.4.4, respectively, show the static test results for 90-degree (end-compression) and 60 degree (oblique) cases, along with the prediction of the F-d model. There is good agreement between the computer model and the test data.

In summary, the 1/8 scale model static test program identified the required design changes to the internal structure of the impact limiters. The 1/8 scale model tests showed that the load-compliance characteristics of AL-STAR are insensitive to the changes in the ambient environment. A comparison of the test results with the mathematical model predictions from the F-d model indicated that the mathematical model was in good agreement with 1/8-scale static crush tests whenever the backbone structure performed as required (i.e. remained elastic). Since the crush geometry of the scale model was *not altered* by the strengthening of the backbone, any subsequent reinforcing of the backbone did not alter the F-d relationship for the impact limiter. The two successful static tests that showed excellent agreement with the computer F-d model, therefore, continued to serve as a valid benchmark of the numerical model after the backbone is stiffened. The reinforced backbone structure is incorporated into the final design drawings for the AL-STAR, and was confirmed as acceptable during the dynamic (1/4-scale) model drop tests. Subsequent to the one-quarter scale dynamic tests and the analytical correlation (Phases 4-6), three additional 1/8<sup>th</sup> scale confirmatory static tests were performed on impact limiters that included the internal backbone structure and the final crush material orientations used in the quarter-scale drop tests and in the analytical correlation. These additional confirmatory static tests were performed at room temperature. The tests simulated the crush orientation corresponding to the side drop, the “center-of-gravity-over corner” drop, and the end drop, respectively. Force-deflection results from the static test are compared with the predictions from the theory for the 1/8<sup>th</sup>-scale impact limiters. Subsection 2.A.10 discusses the results obtained from these three additional static tests.

#### 2.A.5 Phase 4: 9 Meter Quarter-Scale Model Drop Tests

The one-quarter scale model dynamic tests provide physical confirmation of the HI-STAR impact limiter design and the performance of the attachment system.

In the 1/4 scale model drop test program, an instrumented scale model of the HI-STAR 100 dual-purpose cask was assembled with the top and bottom AL-STAR impact limiters, raised to a height of 9 meters (measured from the lowest point on the package), and then released to free fall onto an unyielding concrete and steel armor target (unyielding target). The impact limiter attachment system is reproduced in the model using the appropriate scale for bolt diameters, etc.

A detailed description of the quarter-scale model, instrumentation, data acquisition, and data processing is presented in a proprietary Holtec document [2.A.7]; a concise self-contained summary is provided in the following.

#### 2.A.5.1 Test Plan:

The drop test program was performed at the drop testing facilities at the Oak Ridge National Laboratory. The target at the ORNL facility complies with guidance of IAEA Safety Series 37, Article A-618.

The quarter-scale model testing of the package required the design and fabrication of scale models of AL-STAR, the HI-STAR overpack, and the multi-purpose canister. The quarter-scale replicas of AL-STAR were prepared using the scaling procedure described previously in the context of the 1/8 scale model. In the scale model for the MPC and the overpack, the emphasis is in scaling the weight and moment of inertia, because it is these properties (translational as well as rotational) which are key to the response in the drop event. A schematic of the MPC design used in the scale model is shown in Figure 2.A.5.1. The weight of the MPC replica was set at 1,380 lbs (to simulate an 88,320 lb loaded multi-purpose canister).

The overpack scale model likewise is a cylindrical body whose length and outside diameter are 1/4, whose weight is 1/64, and whose mass moment of inertia is 1/1024 of the respective design parameters in the full-size hardware, as summarized below:

Key Quarter Scale HI-STAR Overpack Model Data			
Length (inch)	O.D. (nominal) (inch)	Overpack Plus MPC Weight (lb.)	Mass Moment of Inertia About a Transverse Centroidal Axis (Overpack Plus MPC) (lb.-in <sup>2</sup> )
50.7813	21	3,733	1.351E+06

Figures 2.A.5.2 through 2.A.5.4 illustrate the principal geometric data of the quarter-scale overpack model. It is evident from the above description that the quarter-scale model is, from a geometrical and inertia standpoint, a quarter-scale emulation of a 84" diameter x 203.125" long, 238,900 lb. (approximate) HI-STAR system (overpack and loaded MPC). Finally, the attachment bolts which join the impact limiter to the overpack are also scaled down to 25% of their size in the full-size hardware (in both diameter and thread engagement length), as can be seen from Figures 2.A.5.3 and 2.A.5.4 or the applicable drawing in Section 1.4.

The one-quarter scale drop tests were performed with four discrete orientations of the cask longitudinal axis with respect to the impact surface, as defined below.

Test A – Vertical Drop (Top End): The cask is dropped such that the deceleration of the cask upon impact is essentially vertical.

Test B: Center of Gravity-Over-Corner (CGOC): For HI-STAR 100, C.G.-over-corner means an orientation wherein the axis of the cask is at 67.5° from the horizontal at the instant of release at the 9-meter height. This test seeks to establish the adequacy of the impact limiter under non-symmetric impact loading.

Test C – Side Drop: The cask is held horizontal with the lowest point on the package 9 meters above the target surface when released for free fall. In this test, both impact limiters participate, and the impact impulse is essentially equally divided between them.

Test D – Slapdown: In this test, the cask axis is held at 15° from the horizontal with the lowest point of the cask assembly at 9 meters from the impact surface. The orientation is such that the top end impact limiter impacts the surface first and the bottom end impact limiter experiences the secondary impact.

Each of the four tests has distinct impact characteristics. For example, in the “side drop” test both impact limiters will strike the target simultaneously; only one impact limiter sustains impact in the “end drop” test. The CGOC test involves a primary impact on one impact limiter at an angle such that the gravity vector is oriented with a line passing through the cask center of gravity and the lowest corner of the limiter. Finally, the slapdown test involves impact at both impact limiters with a very slight time separation. These four tests are deemed to adequately represent the limiting impact scenarios under the hypothetical accident conditions of 10CFR71.73.

The torque values used to secure the attachment bolts in the scale model package warrant special mention. The impact limiter attachment bolts serve two major functions during transportation:

1. During normal transport, the attachment bolts ensure that the impact limiters remain attached to the HI-STAR 100 overpack during a 10g axial deceleration as mandated by 10CFR71.45, and during exposure to normal vibratory loading that may reasonably be expected during the course of a normal transport operation. To ensure against loss of attachment due to vibratory loading during normal transport, an initial bolt pre-stress of 30,000 psi has been set, based on common engineering practice. For the bolt diameters specified for the HI-STAR 100 package, the pre-load torque is 245 ft-lb and 1,500 ft-lb for the top and bottom impact limiter attachment bolts, respectively.
2. During the hypothetical accident, the attachment bolts ensure that the impact limiters remain attached to the HI-STAR 100 overpack during and after the impact with the unyielding surface.

The bottom impact limiter is attached to the overpack by 16 bolts aligned with the longitudinal axis of the overpack and arranged in a circular pattern (Figure 2.A.5.4 shows the bottom view of the one-quarter scale replica). These bolts perform their function by developing tensile stress to resist loading during the hypothetical accident. Because of close clearances with the overpack shielding, the bottom impact limiter also has a set of eight circumferentially arranged alignment

pins that fit into mating holes in the overpack bottom plate. These mating holes are plugged when the impact limiter is not in place.

The top impact limiter is attached to the overpack using twenty radial bolts that are designed to resist relative motion and transfer loads by shear (Figure 2.A.5.3 shows the top view of the one-quarter scale replica).

Although the attachment analyses do not require pre-load (by application of an initial bolt torque) to demonstrate that the required performance during normal transport conditions is achieved, the presence of pre-load serves only to enhance the performance of bolting which resists loads by developing tensile bolt forces (bottom impact limiter attachment bolts). Pre-stress in the bottom impact limiter attachment bolts serves to develop an interfacial pressure between the two components being joined together. This interfacial pressure acts as a reserve against separation at the interface of the impact limiter and the overpack when the external force or moment act to separate them during the drop event. The actual tensile stress bolt will rise significantly over the initial pre-stress if and only if the external load acting to break apart the interface is large enough to cancel out the interfacial pressure.

The effect of pre-load on the performance of bolting that resists loads by shear (top impact limiter attachment bolts) is different. The presence of both tensile stress (due to bolt pre-load) and shear stress in the bolt (due to the impact loads in a drop event) will increase the maximum principal stress in the bolt, which will consequently reduce the shear capacity of the bolts. Applying a pre-load in excess of the required amount in the 1/4 scale HI-STAR 100 drop tests will therefore result in a conservative evaluation of the top impact limiter attachment bolts.

Based on the initial torque values set in the full-scale package, the appropriate bolt pre-load torque for the 1/4-scale impact limiter attachment bolts is (to the nearest foot-pound):

Top impact limiter (radial) bolts: 4 ft-lb. (full scale equivalent = 245 ft.-lb)  
Bottom impact limiter (axial) bolts: 23 ft-lb. (full scale equivalent =1500 ft.-lb.)

Since a bolt pre-load will enhance the performance of bolts (located at the bottom impact limiter interface) that resist loading by developing tensile stress, the bolt torque was conservatively set at 20 ft-lb. or below for the bottom impact limiter bolts. Since a bolt pre-load will degrade the performance of bolts (located at the top impact limiter interface) that resist loading by developing shear stress, the bolt torque was conservatively set at 4 ft-lb. or above for the top impact limiter bolts.

The end drop onto the top impact limiter tests the resistance of the twenty radial attachment bolts against failure from shear. The use of an initial torque value (15 ft-lb.), in excess of 4 ft-lb., is conservative for evaluation of the performance of the bolts to resist shearing strains (i.e., as noted earlier, due to an interaction relation between tension and shear, the presence of any tensile strain will reduce the allowable shear strain prior to failure).

The C.G. over corner drop used an initial torque of 15 ft-lb., a value below the mandated value of 20 ft-lb. on the bottom impact limiter. This is again conservative for the evaluation of the performance of the bottom impact limiter attachment bolts, since the presence of additional prestress would enhance the ability of the bolts to retain the impact limiter in position.

The slapdown test was performed using low initial bolt torque values for both impact limiters that simulated "hand-tight" values. Thus, there is almost no contribution from pre-load on the bolts on either impact limiter. In the slapdown drop, the bottom impact limiter experienced the largest deceleration. This test demonstrated that the use of a lower pre-load on the most highly loaded attachment bolt does not affect the ability of the bolts to perform their required function.

Finally, the final side drop used the bolt pre-loads that correlate with the final bolt pre-loads specified (top impact limiter - 4 ft-lb.; bottom impact limiter - 20 ft-lb.) for the one-quarter scale tests.

A minimum of five calibrated unidirectional accelerometers was installed on the test package for each test. Schematics of the accelerometer locations and numbering system for all four tests are presented in Figures 2.A.5.5 and 2.A.5.6.

The accelerometers are placed at three axial locations along the height of the overpack model and at different circumferential locations at each axial location. The placement of the accelerometers axially reflects locations consistent with the detailed 2-D finite element analyses of the MPC that conservatively neglected the effect of stiffening provided to the MPC shell by the MPC baseplate. Figure 2.A.5.2 shows the three cutouts of the outer 5/8" thick cylinder that are machined flat to position the accelerometers. The following table provides the locations of the accelerometers.

ACCELEROMETER LOCATIONS FOR ONE-QUARTER SCALE DROP TESTS								
NUMBER	TOP END DROP		SIDE DROP		SLAPDOWN		CG-OVER-CORNER	
	Axial (inch)	Peripheral (degrees)	Axial (inch)	Peripheral (degrees)	Axial (inch)	Peripheral (degrees)	Axial (inch)	Peripheral (degrees)
1	44.781	0	5	0	44.781 25	0	5	0
2	25	0	25	0	25	0	5	+120
3	5	0	44.781	0	5	0	5	-120
4	44.781	+120	25	+90	44.781	+120	44.781	0
5	44.781	-120	25	-90	44.781	-120	44.781	+120
6	5	+120	--	--	5	+120	44.781	-120

## Notes:

1. All accelerometer axial distances measured from top end surface of overpack model (without impact limiters in place).
2. Peripheral locations measured from plane containing accelerometer #1; clockwise direction, viewed from Section A-A in Figures 2.A.5.5 and 2.A.5.6, is positive.

In addition to recording the deceleration during impact, a high-speed camera and a video camera were used to record the test events. The high-speed camera was used to confirm orientation angles just prior to impact and to aid in the evaluation of extent of crush subsequent to the test. The tests were conducted by attaching the ¼ scale package to a 15-ton mobile crane through appropriate rigging and lifting the package to the required height. An electronically activated guillotine-type cable cutter device was used for releasing the package for free fall. An array of photographs labelled Figures 2.A.5.7 through 2.A.5.13 provide pre-test and post-test visuals of the package. These photographs show quite clearly that the post-crush impact limiters maintained their own physical integrity and the attachments to the overpack scale model suffered no failures.

The following acceptance criteria for the scale model dynamic drop tests were identified in the Test Plan [2.A.11]:

- Filtered decelerations limited to a maximum of 60g's (after scaling to full-scale geometry) for all drop orientations.
- No impact of the cask body on the target surface.
- No separation of impact limiters from the cask body through the entire drop event.

#### 2.A.5.2 Results of First Series of Drop Tests

The first series of three one-quarter scale drop tests (types A, B, and C denoted above) were performed in August 1997 and produced significant information [2.A.5]. Table 2.A.1 shows the maximum filtered decelerations registered in the three one-quarter scale tests after the test results are scaled up to the full-scale AL-STAR (by dividing test results by four).

Table 2.A.1: Peak Decelerations from August 1997 Tests

Test I.D.	Orientation	Deceleration (g)
A.	End Drop	134
B.	C.G.-Over-Corner	37.84
C.	Side Drop	51.3

The peak filtered deceleration in the first end-drop test was clearly above the 60g-design limit established for the HI-STAR 100 design. The reasons for this discrepancy were determined to be the use of a low value of the dynamic multiplier assumed in designing the impact limiter, and the lack of pre-crush of the honeycomb material. Numerical analyses also indicated that the honeycomb compression modulus was dependent on the impact limiter velocity during the drops. This confirms laboratory data available in the historical literature [2.A.9]. The velocity and deceleration information obtained from the first round dynamic drop tests enabled development of a simple dynamic correlation multiplier to be applied to the honeycomb material's static F-d behavior. This multiplier is an additional "experimentally based" input term in the computer prediction model for simulation of dynamic drop events [2.A.6]. Data from the initial test series shows that this multiplier is independent of test orientation and is a function of the ratio of crush velocity during the crushing process divided by the impact velocity at the initiation of crush. Based on the numerical analysis of the August 1997 tests, the honeycomb material was appropriately revised with new crush strengths and new sets of ¼ scale model impact limiters were manufactured. The correlation of the August 1997 quarter-scale tests with the numerical results from the computer model is presented in section 2.A.6.

In summary, the chief contribution of the August tests, therefore, lay in providing the database to quantify the crushing characteristic of the honeycomb material under dynamic conditions [2.A.6]. Since none of these tests is ascribed to confirmation of the final performance of the AL-STAR impact limiters, no accelerometer raw or filtered results are included herein. The full set of acceleration data (both raw and filtered) is provided in [2.A.5].

### 2.A.5.3 Results of the Second Series of Drop Tests

The second round of one-quarter scale dynamic drop tests, conducted in December 1997 and February 1998, using the new (lower crush strength) impact limiter materials, occurred in three phases. The first phase consisted of the top end drop, CGOC drop, and side drop tests. While the decelerations in all cases were within the design limit, the attachment system for the bottom impact limiter did not survive the side drop test. The attachment system was redesigned prior to the remaining (slapdown) test. The slapdown test is considered to be the most definitive test of the cask/impact limiter attachment integrity. The slapdown test was successfully completed, with the bottom impact limiter remaining in place during and after the secondary impact, on December 29, 1997 in Phase 2 of the second test series. In order to confirm the adequacy of the attachment system under side drop conditions, the side drop test was repeated in February 1998 during Phase 3. This test reconfirmed the attachment system integrity.

The results from the second round test series demonstrates that the HI-STAR 100 package meets all test acceptance criteria, namely:

- Appropriately filtered decelerations of less than 60g's (after appropriate scaling to reflect the full-size mass and geometry) for all tested orientations;
- All attachment bolts remained intact, ensuring that the impact limiters do not separate from the cask body through and after the drop event;
- No impact of the cask body on the target surface.

Figures 2.A.5.14 through 2.A.5.21, drawn from reference 2.A.7, provide the raw (unfiltered) and filtered deceleration time-histories for each of the four drop scenarios for the key accelerometers used to assess package performance. The accelerometer station numbers indicated in these accelerograms are located by referring to Figures 2.A.5.5 or 2.A.5.6, as applicable. The test report [2.A.7] provides the necessary background to justify the use of this data to evaluate package performance. The following remarks are pertinent concerning the results presented in Figures 2.A.5.14 through 2.A.5.21.

#### End Drop Decelerations (Figures 2.A.5.14, 2.A.5.15, and 2.A.5.15a-c)

All accelerometers for this test recorded decelerations in the direction of crush. Two accelerometers were subsequently determined to be defective (documented in [2.A.7]). The figures show the raw, the filtered response at 450Hz cut-off frequency, and a combined plot of the raw and filtered data covering a reduced time period. All of these results are obtained from the records from the working accelerometers. All working accelerometers gave essentially identical response; the final evaluation of performance presented herein is the average of the response from the accelerometers deemed to be recording correctly. Figures 2.A.5.15b and 2.A.5.15c demonstrate that the sensitivity to cut-off filter frequency is small even up to 1250Hz.

#### Center of Gravity Over Corner Decelerations (Figures 2.A.5.16, 2.A.5.17, and 2.A.5.17a)

The CGOC test was performed immediately after the end drop using the same set of accelerometers. The evaluation of the data after this test clearly determined that the same two accelerometers deemed suspect in the end drop test was also providing erroneous data here. Subsequent independent plate impact tests that definitively showed that these accelerometers were indeed faulty are documented in [2.A.7]. The acceleration data in the figures represents the vertical acceleration obtained by appropriate combination of the raw time data from the longitudinal and lateral mounted accelerometers on the inclined scale model cask. The raw vertical accelerations were then subject to filtering to remove non-rigid body behavior. Raw, filtered, and combined raw and filtered data over the strong response time period are presented.

## Slap Down Decelerations (Figures 2.A.5.18, 2.A.5.19, and 2.A.5.19a)

Although the initial release of the package was at an angle of 15 degrees from the horizontal, the high-speed camera showed that impact occurred with the overpack longitudinal axis at an angle of 7.2 degrees from the horizontal. The numerical simulation of this test reflected the actual angle of impact rather than the initial setting at nine meters. The results for all accelerometers (raw data and filtered) are provided in [2.A.7]. The raw and filtered data presented in the figures here represent the deceleration at the bottom end of the package that experiences the larger magnitude secondary impact. Numerical analysis demonstrated that the peak deceleration from secondary impact is insensitive to impact angles between 5 and 12 degrees from the horizontal and decreases as the angle increases above 12 degrees. Raw, filtered, and combined raw and filtered data over the strong response time period are presented.

## Side Drop Decelerations (Figures 2.A.5.20, 2.A.5.21, and 2.A.5.21a)

Both impact limiters are supposed to impact the target simultaneously in this test. An evaluation of the individual accelerometer data and an examination of the high-speed camera film clearly indicated that there was a small angle existing between the overpack longitudinal axis and the target horizontal surface at the moment of impact. This caused the expected result that accelerometer readings at one end of the package were slightly higher than readings at the other end. The results for raw and filtered data represent results obtained by averaging the data from the accelerometers at the ends of the package. Raw, filtered, and combined raw and filtered data over the strong response time period are presented.

The filter frequency used for the End Drop and CGOC Drop is 450 Hz. The filter frequency used for the Slap Down and Side Drops was 350 Hz. These filter frequencies were established by examination of the power spectral density function for each raw data trace that clearly showed that the majority of the energy occurred at frequencies well below the cut-off frequency. Independent confirmation of the appropriateness of the cut-off frequencies was made by determining the lowest frequency of elastic vibration of the package acting as either a bar or a simply supported beam. As described above, the sensitivity to cut-off frequency was examined for the end drop case by re-analyzing the data for three cut-off frequencies.

Table 2.A.2 provides the peak deceleration data culled from the above-mentioned accelograms for the four drop scenarios after filtering to remove high frequency effects. The table contains the results from the actual 1/4-scale experiments scaled up to the full-size packaging. The test report [2.A.7] provides the detailed information on this final one-quarter scale dynamic drop test series with raw and filtered outputs from all accelerometers. The test report also includes details on the filtering methodology, on the data reduction, and on the evaluation of the performance of the various accelerometers used in each of the tests.

In all of the four final one-quarter scale dynamic drop tests, the impact limiter attachments successfully performed without a single attachment bolt failure (ensuring that the impact limiters did not separate from the overpack), rigid body decelerations were below 60 g's, and the cask body did not contact the unyielding target surface. Also, additional crush margin remained in the aluminum honeycomb material.

Table 2.A.2: Peak Decelerations from AL-STAR™ Drop Tests (Second Series)

Test Case	Orientation	Peak Decelerations (g)
A	End-Drop	53.9
B	C.G.-over-Corner	38.8
C	Side Drop	45.7
D	Slap-Down	59

#### 2.A.6 Phase 5: Numerical Prediction Model for Dynamic Analysis

The numerical prediction model for dynamic drop events utilizes the previously discussed force-crush (F-d) model and incorporates the information into the dynamic equations of equilibrium. Using the procedure discussed previously, the static F-d curves for the AL-STAR impact limiter under the four drop scenarios are readily constructed. Figures 2.A.6.1 to 2.A.6.4, respectively, provide the static force vs. crush plots for the full scale impact limiter with test orientations for drop cases A, B, C, and D (primary impact). An appropriate analytical fit for each curve is developed using the commercial graphing package Deltagraph [2.A.8]. Figures 2.A.6.1 through 2.A.6.4 also provide curves for upper and lower bound material strengths.

We now discuss the application of the F-d model to the prediction of impact limiter performance in a dynamic drop environment. In symbolic form, we can write the static resistive (crush) force,  $F$ , as a function of the crush depth,  $\Delta$ , where a zero value for  $\Delta$  represents an uncrushed condition.

$$F = f(\Delta)$$

The above symbolic formula represents the data on Figures 2.A.6.1 to 2.A.6.4 in analytical form. We have previously explicitly discussed the mathematical concepts underlying the above formulation by referencing the particular case of a side drop. In general, the static F-d curve can be expressed as a sum of local crush pressures multiplied by interface areas where the interface areas may be a function of the current crush. That is, the mathematical relation for static compression (which is validated by comparison to static testing) is also expressible in the form

$$f(\Delta) = \sum_i p_i A_i$$

where  $p_i$  are the crush pressures of the materials participating in the crush and  $A_i$  are the interface areas associated with the different crush strengths. The determination of the areas  $A_i$  as a function of crush depth,  $\Delta$ , has previously been discussed within the context of interpenetration.

The dynamic model for simulating a packaging drop event consists of solving the classical Newtonian equations of motion. In the case of a unidirectional impact such as an end drop ( $\theta=90^\circ$ ), side drop ( $\theta=0$ ), or CGOC drop, the equation of motion simply reduces to:

$$M \frac{d^2 \Delta}{dt^2} = \text{Force} + Mg$$

where:  $M$  = mass of system undergoing deceleration

$d^2\Delta/dt^2$  = second derivative of package movement (which is equal to the impact limiter crush because the target is immovable and rigid).

The resistive “Force” opposes the downward movement and is given by the static force-crush functional relationship (appropriate for the drop orientation) multiplied by a dynamic multiplier  $Z$ . As noted earlier, there is historical evidence that metal honeycomb crush pressure is a linear function of velocity [2.A.9]. The Holtec correlation of the August 1997 test data by numerical simulation [2.A.6] also confirmed that the best correlation is achieved if the dynamic multiplier is represented by a linear function of local crush velocity ( $d\Delta/dt$ ). Introducing the dynamic multiplier, the dynamic equation of force equilibrium for a case involving only primary impacts becomes

$$M \frac{d^2 \Delta}{dt^2} = ZF + Mg = Zf(\Delta) + Mg$$

The above equation is a second order non-linear differential equation in the time coordinate  $t$ , which can be solved for the post-contact event using any standard equation solver package. The initial condition is: @  $t = 0$ ,  $\Delta = 0$ ,  $d\Delta/dt = V_o$  (approach velocity at impact). We note that since the acceleration is an explicit function of both deformation and velocity, maximum acceleration will not, in general, occur at the instant when the velocity of the package is zero.

If the impact event involves both primary and secondary impacts, as is the case for the slapdown event (indeed any event wherein  $\theta < 67.5^\circ$ ), then both the mass  $M$  and rotational moment of inertia  $I$  are involved. The modeling of a dual impact event is only slightly more involved than

the single variable modeling of the single impact case discussed above. Figure 2.A.6.5 pictorially illustrates the sequence of events leading to an appropriate mathematical model. Figure 2.A.6.6 provides the appropriate free-body diagrams associated with each portion of the event.

In the first step, the inertia force of the falling package is resisted by the crush force developed at the primary impact location. While the downward momentum of the package is dissipated by the resistive force, the package also experiences the overturning couple produced by the non-collinearity of the inertia force (which acts at the centroid) and the resistive force which acts at the primary impact zone (Figure 2.A.6.5(a)). The dynamic equation of force equilibrium is given above in terms of the downward movement of the package centroid and the resistive force static compression curve, modified by the dynamic factor  $Z$ , appropriate to the initial orientation at primary impact. The package decelerates and then begins to overturn, in effect pivoting about the initial point of contact in the primary impact region, gathering angular momentum as the second impact limiter (mounted at the far end) approaches the target surface. Referring to Figure 2.A.6.5(b), the dynamic equation insuring moment equilibrium during the overturning (before the initiation of the secondary impact) phase can be written as

$$I_p \frac{d^2\phi}{dt^2} = -MgR \cos(\phi)$$

where  $I_p$ : moment of inertia of the package about the pivot point  
 $\phi$  : angular acceleration with respect to the horizontal plane  
 $R$ : radial distance of the package C.G. with respect to the pivot point.

The initial conditions for this phase are:  $t = 0$ ,  $\phi = \theta$ ,  $d\phi/dt = 0$  where  $t$  is now redefined at the initiation of rotational motion.

Finally, the secondary impact commences wherein the angular momentum of the package plus any linear momentum not dissipated by the primary impact is dissipated by the crushing of the second impact limiter. During the secondary impact phase, the equation of dynamic moment equilibrium can be written by inspection of Figure 2.A.6.5(c):

$$I_p \frac{d^2\phi}{dt^2} = -MgR \cos(\phi) + Zf(D\phi)D$$

where  $f(D\phi)$  is the static resistive force at the secondary impact location under compression  $D\phi$ ,  $Z$  is the current dynamic multiplier appropriate to the secondary impact location,  $D$  is the moment arm, and  $I_p$  is the moment of inertia of the package about the pivot point. During this phase of the motion, the equation of dynamic force equilibrium is modified to reflect dynamic resistive forces from both impact limiters since the entire package may continue to move toward

the target surface with both impact limiters providing a dynamic resistive force. Therefore, during the final phase of the impact event, the dynamic force equilibrium equation can be written as

$$M \frac{d^2 \Delta}{dt^2} = Z_1 F_1 + Z_2 F_2 + Mg$$

where  $Z_i$  and  $F_i$  ( $i=1,2$ ) represent the dynamic multiplier and static compression force appropriate to the primary and secondary impact limiter behavior during the final phase of the event. The dynamic multipliers  $Z_i$  ( $i=1,2$ ) reflect the current value of the local crush velocities at each of the limiters.

The above formulation assumes, for simplicity, that the pivot point does not slide during the overturning or secondary impact phases.

It is evident from the foregoing that the impact limiter is essentially simulated by a non-linear spring whose static force-deformation curve is known a priori (from the F-d model) as a function of the drop orientation. The solution of this rigid body dynamics problem featuring up to two non-linear springs can be determined using any one of several standard software packages available in the public domain. Holtec International utilizes the commercial package WORKING MODEL [2.A.10], which has been validated in the company's QA system for this purpose.

The dynamic simulation model, constructed in the manner of the foregoing, was utilized to simulate all seven one-quarter scale drop events (three in the first series, four in the second series). In order to develop a high level of confidence, it was decided that the model should be validated at all three levels, namely, a comparison of acceleration, crush, and duration of impact. In other words, to be acceptable, the numerical prediction model must predict  $\alpha_{\max}$ , maximum crush sustained  $d_{\max}$ , and the duration of impact, with reasonable accuracy. Since the actual crush  $d_{\max}$  could be measured, and the duration of impact and  $\alpha_{\max}$  were available from accelerometer data, comparison between theory and experiment with respect to all three key indicators was possible. Tables 2.A.3 and 2.A.4 provide the results in a concise form for all of the one-quarter scale dynamic drop tests for the first and second series, respectively.

Note that in the tables, the comparison is made after scaling up the model results to reflect a full-scale package.

Table 2.A.3: Comparison Between Test Data and Prediction Model Results (First Test Series)

Case I.D.	Deceleration (g's)		Total Crush Depth (inch)		Impact Duration (milli-seconds)	
	Predicted	Measured	Predicted	Measured	Predicted	Measured
A. End-Drop	134.2	134.0	2.42	2.42	3.5	Not measured
B. C.G.O.C.	37.8	37.84	16	16	13.25	16.6
C. Side Drop	50.5	51.3	9.1	9.51	8.25	10.74

Table 2.A.4: Comparison Between Test Data and Prediction Model Results (Second Test Series)

Case I.D.	Deceleration (g's)		Total Crush Depth (inch)			Impact Duration (milli-seconds)	
	Predicted	Measured	Predicted	Measured	Max. Available	Predicted	Measured
A. End Drop	53.0	53.9	11.3	10.6	17.659	38.8	37.2
B. C.G.-Over-Corner	38.7	38.8	12*	9.82*	25.06	51.0	61/45.2
C. Side Drop	43.5	45.7	10.9	12.5	16	38.5	53.1 (averaged value)
D. Slap-Down							
Primary	46.4	49.0	9.50	10.7	16	48.5	44.4
Secondary	59.9	59.0	12.8	13.5	16	35.8	41.2

\* For C.G.-Over-Corner, only crush at the external interface is measured.

It is evident from both Tables 2.A.3 and 2.A.4 that the numerical prediction model is robust in predicting all seven impact tests. Not only are peak values of  $\alpha_{max}$  for each test predicted with good agreement, but also the crush depth and impact duration is also reliably simulated.

A perusal of the numerical results in Table 2.A.4 yields two additional insights into the behavior of AL-STAR which are most helpful in the “fine tuning” of the full-scale AL-STAR design:

- i. The maximum deceleration,  $\alpha_{max}$ , predicted as well as measured, under the most limiting scenario (slapdown), is close to the permissible limit of 60g's.
- ii. The maximum crush, predicted as well as measured, in all drop scenarios, is well below the available limit (i.e., the value at which the crush material will “lock up”).

The state-of-the-art manufacturing technology for aluminum honeycombs permits the material to be manufactured within a total tolerance range of 12 to 13% (between the maximum and minimum values). The above observations suggest that the upper and lower bound range of crush pressures for the honeycomb material in the AL-STAR impact limiter should be set at 95% and 82% of the values of honeycomb material used in the second series quarter-scale tests.

Finally, the agreement between the predictions and measured data in the above correlation effort fosters a high level of confidence in the numerical model, which can now be used to conduct sensitivity studies.

#### 2.A.7 Phase 6: Simulation of the Effects of Material Crush Strength Variation, Package Mass Tolerances, and Oblique Drop Orientations

Having ensured the technical reliability of the numerical prediction model, it is now necessary to evaluate the system behavior under all "limiting conditions". As noted earlier, the impact limiter materials are insensitive to environmental temperature changes within the limits of  $-20^{\circ}$  F and  $100^{\circ}$  F. Therefore, limiting conditions are broadly defined here as arising from two sources:

- i. Variation in the impact limiter honeycomb crush strength due to material manufacturing tolerance.
- ii. Variation in the package weight (due to different MPC types that may be transported in the HI-STAR 100 overpack, and manufacturing tolerances in fabrication of the overpack and impact limiters).
- iii. Variation in package angle of impact with the target.

To examine all limiting scenarios, additional simulations using the mathematical model were performed. The crush strength of the honeycomb material was varied within the range permitted in the Holtec Drawing 1765. The packaging weight was set at its upper bound and lower bound value (upper bound weight is 280,000 lb., and lower bound weight is 270,000 lb. based on values listed in Table 2.2.1). Three additional drop orientations (30 degree, 45 degree, and 60 degree orientation angle, measured from the horizontal) that were not the subject of tests were also analyzed numerically using input crush strength data that would maximize the decelerations with an average weight. The purpose of these additional simulations with varied drop angle is to ascertain which, if any, oblique drop orientation merits detailed finite element stress analysis to meet the requirements of the Regulatory Guide. Figures 2.A.7.1-2.A.7.3 provide the static crush force vs. crush depth information used in the dynamic simulation of these accident events. Table 2.A.5 provides key output data, peak decelerations and maximum crush, as obtained from these numerical simulations.

Table 2.A.5: Sensitivity of Package Response to Package Weight, Crush Material Strength Variations, and Package Orientation at Impact

Orientation	Case	Deceleration (g's)	Maximum Total Crush (2-interfaces) (inch)	Available Crush Stroke (inch)
End Drop	Max. Strength, Min. Weight	52.85	11.4	17.659
	Min. Strength, Max. Weight	46.3	12.8	17.659
C.G. Over Corner	Max. Strength, Min. Weight	38.25	17.0	25.06
	Min. Strength, Max. Weight	35.6	18.5	25.06
Side Drop	Max. Strength, Min. Weight	42.5	11.2	16
	Min. Strength, Max. Weight	37.5	12.7	16
Slap Down (secondary impact bounds)	Max. Strength, Min. Weight	58.5	13.2	16
	Min. Strength, Max. Weight	52.6	15.1	16
Oblique Drop – 30 degrees	Max. Strength, Min. Weight	36.44	19.57	24.1
Oblique Drop – 45 degrees	Max. Strength, Min. Weight	35.62	22.39	25.72
Oblique Drop – 60 degrees	Max. Strength, Min. Weight	38.01	19.2	25.65

The following conclusions are readily derived from Table 2.A.5 results:

- i. The maximum value of  $\alpha_{\max}$  is less than 60g's in all cases.
- ii. The total crush of the impact limiter is below the available "stroke", i.e., the overpack body will not contact the unyielding target surface nor will any "lock-up" of the crush material occur.
- iii. The three oblique drop simulations considered all produce approximately the same vertical deceleration from the primary impact. The decelerations resulting from the subsequent secondary impact, after rotation of the HI-STAR 100, are all below the value obtained from the simulation of the "slapdown" at low angles of

impact. If the “limiting” oblique drop is considered as the simulation providing maximum deceleration perpendicular to the longitudinal axis of the cask, then the drop most likely to develop the largest bending of the overpack in the oblique orientation is at 30 degree orientation (from the horizontal axis). Therefore, this case is subjected to detailed stress analysis in Section 2.7 with the applied impact loading (along and perpendicular to the cask axis) balanced solely by the cask inertia forces and moments.

In conclusion, the above work provides full confidence that the HI-STAR 100 packaging will perform in the manner set forth in the NRC regulations (10CFR71.73) under all conceivable hypothetical accident conditions of transport.

#### 2.A.8 One-Foot Drop

Paragraph 2.6 of Reg. Guide 7.8 requires evaluation of the package response under a one-foot drop onto a flat unyielding surface in a position that is expected to inflict maximum damage.

Using the prediction model, the maximum deceleration sustained by the package under the one-foot end and side drop scenarios, the latter expected to produce maximum stress in the fuel basket, was computed. Table 2.A.6 provides summary results for the limiting case of minimum package weight and upper bound material crush strength (so as to maximize the decelerations).

Table 2.A.6: Peak Decelerations Under One-Foot Drop Event

Scenario	Max. Deceleration in g's	Crush (inch)	Duration of Impact (milli-seconds)
90° End Drop	17.25	0.85	20.0
0° Side Drop	11.45	1.33	26.0

#### 2.A.9 Equivalent Dynamic Factor (EDF)

It is instructive to compute an effective equivalent dynamic factor on the predicted static crush force corresponding to the instant of maximum deceleration during the drop event. Table 2.A.7 presents the pseudo-deceleration (obtained by dividing the static force by the mass of the package) and the predicted deceleration; the ratio of the two is the “equivalent dynamic factor” (EDF). The EDF is also equal to the peak dynamic crush force divided by the static resistance force at the coincident instance of crush when the dynamic crush force is maximized. Note that the differences in package weight used in the table below reflect the actual weight of the impact limiters used in each one-quarter scale drop test (after increasing to full-scale equivalent values).

Table 2.A.7: Equivalent Dynamic Factor (EDF) for Different Drop Scenarios

Scenario	Predicted Force (lbs) $\times 10^{-7}$		Participating Package Weight (lbs)	Predicted Max. Deceleration		EDF
	Static	Dynamic		Pseudo- Accn (static)	Dynamic (from Table 2.A.4)	
End Drop	1.0785	1.454	274,336	39.313	53	1.348
CGOC Drop	0.8	1.059	273,680	29.231	38.7	1.324
Side Drop	0.4	0.597	137,270*	29.14	43.5	1.493
Slapdown	0.345	0.6607	†	†	59.9	1.915

\* Only half of the total package weight participates at each impact limiter.

† Indeterminate for this drop configuration.

The last column of the above table demonstrates that the EDF, as defined above, is not a constant value independent of drop orientation.

#### 2.A.10 Additional 1/8<sup>th</sup> Scale Static Tests

Three additional static crush tests on 1/8<sup>th</sup> scale impact limiters have been performed subsequent to the completion of all quarter-scale dynamic testing and theoretical correlation. The F-d test results for each of three impact limiter orientations are compared with the analytical F-d predictions in Figures 2.A.10.1-2.A.10.3. Figure 2.A.10.1 compares test results with theoretical prediction for the crush orientation corresponding to a side impact, Figure 2.A.10.2 presents the results for the Center-of-Gravity-Over-Corner impact orientation, and Figure 2.A.10.3 presents results for the end impact orientation. In all tests, the crush material orientation and location duplicated the final configurations subjected to quarter-scale tests. The internal backbone structure was also faithfully reproduced. The welds were also scaled to the extent practical given the thin material gages used for the one-eighth-scale model. In the three figures, the solid line without symbols represents the predictions of the theory developed for the F-d curves, while filled circles represent test results. Within the range tested for each orientation, good agreement is observed between theory and test for the side and CGOC crush orientation. For the end drop orientation, however, the tested results suggest that inclusion of some elastic behavior at the cask-impact limiter interface into the theory might improve the static correlation. The dynamic test results presented in Table 2.A.4, however, demonstrate conclusively that the prediction of peak deceleration, extent of crush, and impact duration would not be affected by these elastic effects that “smooth” the abrupt “staircase” shape of the F-d curve.

### 2.A.11 Conclusions

The AL-STAR impact limiter design was subjected to a series of static and dynamic tests to validate its functional performance. The 1/8 model static tests conducted under cold and hot, as well as ambient conditions, confirmed that AL-STAR's functional characteristics are independent of the environmental temperature conditions in the range specified in 10CFR71.73. The successful static tests on the 1/8 scale model (namely, end test and 60° oblique test) also correlated well with the theoretical force-crush model developed by Holtec. Subsequent static tests, performed after the final successful one-quarter scale dynamic tests, provided additional confirmation of the validity of the fundamental F-d model.

The static compression tests were followed by quarter-scale drop tests. The first series, in August 1997, consisting of three tests, provided the necessary test data to determine the dynamic multiplier applicable to the honeycomb materials. The numerical model for simulating the dynamic crushing of AL-STAR showed good agreement with the first test series data when the correct dynamic factor was incorporated in the computer model (Table 2.A.3).

While the prediction model for simulating AL-STAR crushing under 9-meter drop conditions was extremely well correlated, the peak deceleration under the end- drop condition in the August 1997 tests exceeded the acceptance criteria.

The second series of tests wherein the crush strength of the honeycomb was lowered (as selected by the prediction model), performed as expected. The agreement between the test data and the prediction model is high (Table 2.A.4).

The prediction model for AL-STAR therefore stands correlated with seven (7) quarter-scale drop events. The first three tests used different honeycomb crush strength materials than the last four, proving the ability of the prediction model to predict the AL-STAR crush performance for a wide range of crush material properties. The backbone structure of AL-STAR, enhanced after the 1/8-model static compression tests, performed as designed in all seven quarter-scale drop tests.

Finally, the AL-STAR-to-overpack attachment system remained intact and the cask did not contact the unyielding target during all four final dynamic tests.

2.A.12 References

- [2.A.1] ANSYS 5.3 Ansys Inc., 1996.
- [2.A.2] CADKEY, Version 7, 1996.
- [2.A.3] Project Procedure No. HPP-5014-5, HI-STAR Aluminum Honeycomb 1/8 Scale Impact Limiter Static Test Procedure.
- [2.A.4] HI-STAR 1/8 Scale Impact Limiter Test Report, HI-961501, Holtec International, June 1996.
- [2.A.5] Holtec Report HI-971774, Revision 1, "Impact Limiter Test Results – 30' Drop Tests" – August 1997
- [2.A.6] Holtec Report HI-971823, Revision 0, "Improved Correlation of ORNL 30' Drop Tests" – August 1997
- [2.A.7] Holtec Report HI-981891, Revision 3, "Impact Limiter Test Report - Second Series", 2007.
- [2.A.8] Deltagraph Pro 3.5, Deltapoint Software, 1995.
- [2.A.9] J.M. Lewallen and E.A. Ripperger, Energy Dissipating Characteristics of Trussgrid Aluminum Honeycomb, SMRL RM-5, University of Texas Structural Mechanics Research Laboratory, 1962.
- [2.A.10] Working Model 3.0, Knowledge Revolution, 1995.
- [2.A.11] HI-STAR 100 Impact Limiter Test Program, Holtec Report No. HI-951278.

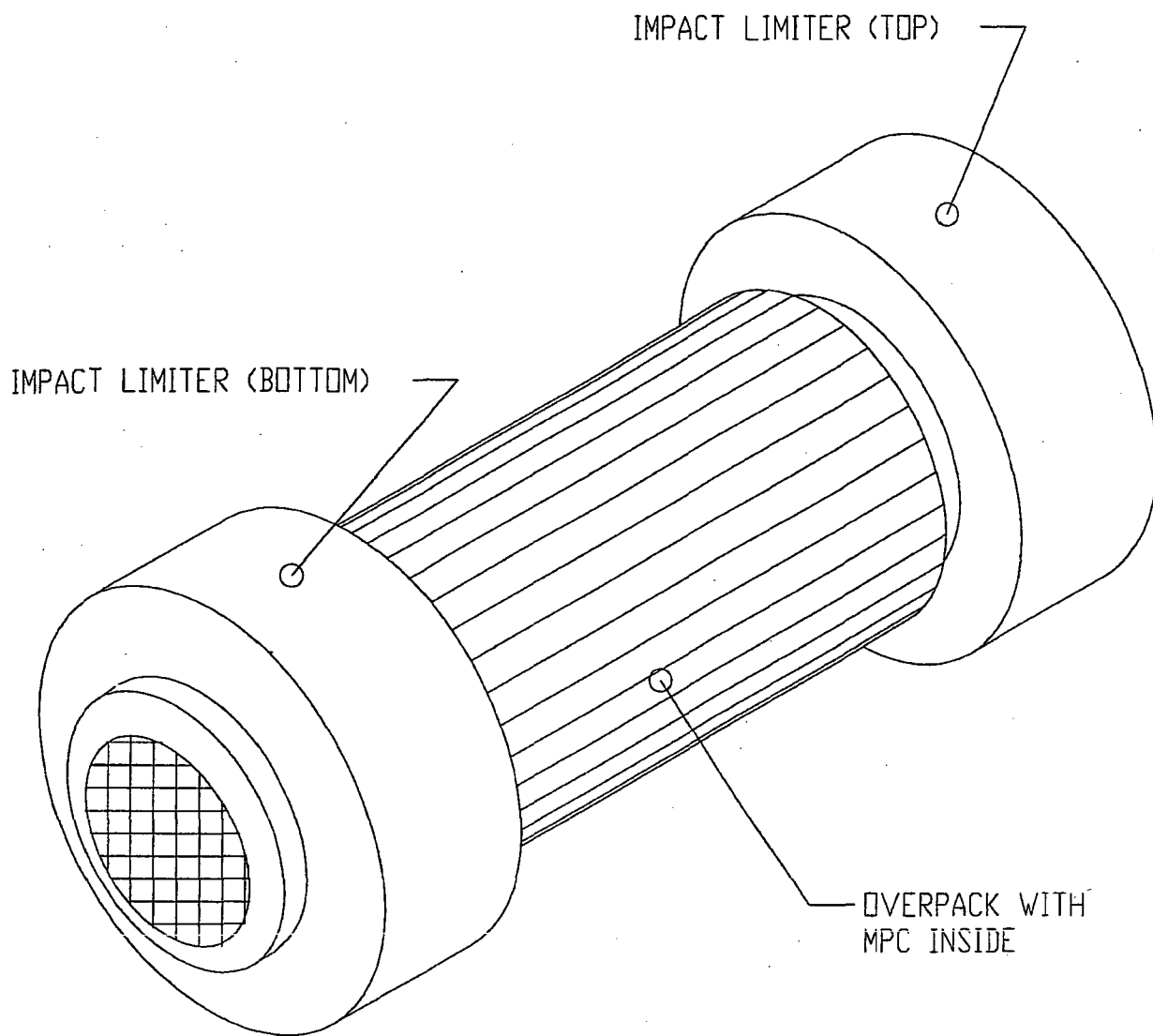


FIGURE 2.A.1.1; HI-STAR 100 PACKAGE WITH TOP AND BOTTOM IMPACT LIMITERS

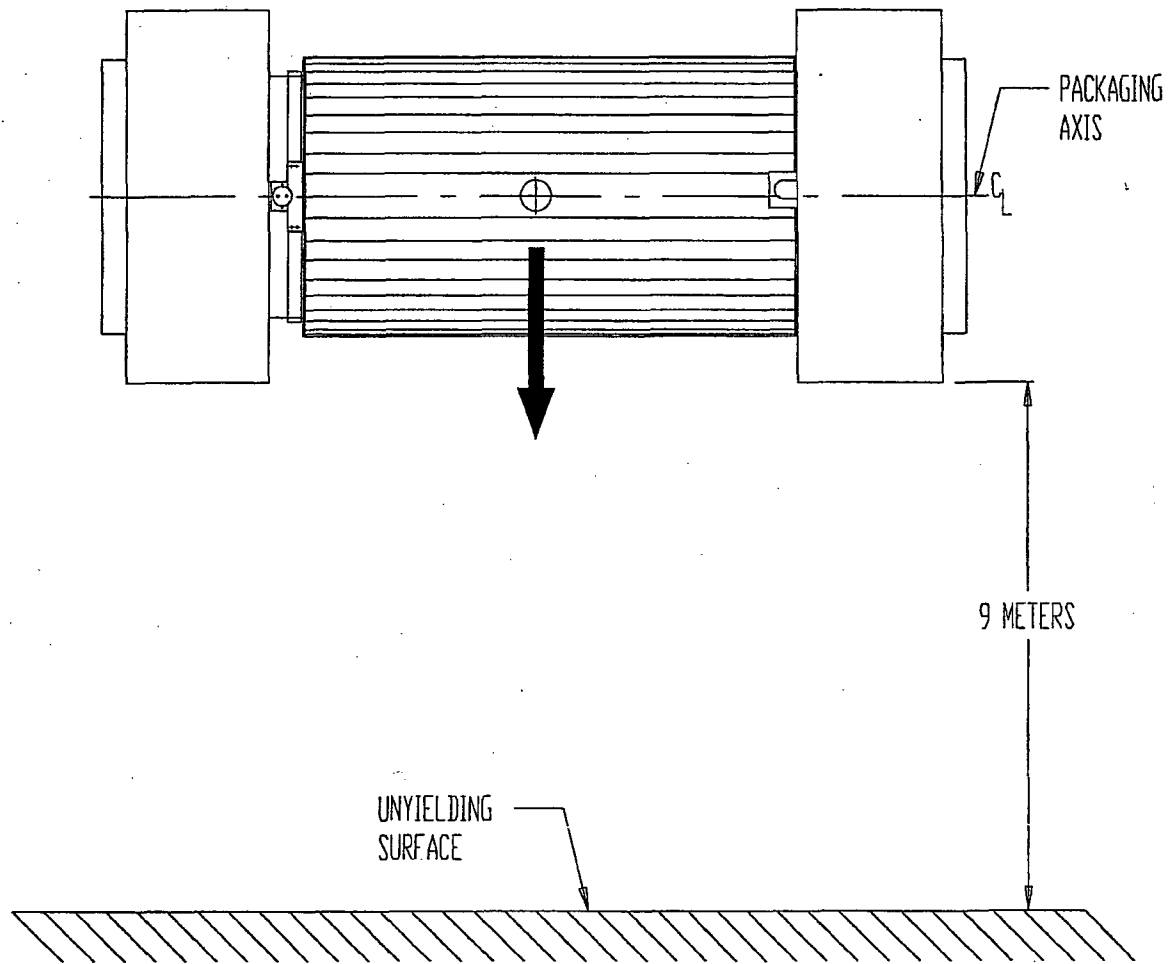


FIGURE 2.A.1.2; DROP FROM 9 METERS ON TO AN ESSENTIALLY UNYIELDING SURFACE (HYPOTHETICAL ACCIDENT CONDITION)

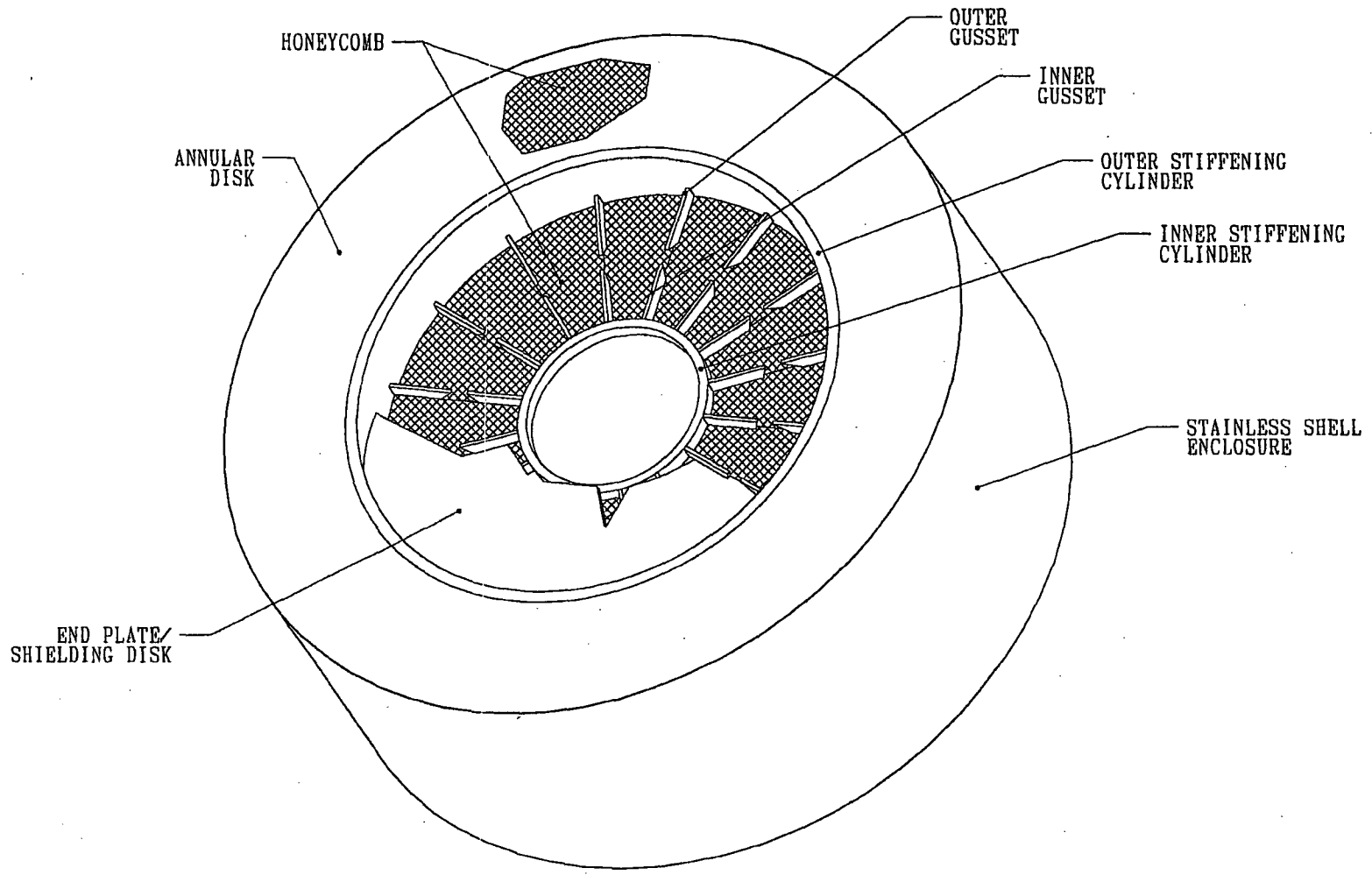


FIGURE 2.A.1.3; PICTORIAL VIEW OF AL-STAR  
(WITH A PORTION REMOVED)

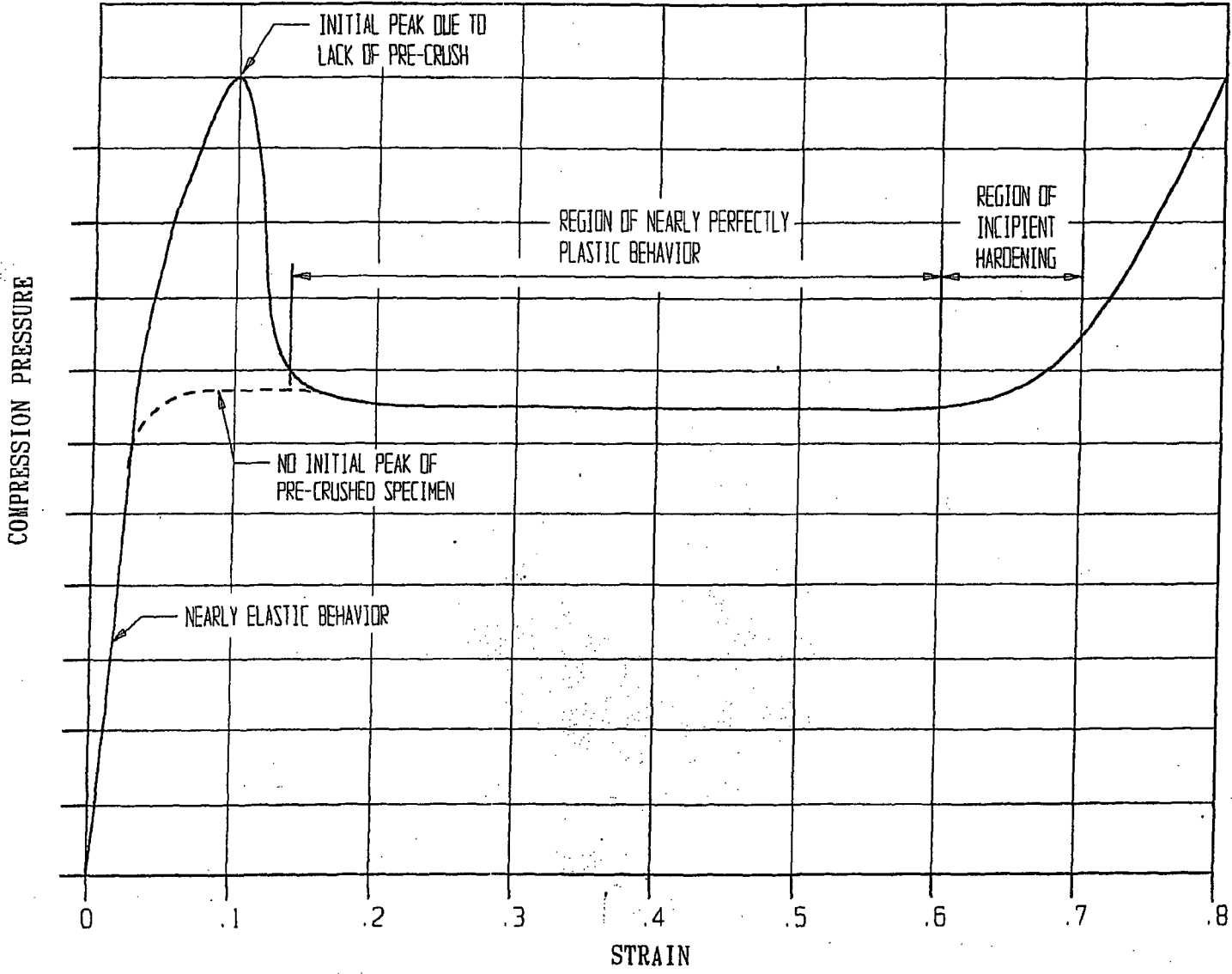
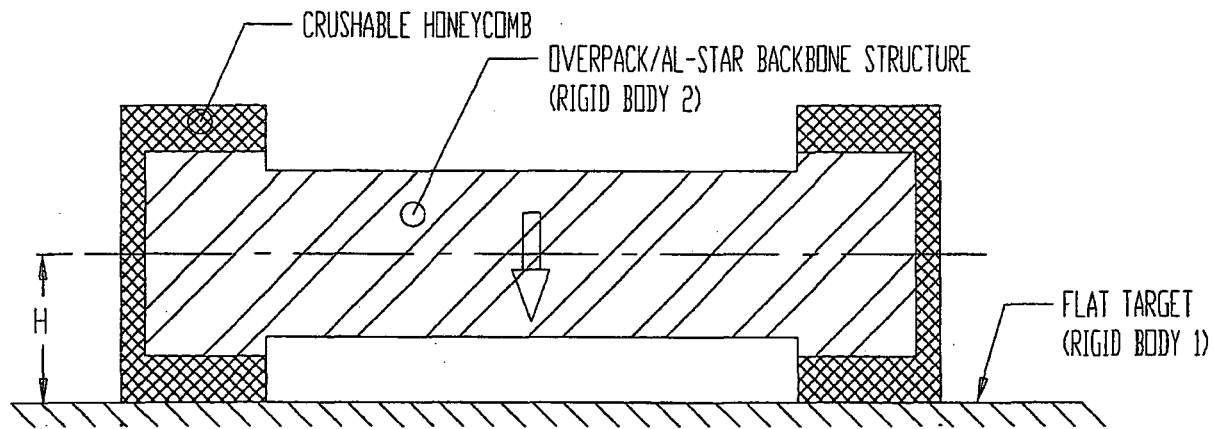


FIGURE 2.A.2.1; PRESSURE-CRUSH STRAIN CURVE (STATIC TESTING)

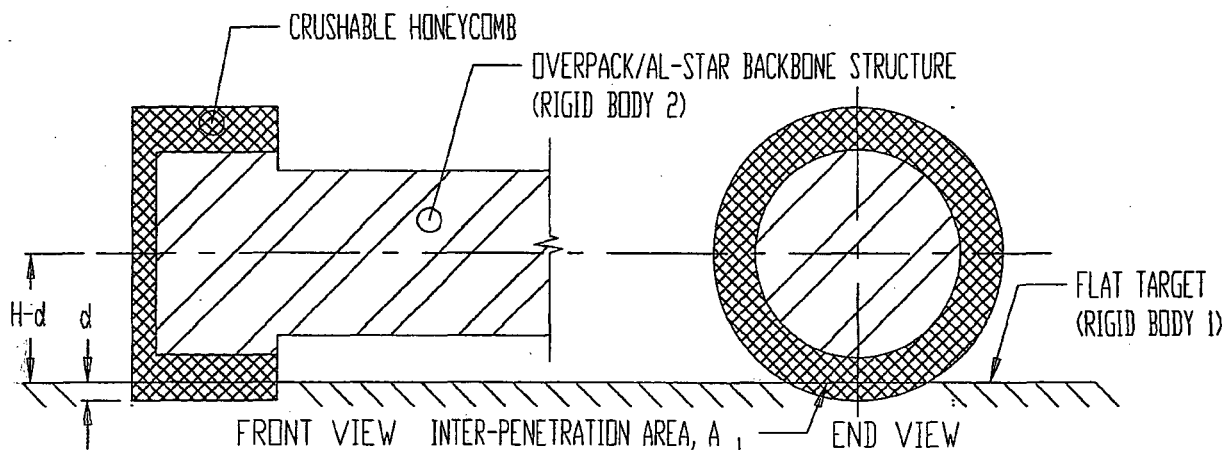
REPORT HI-951251

REVISION 16  
5014\HI951251\2\_H\_2

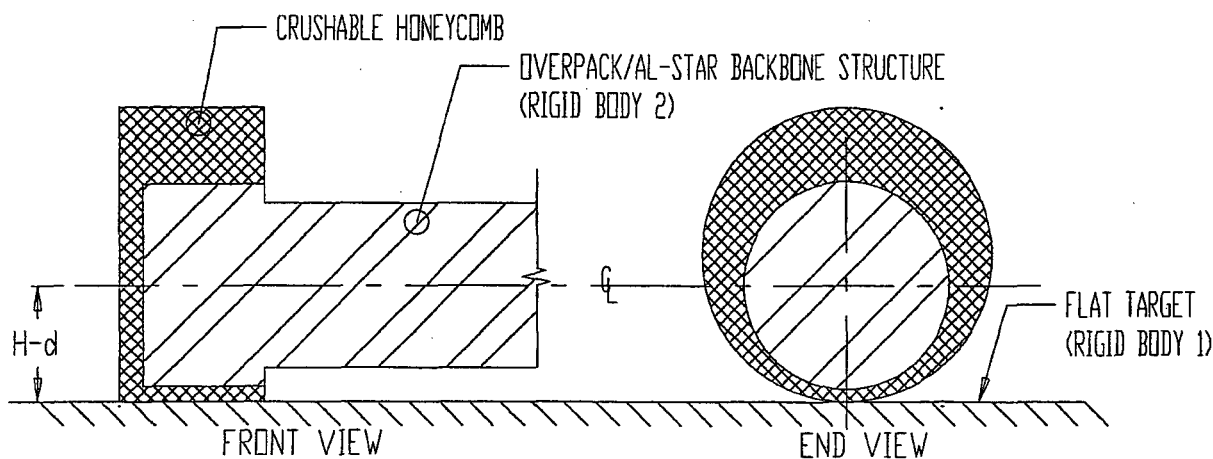
NON-PROPRIETARY VERSION



(a) TWO RIGID BODIES APPROACH EACH OTHER WITH A SOFT CRUSHABLE METAL MASS BETWEEN THEM (INITIATION OF CRUSHING)



(b) SCENARIO ONE: CRUSHING OCCURS AT THE AL-STAR/TARGET INTERFACE; DEFORMATION =  $d$ ; NO CRUSH AT AL-STAR BACKBONE/HONEYCOMB INTERFACE



(c) SCENARIO TWO: CRUSHING OCCURS AT THE AL-STAR BACKBONE/HONEYCOMB INTERFACE.; NO CRUSH AT THE AL-STAR/TARGET INTERFACE

FIGURE 2.A.3.1; ILLUSTRATION OF THE FORCE-CRUSH MODEL CONSTRUCTION USING THE EXAMPLE OF THE SIDE DROP EVENT.

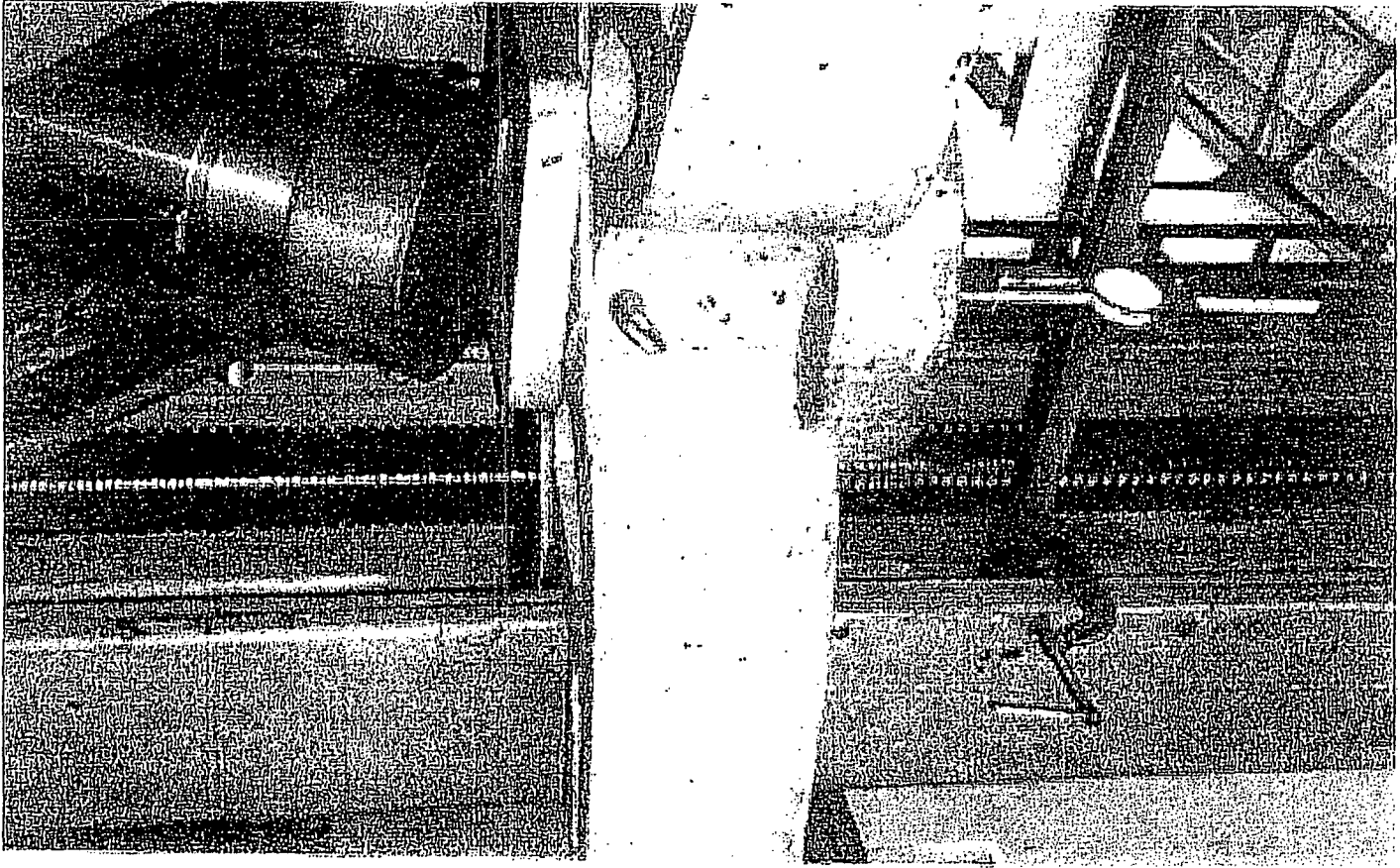


FIGURE 2.A.41; TEST FIXTURE

REPORT HI-951251

REVISION 10

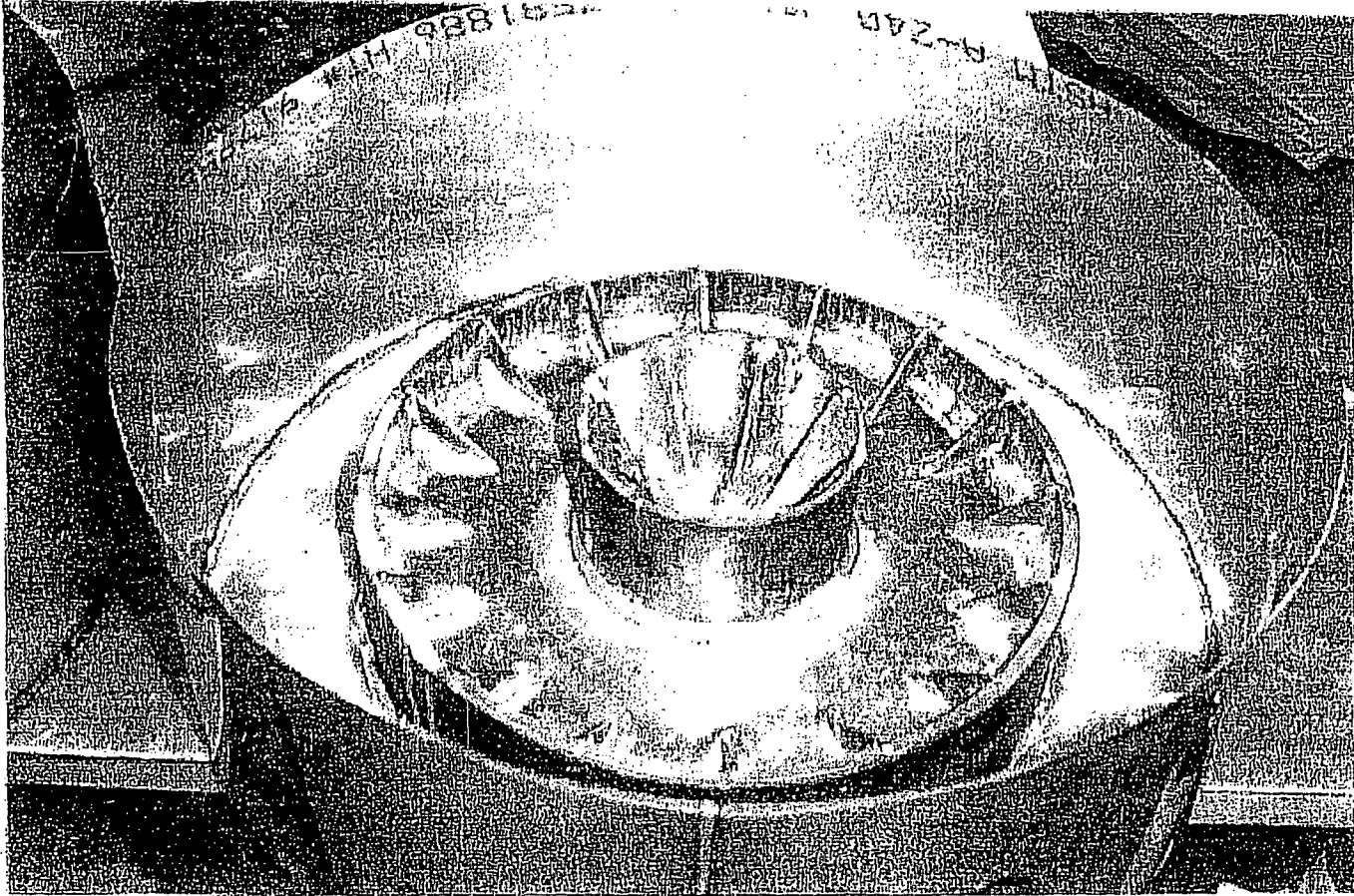


FIGURE 2.A.4.2 ; INTERNAL STIFFENING STRUCTURE IN 1/8 SCALE MODEL

REPORT HI-951251

REVISION 10

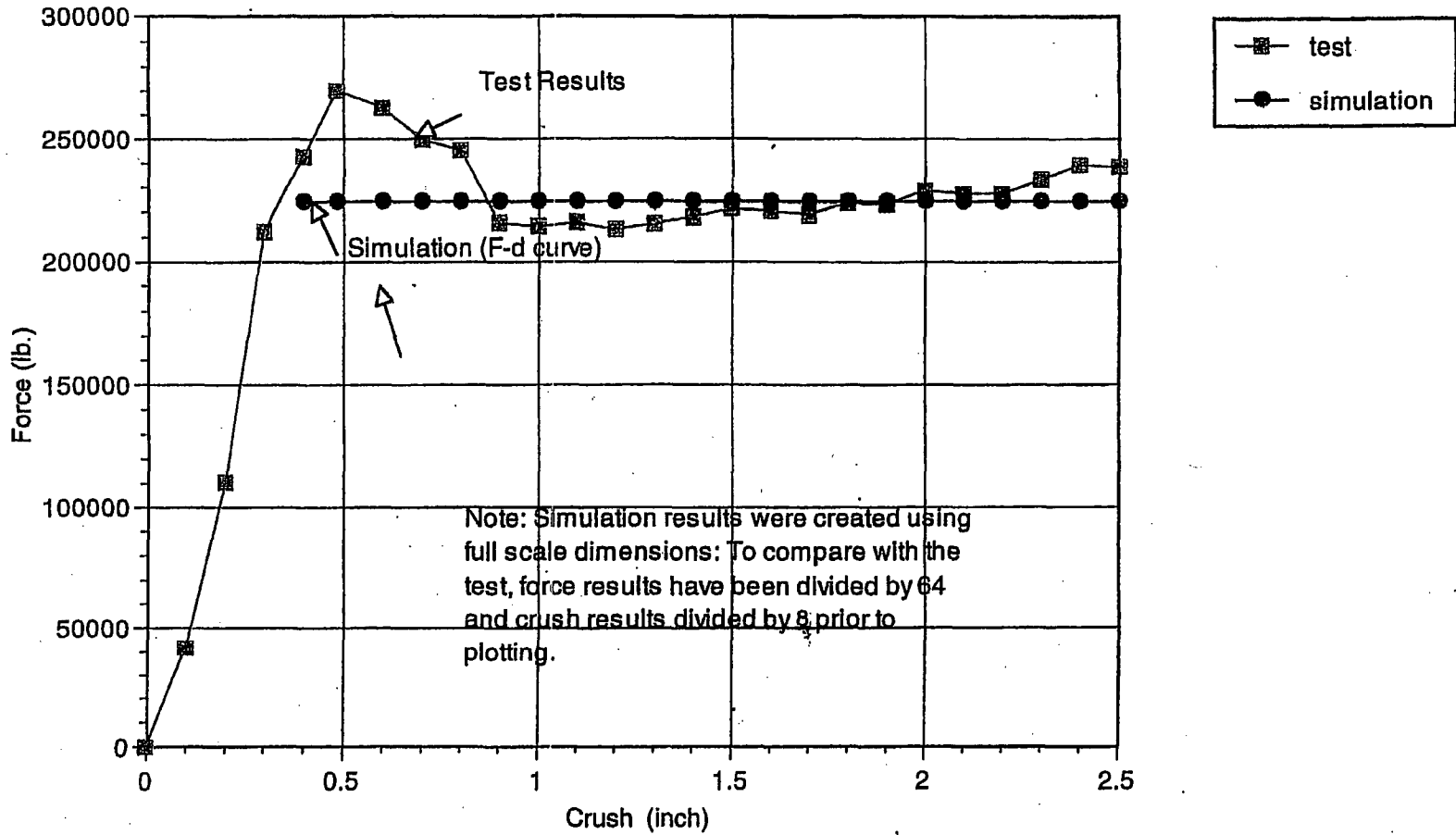


FIGURE 2.A.4.3 : 1/8th Scale Initial Impact Limiter Configuration - Comparison of Static Force-Crush Data from Test and Simulation - END DROP

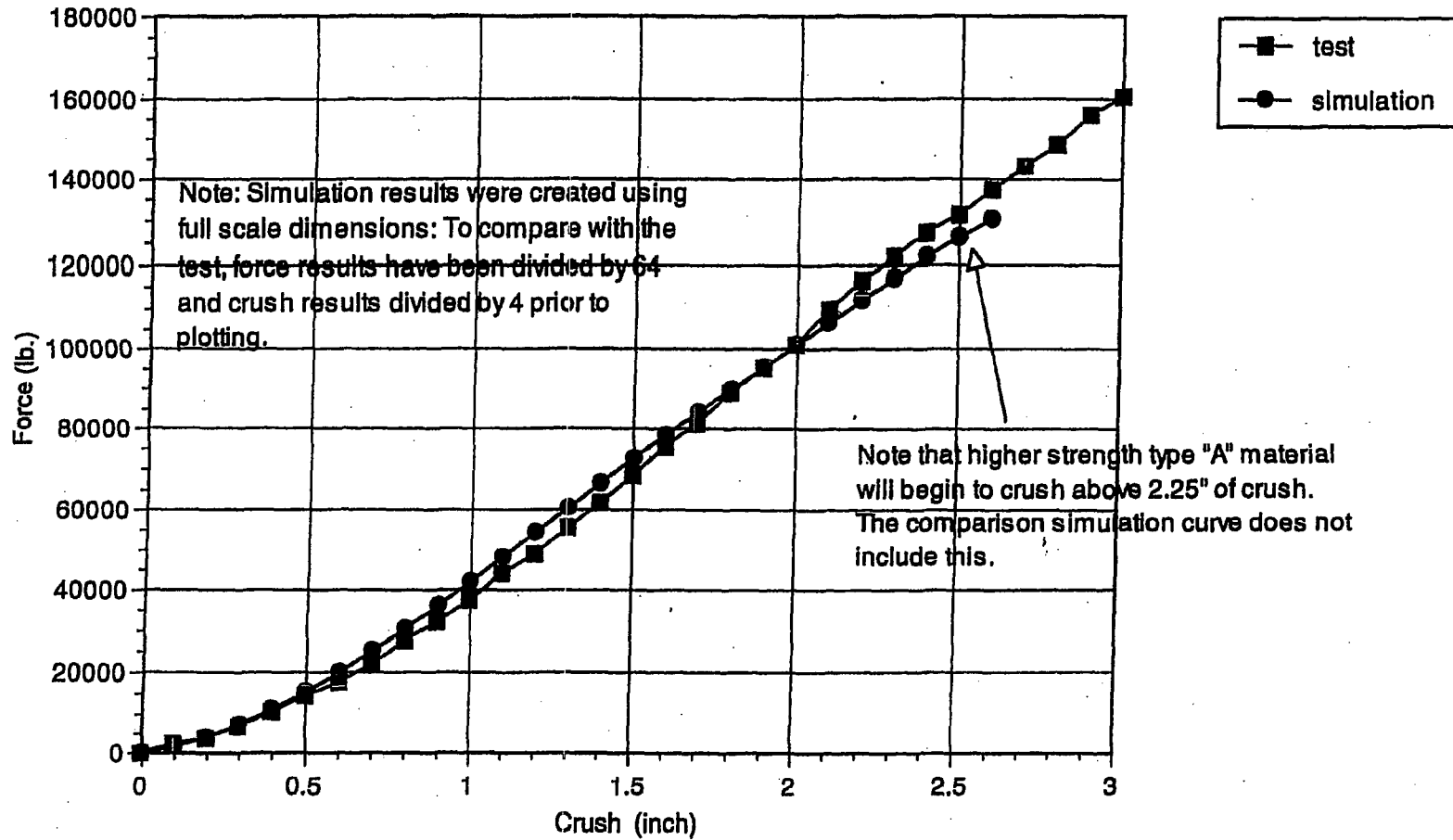


FIGURE 2A.4.4 : 1/8th Scale Initial Impact Limiter Configuration - Comparison of Static Force-Crush Data from Test and Simulation - 60 DEGREE CRUSH

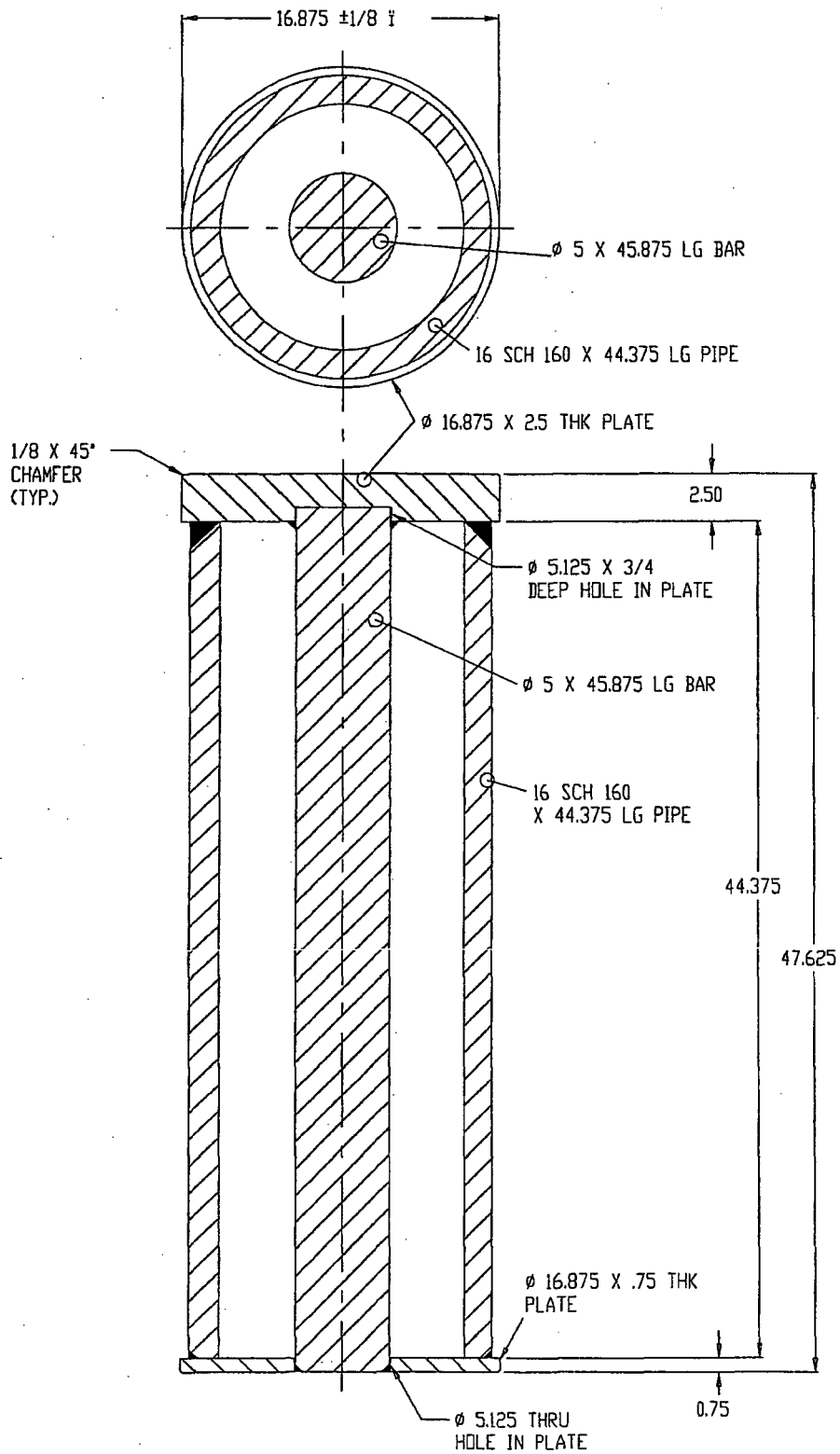


FIGURE 2.A.5.1: QUARTER SCALE MODEL OF LOADED MPC FOR QUARTER SCALE DROP TEST EXPERIMENT

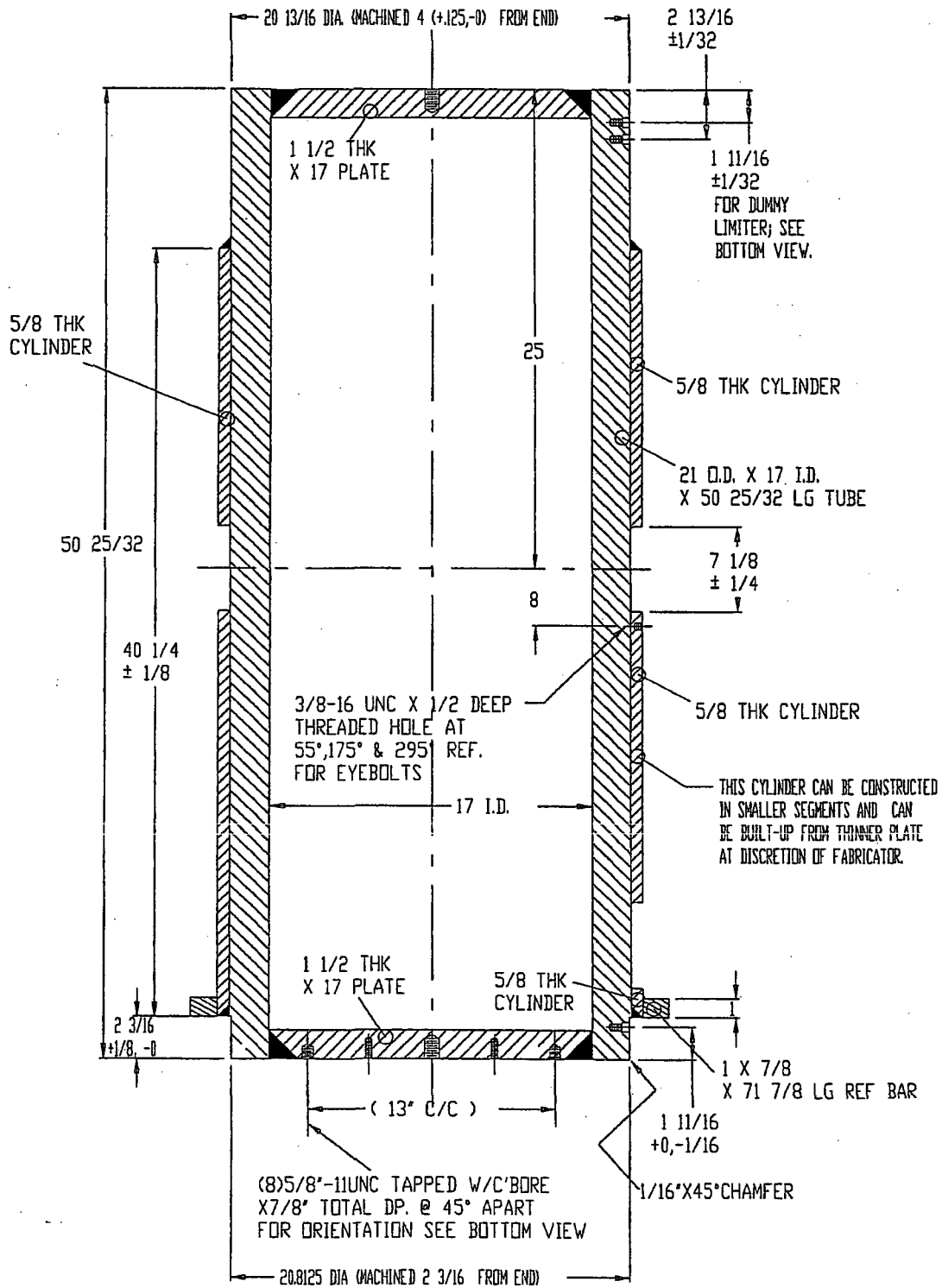


FIGURE 2.A.5.2; OVERPACK QUARTER SCALE MODEL (CROSS SECTION VIEW)

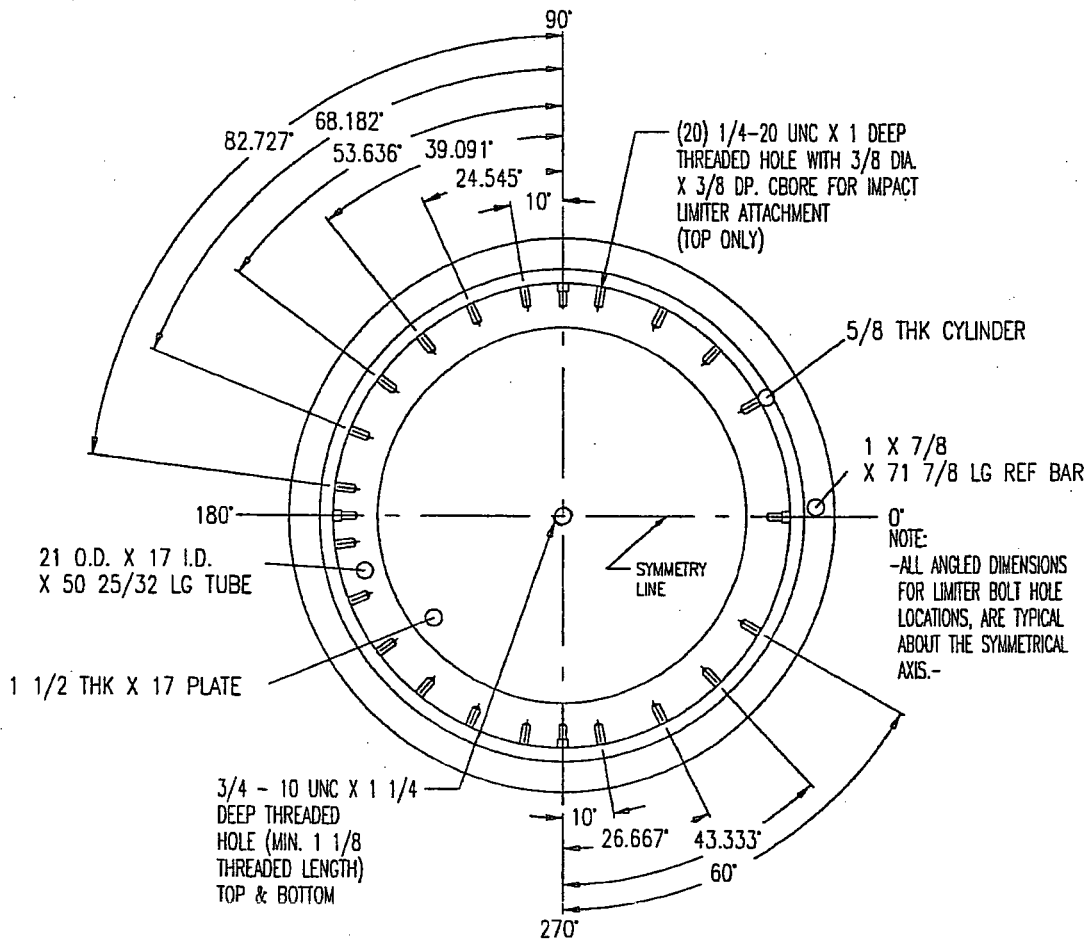


FIGURE 2.A.5.3; OVERPACK QUARTER SCALE MODEL (TOP VIEW)

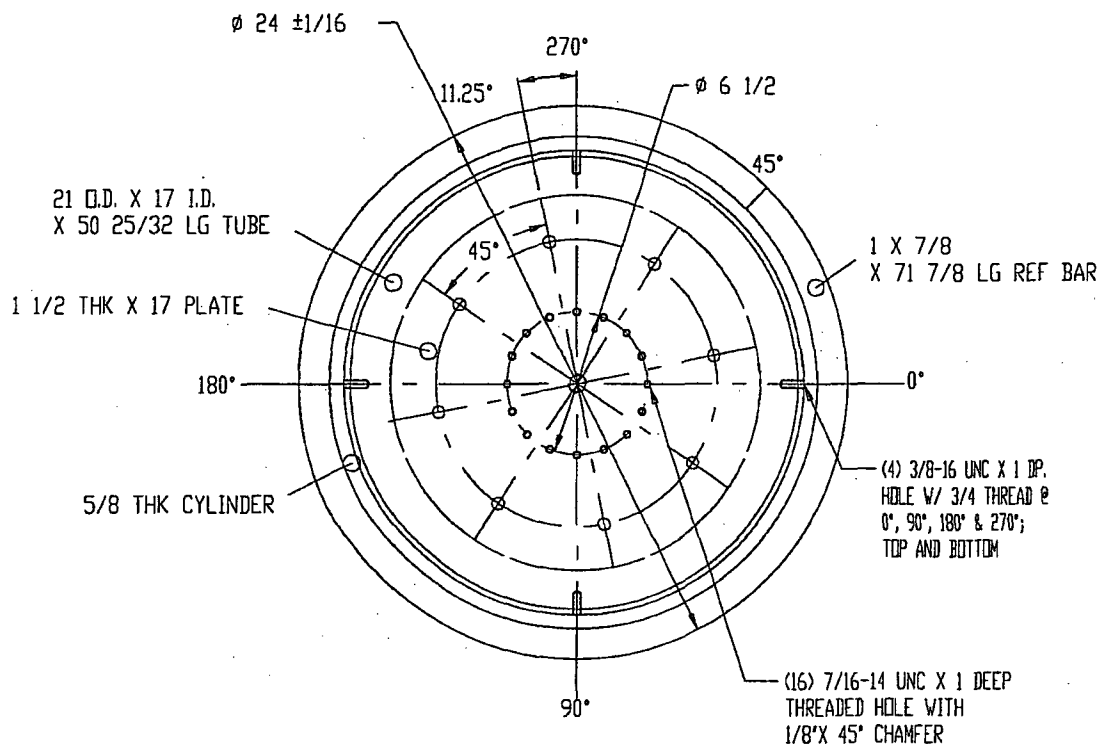
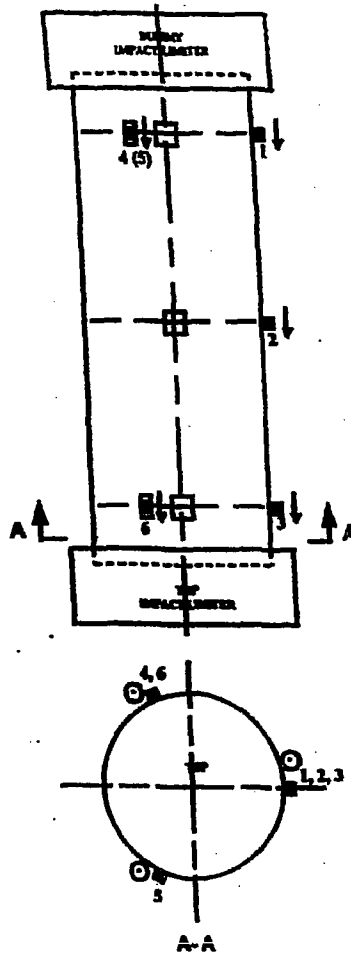


FIGURE 2.A.5.4; OVERPACK QUARTER SCALE MODEL (BOTTOM VIEW)



(a) Accelerometer Location - Top End Drop

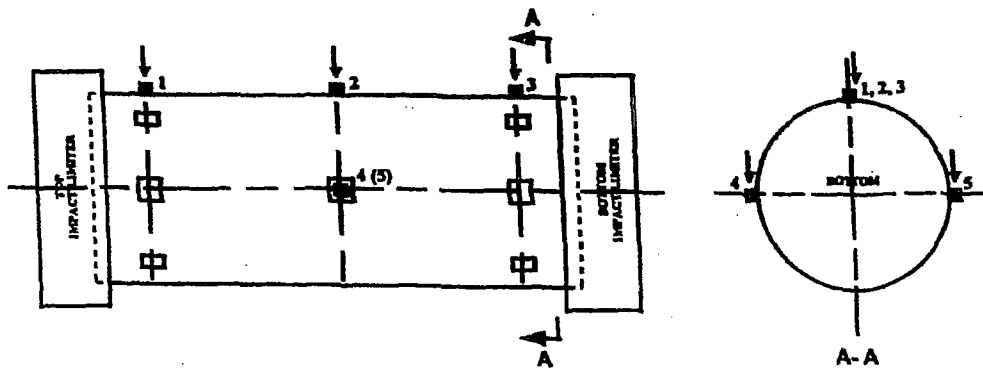
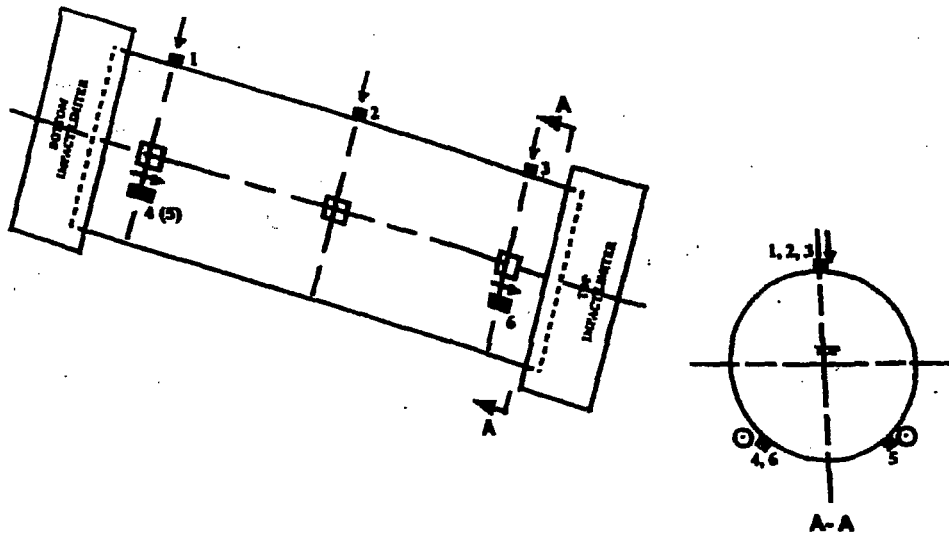
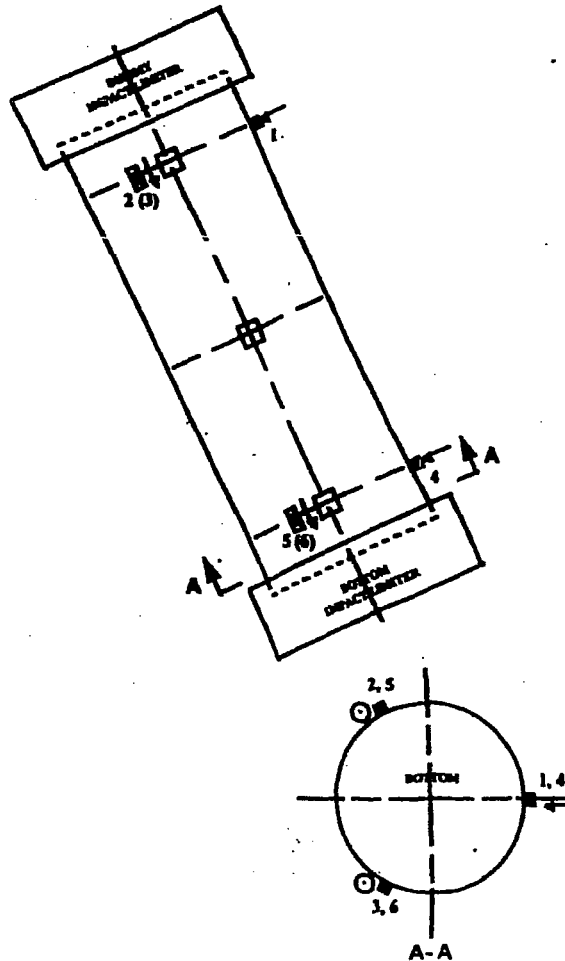


FIGURE 2A.5.5 : ACCELEROMETER LOCATIONS FOR END AND SIDE DROPS



(c) Accelerometer Location - Slap Down Drop



HI-951251

REV. 10

FIGURE 2A.5.6; ACCELEROMETER LOCATIONS FOR SLAP DOWN AND CGOC DROPS  
Revision 15 issued October 11, 2010

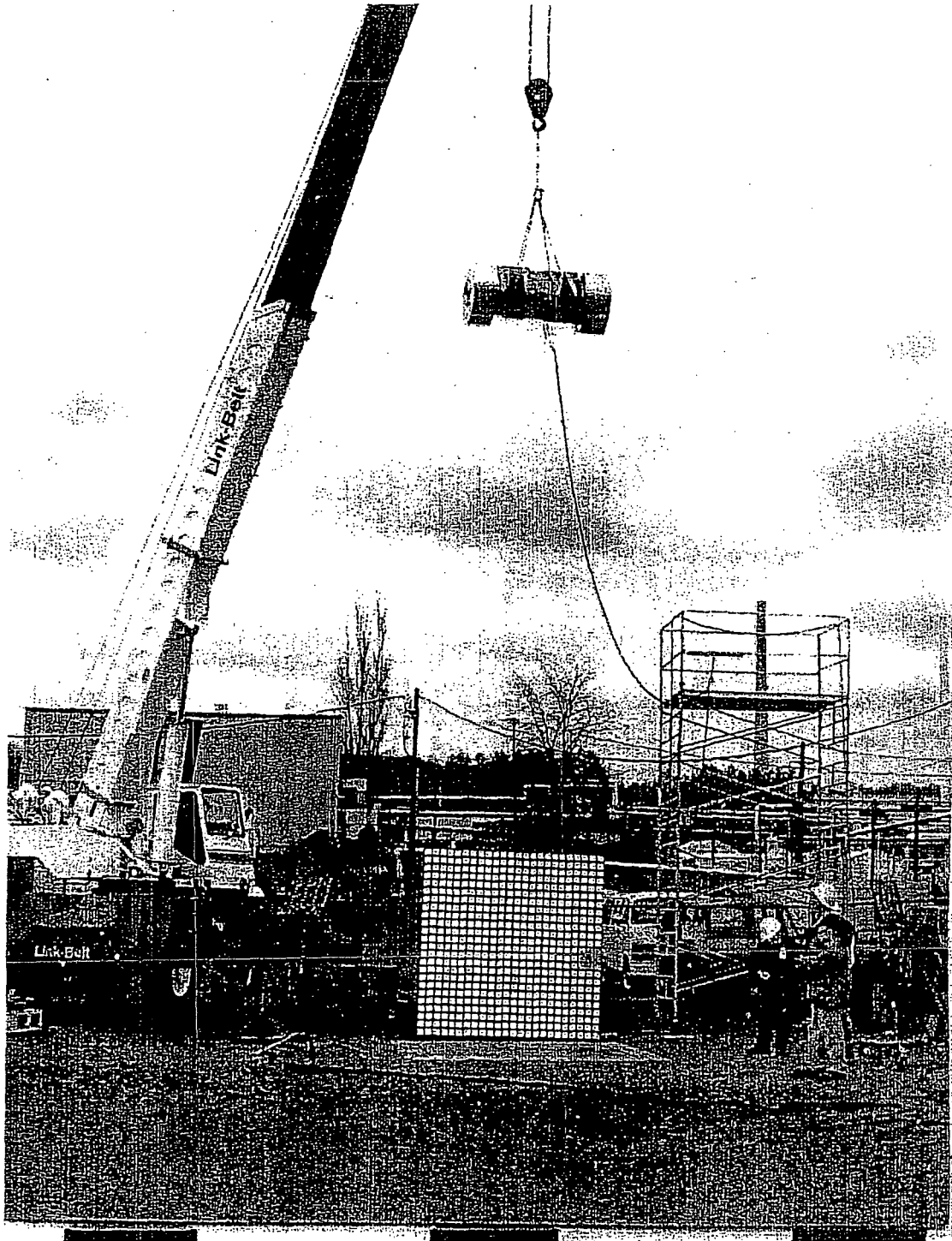


**FIGURE 2.A.5.7 : ¼ SCALE HI-STAR 100 PACKAGING  
AT 30 FT (9 M) PRIOR TO SIDE DROP**

HI-951251

REV. 10



FIGURE 2.A.5.8 ; ¼ SCALE BOTTOM IMPACT LIMITER AFTER SIDE DROP

HI-951251

REV. 10

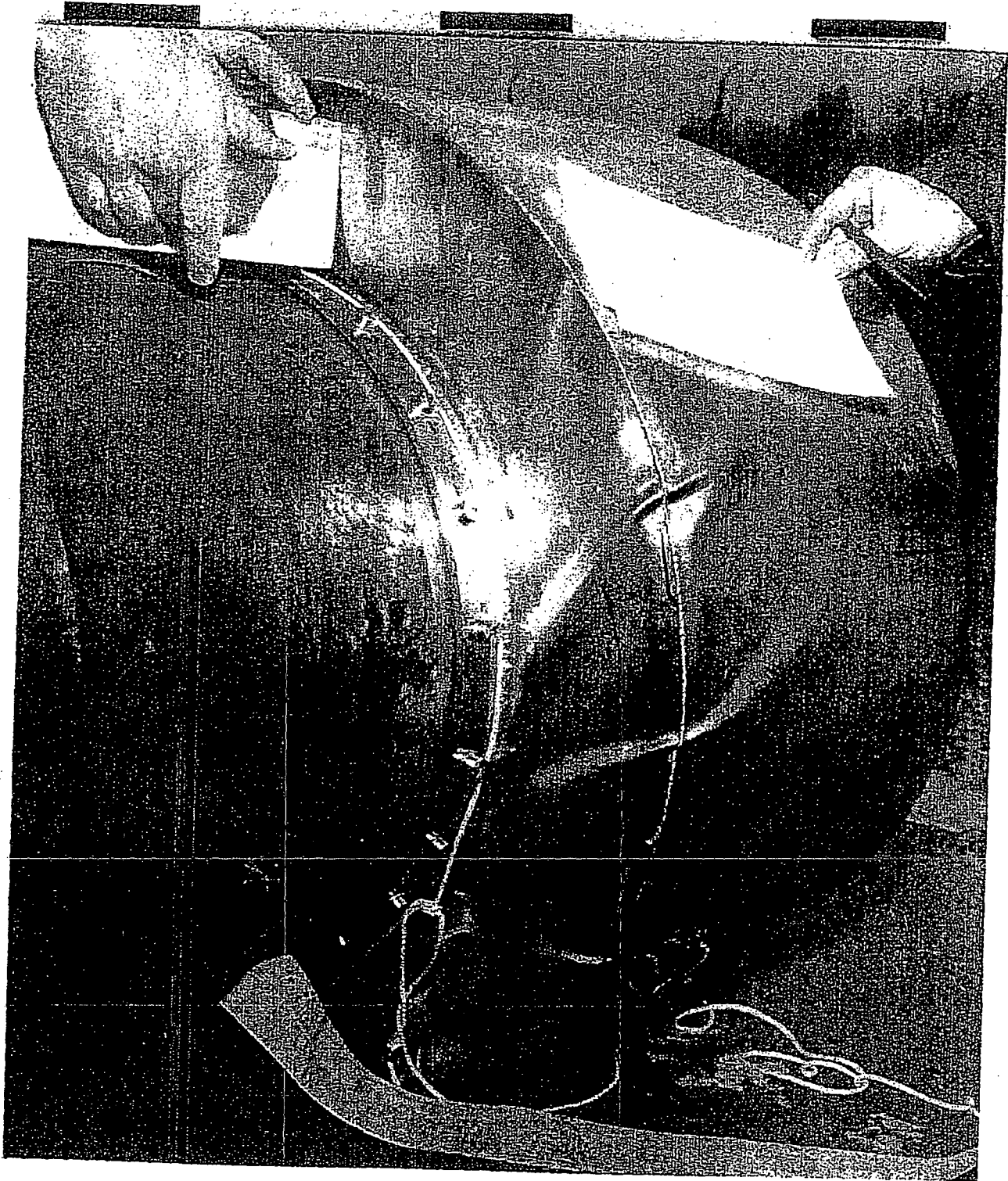


FIGURE 2.A.5.9 : 1/4 SCALE TOP IMPACT LIMITER AFTER SIDE DROP

HI-951251

REV. 10

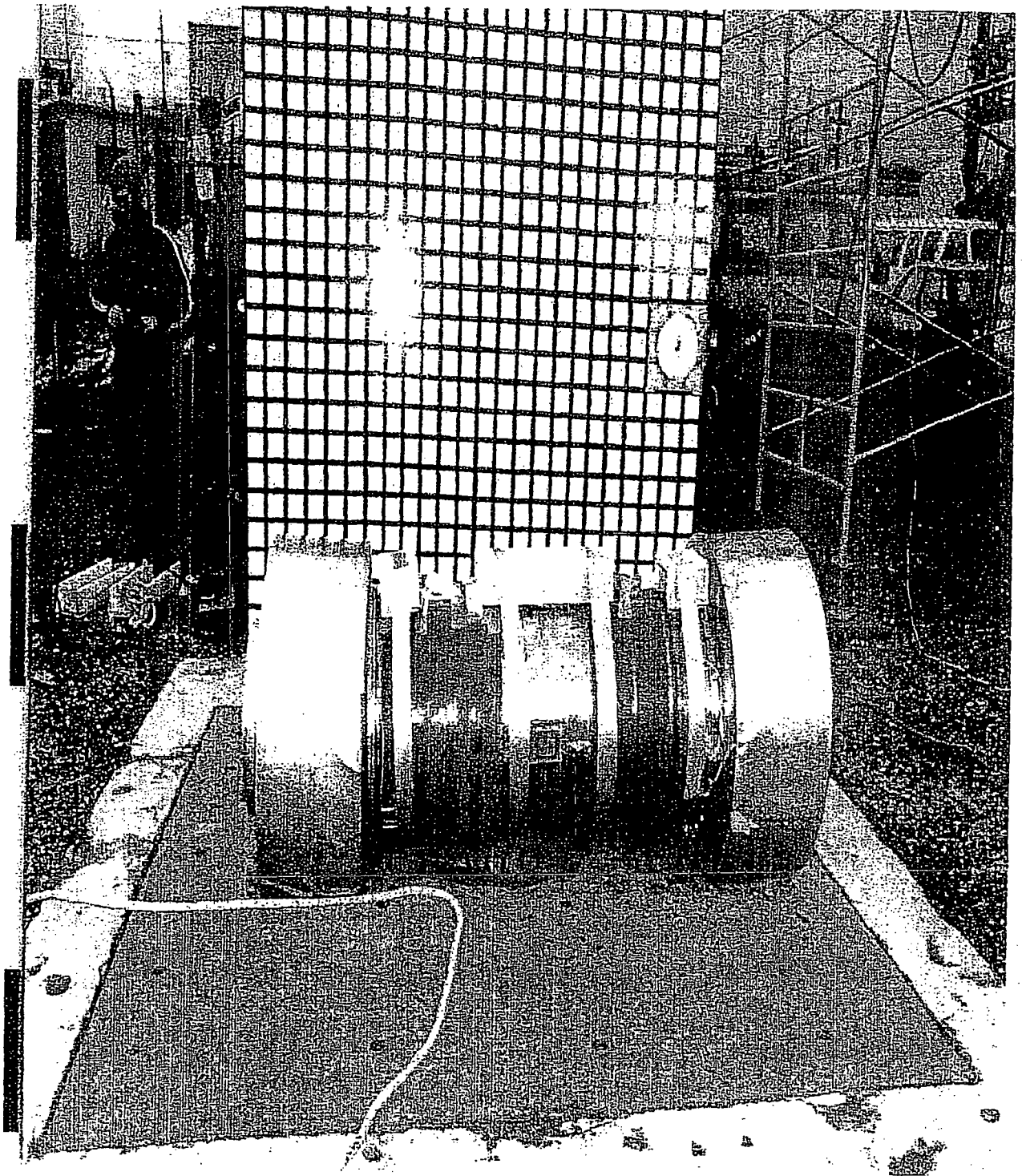


FIGURE 2.A.5.10 ; 1/4 SCALE HI-STAR 100 PACKAGING AFTER SLAP DOWN DROP

HI-951251

REV. 10

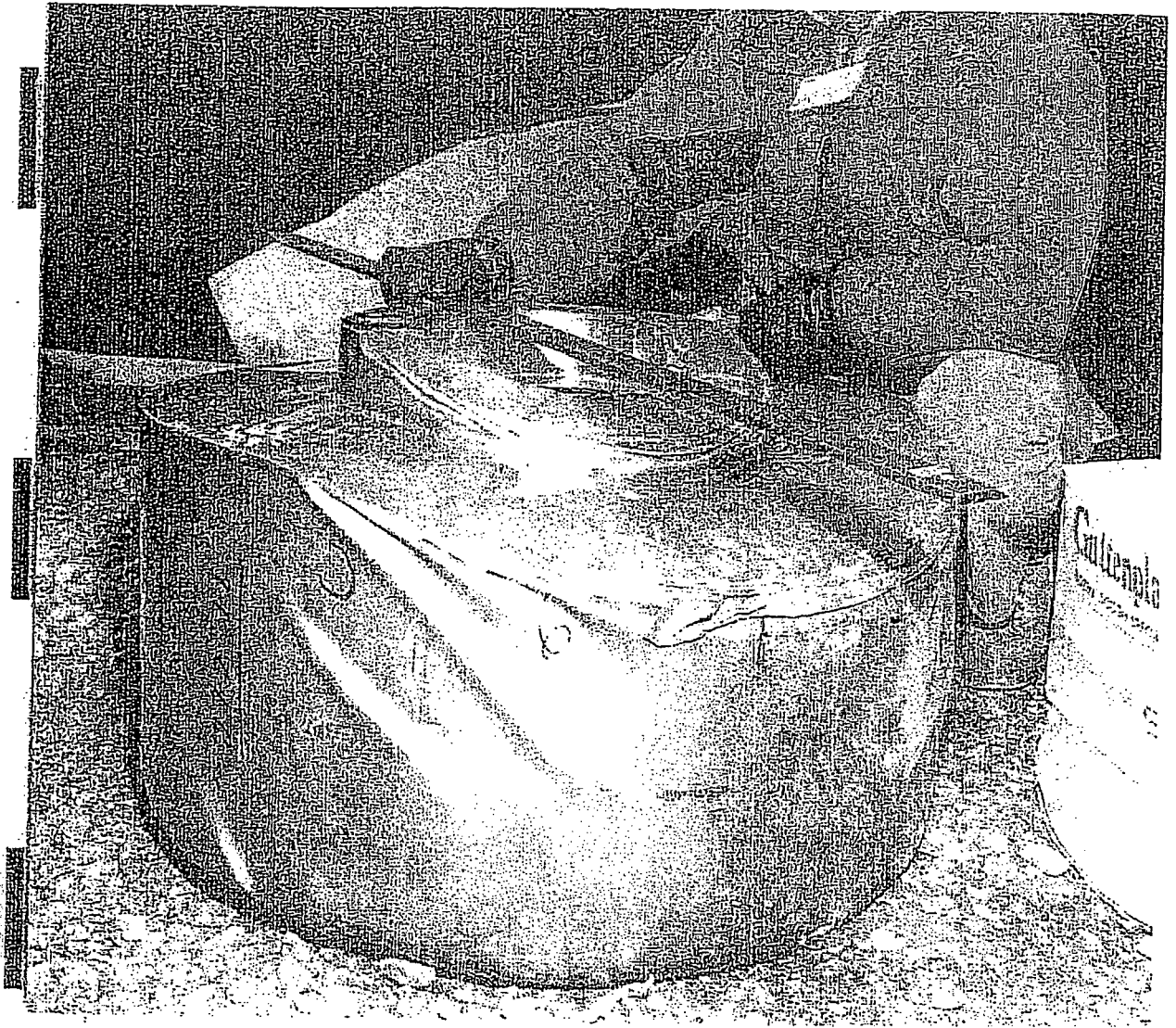


FIGURE 2.A.5.11 ; 1/4 SCALE IMPACT LIMITER AFTER C.G. OVER CORNER DROP

HI-951251

REV. 10

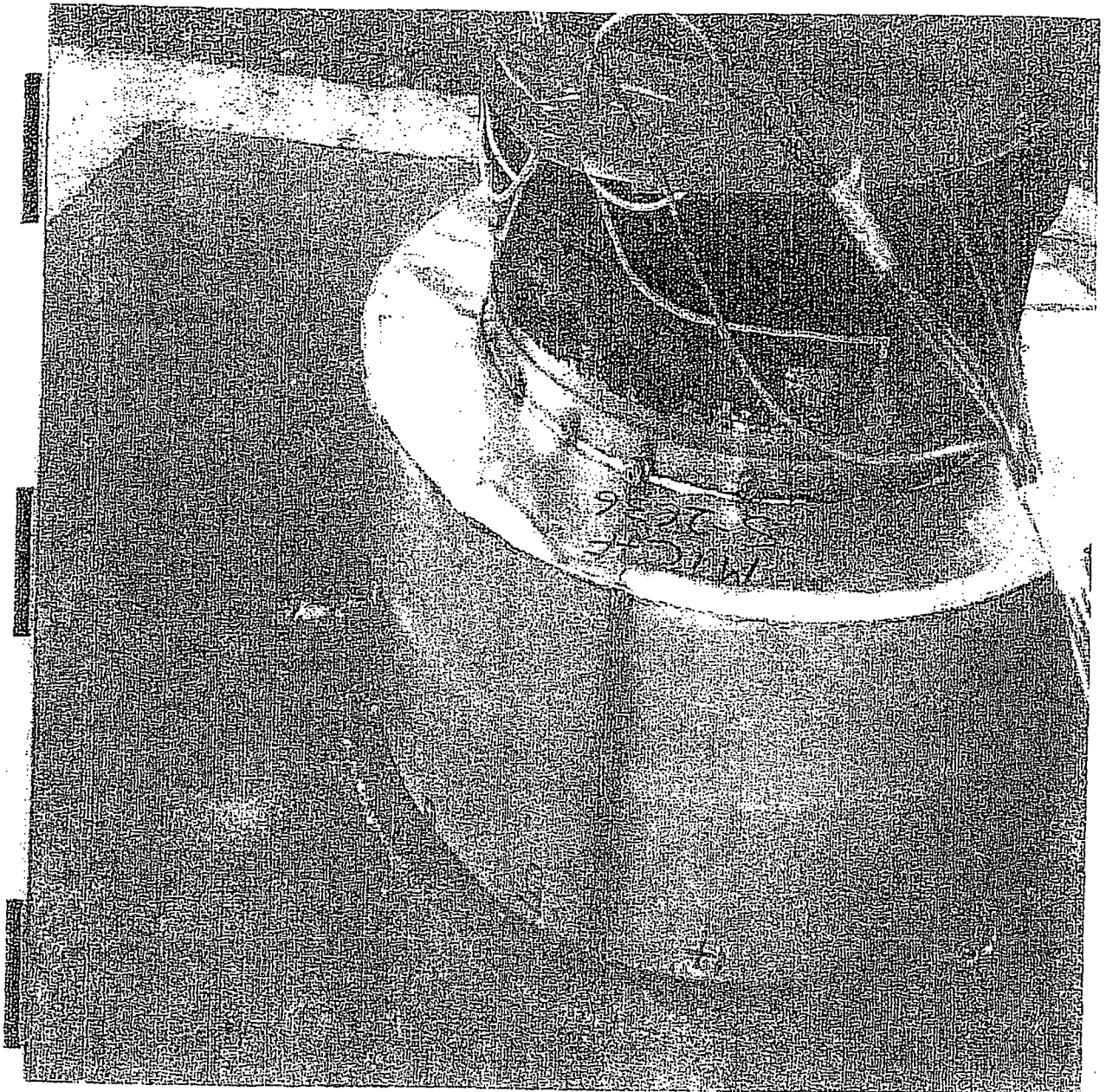


FIGURE 2.A.5.12 ; 1/4 SCALE HI-STAR 100 PACKAGING AFTER TOP END DROP

HI-951251

REV. 10

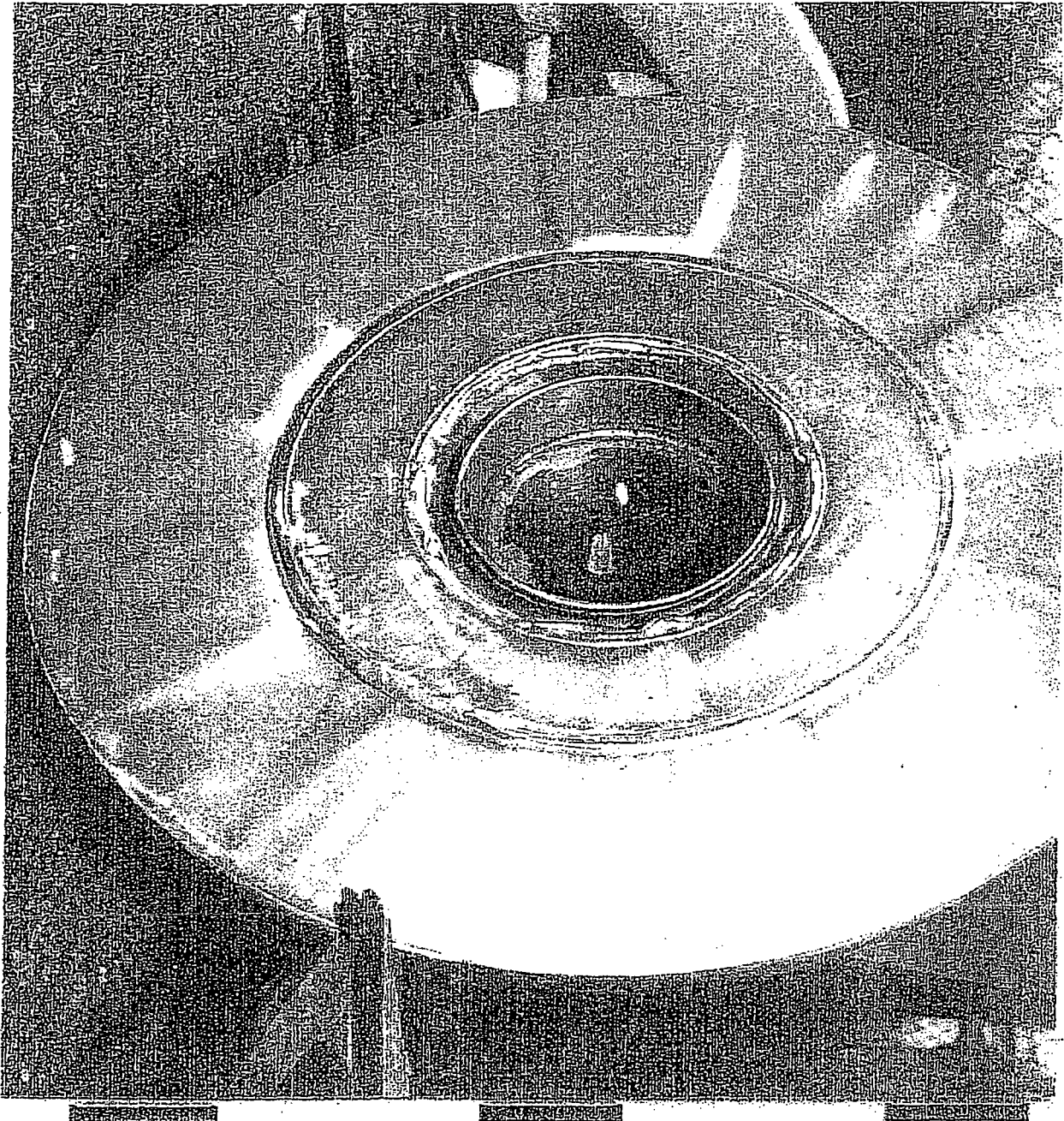


FIGURE 2.A.5.13 : 1/4 SCALE IMPACT LIMITER TOP END DROP

HI-951251

REV. 10

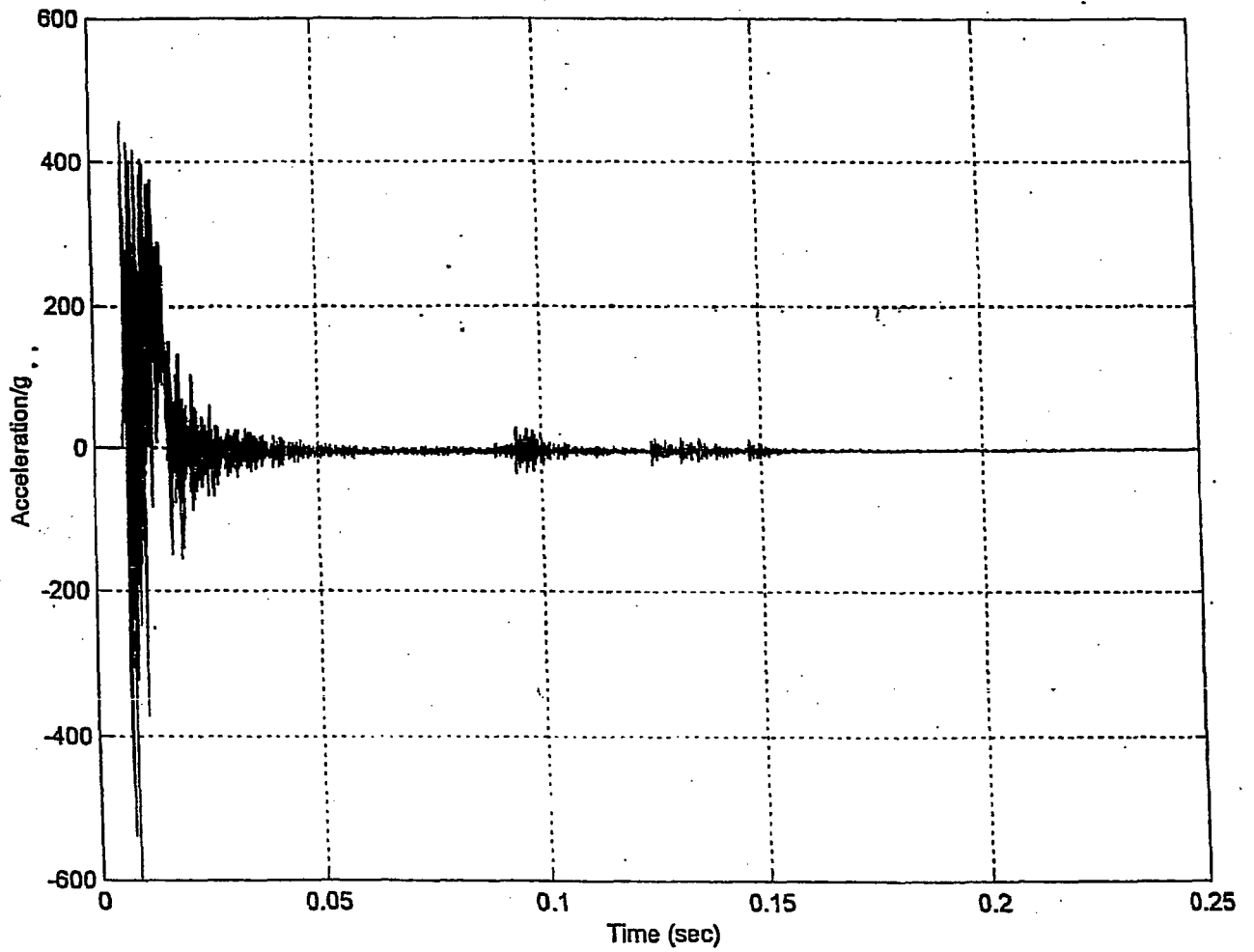


FIGURE 2.A.5.14 ; ACCELERATION RAW DATA FOR TOP END DROP

HI-951251

REV. 10

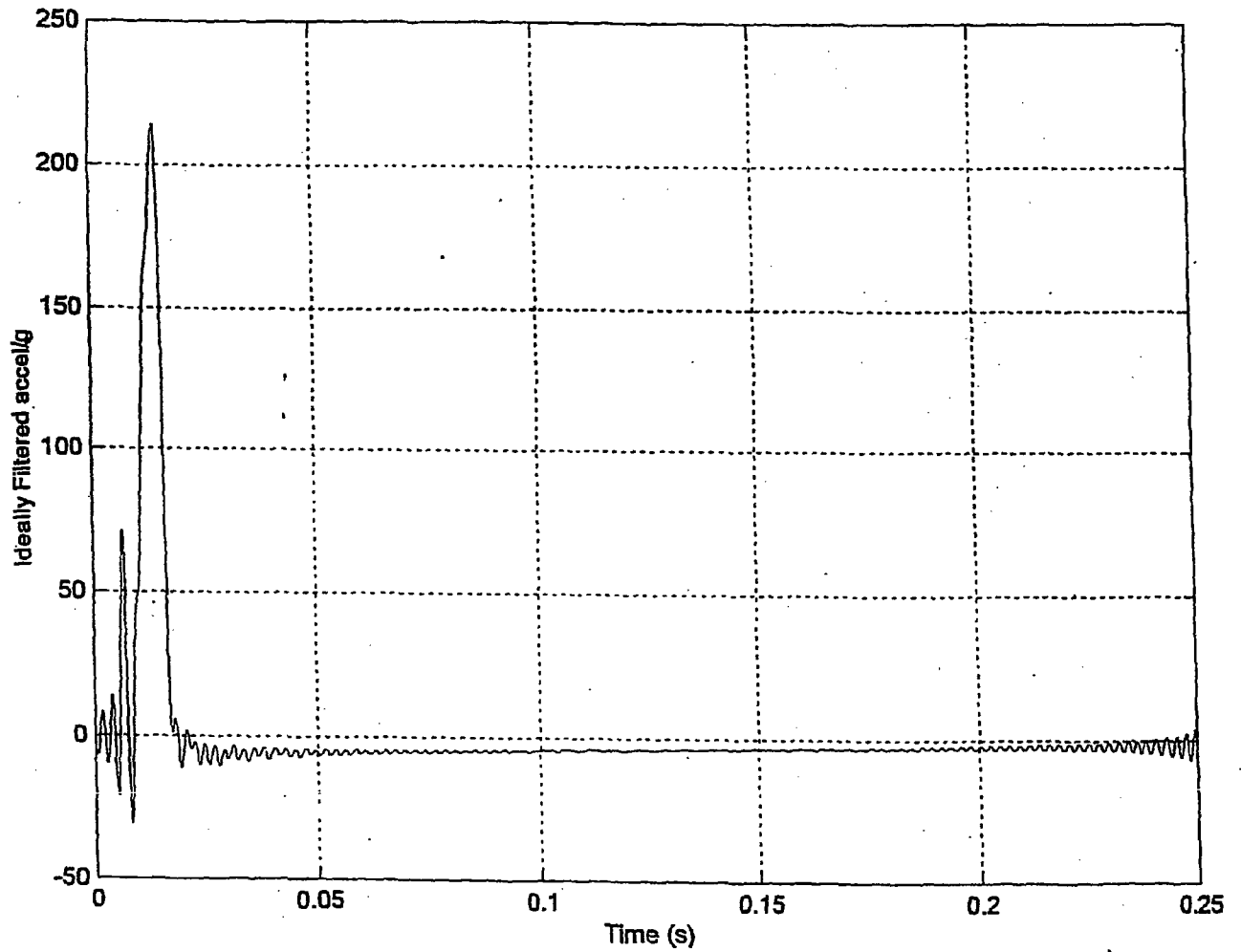


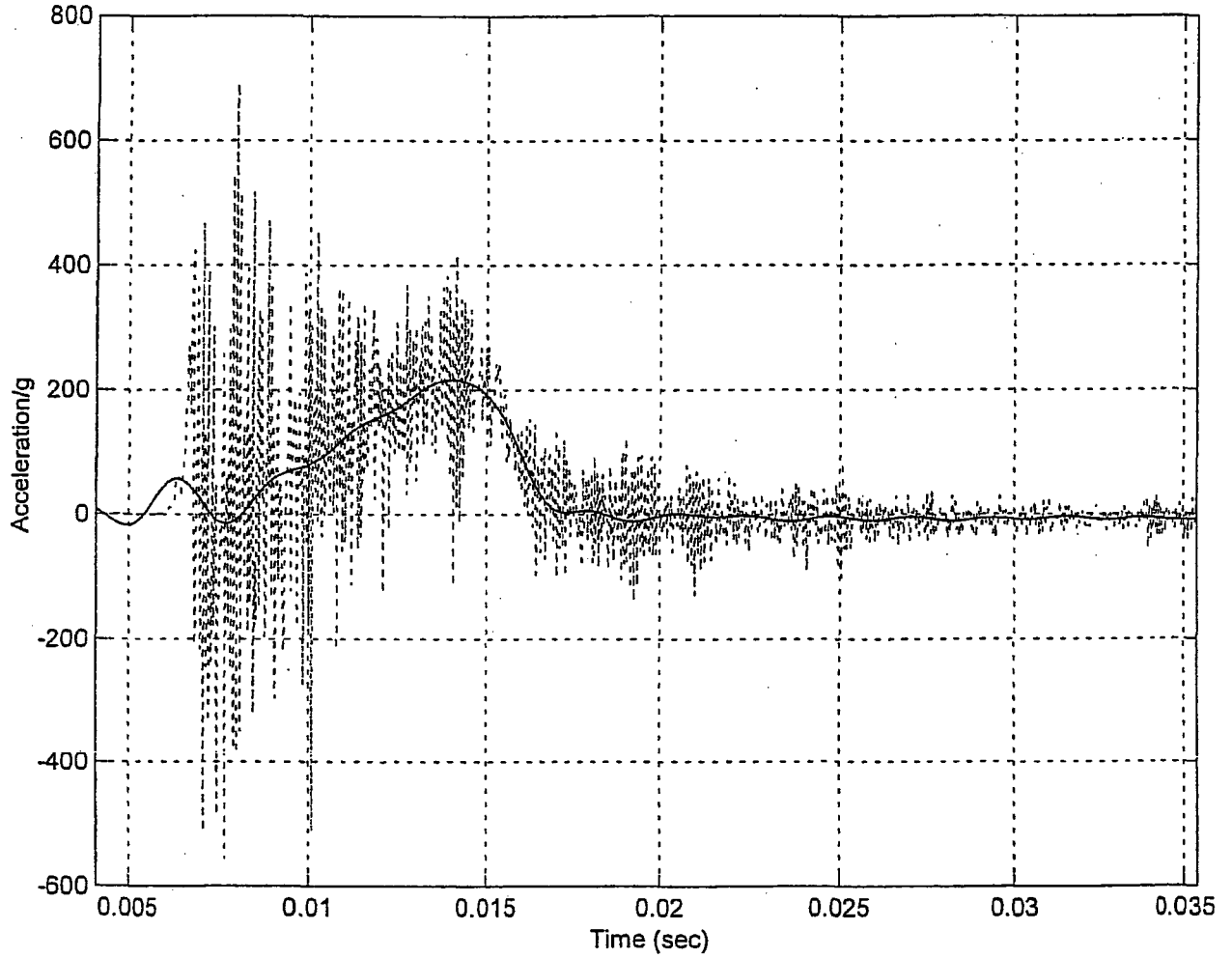
FIGURE 2.A.5.15 ; ACCELERATION DATA FILTERED AT 450 Hz FOR TOP END DROP

HI-951251

REV. 10

**FIGURE 2.A.5.15A ; TOP END DROP**

Filtered (—) and Unfiltered (...) Accelerations, Cutoff Freq. = 450 Hz  
Max. Filtered Acceleration = 216.0534g, at time = 0.014008 s

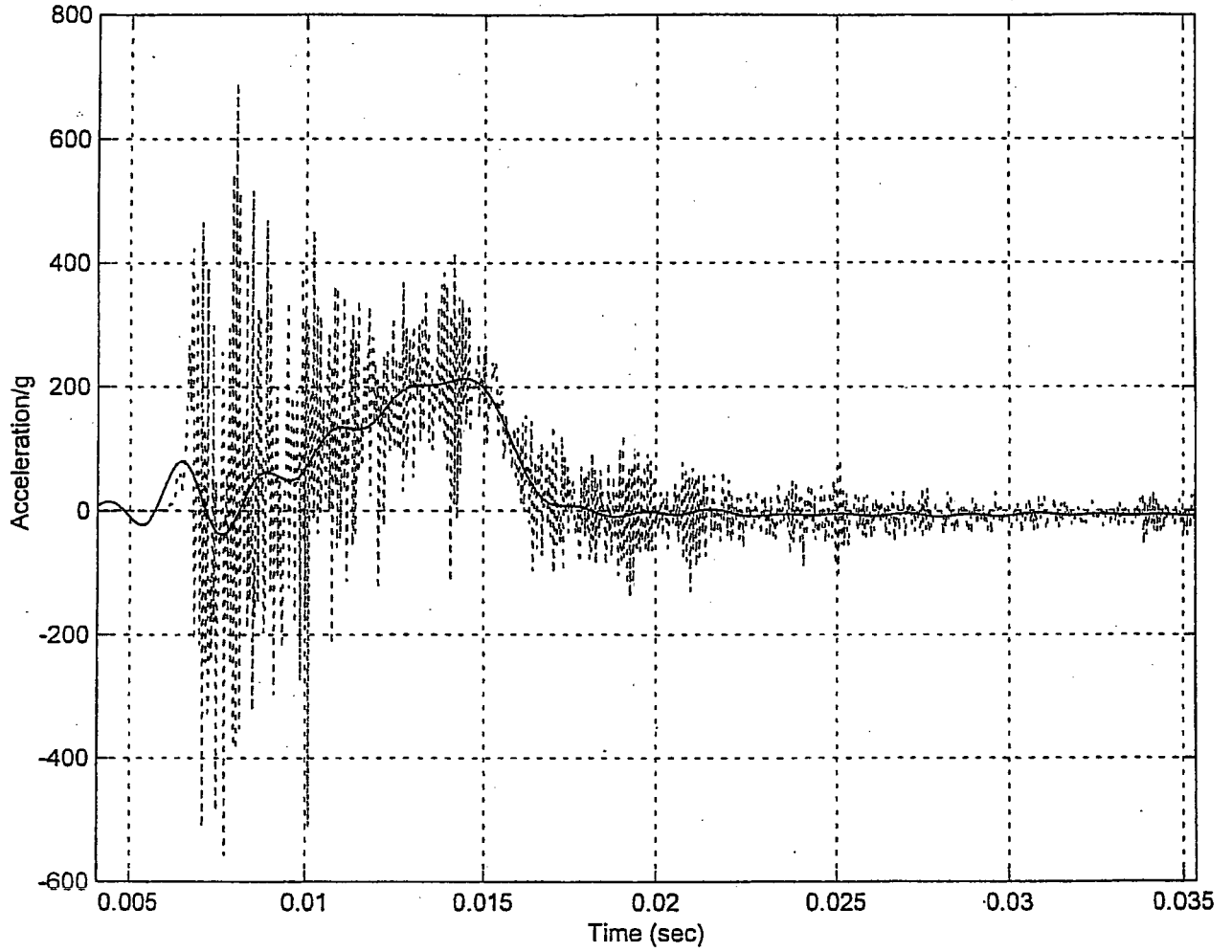


HI-951251

REV. 10

FIGURE 2.A.5.15B ; TOP END DROP

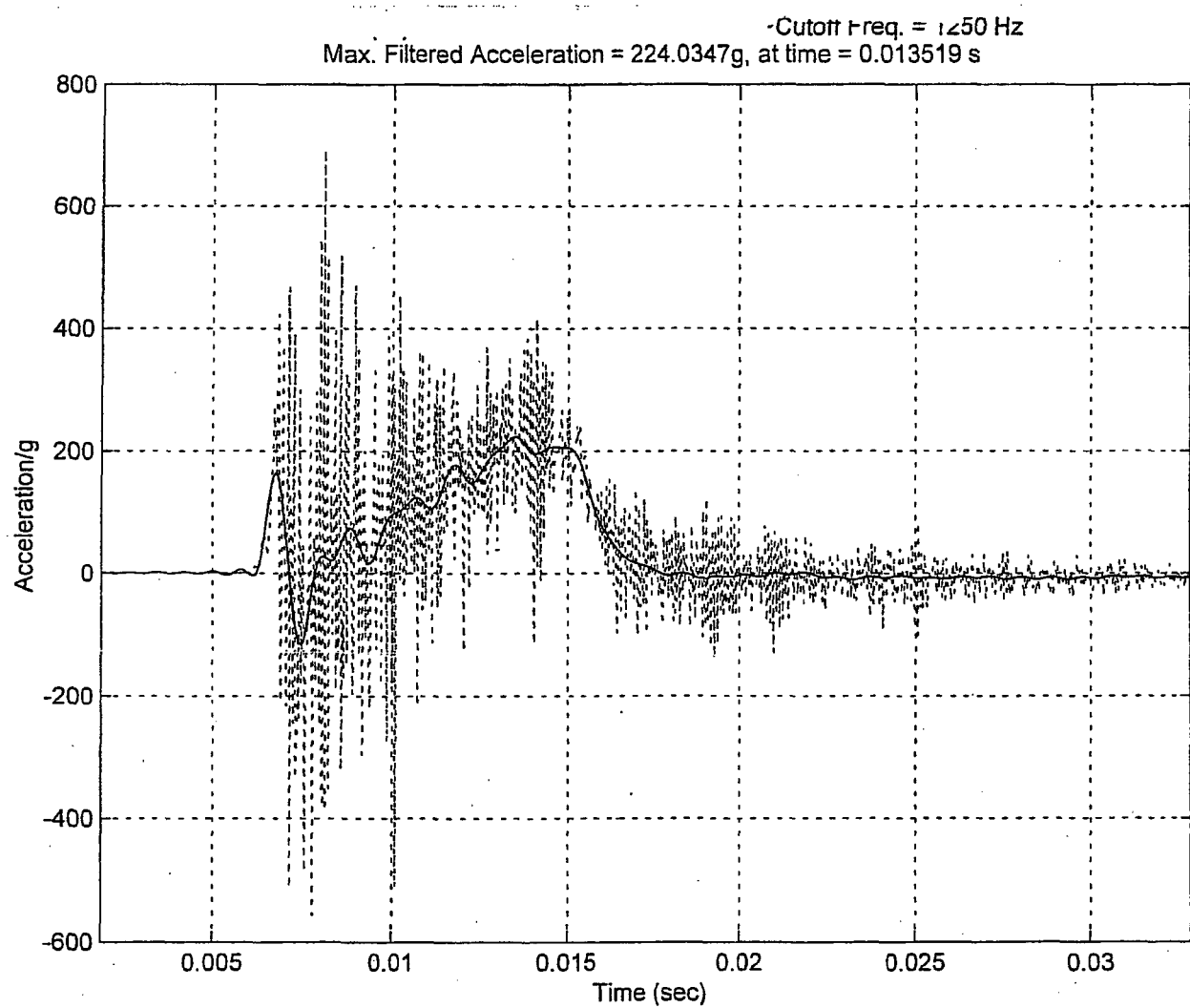
Filtered (—) and Unfiltered (...) Accelerations, Cutoff Freq. = 550 Hz  
Max. Filtered Acceleration = 213.7848g, at time = 0.014465 s



HI-951251

REV. 10

FIGURE 2.A.5.15C : TOP END DROP



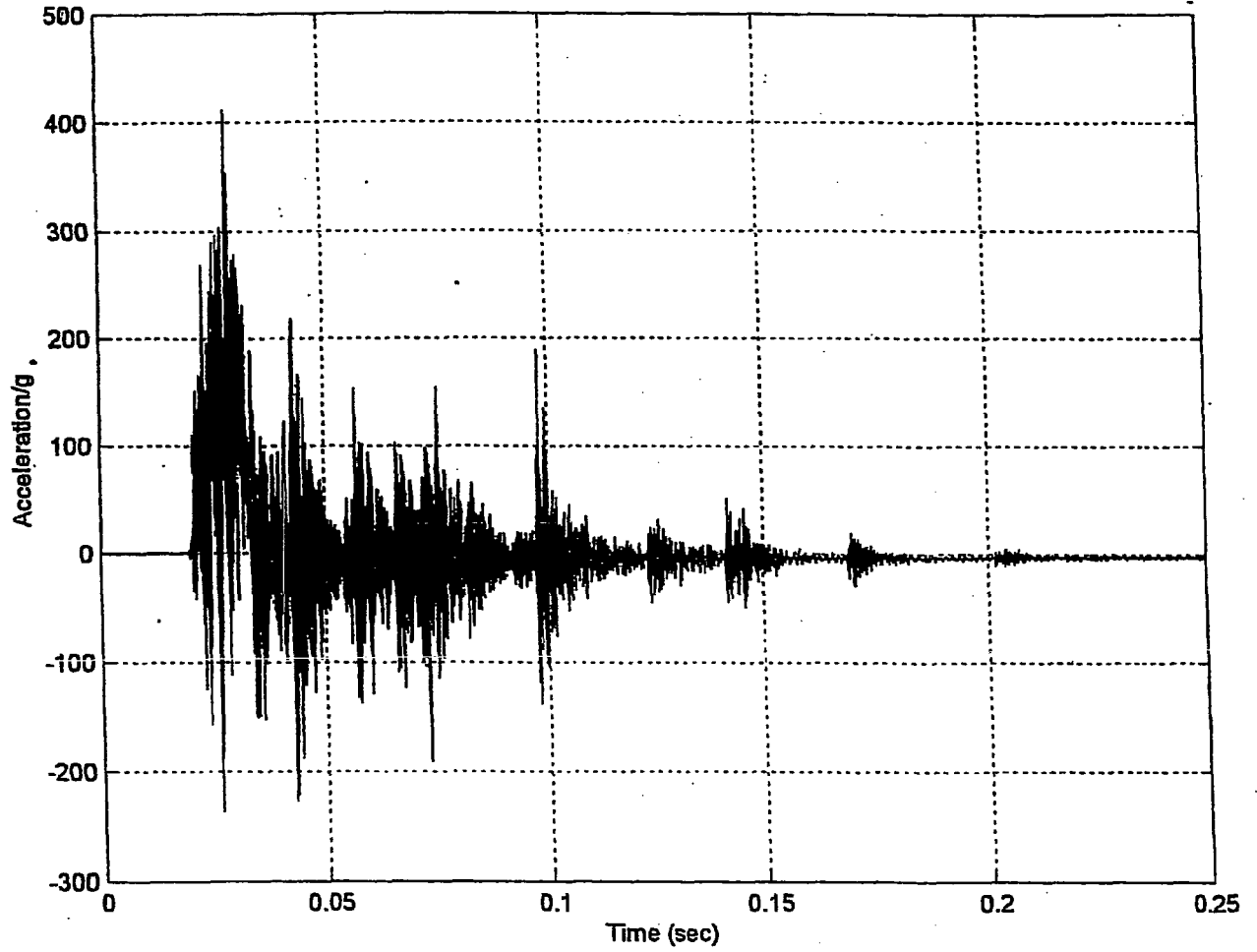


FIGURE 2.A.5.16 : ACCELERATION RAW DATA FOR C.G. OVER CORNER DROP

HI-951251

REV. 1

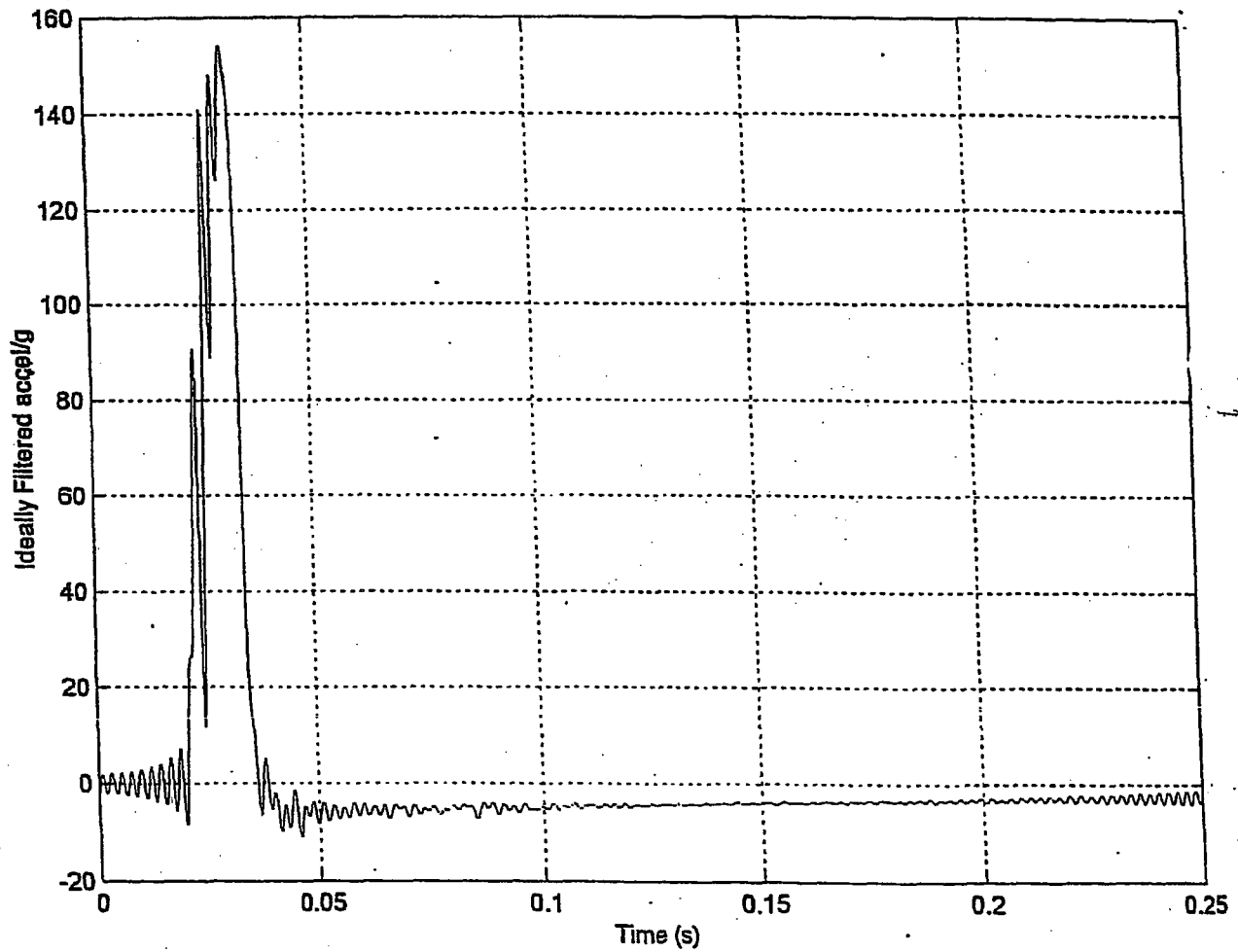


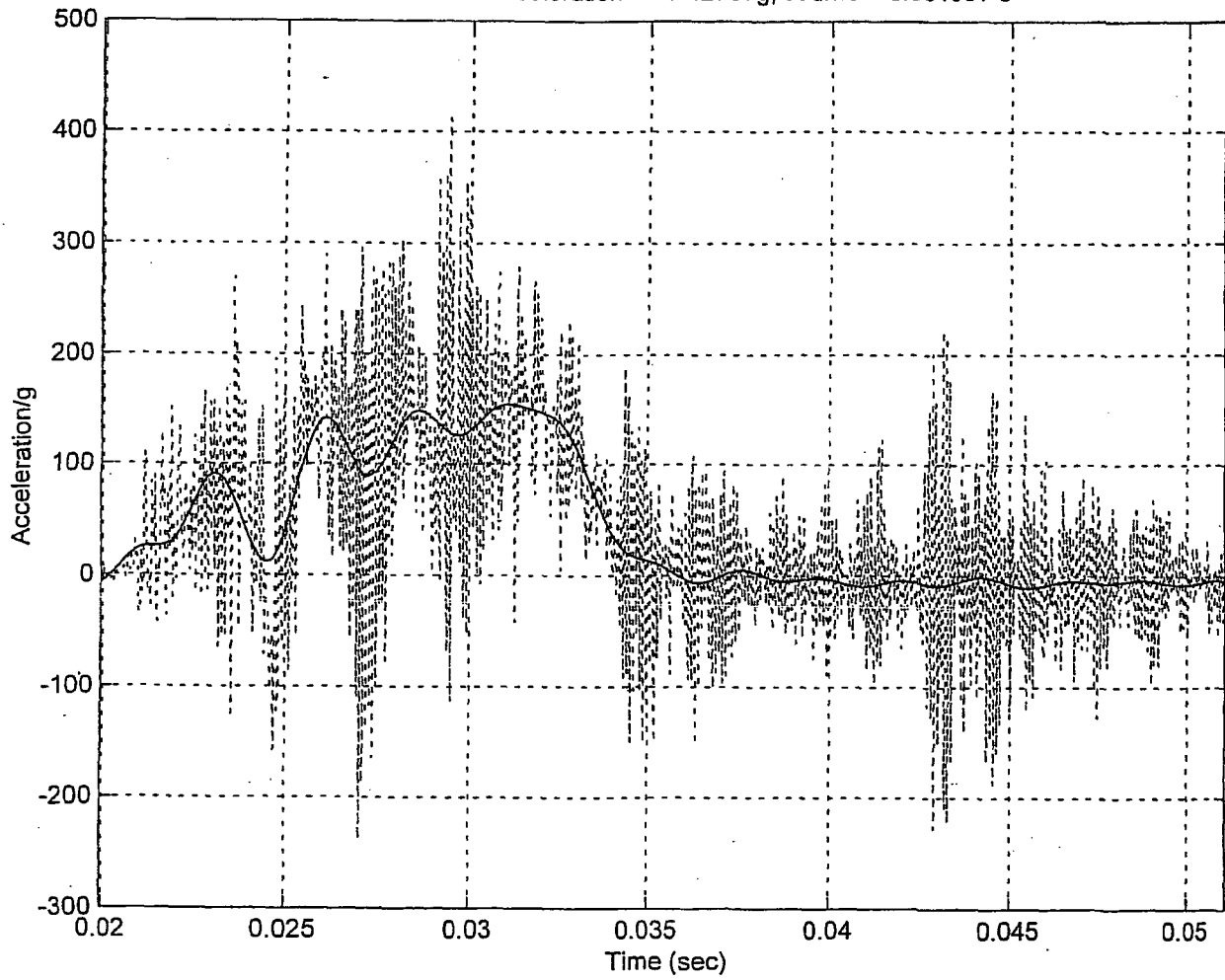
FIGURE 2.A.5.17 ; ACCELERATION DATA FILTERED AT 450 Hz FOR C.G. OVER CORNER

HI-951251

REV. 10

**FIGURE 2.A.5.17A : CG OVER CORNER**

Filtered (—) and Unfiltered (...) Accelerations, Cutoff Freq. = 450 Hz  
Max. Filtered Acceleration = 154.2797g, at time = 0.031097 s



HI-951251

REV. 10

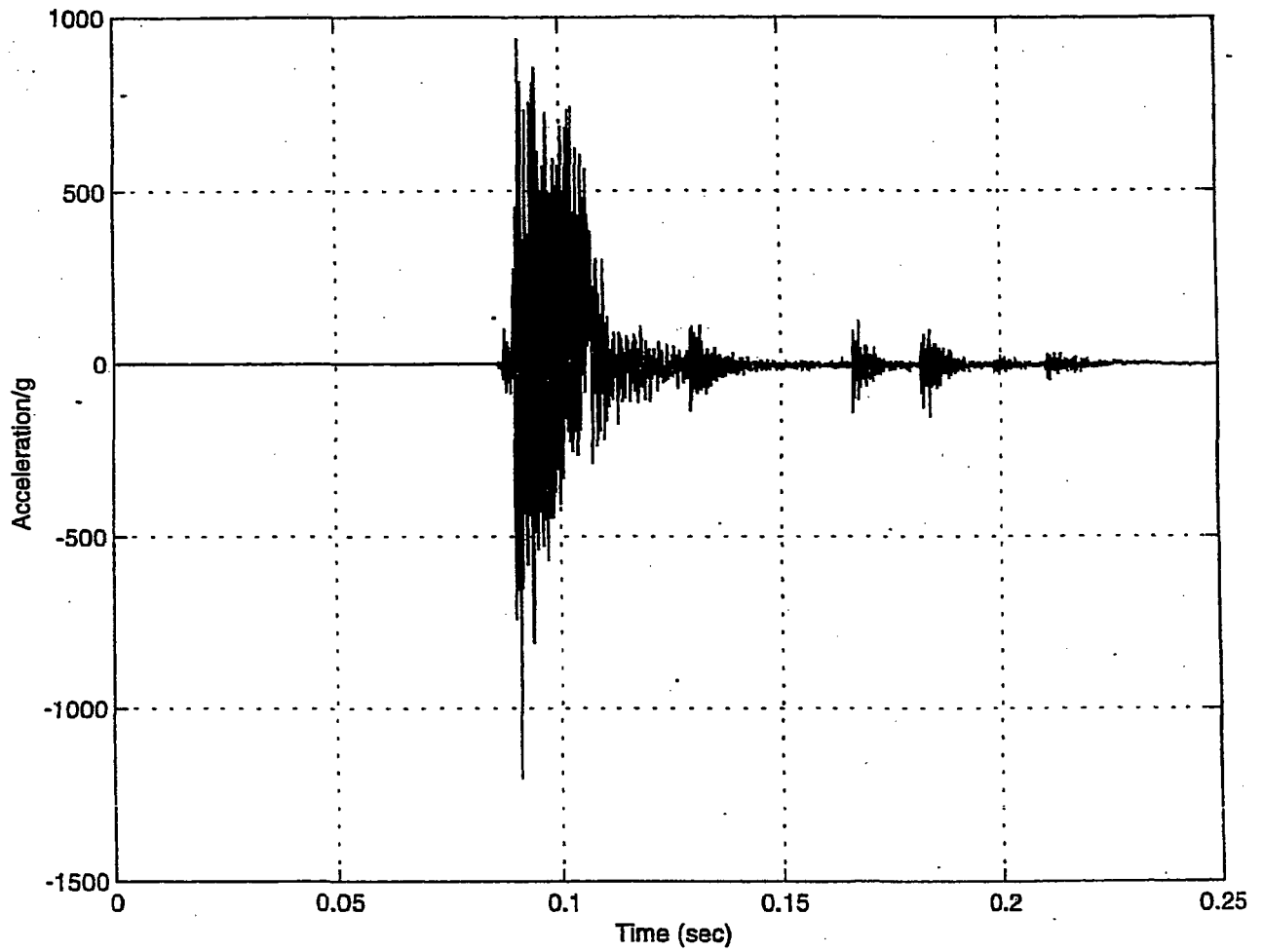


FIGURE 2.A.5.18 ; ACCELERATION RAW DATA AT BOTTOM END DURING SLAPDOWN DROP

HI-951251

REV. 10

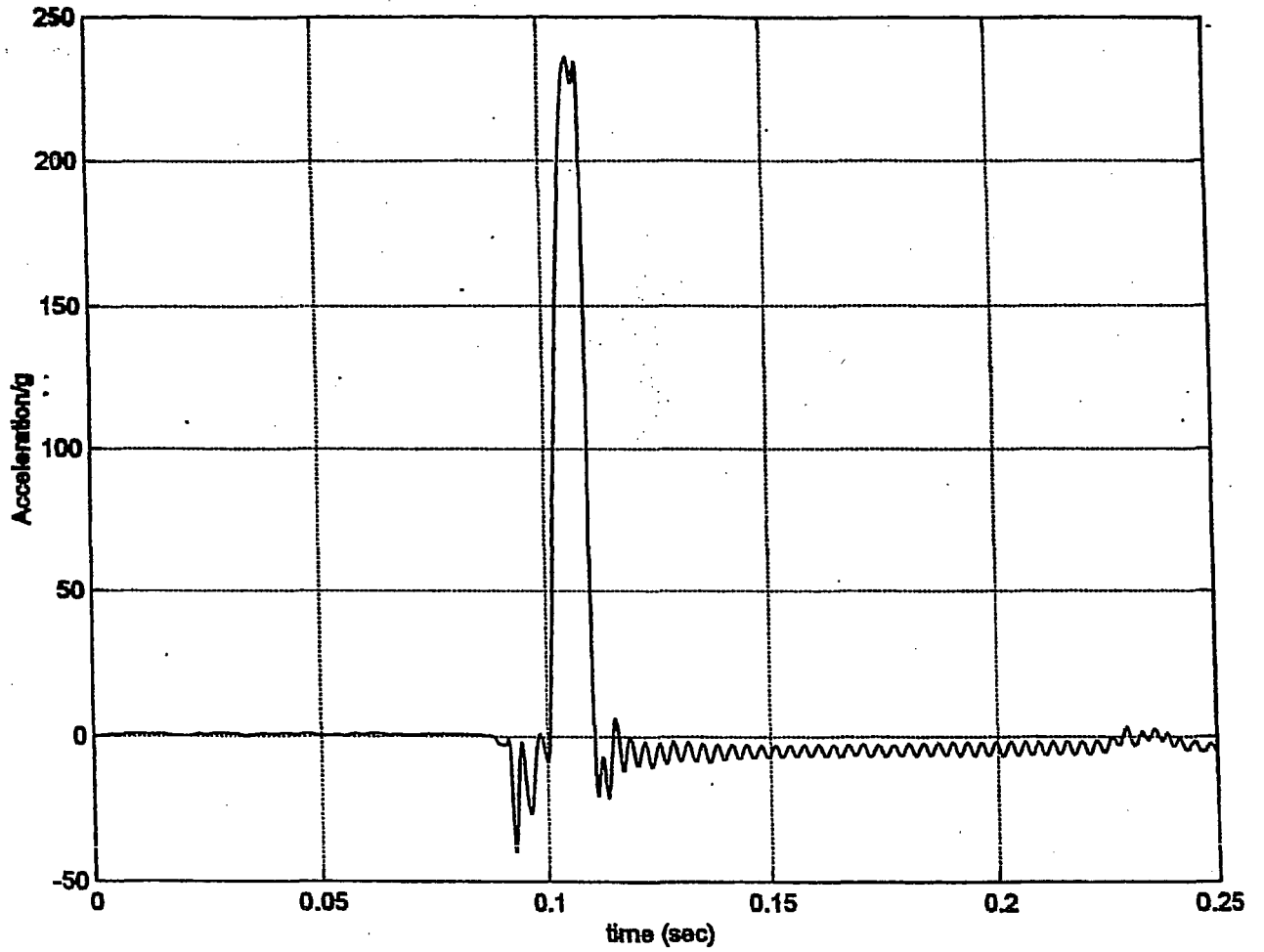


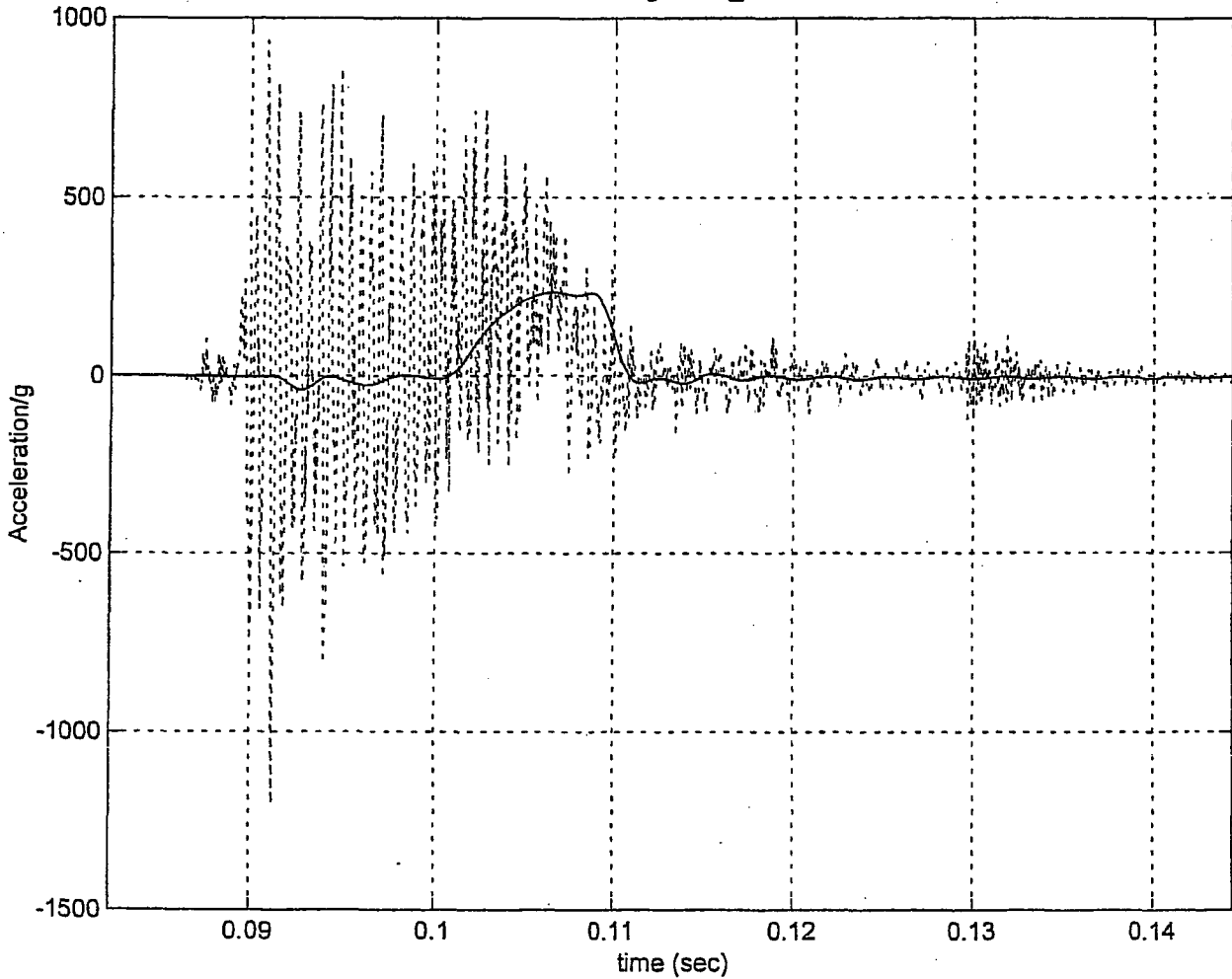
FIGURE 2.A.5.19 ; ACCELERATION DATA FILTERED AT 350 Hz FOR SLAPDOWN DROP

HI-951251

REV. 10

**FIGURE 2.A.5.19A ; SLAP DOWN**

Filtered (—) and Unfiltered (...) Accelerations, Cutoff Freq. = 350 Hz  
Maximum Accel: for 1/4 scale model 236g; for prototype 59g  
From Program sl\_bw1.m



HI-951251

REV. 10

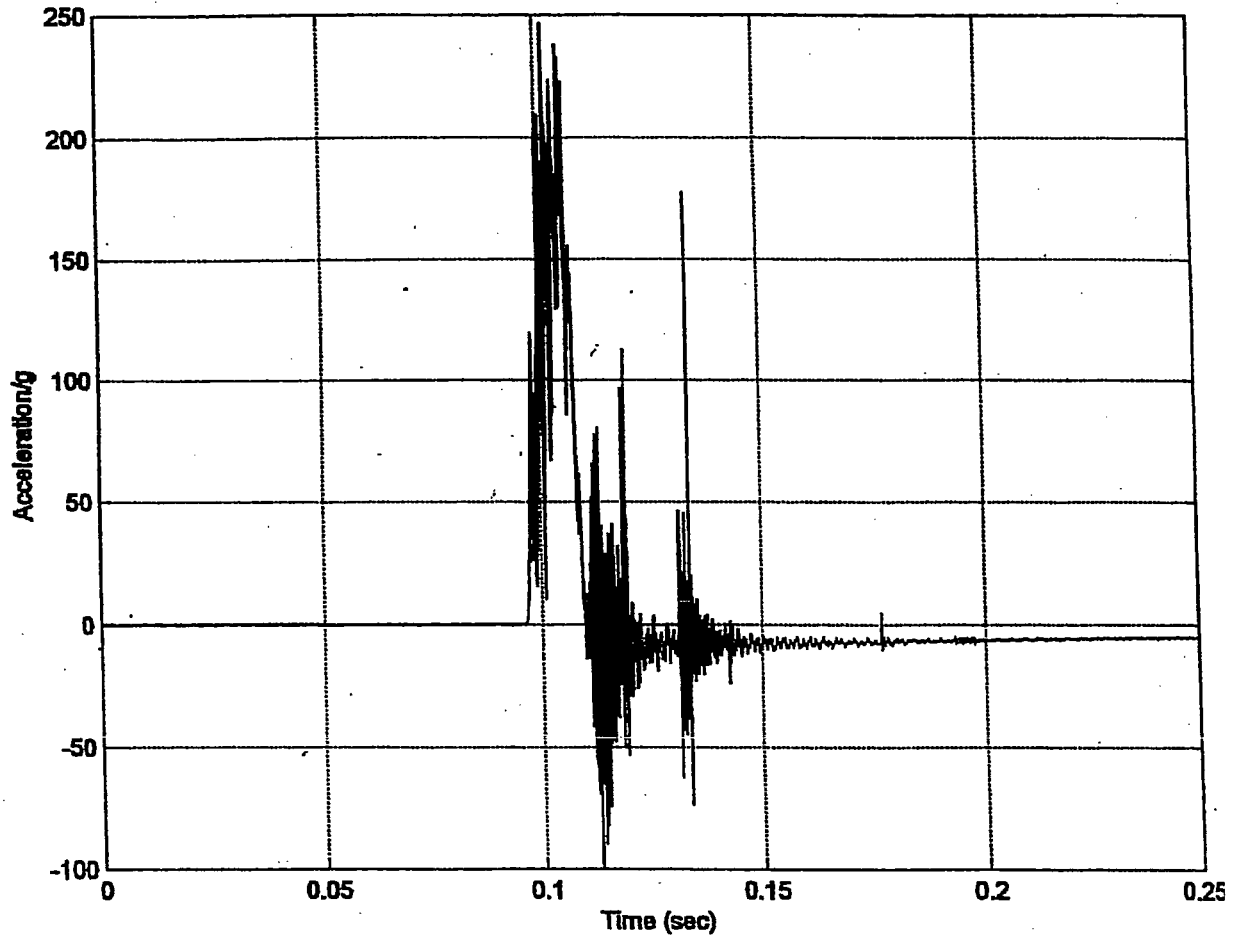


FIGURE 2.A.5.20 : ACCELERATION RAW DATA FOR SIDE DROP

HI-951251

REV. 10

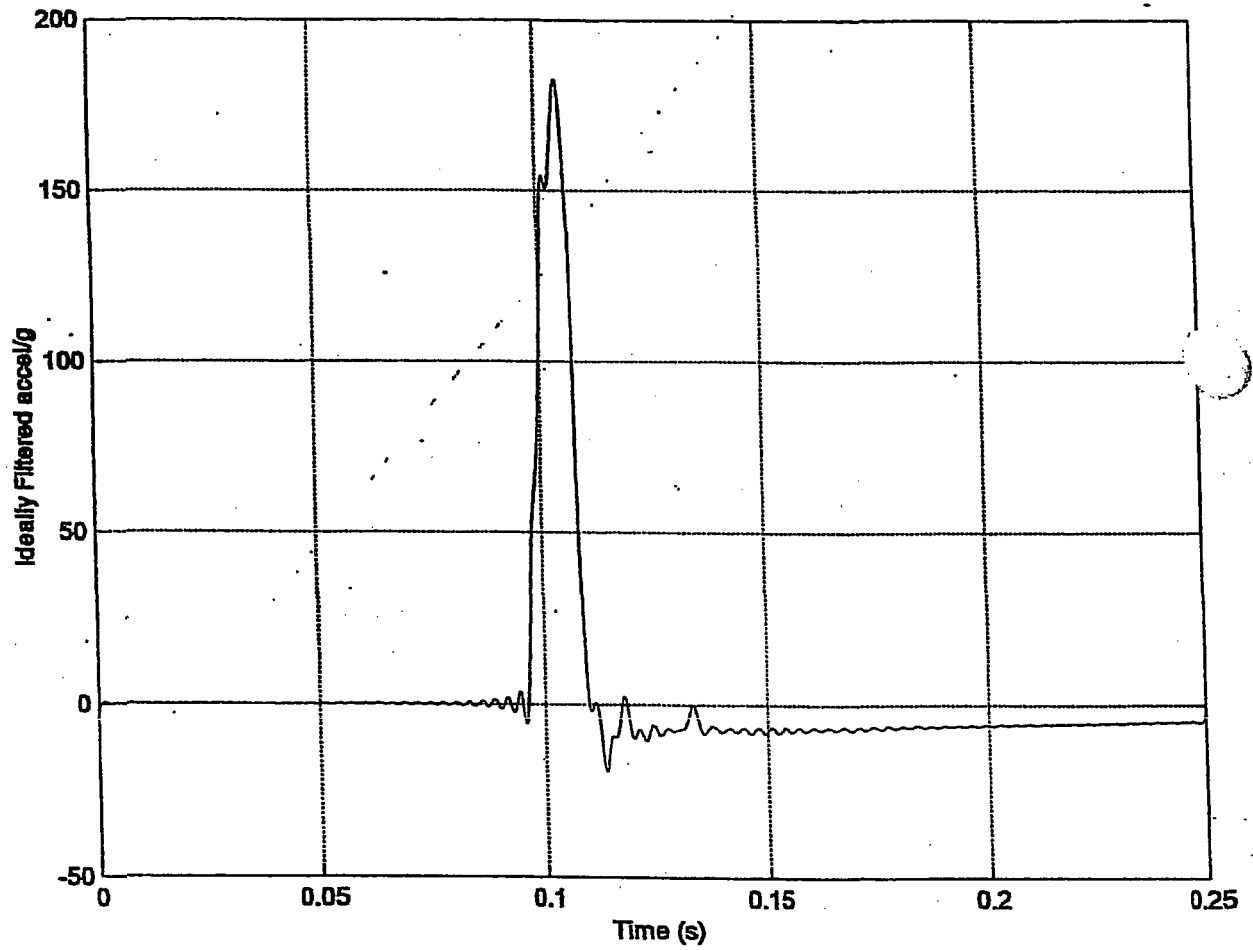


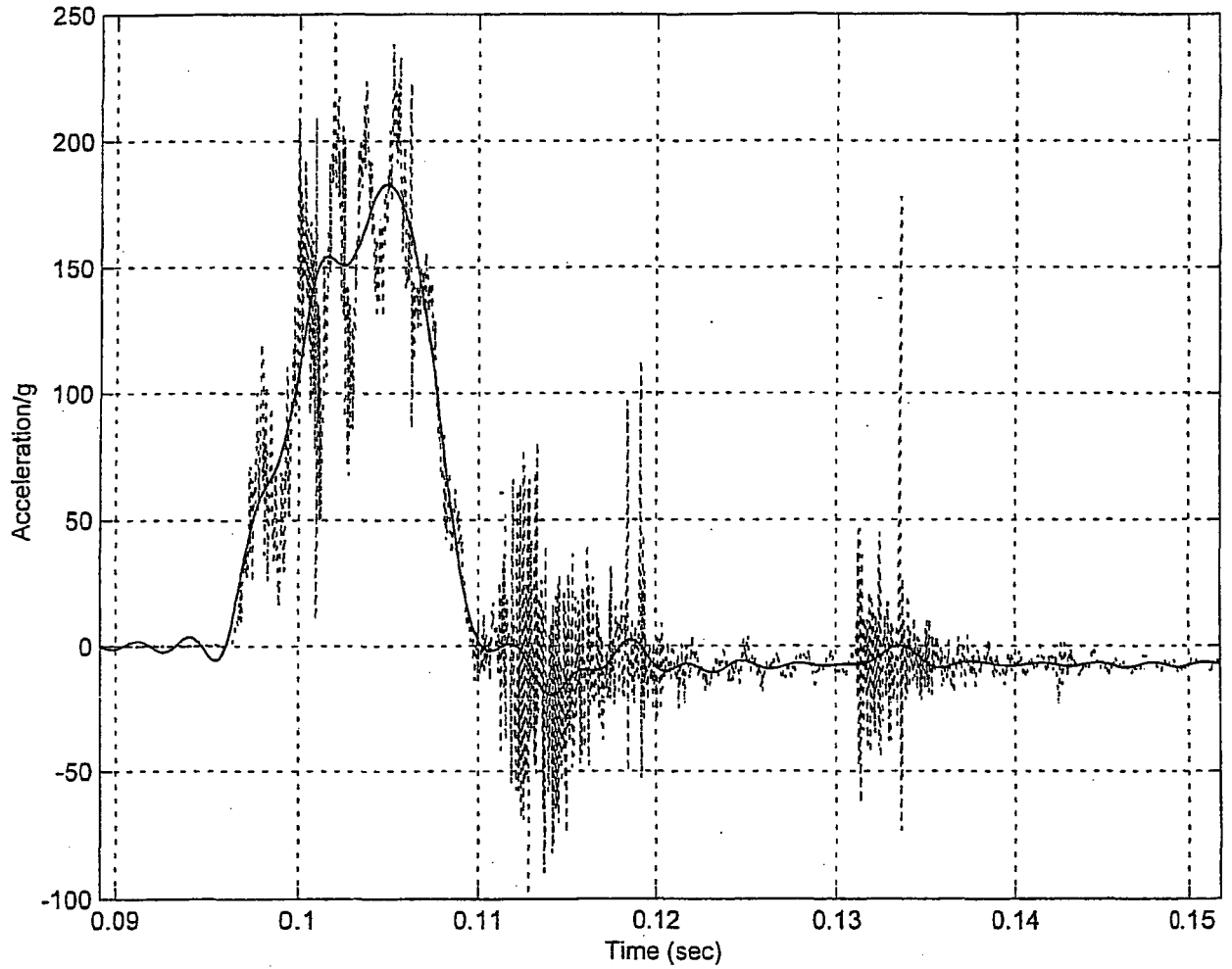
FIGURE 2.A.5.21; ACCELERATION DATA FILTERED AT 350 Hz FOR SIDE DROP

HI-951251

REV. 10

FIGURE 2.A.5.21A

Filtered (—) and Unfiltered (...) Accelerations, Cutoff Freq. = 350 Hz  
Max. Filtered Acceleration = 182.6244g, at time = 0.10492 s



HI-951251

REV. 10

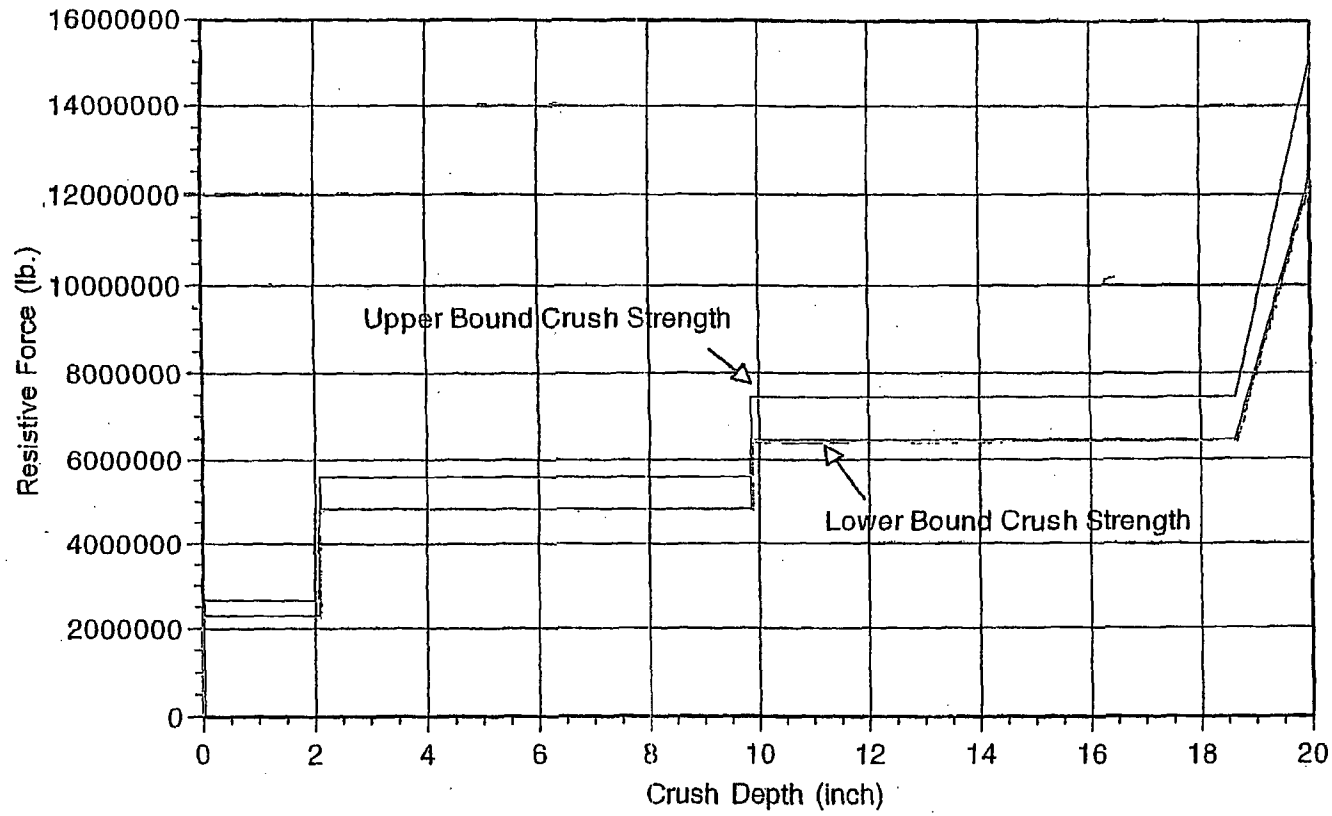


FIGURE 2.A.6.1 ; - Impact Limiter Force vs. Crush Depth ( $\theta = 90$  degrees)

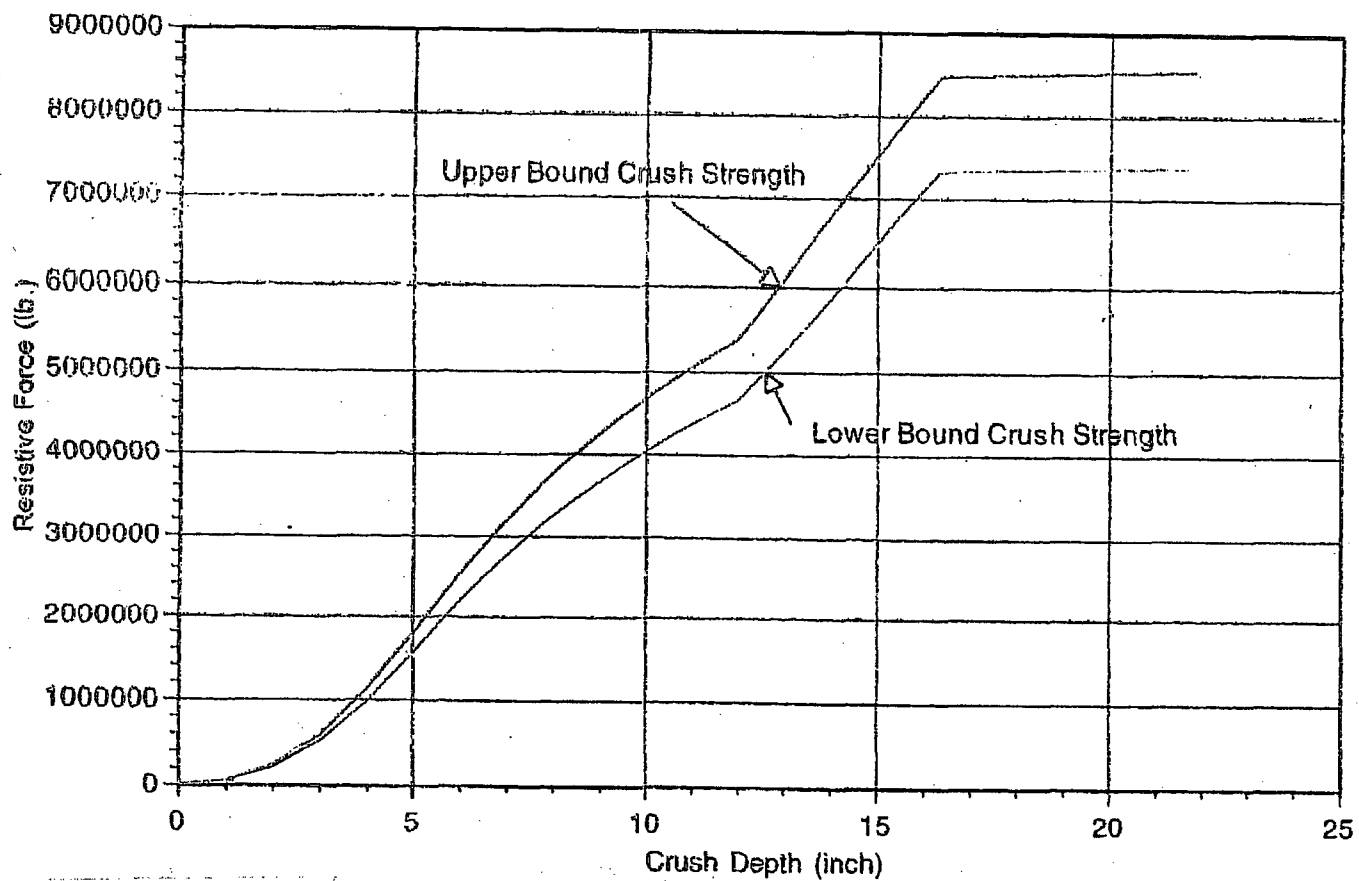


FIGURE 2.A.6.2 ; Impact Limiter Force vs. Crush Depth ( $\theta = 67.5$  degrees)

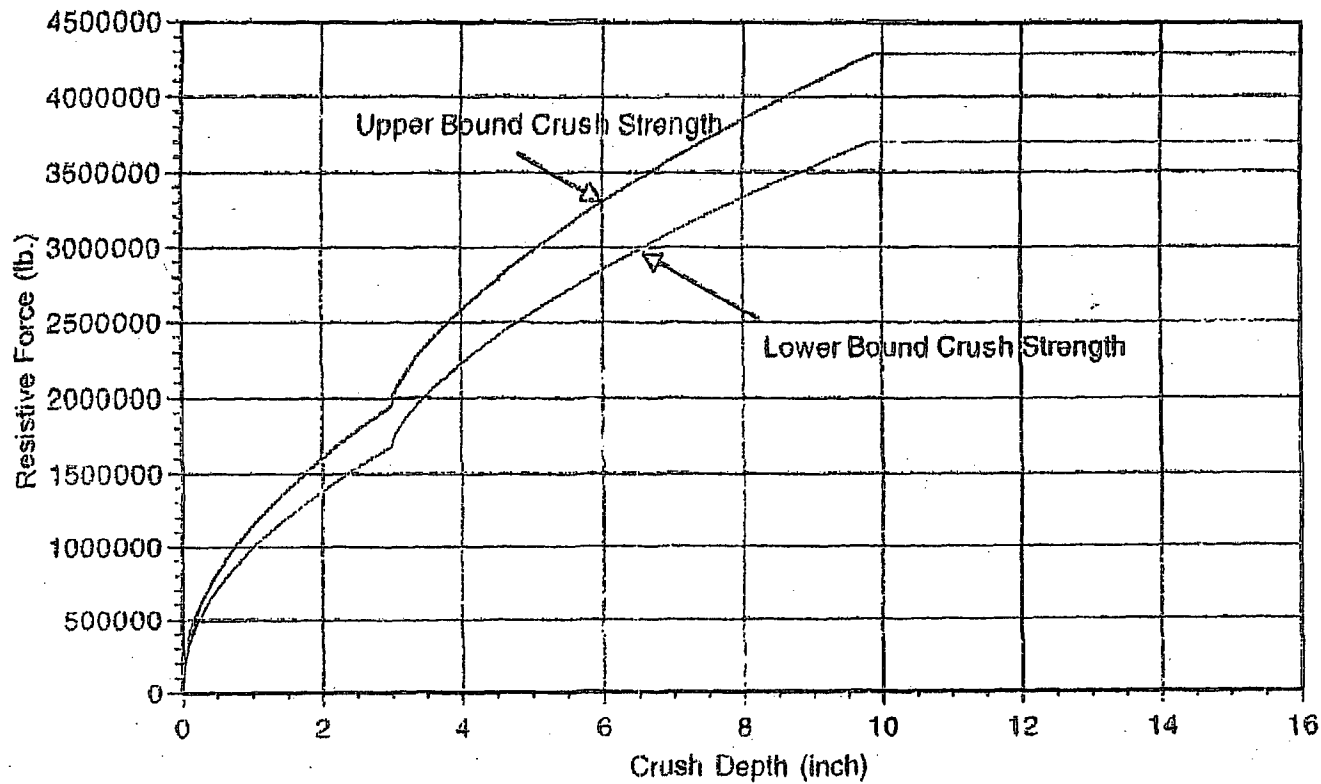


FIGURE 2A.6.3 : - Impact Limiter Force vs. Crush Depth ( $\theta = 0$  degrees)

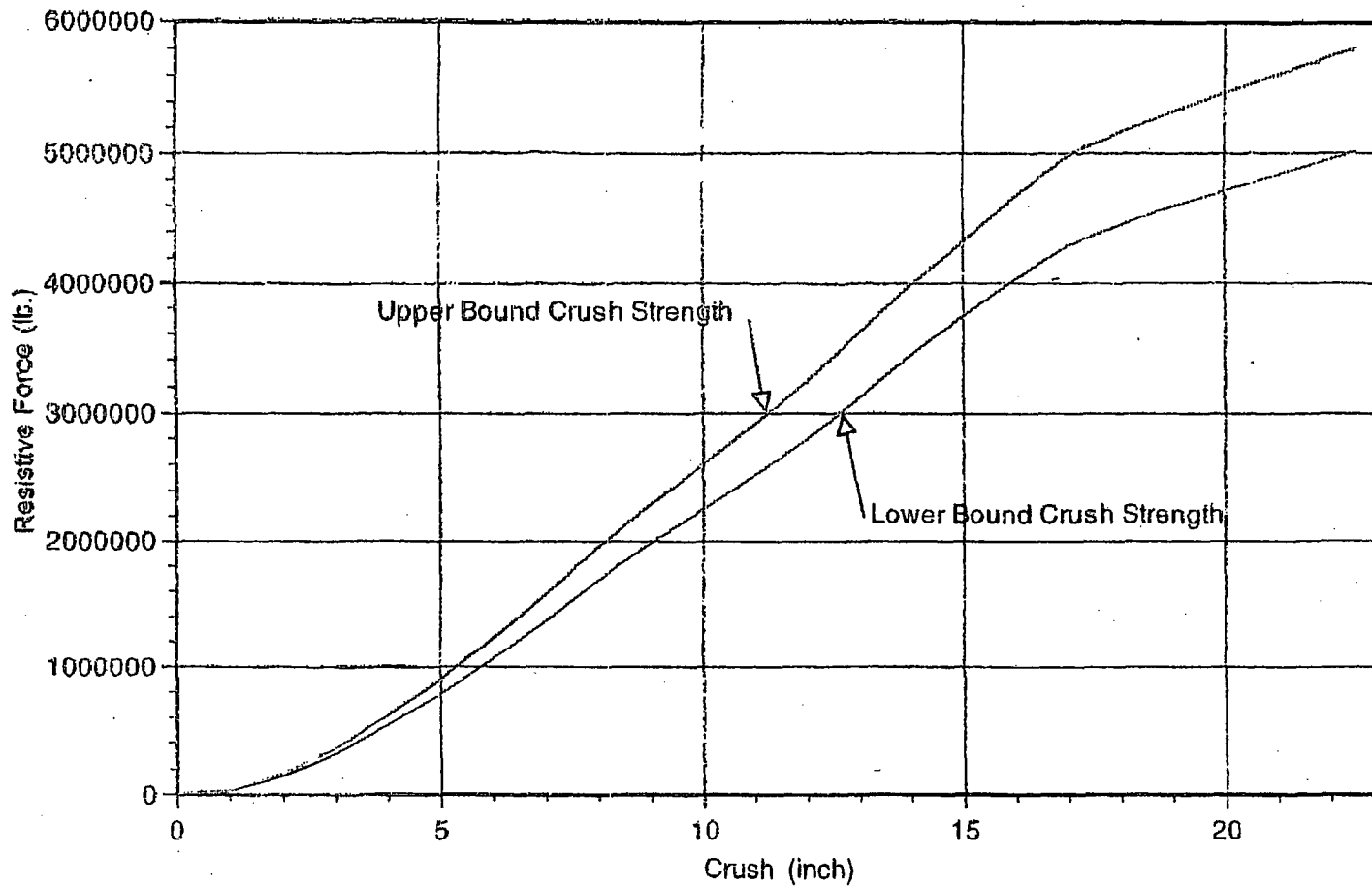
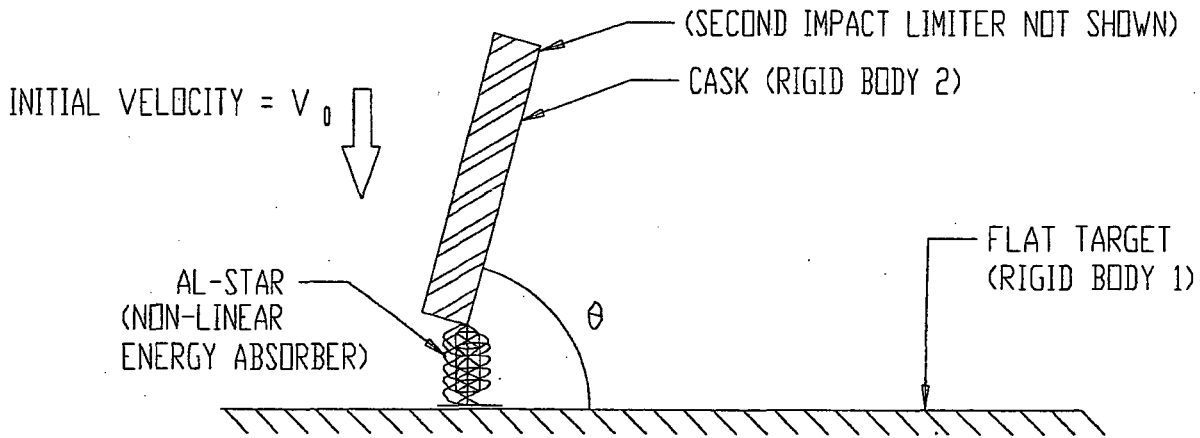
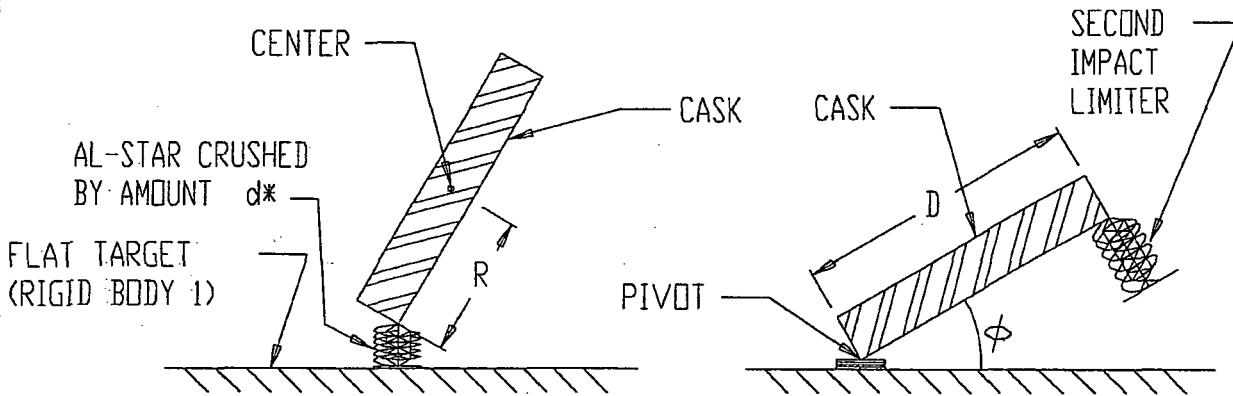


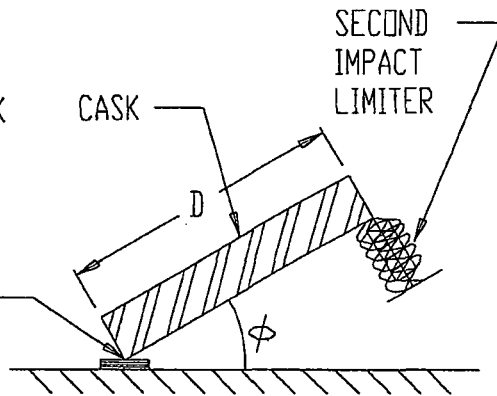
FIGURE 2.A.6.4 : Impact Limiter Force vs. Crush Depth ( $\theta = 15$  degrees)



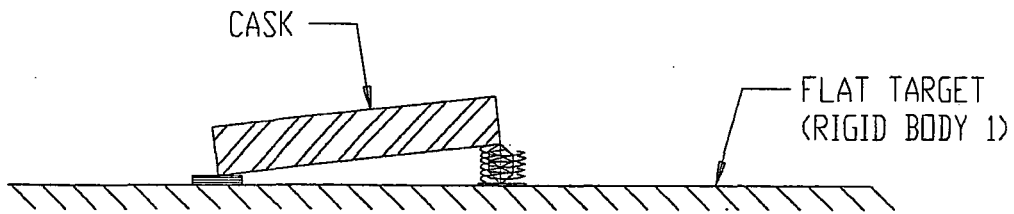
(a) INITIATION OF IMPACT AT AN OBLIQUE ANGLE ( $\theta \approx 67.5^\circ$ )



(b) CONCLUSION OF PRIMARY IMPACT; AXIAL VELOCITY  $\approx 0$

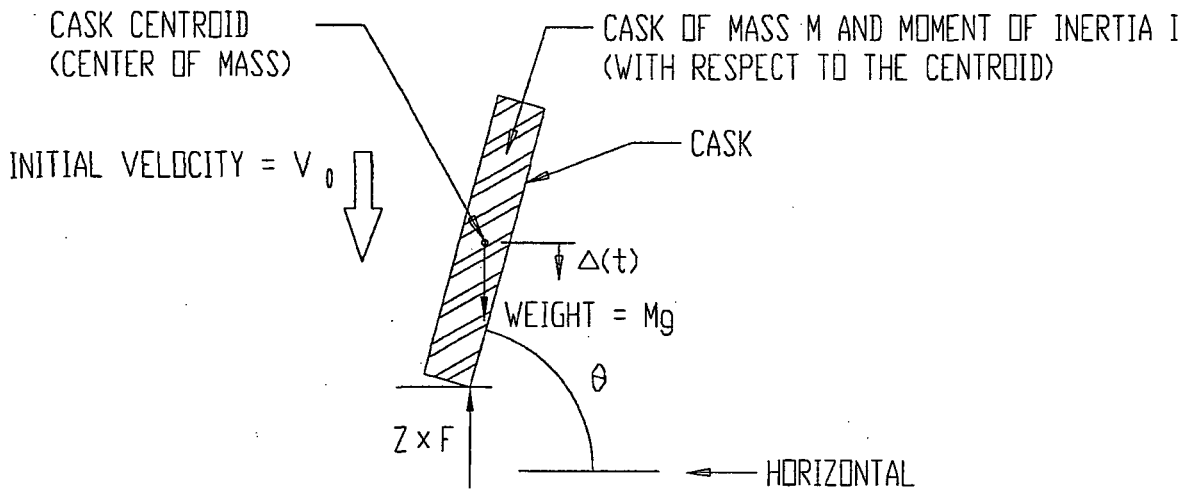


(c) PACKAGE PIVOTS ABOUT THE FIRST COLLISION LOCATION

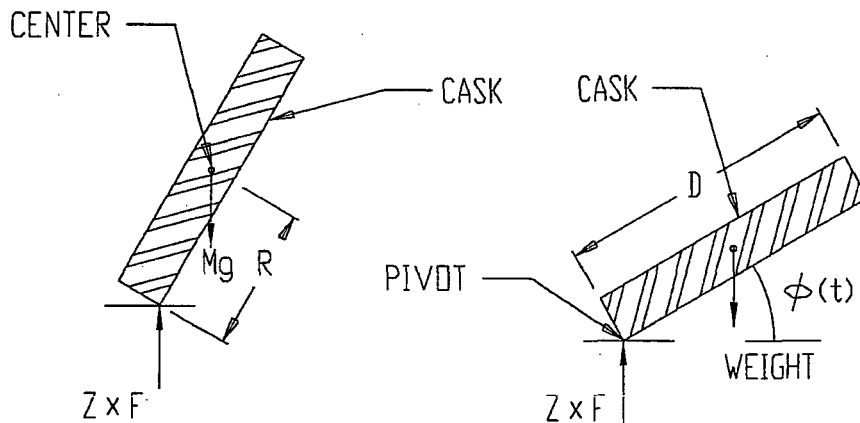


(c) SECONDARY IMPACT AT THE SECOND IMPACT LIMITER

FIGURE 2.A.6.5; DYNAMIC MODEL FOR DUAL IMPACT SCENARIOS

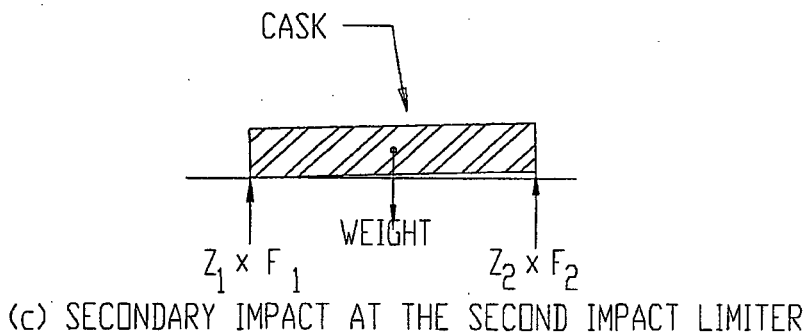


(a) INITIATION OF IMPACT AT AN OBLIQUE ANGLE ( $\theta \approx 67.5^\circ$ )



(b) CONCLUSION OF PRIMARY IMPACT;  
AXIAL VELOCITY  $\approx 0$

(c) PACKAGE PIVOTS ABOUT THE  
FIRST COLLISION LOCATION



(c) SECONDARY IMPACT AT THE SECOND IMPACT LIMITER

FIGURE 2.A.6.6; FREE-BODY DIAGRAM FOR IMPACT SCENARIOS

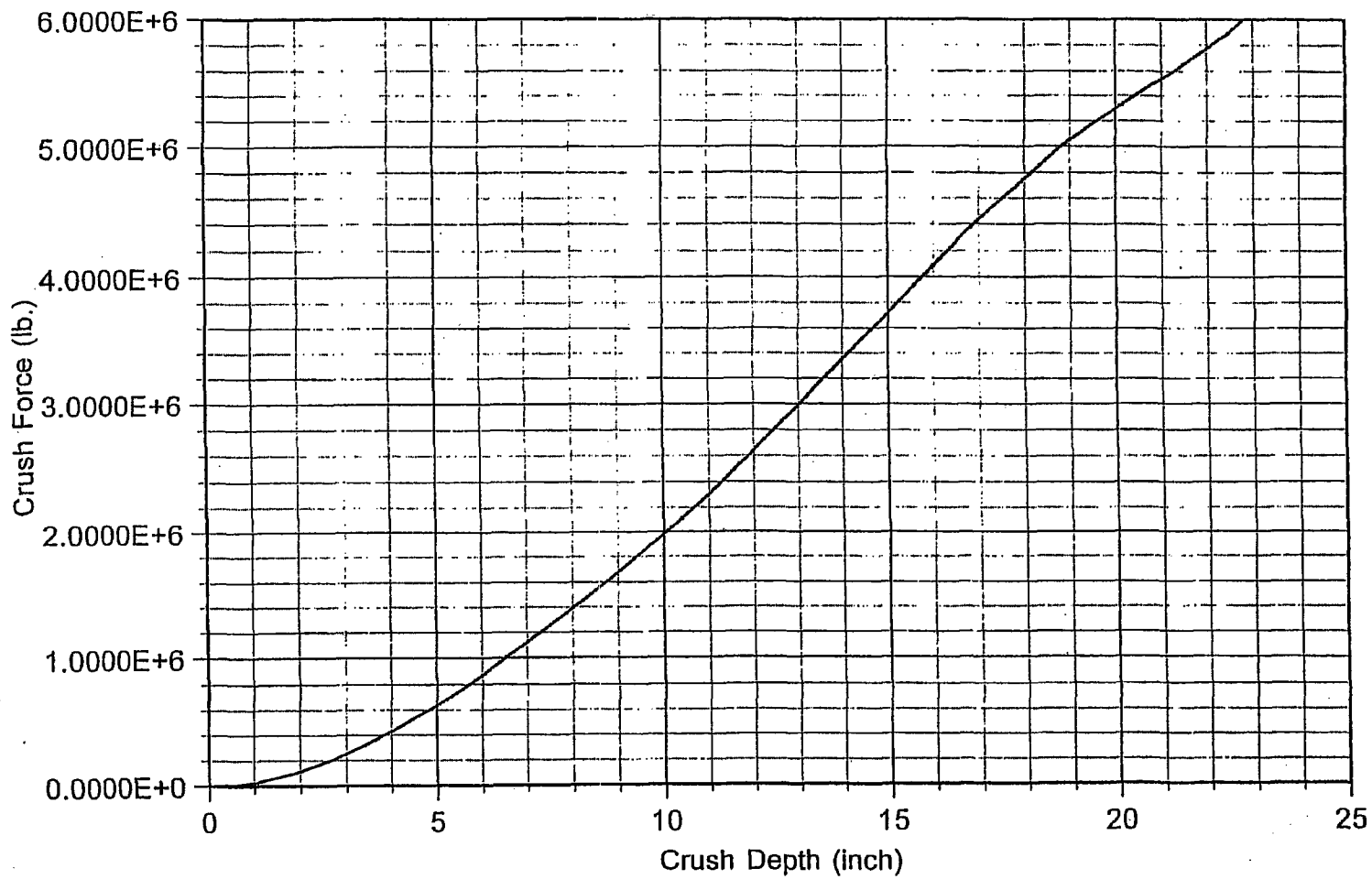


FIGURE 2.A.7.1 ; Static Crush Force vs Crush Depth - Impact at 30 Degrees with Horizontal Target

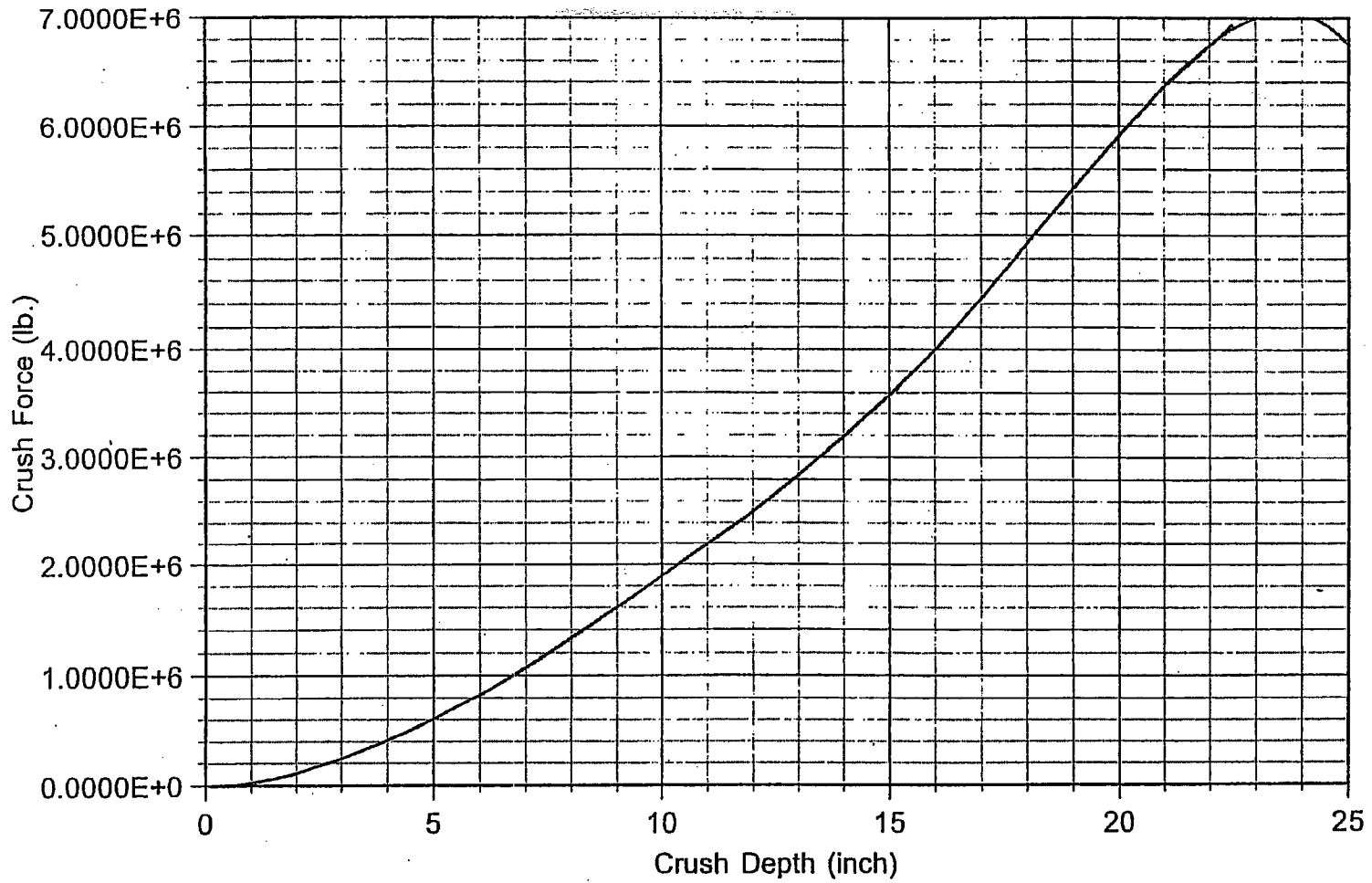


FIGURE 2.A.7.2 ; Static Crush Force vs Crush Depth - Impact at 45 Degrees with Horizontal Target

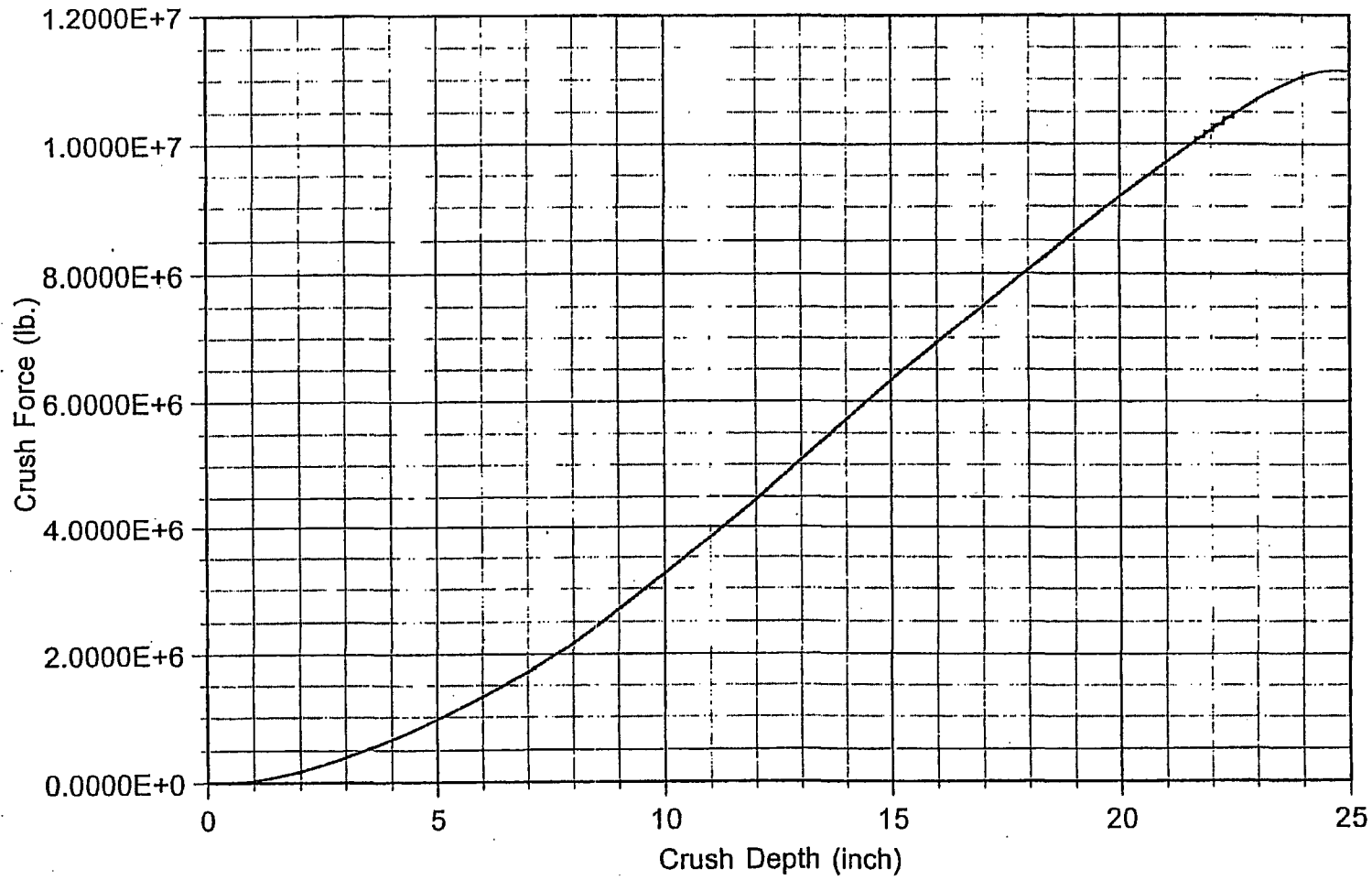


FIGURE 2.A.7.3 ; Static Crush Force vs Crush Depth - Impact at 60 Degrees with Horizontal Target

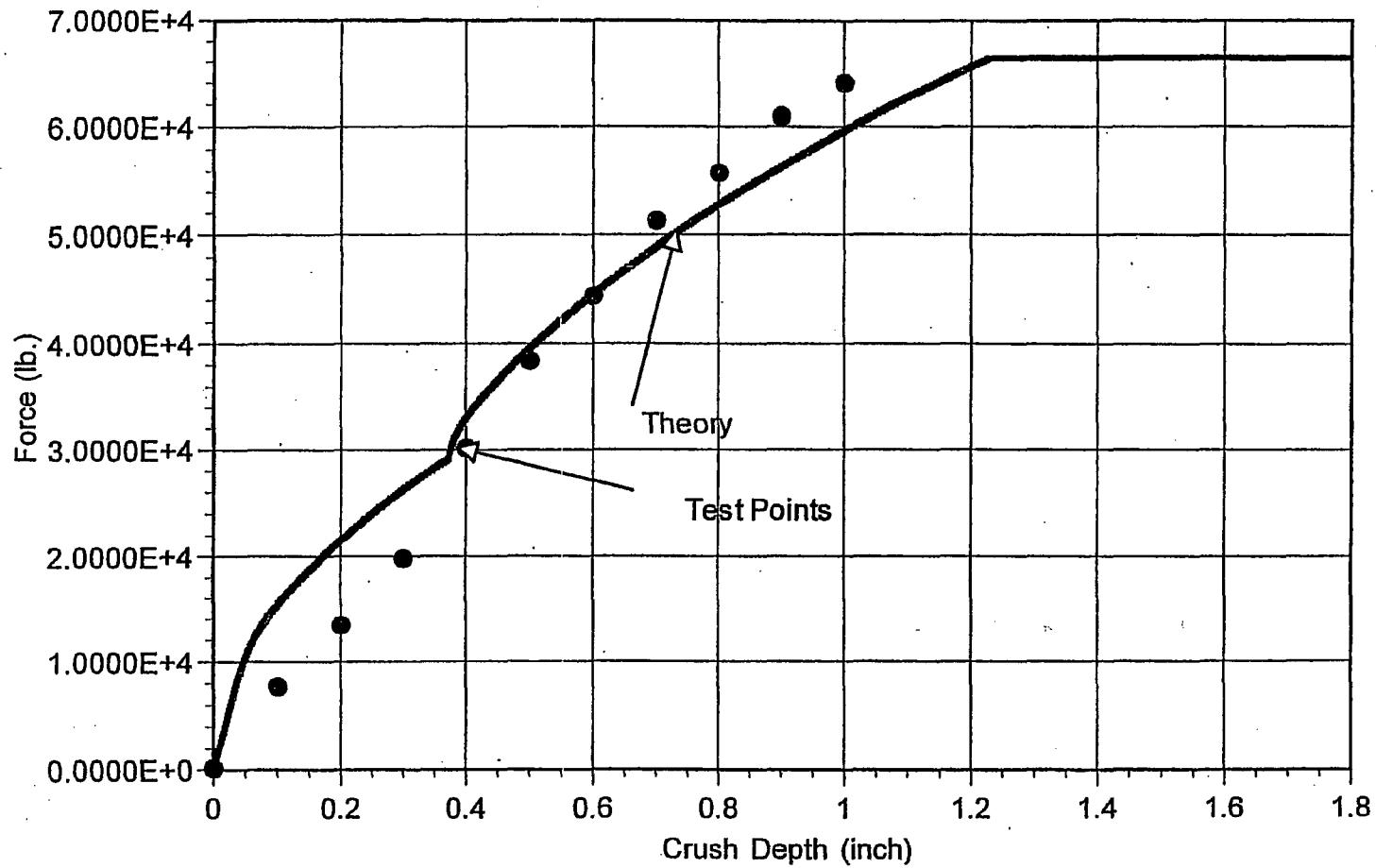


FIGURE 2.A.10.1 ; 1/8th Scale Impact Limiter - Crush Force vs. Crush Depth - Side Orientation -  
HI-951251 REV. 10

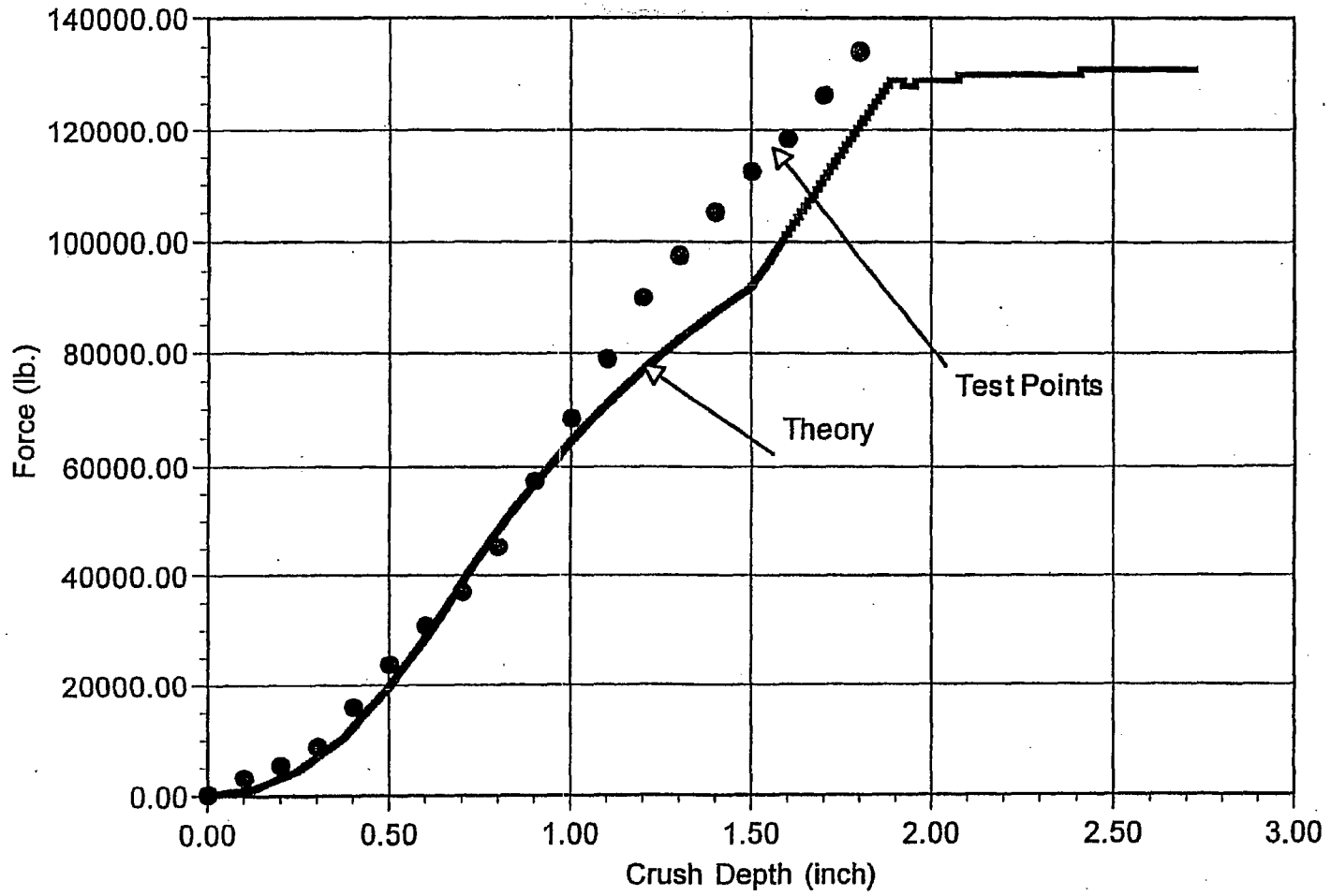


FIGURE 2.A.10.2 ; 1/8th Scale Impact Limiter - Crush Force vs. Crush Depth - Center of Gravity Over Corner Orientation  
HI-951251 REV. 10

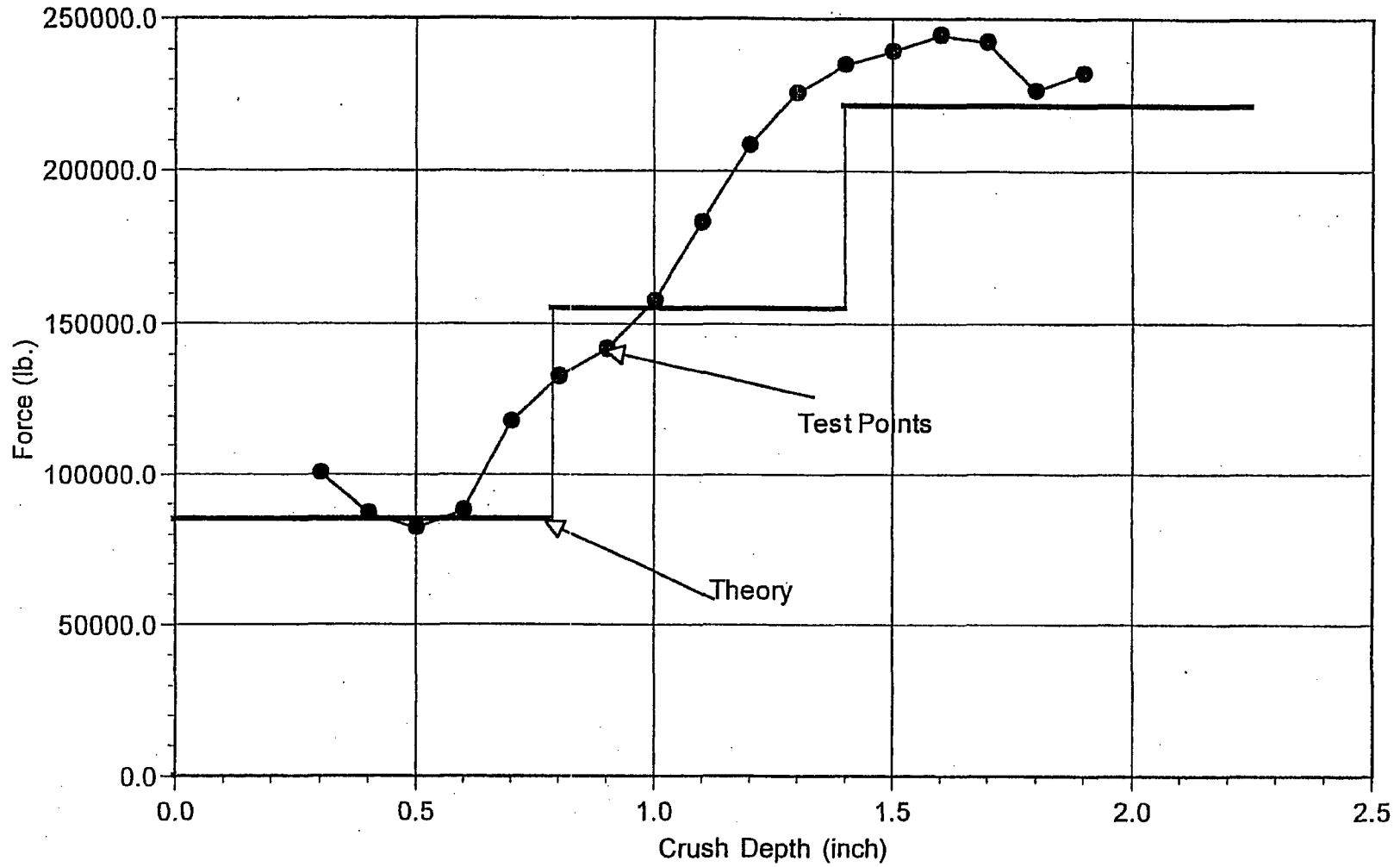


FIGURE 2.A.10.3 : 1/8th Scale Impact Limiter - Crush Force vs. Crush Depth - End Orientation  
HI-951251 REV. 10

## Appendix 2.B

**SUMMARY OF RESULTS FOR STRUCTURAL INTEGRITY OF DAMAGED FUEL  
CANISTERS****2.B.1 Introduction**

Damaged Fuel Canisters or Containers (DFCs) to be deployed in the HI-STAR 100 System transport package have been evaluated to demonstrate that the canisters are structurally adequate to support the mechanical loads postulated during normal lifting operations while in long-term storage, and during a hypothetical end drop accident condition. The evaluations address the following damaged/failed fuel canisters for transportation in the Hi-STAR 100 System:

- Holtec-designed DFC for Dresden Unit 1 and Humboldt Bay fuel
- Transnuclear designed DFC for Dresden Unit 1 fuel
- Dresden Unit 1 Thoria Rod Canister
- Holtec-designed DFC for Trojan plant fuel
- Sierra Nuclear Corporation (SNC)-designed Failed Fuel Can for Trojan plant fuel

**2.B.2 Methodology**

The structural load path in each of the analyzed canisters was evaluated using basic strength of materials formulations. The various structural components were modeled as axial or bending members and stresses computed. Depending on the particular DFC, the load path includes components such as the container sleeve and collar, various weld configurations, load tabs, closure components and lifting bolts. Axial plus bending stresses were computed, together with applicable bearing stresses and weld stresses. Comparison with appropriate allowable strengths at temperature was performed. Input data for all applicable DFC's came from the drawings. The design temperature for lifting evaluation was 150°F (since the DFC is in the spent fuel pool). The design temperature for accident conditions is 725°F.

For the SNC-designed Trojan Failed Fuel Can, the existing calculations prepared by SNC were reviewed by Holtec and determined to bound the loadings applicable to the HI-STAR 100 System. Therefore, no new calculations were prepared for the Trojan Failed Fuel Can.

**2.B.3 Acceptance Criteria**

The upper closure assembly must meet the requirements set forth for special lifting devices used in nuclear applications [1]. The remaining components of the damaged fuel canister are governed by the stress limits of the ASME Code Section III, Subsection NG and Section III, Appendix F, as applicable [2].

#### 2.B.4 Assumptions

Buckling is not a concern during an accident since during a drop, the canister will be supported by the walls of the fuel basket.

The strength of welds is assumed to decrease the same as the base metal as temperatures increase.

An inertia load factor 1.15 is applied to all loads during a lifting analysis, except for the lifting analysis of the Trojan failed fuel can which assumes a 10% dynamic load factor.

#### 2.B.5 Summary of Results

Table 2.B.1 presents minimum safety factors for each DFC from among all of the computations and evaluations performed on the different damaged fuel canisters to be certified for transport in the HI-STAR 100 System.

#### 2.B.6 References

- [1] ANSI N14-6-1993, "American National Standard for Special Lifting Devices for Shipping Containers Weighing 10,000 Pounds (4,500 kg) or More for Nuclear Materials", ANSI, Inc.
- [2] ASME Boiler and Pressure Vessel Code, Section III, Subsection NG and Appendix F, 1995.

Table 2.B.1

## SUMMARY OF SAFETY FACTORS FOR DAMAGED FUELCONTAINERS

Unit – (Maximum weight including contents -lbs)	Component	Calculated Stress (ksi)	Allowable Stress (ksi)	Safety Factor = (Allowable Value)/(Calculated Value)	Remarks
Holtec-designed Dresden (BWR) DFC	Lifting – Upper Closure Assembly	1.687	1.9251	1.141	Allowable weld stress includes a 0.35 quality factor
	60g end drop	10.667	37.920	3.6	Level D stress limits
Transnuclear DFC (550 lb.)	Lifting – Lid Frame Assembly	0.526	4.583	8.7	Bearing Stress
	60g end drop	12.316	37.920	3.1	Level D stress limits
Dresden Thoria Rod Canister (390 lb.)	Lifting – Lid Frame Assembly	0.3735	4.583	12.27	Bearing Stress
	60g end drop	8.733	37.920	4.3	Level D stress limits
Holtec-designed Trojan DFC (1680 lb.)	Lifting – Lifting Bolt	13.702	25.000	1.825	
	60g end drop	11.618	26.586	2.3	Spot welds
Trojan Failed Fuel Can	Lifting – Lifting Bar	6.2	6.37 <sup>†</sup>	1.03	Bending Stress
	124g end drop	8.25	11.7	1.42 <sup>††</sup>	Level D stress limits

<sup>†</sup> Allowable stress is equal to 1/3 of yield stress per [1].

<sup>††</sup> Conservatively based on bounding 124g vertical end drop used in SNC calculations. Per Table 2.1.10, the design basis deceleration for the HI-STAR 100 is 60g.

APPENDIX 2.C:  
EVALUATION OF AN IMPROVED HI-STAR 100 IMPACT LIMITER DESIGN  
BASED ON LS-DYNA DROP SIMULATIONS

**THIS APPENDIX IS PROPRIETARY IN ITS ENTIRETY**

## SUPPLEMENT 2.I: HI-STAR HB STRUCTURAL EVALUATION

### 2.I.0 OVERVIEW

In this supplement, the structural adequacy of the HI-STAR HB is evaluated pursuant to the guidelines of NUREG-1617 and the requirements of 10CFR71. The organization of this supplement mirrors the format and content of Chapter 2 except it only contains material directly pertinent to the HI-STAR HB.

The HI-STAR HB is a shortened version of the HI-STAR 100 that is evaluated in Chapter 2. All dimensions (radius, thickness) of the HI-STAR HB are identical to those of the HI-STAR 100 except for the overall length of the layered cylinders, the threaded diameter of the lifting trunnions, and the enclosure shell radial gussets. The impact limiters are identical in all respects except for the crush strengths of the internal aluminum honeycomb material, which are reduced to ensure that the deceleration limits are met with the lighter weight HI-STAR HB. The HI-STAR HB is configured to carry the MPC HB that has the appropriate length and fuel basket design to carry 80 spent fuel assemblies from the closed Humboldt Bay Nuclear Plant. The qualification of the MPC HB to withstand a 60g deceleration has been documented in the Part 72 license for Humboldt Bay (Humboldt Bay ISFSI, Pacific Gas and Electric Company, Final Safety Analysis Report Update, Revision 0 January 2006, NRC Docket No. 72-27). Therefore, no new analyses of the MPC HB are required in this Supplement 2.I as long as the maximum cask deceleration remains bounded by 60g.

The applicable design codes and standards, and the design criteria for the HI-STAR HB are identical to those applied to the HI-STAR 100. Therefore, since the differences between the HI-STAR HB and HI-STAR 100 are limited to:

- Shorter overall length;
- Lower package weight;
- Reduced strength of impact limiter crush materials;
- Smaller diameter threads on lifting trunnions;
- Decreased number and length of enclosure shell radial gussets,

the supplement is focused on documenting the results from new evaluations required because of the reported differences in length, weight, impact limiter crush strength, thread diameter, and enclosure shell geometry. The reduced length and weight of the HI-STAR HB ensures that all stress-based evaluations performed on the HI-STAR 100 produce safety factors that are lower bounds for the same evaluation on the HI-STAR HB, except for the trunnion analysis discussed below. Therefore, no stress-based calculations need to be performed, except those that involve deceleration limits, because of the change in impact limiters, those that involve the lifting trunnions, because of the smaller diameter threads, and those that involve the enclosure shell, because of the modifications to the radial gussets; this supplement focuses only on providing summaries for the new evaluations performed for the HI-STAR HB, which are documented in Holtec calculation packages HI-2084158 [2.1.7.2] and HI-2033042 [2.1.7.3].

## **2.1.1 STRUCTURAL DESIGN**

### **2.1.1.1 Discussion**

The general discussion presented in Subsection 2.1.1 applies to the HI-STAR HB package. Drawings for the components of the HI-STAR HB package are provided in Section 1.I.4.

### **2.1.1.2 Design Criteria**

The HI-STAR HB package meets the design criteria espoused in Section 2.1.2 in its entirety. For the HI-STAR HB overpack, however, the option to replace the SA203-E plate used for the 2.5" thick inner shell with comparable SA350 LF3 ring forgings, stacked to form the inner shell and welded together with full penetrant welds, has been added to the drawings. The Nil Ductility Transition Temperature is still required to be less than -70 degrees F when this option is used (per Subsection 2.1.2.3). Accordingly, Table 2.1.22 lists SA350 LF3 as an optional material for the inner shell. Similarly, Table 2.1.23 lists SA350 LF3 as an option for the port cover plates.

## **2.1.2 WEIGHTS AND CENTERS OF GRAVITY**

Table 2.I.2.1 provides the weights of HI-STAR HB components as well as the total package weight. The weight of the impact limiter is also provided. Table 2.I.2.1 also provides the location of the calculated center of gravity for the HI-STAR HB package.

### **2.I.3 MECHANICAL PROPERTIES OF MATERIALS**

Materials for the HI-STAR HB package are identical to those used for the HI-STAR 100 package.

### **2.I.4 GENERAL STANDARDS FOR ALL PACKAGES**

The HI-STAR HB is a shorter and lighter version of the HI-STAR 100. Therefore, the features presented in Section 2.4 apply to the HI-STAR HB.

### **2.I.5 LIFTING AND TIE-DOWN STANDARDS**

#### **2.I.5.1 Lifting Devices**

The lifting devices for the HI-STAR HB package are identical to those for the HI-STAR 100, except that the threaded portion of the lifting trunnions has a slightly smaller diameter. Therefore, even though the HI-STAR HB is lighter than the HI-STAR 100, the safety factors for the HI-STAR HB lifting trunnions and the top flange interface are recalculated based on the smaller trunnion diameter.

The embedded trunnion is analyzed as a cantilever beam in the same manner as described in Subsection 2.5.1.1. Calculations demonstrate that the stresses in the trunnions comply with NUREG-0612 provisions.

Specifically, the following results are obtained:

Safety Factors from HI-STAR HB Lifting Trunnion Stress Analysis for a Bounding Lifted Load of 161,200 lb			
Item	Value (ksi) or (lb) or (lb-in)	Allowable (ksi) or (lb) or (lb-in)	Safety Factor
Bending stress (Comparison with Yield Stress/6)	11.2	24.5	2.19
Shear stress (Comparison with Yield Stress/6)	4.76	14.7	3.09
Bending Moment (Comparison with Ultimate Moment/10)	208,600	574,400	2.75
Shear Force (Comparison with Ultimate Force/10)	92,690	282,500	3.05

We note from the above that all safety factors are greater than 1.0. A factor of safety of exactly 1.0 means that the maximum stress, under apparent lift load  $D^*$ , is equal to the yield stress in tension or shear divided by 6, or that the section moment or shear force is equal to the ultimate section moment capacity or section force capacity divided by 10.

It is also important to note that safety factors associated with satisfaction of 10CFR71.45(a) are double those reported in the table since 10CFR71.45 only requires a factor of safety of 3 on the yield strength.

The top flange interface with the trunnion under the lifted load is analyzed in the same manner as described in Subsection 2.5.1.2.2. The interface region is conservatively considered as subject to the provisions of NUREG-0612, and the thread shear stress and bearing stress are compared to 1/6 of the top forging yield stress in shear or compression. The following table summarizes the results:

Top Flange B Minimum Safety Factors (Interface with Trunnion) for HI-STAR HB			
Item	Value (ksi)	Allowable (ksi)	Safety Factor
Bearing Stress (NUREG-0612 Comparison)	2.555	5.975	2.34
Thread Shear Stress (NUREG-0612 Comparison)	2.466	3.585	1.45
Stress Intensity (NB Comparison)	5.655	34.6	6.12

It is noted from the above that all safety factors are greater than 1.0 and that the safety factors for bearing stress and thread shear stress represent the additional margin over the factor of safety inherent in the member by virtue of the load multiplier mandated in NUREG-0612.

#### 2.1.5.2 Tie-Down Devices

Since the HI-STAR HB is shorter and lighter, but otherwise identical to the HI-STAR 100, the tie-down devices and the resulting tables of reaction loads in Section 2.5 bound those for the HI-STAR HB. The span between tie-down locations is less, reflecting the shorter overall length of the HI-STAR HB. The equilibrium equations presented in Subsection 2.5.2 also apply to the HI-STAR HB. No new analyses are performed.

#### 2.1.5.3 Failure of Lifting and Tie-Down Devices

The discussion in Subsection 2.5.3 for the HI-STAR 100 also applies to the HI-STAR HB, except for the following. New calculations have been performed for the HI-STAR HB to demonstrate that the ultimate load carrying capacity of the lifting trunnions is governed by the cross section of the trunnion external to the overpack top forging rather than by any section within the top forging. It is concluded that the trunnion shank reaches ultimate load capacity limit prior to the top forging reaching its corresponding ultimate load capacity limit. Loss of the external shank of the lifting trunnion will not cause loss of any other structural or shielding function of the HI-STAR HB overpack; therefore, the requirement imposed by 10CFR71.45(a) is satisfied.

The following safety factors are established:

$$\frac{\text{(Ultimate Bearing Capacity at Trunnion/Top Forging Interface)}}{\text{(Ultimate Trunnion Load)}} = 1.04$$

$$\frac{\text{(Ultimate Moment Capacity at Trunnion/Top Forging Thread Interface)}}{\text{(Ultimate Trunnion Moment Capacity)}} = 1.51$$

**2.1.5.4 Lifting of Humboldt Bay Damaged Fuel Container**

The Humboldt Bay Damaged Fuel Container (DFC) has been analyzed in [2.1.5.1] for structural integrity during a lifting operation consistent with the methodology described in Appendix 2.B of the SAR. In order to lift the HB DFC and its contents, the DFC lid is temporarily removed and a specially designed lifting tool is installed in its place. The lifting tool connects to the DFC through the four machined slots (one per side) near the top of the DFC tube. Once the DFC has been moved to its new location, the lifting tool is disengaged and the DFC lid is re-installed. The minimum safety factor for the HB DFC during lifting is provided in the following table, and shows that the factor of safety is greater than 1.0.

Unit	Component	Calculated Stress (ksi)	Allowable Stress (ksi)	Safety Factor = (Allowable Value)/(Calculated Value)
Holtec Designed HB DFC	Lifting – DFC Top Ring	19.042	30.000	1.575

**2.1.6 NORMAL CONDITIONS OF TRANSPORT**

The HI-STAR HB package, when subjected to the normal conditions of transport specified in 10CFR71.71, meets the design criteria in Subsection 2.1.2 (derived from the stipulations in 10CFR71.43 and 10CFR71.51). The HI-STAR HB is identical to the HI-STAR 100 in all respects except for the length of the overpack (and the MPC HB), the crush strength of the impact limiter material, the lifting trunnion thread diameter, and the configuration of the enclosure shell radial gussets; the total package weight is bounded by the package weights listed for the HI-STAR 100. Component diameters and thicknesses for the HI-STAR HB overpack and its closures are identical to those of the HI-STAR 100. Therefore, with the exception of the

lifting trunnions and the enclosure shell, all stress analysis results associated with the HI-STAR HB overpack are bounded by the available results for the HI-STAR 100. No new analyses are reported in this supplement except for those associated with the performance of the impact limiter, the lifting trunnions, and the enclosure shell. Stress results for the MPC HB have been reported in detail in the Humboldt Bay ISFSI FSAR [2.I.6.1]; the MPC HB analyses were performed using the design basis deceleration.

#### 2.I.6.1 Heat

Consistent with Regulatory Guide 7.9, the thermal evaluation of the HI-STAR HB is performed in Supplement 3.I and sets material temperatures, which are used in the structural evaluations discussed in this section and in Section 2.I.7. As the Humboldt Bay fuel is “old and cold”, the operating temperatures are at or below comparable temperatures for the HI-STAR 100 analyses. This adds additional margins since the allowable strengths will generally be higher in a comparable strength analysis using the HI-STAR HB.

Design pressures and design temperatures for all conditions of transport are listed in Tables 2.1.1 and 2.1.2, respectively. Since the design pressures and temperatures for the HI-STAR 100 and the HI-STAR HB are the same, and the HI-STAR HB is shorter than the HI-STAR 100, the stress analyses for the HI-STAR 100 in Section 2.6 give bounding results for the HI-STAR HB, except for the overpack enclosure shell.

In the HI-STAR HB, the number and length of the enclosure shell radial gussets have been reduced significantly as compared to the HI-STAR 100 (see drawings in Section 1.I.4). Therefore, a new analysis has been performed for the HI-STAR HB to demonstrate the structural integrity of the overpack enclosure shell and the overpack enclosure return under a bounding internal pressure. It is shown that large safety factors exist against overstress due to an internal pressure developing from off-gassing of the neutron shield material combined with a reduced external pressure. The minimum safety factors are summarized below:

Location	Calculated Stress (ksi)	Allowable Stress (ksi)	Safety Factor
Enclosure Shell	1.00	26.3	26.3

Return (bottom)			
Enclosure Shell Return (top)	3.55	26.3	7.42
Enclosure Shell	4.32	17.5	4.05
Weld Shear	0.46	10.5	22.8

The change in the enclosure shell radial gussets also has a minor effect on the global response of the HI-STAR HB overpack to a lateral drop because of the change in the gross metal cross section. Specifically, the area moment of inertia of the HI-STAR HB, at a cross section through the enclosure shell cavity, is roughly 5% lower than the HI-STAR 100 due to the difference in the enclosure shell radial gussets. However, this small decrease in the gross section properties is completely offset by the almost 40% decrease in the cask containment cavity length. The net effect of the change in the enclosure shell radial gussets and the shorter cavity length is a HI-STAR HB overpack that is stronger in bending than the HI-STAR 100 overpack.

In summary, because of the lower weight and shorter length, all stress analyses performed for the HI-STAR 100 using the bounding deceleration inputs give stress results that are equal to or greater than results using the HI-STAR HB.

#### 2.I.6.1.1 Manufacturing Deviations

This subsection addresses specific manufacturing deviations that have occurred and potentially have an adverse impact on the structural performance of the HI-STAR HB.

HI-STAR HB Serial # 1020-012 has five closure lid bolt holes (out of 54) with useable thread lengths less than the minimum length specified on the licensing drawing. The worst case hole has a useable thread length of 1.5" compared to the design basis length of 3.25". At these five locations the preload torque on the overpack closure plate bolts is reduced to a maximum of 750 ft-lb. The remaining 49 bolts are torqued per the requirements of Table 7.1.1. This deviation has been evaluated and determined to be acceptable because:

- i) the preload force associated with the 49 fully threaded hole locations is sufficient to maintain compression on the closure plate seals during normal operation of the HI-STAR HB system and to prevent gross unloading of all bolts during hypothetical accident conditions, and;
- ii) the thread engagement lengths at the 5 non-conforming hole locations are sufficient to meet ASME Section III, Subsection NB stress limits at 750 ft-lb of torque.

#### 2.I.6.2 Cold

No new or modified calculations or discussions are required for this subsection.

#### 2.I.6.3 Reduced External Pressure

No new or modified calculations or discussions are required for this subsection. The stress analysis of the overpack enclosure shell in Subsection 2.I.6.1 conservatively bounds the effect of reduced external pressure (3.5 psia) by considering a higher pressure inside the enclosure shell cavity.

#### 2.I.6.4 Increased External Pressure

No additional analyses need be performed here to demonstrate package performance of the HI-STAR HB.

#### 2.I.6.5 Vibration

No new or modified calculations or discussions are required for this subsection.

#### 2.I.6.6 Water Spray

The condition is not applicable to the HI-STAR HB System per Reg. Guide 7.8 [2.1.2].

#### 2.I.6.7 Free Drop

The structural analysis of a 1-foot side drop has been performed for the HI-STAR 100 in Subsections 2.6.1 and 2.6.2 for heat and cold conditions of normal transport. As demonstrated in

Subsections 2.6.1 and 2.6.2, safety factors are well over 1.0. Since the HI-STAR HB is shorter and lighter than the HI-STAR 100, the safety factors determined in Subsections 2.6.1 and 2.6.2 are lower bounds for comparable safety factors for the HI-STAR HB. As final verification, the decelerations for the free drop for the HI-STAR HB are determined in Section 2.I.7 and shown to be less than the design basis limits for the 1-foot free drop. Results for the 1-foot drop simulations are presented in Table 2.I.7.2.

2.I.6.8 Corner Drop

This condition is not applicable to the HI-STAR HB System per [2.1.2].

2.I.6.9 Compression

The condition is not applicable to the HI-STAR HB System per [2.1.2].

## 2.1.7 HYPOTHETICAL ACCIDENT CONDITIONS

The hypothetical accident conditions, as defined in 10CFR71.73 and Regulatory Guide 7.9, have been applied to the HI-STAR 100 System in the required sequence in Subsection 2.7.

It is shown in the following subsections that the HI-STAR HB System also meets the standards set forth in 10CFR71, when it is subjected to the hypothetical accident conditions specified in 10CFR71.73.

### 2.1.7.1 Free Drop

In this subsection the performance and structural integrity of the HI-STAR HB System is evaluated for the most severe drop events. The drop events that are potentially most damaging are the end drops (top or bottom), the side drop, the orientation for which the center of gravity is directly over the point of impact, an oblique drop where the angle of impact is somewhere between center of gravity over corner and a near side drop, and an orientation where package rotation after an impact at one end induces a larger impact deceleration when the other end impacts the target (i.e., slapdown).

As has been noted, the HI-STAR HB is shorter and lighter than the HI-STAR 100, but is identical to the HI-STAR in all other aspects of geometry. The impact limiter crush strengths are adjusted from those used in the HI-STAR 100 in order to ensure that the design basis deceleration limits for the HI-STAR family continue to be met. In Section 2.7, the analysis was performed in two parts. Initially, 1/8 and 1/4 scale testing was performed to establish the characteristics of the impact limiter and to demonstrate that the experimentally obtained decelerations for all orientations of the cask were below the design basis. Analytical models were developed and demonstrated to be capable of predicting the observed responses from the experimental results. These models were used to evaluate sensitivity to crush strength change and cask weight change. Once it was established that the impact limiter configuration and crush strengths successfully limited the rigid body decelerations of the cask to below the prescribed limits, various strength analyses were performed to assess the state of stress in the cask components and ensure that the proscribed stress limits were satisfied.

As the impact limiter for the HI-STAR HB has the same geometry as the HI-STAR 100 with the sole difference being the impact limiter crush material, no qualification testing is employed. In lieu of testing, the same analytical methodology (the differential equation method) is used to simulate the free drop tests and demonstrate the performance of the impact limiter for the HI-STAR HB. The key features of the differential equation method are presented in [2.I.7.1], which summarizes, in a single document, the general analysis method as it was first implemented for the HI-STAR 100 license under 10CFR71.

The drop analysis of the HI-STAR HB Package using the differential equation method differs from the drop analysis for the HI-STAR 100 only to the extent that:

- the axial length of the cylindrical body is reduced;
- the nominal strength of the energy absorbing honeycomb material is reduced;
- the mass of the package is reduced.

Sheet 1 of Holtec drawing C1765 (Rev. 4) provides the reduced nominal crush strengths used in the impact limiters for the HI-STAR HB.

The dynamic multipliers (or dynamic correlation function), which were originally determined for the HI-STAR 100, remain valid for the HI-STAR HB Package for the following reasons. The Hexcel manufacturer's catalog states that dynamic crush strengths are a function of impact velocity only; there is no information suggesting that the dynamic multipliers in the differential equation method are a function of crush material strength. Therefore, the drop analyses for the HI-STAR HB impact limiters use the same dynamic multipliers (represented as a linear function of the concomitant crush velocity) that were used for the HI-STAR 100. More information on the dynamic multipliers, including the explicit form of the dynamic correlation function, is provided in [2.I.7.1].

The results from the four free drop simulations of the HI-STAR HB are documented in Table 2.I.7.1 using the nominal strengths of the honeycomb energy absorbing material. Because of the reduced length of the HI-STAR HB Package, the CGOC and slapdown angles are 58.63 degrees

and 6 or 10 degrees from the target plane, respectively. For the slapdown, the maximum deceleration of the secondary impact (after filtering to eliminate oscillations exceeding a frequency of 350 Hz) was slightly larger at a 10 degree initial angle than it was at 6 degrees; the maximum crush, however, was larger at 6 degrees as the initial orientation angle of the cask. Therefore, simulations using nominal crush strength are reported for both orientations, although sensitivity studies were performed only for the 6 degree initial orientation. The results show that the HI-STAR HB impact limiters effectively protect the HI-STAR HB cask under the postulated 30-foot drop events by maintaining the peak cask rigid body deceleration below the design basis limit of 60 g's. Since the peak decelerations are below the values computed for the HI-STAR 100, it is assured that the pin/bolt connections between the HI-STAR HB impact limiters and the HI-STAR HB body maintain their structural integrity.

Consistent with the requirements for 1-foot free drops as part of the Normal Conditions of Transport, two free drops (end drop and side drop) are also analyzed for the HI-STAR HB Package using the nominal strengths (plus 15%) specified for the honeycomb energy absorbing material. The maximum decelerations sustained by the Package, as well as the maximum impact limiter crush and impact durations, are summarized in Table 2.1.7.2. Finally, Table 2.7.1.3 presents the results of some additional parametric simulations that set upper and lower limits on permitted variation of the strength properties for the honeycomb material. The analyses leading to the reported results are documented in a supporting calculation package [2.1.7.2].

Analysis of the HB DFC to be transported in the HI-STAR 100 HB package is performed in [2.1.5.1] to demonstrate structural integrity under end drop condition consistent with those described in Appendix 2.B of the SAR. The safety factor for the HB DFC during a 60g end drop is provided in the following table, and shows that the factor of safety is greater than 1.0.

Unit	Component	Calculated Stress (ksi)	Allowable Stress (ksi)	Safety Factor = (Allowable Value)/(Calculated Value)	Remarks
Holtec Designed HB DFC	60g End Drop	13.260	26.586	2.00	Spot Welds

#### 2.I.7.2 Puncture

No new or modified calculations need be performed to qualify the HI-STAR HB, as the structure at the puncture locations is unchanged from the HI-STAR 100.

#### 2.I.7.3 Thermal

Thermal evaluation of the fire accident is presented in Supplement 3.I. No new or modified structural calculations need be performed to qualify the HI-STAR HB for the fire accident.

#### 2.I.7.4 Immersion - Fissile Material

No new or modified calculations need be performed to qualify the HI-STAR HB.

#### 2.I.7.5 Immersion - All Packages

No new or modified calculations need be performed to qualify the HI-STAR HB.

#### 2.I.7.6 Summary of Damage

The results presented in Subsections 2.I.7.1 through 2.I.7.5 show that the HI-STAR HB System meets the requirements of 10CFR71.61 and 10CFR71.73. The results from simulation of the hypothetical drop conditions produce deceleration levels that are below the design basis levels for the HI-STAR 100 for crush strength variations of plus or minus 15% of the nominal values specified for the HI-STAR HB impact limiters. Therefore, safety factors for the HI-STAR HB are greater than 1.0 by virtue of comparison with the corresponding calculations for the HI-STAR 100 for the Hypothetical Accident Conditions of Transport. Therefore, the HI-STAR 100 HB package, under the Hypothetical Accident Conditions of Transport, has adequate structural integrity to satisfy the subcriticality, containment, shielding, and temperature requirements of 10CFR71.

### 2.I.8 SPECIAL FORM

This section is not applicable to the HI-STAR HB System. This application does not seek approval for transport of special form radioactive material as defined in 10CFR71.4.

### 2.1.9 FUEL RODS

The Humboldt Bay fuel is shorter than the design basis fuel carried by the HI-STAR 100; therefore, the computations and conclusions in Section 2.9 encompass the HI-STAR HB. The presence of "Undamaged Fuel Assemblies", which are defined in Table 1.0.1 will have no significant effect on the structural response of the HI-STAR HB. This is because the only fuel parameters that have an influence on the structural analyses are the fuel mass and center of gravity height. Therefore, since an undamaged fuel assembly has essentially the same mass as an intact fuel assembly, and the exterior fuel rods serve to confine the interior fuel rods (with cladding in unknown condition) preventing them from dislocating and falling to the bottom of the fuel basket, the presence of undamaged fuel assemblies has no significant effect on the total amount of stored fuel mass or the center of gravity height used as input in the drop analysis for the HI-STAR HB.

### 2.1.10 MISCELLANEOUS ITEMS

No new appendices are introduced in Supplement 2.I. Also, since the HI-STAR 100 Package meets applicable NUREG 1617/10CFR71 requirements, so does the HI-STAR HB.

### 2.1.11 REFERENCES

- [2.1.5.1] Miscellaneous Calculations for the HI-STAR HB, HI-2033042, Rev. 4.
- [2.1.6.1] Pacific Gas and Electric Company, NRC Docket Number 72-27, Humboldt Bay ISFSI, Final Safety Analysis Report Update, Revision 0, January 2006.
- [2.1.7.1] A Classical Dynamics Based and Experimentally Benchmarked Impact Response Computation Methodology for AI-STAR Equipped Casks, HI-2084137, Rev. 0.
- [2.1.7.2] Calculation Package for HI-STAR HB Drop Analyses, HI-2084158, Rev. 0.
- [2.1.7.3] Miscellaneous Calculations for the HI-STAR HB, HI-2033042, Rev. 4.

<i>Table 2.I.2.1 Weights and Center of Gravity of HI-STAR HB Package</i>			
<i>Item</i>	<i>Component Weight (lb.)</i>	<i>Total Weight (lb.)</i>	<i>Location of C.G. above base of cask (inch)</i>
<i>Impact Limiter</i>	<i>13,000</i>	<i>26000</i>	<i>-</i>
<i>MPC HB</i>	<i>59,000*</i>	<i>-</i>	<i>-</i>
<i>HI-STAR HB (with loaded MPC HB)</i>	<i>161,200</i>	<i>-</i>	<i>-</i>
<i>Total Package Weight</i>	<i>-</i>	<i>187,200</i>	<i>-</i>
<i>Loaded Package Center of Gravity</i>	<i>-</i>	<i>-</i>	<i>61.4</i>

*\* Includes approximately 32,000 lb of fuel*

**Table 2.I.7.1 –HI-STAR HB 30' DROP RESULTS**

CONFIGURATION	MAXIMUM DECELERATION (G'S)	MAXIMUM CRUSH (INCH)	DURATION OF IMPACT (SEC.)	COMMENTS
30' TOP END DROP	56.5	13.1	0.0425	Avg. strength=694 psi
30' BOTTOM END DROP	45.6	13.8	0.047	Strength=390 psi
30' SIDE DROP	34.8	13.4	0.0485	-
30' CGOC	33.75	22	0.0665	Bottom down
30' SLAPDOWN - 6 DEGREES	45.06*	15.08	0.0705	Secondary impact limiter
30' SLAPDOWN - 10 DEGREES	45.88*	14.93	0.0964	Secondary impact limiter
30' SLAPDOWN - 6 DEGREES	33.52*	11.43	-	Primary impact limiter
30' SLAPDOWN - 10 DEGREES	30.57*	13.82	-	Primary impact limiter

\*Reported result is subsequent to filtering to remove high frequency effects above 350 Hz.

**Table 2.I.7.2 –HI-STAR HB 1' DROP RESULTS**

COMMENTS	MAXIMUM DECELERATION (G'S)	MAXIMUM CRUSH (INCH)	DURATION OF IMPACT (SEC.)	COMMENTS
1' TOP END DROP	14	1.07	0.0254	Crush strength increased by 15%
1' SIDE DROP	10	1.55	0.0305	Crush strength increased by 15%

**Table 2.I.7.3 –HI-STAR HB 30' DROP RESULTS –SENSITIVITY ANALYSES**

CONFIGURATION	MAXIMUM DECELERATION (G'S)	MAXIMUM CRUSH (INCH)	DURATION OF IMPACT (SEC.)	COMMENTS
30' TOP END DROP	59	12.4	0.040	15% increase in crush strength
30' BOTTOM END DROP	44.3	14.8	0.050	15% decrease in crush strength
30' SIDE DROP	38.5	12.2	0.0435	15% increase in crush strength
30' SIDE DROP	43*	15.2*	0.053	15% decrease in crush strength
30' CGOC	36.75	20.75	0.0608	15% increase in crush strength
30' CGOC	30.55	23.75	0.0728	15% decrease in crush strength
30' SLAPDOWN -6 DEGREES	49.17**	13.6	0.0718	Secondary IL – 15% increase in crush strength
30' SLAPDOWN -6 DEGREES	34.9**	10.43	-	Primary IL – 15% increase in crush strength
30' SLAPDOWN -6 DEGREES	38.82**	17.08	0.0842	Secondary IL – 15% decrease in crush strength
30' SLAPDOWN -6 DEGREES	30.28**	12.88	-	Primary IL – 15% decrease in crush strength

\* 1050 psi material experiences minimal lockup so peak deceleration value rises but remains below the design basis limit.

\*\* No filtering performed on deceleration time histories.